The Isolation, Characterisation and Chemotaxonomic Significance of Secondary Metabolites from Selected South African *Laurencia* spp. Rhodophyta

A Thesis Submitted in Fulfillment of the Requirements for the Degree of

DOCTOR OF PHILOSOPHY (PHARMACY)

of

RHODES UNIVERSITY

By

Jameel Fakee

February 2015

Acknowledgements

It is only imperative to acknowledge the many people who have assisted me in the completion of this thesis to whom I offer my sincerest thanks and gratitude:

- My research supervisor Professor Denzil Beukes. A man who has served as a figure of inspiration, hope and unwavering support for many years. The lessons he has taught me will be with me for life. Thank you for believing in me.
- Professor John Bolton and Dr. Caitlynne Francis from the University of Cape Town for tireless collaborative efforts.
- Mr. and Mrs. Morley from the Pharmacy Faculty for their continuous assistance.
- Prudence for providing a conducive working environment in the lab.
- Dr. Marietjie Stander from Stellenbosch University for assistance with mass spectrometry.
- The Henderson Scholarship Trust and Rhodes University for generous funding.
- Professor Walker and fellow colleagues in the Faculty of Pharmacy for their unflinching support.
- Maynard Chiwakata for always being my right hand man. A selfless person who I have had the pleasure of forging an eternal brotherhood with.
- To all my wonderful friends including Nabeela Sader, Taherah Moola and Mohammed Adam. They have undoubtedly served as pillars of strength and their diligent support has, without a doubt, been the sole reason for my success.
- Farida and Hayat Ticklay for their consistent support and mentorship throughout my academic journey.
- Yasmin Farrelly and family for always believing in me and providing assistance in more ways than one.
- Finally to my entire family, especially my loving parents **Amina** and **Asgar Fakee** who have sacrificed dearly for me to achieve this dream. I thank each and every one of you for being behind me in my ventures and providing me with strength as well as self belief. I hope I have managed to make you all proud.

Thank you!

In all things of nature there is something of the marvelous

Aristotle

Table of contents

Table of contents

List of figures

List of tables

List of schemes

List of abbreviations

ax	Axial
BBI	Broadband Inverse
°C	Degrees celsius
COSY	^{1}H-^{1}H Homonuclear Correlation Spectroscopy
d	Doublet
dd	Double doublet
dt	Doublet triplet
DQD	Digital Quadrature Detection
DEPT	Distortionless Enhancement of Polarisation Transfer
dq	Doublet quartet

EtOAc	Ethyl acetate
eq	Equatorial
gem	Geminal
HMBC	Heteronuclear Multiple Bond Correlation
HPLC	High Performance Liquid Chromatography
HRAPCIMS	High Resolution Atmospheric Pressure Chemical Ionisation Mass Spectrometry
HREIMS	High Resolution Electron Impact Mass Spectrometry
HRESIMS	High Resolution Electron Spray Ionisation Mass Spectrometry
HRGCEIMS	High Resolution Gas Chromatography Electron Impact Mass Spectrometry
HSQC	Heteronuclear Single Quantum Coherence
Hz	Hertz
Imp	Impurity
IR	Infra-red
J	Spin-Spin coupling constant (Hz)
m	Multiplet
m/z	Mass to charge ratio
MHz	Megahertz
mult	Multiplicity
M_r	Molecular weight
NMR	Nuclear Magnetic Resonance
NOESY	Nuclear Overhauser Enhancement Spectroscopy
q	Quartet
quin	Quintet
s	Singlet
sex	Sextet
Sp.	Species (Singular)
Spp.	Species (Plural)
t	Triplet
td	Triplet doublet
δ_H	Proton chemical shift
δ_C	Carbon chemical shift

Abstract

Bioprospection of marine organisms as a potential source for lead drugs is becoming increasingly popular. The secondary metabolome of these organisms consists of structurally diverse molecules possessing unprecedented carbon skeletons, the biosynthesis of which occurs *via* complex metabolomic pathways driven by specialist enzymes. This structural novelty is highly influential on the favourable bioactivity these compounds display. A prominent example of such a compound is trabectedin marketed as Yondelis®. Registered for the treatment of soft tissue sarcomas, this marine drug was developed from extracts of the tunicate *Ecteinascidia turbinata*.

South Africa is renowned for possessing a highly diverse marine biota including several endemic species of marine red algae belonging to the *Laurencia sensu stricto* genus, which falls within the *Laurencia* complex. Despite having a good reputation for fascinating secondary metabolites, the taxonomy of *Laurencia* natural products is proving challenging for reasons including the presence of cryptic species, as well as individual species displaying morphological variability.

The aim of this study was thus to isolate secondary metabolites from various South African *Laurencia* spp. and subsequently assess their chemotaxonomic significance by analysis of a parallel plastid *rbc*L phylogeny study of *Laurencia* spp.

This study reports the first phycochemical investigation into ***Laurencia natalensis*** Kylin, ***Laurencia* cf. *corymbosa*** J.Agardh, ***Laurencia complanata*** (Suhr) Kützing, ***Laurencia sodwaniensis*** Francis, Bolton, Mattio and Anderson submitted, ***Laurencia multiclavata*** Francis, Bolton, Mattio and Anderson submitted, and a South African specimen of ***Laurenciella marilzae*** Gil-Rodríguez, Sentíes, Díaz-Larrea, Cassano and M.T. Fujii (basionym: *Laurencia marilzae*) originally described from Spain. Additionally, the chemical profiles of previously explored species ***Laurencia flexuosa*** Kützing and ***Laurencia glomerata*** Kützing were re-investigated.

The organic extracts of the above species afforded 31 compounds belonging to a wide array of structural classes including halo-chamigranes, linear C_{15} acetogenins, indole alkaloids, cuparanes and cyclic bromo-ethers. A new tri-cyclic keto-cuparane (**4.4**) was isolated from *L.* cf. *corymbosa* alongside the new cuparanes **4.1** and **4.7**.

Algoane (**5.9**), a unique marker compound isolated from *L. natalensis*, was previously only reported from a sea-hare. Such marker compounds which are exclusive to an individual algal species increase the ease of their subsequent identification.

The feasibility of chemotaxonomy as an additional tool to classify *Laurencia* spp. was established as broad predictions of a specimen's phylogeny, based on representatives of its secondary metabolome, proved viable. The study specimens were shown to possess similar chemical profiles to their sister species e.g. *L. complanata*, *L. sodwaniensis* and *L. multiclavata* produced similar metabolites to their sister species as inferred by an *rbc*L phylogeny tree.

Finally, a ^{1}H NMR profiling study on the crude organic extracts of various *Laurencia* spp. generated distinctive, reproducible spectra, exposing the value of NMR spectroscopy as a rudimentary species discernment tool.

Chapter 1

General introduction

A noticeable increase in the interest of natural products as potential drug leads has led to immense bioprospection of many marine organisms resulting in the expansion of marine natural product libraries (Blunt *et al*., 2014). Marine macroalgae in particular have generated over 3000 new chemical structures in the last 40 years, most of which were isolated from the phylum Rhodophyta (Leal *et al*., 2013).

Within the *Laurencia* complex, the genus *Laurencia sensu stricto* (referred to as *Laurencia* spp. henceforth) is reputable for producing a varied collection of fascinating chemistry with over 500 new metabolites documented (de Carvalho *et al*., 2006). Unfortunately factors such as high morphological variability amongst individual species make the classification and or identification of members within this genus increasingly difficult (Wang *et al*., 2013). Such was the case for *Laurencia pacifica* which was seen to possess a number of different distinctive forms (Fenical and Norris, 1975).

Laurencia spp. produce compounds including sesquiterpenes, diterpenes, C_{15} acetogenins and *N*-methyl indoles (Wang *et al*., 2013). The majority of these compounds are halogenated; bromine being the most common. Their biosynthesis is undoubtedly controlled by tailored enzymes which possess multifunctional roles (Schwab, 2003). The enzymes themselves are products of inherent genetic sequences within the algae and consequently this phenotypic status endorses the use of the resultant secondary metabolites as phylogenetic markers (Masuda *et al*., 1997).

The high incidence of untapped macroalgae endemic to the South African coastline, especially of the *Laurencia* genus, inspired a unique, systematic study of a select number of these species in terms of isolating and characterising the natural products they produce, and subsequently assessing their chemotaxonomic value. This study was done in parallel with Francis (2014) who focused on defining *Laurencia* spp. phylogeny along the South African coastline by means of morpho-anatomical and DNA *rbc*L marker classification. Our main goal was to assess whether there is a clear correlation between genetically similar *Laurencia* spp. and the secondary metabolites they produce i.e. will sister species produce identical metabolites?

The *Laurencia* spp. employed in this study were collected at various locations along the South African coastline as depicted in (Figure 1.1).

Figure 1.1: Collection sites, along the South African seaboard, of various *Laurencia* spp. analysed in this study[1]

The specific research objectives of the study were to:

- Isolate and fully characterise secondary metabolites from the crude organic extracts of South African specimens of:
  - *Laurencia natalensis* Kylin
  - *Laurencia* cf. *corymbosa* J.Agardh
  - *Laurencia complanata* (Suhr) Kützing
  - *Laurencia sodwaniensis* Francis, Bolton, Mattio and Anderson submitted
  - *Laurencia multiclavata* Francis, Bolton, Mattio and Anderson submitted
  - *Laurencia flexuosa* Kützing
  - *Laurencia glomerata* Kützing
  - *Laurenciella marilzae* (Gil-Rodríguez, Sentíes, Díaz-Larrea, Cassano and M.T.Fujii) (basionym: *Laurencia marilzae*)

[1] Image adapted from Google maps © 2015 NASA, Accessed 02/01/2015,
Available at: https://www.google.com/maps/@29.9524212,24.5703502,1335784m/data=!3m1!1e3

- Based on an *rbc*L inferred *Laurencia* spp. phylogeny tree, investigate the chemotaxonomic significance of the isolated compounds by assessing whether genetically similar species produce similar secondary metabolites.

- Conduct a ^{1}H NMR profiling study on the crude organic extracts of the abovementioned *Laurencia* spp., including *L.* cf. *elata* and *L. peninsularis*, in an attempt to establish rudimentary spectroscopic species delineation methods based on unique chemical profiles of members within the genus.

This thesis is divided into 12 stand alone chapters each possessing their own references. As a result some references will be duplicated.

A brief literature review is presented in the next chapter (Chapter 2) followed by a detailed account of the secondary metabolites isolated from seven South African *Laurencia* spp. (Chapters 3-9). Thereafter, the chemotaxonomic significance of the compounds isolated is presented (Chapter 10) followed by results of a ^{1}H NMR profiling study, exploring the use of crude organic extracts for discriminating between *Laurencia* spp. (Chapter 11). Chapter 12 contains concluding remarks in the context of the study aims.

Appendix 1 reports the natural product chemistry, for the first time, of a South African specimen of the re-classified *Laurenciella marilzae*. A proposed biosynthetic scheme of the majority of the isolated metabolites is presented in Appendix 2.

Finally, a Compact Disc (CD) accompanies this thesis which contains all the relevant supplementary data. When any reference is made to spectroscopic data which is not presented within the text, it can be found within the supplementary data. The CD also contains an eCopy of the thesis to assist where image clarity is lost in the printed hardcopy.

References

Blunt, J. W.; Copp, B. R.; Keyzers, R. A.; Munro, M. H. G.; Prinsep, M. R. Marine natural products. *Natural Product Reports* **2014**, *31*, 160-258.

de Carvalho, L. R.; Fujii, M. T.; Roque, N. F.; Lago, J. H. G. Aldingenin derivatives from the red alga *Laurencia aldingensis*. *Phytochemistry* **2006**, *67*, 1331-1335.

Fenical, W.; Norris, J. N. Chemotaxonomy in marine algae: chemical separation of some *Laurencia* species (Rhodophyta) from the Gulf of California. *Journal of Phycology* **1975**, *11*, 104-108.

Francis, C. M. **2014**. Systematics of the *Laurencia* complex (Rhodomelaceae, Rhodophyta) in southern Africa. PhD Thesis. University of Cape Town, Cape Town, South Africa.

Leal, M. C.; Munro, M. H. G.; Blunt, J. W.; Puga, J.; Jesus, B.; Calado, R.; Rosa, R.; Madeira, C. Biogeography and biodiscovery hotspots of macroalgal marine natural products. *Natural Product Reports* **2013**, *30*, 380-1390.

Masuda, M.; Abe, T.; Sato, S.; Suzuki, T.; Suzuki, M. Diversity of halogenated secondary metabolites in the red alga *Laurencia nipponica* (Rhodomelaceae, Ceramiales). *Journal of Phycology* **1997**, *33*, 196.

Schwab, W. Metabolome diversity: too few genes, too many metabolites? *Phytochemistry* **2003**, *62*, 837-849.

Wang, B. G.; Gloer, J. B.; Ji, N, Y.; Zhao, J. C.; Halogenated organic molecules of Rhodomelaceae origin: Chemistry and Biology. *Chemical Reviews* **2013**, *113*, 3632-3685.

Chapter 2

Literature review

2.1 Natural products

A natural product or secondary metabolite can be described as any compound produced by an organism *via* a secondary metabolic pathway and is considered to be uninfluential on growth, development or reproduction of the organism. It may however augment the organism's chances of survival by adopting a defensive or chemo-attractant role. Conversely, primary metabolites such as sugars, amino acids and lipids are critical for the normal functioning of the cell and hence imperative for the survival of the organism (Maplestone *et al.*, 1992; Dewick, 2002).

Natural products are viewed as one of the most prolific sources of prospective drug lead compounds (Mishra and Tiwari, 2011). These compounds boast complex as well as novel structural attributes which are seen to be unique compared to those produced using a standard combinatorial type approach (Butler, 2004).

The impressive activity of natural products *vs.* synthetic counterparts comes as a result of an increase in the number of chiral centres, greater structural rigidity, a higher incidence of hetero-atoms, aromatic rings and complex cage like structures as well as more sites for hydrogen bond donation and acceptance (Yuliana *et al*., 2011).

Unavoidable drawbacks of natural products as drug leads include factors such as compound instability, erroneous sourcing of organisms containing the desired compounds, complex structure elucidation processes as well as difficulty up scaling their production (Yuliana *et al*., 2011).

2.1.1 Natural products in history

Ancient records of natural product usage were found on clay tablets originating from Mesopotamia (2600 BC). These contained details of oils extracted from *Commiphora* spp. (myrrh) and *Cupressus sempervirens* (cypress) which are still recognised today for their acclaimed effectiveness against respiratory tract infections (Cragg and Newman, 2005).

The *Ebers Papyrus* (2900 BC) originating from Egypt possessed over 500 documented herbal remedies (Cragg and Newman, 2005), while the well established Indian traditional healing practice known as Ayurveda, highlights the use of plant-based remedies amongst others for the treatment of various illnesses (Mukherjee *et al*., 2012).

The Greek philosopher and natural scientist Theophrastus (300 BC) wrote a dissertation entitled *Historia Plantarium*. This collection provided physicians with details on plant taxonomy as well as plant remedies for a variety of different illnesses (Cragg and Newman, 2005).

Ibn Sina (Avicenna), a Persian physician and Islamic scholar, wrote close to 40 books relating to medical science. His piece entitled *Canon Medicinae* was one of the more renowned, containing clear evidence of the use of natural products for the treatment of multitudes of diseases (Cragg and Newman, 2005).

2.1.2 Distinction between primary and secondary metabolism

It is essential to be acquainted with the biosynthetic origin of secondary metabolites *vs*. that of primary metabolites. Primary metabolites are those compounds which are produced within a living organism as direct products of biosynthetic and/or catabolic processes involving proteins, carbohydrates, nucleic acids and fats (all essential to living organisms) (Haefner, 2003).

On the contrary, secondary metabolites are molecules formed *via* unique metabolic pathways which are deemed as being less essential for the survival of the organism than primary metabolites. These pathways are often seen to be unique to a particular organism or species and hence can be viewed as a form of expressing identity. The rationale for their production has come under great scrutiny over the years and the role they play in contributing toward the organism's survival must not be over looked (Maplestone *et al*., 1992).

Secondary metabolites are thought to be produced in response to environmental cues. It is hypothesised that organisms produce them for defensive purposes, as they have displayed antiherbivory, antifouling and ichthyotoxic effects amongst others (Colegate and Molyneux, 2008). Their biosynthesis involves either the shikimate, acetate, alkaloid, mevalonate or methylerythritol phosphate pathway (Dewick, 2002), each pathway generating structurally varied products.

2.1.3 Clinically significant natural products

Many well-known drugs on the market today originate from natural sources. These compounds have played a significant role in either the management or cure of disease. Furthermore, they have forwarded invaluable knowledge on structural originality which researchers can apply to modern day thinking in the drug discovery process (Mishra and Tiwari, 2011).

The active constituent of *Digitalis purpurea*, digitoxin (**2.1**), had been isolated in the 18th century. It was found to improve cardiac contractility and consequently has been used, along with its analogues, for the management of congestive cardiac disease (DerMarderosian and Beutler, 2002).

Perhaps one of the most renowned natural product derived drug to date is acetylsalicylic acid (**2.2**) commonly known as aspirin. It is derived from salicin, found in the bark of the willow tree *Salix alba*, and has made its name as an effective analgesic agent (DerMarderosian and Beutler, 2002).

Analyses of the chemical constituents of the opium poppy, *Papaver somniferum*, displayed numerous alkaloids including morphine (**2.3**), a potent opioid analgesic whose role in pain management is well established. Other derivatives such as heroin and codeine also stem from the opium poppy (DerMarderosian and Beutler, 2002).

Quinine (**2.4**), isolated from the bark of the *Cinchona succirubra* tree, had formally been used by the British to treat malaria in the 19th century (DerMarderosian and Beutler, 2002).

The *L*-histidine derived alkaloid pilocarpine (**2.5**) found in *Pilocarpus jaborandi* (Rutaceae) has been used as a clinical drug for over a century treating various glaucomas. An oral preparation of pilocarpine is now available and is indicated for use in xerostomia as well as management of Sjörgen's syndrome (DerMarderosian and Beutler, 2002).

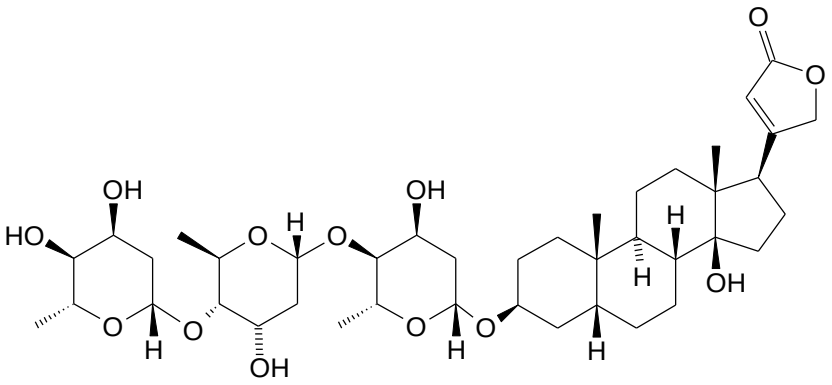

2.1
Digitoxin

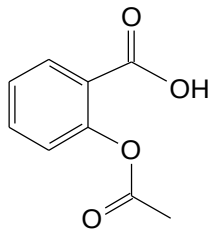

2.2
Aspirin

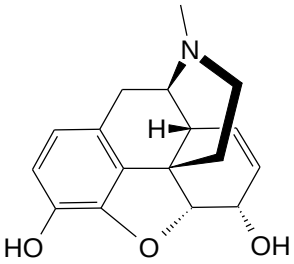

2.3
Morphine

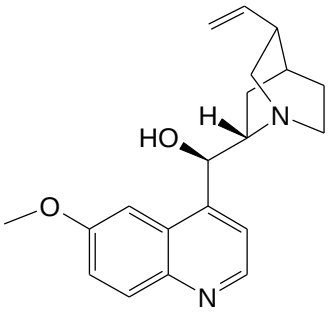

2.4
Quinine

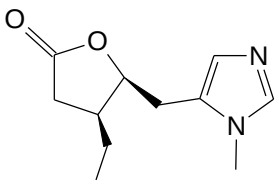

2.5
Pilocarpine

Figure 2.1: Clinically significant compounds derived from natural products

2.1.4 Natural products from marine algae

Natural products are found in an assortment of marine organisms including sponges, marine algae and tunicates (Blunt *et al.*, 2014).

Marine algae are classified as either microalgae or macroalgae. In excess of 30 000 species of macroalgae (seaweed) have been identified (Faulkner, 2002) and they are seen to play significant ecological roles such as the provision of the majority of atmospheric oxygen.

Natural products from marine sources are structurally diverse, complex molecules which include terpenes, linear acetogenins, peptides, indoles, cyclic polyketides, hydrocarbons and phenols (Haefner, 2003). The majority of these secondary metabolites are halogenated, of which the most common halo-substituents are seen to be bromine followed by chlorine. This reflects the abundant nature of bromide and chloride ions in the ocean (Butler and Sandy, 2009). The halogenated nature of these compounds contributes significantly to the vast assortment of biological activities which they display including antibacterial, antifungal, antiviral, anti-inflammatory, antiproliferative, antifouling, antifeedant, cytotoxic, ichthyotoxic and insecticidal activity (Blunt *et al.*, 2014).

2.1.5 Drug discovery and marine natural products

The fact that approximately 70% of the earth's surface is made up entirely of water, in addition to the serendipitous discovery of penicillin by Alexander Fleming in 1928, sparked a global pharmaceutical interest to explore natural products as potential drug leads, particularly from the marine environment. It was seen that there was a greater chance of finding exclusive biodiversity from marine sources and hence prospective drug leads (Haefner, 2003). A testament to this interest is the initiation of several natural product discovery (NPD) programs by major pharmaceutical companies in an attempt to obtain lead compounds for various diseases (Ojima, 2008; Baker *et al.*, 2007).

The aquatic environment became more accessible for investigation due to advancements in snorkelling techniques as well as the introduction of SCUBA diving in the early 1970s (Alejandro *et al.*, 2010). Organisms scrutinised include sponges, tunicates, algae and bryozoans amongst others (Blunt *et al.*, 2014). Regrettably, the initiation of high throughput screening (HTS) encouraged the hasty demobilisation of numerous NPD programs by pharmaceutical companies (Nussbaum *et al.*, 2006).

Some of the challenges faced included failure in total syntheses of the compounds isolated due to their structural complexity. In addition, marine organisms are difficult to classify hence finding the same species and re-isolating the same compound proves challenging (Faulkner, 1977).

Nonetheless, advancements in spectroscopic techniques, amplification of instrumentation sensitivity and the advent of chemotaxonomic as well as genomic means of classifying marine organisms reinitiated the interest in natural product based drug discovery (Baker *et al*., 2007).

A prominent example of a successful compound isolated from the marine environment is trabectedin (**2.6**) (Cuevas and Francesch, 2009). This compound, isolated from the sea squirt *Ecteinascidia turbinata*, was the first marine anticancer drug to be approved in the European Union (Alejandro *et al*., 2010).

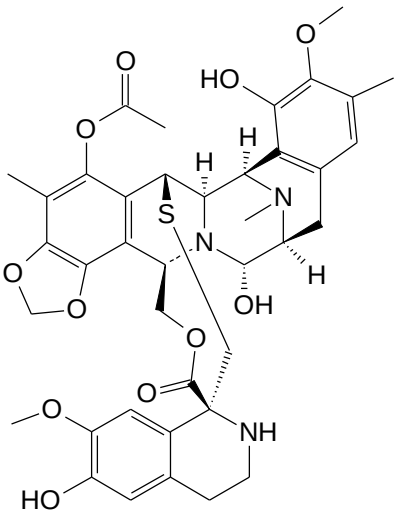

2.6

Figure 2.2: The marine anticancer drug trabectedin

2.1.6 South African marine algae

The South African coastline stretches a little under 4000 km (Griffiths *et al*., 2010) with a diverse population of endemic seaweed flora. In excess of 12 000 marine plants and animals exist along the southern African seaboard (Branch *et al*., 1994) with more than 50% of the seaweeds found on the west coast being confined to the southern African region (Stegenga *et al*., 1997). A total of 803 species are acknowledged of which 101 are brown algae, 149 are green algae and 553 are red algae (Bolton, 2010).

A major contributing factor to this phenomenon is the Agulhas current (Figure 2.3) which flows down the east coast of Africa and brings with it warm water from the Indian ocean to the southern African shoreline. It is regarded as one of the strongest currents in the world and its direction of flow refreshes the nutrients along the southern African coast. The mixing of this warm current with the colder Benguela current along the western seaboard creates a unique oceanic environment allowing algae to flourish.

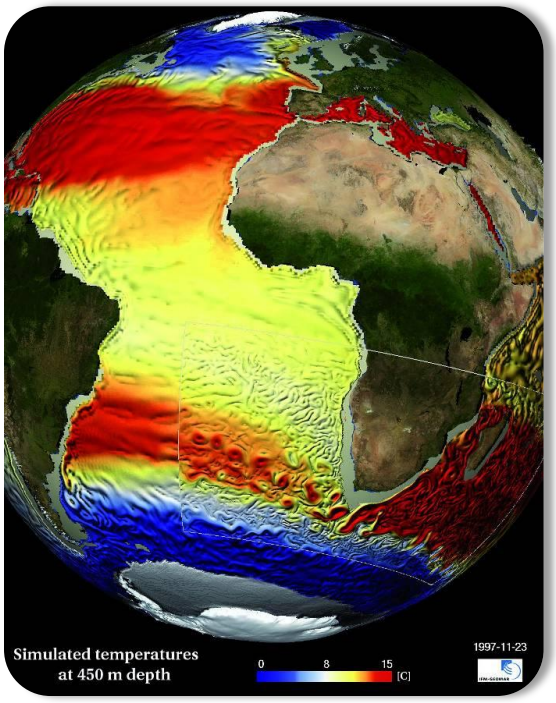

Figure 2.3: A depiction of the Agulhas current[1]

(Accessed 26/10/2014), Available at: http://inside.hlrs.de/_old/htm/Edition_01_11/article_06.html

[1] Image courtesy of Arne Biastoch © 2015, Leibniz Institute of Marine Sciences, Kiel, Germany.

Griffiths *et al*., (2010) show South Africa to have a total of nine marine bioregions, five of which are coastal including the Namaqua, South-western Cape, Agulhas, Natal and Delagoa bioregions (Figure 2.4).

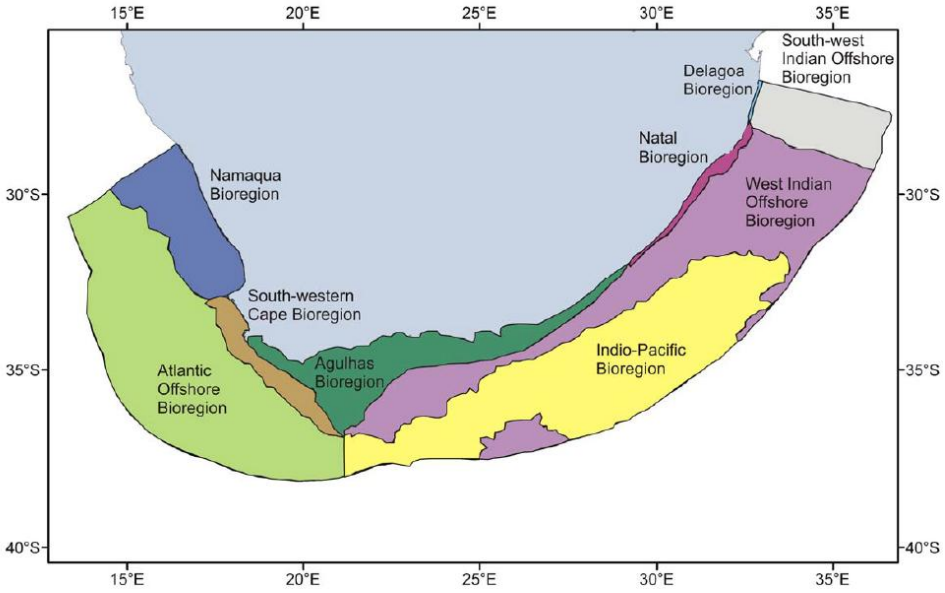

Figure 2.4: Nine bioregions of South Africa (Griffiths *et al*., 2010)[2]

Research interests into the natural product chemistry of South African marine algae have consequently risen, with novel compounds such as the procoralides (**2.7** and **2.8**) reported from *Plocamium corallorhiza* (Knott *et al*., 2005). Additionally, Phaeophyta such as *Sargassum* sp. have afforded compounds such as sargahydroquinoic acid (**2.9**) (Afolayan, 2008).

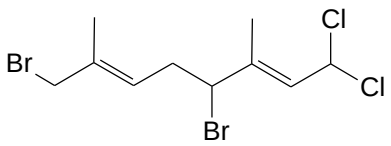

2.7

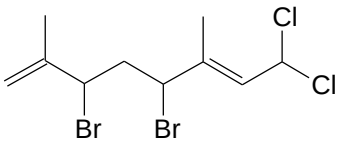

2.8

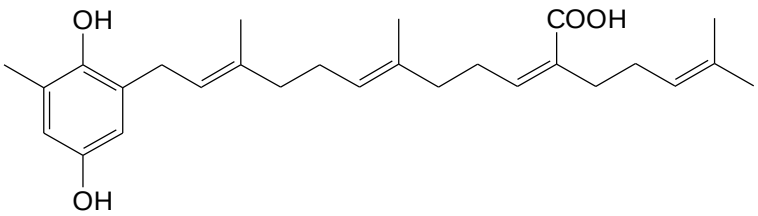

2.9
Sargahydroquinoic acid

[2] Image courtesy of Charles Griffiths © 2015, University of Cape Town, South Africa

2.2 *Laurencia* species

The *Laurencia* complex consists of five genera with a sixth recently discovered. These include *Laurencia sensu stricto, Chondrophycus, Osmundea, Palisada, Yuzura* and the newly discovered genus *Laurenciella* gen. nov. (basionym: *Laurencia marilzae*)[3] (Cassano *et al*., 2012).

According to the database AlgaeBase™ (Guiry and Guiry, 2015) the *Laurencia* genus within the complex consists of 421 documented species, 131 of which are taxonomically accepted. These taxa are widely distributed particularly within tropical and temperate regions with the majority of the species found within the southern hemisphere (Francis, 2014).

Given the fascinating secondary metabolites *Laurencia* spp. produce (Wang *et al*., 2013) it is advantageous, especially to the natural product chemist, that delineation of species within this genus is on an increase (Martin-Lescanne *et al*., 2010).

Furthermore, the integrity of *Laurencia* spp. systematics has been consolidated by the use of genetic markers especially *rbc*L sequences for species delineation (Nam, 2006), however, failures in standardising innate morphological traits amongst the species is still of concern (Francis, 2014).

2.2.1 Occurrence in South Africa

As previously mentioned (Figure 2.3) the east and southern coastal regions of southern Africa are enriched with temperate, nutrient rich waters which provide ideal conditions for *Laurencia* spp. to thrive in.

Francis, (2014) confirms the identity of nine previously described South African *Laurencia* spp. including five newly discovered species (Table 2.1), by morpho-anatomical as well as *rbc*L sequencing methods. Of these, seven possess their type locality within South Africa with *L. complanata, L. flexuosa, L. natalensis, L. pumila and L. peninsularis* deemed southern African endemic.

The distribution of these species is as displayed below (Table 2.1). Note that most of the *Laurencia* spp. flourish either on the eastern or southern seaboard as a result of the temperate waters within those regions.

[3] Appendix 1 discusses the natural product chemistry of a South African specimen of *Laurenciella marilzae*.

Table 2.1: Occurrence of *Laurencia* spp. in South Africa

(Stegenga *et al*., 1997; Bolton and Anderson, 1997; De Clerck *et al*., 2005, Francis, 2014)

South African *Laurencia* spp.	**Distribution**[4]
Laurencia brongniartii J. Agardh	EC
Laurencia complanata (Suhr) Kützing	SC, EC
Laurencia cf. *corymbosa* J. Agardh	SC, EC
Laurencia cf. *elata* (C. Agardh)	SC
Laurencia flexuosa Kützing	WTZ, SC, EC
Laurencia glomerata Kützing	WC, EC
Laurencia natalensis Kylin	WTZ, SC, EC
Laurencia stegengae Francis, Bolton, Mattio and Anderson submitted	WTZ, SC
Laurencia pumila (Grunow) Papenfuss	SC, EC
Laurencia dehoopiensis Francis, Bolton, Mattio and Anderson submitted	SC
Laurencia dichotoma Francis, Bolton, Mattio and Anderson submitted	EC
Laurencia digitata Francis, Bolton, Mattio and Anderson submitted	SC, EC
Laurencia multiclavata Francis, Bolton, Mattio and Anderson submitted	SC, EC
Laurencia sodwaniensis Francis, Bolton, Mattio and Anderson submitted	EC

South Africa is consequently recognised as a unique geographical location for *Laurencia* spp. as a variety of taxa with high levels of endemism thrive along its shoreline.

This exclusive bio-geography was the underlying motivation for this study wherein valuable contributions are made *via* primary phycochemical exposure of various South African *Laurencia* spp. coupled with a detailed assessment of their chemotaxonomic value based on comparisons to *rbc*L phylogenetic studies constructed in parallel by Francis, (2014).

Species which have previously been investigated for their natural product chemistry such as *L. glomerata* (Elsworth and Thomson, 1989) and *L. flexuosa* (Mann, 2008) were re-assessed for metabolite constancy as well as new chemistry.

[4] WC (West Coast), WTZ (Western Transition Zone from Cape Point to Cape Agulhas, SC (South Coast), EC (East Coast)

2.2.2 Compounds from *Laurencia* spp.

Laurencia spp. have been shown to produce a vast number of secondary metabolites with structural classes including sesquiterpenes, diterpenes, triterpenes, indole alkaloids and C_{15} acetogenins each showing an assortment of carbon skeletons as seen below in (Table 2.2).

Table 2.2: Various structural classes isolated from *Laurencia* spp. (Wang *et al*., 2013).

Sesquiterpenes	**Diterpenes**	**Triterpenes**	**Indole alkaloid**	**C_{15} acetogenins**
Bisabolene	Irieane	Dioxybicyclodecane	Indole	Linear
Brasilane	Labdane	Dioxybicycloundecane	*Bis*-indole	5 membered cyclic ethers
Chamigrane	Parguerane			6 membered cyclic ethers
Cuparane				7 membered cyclic ethers
Eudesmane				8 membered cyclic ethers
Laurane				12 membered cyclic ethers
Snyderane				Manenone

Halogenated metabolites produced by *Laurencia* spp. exist within cellular bodies commonly known as *corps en cerise*. These are cherry like bodies which serve to store and sequester toxic metabolites produced by the algae (Hay and Fenical, 1988). Each *Laurencia* spp. possesses a distinctive number of *corps en cerise* per cell and these bodies are only present in species of *Laurencia* and *Laurenciella* within the *Laurencia* complex (Garbary and Harper, 1998). They tend to concentrate within cellular tissue which is prone to herbivory, such as those of the outer cortex of the plant. *Laurencia* spp. which do not produce halogenated metabolites are deficient of these vesicles (Hay and Fenical, 1988).

Structural representatives from each chemical class of secondary metabolites found in *Laurencia* spp. are displayed overleaf (Figure 2.5).

Sesquiterpenes

Bisabolene

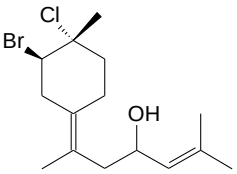

2.10

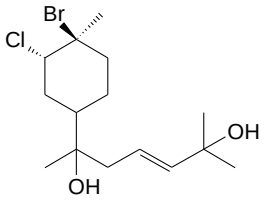

2.11

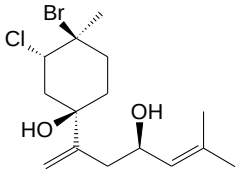

2.12

Brasilane

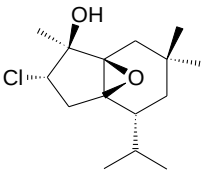

2.13

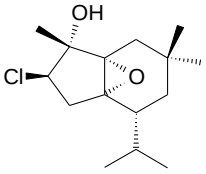

2.14

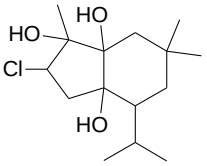

2.15

Chamigrane

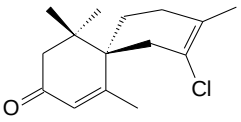

2.16

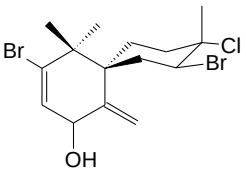

2.17

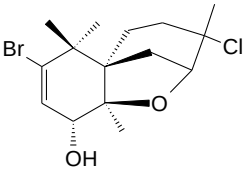

2.18

Cuparane

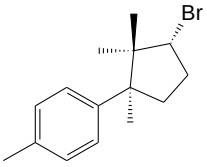

2.19

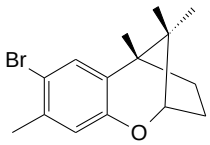

2.20

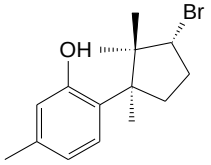

2.21

Eudesmane

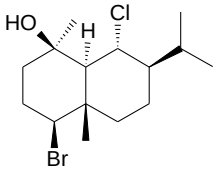

2.22

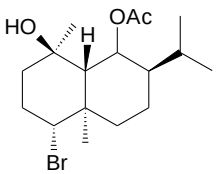

2.23

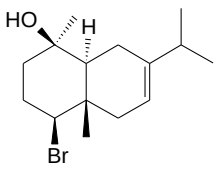

2.24

Figure 2.5: *Laurencia* spp. compounds isolated from various structural classes (Wang *et al*., 2013)

Laurane

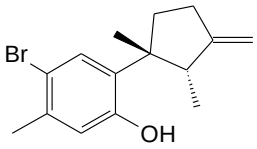

2.25

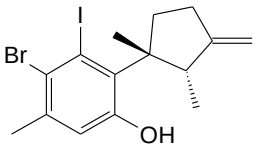

2.26

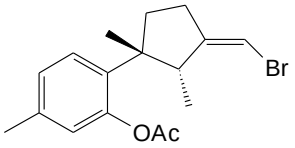

2.27

Snyderane

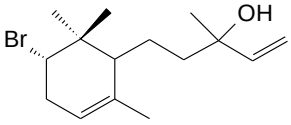

2.28

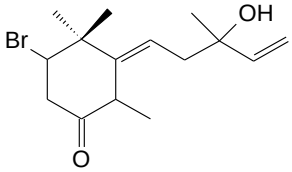

2.29

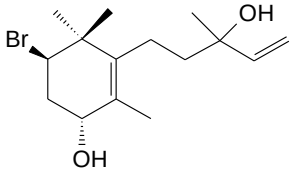

2.30

Diterpenes

Irieane

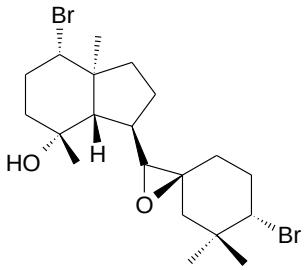

2.31

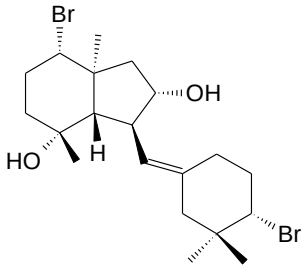

2.32

Labdane

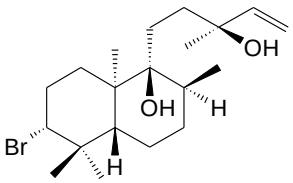

2.33

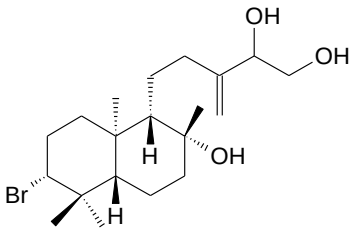

2.34

Parguerane

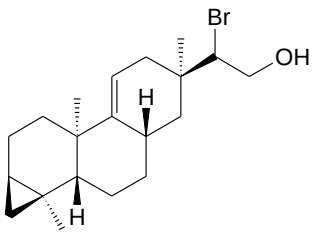

2.35

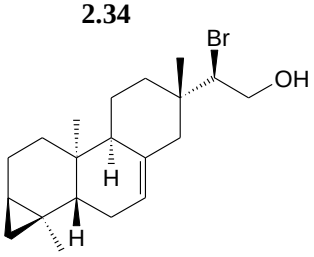

2.36

Figure 2.5: Continued

Triterpenes

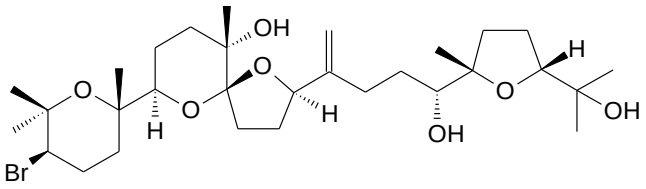

2.37

Indole alkaloids

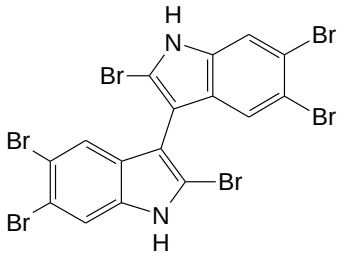

2.38

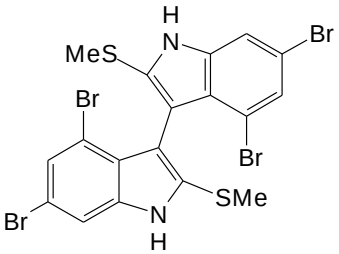

2.39

C_{15} acetogenins

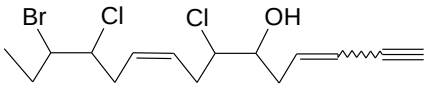

2.40

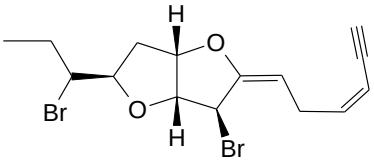

2.41

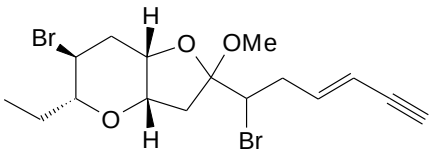

2.42

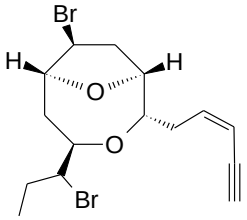

2.43

Figure 2.5: Continued

2.2.3 Biosynthesis of secondary metabolites

A large number of *Laurencia* spp. metabolites are brominated. Dissolved oceanic bromide salts are regarded as the source of bromine utilised by the algae for secondary metabolite synthesis (Butler and Carter-Franklin, 2004).

Suzuki *et al*., (2009) confirmed this theory by culturing three species of *Laurencia* (*L. okamurai*, *L. japonensis* and *L. nipponica*) in a medium containing a radio-labelled $Na^{82}Br$ salt. After a specific culture period, the resultant compounds isolated were seen to contain the radio-labelled ^{82}Br halogen by TLC-ARLG (Thin layer chromatography auto radio luminography) imaging, proving that the algae utilise external bromide ion for secondary metabolite synthesis.

The process by which bromine is introduced into the molecule relies heavily on an enzyme known as Vanadium-bromoperoxidase (V-BrPO) (Butler and Carter-Franklin, 2004) which catalyses the oxidation of bromide by H_2O_2. Crude preparations of this particular enzyme have been isolated from *Laurencia nipponica* and were successfully employed in bromo-ether cyclisation reactions with laurediol precursors (Fukuzawa *et al*., 1994). The enzyme bound electrophilic halogenating species, commonly known as the bromonium ion (Br^+) is key in the formation of *Laurencia* brominated metabolites such as cyclic bromo-ethers from linear C_{15} acetogenins (Figure 2.6).

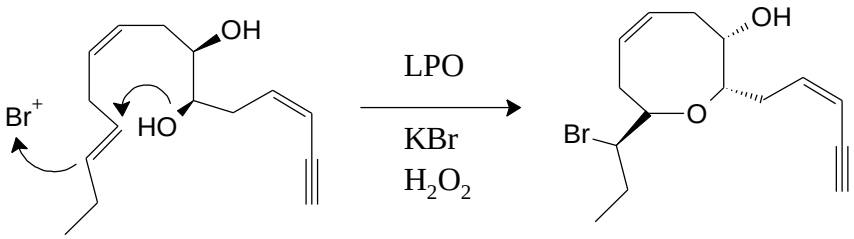

Laurediol Pre-laureatin

Figure 2.6: Proposed formation of pre-laureatin *via* a peroxidase catalysed bromonium ion induced cyclisation[5] (Ishihara *et al*., 1995; Butler and Carter-Franklin, 2004)

.

[5] Commercially available lactoperoxidase (LPO) was used as an analogue to V-BrPO

2.3 References

Afolayan, A. F. **2008**. Isolation and characterisation of anti-plasmodial metabolites from South African marine algae. M.Sc thesis. Rhodes University, Grahamstown.

Alejandro, M.; Glaser, K. B.; Cuevas, C.; Jacobs, R. S.; Kem, W.; Little, R. D.; McIntosh, J. M.; Newman, D. J.; Potts, B. C.; Shuster, D. E. The odyssey of marine pharmaceuticals: a current pipeline perspective. *Trends in Pharmaceutical Sciences* **2010**, *31*, 255-265.

Baker, D. D.; Chu, M.; Oza, U.; Rajgarhia, V. The value of natural products to future pharmaceutical discovery. *Natural Product Reports* **2007**, *24*, 1225-1244.

Blunt, J. W.; Copp, B. R.; Keyzers, R. A.; Munro, M. H. G.; Prinsep, M. R. Marine natural products. *Natural Product Reports* **2014**, *31*, 160-258.

Bolton, J. J.; Anderson, R. J. Marine vegetation. In Cowling, R.M., Richardson, D.M. & Pierce, S.M. (Eds) *Vegetation* of *Southern Africa*; Cambridge, Cambridge University Press. **1997**, 348-370.

Bolton, J. J. Seaweed systematics and diversity in South Africa: an historical account. *Transactions of the Royal Society of South Africa* **2010**, *54*, 167-177.

Branch, G. M.; Griffiths, C. L.; Branch, M. L.; Beckley, L. E. *Two oceans: A guide to the marine life of Southern Africa*, David Philips Publishers, South Africa, **1994**, 1-2.

Butler, M. S. The role of natural product chemistry in drug discovery. *Journal of Natural Products* **2004**, *67*, 2141–2153.

Butler, A.; Sandy, M. Mechanistic considerations of halogenating enzymes. *Nature* **2009**, *460*, 848-854.

Butler, A.; Carter-Franklin, J. N. The role of vanadium bromoperoxidase in the biosynthesis of halogenated marine natural products. *Natural Product Reports* **2004**, *21*, 180-188.

Cassano, V.; Gil-Rodríguez, M. C.; Sentíes, A.; Díaz-Larrea, J.; Fujii, M. T. Molecular support for the establishment of the new genus *Laurenciella* within the *Laurencia* complex (Ceramiales, Rhodophyta). *Botanica Marina* **2012**, *55*, 349–357.

Colegate, S. M.; Molyneux, R. J. *Bioactive Natural Products: Detection, Isolation and Structure Determination*; CRC Press: Boca Raton, FL, USA, **2008**, 421-437.

Cragg, G. M.; Newman, D. J. Biodiversity: A continuing source of novel drug leads. *Pure Applied Chemistry* **2005**, *77*, 7-24.

Cuevas, C.; Francesch, A. Development of Yondelis® (trabectedin, ET-743). A semi-synthetic process solves the supply problem. *Natural Product Reports* **2009**, *26*, 322-337.

De Clerck, O.; Bolton, J. J.; Anderson, R. J.; Coppejans, E.. *Guide to the seaweeds of KwaZulu-Natal*. *Scripta Botanica Belgica 33*. National Botanic Garden of Belgium, VLIZ: Flanders Marine Institute and Flemish Community **2005**, 1-294.

DerMarderosian, A.; Beutler, J. A. *The Review of Natural Products*, 2nd ed.; Facts and Comparisons; Seattle, WA, USA, **2002**, 13-43.

Dewick, P. M. *Medicinal Natural Products: A Biosynthetic Approach*, 2nd ed.; John Wiley and Son: West Sussex, UK, **2002**, 520.

Elsworth, J. F.; Thomson, R. H. A new chamigrane from *Laurencia glomerata*. *Journal of Natural Products* **1989**, *52*, 893-895.

Faulkner, D. J. Interesting aspects of marine natural products chemistry. *Tetrahedron* **1977**, *33*, 1421-1433

Faulkner, D. J. Marine natural products. *Natural Product Reports* **2002**, *19*, 1-48.

Francis, C. M. **2014**. Systematics of the *Laurencia* complex (Rhodomelaceae, Rhodophyta) in southern Africa. PhD Thesis. University of Cape Town, Cape Town, South Africa.

Fukuzawa, A.; Aye, M.; Takasugi, Y.; Nakamura, M.; Tamura, M.; Murai, A. Enzymatic Bromo-ether cyclisation of laurediols with bromoperoxidase. *Chemistry Letters* **1994**, *23*, 2307-2310.

Garbary, D. J.; Harper, J. T. A phylogenetic analysis of the *Laurencia* complex (Rhodomelaceae) of the red algae. *Cryptogamie Algologie* **1998**, *19*,185-200.

Griffiths, C. L.; Robinson, T. B.; Lange, L.; Mead, A. Marine biodiversity in South Africa: An evaluation of current states of knowledge. *PLoS ONE* **2010**, *5*, 1-14

Guiry, M. D.; Guiry, G. M. *AlgaeBase* **2015**. World-wide electronic publication. National University of Ireland, Galway. http://www.algaebase.org; Accessed 10/01/2015.

Haefner, B. Drugs from the deep: Marine natural products as drug candidates. *Drug Discovery Today* **2003**, *8*, 536-544.

Hay, M. E.; Fenical, W. Marine plant-herbivore interactions: The ecology of chemical defense. *Annual Review of Ecology and Systematics* **1988**, *19*, 111-145.

Ishihara, J.; Kanoh, N,; Murai, A. Enzymatic reaction of (3*E*, 6*S*, 7*S*)-laurediol and the molecular modelling studies on the cyclisation of laurediols. *Tetrahedron Letters* **1995**, *36*, 797-740.

Knott, M. G.; Mkwananzi, H.; Arendse, C. E.; Hendricks, D. T.; Bolton, J. J.; Beukes, D. R. Plocoralides A-C, polyhalogenated monoterpenes from the marine alga *Plocamium corallorhiza*. *Phytochemistry* **2005**, *66*, 1108-1112.

Mann, M. G. A. **2008**. An investigation of the antimicrobial and antifouling properties of marine algal metabolites. M.Sc thesis. Rhodes University, Grahamstown.

Maplestone, R. A.; Stone, M. J.; Williams, D. H. The evolutionary role of secondary metabolites - A review. *Gene* **1992**, *115*, 151–157.

Martin-Lescanne, J.; Rousseau, F.; De Reviers, B.; Payri, C.; Couloux, A.; Cruaud, C.; Le Gall, L. Phylogenetic analyses of the *Laurencia* complex (Rhodomelaceae, Ceramiales) support recognition of five genera: *Chondrophycus, Laurencia, Osmundea, Palisada* and *Yuzurua* stat. nov. *European Journal of Phycology* **2010**, *45*, 51-61.

Mishra, B. B.; Tiwari, V. K. Natural products: An evolving role in future drug discovery. *European Journal of Medicinal Chemistry* **2011**, *46*, 4769–4807.

Mukherjee, P. K.; Nema, N. K.; Venkatesh, P.; Debnath, P. K. Changing scenario for promotion and development of Ayurveda - way forward. *Journal of Ethnopharmacology* **2012**, *143*, 424-434.

Nam, K. W. Phylogenetic re-evalution of the *Laurencia* complex (Rhodophyta) with a description of *L. succulenta* sp. nov. from Korea. *Journal of Applied Phycology* **2006**, *18*, 679-697.

Nussbaum, F. V.; Brands, M.; Hinzen, B.; Weigand, S.; Habich, D. Antibacterial natural products in medicinal chemistry - exodus or revival? *Angewandte Chemie International Edition* **2006**, *45*, 5072-5129.

Ojima, I. Modern natural products chemistry and drug discovery. *Journal of Medicinal Chemistry* **2008**, *51*, 2587-2588.

Stegenga, H.; Bolton, J. J.; Anderson, R. J. Seaweeds of the South African west coast; *Contributions from the Bolus herbarium* **1997**, *18*, 1-655.

Suzuki, M.; Takahashi, Y.; Nakano, S.; Abe, T.; Masuda, M.; Ohnishi, T.; Noya, Y.; Seki, K. An experimental approach to study the biosynthesis of brominated metabolites by the red algal genus *Laurencia*. *Phytochemistry* **2009**, *70*, 1410-1415.

Wang, B. G.; Gloer, J. B.; Ji, N, Y.; Zhao, J. C.; Halogenated organic molecules of Rhodomelaceae origin: Chemistry and Biology. *Chemical Reviews* **2013**, *113*, 3632-3685.

Yuliana, N. D.; Khatib, A.; Choi, Y. H.; Verpoorte, R. Metabolomics for bioactivity assessment of natural products. *Phytotherapy Research* **2011**, *25*, 157-169.

Chapter 3

Secondary metabolites from *Laurencia glomerata*

Abstract

South African specimens of *Laurencia glomerata* have previously been investigated for their natural product chemistry by Elsworth and Thomson (1989) and Knott (2011). A re-investigation into the chemistry of this species afforded two known compounds isolated for the first time from this species i.e. the cyclohexadiene **3.5** (*iso*-dihydrolaurene), and prepacifenol epoxide (**3.15**). Chamigranes **3.1**, **3.9** and **3.17**, including a linear acetogenin **3.7** were isolated as typical *L. glomerata* metabolites. The re-isolation of these compounds is a good representation of the metabolite constancy within this particular species.

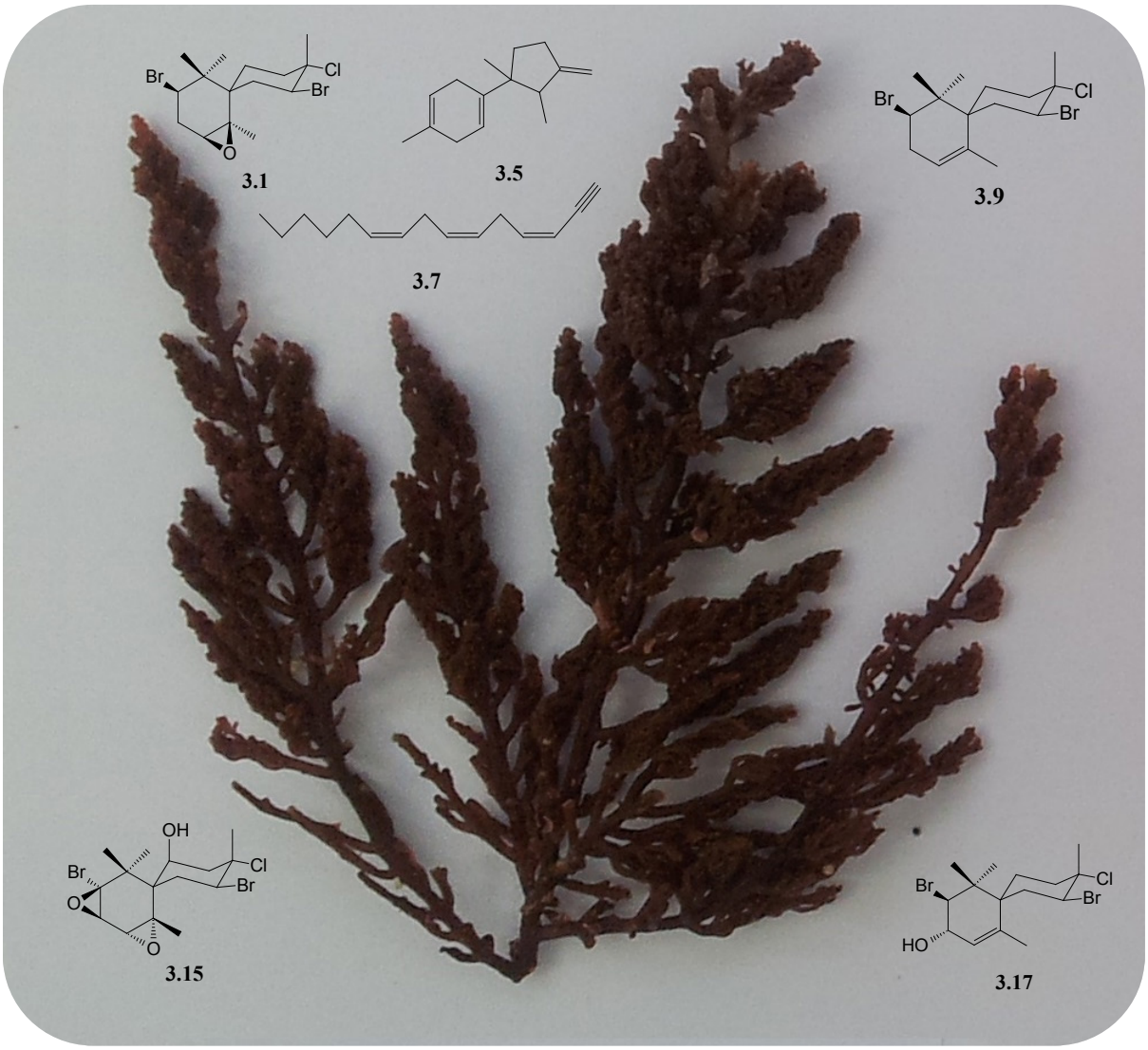

Chapter 3

Secondary metabolites from *Laurencia glomerata*

3.1 Introduction

Laurencia glomerata is a mainly South African endemic species, with specimens collected and documented from the south Cape peninsula of Southern Africa extending eastward (Stegenga *et al*., 1997). This bushy species is known for its dark red hue and stubby terminal branchlets, hence the name (*glomerata*: a tight grouping of). The plants grow anywhere between 15-40 cm high and are generally epilithic (grow on rocky surfaces) (Stegenga *et al*., 1997). During its fertile stage, *L. flexuosa* can be confused for *L. glomerata* thus caution should be taken during collection. *L. glomerata* can be distinguished from fertile *L. flexuosa* by intricate identification of densely crowded higher order branching patterns (De Clerck, 2005).

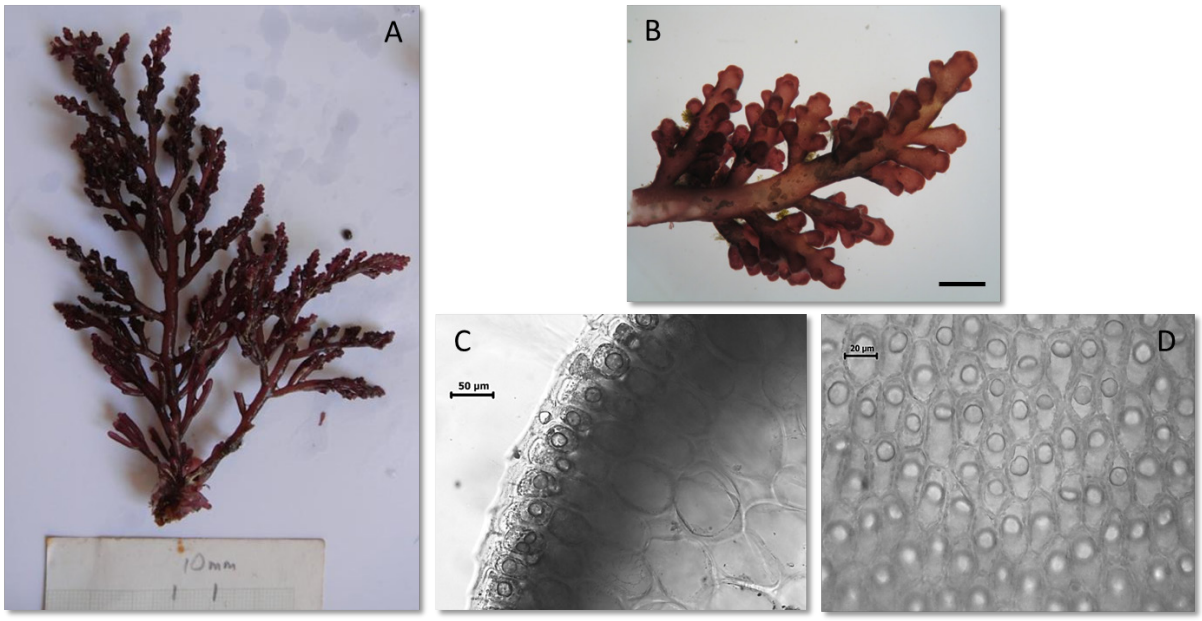

Figure 3.1: *Laurencia glomerata*[1] (Caitlynne Francis © 2014)

A) Habit.

B) Depiction of branchlet pattern (8x). *Scale bar: 1cm =360µm*

C) Cross section of thallus showing outermost cortical cells (with visible *corps en cerise*) and cortical cells (20x).

D) *Corps en cerise* in outermost cortical cells (Usually one per cell) (40x).

[1] Image plates courtesy of Caitlynne Francis © 2014, University of Cape Town, South Africa

3.2 Results and Discussion

3.2.1 Extraction and isolation of metabolites from *L. glomerata* (NDK130821-10, Noordhoek)

The alga was extracted initially with MeOH at room temperature followed by a combination of CH_2Cl_2 and MeOH in a 2:1 ratio, at 40 ^oC. The extracts were combined and the organic phase was collected after the initiation of phase separation with de-ionised water[2]. The resultant organic extract was dried *in vacuo*, affording a crude isolate of weight 0.85 g which equates to 2.0% yield of the dry algal material.

The crude organic extract was further fractionated into nine separate fractions on silica gel using step gradient column chromatography (Scheme 3.1). The effectiveness of this method was evident as fractions whose ^1H NMR signals were not apparent in the crude spectrum became clearly visible after fractionation (Figure 3.2). From (Figure 3.2) the more none polar fractions A, B and C displayed NMR resonances of interest, with subsequent fractions showing typical chlorophyll (fraction D) and sugar type resonances (fractions E-H).

Since the majority of *Laurencia* spp. secondary metabolites fall within the non-polar to intermediate polarity range, fractions A, B and C were selected for further purification *via* silica gel column chromatography and normal phase HPLC to yield compounds **3.5**, **3.7**, **3.9**, **3.15** and **3.17** while compound **3.1** crystallised out of various chromatographic fractions (Figure 3.1).

[2] An identical extraction procedure is used for algae in subsequent chapters

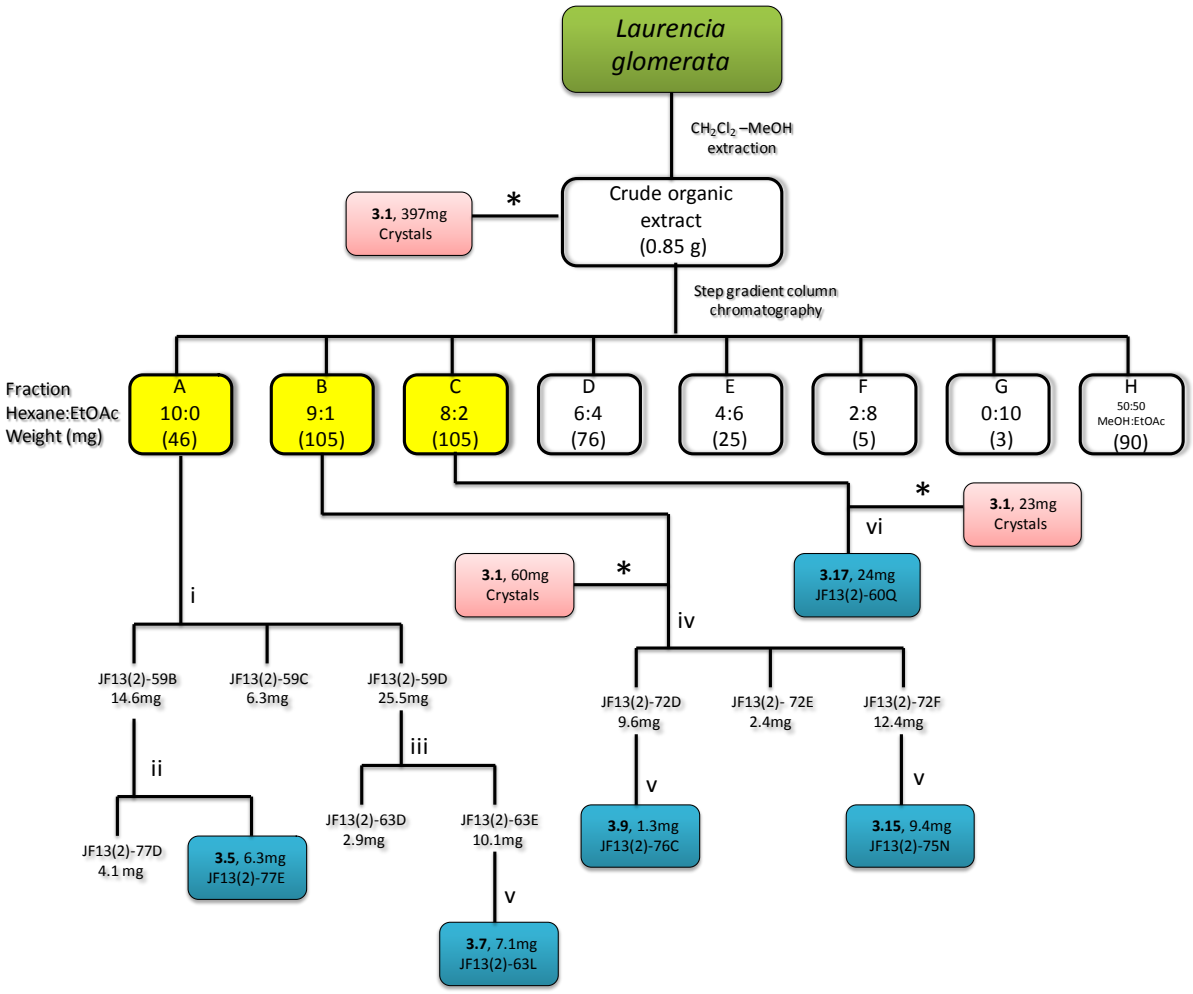

Scheme 3.1: Isolation scheme of metabolites from *L. glomerata* (NDK130821-10)

Conditions: i) Silica gel column chromatography (100% hexane); ii) Normal phase HPLC (100% hexane); iii) Normal phase HPLC (9:1 hex:EtOAc); iv) Silica gel column chromatography (9:1 hex:EtOAc); v) Normal phase HPLC (19:1 hex:EtOAc); vi) Normal phase HPLC (4:1 hex:EtOAc)

* Addition of hexane induced crystallisation of compound **3.1**

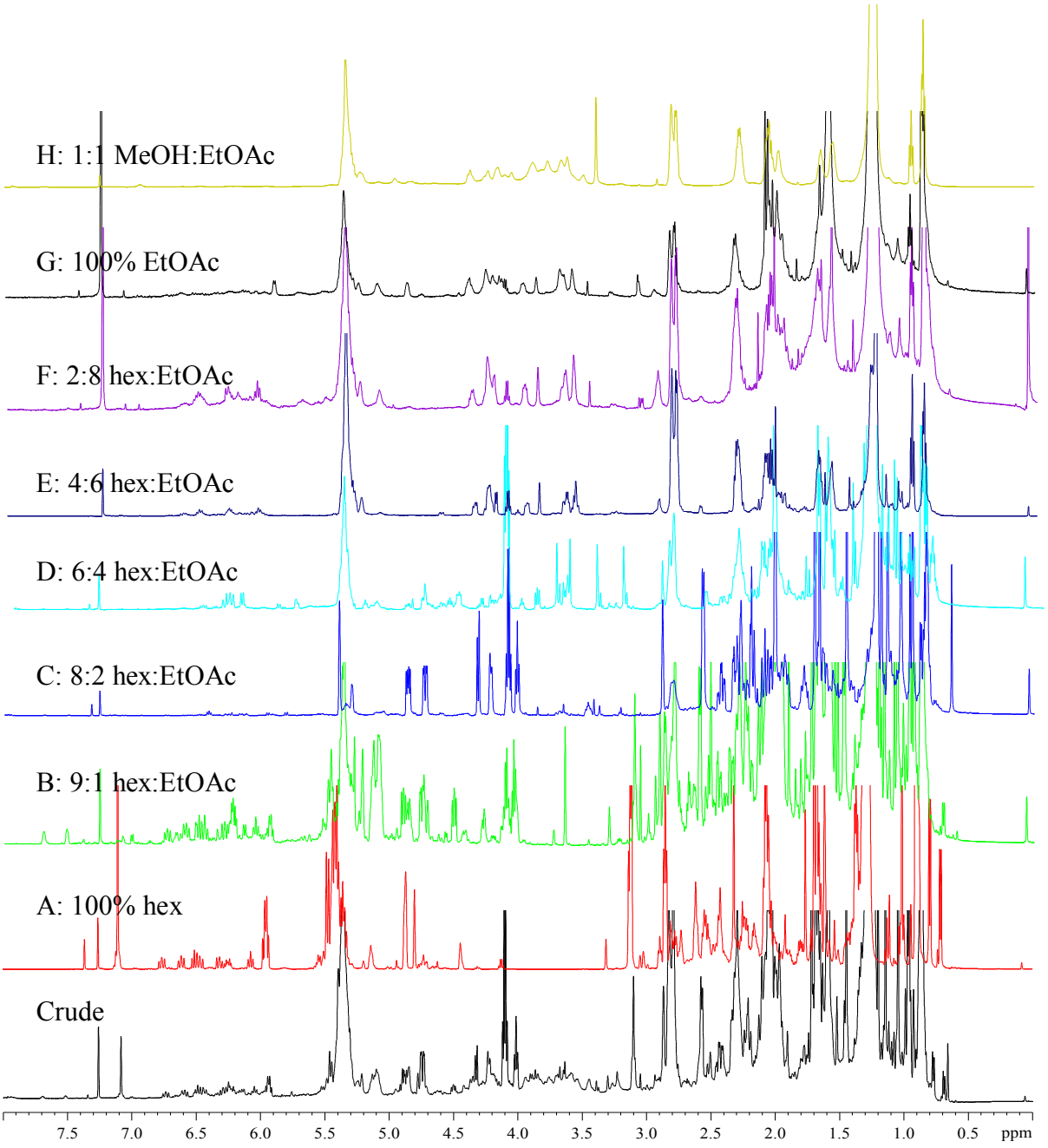

Figure 3.2: ^{1}H NMR spectra ($CDCl_3$, 600 MHz) of the crude organic extract of *L. glomerata* (NDK130821-10) and step gradient column fractions A-H

3.2.2 Structure elucidation of metabolites[3]

3.2.2.1 Compound 3.1

After reconstitution with hexane, compound **3.1** immediately crystallised out of the crude extract, as well as step gradient column fractions B and C, to afford a green tinged crystalline material. Recrystallisation with hexane yielded white plate like crystals.

The ^{1}H NMR spectrum (Figure 3.3) of the crystalline material together with an edited HSQC spectrum (Figure 3.4) were key in identifying three sets of diastereotopic methylene resonances at δ_H 1.67; 1.98, δ_H 2.38; 2.47, δ_H 2.10; 2.84, and one enantiotopic methylene resonance at δ_H 2.61 (dd, J = 7.7, 3.0 Hz). A total of three methine moieties were detected at δ_H 4.77 (dd, J = 13.3, 4.7 Hz), δ_H 2.92 (t, J = 3.0 Hz) and δ_H 4.06 (t, J = 7.7 Hz). Four methyl singlets between δ_H 1.0-2.0 were suggestive of a sesquiterpene skeleton.

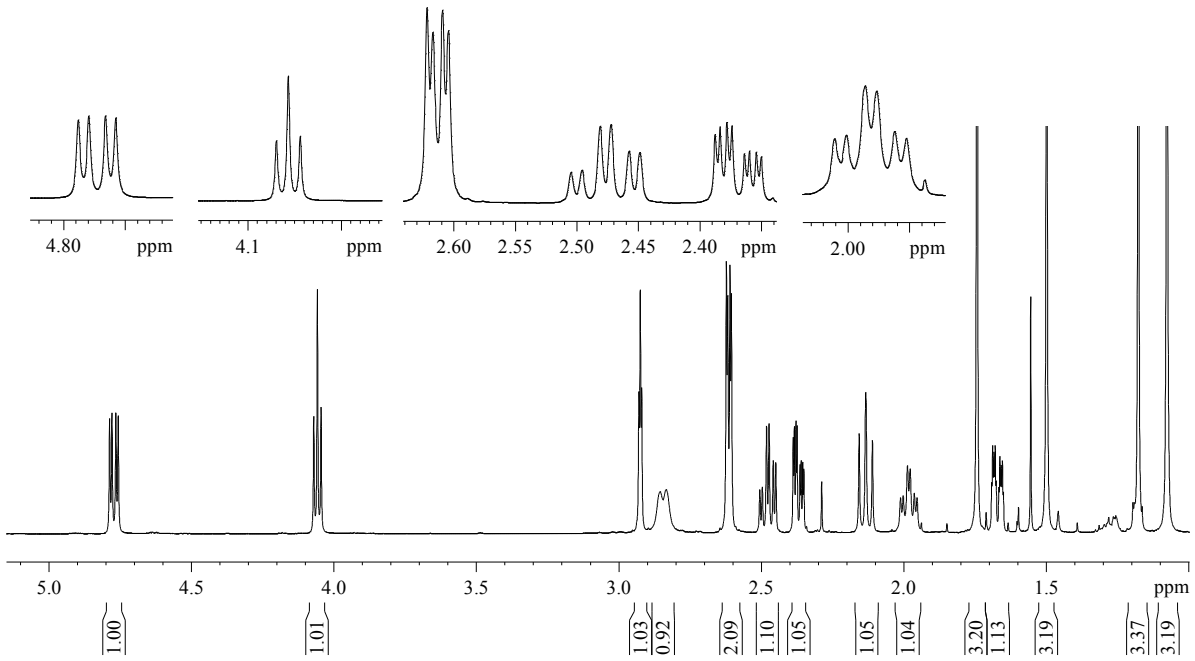

Figure 3.3: ^{1}H NMR spectrum ($CDCl_3$, 600 MHz) of compound **3.1**

The ^{13}C NMR spectrum (Figure 3.5) displayed 14[4] well resolved signals which, together with the edited HSQC and DEPT-135 spectra, allowed for the recognition of four methyl (δ_C 21.3, 24.0, 25.8 and 27.3), four methylene (δ_C 26.2, 32.7, 39.1 and 40.4), three methine (δ_C 57.6,

[3] Where possible, the structure elucidation of compounds belonging to similar structural classes are discussed in succession.
[4] Following a sesquiterpenoid skeleton in **3.1**, a 15th quaternary carbon was identified which had the same ^{13}C NMR chemical shift as the methine carbon at δ_C 62.0.

62.0 and 62.1) and four quaternary (δ_C 42.3, 44.6, 62.0 and 71.1) carbon signals for compound **3.1**.

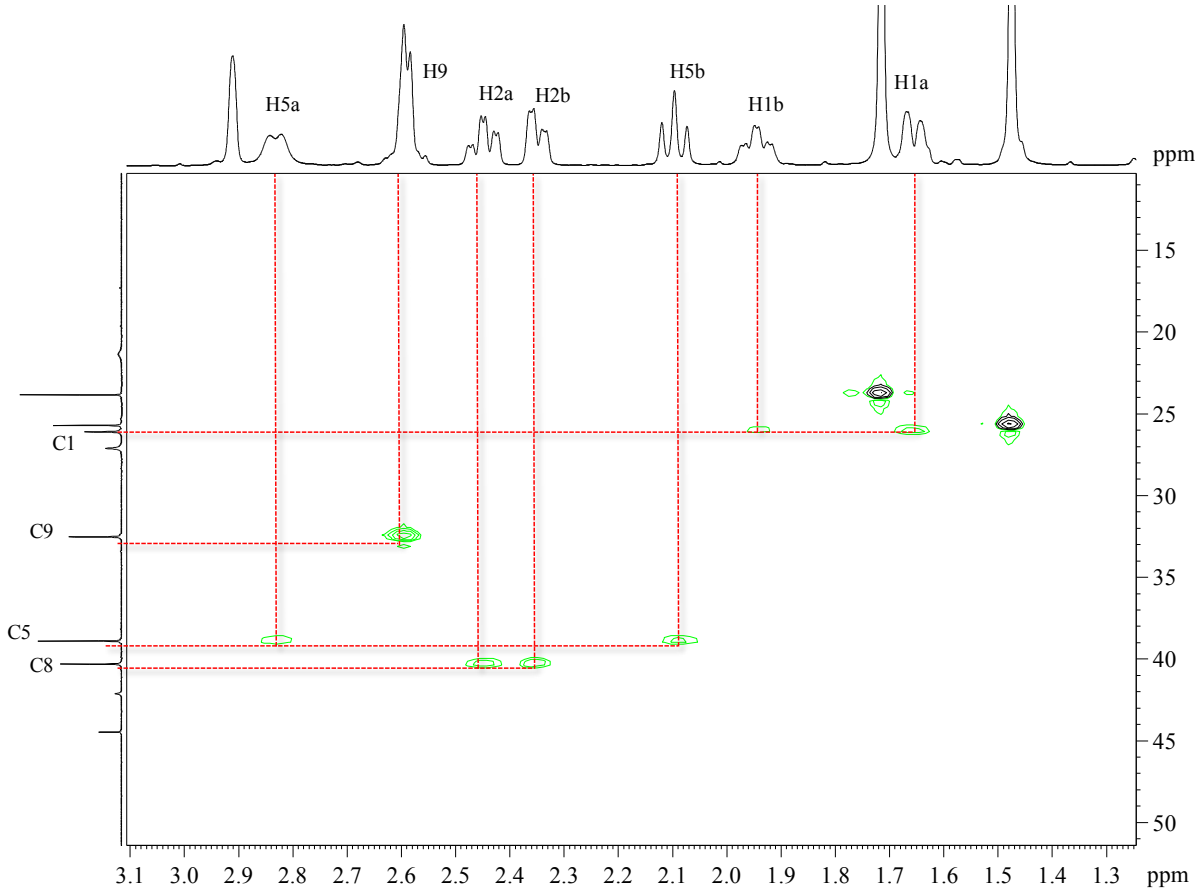

Figure 3.4: Partial *edited* HSQC spectrum of compound **3.1** showing methylene correlations

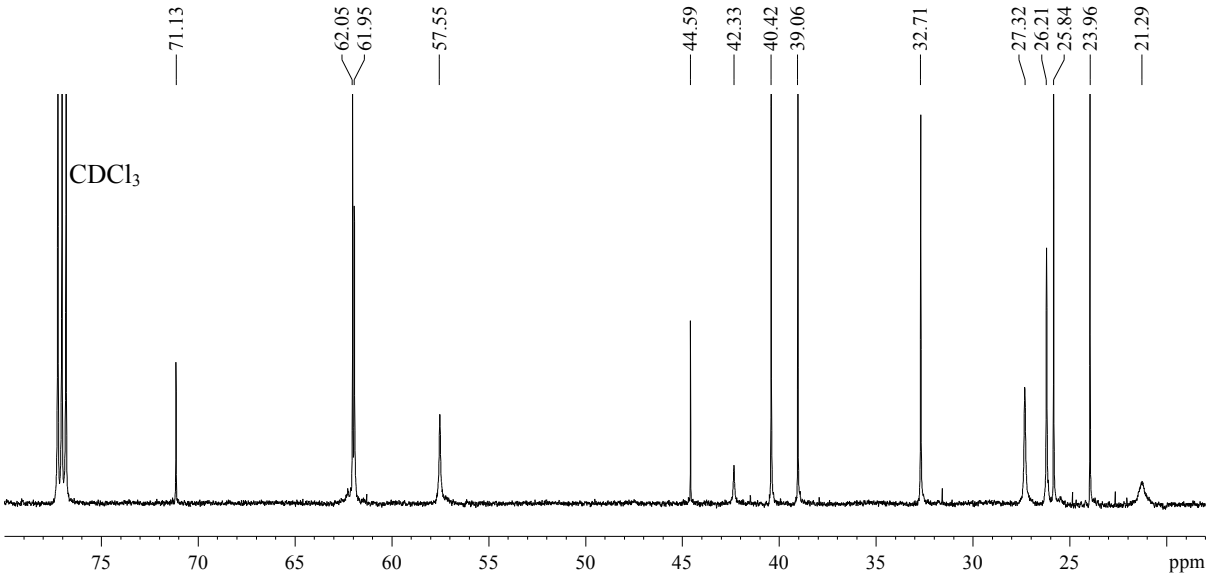

Figure 3.5: ^{13}C NMR spectrum ($CDCl_3$, 150 MHz) of compound **3.1**

The above NMR data supported a chamigrane sesquiterpene structure with a spiro [5.5] undecane arrangement. This was confirmed by HMBC data which showed correlations from the *gem*-dimethyl moiety (δ_H 1.08 and δ_H 1.18) to two quaternary carbon resonances (δ_C 42.3 and δ_C 44.6), (Figure 3.6). The chamigrane class of sesquiterpenoid metabolites are typically produced by *Laurencia* spp. (Wang *et al*., 2013).

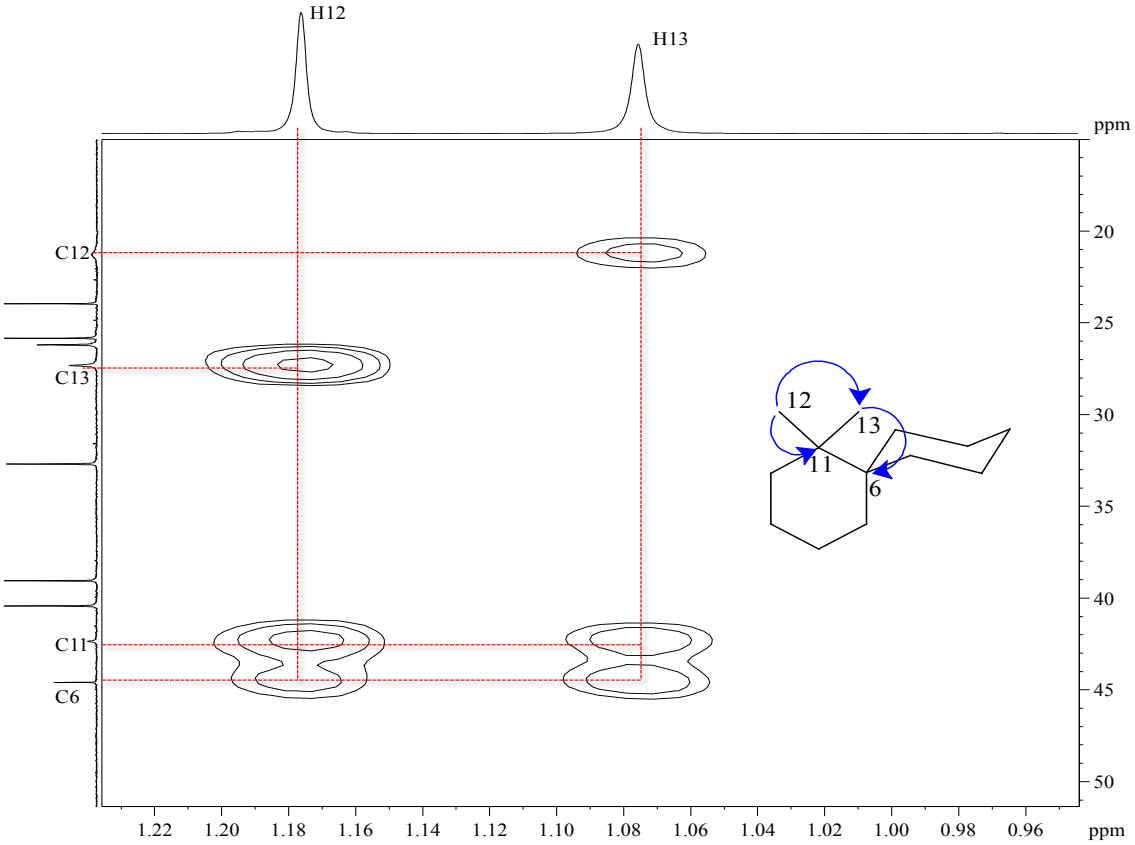

Figure 3.6: Partial HMBC spectrum of compound **3.1** showing key correlations

Compound **3.1** was identified as a previously isolated metabolite, *3-chloro-4,10-dibromo-7,8-epoxychamigrane*, discovered from a *Laurencia* sp. in the Gulf of California (Howard and Fenical, 1975), with the crystal structure reported by Cowe *et al*., (1989).

Analysis of the NOESY spectrum of compound **3.1** allowed for confident assignment of stereocentres as shown below (Figure 3.7). This allowed for a distinction to be made between compound **3.1** and the corresponding epoxy-epimer about C7/C8, compound **3.2**, which was isolated by Ojika *et al*., (1982) from *Laurencia okamurai*. The relative configuration displayed in compound **3.1** is further justified as ^{1}H NMR data was consistent with that provided by Howard and Fenical (1975).

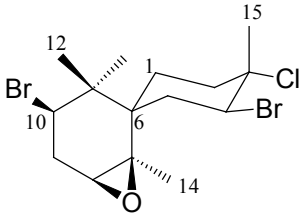

3.1

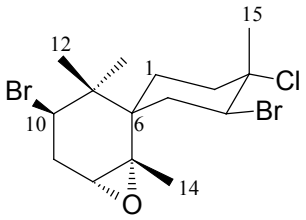

3.2

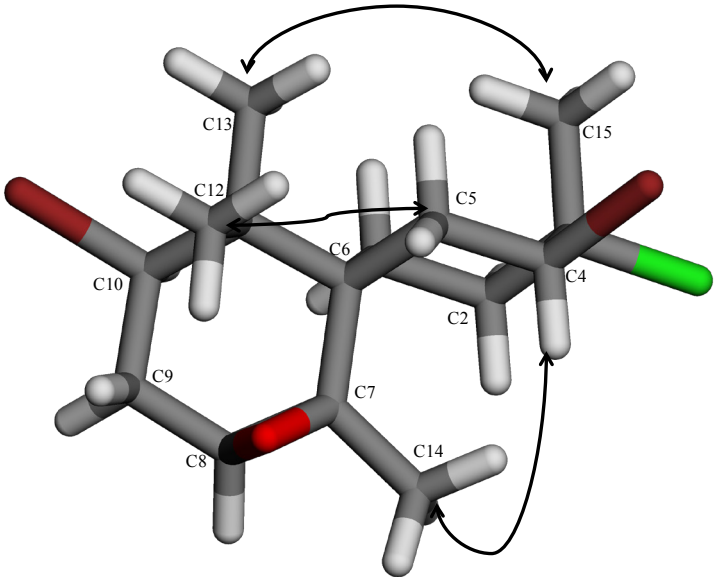

Figure 3.7: Key NOESY correlations in compound **3.1**

After exhaustively analysing the ^{13}C NMR data of compound **3.1**, it became evident that an informed re-assignment of the positioning of reported carbon chemical shifts was required. Unambiguous COSY and HMBC correlations obtained for compound **3.1** in this study conflicted with those reported by Bano *et al*., (1987) as shown in compound **3.1a** (Figure 3.8), especially regarding positions C6, C10 and C11.

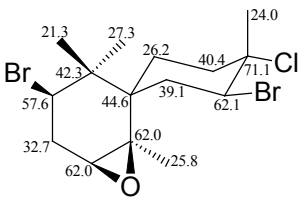

3.1
This study

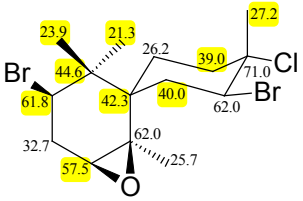

3.1a
Bano *et al*., 1987

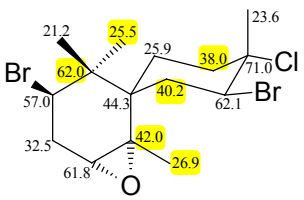

3.2
Crews *et al*., 1984

Figure 3.8: ^{13}C NMR shift comparisons of compound **3.1**[5]
(Dubious allocations are highlighted yellow)

[5] All shifts reported in $CDCl_3$

Possible mis-assignments are also present within the epoxy epimer, compound **3.2**. The ^{13}C NMR data for **3.2** is absent in reports by the authors who isolated it (Ojika *et al*., 1982), but Crews *et al.,* (1984) provide its ^{13}C NMR data after obtaining a semi-synthetic analogue prepared by Howard and Fenical (1975).

COSY correlations in compound **3.1** (Figure 3.9) between H8, H9 and H10 prove a (-OCH-CH_2-CHBr-) spin system. This is validated as C12 and C13 methyl protons show clear ^3J HMBC correlations to the bromo-methine at C10 where the chemical shift is δ_C 57.6 and not δ_C 61.8 as suggested by Bano *et al*., (1987).

The spiro-centre at C6 in compound **3.1** clearly possesses a quaternary carbon with a chemical shift of δ_C 44.6 and not δ_C 42.3 according to Bano *et al*., (1987). This is supported by unambiguous ^3J HMBC correlations from methyl moieties at C13 and C14.

In contrast to **3.1a**, the ^{13}C NMR chemical shift of the *gem*-dimethyl quaternary carbon at C11 should be δ_C 42.3 and not δ_C 44.6, as both methyl groups C12 and C13 display strong ^2J HMBC correlations to C11 (δ_C 42.3).

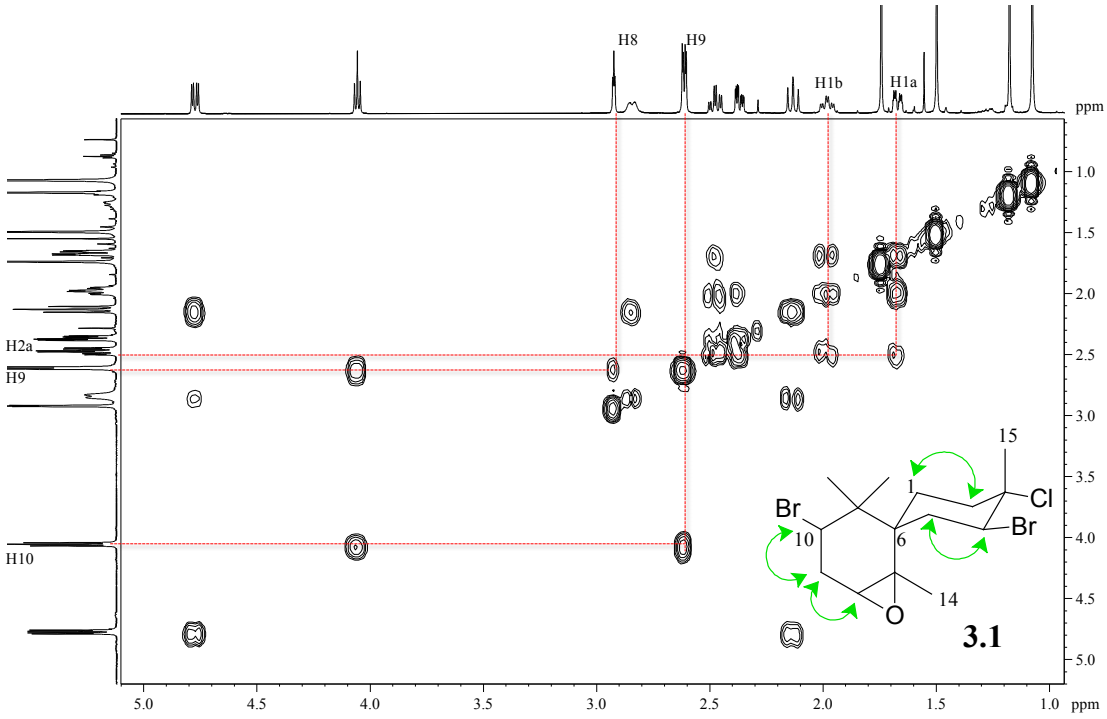

Figure 3.9: ^1H-^1H COSY correlations of compound **3.1**

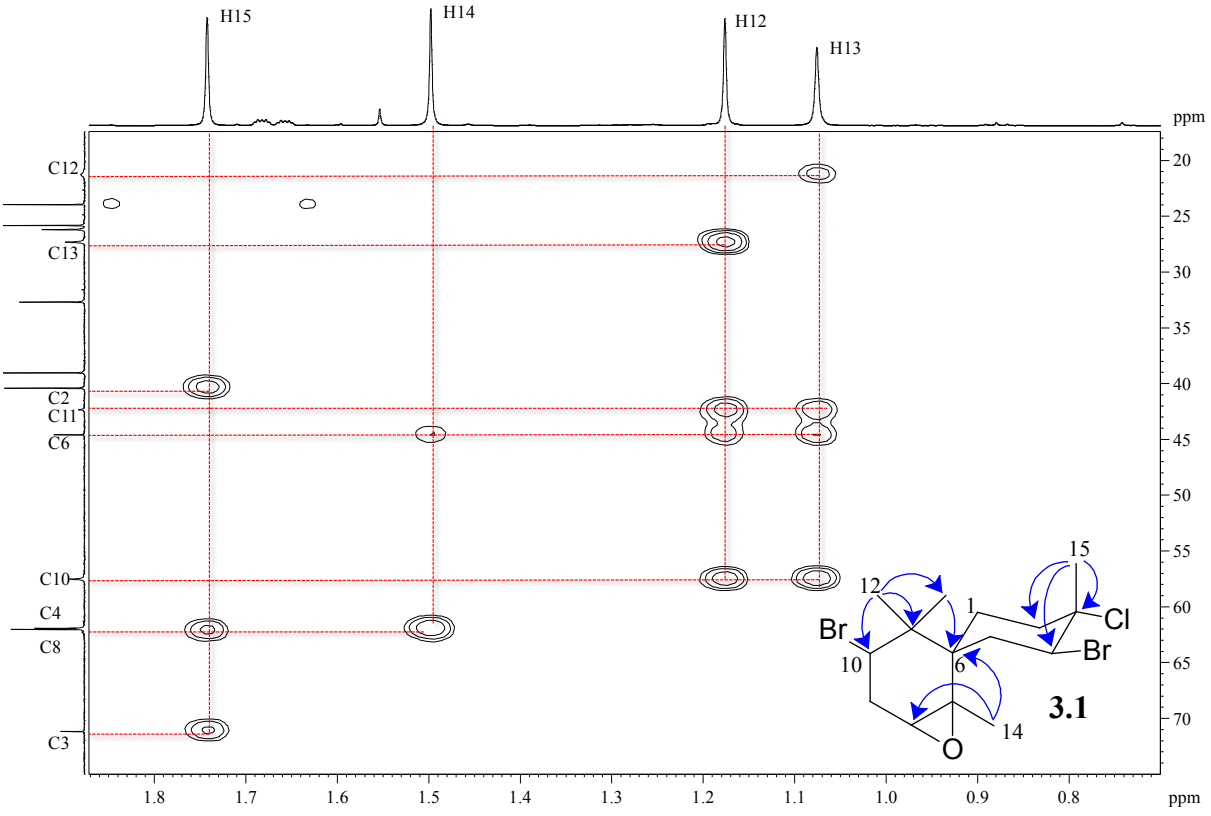

Figure 3.10: Partial HMBC spectrum of compound **3.1** showing key correlations

As only 14 carbon signals were apparent in the ^{13}C NMR spectrum of compound **3.1**, it was evident that two carbon atoms within the molecule possessed the same chemical shift. Bano *et al*., (1987) and Crews *et al.,* (1984) both report two carbon resonances at δ_C 62.0. Following the comprehensive 2D NMR assignments of carbon chemical shifts in compound **3.1** it was realised that C7 remained unassigned and hence ought to be δ_C 62.0.

The NMR solvent was changed from $CDCl_3$ to acetone $[(CD_3)_2CO]$ in hope that the postulated duo of carbons resonating at δ_C 62.0 separate out into individual signals, however, despite the ^{13}C NMR spectrum showing marked shift changes, it was presumed that the C7 and C8 still possessed the same chemical shift as again, only 14 carbon signals materialised with no HMBC evidence of a distinct, hidden quaternary signal. Furthermore, a proton coupled ^{13}C NMR experiment failed to clarify the region between δ_C 55.0 and δ_C 65.0.[6]

Since a postulation was made of the carbon chemical shift at C7 (δ_C 62.0) more proof of an epoxy functionality between C7 and C8 was necessary. Such confirmation was bestowed by cleavage of the epoxy ring with $BF_3.Et_2O$.

[6] Supplementary data

The corresponding dehydrohalogenated ketone, compound **3.3**, was produced (Selover and Crews, 1980) together with the ring contracted cyclopentanyl aldehyde compound **3.4** (Howard and Fenical, 1975) as shown below in (Scheme 3.2).

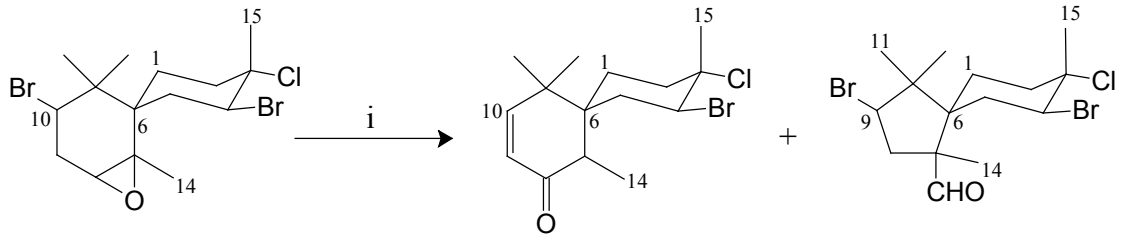

3.1 **3.3** **3.4**

Scheme 3.2: Epoxy cleavage of compound **3.1**

Conditions: i) $BF_3.Et_2O$ in anhydrous Et_2O. Stir for 18 h from -78 °C to RT

Indicative signs of the formation of the α,β unsaturated ketone **3.3**, arose from the ^{1}H NMR spectrum (Figure 3.11) wherein coupled (J = 10.2 Hz) olefinic doublets emerged at δ_H 5.82 and δ_H 6.43. A carbonyl signal at δ_C 201.5 as well as an IR carbonyl stretch at 1681 cm^{-1} validated the presence of a carbonyl moiety in compound **3.3**.

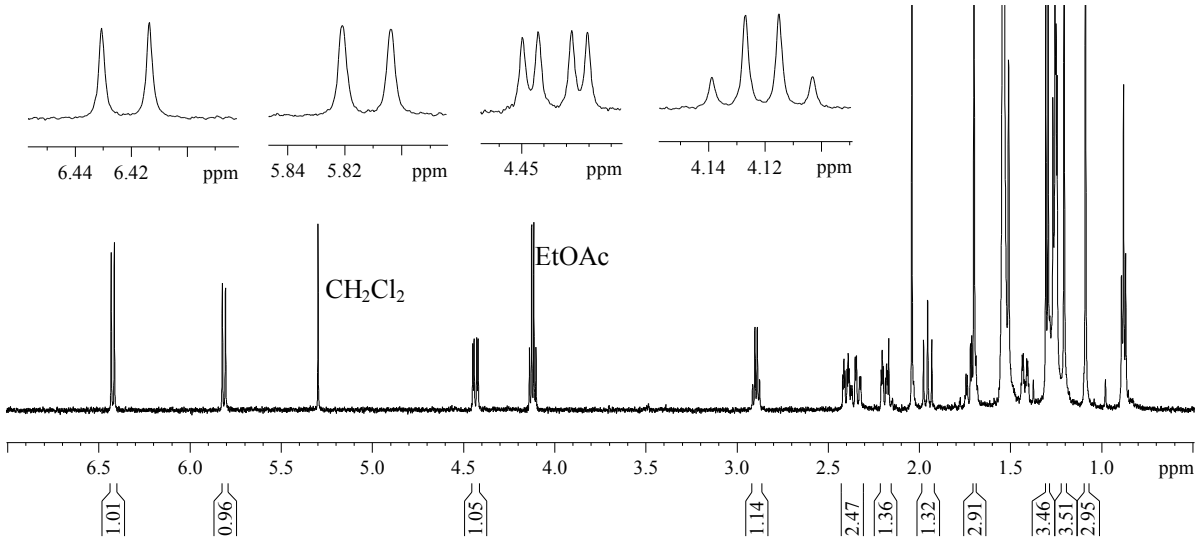

Figure 3.11: ^{1}H NMR spectrum ($CDCl_3$, 600 MHz) of compound **3.3**

Compound **3.4** showed a distinctive aldehyde singlet in its ^{1}H NMR spectrum (Figure 3.12) at δ_H 9.79. A condensed five-membered alicycle was confirmed by examining $^{2,3}J$ HMBC correlations within the pentacyclic ring from methyl moieties positioned at C7 and C10.

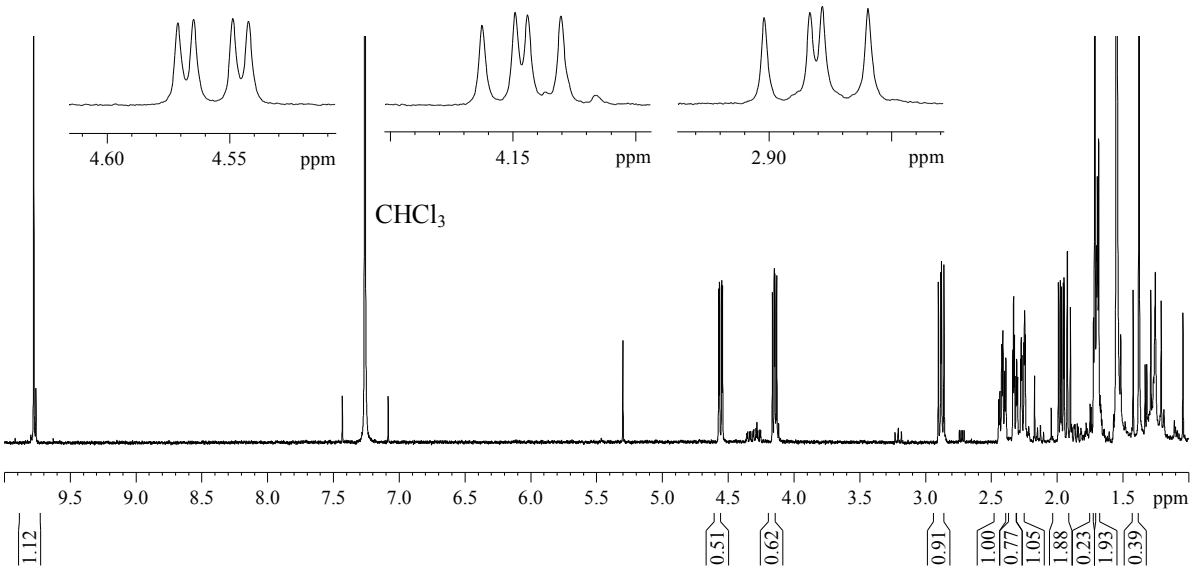

Figure 3.12: ^{1}H NMR spectrum ($CDCl_3$, 600 MHz) of compound **3.4**

The aldehyde functionality at C13 was clearly visible in the ^{13}C NMR spectrum of compound **3.4** peaking at δ_C 203.5 (Figure 3.13).

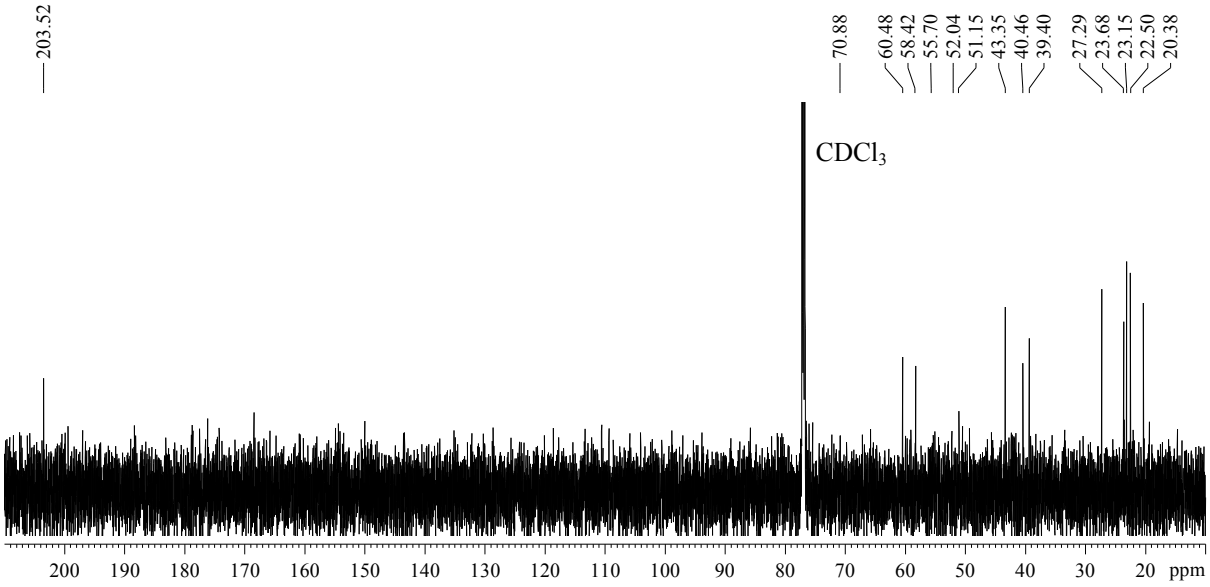

Figure 3.13: ^{13}C NMR spectrum ($CDCl_3$, 150 MHz) of compound **3.4**

Given that the carbon chemical shift at C7 in compound **3.1** was hypothesised, the resultant products cleared any ambiguity surrounding the presence of an epoxy ring and added integrity to the proposed chemical shift of δ_C 62.0 at C7.

Furthermore Crews *et al*., (1985) show the use of the attached proton test (APT) NMR experiment in ascertaining the carbon chemical shift at C7, wherein it was confirmed as being δ_C 62.0.

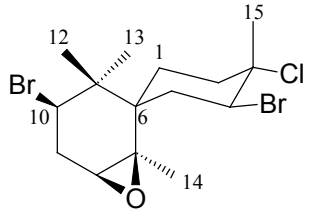

3.1

Table 3.1: NMR spectroscopic data of compound **3.1**

Carbon No	δ_C	δ_C mult	δ_H, mult, J (Hz)	COSY	HMBC	NOESY
1a	26.2	CH_2	1.67, dq, 15.2, 5.7	H1b, H2a	-	H1b, H13, H14
1b			1.98, dt, 15.2, 5.7	H1a, H2a, H2b	-	H1a, H13
2a	40.4	CH_2	2.47, dt, 14.6, 5.7	H1a, H1b	C1, C3, C15	H2b, H14
2b			2.38, dd, 14.6, 2.9	H1b	C1, C3, C4, C6, C15	H2a, H15
3	71.1	C	-	-	-	-
4	62.1	CH	4.77, dd, 13.3, 4.7	H5a, H5b	C3, C5, C15	H5a, H14
5a	39.1	CH_2	2.84, br d, 13.3	H4, H5b	-	H4
5b			2.10, t, 13.3	H4, H5a	C4, C7, C6, C11	H1a, H12, H13, H15
6	44.6	C	-	-	-	-
7	62.0	C	-	-	-	-
8	62.0	CH	2.92, t, 3.0	H9	C9, C10, C14	H9, H14
9	32.7	CH_2	2.61, dd, 7.7, 3.0	H8, H10	C7 or C8, C10, C11	H8, H10, H12, H13
10	57.6	CH	4.06, t, 7.7	H9, H12	C6, C8, C9, C12, C13	H1a, H9, H13
11	42.3	C	-	-	-	-
12	21.3	CH_3	1.18, s	H10	C6, C11, C13	H5a, H5b, H9
13	27.3	CH_3	1.08, s	-	C6, C11, C2	H1a, H1b, H5b, H15
14	25.8	CH_3	1.50, s	-	C6, C7 or C8	H2a, H4, H8
15	24.0	CH_3	1.74, s	-	C2, C3, C4	H1a, H2b, H5b, H13

3.2.2.2 Compound 3.9

Compound **3.9** also portrayed a similar chamigrane skeleton to compound **3.1** with the exception of an absent epoxy-methine signal (δ_H 2.92, t, J = 3.0), and the emergence of an unsaturated functionality observed as a prominent deshielded olefinic singlet at δ_H 5.23 in the ^{1}H NMR spectrum (Figure 3.14).

A quaternary carbon at δ_C 140.2 [7] (C7) in **3.9** confirmed the reduced nature of **3.9** *vs*. **3.1**, with compound **3.9** manifesting as the de-oxygenated derivative of compound **3.1**.

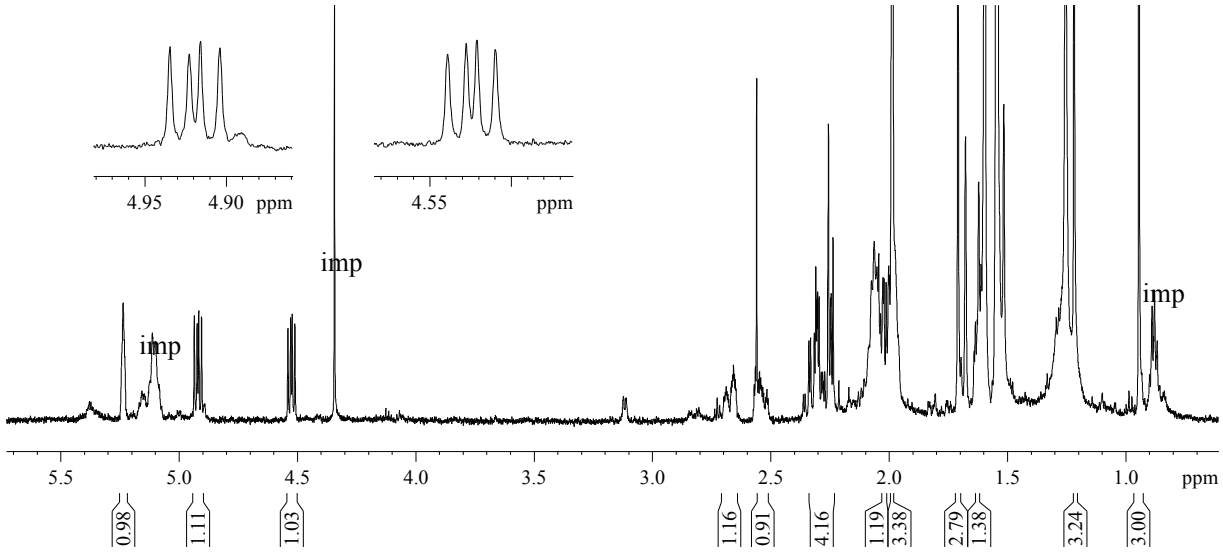

Figure 3.14: ^{1}H NMR spectrum ($CDCl_3$, 600 MHz) of compound **3.9**[8]

Although NMR data did not reflect the olefinic carbon signal at C8 (δ_C 123.0), similarities in the 1D and 2D NMR analyses were sufficient enough to elucidate the structure of compound **3.9** as the olefinic chamigrane derivative of compound **3.1**.

The relative configuration at C10 was assigned by considering the coupling constant of H10 (d, J = 11.1, 7.0 Hz) as compared to that observed for compound **3.1**.

[7] Carbon shifts deduced by HMBC correlations
[8] "imp" indicates a signal due to an impurity, and will be used henceforth to mark out peaks due to impurities

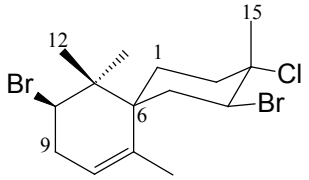

3.9

The reduced chamigrane, compound **3.9**, was isolated from a specimen of *Laurencia* sp. by Howard and Fenical (1975) as well as from *Laurencia implicata* by Wright *et al*., (1991).

Interestingly, Suzuki *et al*., (1979) reported a series of similar chamigrenes (compounds **3.10**-**3.14**), including compound **3.9**, from *Laurencia glandulifera*.

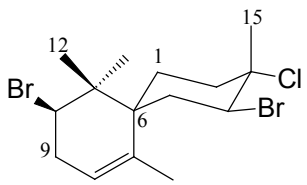

3.9

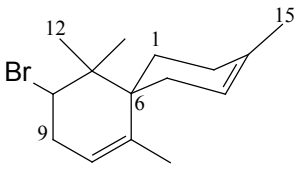

3.10

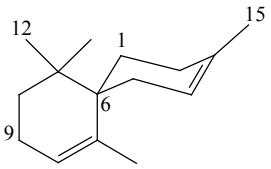

3.11

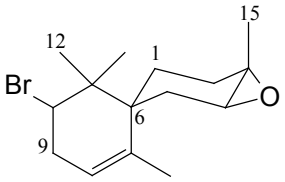

3.12

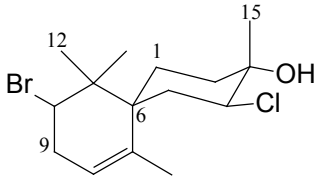

3.13

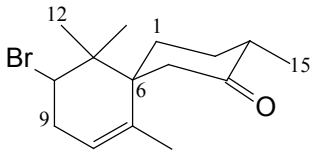

3.14

Howard and Fenical (1975) reported the conversion of compound **3.9** to quantitative yields of compound **3.2** using *m*-chloroperbenzoic acid. This conversion was attempted so as to further validate the elucidated structure, however attempts were unsuccessful possibly due to the relatively diminutive quantity of compound **3.9** that was available for the reaction (~1mg).

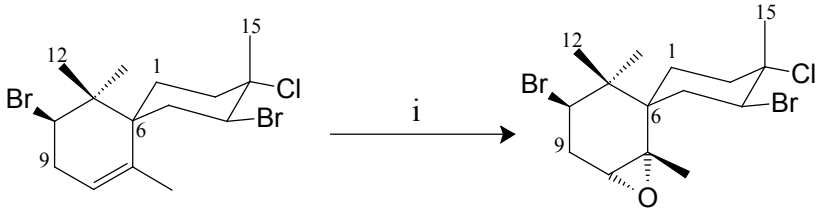

3.9 **3.2**

Scheme 3.3: Attempt at converting compound **3.9** to the epoxy derivative **3.2**

Conditions: i) *m*-chloroperbenzoic acid in refluxing chloroform (equimolar), Stir at 30 ^{o}C overnight

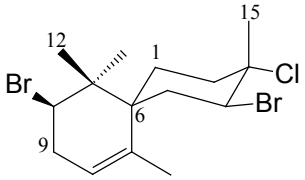

3.9

Table 3.2: NMR spectroscopic data of compound **3.9**

Carbon No	δ_C[9]	δ_C mult	δ_H, mult, J (Hz)
1a	31.6	CH_2	1.61. m
1b			2.01, m
2a	40.4	CH_2	2.24, m
2b			2.31, m
3	71.8	C	-
4	62.8	CH	4.92, d, 11.2, 7.0
5a	39.8	CH_2	2.24, m
5b			2.35, m
6	47.0	C	-
7	140.2	C	-
8	123.0[10]	CH	5.23, m
9a	36.3	CH_2	2.54, m
9b			2.67, m
10	60.8	CH	4.52, d, 11.1, 7.0
11	43.0	C	-
12	17.1	CH_3	0.94, s
13	24.1	CH_3	1.22, s
14	25.5	CH_3	1.98, s
15	23.9	CH_3	1.72, s

[9] Deduced via HMBC analysis
[10] Not observed in this study; as reported by Wright *et al.*, (1991)

3.2.2.3 Compound 3.15

A combination of four methyl singlets (δ_H 0.98, 1.49, 1.54 and 1.92) in the ^{1}H NMR spectrum (Figure 3.15), as well as 15 carbon resonances in the ^{13}C NMR spectrum (Figure 3.16) confirmed the adoption of a C_{15} chamigrane skeleton in compound **3.15**.

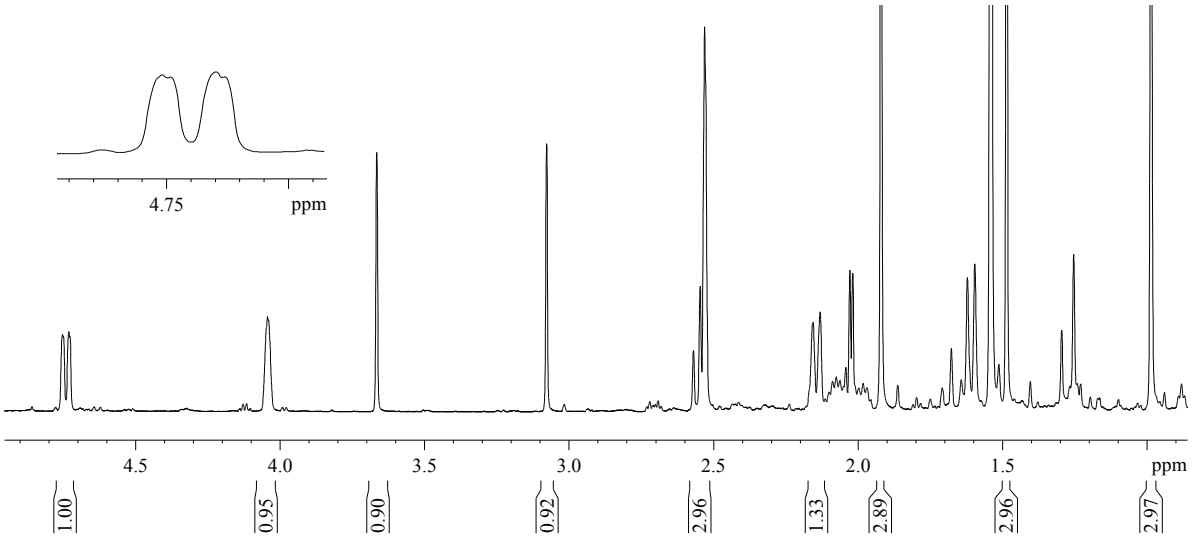

Figure 3.15: ^{1}H NMR spectrum ($CDCl_3$, 600 MHz) of compound **3.15**

Taking into account a quaternary carbon at δ_C 75.5, an extra epoxy-methine resonance at (δ_H 3.66; δ_C 55.6) and a methine signal at (δ_H 4.04; δ_C 69.9), it was established that compound **3.15** was in fact similar to compound **3.1** except for the presence of additional epoxy ring as well as a secondary alcoholic functionality.

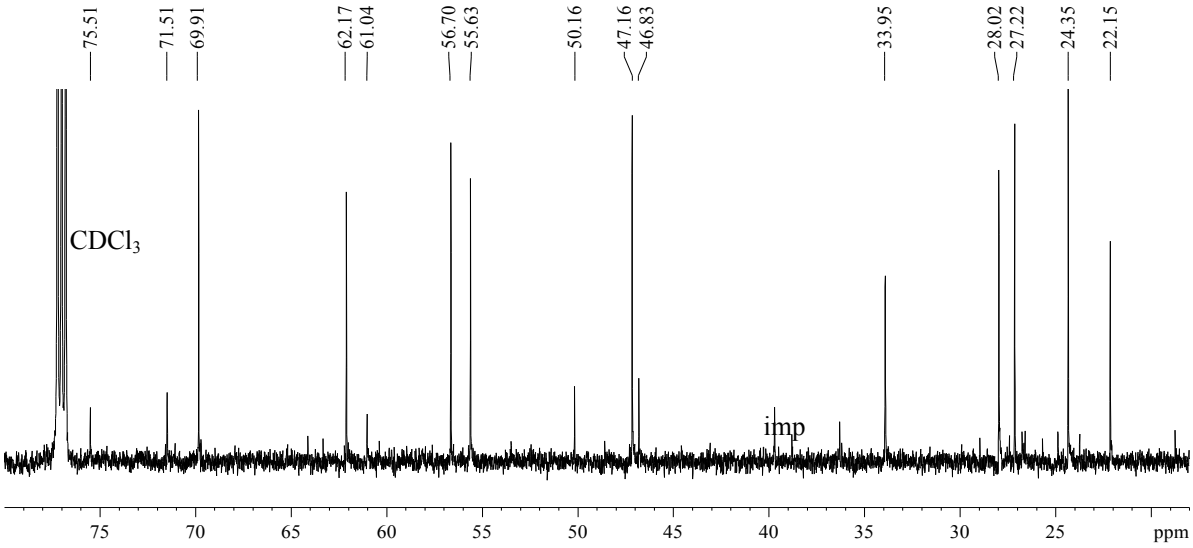

Figure 3.16: ^{13}C NMR spectrum ($CDCl_3$, 150 MHz) of compound **3.15**

A *trans* epoxy configuration was established at C8 and C9 based on the absence of coupling between protons H8 and H9. Furthermore H4 was assigned as axial after considering its coupling constant (dd, J = 13.6, 2.3 Hz). Compound **3.15** (Figure 3.17) was previously reported by Faulkner *et al*., (1974) as prepacifenol epoxide.

Compound **3.16** was isolated as a 1-dehydroxy analogue of compound **3.15** by Kimura *et al*., (1999) from a Hawaiian example of *Laurencia nidifica*.

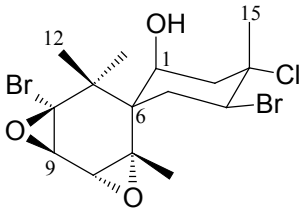

3.15

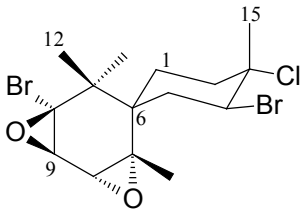

3.16

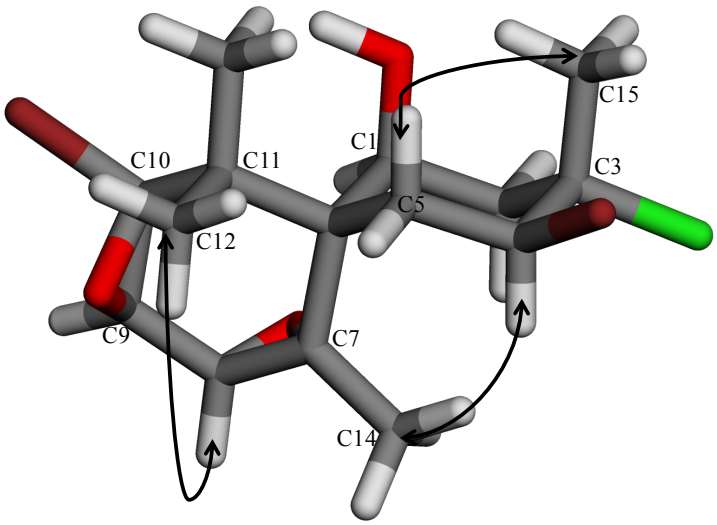

Figure 3.17: Key NOESY correlations in compound **3.15**

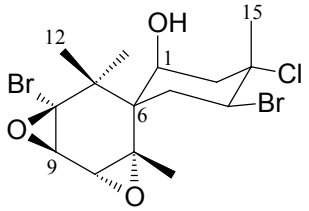

3.15

Table 3.3: NMR spectroscopic data of compound **3.15**

Carbon No	δ_C	δ_C **mult**	δ_H, **mult, J (Hz)**
1	69.9	CH	4.04, br s
2	47.2	CH_2	2.53, m
3	71.5	C	-
4	62.2	CH	4.74, dd, 13.8, 2.3
5a	34.0	CH_2	2.13, d, 13.8
5b			2.54, m
6	50.2	C	-
7	61.0	C	-
8	56.7	CH	3.07, s
9	55.6	CH	3.66, s
10	75.5	C	-
11	47.2	C	-
12	24.4	CH_3	0.98, s
13	27.2	CH_3	1.54, s
14	22.2	CH_3	1.49, s
15	28.0	CH_3	1.92, s

3.2.2.4 Compound 3.17

Altogether, four methine signals were detected in the ^{1}H NMR spectrum (Figure 3.18) of compound **3.17** i.e. an olefinic singlet at δ_H 5.44, a double doublet at δ_H 4.90 (J = 12.5, 6.7 Hz), and two coupled doublets with a coupling constant of 8.5 Hz at δ_H 4.26 and δ_H 4.35. Once again, four distinct methyl signals were seen further upfield between δ_H 0.95-2.10 allowing for the inference of yet another chamigrane type system.

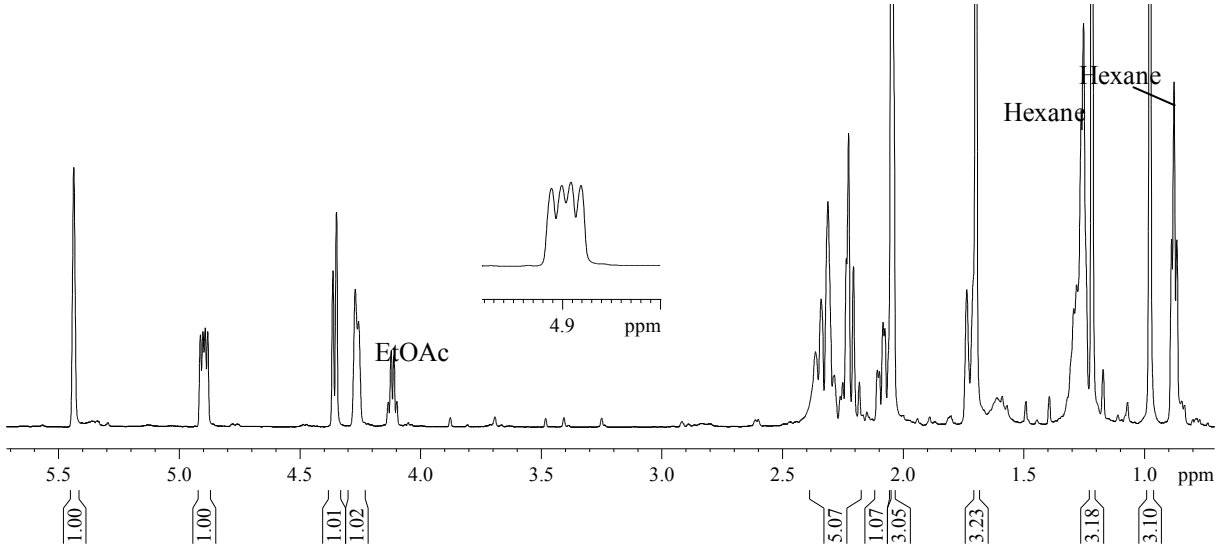

Figure 3.18: ^{1}H NMR spectrum ($CDCl_3$, 600 MHz) of compound **3.17**

The ^{13}C NMR spectrum (Figure 3.19) of compound **3.17** was essential in identifying unsaturated olefinic carbons at δ_C 143.3 and δ_C 125.3. A hydroxymethine signal at δ_C 73.2 in conjunction with two bromo-methine signals at δ_C 62.6 and δ_C 71.0 confirmed a dibromo, hydroxy olefin chamigrane. Compound **3.17** was previously reported by Fenical (1976) from *Laurencia pacifica*.

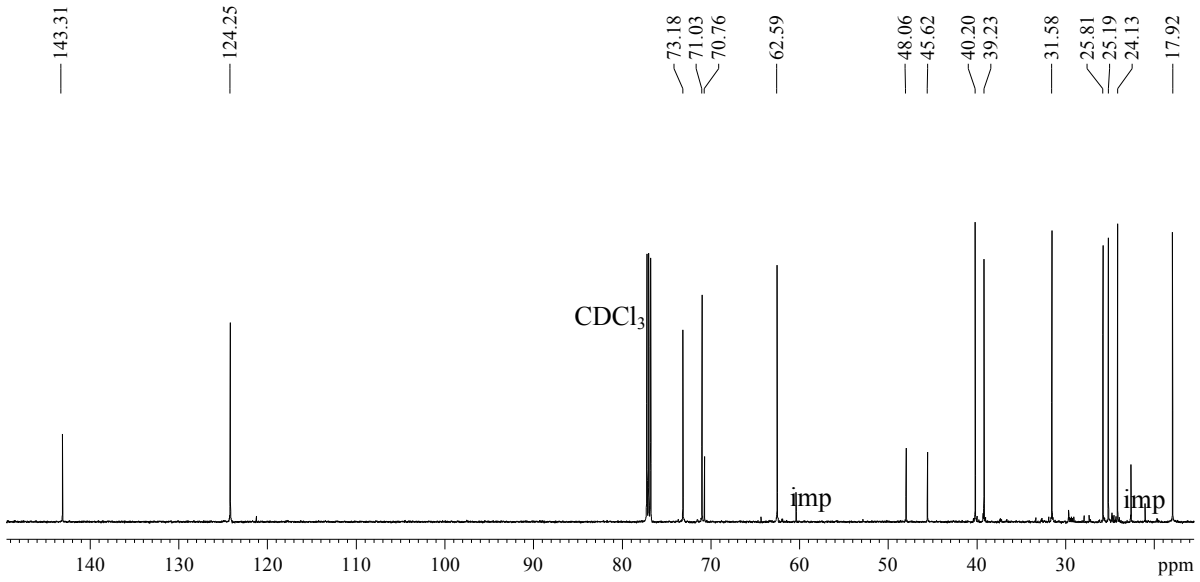

Figure 3.19: ^{13}C NMR spectrum ($CDCl_3$, 150 MHz) of compound **3.17**

NOESY cross peaks, as well as consideration of the coupling constants at H8, H9 and H10 confirmed the relative configuration of the substituents at C9 and C10 as *trans*-equatorial. A related stereogenic chamigrene, compound **3**.**18**, was also isolated by König and Wright (1997) from an Australian sample of *Laurencia rigida*.

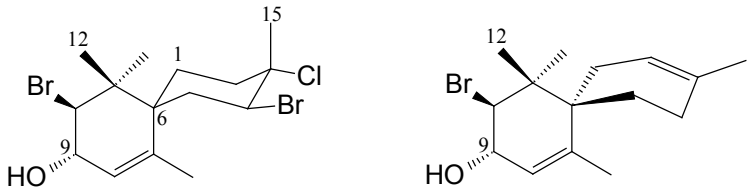

3.17 **3.18**

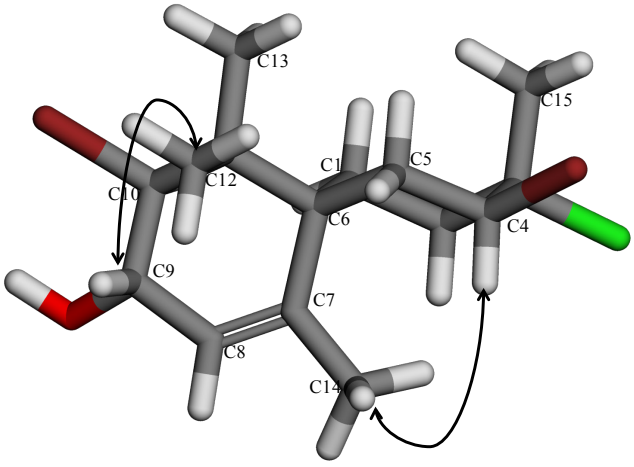

Figure 3.20: Key NOESY correlations in compound **3.17**

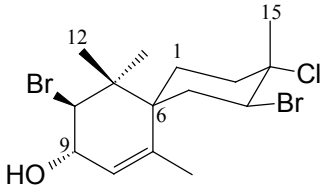

3.17

Table 3.4: NMR spectroscopic data of compound **3.17**

Carbon No	δ_C	δ_C **mult**	δ_H, **mult, J (Hz)**
1a	31.6	CH_2	1.73, m
1b			2.08, m
2	40.4	CH_2	2.32, m
3	70.8	C	-
4	62.6	CH	4.89, dd, 12.2, 6.2
5	39.2	CH_2	2.21, m
6	48.1	C	-
7	143.3	C	-
8	124.2	CH	5.44, s
9	73.2	CH	4.26, d, 8.5
10	71.0	CH	4.35, d, 8.5
11	45.6	C	-
12	17.9	CH_3	0.98, s
13	25.2	CH_3	1.22, s
14	25.8	CH_3	2.05, s
15	24.1	CH_3	1.70, s

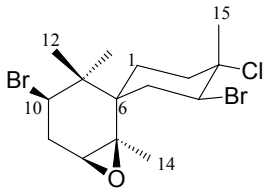

3.1

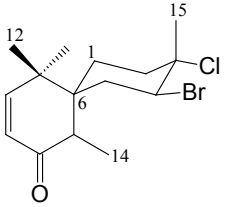

3.3

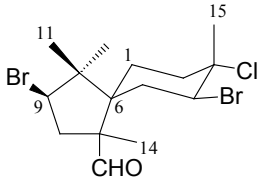

3.4

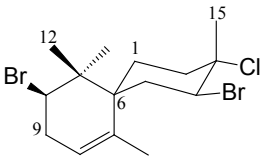

3.9

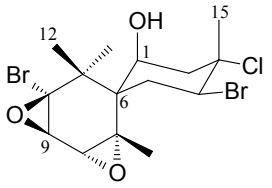

3.15

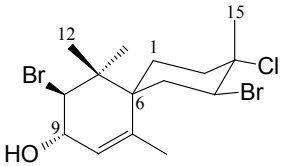

3.17

Table 3.5: ^{1}H and ^{13}C NMR data of chamigranes and derivatives thereof[11] from *L. glomerata*

Proton No	3.1	3.3	3.4	3.9	3.15	3.17
1a	1.67, d, 15.2, 5.7	1.43, dq, 15.0, 2.9	1.70, m	1.61. m	4.04, br s	1.73, m
1b	1.98, dt, 15.2, 5.7	1.71, m	-	2.01, m		2.08, m
2a	2.47, dt, 14.6, 5.7	2.19, td, 14.8, 4.1	2.32, td, 14.1, 4.0	2.24, m	2.53, m	2.32, m
2b	2.38, dd, 14.6, 2.9	2.35, dt, 14.8, 4.1	2.42, dt, 14.1, 4.0	2.31, m	-	-
3	-	-	-	-	-	-
4	4.77, dd, 13.3, 4.7	4.45, dd, 13.3, 4.5	4.56, dd, 13.4, 3.6	4.92, d, 11.2, 7.0	4.74, dd, 13.8, 2.3	4.89, dd, 12.2, 6.2
5a	2.84, br d, 13.3	1.98, t, 13.3	1.92, t, 14.6	2.24, m	2.13, d, 13.8	2.21, m
5b	2.10, t, 13.3	2.40, dt, 13.3, 4.5	2.26, td, 14.6, 3.1	2.35, m	2.54, m	-
6	-	-	-	-	-	-
7	-	2.90, q, 7.8	-	-	-	-
8a	2.92, t, 3.0	-	1.97, dd, 14.1, 8.4	5.23, m	3.07, s	5.44, s
8b	-	-	2.88, dd, 14.1, 8.4	-		-
9a	2.61, dd, 7.7, 3.0	5.82, d, 10.2	4.15, dd, 11.3, 8.4	2.54, m	3.66, s	4.26, d, 8.5
9b	-	-	-	2.67, m		-
10	4.06, t, 7.7	6.43, d, 10.2	-	4.52, d, 11.1, 7.0	-	4.35, d, 8.5
11	-	-	0.88, s	-	-	-
12	1.18, s	1.09, s	0.98, s	0.94, s	0.98, s	0.98, s
13	1.08, s	1.21, s	9.79, s	1.22, s	1.54, s	1.22, s
14	1.50, s	1.30, d, 8.1	1.38, s	1.98, s	1.49, s	2.05, s
15	1.74, s	1.70, s	1.71, s	1.72, s	1.92, s	1.70, s

Carbon No	3.1	3.3	3.4	3.9	3.15	3.17
1	26.2	28.3	27.3	31.6	69.9	31.6
2	40.4	37.7	40.5	40.4	47.2	40.4
3	71.1	71.8	71.0	71.8	71.5	70.8
4	62.1	59.7	60.5	62.8	62.2	62.6
5	39.1	37.1	39.4	39.8	34.0	39.2
6	44.6	43.1	56.0	47.0	50.2	48.1
7	62.0	44.1	52.0	140.2	61.0	143.3
8	62.0	201.5	43.4	123.0	56.7	124.2
9	32.7	123.8	58.4	36.3	55.6	73.2
10	57.6	156	51.2	60.8	75.5	71.0
11	42.3	39.1	20.4	43.0	47.2	45.6
12	21.3	25.4	22.6	17.1	24.4	17.9
13	27.3	25.2	203.5	24.1	27.2	25.2
14	25.8	15.4	23.2	25.5	22.2	25.8
15	24.0	23.7	23.7	23.9	28.0	24.1

[11] Although compound **3.4** is not of the chamigrane class, it was useful including it within this summary for NMR chemical shift comparison.

3.2.2.5 Compound 3.5

The ^{1}H NMR spectrum of compound **3.5** (Figure 3.21) reflected three methyl signals, two of which were singlets at (δ_H 1.00; δ_H 1.66) and one doublet at δ_H 0.78 (d, J = 7.3 Hz). Further downfield, a pair of olefinic signals at δ_H 5.41 and δ_H 5.43 as well as a methylidene moiety at δ_H 4.79 and δ_H 4.86 were identified.

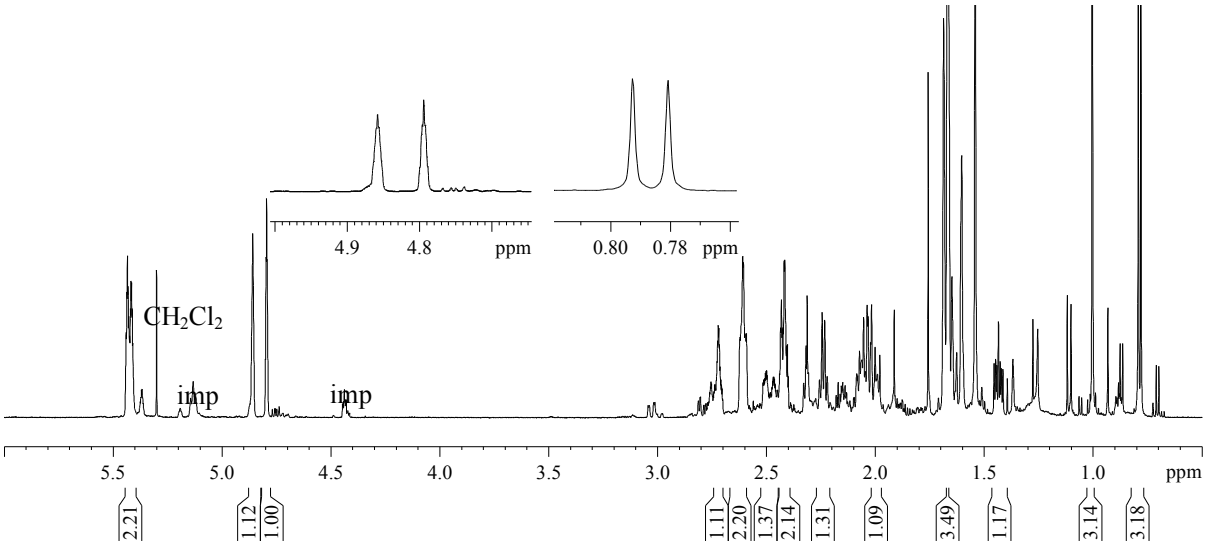

Figure 3.21: ^{1}H NMR spectrum ($CDCl_3$, 600 MHz) of compound **3.5**

A combined analysis of ^{13}C (Figure 3.22) as well as 2D NMR data permitted the assignment of four quaternary (δ_C 49.8, 130.9, 139.2 and 158.0), three methine (δ_C 48.8, 117.8 and 118.9), five methylene (δ_C 27.4, 28.6, 31.7, 32.8 and 105.3) and three methyl (δ_C 17.5, 22.9 and 25.8) carbon signals.

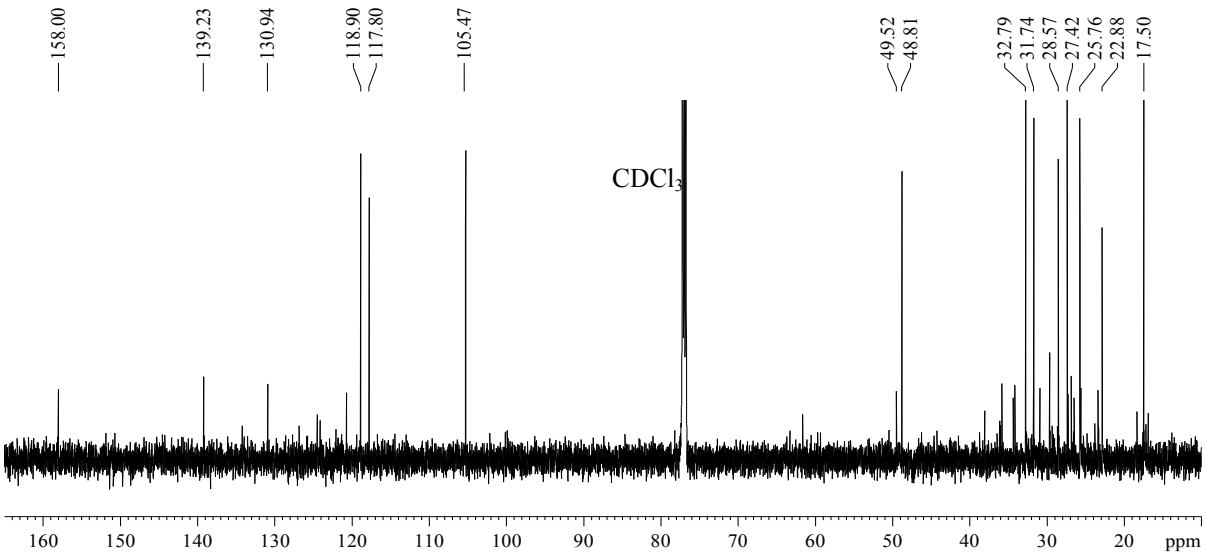

Figure 3.22: ^{13}C NMR spectrum ($CDCl_3$, 150 MHz) of compound **3.5**

Compound **3.5** was identified as *iso*-dihydrolaurene, previously isolated by Suzuki *et al*., (1982). It differs from dihydrolaurene (**3.6**) due to a double bond migration from $\Delta^{6,7}$ to $\Delta^{6,11}$. This was confirmed *via* distinct COSY correlations in compound **3.5** between the neighbouring methylene and olefin groups (H7, H8) and (H10, H11).

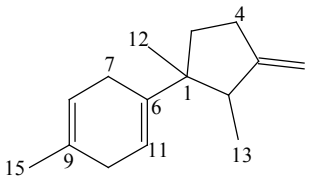

3.5
iso-dihydrolaurene

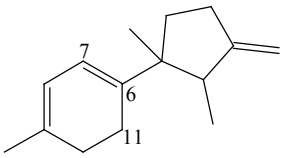

3.6
Dihydrolaurene

Suzuki *et al*., (1982) reported the isolation of compound **3.5** from a *Laurencia nipponica* sample collected from Japanese waters. This is the first report of *iso*-dihydrolaurene (compound **3.5**) from *Laurencia glomerata*.

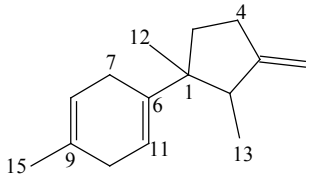

3.5

Table 3.6: NMR spectroscopic data of compound **3.5**

Carbon No	δ_C	δ_C mult	δ_H, mult, J (Hz)
1	49.5	C	-
2	48.8	CH	2.24, q, 7.2
3	158.0	C	-
4	28.6	CH_2	2.42, m
5a	32.8	CH_2	2.02, m
5b			1.43, m
6	139.2	C	-
7a	27.4	CH_2	2.47, m
7b			2.72, m
8	118.9	CH	5.41, m
9	130.9	C	-
10	31.7	CH_2	2.61, m
11	117.8	CH	5.43, m
12	25.8	CH_3	1.00, s
13	17.5	CH_3	0.78, d, 7.1
14a	105.5	CH_2	4.79, m
14b			4.86, m
15	22.9	CH_3	1.66, s

3.2.2.6 Compound 3.7

Compound **3.7** was isolated as a viscous non polar oil. The ^{1}H NMR spectrum (Figure 3.23) contained a complex cluster of olefinic signals in the region of δ_H 5.0-6.0 suggesting the presence of unsaturated functionalities. A terminal methyl flanked by a methylene group was deduced from a broad triplet at δ_H 0.89 (t, J = 7.1 Hz). A broad singlet was also observed at δ_H 3.11 typical of a terminal alkyne proton.

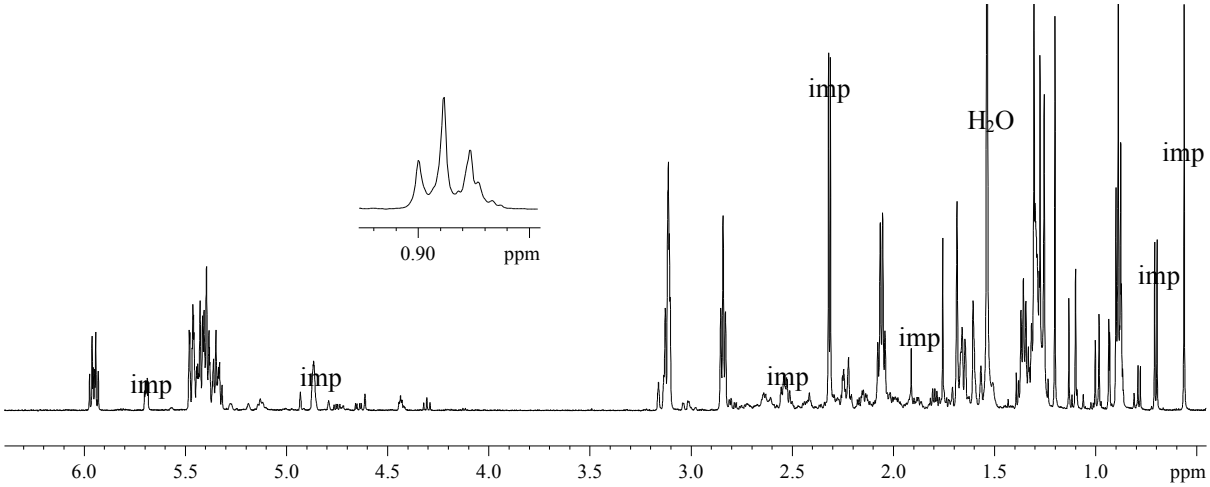

Figure 3.23: ^{1}H NMR spectrum ($CDCl_3$, 600 MHz) of compound **3.7**

The ^{13}C NMR spectrum (Figure 3.24) of compound **3.7** exhibited 15 signals including resonances characteristic of a terminal conjugated alkenyne moiety (δ_C 81.8, 80.3, 108.3 and 143.7), the ≡C-H functionality of which was further confirmed by an IR stretch at ~3300 cm^{-1} (Figure 3.25).

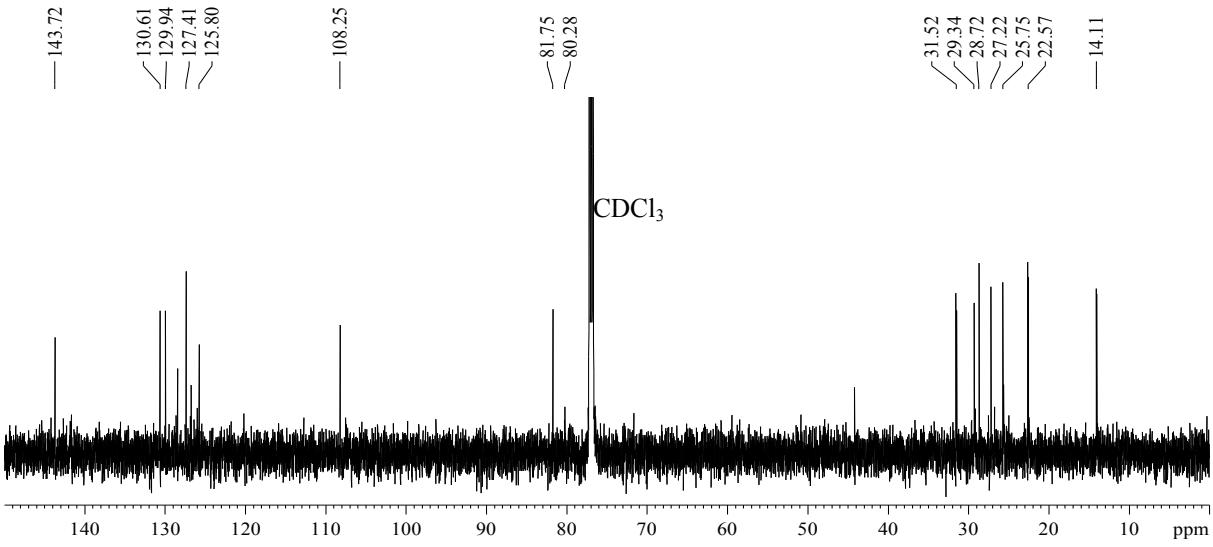

Figure 3.24: ^{13}C NMR spectrum ($CDCl_3$, 150 MHz) of compound **3.7**

A further two double bonds (δ_C 125.8, 127.4, 129.9 and 130.6) and five methylene moieties (δ_C 28.7, 29.3, 31.5, 25.8 and 27.2) were deduced from an edited HSQC spectrum in conjunction with the ^{13}C NMR spectrum.

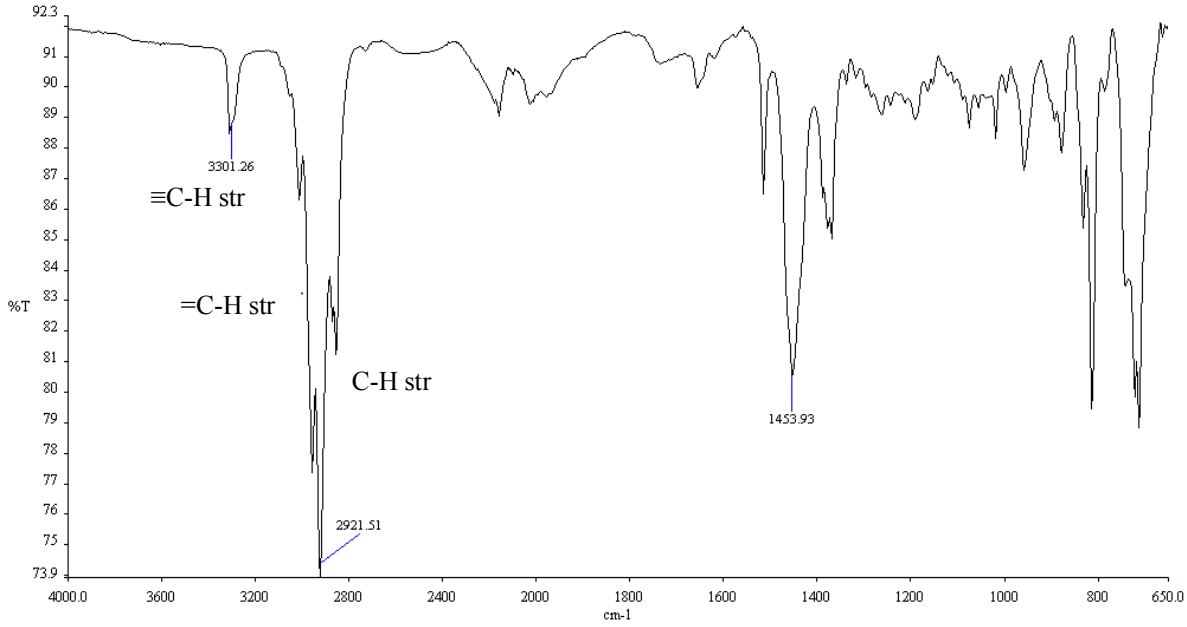

Figure 3.25: IR spectrum of compound **3.7**

Compound **3.7** was identified as neolaurencenyne, a non-terpenoid linear acetogenin previously isolated from *Laurencia okamurai* and successfully synthesized by Kigoshi *et al.*, (1981). Compounds within this particular structural class are thought to be precursors to the more complex cyclic acetylenic ethers as will be shown later. The orientation of the terminal alkyne about $\Delta^{3,4}$ was assigned as *cis*, deduced by the assessment of the carbon chemical shift at C2 with *cis* systems resonating at ~ δ_C 80 and *trans* systems at ~ δ_C 76 (Kigoshi *et al.*, 1982).

A biosynthetically significant metabolite exposing the precursor nature of **3.7** is the $\Delta^{6,7}$ hydroxy-chloro derivative (**3.8**) of neolaurencenyne, isolated by Norte *et al.*, (1991) from a Spanish sample of *Laurencia pinnatifida*. This compound displays the enzyme driven substitution of the olefin within **3.7**.

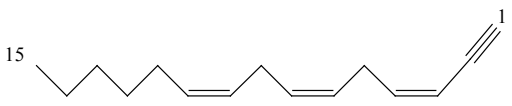

3.7

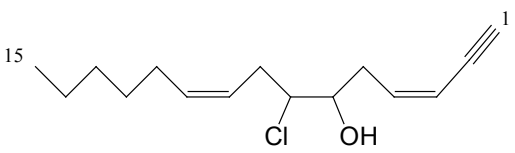

3.8

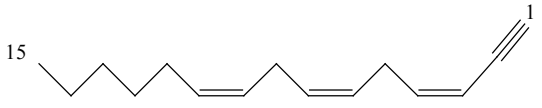

3.7

Table 3.7: NMR spectroscopic data of compound **3.7**[12]

Carbon No	δ_C	δ_C mult	δ_H, mult, J (Hz)
1	81.8	CH	3.11, m
2	80.2	C	-
3	108.3	CH	5.48, m
4	143.7	CH	5.96, m
5	25.7	CH_2	2.84, m
6	125.8	CH	5.41, m
7	127.4	CH	5.36, m
8	27.3	CH_2	2.06, m
9	129.9	CH	5.45, m
10	130.6	CH	5.41, m
11	28.7	CH_2	3.11, m
12	29.3	CH_2	1.37, m
13	31.5	CH_2	1.28, m
14	22.5	CH_2	1.31, m
15	14.1	CH_3	0.89, t, 7.1

[12] The majority of signal multiplicity in the ^{1}H NMR spectrum of compound **3.7** could not be established due to abundant overlapping of peaks. Such is a common phenomenon associated with hydrocarbon chains attributable to the presence of several magnetically equivalent spin-systems. Resultant signals were thus reported as multiplets.

3.3 Experimental

3.3.1 General experimental

NMR experiments were performed on a Bruker® Avance 600 MHz spectrometer using standard pulse sequences with $CDCl_3$ as the solvent. All spectra were referenced according to residual proton residues in deuterated solvent ($CHCl_3$ δ_H 7.26, $CDCl_3$ δ_C 77.0).

All solvents used were of chromatography grade (LiChrosolv®), obtained from Merck®, Darmstadt, Germany while column chromatography was performed using Merck® Silica gel 60 (0.040-0.063 mm), Germany.

HPLC was performed using a semi-preparative normal phase Whatman Partisil® 10 M9/50 (9.5 mm x 500 mm) column and a Rheodyne® manual injector containing a Waters® HPLC pump with a Spectra physics® RI detector attached to a Ridenki® chart recorder.

3.3.2 Plant material (*L. glomerata*, NDK130821-10)

Laurencia glomerata was collected by hand at Noordhoek beach in the south-east coastal region of South Africa in August 2013. A voucher specimen is kept in the seaweed sample repository at the School of Pharmacy, University of the Western Cape. Identification of the alga was done by Professor John Bolton with the Department of Biological Sciences at the University of Cape Town, South Africa.

3.3.3 Extraction and isolation

The algal material, with a dry mass of 41.6 g, was initially steeped in MeOH at room temperature for one hour, after which it was extracted three times with CH_2Cl_2-MeOH (2:1, 770 mL[13] x 3) at a constant temperature of 40 ^oC.

The combined organic phases were collected (after an adequate amount of water was added for phase separation) and concentrated under reduced pressure to produce a crude extract of 0.85 g which corresponds to a 2% yield [Weight of crude/ (Weight of dry mass + Weight of Crude)].

[13] The volume of solvent used was variable for each alga within subsequent chapters. An amount sufficient to submerge the algae fully was used in each case.

Fractionation of the crude was further carried out *via* hexane:EtOAc step gradient column chromatography (50 mL solvent per fraction) to yield eight fractions **A**-**H**. (**A** 100% hexane; **B** 9:1 hex:EtOAc, **C** 8:2 hex:EtOAc, **D** 6:4 hex:EtOAc, **E** 4:6 hex:EtOAc, **F** 2:8 hex:EtOAc, **G** 100% EtOAc, **H** 1:1 MeOH:EtOAc).

Fractions A, B and C were further purified via silica gel column chromatography and/or normal phase HPLC to yield compounds **3.1** (480 mg, 1.130%), **3.5** (6.3 mg, 0.015%), **3.7** (7.1 mg, 0.017%), **3.9** (1.3 mg, 0.003%), **3.15** (9.4 mg, 0.022%) and **3.17** (24 mg, 0.052%).

3.3.4 Compounds isolated[14]

3.3.4.1 Compound 3.1(JF13(2)-58)

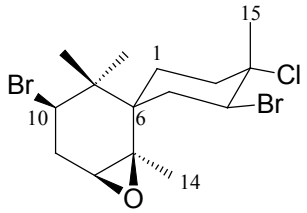

3.1

3-chloro-4, 10 dibromo-7,8 epoxychamigrane OR *(1R*,4R*,6S*)-3',4-dibromo-4'-chloro-1,3,3,4'-tetramethyl-7-oxaspiro[bicyclo[4.1.0]heptane-2,1'-cyclohexane]* (**3.1**): White plate like crystals; ^{1}H and ^{13}C NMR ($CDCl_3$) data available in Table 3.1. As previously reported by Howard and Fenical, (1975).

*Cleavage of the epoxy group compound in **3.1** to produce compounds **3.3** and **3.4***

Compound **3.1** (15 mg) was dissolved in dry Et_2O (15 mL). In a separate round bottomed flask, $BF_3.Et_2O$ (2 mL) was added to Et_2O (15 mL) and cooled to -70 ^{o}C in a dry ice/acetone bath. The previously prepared solution of compound **3.1** was gradually added to the $BF_3.Et_2O$ solution after which stirring occurred for 18 hours under a N_2 stream, allowing the vessel to slowly achieve room temperature. The reaction mixture was quenched with $NaHCO_3$ (30 mL), filtered and dried under vacuum. The resultant crude mixture was purified *via* normal phase HPLC (4:1 Hex: EtOAc) yielding pure compounds **3.3** (6.1 mg, 40.6%) and **3.4** (2.3 mg, 15.3%).

[14] The numbering of the compounds within this thesis is as per that most commonly seen within the literature. Consequently, the compound names (generated by ACD/ChemSketch®) may not possess similar numbering.

3.3.4.2 Compound 3.5 (JF13(2)-77E)

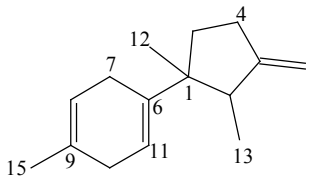

3.5

Iso-dihydrolaurene OR *1-(1,2-dimethyl-3-methylidenecyclopentyl)-4-methylcyclohexa-1,4-diene* (**3.5**): Colourless oil; ^{1}H and ^{13}C NMR ($CDCl_3$) data available in Table 3.6. As previously reported by Suzuki *et al*., (1982).

3.3.4.3 Compound 3.7 (JF13(2)-63(12))

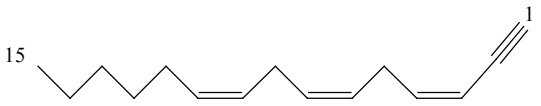

3.7

Neolaurencenyne OR *(3Z,6Z,9Z)-pentadeca-3,6,9-trien-1-yne* (**3.7**): Colourless oil; ^{1}H and ^{13}C NMR ($CDCl_3$) data available in Table 3.7. As previously isolated by Kigoshi *et al*., (1981).

3.3.4.4 Compound 3.9 (JF13(2)-76C)

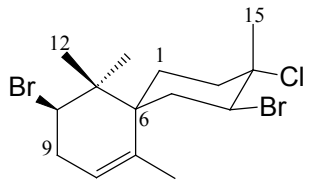

3.9

3-chloro-4,10-dibromo-chamigrene OR *(4R*)-4,8-dibromo-9-chloro-1,5,5,9-tetramethylspiro [5.5]undec-1-ene* (**3.9**): Amorphous white solid; ^{1}H and ^{13}C NMR ($CDCl_3$) data available in Table 3.2. As previously reported by Howard and Fenical (1975).

3.3.4.5 Compound 3.15 (JF13(2)-72F)

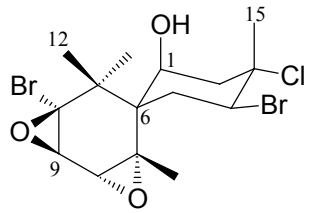

3.15

Prepacifenol epoxide OR *1- hydroxy-3-chloro-4, 10 dibromo-7,8:9,10 diepoxychamigrane* (**3.15**): White crystals; ^{1}H and ^{13}C NMR ($CDCl_3$) data available in Table 3.3. As previously reported by Faulkner *et al*., (1974).

3.3.4.6 Compound 3.17 (JF13(2)-60Q)

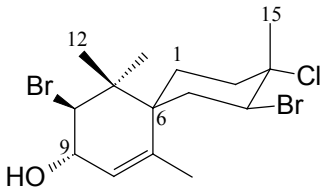

3.17

3-chloro- 4,10-dibromo-9-hydroxy-chamigrene OR *(3S*,4S*)-4,8-dibromo-9-chloro-1,5,5,9-tetramethylspiro[5.5]undec-1-en-3-ol* (**3.17**): White crystals; ^{1}H and ^{13}C NMR ($CDCl_3$) data available in Table 3.4. As previously reported by Fenical (1976).

3.4 References

Bano, S.; Ali, M. S.; Ahmad, V. U. Marine Natural Products Vl.A halogenated chamigrene epoxide from the red alga *Laurencia pinnatifida*. *Planta Medica* **1987**, *53*, 508.

Cowe, H. J.; Cox, P. J.; Howie, R. A. Structure of *2,10-dibromo-3-chloro-7R,8S-epoxychamigrene*. *Zeitschrift fuer Kristallographie* **1989**, *188*, 1-4.

Crews, P.; Naylor S.; Hanke, J. F.; Hogue, R. E.; Kho, E.; Braslau, R. Halogen regiochemistry and substituent stereochemistry determination in marine monoterpenes by ^{13}C NMR. *Journal of Organic Chemistry* **1984**, *49*, 1371-1377.

Crews, P.; Naylor, S.; Myers, B. L.; Loo, J.; Manes, L. V. Residually coupled attached proton test in the carbon-13 NMR assignment of natural products. *Magnetic Resonance in Chemistry* **1985**, *23*, 684-687.

De Clerck, O.; Bolton, J. J.; Anderson, R. J.; Coppejans, E. *Guide to the seaweeds of KwaZulu-Natal*. *Scripta Botanica Belgica 33*. National Botanic Garden of Belgium, VLIZ: Flanders Marine Institute and Flemish Community, **2005**, 1-294.

Elsworth, J. F.; Thomson, R. H. A new chamigrane from *Laurencia glomerata*. *Journal of Natural Products* **1989**, *52*, 893-895.

Faulkner, J. D.; Stallard, M. O.; Ireland, C. Prepacifenol epoxide, a halogenated sesquiterpene diepoxide. *Tetrahedron Letters* **1974**, *40*, 3571-3574.

Francis, C. M. **2014**. Systematics of the *Laurencia* complex (Rhodomelaceae, Rhodophyta) in southern Africa. PhD Thesis. University of Cape Town, Cape Town, South Africa.

Fenical, W. Chemical variation in a new bromochamigrene derivative from the red seaweed *Laurencia pacficia*. *Phytochemistry* **1976**, *15*, 511-512.

Howard, B. M.; Fenical, W. Structures and chemistry of two new halogen-containing chamigrene derivatives from *Laurencia*. *Tetrahedron Letters* **1975**, *21*, 1687-1690.

Kigoshi, H.; Shizuri, Y.; Niwa, H.; Yamada, K. Laurencenyne, a plausible precursor of various nonterpenoid C_{15}-compounds, and neolaurencenyne from the red alga *Laurencia okamurai*. *Tetrahedron Letters* **1981**, *2,* 4729-4732.

Kigoshi, H.; Shizuri, Y.; Niwa, H.; Yamada, K. Isolation and structures of trans-laurencenyne, a possible precursor of the C_{15} halogenated cyclic ethers, and trans-neolaurencenyne from Laurencia okamurai. *Tetrahedron Letters* **1982**, *23*, 1475-1476.

Kimura, J.; Kamada, N.; Tsujimoto, Y. Fourteen chamigrane derivatives from a red alga, *Laurencia nidifica*. *Bulletin of the Chemical Society of Japan* **1999**, *72*, 289-292.

Knott, M. G. **2011** Isolation, structural characterisation and anti-cancer activity of natural products from selected South African marine algae. Ph.D thesis. Rhodes University, Grahamstown.

König, G. M.; Wright, A. D. *Laurencia rigida*: chemical investigations of its antifouling dichloromethane extract. *Journal of Natural Products* **1997**, *60*, 967-970.

Norte, M.; Gonzalez, A. G.; Cataldo, F.; Rodriguez, M, L.; Brito, I**.** New examples of acyclic and cyclic C-15 acetogenins from *Laurencia pinnatifida*. Reassignment of the absolute configuration for *E* and *Z* pinnatifidienyne. *Tetrahedron* **1991**, *47*, 9411-9418.

Ojika, M.; Shizuri, Y.; Yamada, K. A halogenated chamigrane epoxide and six related halogen-containing sesquiterpenes from the red alga *Laurencia okamurai*. *Phytochemistry* **1982**, *21*, 2410-2411.

Selover, S. J.; Crews, P. Kylinone, a new sesquiterpene skeleton from the marine alga *Laurencia pacifica*. *Journal of Organic Chemistry* **1980**, *45*, 69-72.

Stegenga, H.; Bolton, J. J.; Anderson, R. J. Seaweeds of the South African west coast; *Contributions from the Bolus Herbarium* **1997**, *18*, 1-655.

Suzuki, M.; Kurosawa, E.; Furusaki, A. The absolute configurations of halogenated chamigrene derivatives from the marine alga, *Laurencia glandulifera* Kützing. *Tetrahedron* **1979**, *35*, 823-831.

Suzuki, T.; Kikuchi, H.; Kurosawa, E. Six new sesquiterpenoids from the red alga *Laurencia nipponica* Yamada. *Bulletin of the Chemical Society of Japan* **1982**, *55*, 1561-1563.

Wang, B. G.; Gloer, J. B.; Ji, N, Y.; Zhao, J. C.; Halogenated organic molecules of Rhodomelaceae origin: Chemistry and Biology. *Chemical Reviews* **2013**, *113*, 3632-3685.

Wright A. D.; König, G. M.; Sticher, O. New sesquiterpenes and C_{15} acetogenins from the marine red alga *Laurencia implicata*. *Journal of Natural Products* **1991**, *54*, 1025-1033.

Chapter 4

Secondary metabolites from *Laurencia* cf. *corymbosa*

Abstract

This, the first phycochemical analysis of *Laurencia* cf. *corymbosa*, revealed known brominated, hydroxy cuparane compounds **4.5** and **4.6**, including new isomers **4.1** and **4.7**, and the new cyclic keto-cuparane, **4.4**. A known epoxy chamigrane (**4.8**) was also isolated together with *L. glomerata* metabolites neolaurencenyne **3.7** and the dibromo-epoxychamigrane **3.1**.

Chapter 4

Secondary metabolites from *Laurencia* cf. *corymbosa*

4.1 Introduction

Laurencia cf. *corymbosa* is distributed along the southern coast of Africa from De Hoop to Port Alfred (Francis, 2014). This species is epilithic and plant colour varies from maroon to purple. Plants can reach anywhere between 5-15 cm high with terminal branchlets showing a corymboid nature (*corymbosa*: grape like cluster). The cortical cells are known for possessing one *corps en cerise* and in its non fertile stage can be confused for *Laurencia obtusa* (Francis, 2014). Francis, (2014) shows a number of morphological variants present for this species however divergences among their DNA sequences are insignificant. The species is hence described as cf. *corymbosa* i.e. comparable to.

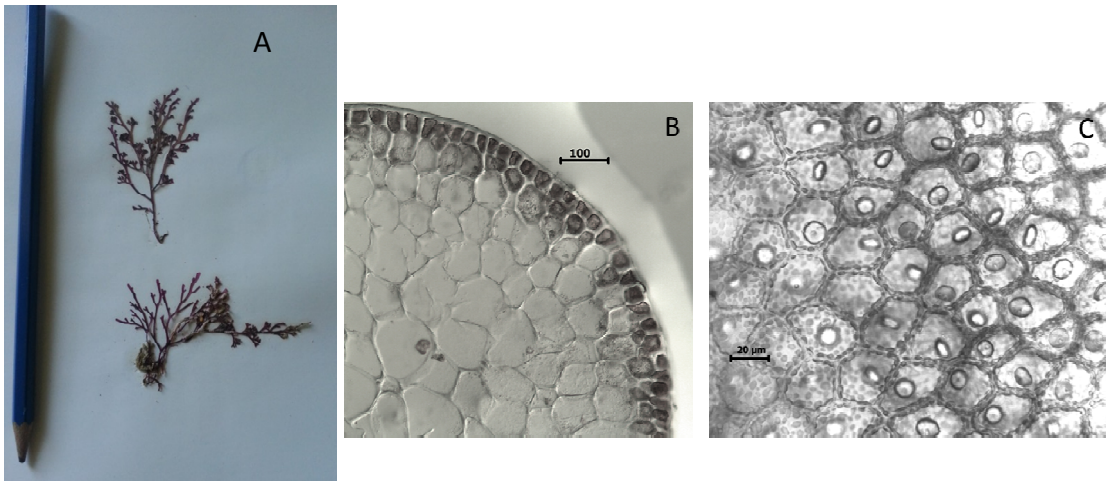

Figure 4.1: *Laurencia* cf. *corymbosa*[1] (Caitlynne Francis © 2014)

A) Habit.

B) Cross section through thallus with outermost cortical cells and spaces between medullary and cortical cells in view.

C) Cortical cells show one *corps en cerise* per cell (40x).

[1] Image plates courtesy of Caitlynne Francis © 2014, University of Cape Town, South Africa

4.2 Results and Discussion

4.2.1 Extraction and isolation of metabolites from *L.* cf. *corymbosa* (NDK130821-11, Noordhoek)

Following our standard extraction and fractionation protocol (section **3.2.1**, page 54), the alga afforded a crude isolate of 1.17 g equating to a 3.9% yield of the dry algal material (Scheme 4.1). From (Figure 4.2), fractions A, B and D displayed peaks of interest and were further purified by a combination of silica gel column chromatography and normal phase HPLC to yield compounds **3.1**, **3.7**, **4.1**, **4.4**, **4.5-4.8**. Fractions E-H displayed typical fatty acid and sugar type resonances.

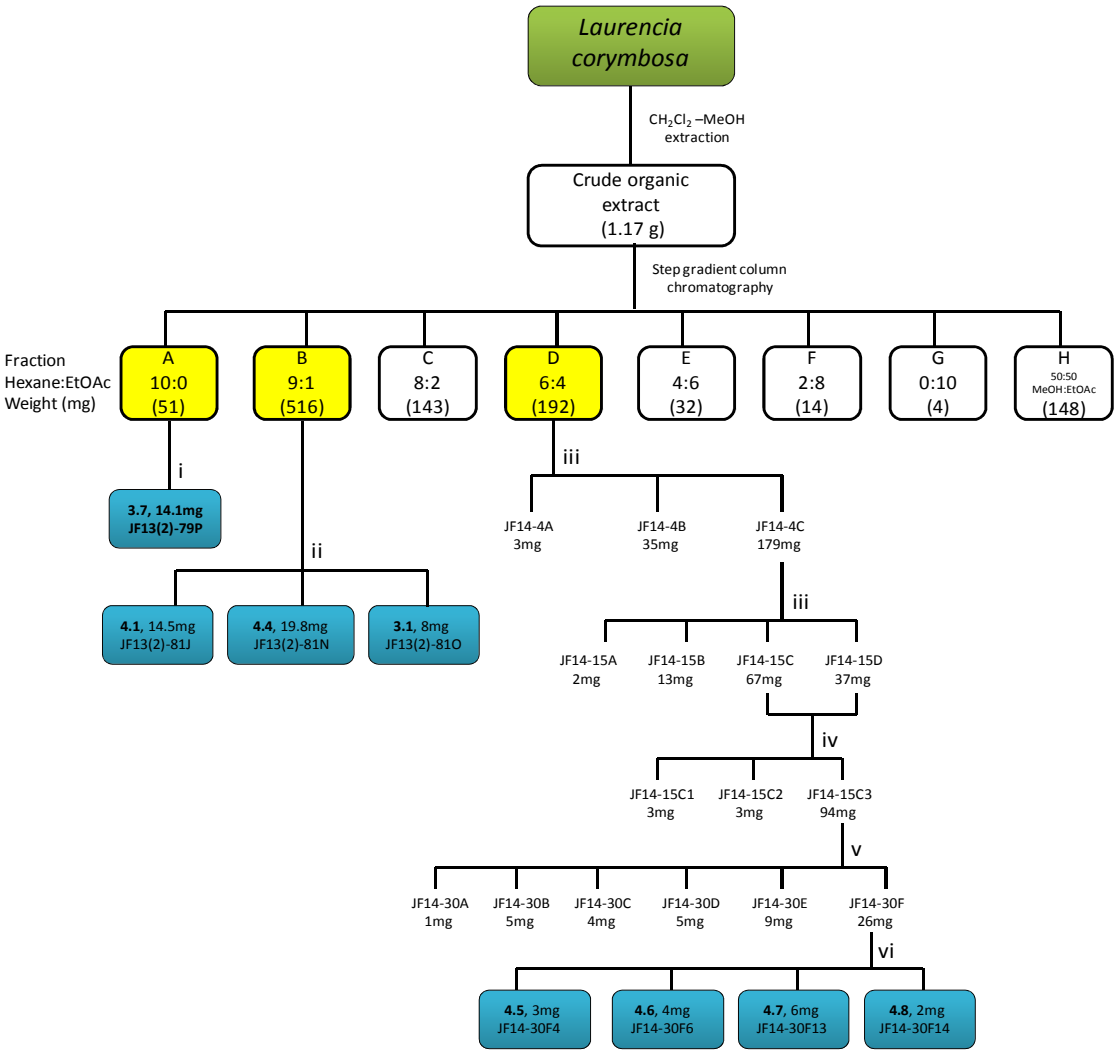

Scheme 4.1: Isolation scheme of metabolites from *L.* cf. *corymbosa* (NDK130821-11)

Conditions: i) Normal phase HPLC (100% hexane); ii) Normal phase HPLC (19:1 hex:EtOAc); iii) Silica gel column chromatography (3:2 hex:EtOAc); iv) Silica gel column chromatography (3:1:1 hex:EtOAc:CH_2Cl_2); v) Normal phase HPLC (3:2 hex:EtOAc); vi) Normal phase HPLC (7:3 hex:EtOAc)

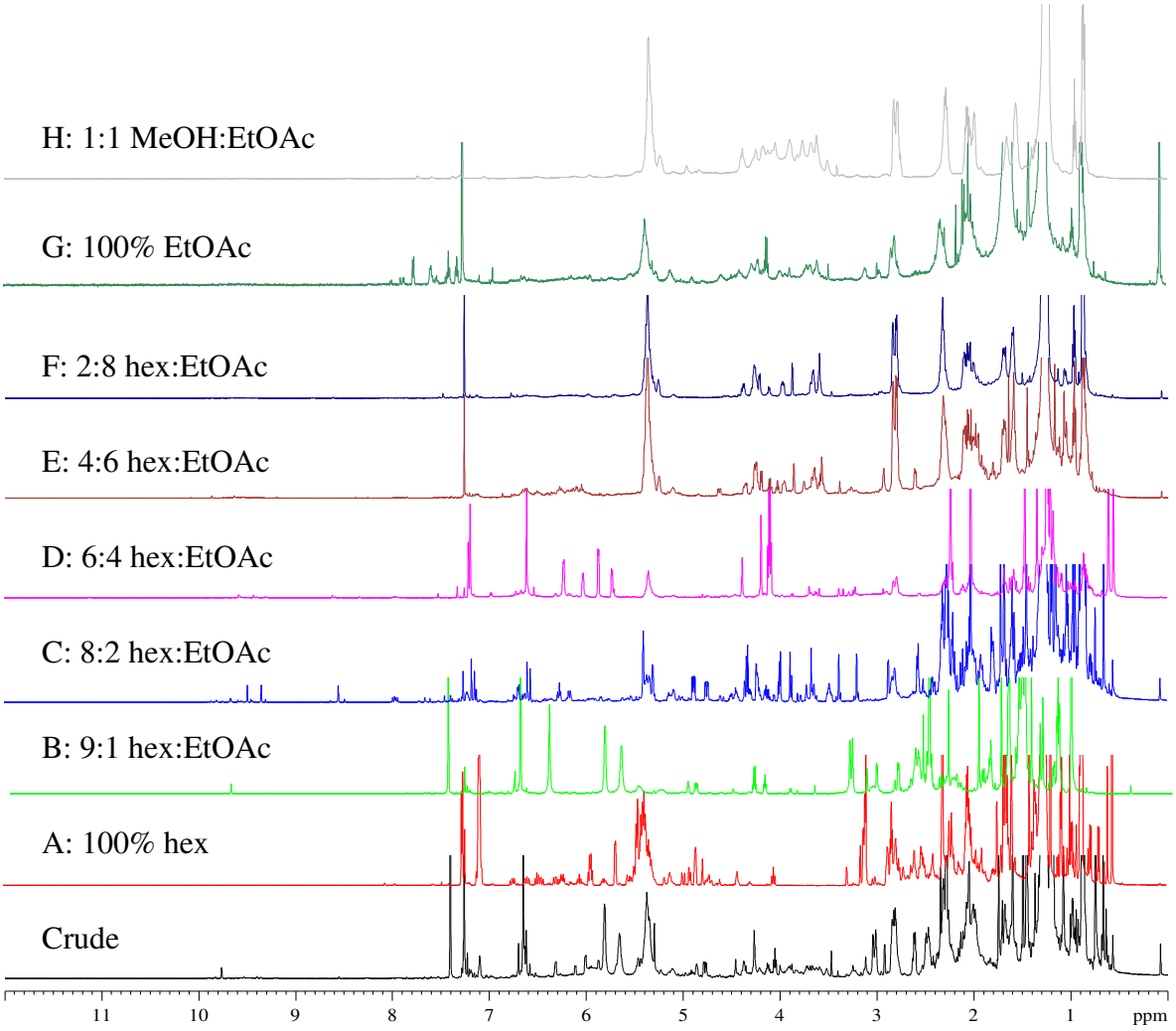

Figure 4.2: ^{1}H NMR spectra ($CDCl_3$, 600 MHz) of the crude organic extract of *L.* cf. *corymbosa* (NDK130821-11) and step gradient column fractions A-H

4.2.2 Structure elucidation of metabolites

4.2.2.1 Compound 4.1

Compound **4.1**, a colourless oil, showed molecular ion cluster at *m/z* 294 and 296 in its HRGCESIMS spectrum (Figure 4.3). This is indicative of the presence of a single isotopic halo-substituent within the molecule[2]. The molecular formula was deduced as $C_{15}H_{19}O^{79}Br$ with a calculated double bond equivalent of six. A total of 15 signals in the ^{13}C NMR spectrum (Figure 4.4), deduced together with HSQC and HMBC data, as well as a broad hydroxy stretch in the IR spectrum (Figure 4.5) added integrity to the molecular formula.

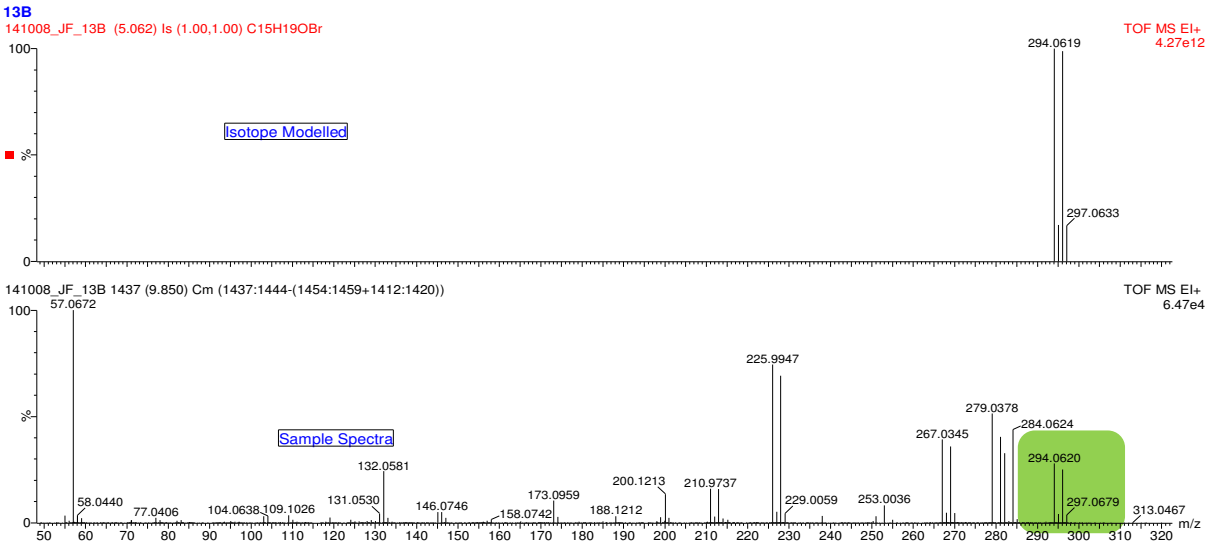

Figure 4.3: HRGCEIMS spectrum of compound **4.1**

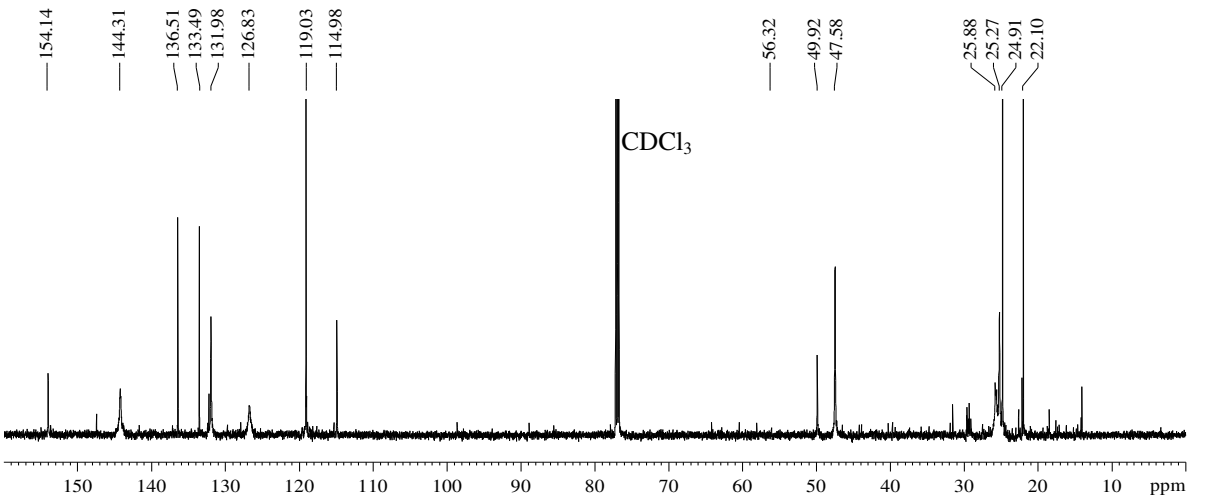

Figure 4.4: ^{13}C NMR spectrum ($CDCl_3$, 150 MHz) of compound **4.1**

[2] See Appendix 4 for halogen abundance patterns in mass spectrometry

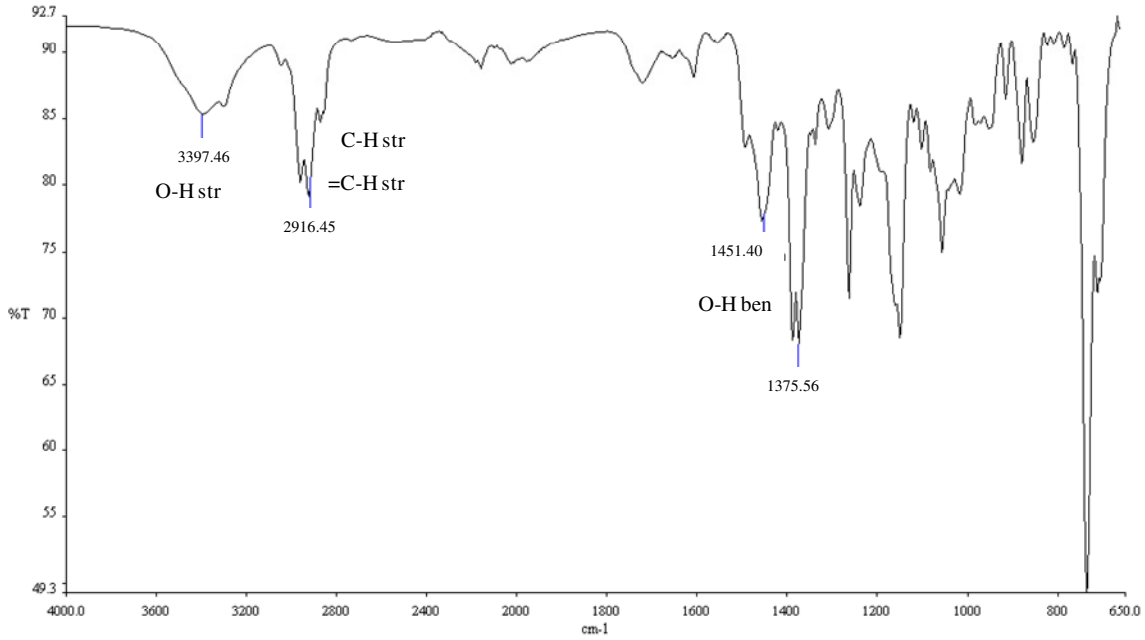

Figure 4.5: IR spectrum of compound **4.1**

The relatively simple ^{1}H NMR spectrum (Figure 4.6) displayed four methyl resonances between δ_H 0.5-2.5 suggesting a sesquiterpenoid skeleton. The ^{1}H NMR spectrum also showed aromatic singlets between δ_H 6.5-7.5, two deshielded broad olefinic singlets between δ_H 5.5-6.5 and mutually coupled (J = 16.1 Hz) allylic methylene doublets at δ_H 2.5 and δ_H 3.0.

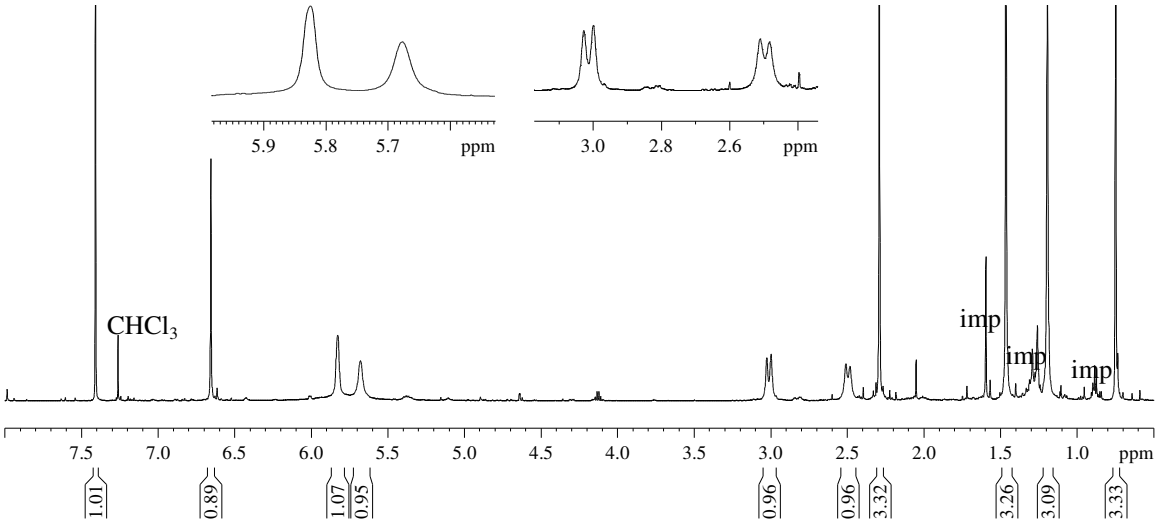

Figure 4.6: ^{1}H NMR spectrum ($CDCl_3$, 600 MHz) of compound **4.1**

Compound **4.1**, a new compound, was identified as being isomeric to **4.2** (*iso*-allolaurinterol) isolated by Dias *et al*., (2009) from *Laurencia filiformis*. Compound **4.2** shows a methyl shift from C5 to C4, whereas compound **4.1** exhibits the presence of a broad olefin singlet at C4 (δ_H 5.67) and a *gem*-dimethyl moiety at C5.

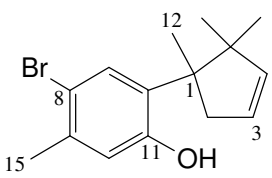

4.1

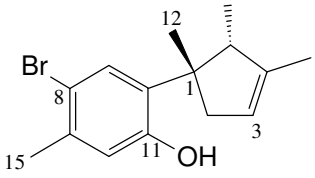

4.2
iso-allolaurinterol

Knowing that aromatic hydroxyl substituents are more deshielded than bromo-substituents (Kladi *et al*., 2005), critical assessment of HMBC correlations from the methyl substituents at C1 and C9 to various carbon centres on the aromatic ring (Figure 4.7) allowed for the establishment of the positions of the bromine and hydroxy functions.

Moreover, the proposed substituent locations in compound **4.1** are typical amongst metabolites isolated from *Laurencia* spp. as is shown by Dias *et al*., (2009) in **4.2** as well as Yu *et al*., (2014) and Yamada *et al*., (1969).

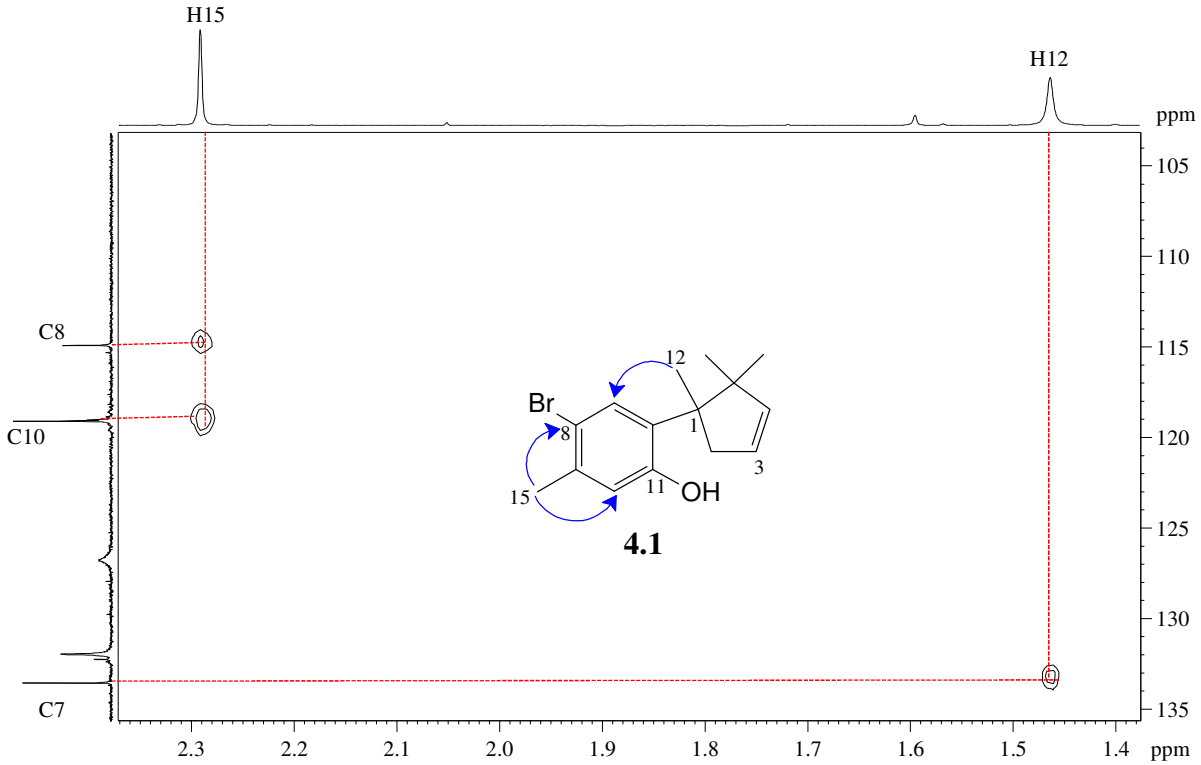

Figure 4.7: Partial HMBC spectrum of compound **4.1** showing key correlations

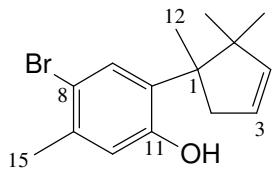

4.1

Table 4.1: NMR spectroscopic data of compound **4.1**

Carbon No	δ_C	δ_C **mult**	δ_H, **mult, J (Hz)**	**COSY**	**HMBC**
1	56.3	C	-	-	-
2a	47.6	CH_2	3.01, d, 16.1	H2b	-
2b			2.50, d, 16.1	H2a	-
3	126.8	CH	5.83, br s	H2a, H2b	C1*
4	144.3	CH	5.67, br s	H2a, H2b*	-
5	49.9	C	-	-	-
6	133.4	C	-	-	-
7	132.0	CH	7.41, s	H12, H15	C5, C8, C9, C11, C15
8	114.7	C	-	-	-
9	136.5	C	-	-	-
10	119.0	CH	6.65, s	H15	C6, C8, C11, C15
11	154.1	C	-	-	-
12	25.3	CH_3	1.47, s	-	C1, C2, C5, C6
13	25.9	CH_3	1.19, s	-	C4*, C5, C14
14	24.9	CH_3	0.75, s	-	C4, C5, C13
15	22.1	CH_3	2.30, s	H7, H10	C8, C9, C10

* Indicates weak correlation

Acetylation of compound **4.1** (Scheme 4.2), confirmed by acetyl carbon signals δ_C 169.6 and δ_C 21.8 (Figure 4.8), resulted in clearer splitting of olefinic signals H3 and H4 as well as more distinctive splitting of H2 (Figure 4.9).

The HRESIMS spectrum (Figure 4.10) of the acetylated compound, **4.3** showed a molecular ion cluster $[M+H]^+$ at *m/z* 337.0789 (calculated for 337.0803) and 339.0823 confirming the molecular formula $C_{17}H_{21}{}^{79}BrO_2$.

The positions of substituents at C8 and C11 in compound **4.1** were further substantiated as similar 2D correlations were observed in the acetylated derivative, compound **4.3**.

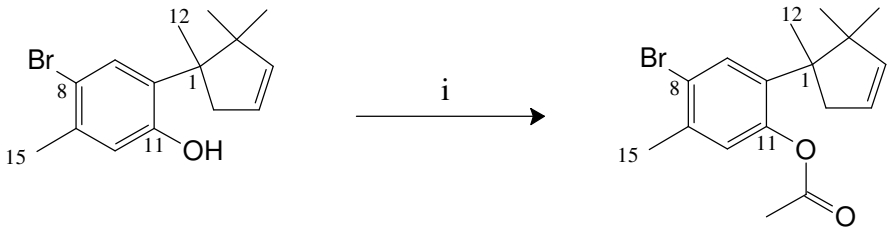

4.1 **4.3**

Scheme 4.2: Acetylation of compound **4.1**

Conditions: i) Pyridine/acetic anhydride, stir overnight at room temperature

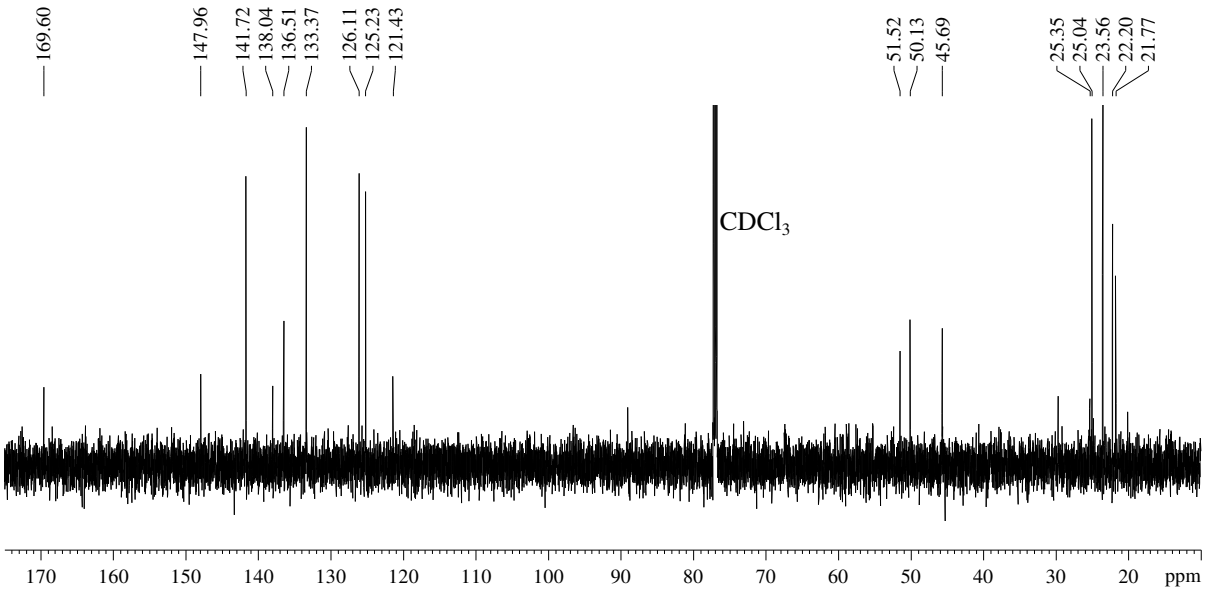

Figure 4.8: ^{13}C NMR spectrum ($CDCl_3$, 150 MHz) of compound **4.3**

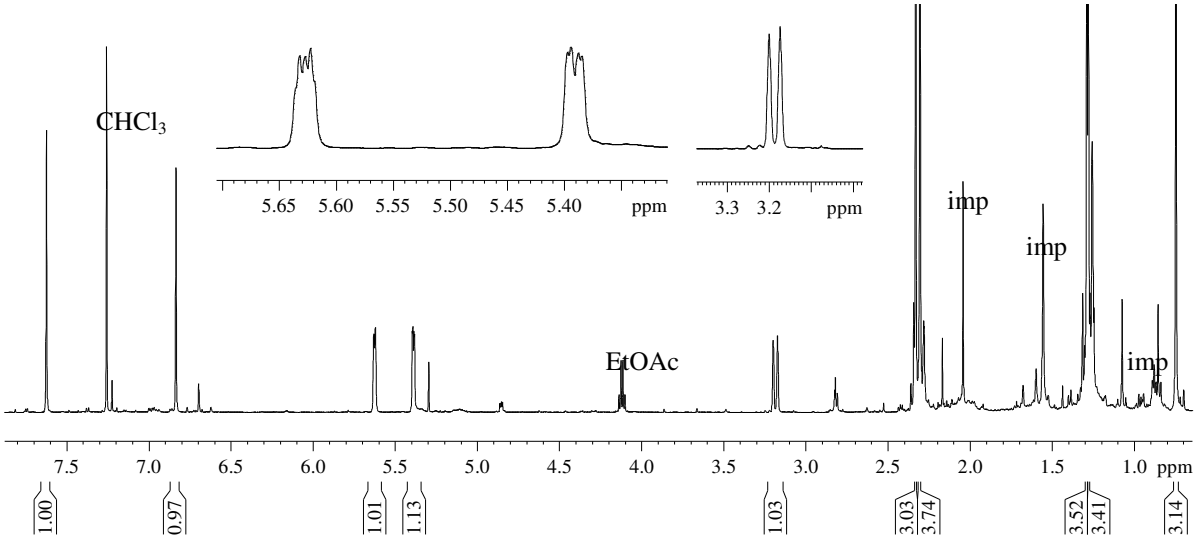

Figure 4.9: ^{1}H NMR spectrum ($CDCl_3$ 600 MHz) of compound **4.3**

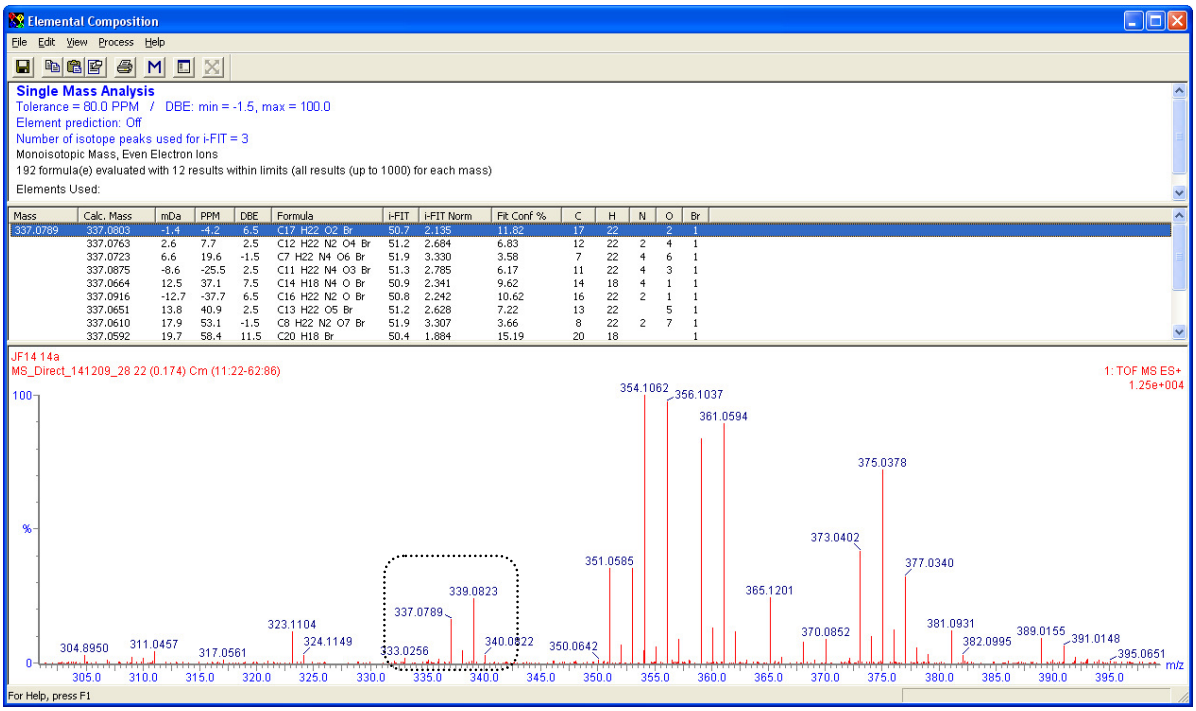

Figure 4.10: Expansion of the HRESIMS spectrum of compound **4.3**

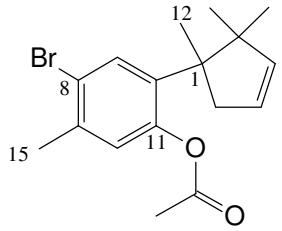

4.3

Table 4.2: NMR spectroscopic data of compound **4.3**

Carbon No	δ_C	δ_C mult	δ_H, mult, J (Hz)	COSY	HMBC
1	51.5	C	-	-	-
2a	45.7	CH_2	3.19, d, 16.1	H2b	C1, C3, C4, C6, C12
2b			2.30, m	H2a	-
3	125.3	CH	5.63, m	H2a, H2b, H4	C2, C4, C5
4	141.7	CH	5.39, dd, 5.9, 2.0	H2a, H2b, H3	C2, C3, C5
5	50.1	C	-	-	-
6	138	C	-	-	-
7	133.4	CH	7.63, s	-	C1, C8, C9, C11, C15
8	121.4	C	-	-	-
9	136.5	C	-	-	-
10	126.1	CH	6.84, s	H15	C6, C8, C11, C15
11	148	C	-	-	-
12	25.4	CH_3	1.28, s	-	C2, C5, C6
13	23.6	CH_3	1.29, s	-	C4, C5, C14
14	25.0	CH_3	0.75, s	-	C4, C5, C13
15	22.2	CH_3	2.33, s	H10	C8, C9, C10
16	169.6	O**C**OCH$_3$	-	-	-
17	21.8	OCO**C**H$_3$	2.31, s	-	C16

4.2.2.2 Compound 4.4

Compound **4.4** was recrystallised in hexane to afford white, needle like crystals. Detailed analysis of the HRGCEIMS spectrum (Figure 4.11) reflected isotopic molecular ion signals at *m/z* 308.0356 (calc. 308.0412) and 310.0346 and, after identifying a total of 15 carbon signals by analysis of the ^{13}C NMR (Figure 4.12) and HMBC spectra, the molecular formula of **4.4** was assigned as $C_{15}H_{17}{}^{79}BrO_2$ with a calculated double bond equivalent of seven.

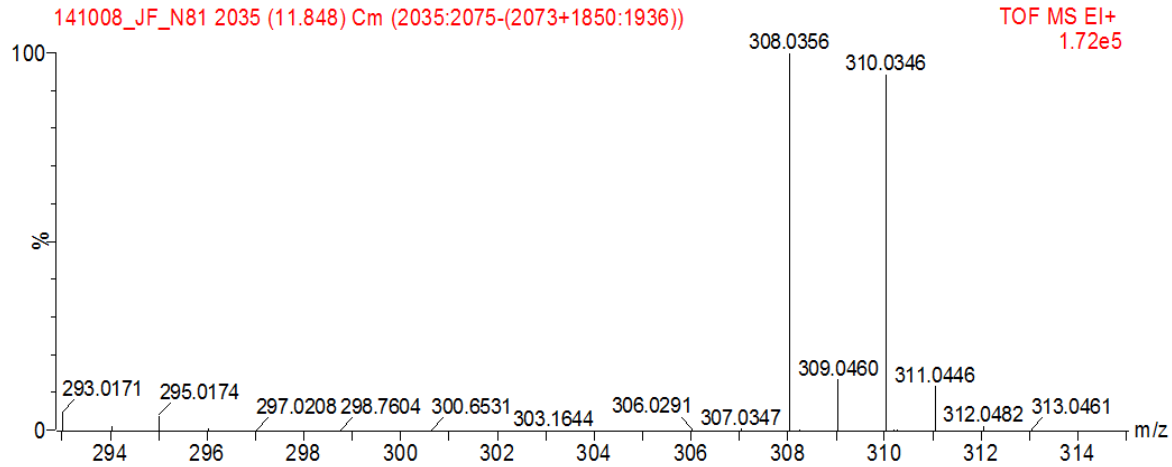

Figure 4.11: Expansion of the HRGCEIMS spectrum of compound **4.4**

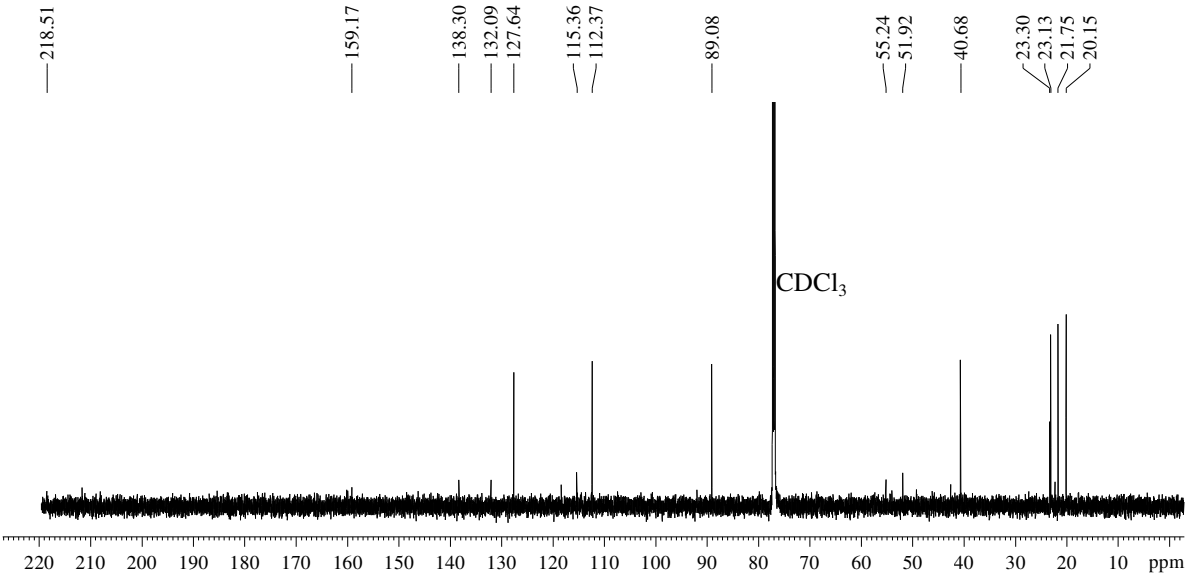

Figure 4.12: ^{13}C NMR spectrum ($CDCl_3$, 150 MHz) of compound **4.3**

The ^{13}C NMR spectrum (Figure 4.12) displayed a deshielded methine signal at δ_C 89.1 as well as a cluster of methyl peaks between δ_C 20-24 similar to those witnessed in compound **4.1**.

The ^{1}H NMR spectrum of **4.4** (Figure 4.13) showed deshielded singlets corresponding to the same tetra-substituted aromatic ring as previously observed in compound **4.1**. The main difference was the appearance of a doublet of doublets at δ_H 4.68 (J = 6.9, 3.5 Hz) and a methylene multiplet at δ_H 2.82.

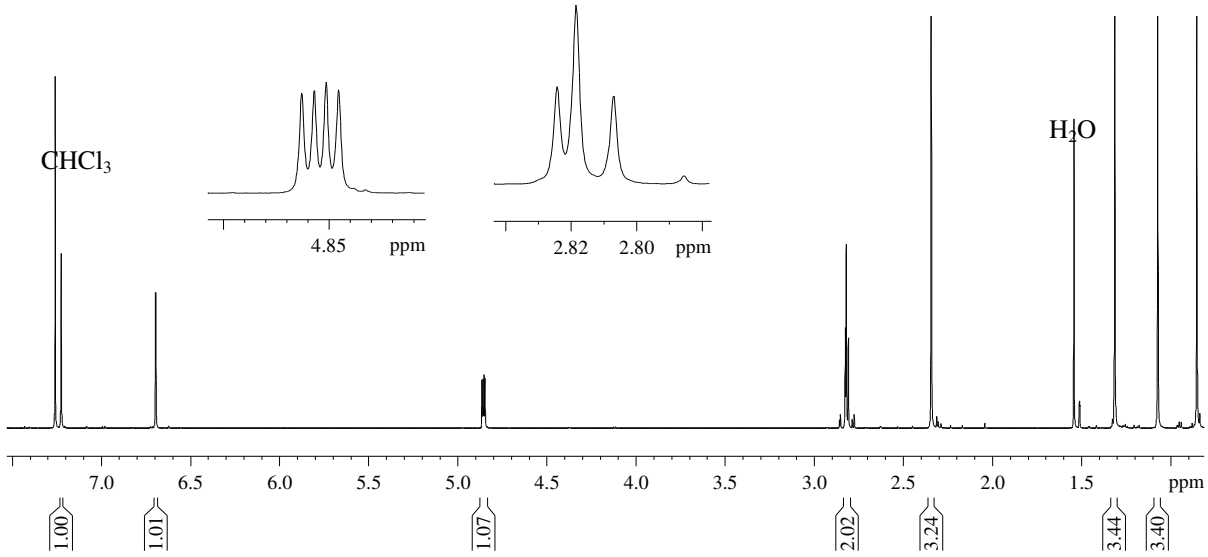

Figure 4.13: ^{1}H NMR spectrum ($CDCl_3$, 600 MHz) of compound **4.4**

With the preceding ^{1}H NMR data, and after careful scrutiny of the ^{13}C NMR, COSY and HMBC spectra, partial structures **A** and **B** (Figure 4.14) were considered.

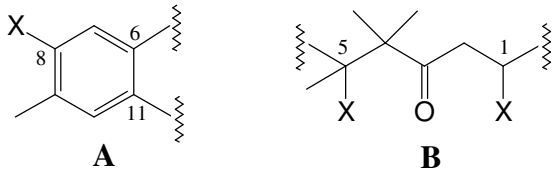

Figure 4.14: Partial structures **A** and **B** of compound **4.4**

Aromatic substructure **A** was similar to that of compound **4.1** with the exception of a more deshielded quaternary carbon at C11 (δ_C 159 *vs*. δ_C 154).

In substructure **B**, COSY NMR data (Figure 4.15) allowed for the construction of a (-CHX-CH_2-) spin system (C1 and C2). The presence of a carbonyl moiety at C3 was supported by

HMBC correlations from the methylene functionality at C2 as well as *gem*-dimethyl moieties on C4 (Figure 4.16). Additionally the IR spectrum (Figure 4.17) reflected a C=O stretch at 1742 cm^{-1} as well, typical of five-membered cyclic ketones.

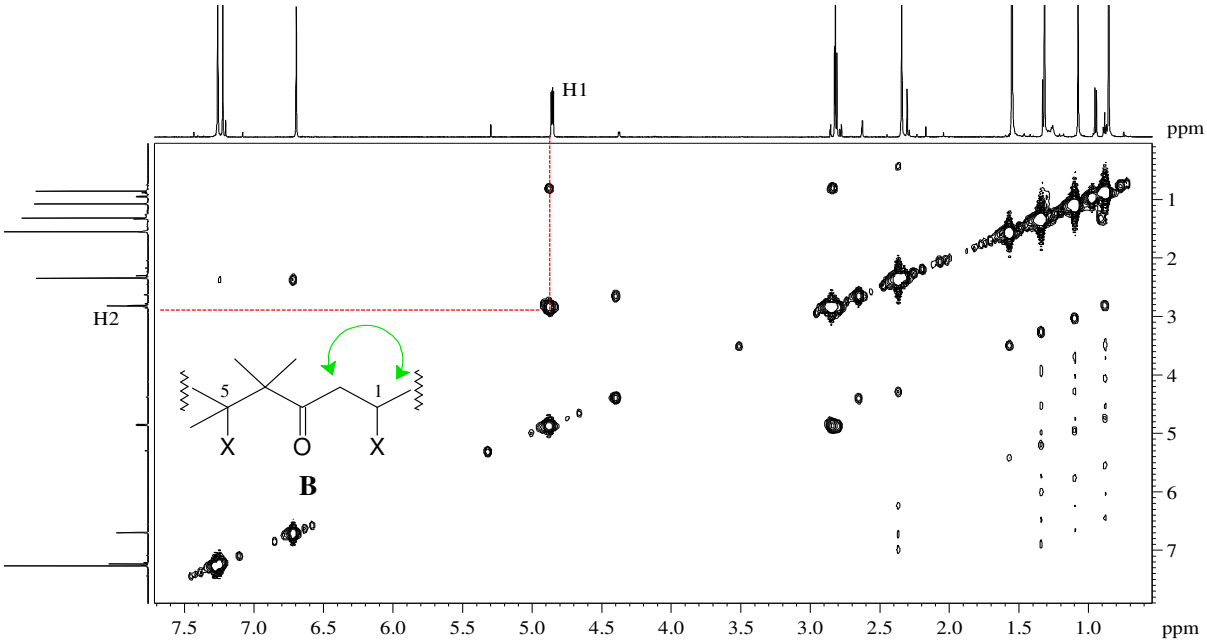

Figure 4.15: ^{1}H-^{1}H COSY spectrum of compound **4.4**

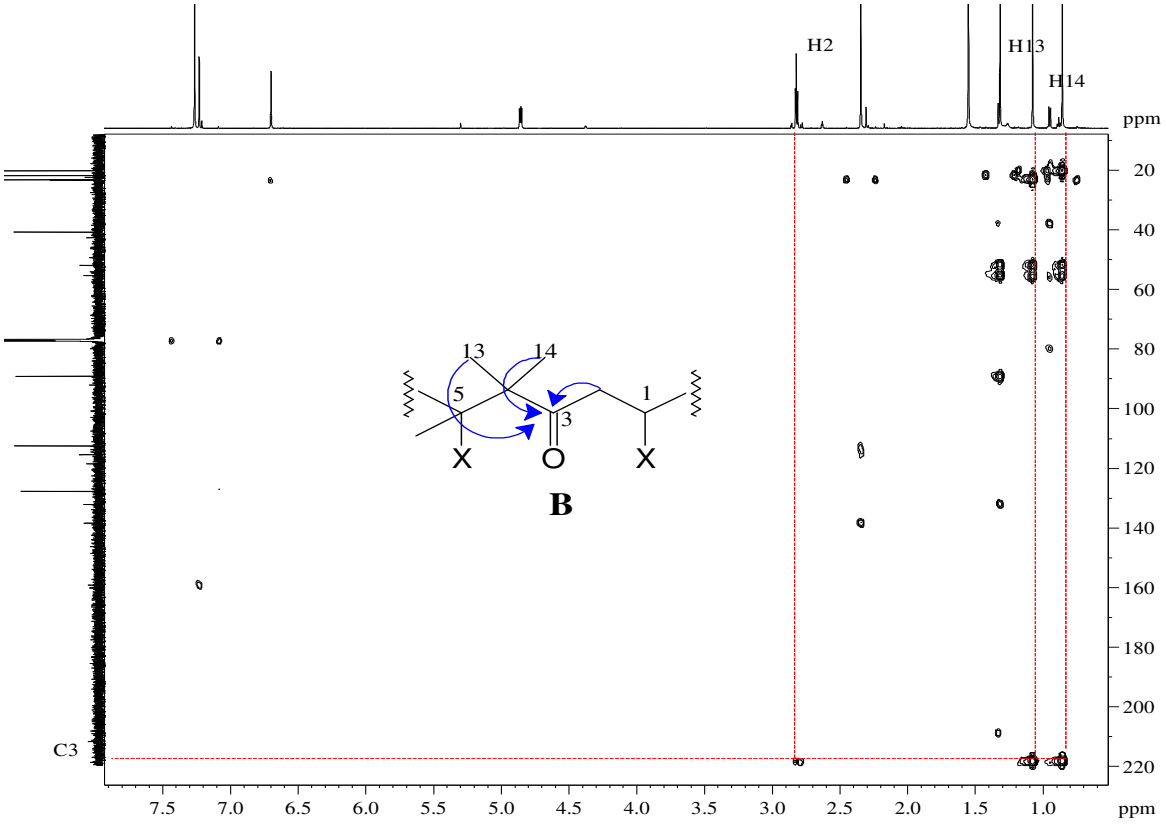

Figure 4.16: Partial HMBC spectrum of compound **4.4**

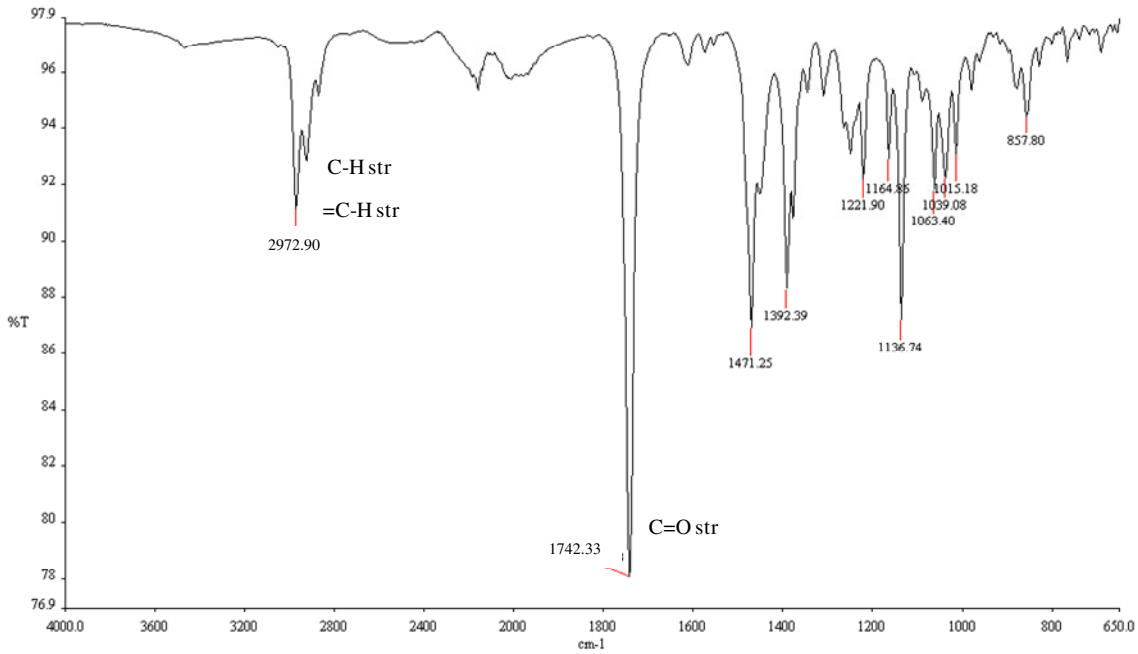

Figure 4.17: IR spectrum of compound **4.4**

The merging of substructures **A** and **B** was achieved by further analysis of the HMBC spectrum where correlations were seen between H12-C6 and H7-C5 as shown below.

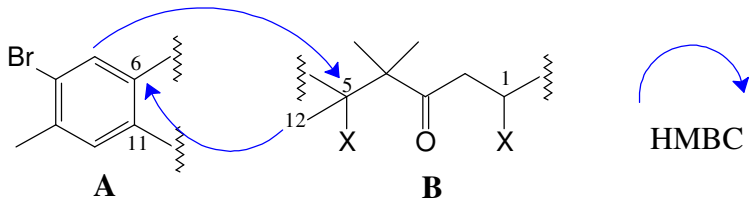

Figure 4.18: Selected HMBC correlations between compound **4.4** substructures **A** and **B**

Since the molecular formula indicated the presence of two oxygen atoms, and considering a carbon chemical shift at δ_C 89.1 (C1), it was proposed that substructure **B** would cyclise to form a cyclopentanyl type system linked to substructure **A** *via* a dihydrofuran like heterocycle.

This was confirmed as the aromatic ring and carbonyl moiety within compound **4.4** accounted for a total of five degrees of unsaturation. The additional two double bond equivalents required by the molecular formula must therefore be accommodated by two additional rings within **4.4** i.e. dihydrofuran ring and cyclopentanyl ring.

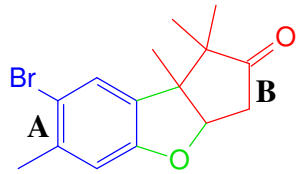

4.4

Figure 4.19: Compound **4.4** with substructures **A** and **B** attached *via* a furan ring

The relative configurations at C1, C4 and C5 were assigned by analysis of NOESY correlations from H1 to H12 and H14.

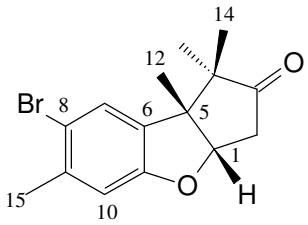

4.4

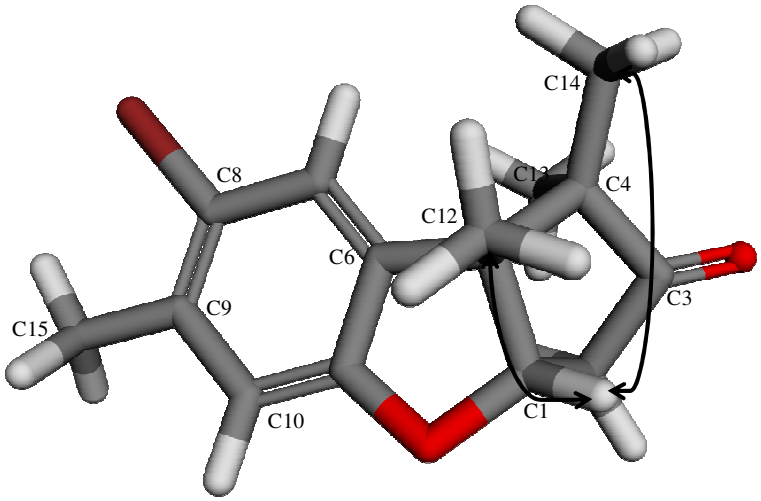

Figure 4.20: Key NOESY correlations in compound **4.4**

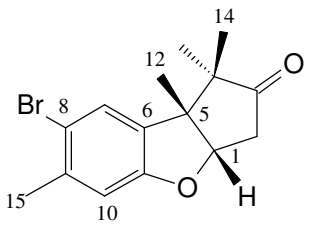

4.4

Table 4.3: NMR spectroscopic data of compound **4.4**

Carbon No	δ_C	δ_C mult	δ_H, mult, J (Hz)	COSY	HMBC	NOESY
1	89.1	CH	4.86, dd, 6.9, 3.5	H2	-	H2, H12, H14
2	40.7	CH_2	2.82, m	H1	C3	H12, H13
3	218.5	C	-	-	-	-
4	51.9	C	-	-	-	-
5	55.2	C	-	-	-	-
6	132.1	C	-	-	-	-
7	127.6	CH	7.23, s	-	C9, C11	H12, H13, H14
8	115.4	C	-	-	-	-
9	138.3	C	-	-	-	-
10	112.4	CH	6.69, s	H15	C15	H15
11	159.2	C	-	-	-	-
12	21.8	CH_3	1.32, s	-	C1, C4, C5, C6	H1, H2, H7
13	23.1	CH_3	0.86, s	H1, H2	C3, C4, C5, C14	H2, H7
14	20.2	CH_3	1.08, s	-	C3, C4, C5, C13	H1
15	23.3	CH_3	2.34, s	-	C8, C9, C10	-

4.2.2.3 Compound 4.5

A doublet at δ_H 5.82 (J = 6.2 Hz) coupled to a doublet of doublets at δ_H 5.62 (J = 6.2, 1.9 Hz) in the ^{1}H NMR spectrum (Figure 4.21) of compound **4.5**, was the only major spin system (-CH-CH-) differentiating the proton spectral data of compound **4.5** and compound **4.4**.

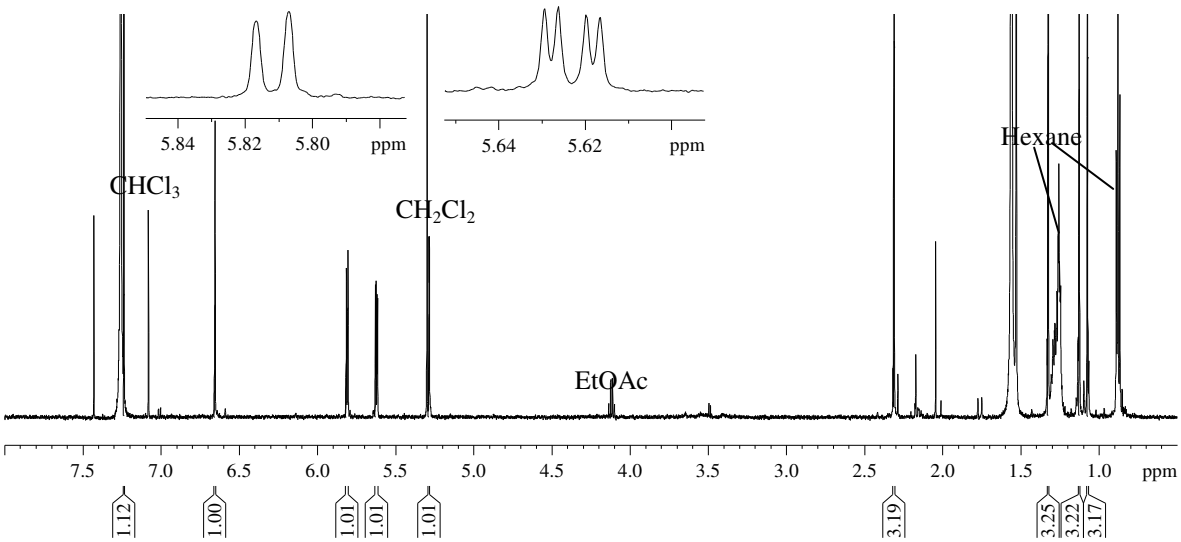

Figure 4.21: ^{1}H NMR spectrum ($CDCl_3$, 600 MHz) of compound **4.5**

With compound **4.5** deficient of a shielded methylene multiplet in the proton NMR spectrum, and with the concurrent disappearance of a deshielded carbonyl correlation in the HMBC spectrum, two deshielded carbon signals[3] at δ_C 124.8 and δ_C 147.7 suggested the presence of an olefin between C2 and C3 as opposed to a carbonyl at C3 as in compound **4.4**. Compound **4.5** was isolated previously from *Laurencia flexuosa* by Mann (2008).

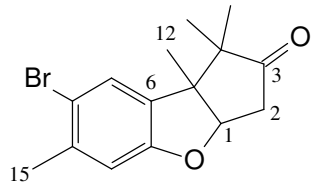

4.4

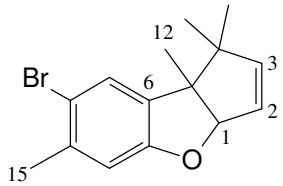

4.5

[3] Determined *via* HMBC analysis

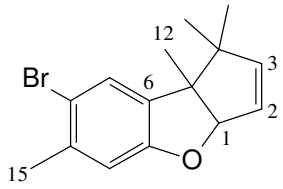

4.5

Table 4.4: NMR spectroscopic data of compound **4.5**

Carbon No	δ_C[4]	**δ_C mult**	**δ_H, mult, J (Hz)**
1	99.3	CH	5.28, d, 1.8
2	124.8	CH	5.62, dd, 5.8, 1.8
3	147.6	CH	5.81, d, 5.8
4	52.0	C	-
5	54.7	C	-
6	133.8	C	-
7	129.0	CH	7.24, s
8	113.1	C	-
9	138.1	C	-
10	112.1	CH	6.66, s
11	157.8	C	-
12	22.3	CH_3	1.33,s
13	26.9	CH_3	1.07, s
14	27.1	CH_3	1.13, s
15	23.1	CH_3	2.31, s

[4] Deduced *via* HMBC NMR data

4.2.2.4 Compounds 4.6 and 4.7

The rudimentary purification of compound **4.6** was achieved *via* HPLC however numerous attempts at purifying compound **4.7** were unsuccessful as co-elution with compound **4.6**, which appeared to be an isomer of compound **4.7**, kept occurring. Despite this the structure of compound **4.7** was still resolved as a mixture with compound **4.6**.

The ^{1}H NMR spectra (Figures 4.22, 4.23) of compounds **4.6** and **4.7** closely resembled that of compound **4.1** except for the withdrawal of the shielded methylene cluster between δ_H 2.5 - 3.0 and the emergence of extra deshielded signals within the region of ~ δ_H 4.2.

Of interest in the ^{1}H NMR spectrum of compound **4.6** (Figure 4.22) was the distinct enhancement in peak splitting of the coupled olefinic doublets at δ_H 5.92 (J = 5.5 Hz) and δ_H 6.13 (J = 5.5 Hz) *vs.* that of the broad signals seen earlier in compound **4.1** (Figure 4.4). The ^{1}H NMR data of these isomers, particularly the additional resonances at ~ δ_H 4.0, implied a structure similar to that of compound **4.1** save for substitution of the methylene group at C2.

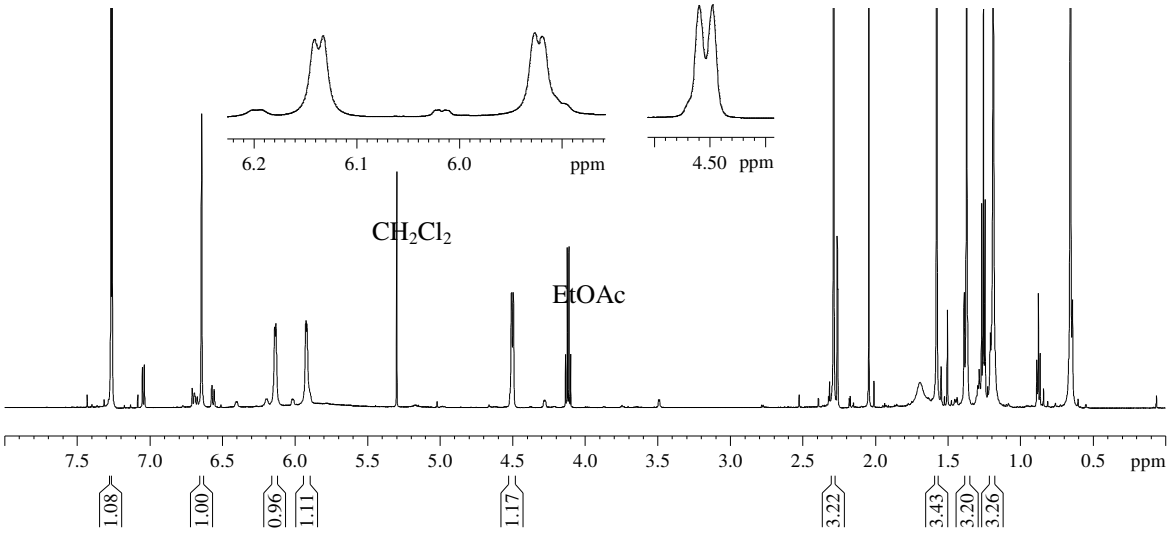

Figure 4.22: ^{1}H NMR spectrum ($CDCl_3$, 600 MHz) of compound **4.6**

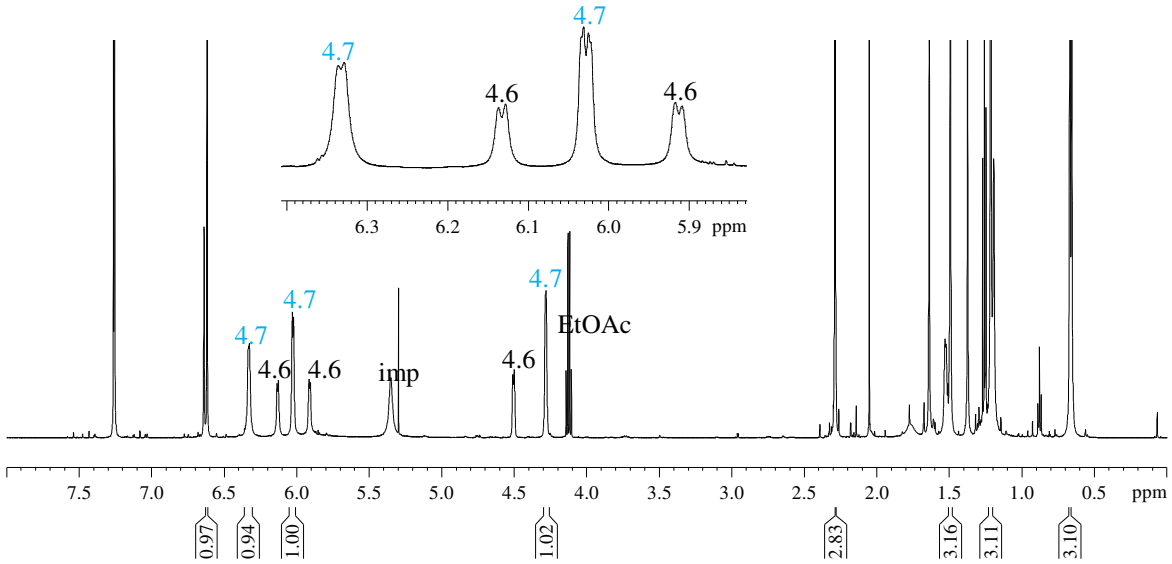

Figure 4.23: ^{1}H NMR spectrum ($CDCl_3$, 600 MHz) of compound **4.7** as a mixture with **4.6**

Upon consideration of a carbon chemical shift at C2 of ~ δ_C 85, it was proposed that the substituent was a hydroxyl moiety. Compound **4.7** is analogous to a hydroxy cuparane isolated by Mann (2008) from *L. flexuosa*.

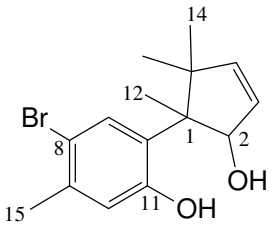

4.7

The HRESIMS spectrum (Figure 4.24) of compound **4.6** displayed the same molecular formula ($C_{15}H_{19}{}^{79}BrO_2$) as compound **4.7** with [M-OH] observed at *m/z* 293.0533 (calculated for 293.0541). The same basic carbon skeleton was proposed in compound **4.6** to that of compound **4.7** however, reasons as to the differences in proton and carbon spectral data in **4.6** *vs*. **4.7** at the positions marked below required further investigation.

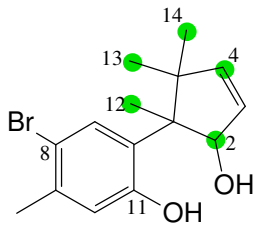

4.6

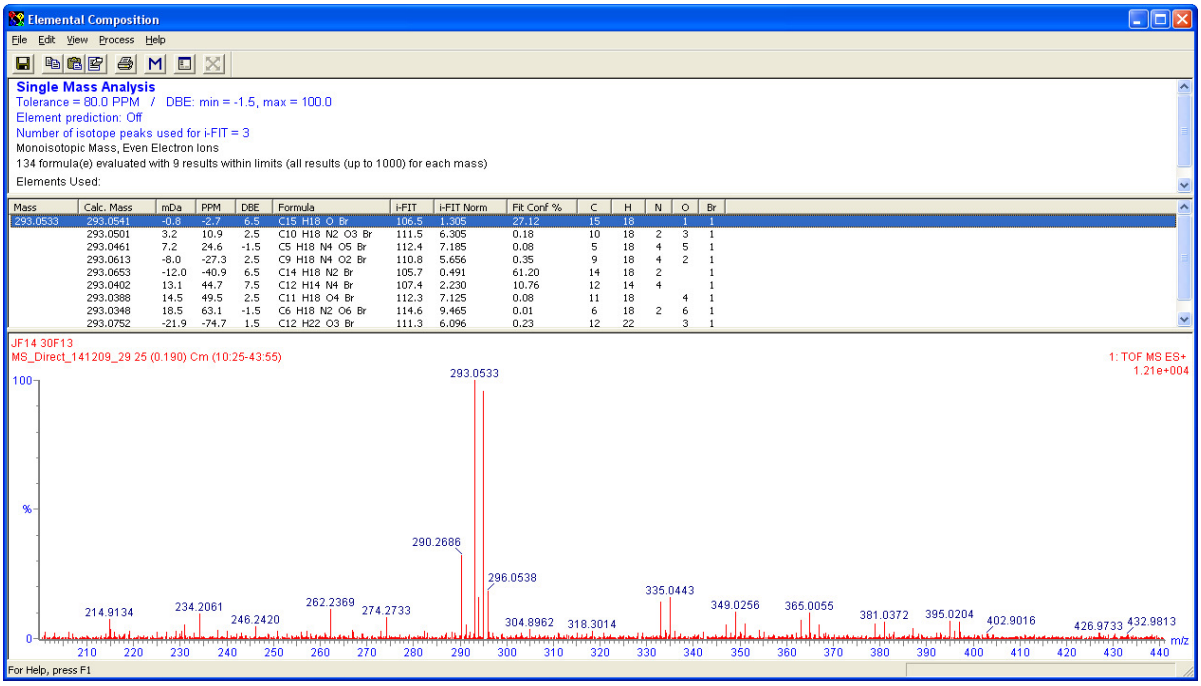

Figure 4.24: Expansion of the HRESIMS spectrum of compound **4.6**

Careful analysis of NOESY NMR data for both compounds revealed evidence that compound **4.6** was a diastereomer of compound **4.7** at C1. This discernment came after clear NOESY cross peaks were seen in compound **4.6** (Figure 4.25) from the hydroxy methine proton H2 (δ_H 4.50) to methyl singlets at H12 (δ_H 1.38) and H13 (δ_H 1.19).

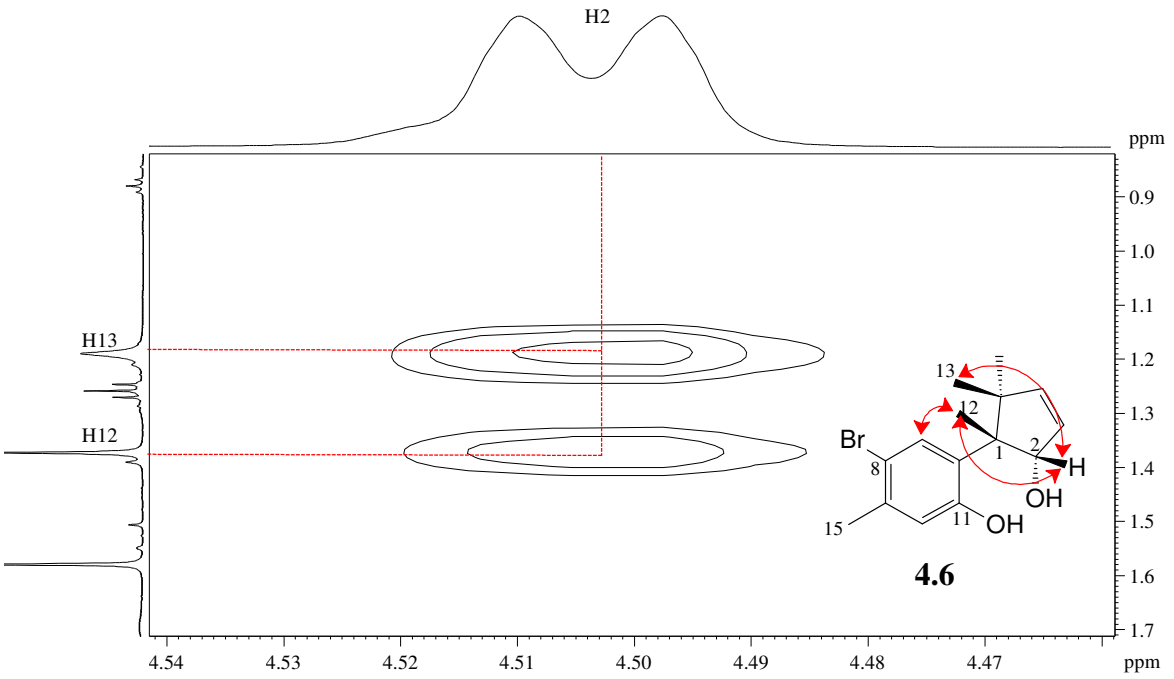

Figure 4.25: Partial NOESY spectrum of compound **4.6** showing key correlations

This was contrary to compound **4.7** (Figure 4.26) wherein the hydroxy-methine at H2 (δ_H 4.28) displayed a NOESY correlation only to the methyl singlet at H14 (δ_H 0.66) but not to H12 (δ_H 1.49).

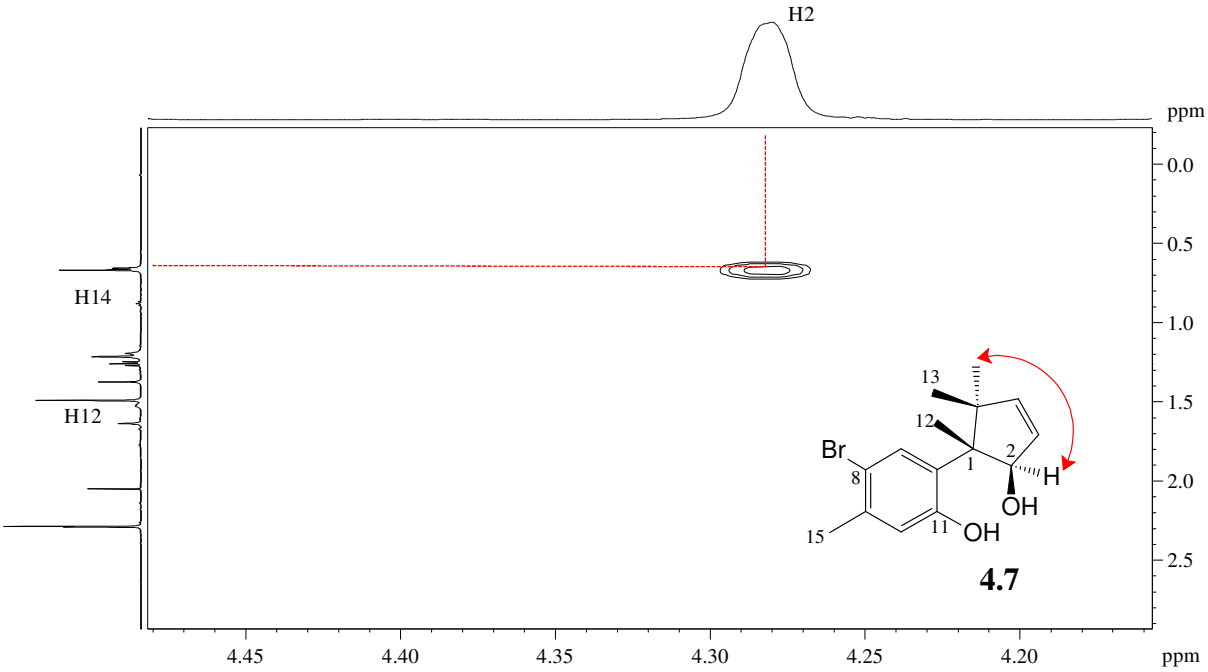

Figure 4.26: Partial NOESY spectrum of compound **4.7** showing key correlations

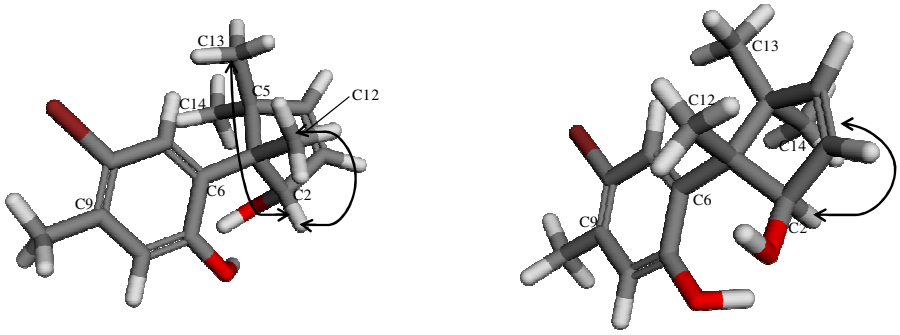

Compound **4.6** Compound **4.7**

Figure 4.27: Key NOESY correlations in compounds **4.6** and **4.7**

Compounds **4.1**, **4.4, 4.5** and **4.6** appear to be part of a proposed biosynthetic series (Figure 4.28) with compound **4.1** serving as a plausible precursor. Conversely, the removal of water on the five membered ring of **4.6** could give rise to **4.1**.

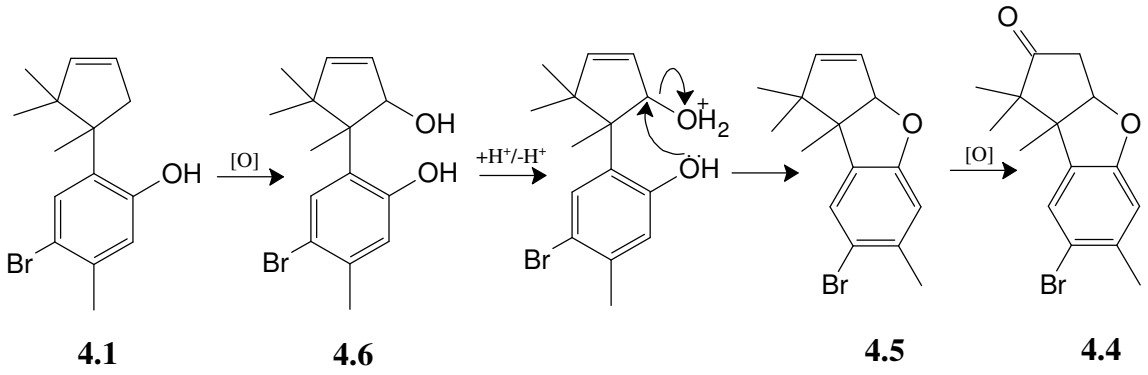

4.1 **4.6** **4.5** **4.4**

Figure 4.28: Proposed biosynthetic pathway of compounds **4.1**, **4.4**, **4.5** and **4.6**

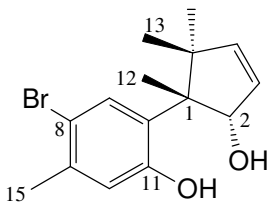

4.6

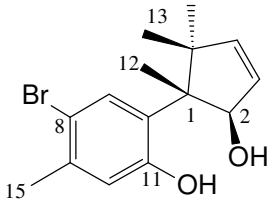

4.7

Table 4.5: NMR spectroscopic data of compounds **4.6** and **4.7**

		Compound **4.6**			Compound **4.7**		
Carbon No	**δ_C mult**	**δ_C**	**δ_H, mult, J (Hz)**	**NOESY**	**δ_C**	**δ_H, mult, J (Hz)**	**NOESY**
1	C	55.2	-	-	56.0	-	-
2	CH	85.3	4.50, d, 7.4	H12, H13	85.6	4.28, br s	H14
3	CH	131.8	5.92, d, 5.5	H4	131.0	6.02, d, 5.5	H4
4	CH	141.4	6.13, d, 5.5	H3	144.6	6.33, d, 5.5	H3
5	C	48.9	-	-	47.1	-	-
6	C	128.7	-	-	129.7	-	-
7	CH	132.2	7.27, s	H12	132.1	7.26, s	H12
8	C	115.5	-	-	115.1	-	-
9	C	137.3	-	-	137.0	-	-
10	CH	119.7	6.64, s	H15	119.0	6.62, s	
11	C	154.0	-	-	153.8	-	-
12	CH_3	23.4	1.38, s	H2, H7, H13	26.4	1.49, s	H7, H13
13	CH_3	23.4	1.19, br s	H2, H12, H14	18.8	1.22, s	H12, H14
14	CH_3	20.3	0.66, s	H13	27.1	0.66, s	H2, H13
15	CH_3	22.2	2.30, s	H10	22.3	2.29, s	H10

4.2.2.5 Compound 4.8

The ^{1}H NMR spectrum of compound **4.8** (Figure 4.29) indicated a similar chamigrane skeleton to that observed in compound **3.1** in chapter 3. Terpenoid shielded methyl moieties were apparent between δ_H 1.0 and δ_H 2.0 together with a cluster of methylene signals between δ_H 2.0-2.8. Curiously, an additional methine signal was observed in the range δ_H 3.7-5.0 suggesting that there was further substitution on the chamigrane skeleton of compound **4.8** versus compound **3.1**.

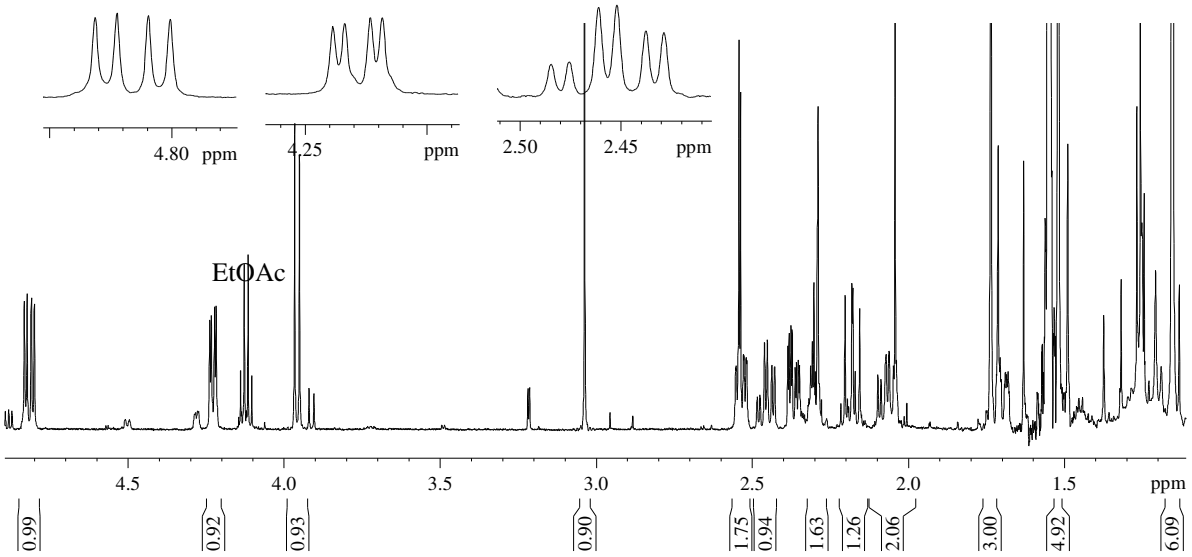

Figure 4.29: ^{1}H NMR spectrum ($CDCl_3$, 600 MHz) of compound **4.8**

Upon the analysis of 2D NMR data of compound **4.8** clear similarities to compound **3.1** were noted, however, COSY and HMBC experiments in particular revealed the presence of a methine moiety at C9 in compound **4.8** *vs.* a methylene function in **3.1**. A carbon chemical shift of δ_C 70.7 at C9 in compound **4.8** strongly supported the possibility of the substituent being a hydroxyl group.

The stereochemistry at C9 and C10 was assigned as in compound **3.17** based on a coupling constant of (J = 9.1 Hz) suggesting a trans-axial arrangement for the methine protons H9 and H10. A coupling constant of (J = 2.8 Hz) at H9 allowed the assignment of the relative configuration at C7/C8. Elsworth and Thomson (1989) report the isolation of compound **4.8** from *Laurencia glomerata*.

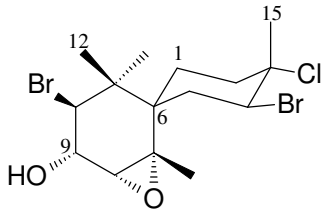

4.8

Table 4.6: NMR spectroscopic data of compound **4.8**

Carbon No	δ_C	δ_C **mult**	δ_H, **mult, J (Hz)**
1	25.4	CH_2	2.06, dt, 14.6, 5.9
2a	40.0	CH_2	2.37, ddd, 14.6, 5.9, 2.1
2b			2.46, dd, 14.6, 5.9
3	70.5	C	-
4	61.9	CH	4.81, dd, 13.3, 5.4
5a	38.8	CH_2	2.18, m
5b			2.53, m
6	44.5	C	-
7	64.8	C	-
8	65.2	CH	3.04, s
9	70.7	CH	4.23, dd, 9.1, 2.8
10	69.9	CH	3.96, d, 9.1
11	42.9	C	-
12	28.5	CH_3	1.16, s
13	20.0	CH_3	1.16, s
14	25.5	CH_3	1.52, s
15	24.0	CH_3	1.74, s

4.2.2.6 Re-isolation of compound 3.1

Compound **JF13(2)-81O**, purified from *L.* cf. *corymbosa* was identified as the crystalline epoxy chamigrane, compound **3.1**, as previously isolated from *Laurencia glomerata* in chapter 3.

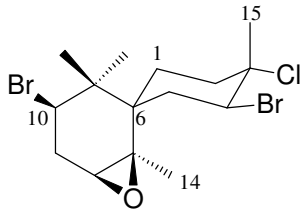

3.1

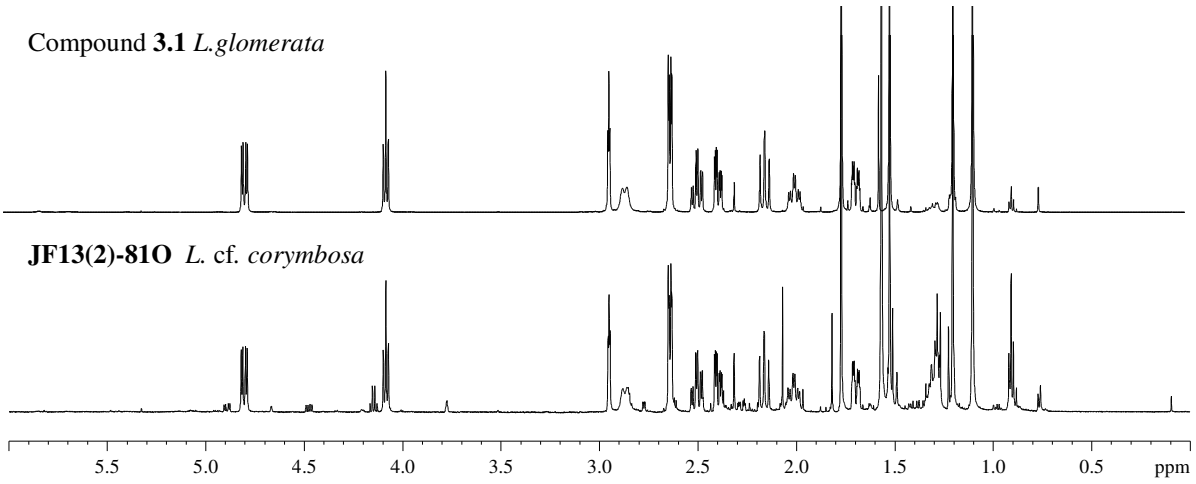

Figure 4.30: ^{1}H NMR spectra ($CDCl_3$, 600 MHz) of compounds **3.1** and **JF13(2)-81O**

4.2.2.7 Re-isolation of compound 3.7

Additionally, compound **JF13(2)-79P** was identical to the previously isolated compound, **3.7** from *Laurencia glomerata*.

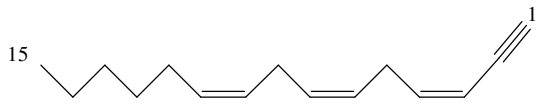

3.7

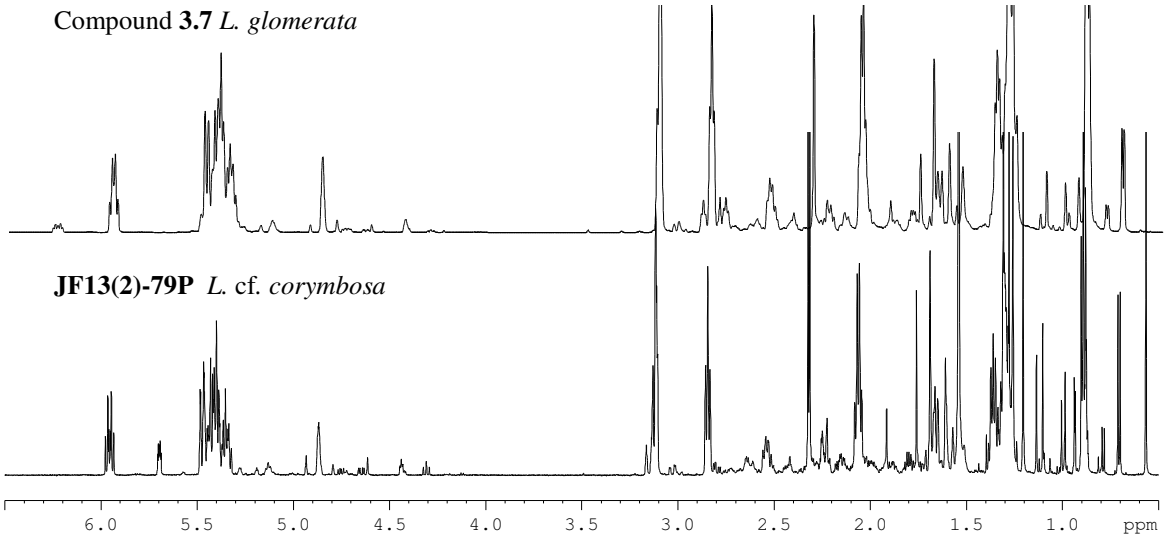

Figure 4.31: ^{1}H NMR spectra ($CDCl_3$, 600 MHz) of compounds **3.7** and **JF13(2)-79P**

4.3 Experimental

4.3.1 General experimental

As per section **3.3.1** in chapter 3, page 54.

4.3.2 Mass spectrometry

4.3.2.1 HRGCEIMS (High resolution gas chromatography electron impact mass spectrometry)

HRGCEIMS spectra were obtained from the Central Analytical Facility, University of Stellenbosch using a Waters® GCT spectrometer. The parameters used are as listed below.

Instrument: Waters® GCT

Column: HP5 (30 m, 0.25 mm ID, 0.25 µm film thickness)

Instrument settings

Injector temperature : 280 °C
Injection volume : 1 µl
Injection mode : Split
Split ratio : 10:1
Carrier gas : Helium
Flow rate : 1 ml/min
MS mode : EI+
Scanning mass range : 35 to 650 m/z
Scan time : 0.15 min
Inter-scan delay : 0.05 min

Oven temperature program:

Oven Ramp	°C/min	Temp (°C)	Hold (min)
Initial		100	1
Ramp 1	15	280	5

4.3.2.2 HRESIMS (High resolution electron spray ionisation mass spectrometry)

HRESIMS spectra were also obtained from the Central Analytical Facility, University of Stellenbosch using a Waters® Synapt G2 spectrometer. The ionisation source varied between ESI+ and ESI- depending on the compound analysed, with a cone voltage of 15V. The lock mass was set with Leucine enkephalin. Sample introduction: ESI probe into a stream of MeOH.

4.3.3 Plant material (*L.*cf. *corymbosa*, NDK130821-11)

L. cf. *corymbosa* was collected by hand at Noordhoek beach in the southern coastal region of South Africa in August 2013. A voucher specimen is kept in the seaweed sample repository at the School of Pharmacy, University of the Western Cape. Identification of the alga was done by Professor John Bolton with the Department of Biological Sciences at the University of Cape Town, South Africa.

4.3.4 Extraction and isolation of metabolites

The same extraction procedure was employed as in section **3.3.3**, chapter 3, page 54 (dry mass 28.7 g, crude extract 1.17 g, 3.9% yield).

Purification of step gradient fractions A, B and D *via* column chromatography and or normal phase HPLC resulted in the isolation of compounds **3.1** (8 mg, 0.027%), **3.7** (14.1 mg, 0.047%), **4.1** (14.5 mg, 0.049%), **4.4** (19.8 mg, 0.066%), **4.5** (3 mg, 0.010%), **4.6** (4 mg, 0.013%) **4.7** (6 mg, 0.020%) **4.8** (2 mg, 0.007%).

4.3.5 Compounds isolated

4.3.5.1 Compound 3.1 (JF13(2)-81O) As per chapter 3, page 55.

4.3.5.2 Compound 3.7 (JF13(2)-79P) As per chapter 3, page 56.

4.3.5.3 Compound 4.1 (JF13(2)-81J)

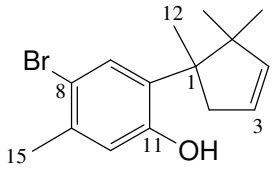

4.1

4-bromo-5-methyl-2-(1,2,2-trimethylcyclopent-3-en-1-yl)phenol (**4.1**): Clear oil; $[\alpha]_D^{25}$ +93.2° (c = 0.005, MeOH); ^1H and ^{13}C NMR ($CDCl_3$) data available in Table 4.1; IR V_{max} 3397; 2916;1375 cm^{-1}; HRGCEIMS *m/z* 294.0620 (Calculated for 294.0619); $C_{15}H_{19}{}^{79}BrO$.

4.3.5.4 Compound 4.3 (JF13(2)-14A)

*Acetylation of compound **4.1** to produce **4.3***

Compound **4.1** (4 mg) was weighed out and placed in a round bottomed flask with 10 drops of pyridine and 20 drops of acetic anhydride. The reaction mixture was left to stir overnight at ambient temperature after which HCl (1M, 12 mL) was used to acidify the mixture. EtOAc (3x10 mL) was used to extract the resultant product after which semi-preparative TLC was used (4:6 hex:EtOAc) to obtain the acetate derivative, compound **4.3**.

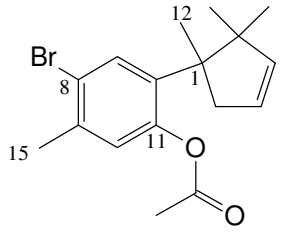

4.3

4-bromo-5-methyl-2-(1,2,2-trimethylcyclopent-3-en-1-yl)phenyl acetate (**4.3**): White solid; $[\alpha]_D^{25}$ +61.2° (c = 0.002, MeOH); ^{1}H and ^{13}C NMR ($CDCl_3$) data available in Table 4.2; IR V_{max} 3402; 2962; 2921; 1742 cm^{-1}; HRESIMS, $[M+H]^+$ at *m/z* 337.0789 (calculated for 337.0803); $C_{17}H_{21}{}^{79}BrO_2$.

4.3.5.5 Compound 4.4 (JF13(2)-81N)

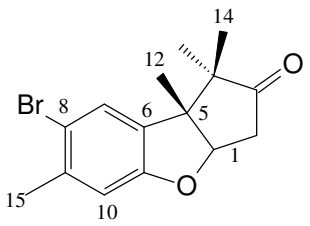

4.4

(3aS,8bR*)-7-bromo-1,1,6,8b-tetramethyl-1,3,3a,8b- tetrahydro- 2H -benzo [b] cyclopenta [d] furan-2-one* (**4.4**): White crystals; $[\alpha]_D^{25}$ -86.5° (c = 0.008, MeOH); ^{1}H and ^{13}C NMR ($CDCl_3$) data available in Table 4.3; IR V_{max} 2972, 1742, 1471, 1392 cm^{-1}; HRGCEIMS *m/z* 308.0356 (Calculated for 308.0412); $C_{15}H_{17}{}^{79}BrO_2$.

4.3.5.6 Compound 4.5 (JF14-30F4)

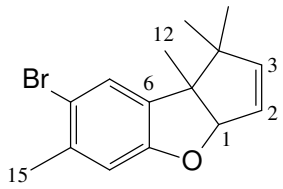

4.5

7- bromo- 1, 1, 6, 8b-tetramethyl-3a, 8b- dihydro- 1H- benzo [b] cyclopenta [d] furan (**4.5**): Colourless oil; ^{1}H and ^{13}C NMR ($CDCl_3$) data available in Table 4.4. As previously reported by Mann (2008).

4.3.5.7 Compound 4.6 (JF14-30F6)

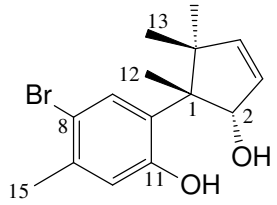

4.6

4-bromo-2-[(1S,5S*)-5 -hydroxy-1,2,2-trimethylcyclopent-3-en-1-yl]- 5 -methylphenol* (**4.6**)[5]: Clear oil; ^{1}H and ^{13}C NMR ($CDCl_3$) data available in Table 4.5; IR V_{max} 3296; 2962; 2151; 1390 cm^{-1}; HRESIMS [M-OH] at *m/z* 293.0533 (calculated for 293.0541); $C_{15}H_{19}{}^{79}BrO_2$.

4.3.5.8 Compound 4.7 (JF14-30F13)

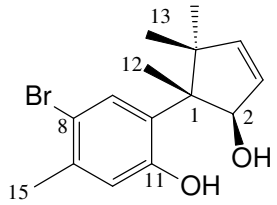

4.7

8 -bromo -6-[(1R,5S*)-2-hydroxy-1,5,5-trimethylcyclopent-3-en-1-yl]-9-methylphenol* (**4.7**): Colourless oil; ^{1}H and ^{13}C NMR ($CDCl_3$) data available in Table 4.5. As previously reported by Mann (2008).

[5] Insufficient viable material for assessment of optical rotation

4.3.5.9 Compound 4.8 (JF14-30F14)

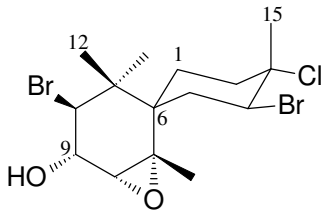

4.8

3-chloro-9-hydroxy, 4, 10 dibromo-7,8 epoxychamigrane OR *(1S*,4S*,5S*,6R*)-3',4-dibromo-4'-chloro-1,3,3,4'-tetramethyl-7-oxaspiro [bicyclo [4.1.0]heptane-2,1'-cyclohexan]-5-ol* (**4.8**): White crystals; ^{1}H and ^{13}C NMR ($CDCl_3$) data available in Table 4.6. As previously reported by Elsworth and Thomson (1989).

4.4 References

Dias, D. A.; White, J. M.; Urban, S. *Laurencia filiformis*: Phytochemical profiling by conventional and HPLC-NMR approaches. *Natural Product Communications* **2009**, *4*, 157-172.

Elsworth, J. F.; Thomson, R. H. A new chamigrane from *Laurencia glomerata*. *Journal of Natural Products* **1989**, *52*, 893-895.

Francis, C. M. **2014**. Systematics of the *Laurencia* complex (Rhodomelaceae, Rhodophyta) in southern Africa. PhD Thesis. University of Cape Town, Cape Town, South Africa.

Kladi, M.; Vagias, C.; Furnari, G., Moreau, D.; Roussakis, C., Roussis, V. Cytotoxic cuparene sesquiterpenes from *Laurencia microcladi. Tetrahedron Letters* **2005**, *46*, 5723-5726.

Mann, M. G. A. **2008**. An investigation of the antimicrobial and antifouling properties of marine algal metabolites. M.Sc thesis. Rhodes University, Grahamstown.

Yamada, K.; Yazawa, H.; Uemura, D.; Toda, M.; Hirata, Y. Total synthesis of (±) aplysin and (±) debromoaplysin. *Tetrahedron* **1969**, *25*, 3509-3520.

Yu, X. Q.; He, W. F.; Liu, D. Q.; Feng, M. T.; Fang, Y.; Wang, B.; Feng, L. H.; Guo, Y. W.; Mao, S. C. A seco-laurane sesquiterpene and related laurane derivatives from the red alga *Laurencia okamurai* Yamada. *Phytochemistry* **2014**, *103*, 162-170.

Chapter 5

Secondary metabolites from *Laurencia natalensis*

Abstract

This chapter reports the first investigation into the natural product chemistry of *Laurencia natalensis*, affording **5.9** (algoane), exclusively isolated from the sea-hare *Aplysia dactylomela*. An isomer of acetoxyintricatol, **5.14**, including the known chamigrane **5.8** (nidificene) were also isolated among two other known precursor type molecules, compounds **5.1** known as (*E*)-γ-bisabolene (precursor to chamigrane type compounds) and **5.5** known as *cis*-laurencenyne (precursor to C_{15} acetogenins).

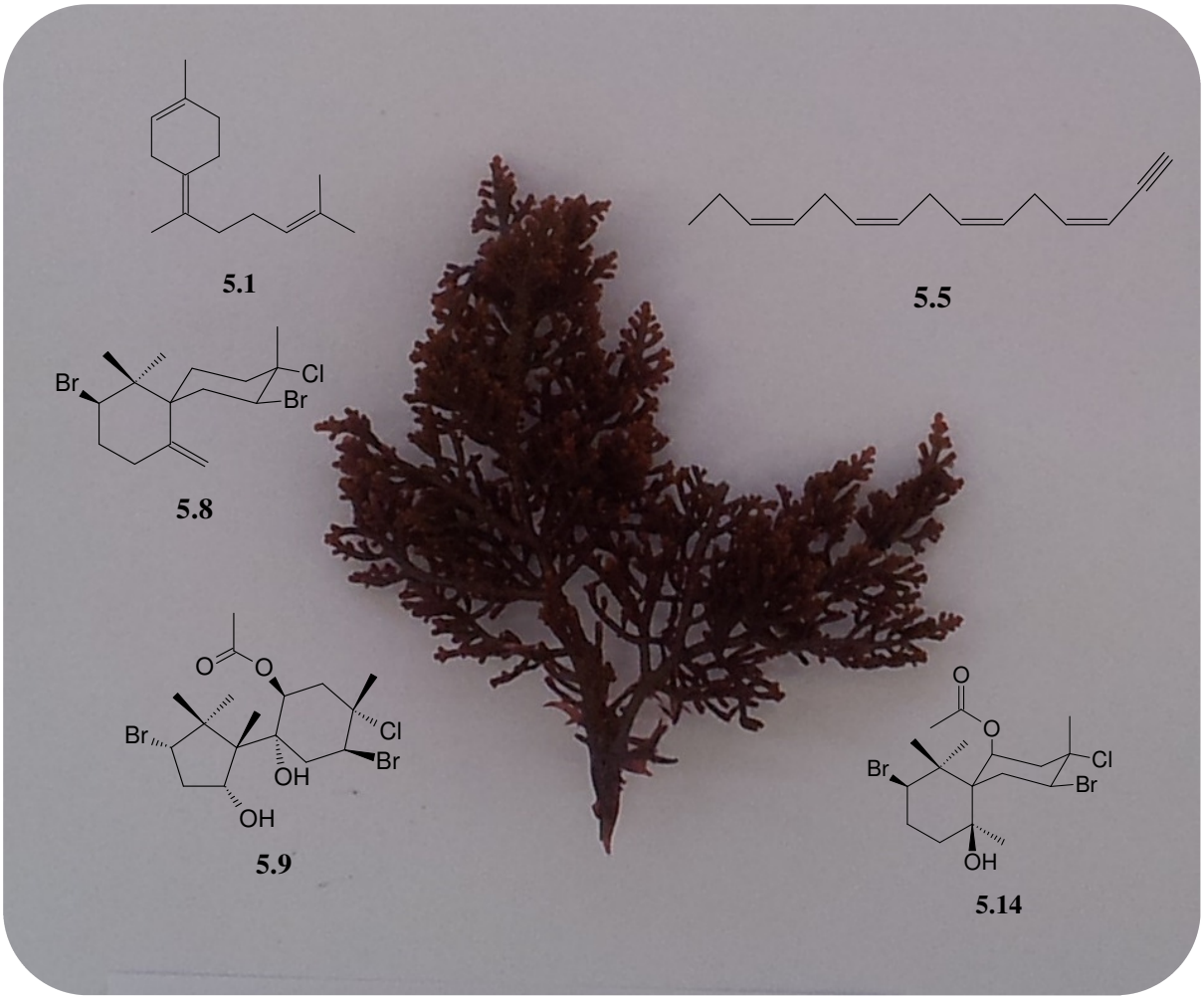

Chapter 5

Secondary metabolites from *Laurencia natalensis*

5.1 Introduction

Laurencia natalensis is distributed along the south and east coast of South Africa and is readily distinguishable due to its characteristic orange tinged branch tips (apices) (Stegenga *et al*., 1997). The plants usually grow 6-8 cm high and are found predominantly on sand covered rocks in temperate inter-tidal waters. The cortical cells show one *corps en cerise* per cell and the plants of this species are much narrower than most other *Laurencia* spp. (Francis, 2014).

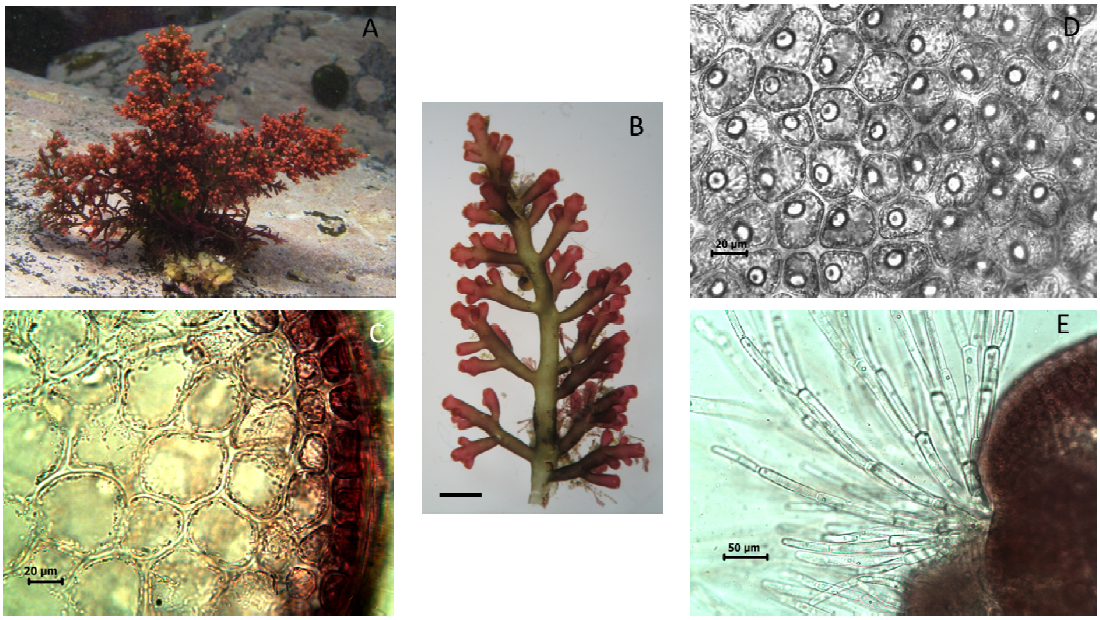

Figure 5.1: *Laurencia natalensis*[1] (Caitlynne Francis © 2014)

A) Habit.

B) Branching pattern subopposite to subverticillate (8x). *Scale bar: 1cm = 200µm*

C) Transverse section through thallus showing outermost cortical and cortical cells (40x).

D) Outermost cortical cells showing one *corps en cerise* per cell (40x).

E) Trichoblasts with one *corps en cerise* per cell (20x).

[1] Image plates courtesy of Caitlynne Francis © 2014, University of Cape Town, South Africa

5.2 Results and Discussion

5.2.1 Extraction and isolation of metabolites from *L. natalensis* (KOS110201-1, Kenton-on-Sea)

The extraction and fractionation procedure was the same as that described in section **3.2.1** (chapter 3, page 54). As shown in the isolation scheme (Scheme 5.1), only fractions A, B and C from the step gradient column were further fractionated. These fractions displayed interesting ^{1}H NMR resonances (Figure 5.2) and were further purified *via* a combination of normal phase HPLC and silica gel chromatography to yield compounds **5.1**, **5.5**, **5.8**, **5.9** and **5.14**.

Compounds **5.9** and **5.14** were purified by preferential solubility wherein addition of 9:1 hex:EtOAc to fraction C precipitated out a crystalline mass which contained two components when analysed by ^{1}H NMR spectroscopy. Continual addition of 9:1 hex:EtOAc to the crystal precipitate allowed for the effective separation of the two components.

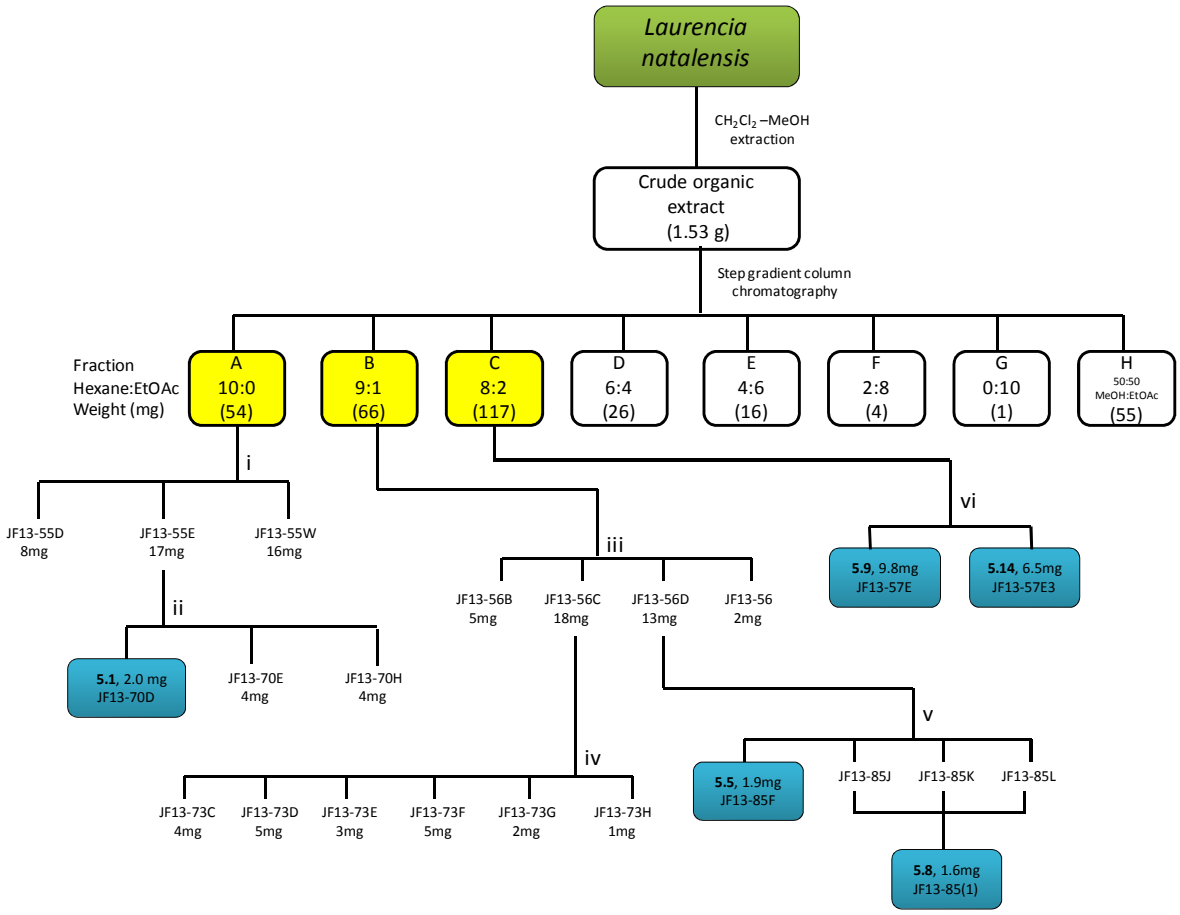

Scheme 5.1: Isolation scheme of metabolites from *L. natalensis* (KOS110201-1)

Conditions: i) Silica gel column chromatography (19:1 hex:EtOAc); ii) Normal phase HPLC (100% hexane); iii) Silica gel column chromatography (9:1 hex:EtOAc); iv) Normal phase HPLC (9:1 hex:EtOAc); v) Normal phase HPLC (19:1 hex:EtOAc); vi) Preferential solubility (9:1 hex:EtOAc)

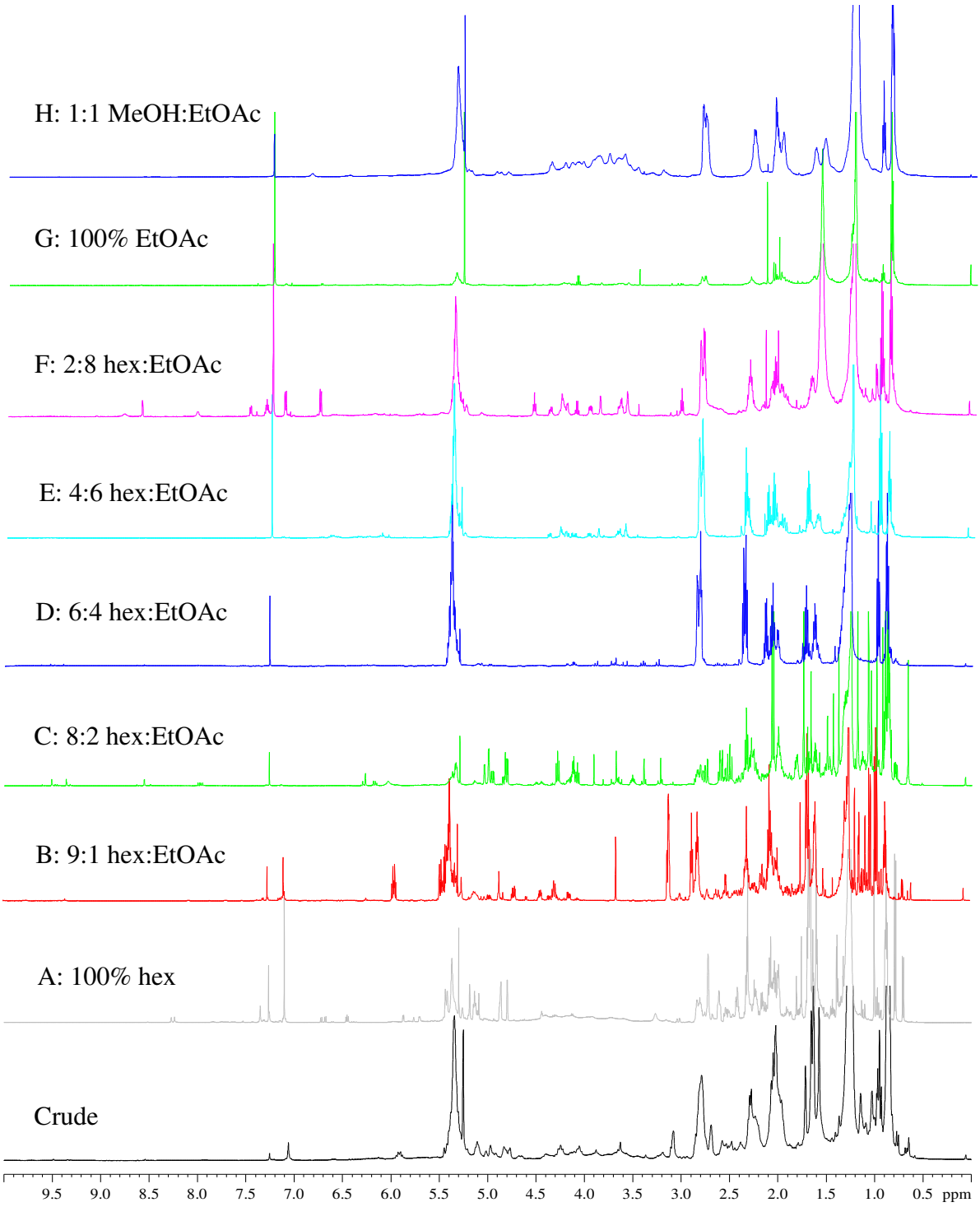

Figure 5.2: ^{1}H NMR spectra ($CDCl_3$, 600 MHz) of the crude organic extract of *L. natalensis* (KOS110201-1) and step gradient column fractions A-H

5.2.2 Structure elucidation of metabolites

5.2.2.1 Compound 5.1

Compound **5.1** displayed an interesting ^{1}H NMR spectrum (Figure 5.3) in that only two deshielded olefinic moieties were witnessed between δ_H 5.0-5.5 amongst a multitude of shielded signals between (δ_H 1.99-2.32). A cluster of four methyl singlets were observed in the region between δ_H 1.60-1.80.

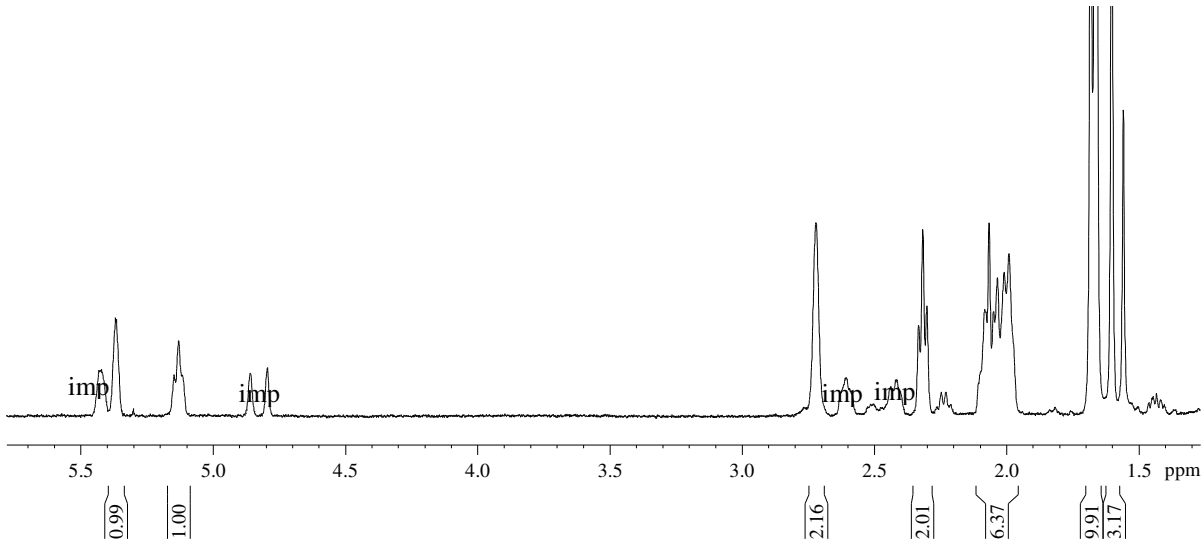

Figure 5.3: ^{1}H NMR spectrum ($CDCl_3$, 600 MHz) of compound **5.1**

The examination of the ^{13}C NMR spectrum (Figure 5.4) of compound **5.1** together with edited HSQC data revealed the presence of four quaternary carbons at (δ_C 125.9, 128.4, 131.5 and 134.3) including two olefinic, protonated carbons at δ_C 120.8 and δ_C 124.5.

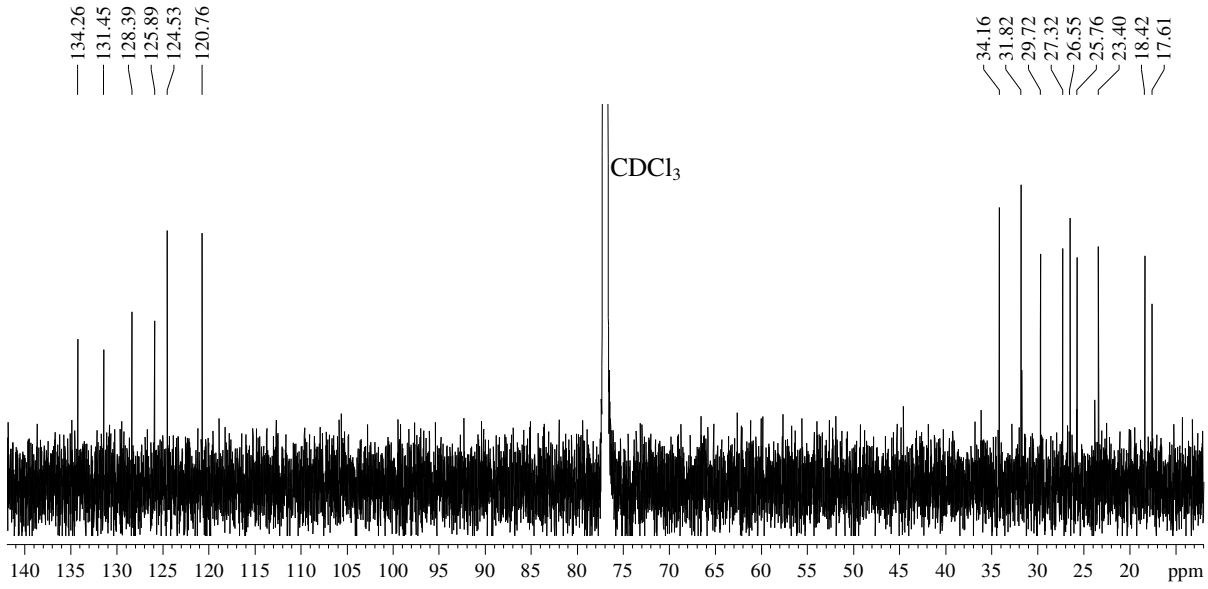

Figure 5.4: ^{13}C NMR spectrum ($CDCl_3$, 150 MHz) of compound **5.1**

Compound **5.1** was identified as (*E*)-γ-bisabolene, a monocyclic, sesquiterpene thought to be a major biosynthetic intermediate in the production of various C_{15} secondary metabolites (Butler and Carter-Franklin, 2004).

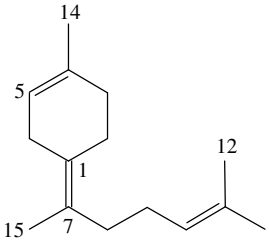

5.1
(*E*)-γ-bisabolene

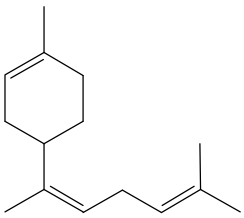

5.2
α-bisabolene

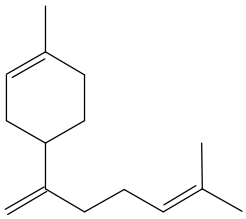

5.3
β-bisabolene

Although identified frequently as a component of essential oils in various plants (Minyard *et al*., 1966), there are no documented reports of the isolation of (*E*)-γ-bisabolene from marine algae in its unsubstituted form.

To the best of our knowledge this is the first documented isolation of (*E*)-γ-bisabolene from seaweed *viz*. *Laurencia natalensis*. However, Kurosawa *et al*., (1980) stated that D. J. Faulkner, in a personal communication, described the isolation of (*E*)-γ-bisabolene from a sample of *Laurencia pacifica.*

Faulkner and Wolinsky (1975) reported the synthesis of (*E*)-γ-bisabolene, presenting NMR data in CCl_4. Negishi *et al*., (2001) presented NMR data for (*E*)-γ-bisabolene for $CDCl_3$ proving useful in the confirmation of the structure of **5.1**.

The assignment of the geometry of compound **5.1** as (*E*)-γ-bisabolene was deduced by comparison of the NMR data of the two isomers presented by Negishi *et al*., (2001).

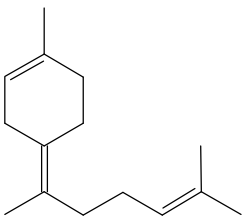

5.1
(*E*)-γ-bisabolene

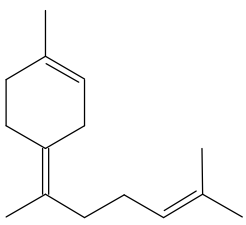

5.4
(*Z*)-γ-bisabolene

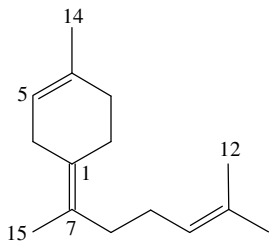

5.1

Table 5.1: NMR spectroscopic data of compound **5.1**

Carbon No	δ_C	δ_C **mult**	δ_H, **mult, J (Hz)**
1	128.4	C	-
2	26.6	CH_2	2.32, t, 6.4
3	31.8	CH_2	1.99, m
4	134.3	C	-
5	120.8	CH	5.37, m
6	29.7	CH_2	2.72, m
7	125.9	C	-
8	34.2	CH_2	2.07, m
9	27.3	CH_2	2.02, m
10	124.5	CH	5.14, t, 6.4
11	131.5	C	-
12	25.8	CH_3	1.68, s
13	17.6	CH_3	1.60, s
14	23.4	CH_3	1.66, s
15	18.4	CH_3	1.66, s

5.2.2.2 Compound 5.5

Compound **5.5** was isolated as a colourless oil. Analogous to compound **3.7** (Figure 3.23, page 51), the ^{1}H NMR spectrum (Figure 5.5) of compound **5.5** showed a complex cluster of unsaturated methine signals between δ 5.0 and δ 6.0 indicating the presence of several olefin functionalities. An ethyl moiety (–CH_2–CH_3) was deduced from a triplet signal at δ_H 0.97 (t, J = 7.6 Hz) coupled to a methylene signal at δ_H 2.08 (quin, J = 7.4 Hz).

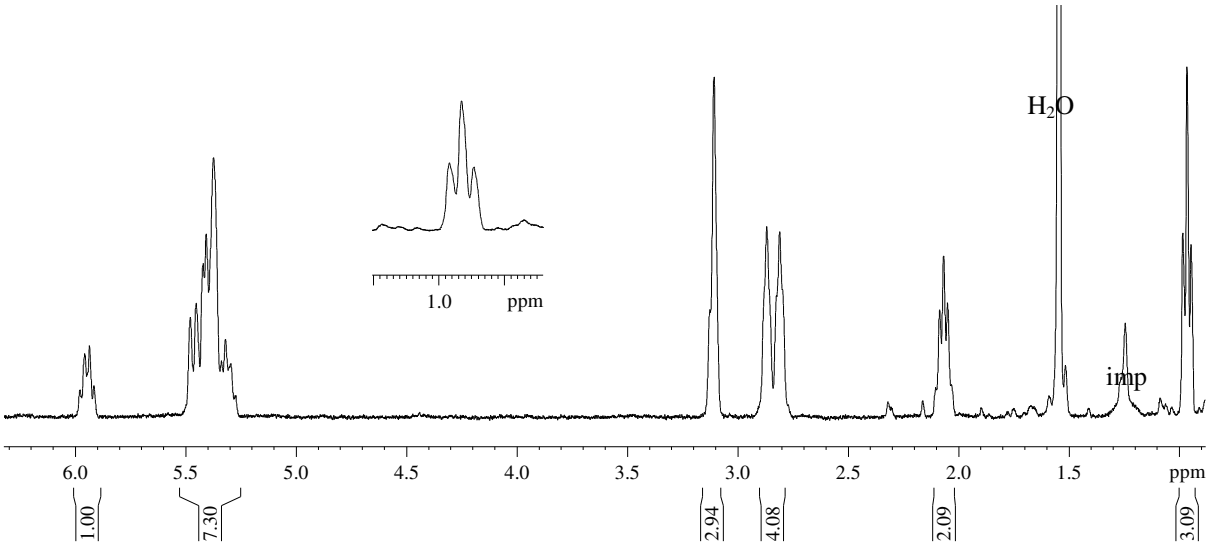

Figure 5.5: ^{1}H NMR spectrum ($CDCl_3$, 600 MHz) of compound **5.5**

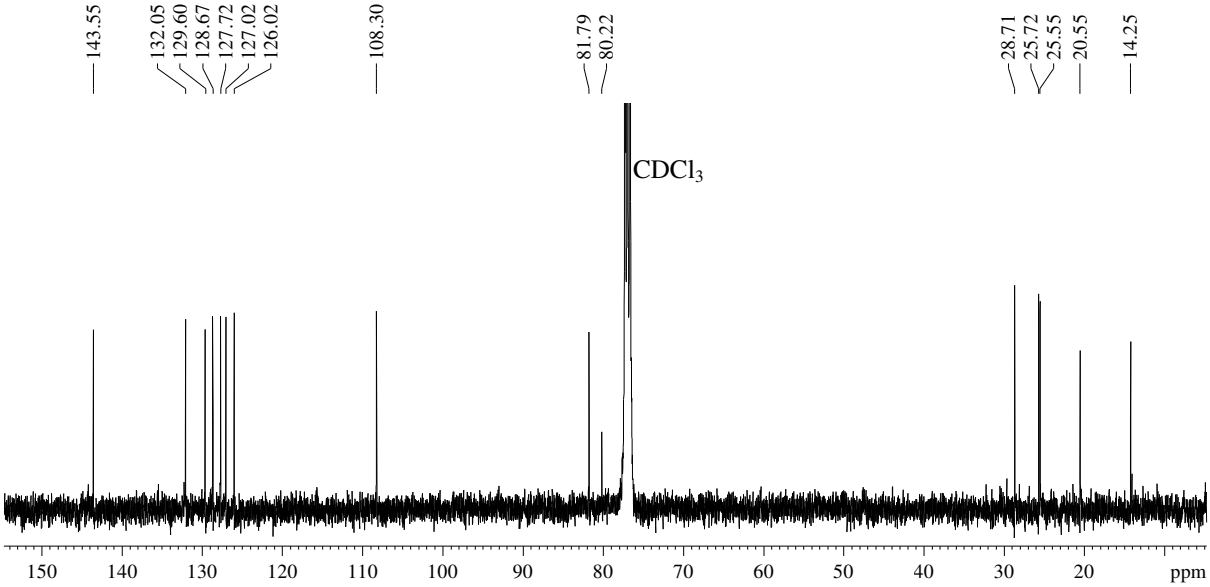

Figure 5.6: ^{13}C NMR spectrum ($CDCl_3$, 150 MHz) of compound **5.5**

The ^{13}C NMR spectrum of compound **5.5** (Figure 5.6), in combination with the DEPT-135 spectrum, showed 15 signals which included resonances characteristic of a terminal alkenyne system (δ_C 143.6, 108.3, 81.8 and 80.2) in addition to signals of a further three double bonds (δ_C 132.1, 129.6, 128.7, 127.7, 127.0, 126.0).

Compound **5.5** was identified as *cis*-laurencenyne by comparison of spectroscopic data with literature values. This linear C_{15} acetogenin with a terminal alkyne moiety was previously isolated by Kigoshi *et al*., (1981) from *Laurencia okamurai*. A total synthesis of compound **5.5** was achieved by Skattebøl *et al*., (2001) using *eicosa-5,8,11,14,17-pentaenoic acid*.

The orientation of the terminal alkyne about $\Delta^{3,4}$ was determined similarly to **3.7**. A carbon chemical shift of δ_C 80.2 at the quaternary carbon (C2) is consistent with a *cis*-alkenyne moiety (Kigoshi *et al*., 1982).

Fukuzawa *et al*., (1993) show the isolation of a diacetate derivative of compound **5.5** about positions C6 and C7 shown below as compound **5.6.** This acetylated compound is a derivative of compound **5.7** known as laurediol, isolated from *Laurencia nipponica* by Kurosawa *et al*., (1972).

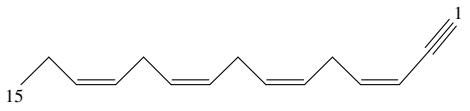

5.5

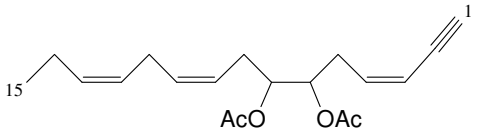

5.6

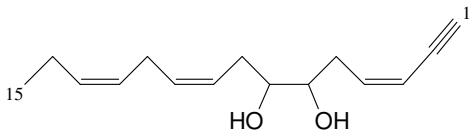

5.7

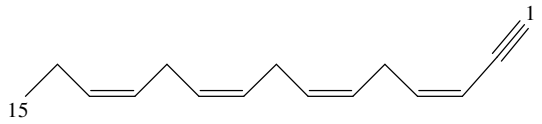

5.5

Table 5.2: NMR spectroscopic data of compound **5.5**[2]

Carbon No	δ_C	δ_C **mult**	δ_H, **mult, J (Hz)**
1	81.8	CH	3.12, m
2	80.2	C	-
3	108.3	CH	5.48, m
4	143.6	CH	5.96, m
5	28.7	CH_2	3.12, m
6	129.6	CH	5.43, m
7	128.7	CH	5.38, m
8	25.7	CH_2	2.88, m
9	127.7	CH	5.38, m
10	127.0	CH	5.32, m
11	25.5	CH_2	2.83, m
12	126.0	CH	5.43, m
13	132.1	CH	5.39, m
14	20.5	CH_2	2.08, quin, 7.4
15	14.3	CH_3	0.97, t, 7.6

[2] Similar difficulties assigning multiplicity of ^{1}H NMR signals were experienced as previously observed in compound **3.7**. Again this is due to the multitude of several magnetically equivalent protons within compound **5.5**

5.2.2.3 Compound 5.8

The most interesting features in the ^{1}H NMR spectrum (Figure 5.7) of compound **5.8** were a pair of halo-methine double doublets at δ_H 4.44 (dd, J = 12.8, 4.6 Hz) and δ_H 4.72 (dd, J = 12.9, 4.8 Hz), as well as a methylidene singlets at δ_H 4.87 and δ_H 5.26. A total of three methyl proton signals within the region δ_H 0.96-1.70 were also noted amongst a multitude of methylene resonances between δ_H 1.5-2.5.

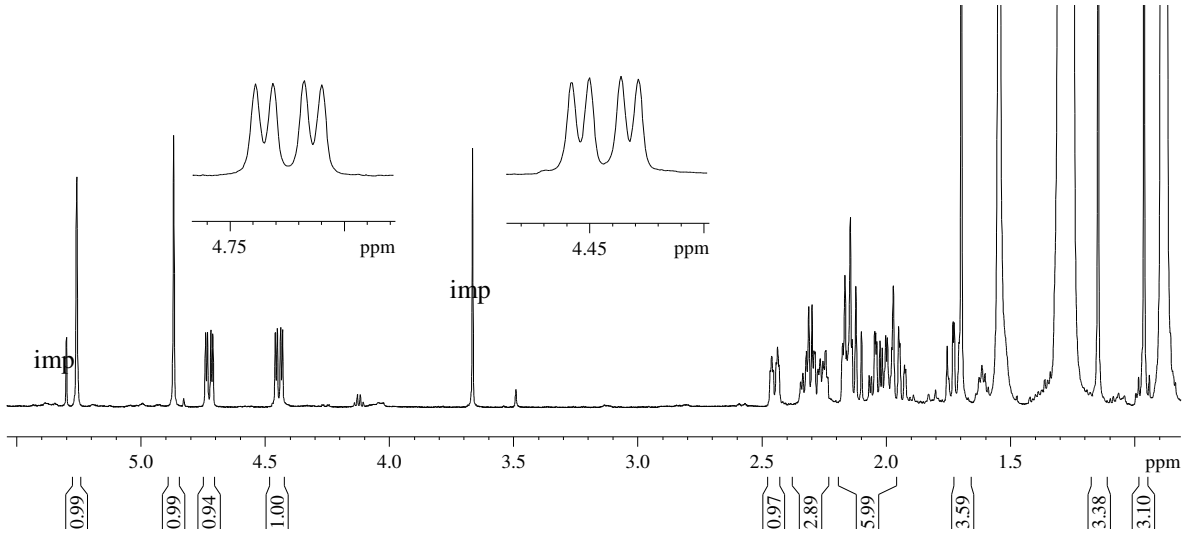

Figure 5.7: ^{1}H NMR spectrum ($CDCl_3$, 600 MHz) of compound **5.8**

The ^{13}C NMR spectrum (Figure 5.8) together with the HSQC and HMBC spectra of compound **5.8** allowed for the identification of four quaternary, two methine, six methylene and three methyl signals.

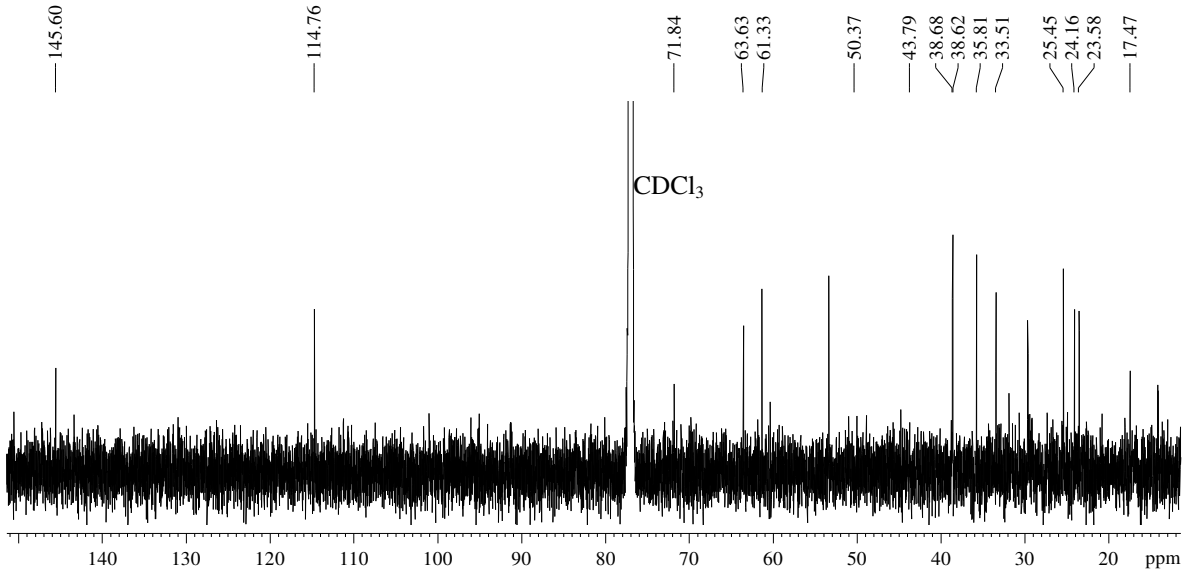

Figure 5.8: ^{13}C NMR spectrum ($CDCl_3$, 150 MHz) of compound **5.8**

The NMR spectral data of compound **5.8** was in accordance with that of nidificene, isolated initially from *Laurencia nidifica* by Waraszkiewicz and Erickson (1974).

Compound **5.8** is isomeric to compound **3.9**, isolated from *Laurencia glomerata*.

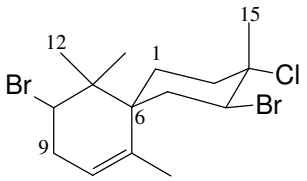

3.9

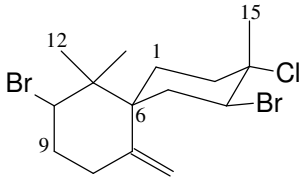

5.8

NOESY assessments of compound **5.8** confirmed a relative configuration as shown in (Figure 5.9). An equatorial bromine at C4 was assigned as unambiguous coupling constants at H4 δ_H 4.72 (dd, J = 12.8, 4.6 Hz) suggested a trans-axial arrangement between H4 and H5a.

A similar equatorial configuration of the bromine atom at C10 was assigned as at C4 based on analogous ^3J coupling constants shown by H10 δ_H 4.44 (dd, J = 12.9, 4.8 Hz) to the neighbouring axial proton H9a.

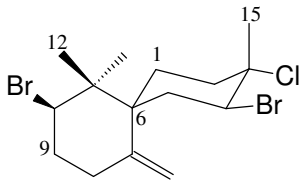

5.8

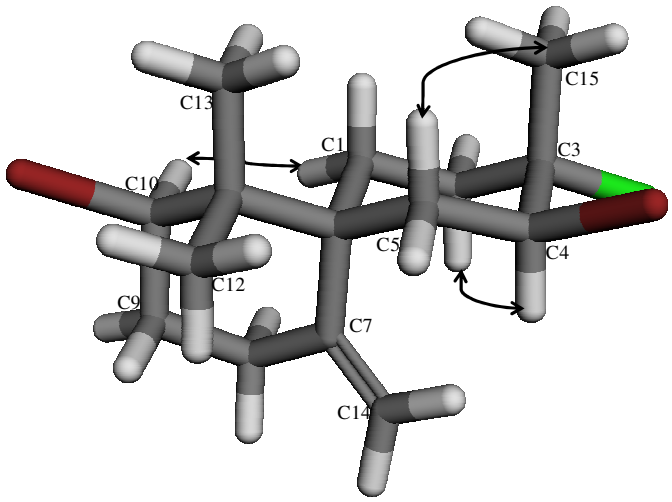

Figure 5.9: Key NOESY correlations in compound **5.8**

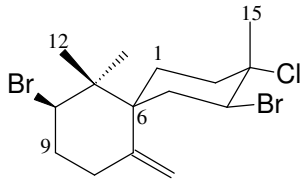

5.8

Table 5.3: NMR spectroscopic data of compound **5.8**

Carbon No	δ_C	δ_C **mult**	δ_H**, mult, J (Hz)**
1a	25.5	CH_2	1.73, m
1b			1.97, m
2a	38.6	CH_2	2.14, m
2b			1.94, m
3	71.8	C	-
4	61.3	CH	4.72, dd, 12.8, 4.6
5a	38.7	CH_2	2.14, m
5b			2.45, m
6	50.4[3]	C	-
7	145.6	C	-
8a	33.5	CH_2	2.16, m
8b			2.31, m
9a	35.8	CH_2	2.03, m
9b			2.26, m
10	63.6	CH	4.44, dd, 12.9, 4.8
11	43.8	C	-
12	17.5	CH_3	0.96, s
13	23.6	CH_3	1.15, s
14a	114.8	CH_2	4.87, s
14b			5.26, s
15	24.2	CH_3	1.70, s

[3] Deduced *via* HMBC NMR data

5.2.2.4 Compound 5.14

Compound **5.14** was isolated as a white crystalline solid. The ^{1}H NMR spectrum (Figure 5.10) reflected a broad methine singlet at δ_H 5.02 and a methine double doublet at δ_H 4.83 (dd, J = 12.8, 4.43 Hz).

Two sets of methylene resonances were observed at δ_H 2.52 (t, J = 13.1 Hz); δ_H 2.28 (d, J = 13.1 Hz), and δ_H 2.77 (dd, J = 14.9, 3.0 Hz); δ_H 2.62 (dd, J = 14.9, 2.9 Hz). Furthermore, five methyl singlet resonances (δ_H 0.92, 1.11, 1.23, 1.76 and 2.08) immediately suggested a sesquiterpene type structure for compound **5.14**.

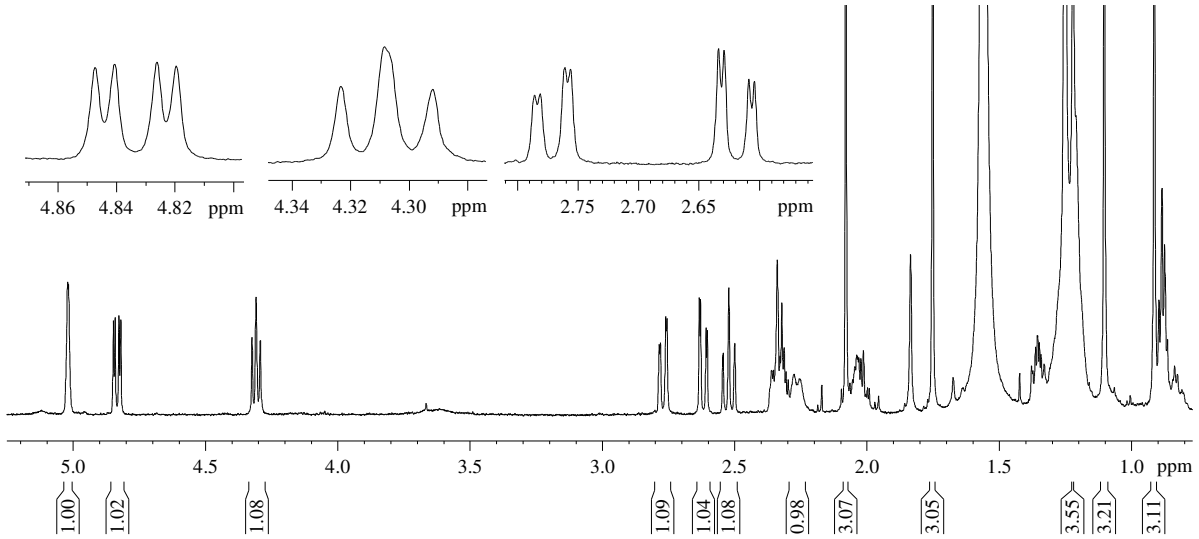

Figure 5.10: ^{1}H NMR spectrum ($CDCl_3$, 600 MHz) of compound **5.14**

The ^{13}C NMR spectrum (Figure 5.11) of **5.14** showed only one unsaturated carbon signal at δ_C 169.0 distinctive of an ester moiety and confirmed by the IR spectrum of compound **5.14** (Figure 5.15) with a carbonyl stretch at 1723 cm^{-1}.

The IR spectrum (Figure 5.12) was also key in indentifying a broad hydroxy stretch at 3514 cm^{-1} implying that compound **5.14** possessed a hydroxyl substituent.

A further five methyls (δ_C 21.3, 21.5, 22.5, 22.5 and 27.4), four methylenes (δ_C 30.6, 32.4, 40.2 and 42.0), three methines (δ_C 59.6, 63.3 and 74.3) and four quaternary carbons (δ_C 47.7, 50.7, 69.6 and 78.2) were deduced from ^{13}C NMR and HSQC data.

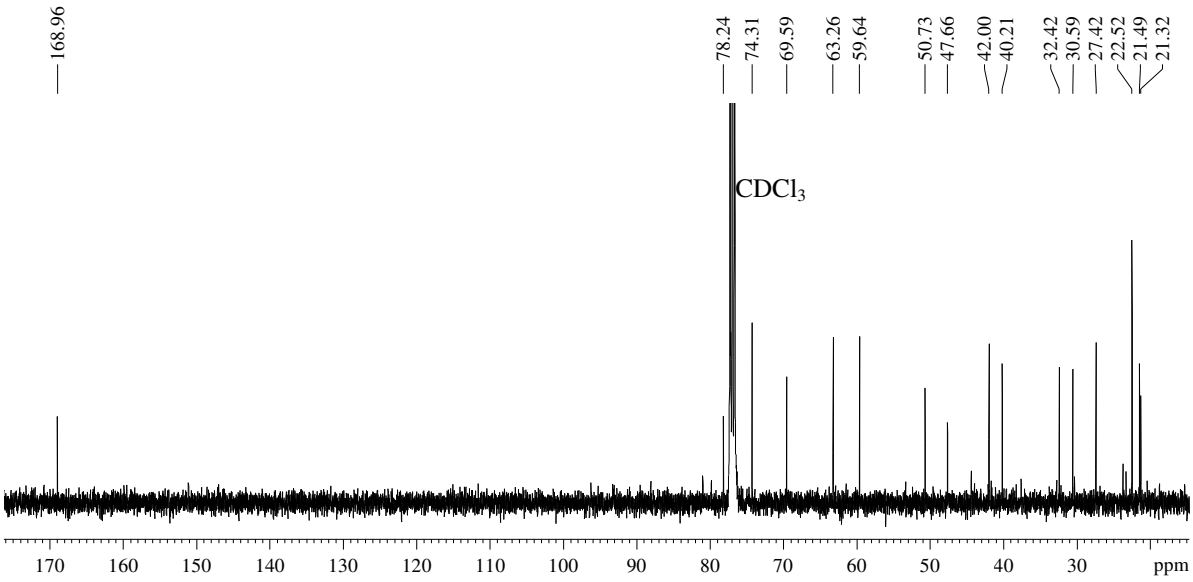

Figure 5.11: ^{13}C NMR spectrum ($CDCl_3$, 150 MHz) of compound **5.14**

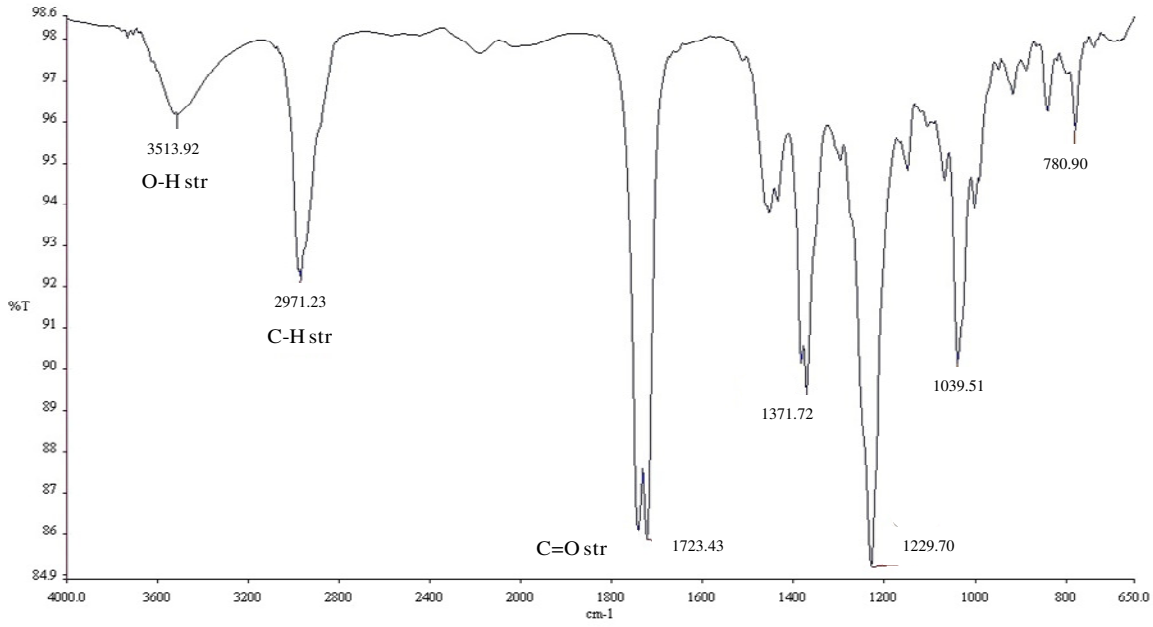

Figure 5.12: IR spectrum of compound **5.14**

With the spectroscopic data above considered, compound **5.14** belonged to the chamigrane class of sesquiterpenes.

The HRESIMS of compound **5.14** (Figure 5.13) provided a molecular ion cluster $[M+Cl]^4$ at *m/z* 506.9704 (calculated for 506.9704), 508.9862, 510.9669 and 512.9618 indicative of a molecular formula of $C_{17}H_{27}{}^{79}Br_2{}^{35}Cl_2O_3$. The isotopic abundance pattern was complementary of a $BrCl_2$ halogenated system (Appendix 4).

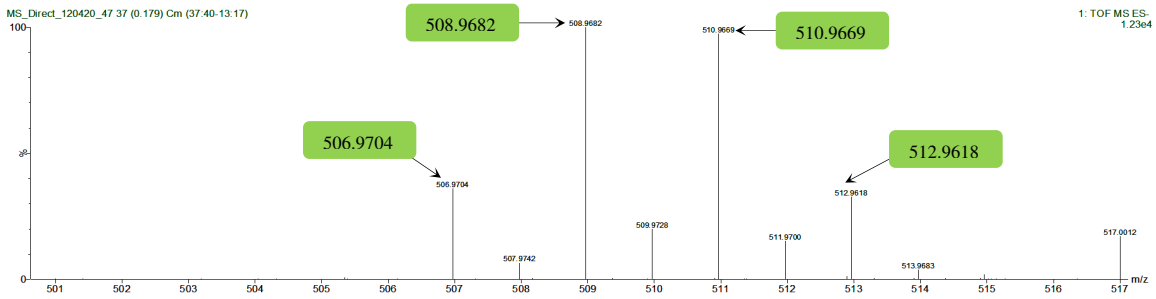

Figure 5.13: Expansion of the HRESIMS spectrum of compound **5.14**

A calculated three degrees of unsaturation confirmed compound **5.14** to be a stereoisomer at position C1 to acetoxyintricatol, a hydroxy-acetyl chamigrane previously isolated by McMillan *et al*., (1974) from *Laurencia implicata*. A detailed account of the NMR data for compound **5.14** is presented for the first time (Table 5.4).

Having analysed the NOESY spectrum of compound **5.14** the relative configuration was assigned as shown in (Figure 5.14). The acetoxy group must be in the axial position as opposed to the isomer, acetoxyintricatol, reported by McMillan *et al*., (1974), based on the chemical shift at H1 and coupling constants at H2, additionally confirmed by NOESY NMR correlations from H1 to both H2a and H2b. The relative configuration at C7 was assigned as being isomeric to acetoxyintricatol after considering strong NOESY correlations from H14 to H10 and H1. The bromo substituent at C4 was assigned as being equatorial after considering the vicinal coupling constants of H4 (dd, J = 13.0, 4.4 Hz) and H5 (t, J = 13.0 Hz). Furthermore H4, which is axial, also showed NOESY correlations to the axial proton H2b (δ_H 2.77).

[4] Dias and Urban (2011) also show the addition of Cl to a sesquiterpene when using HRESIMS (negative)

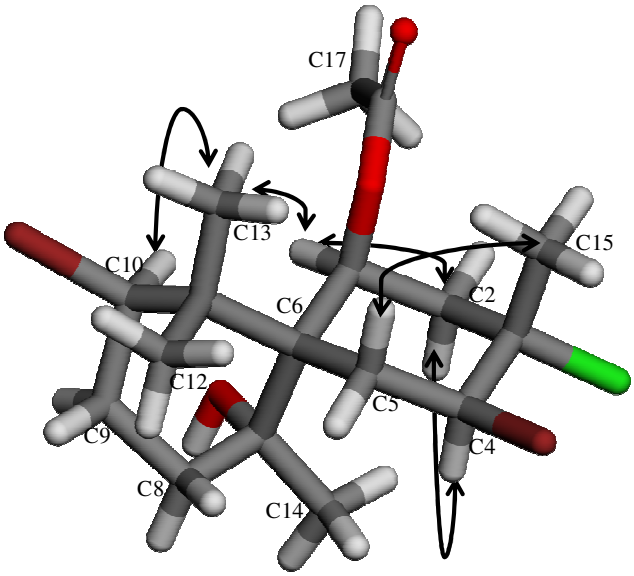

Figure 5.14: Key NOESY correlations in compound **5.14**

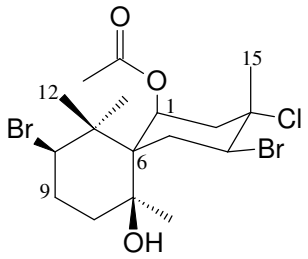

5.14

Table 5.4: NMR spectroscopic data of compound **5.14**

Carbon No	δ_C	δ_C mult	δ_H, mult, J (Hz)	COSY	HMBC	NOESY
1	74.3	CH	5.02, br s	H5	C6	H2a, H2b, H13, H14
2a	42.0	CH_2	2.62, dd, 14.9, 3.0	-	C1	-
2b			2.77, dd, 14.9, 3.0	-	-	H4, H14
3	69.6	C	-	-	-	-
4	59.6	CH	4.83, dd, 13.0, 4.4	H2	C5	H2b
5a	40.2	CH_2	2.52, t, 13.0	-	C3	H15
5b			2.27, d, 13.0	-	-	-
6	50.7	C	-	-	-	-
7	78.2	C	-	-	-	-
8a	32.4	CH_2	2.34, m	H9	-	H9
8b			1.35, m	-	C6	-
9a	30.6	CH_2	2.34, m	-	C8, C10	-
9b			2.02, m	-	-	-
10	63.3	CH	4.31, t, 9.5	H9	C9	H13
11	47.7	C	-	-	-	-
12	22.5	CH_3	1.23, s	-	C6, C10, C11, C13	-
13	21.3	CH_3	0.92, s	-	C12	H5, H10
14	22.5	CH_3	1.11, s	-	C7, C8	H1, H10
15	27.4	CH_3	1.75,s	-	C2, C3, C4	H2a, H5a
16	169.0	O**C**OCH_3	-	-	-	-
17	21.5	OCO**C**H_3	2.08, s	H8	C16	-

5.2.2.5 Compound 5.9

Compound **5.9** was isolated as needle like crystals by a purification process involving preferential solubility. The ^{1}H NMR spectrum (Figure 5.15) of compound **5.9** displayed a series of methine resonances including a triplet corresponding to a bromo-methine at δ_H 4.13 (J = 9.3 Hz), an oxy-methine double doublet at δ_H 4.22 (J = 7.9, 2.9 Hz) and an oxy-methine doublet at δ_H 5.07 (J = 2.3 Hz).

A total of five methyl singlets were identified between δ_H 0.92 and δ_H 2.07. A broad D_2O exchangeable hydroxyl resonance was noticed at δ_H 5.82.

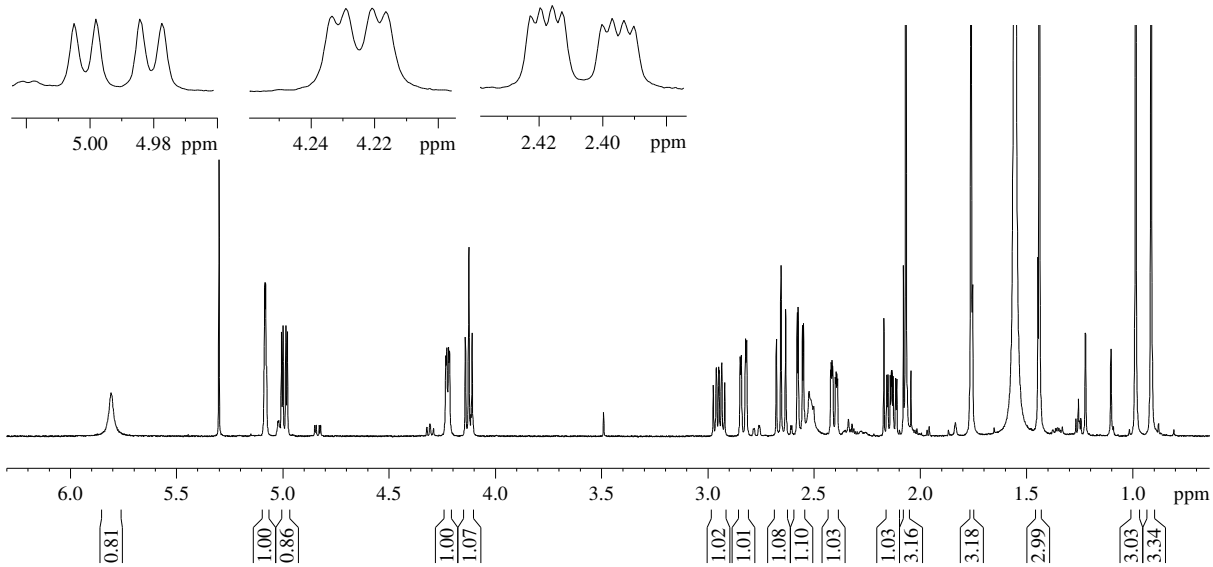

Figure 5.15: ^{1}H NMR spectrum ($CDCl_3$, 600 MHz) of compound **5.9**

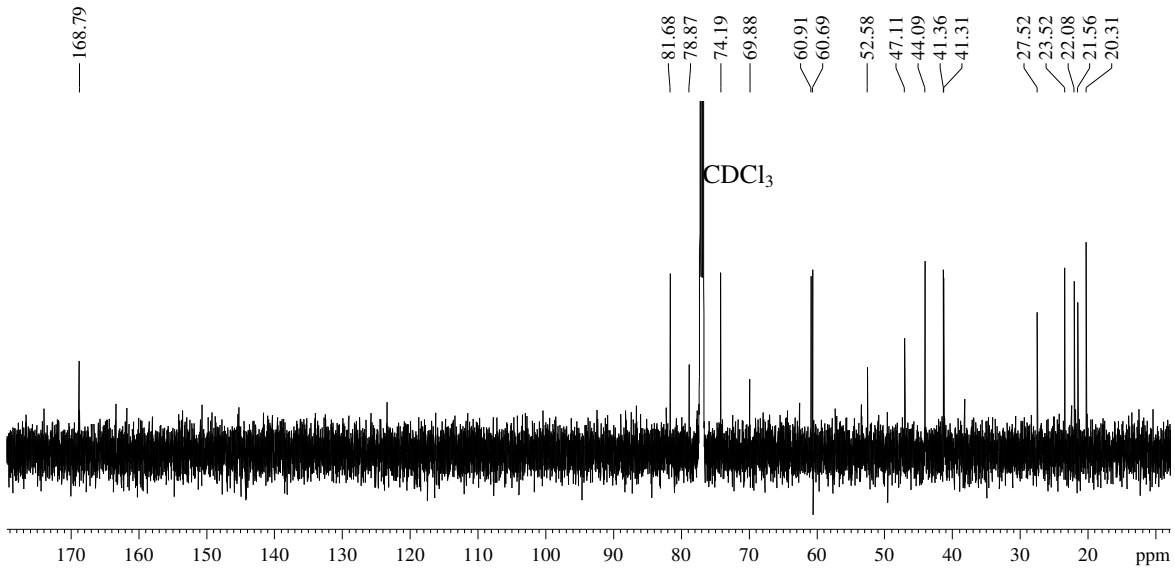

Figure 5.16: ^{13}C NMR spectrum ($CDCl_3$, 150 MHz) of compound **5.9**

Compound **5.9** possessed an acetate moiety after a carbonyl signal at δ_C 168.8 was deduced from the ^{13}C NMR (Figure 5.16) and HMBC spectra. This was confirmed by a C=O stretch in the IR spectrum of compound **5.9** at 1714 cm^{-1}.

HRESIMS was critical in confirming the molecular formula of compound **5.9** as $C_{17}H_{27}{}^{79}Br_2{}^{35}ClO_4$ with a molecular ion signal $[M+H]^+$ observed at *m/z* 489.0039 (calculated for 489.0043). Isotopic signals were also observed at *m/z* 491.0012, 492.9994 and 495.4417 typical of a Br_2Cl halogenated system (Appendix 4).

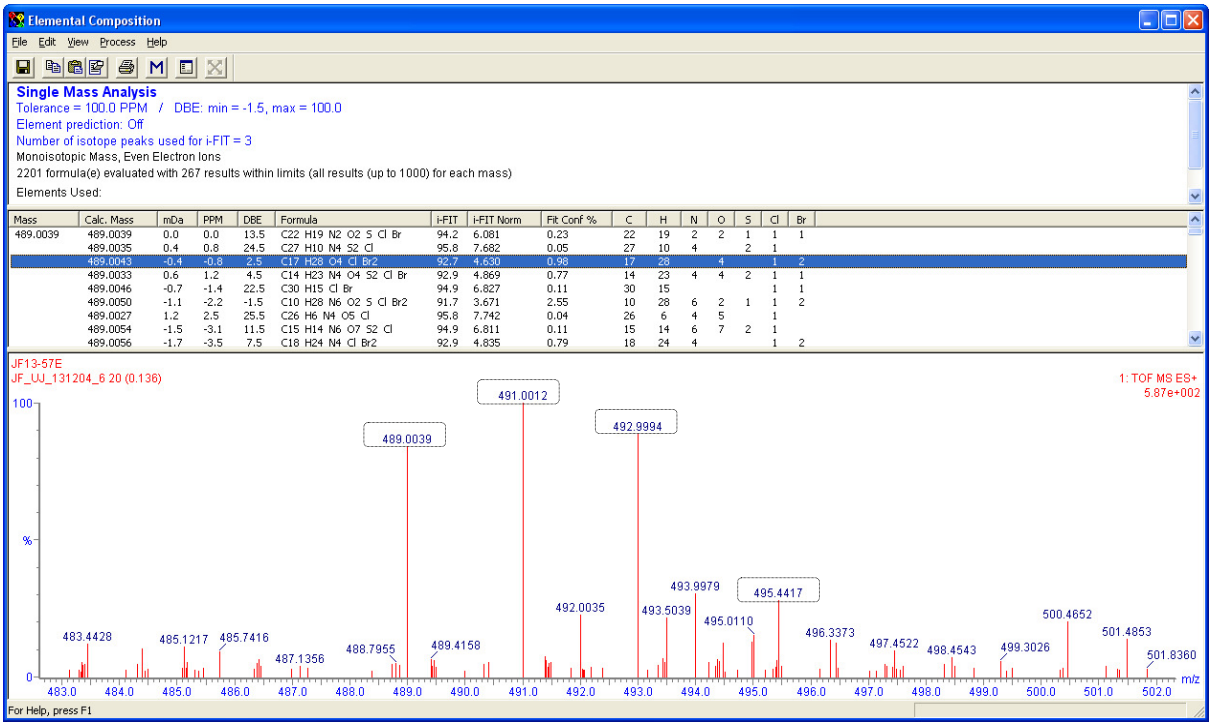

Figure 5.17: Expanded HRESIMS spectrum of compound **5.9**

Since the calculated double bond equivalent of three was already less one due to the carbonyl component, compound **5.9** must contain two cyclic entities.

HMBC data proved paramount in revealing that compound **5.9** adopted a peculiar carbon skeleton mimicking a saturated cuparane which contains cyclopentanyl and cyclohexanyl rings as opposed to the expected spiro-fused chamigrane sesquiterpene entity.

Compound **5.9** was accurately assigned as algoane. This sesquiterpene with an unprecedented carbon skeleton was isolated from the digestive glands of the sea-hare *Aplysia dactylomela* by McPhail *et al*., (1999) who also report its crystal structure.

This marks the first isolation of algoane from a seaweed and hence a prudent postulation of the herbivorous nature of the sea-hare on the alga can be made. Compounds **5.10** and **5.11** were also isolated from the same sea-hare by McPhail *et al*., (1999). Ji *et al*., (2012) isolated a similar carbon skeleton from *Laurencia okamurai* (compound **5.12**) while Hegazy *et al*., (2014) show compound **5.13** from *Aplysia oculifera*, an Egyptian sea-hare.

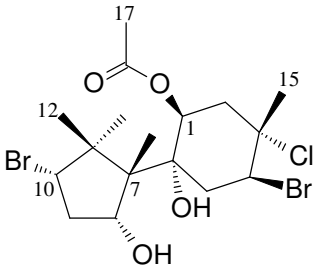

5.9

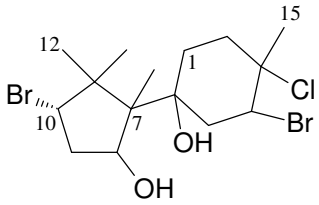

5.10

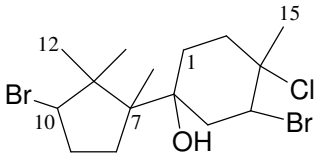

5.11

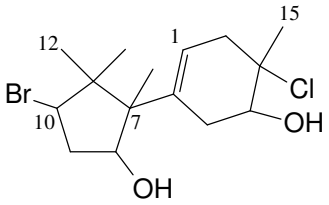

5.12

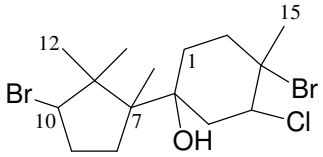

5.13

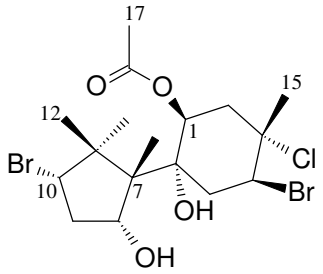

5.9

Table 5.5: NMR spectroscopic data of compound **5.9**

Carbon No	δ_C	δ_C **mult**	δ_H, **mult, J (Hz)**
1	74.2	C	5.07, d, 2.6
2a	41.4	CH_2	2.57, dd, 14.9, 2.6
2b			2.83, dd, 14.9, 2.6
3	69.9	C	-
4	60.7	CH	4.99, dd, 13.0 4.3
5a	41.3	CH_2	2.41, m
5b			2.66, t, 13.0
6	78.9	C	-
7	52.6	C	-
8	81.7	CH	4.22, dd, 9.1, 3.0
9a	44.1	CH_2	2.13, td, 9.1, 3.0
9b			2.95, pent, 8.9
10	60.9	CH	4.13, t, 8.9
11	47.1	C	-
12	22.1	CH_3	0.92, s
13	23.5	CH_3	1.44, s
14	20.3	CH_3	0.99, s
15	27.5	CH_3	1.76, s
$O\underline{\mathbf{C}}OCH_3$	168.8	C	-
$OCO\underline{\mathbf{C}}H_3$	21.5	CH_3	2.07, s

5.3 Experimental

5.3.1 General experimental

As per section **3.3.1** in chapter 3, page 54.

5.3.2 Mass spectrometry

HRESIMS as per section **4.3.2.2** in chapter 4, page 90.

5.3.3 Plant material (*L. natalensis*, KOS110201-1)

L. natalensis was collected by hand at Kenton-on-Sea in the south coast of South Africa in February 2011. A voucher specimen has been stowed away in the seaweed sample repository at the School of Pharmacy, University of the Western Cape. Identification of the alga was done by Professor John Bolton with the Department of Biological Sciences at the University of Cape Town, South Africa.

5.3.4 Extraction an isolation of metabolites

Same extraction procedure as discussed in section **3.3.3**, chapter 3, page 54 (dry mass 26.4 g, crude extract 1.53 g, 5.5% yield).

Normal phase HPLC and silica gel column chromatography were imperative in the purification in the purification of step gradient column fractions A and B to yield compounds **5.1** (2.0 mg, 0.072%), **5.5** (1.9 mg, 0.068%) and **5.8** (1.6 mg, 0.057%).

Fraction C showed an interesting crystal precipitate when 1.5 mL of 9:1 hex:EtOAc was added to it. The dissolved solutes were pipetted off leaving the crystalline material behind. After ^{1}H NMR analysis it was evident that the material consisted of two major components. Further washes of the crystalline material with 0.5 mL aliquots of 9:1 hex:EtOAc resulted in the purification of compounds **5.9** (9.8 mg, 0.360%) and **5.14** (6.5 mg, 0.230%).

5.3.5 Compounds isolated

5.3.5.1 Compound 5.1 (JF13-70D)

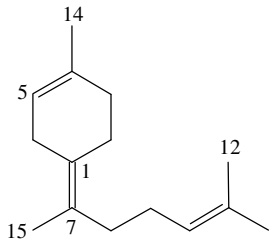

5.1

(*E*)-*γ*-bisabolene OR *(4Z)-1-methyl-4-(6-methylhept-5-en-2-ylidene)cyclohexane* (**5.1**): Clear oil; ^{1}H and ^{13}C NMR ($CDCl_3$) data available in Table 5.1. As previously synthesised by Faulkner and Wolinsky (1975) and Anastasia *et al*., (2001).

5.3.5.2 Compound 5.5 (JF13-85F)

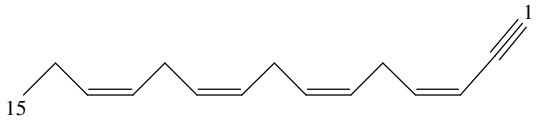

5.5

Cis-laurencenyne OR *(3Z,6Z,9Z,12Z)-pentadeca-3,6,9,12-tetraen-1-yne* (**5.5**): Colourless oil; ^{1}H and ^{13}C NMR data available in Table 5.2. As previously reported by Kigoshi *et al.,* (1981).

5.3.5.3 Compound 5.8 (JF13-85(1))

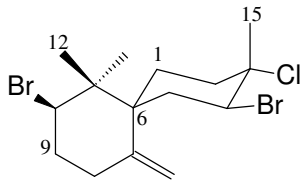

5.8

Nidificene OR *3-chloro-4, 10 dibromo-7-methylidene-chamigrane* (**5.8**): Colourless oil; ^{1}H and ^{13}C NMR data available in Table 5.3. As previously reported by Waraszkiewicz *et al*., (1974).

5.3.5.4 Compound 5.9 (JF13-57E)

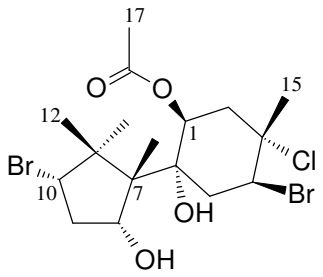

5.9

Algoane (**5.9**): White needle like crystals; ^{1}H and ^{13}C NMR data available in Table 5.5. As previously reported by McPhail *et al*., (1999).

5.3.5.5 Compound 5.14 (JF13-57E3)

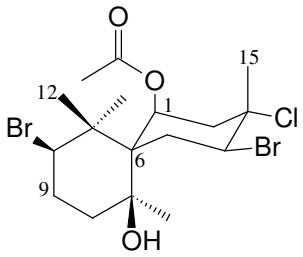

5.14

(8R,11S*)- 4,8 -dibromo -3- chloro- 11 -hydroxy-3, 7 ,7, 11-tetramethylspiro[5.5]undec-1-yl acetate* (**5.14**): White plate like crystals; $[\alpha]_D^{25}$ +97.6 (c = 0.003, MeOH); ; ^{1}H and ^{13}C NMR data available in Table 5.4; IR V_{max} 3513; 2971; 1723 ; 1371; 1229 cm^{-1}; HRESIMS [M+Cl] at *m/z* 506.9704 (calculated for 506.9704); $C_{17}H_{27}{}^{79}Br^{35}Cl_2O_3$.

5.4 References

Butler, A.; Carter-Franklin, J. N. The role of vanadium bromoperoxidase in the biosynthesis of halogenated marine natural products. *Natural Product Reports* **2004**, *21*, 180-188.

Dias, D. A.; Urban, S. Phytochemical studies of the southern Australian marine alga, *Laurencia elata*. *Phytochemistry* **2011**, *72*, 2081-2089.

Faulkner, D. J.; Wolinsky, L. E. A simple synthesis of γ-bisabolene. *Journal of Organic Chemistry* **1975**, *40*, 389-391.

Francis, C. M. **2014**. Systematics of the *Laurencia* complex (Rhodomelaceae, Rhodophyta) in southern Africa. PhD Thesis. University of Cape Town, Cape Town, South Africa.

Fukuzawa, A.; Honma, T.; Takasugi, Y.; Murai, A. Biogenetic intermediates, (3*E* and 3*Z*,12*Z*)-laurediols and (3*E* and 3*Z*)-12,13 dihydrolaurediols, isolated from *Laurencia nipponica*. *Phytochemistry* **1993**, *32*, 1435-1438.

Hegazy, M. E. F.; Moustfa, A. Y.; Mohamed, A. E. H.; Alhammady, M. A.; Elbehairi, S. E. I.; Ohta, S.; Paré, P. W. New cytotoxic halogenated sesquiterpenes from the Egyptian sea hare, *Aplysia oculifera*. *Tetrahedron Letters* **2014**, *55*, 1711-1714.

Ji, N.; Li, X. D.; Miao, F. Sesquiterpenes and acetogenins from the marine red alga *Laurencia okamurai*. *Fitoterapia* **2012**, *83*, 518-522.

Kigoshi, H.; Shizuri, Y.; Niwa, H.; Yamada, K.. Laurencenyne, a plausible precursor of various nonterpenoid C_{15}-compounds, and neolaurencenyne from the red alga *Laurencia okamurai*. *Tetrahedron Letters* **1981**, *2,* 4729-4732.

Kigoshi, H.; Shizuri, Y.; Niwa, H.; Yamada, K. Isolation and structures of trans laurencenyne, a possible precursor of the C_{15} halogenated cyclic ethers, and trans neolaurencenyne from Laurencia okamurai. *Tetrahedron letters* **1982**, *23*, 1475-1476.

Kurosawa, E.; Fukuzawa, A.; Irie, T. *Trans* and *cis*-laurediol, unsaturated glycols from *Laurencia nipponica* Yamada. *Tetrahedron letters* **1972**, *21*, 2121-2124.

Kurosawa, E.; Suzuki, T.; Kikuchi, H. (*E*)-γ-bisabolen-8,9-epoxide and isocycloeudesmol, two new sesquiterpenoids from the marine red alga *Laurencia nipponica* Yamada. *Chemistry Letters* **1980**, *9*, 1267-1270.

McMillan, J.; Paul, I. C.; White, R. H.; Hager, L. P. Molecular structure of acetoxyintricatol: a new bromo compound from *Laurencia intricata*. *Tetrahedron* **1974**, *23*, 2039-2042.

McPhail K. L.; Davies-Coleman M. T.; Copley R. C. B.; Eggleston D. S. New halogenated sesquiterpenes from South African specimens of the circumtropical sea hare *Aplysia dactylomela. Journal of Natural Products* **1999**, *62*, 1618-1623.

Minyard, J. P.; Tumlinson, J. H.; Thompson, A. C.; Hedin, P. A. Constituents of the cotton bud. Sesquiterpene hydrocarbons. *Journal of Agricultural and Food Chemistry* **1966**, *14*, 332-335.

Negishi, E.; Dumond, Y. R.; Anastasia, L. Stereoselective synthesis of exocyclic alkenes by Cu-catalyzed allylmagnesiation, Pd-catalysed alkylation, and Ru-catalysed ring-closing metathesis: highly stereo selective synthesis of (*Z*)- and (*E*)-γ-bisabolenes. *European Journal of Organic Chemistry* **2001**, *16*, 3039-3043.

Skattebøl, L.; Holmeide, A. K.; Sydnes, M. The syntheses of three highly unsaturated marine lipid hydrocarbons. *Journal of the Chemical Society*, *Royal Society of Chemistry* **2001**, *1*, 1942-1946.

Stegenga, H.; Bolton, J. J.; Anderson, R. J. Seaweeds of the South African west coast; *Contributions from the Bolus herbarium* **1997**, *18*, 1-655.

Waraszkiewicz, S. M.; Erickson, K. L. Halogenated sesquiterpenoids from the Hawaiian marine red alga *Laurencia nidifica*: Nidificene and Nidifidiene. *Tetrahedron Letters* **1974**, *23*, 2003-2006.

Chapter 6

Secondary metabolites from *Laurencia complanata*

Abstract

This, the first phycochemical analysis of *Laurencia complanata*, afforded a series of brominated indole, and *N*-methyl indoles (**6.1**-**6.5**), the majority of which have been previously isolated from *Laurencia brongniartii*.

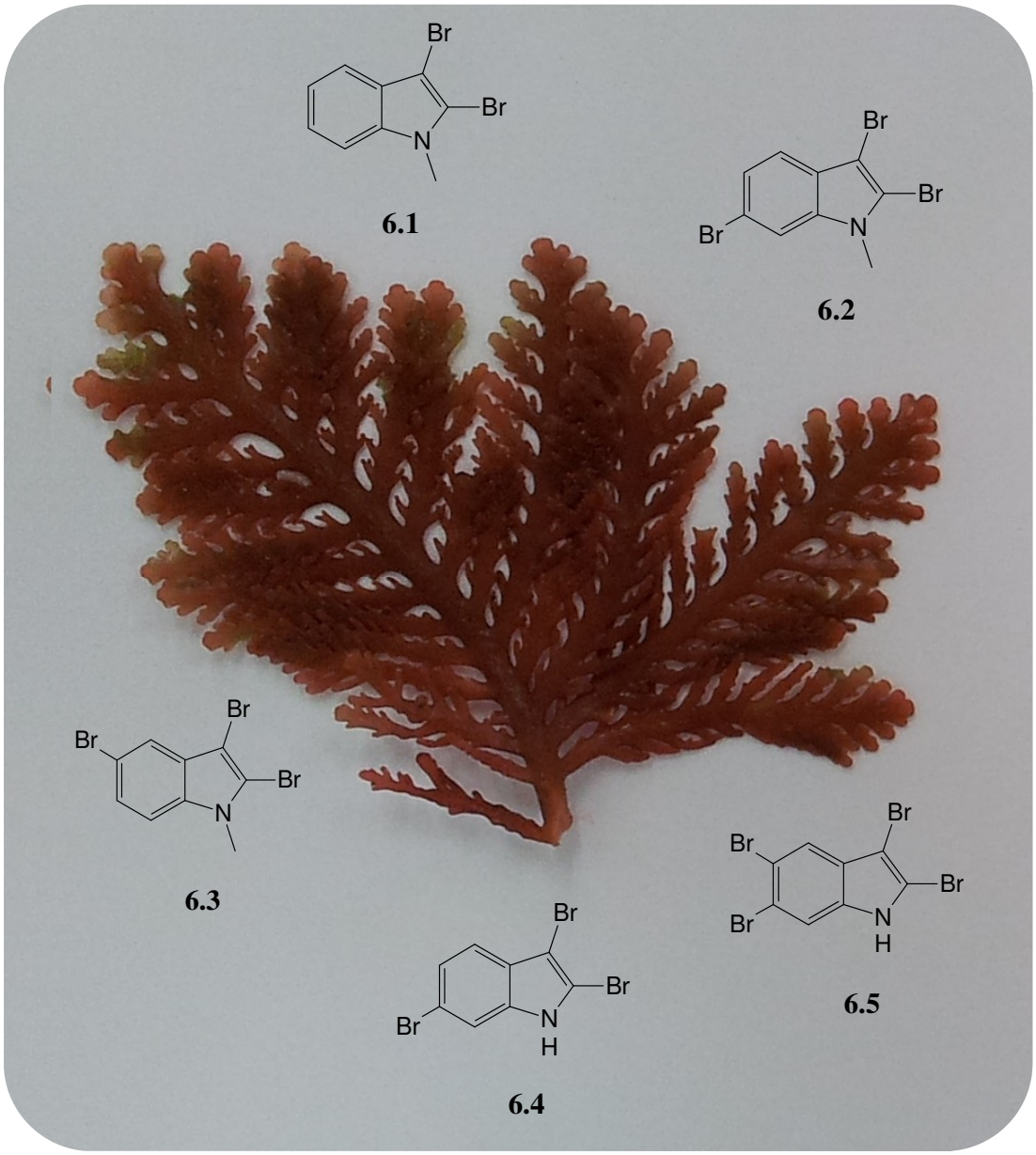

Chapter 6

Secondary metabolites from *Laurencia complanata*

6.1 Introduction

Laurencia complanata is known for its flattened or complanate appearance (*complanata*: flattened out in one plane). Plants are dark red and grow 6-22 cm high with one-two *corps en cerise* per cell (Figure 6.1). This species is mainly epilithic, growing in intertidal and shallow subtidal pools. It is distributed from the east coast of South Africa, extending northward (De Clerck *et al*., 2005; Francis, 2014). *Laurencia complanata* is comparable to *Laurencia brongniartii* as both plants have pinnate arrangements, however, *L. complanata* is known to be larger, existing in lower intertidal waters, whereas the smaller *L. brongniartii* species is more commonly found within deeper reef systems (De Clerck *et al*., 2005; Francis, 2014). Furthermore, Francis (2014) confirms the distinction between the two species *via rbc*L sequence divergence.

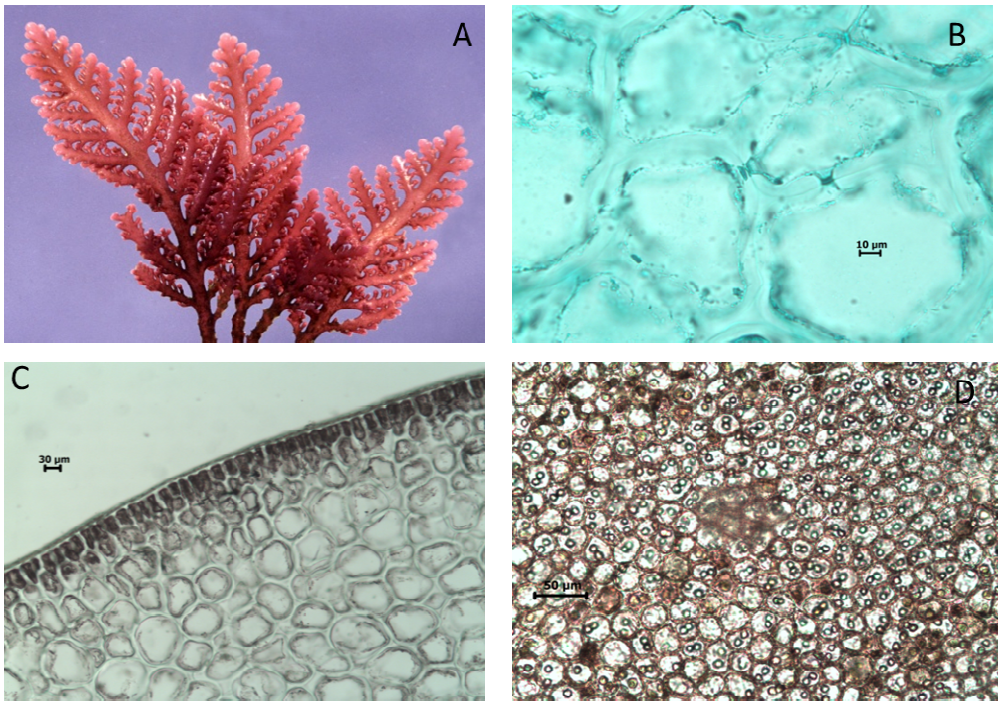

Figure 6.1: *Laurencia complanata*[1] (Caitlynne Francis © 2014)

A) Habit.
B) Secondary pit connections between cortical cells (40x).
C) Transverse section of thallus showing outermost cortical and cortical cells (20x).
D) Outermost cortical cells showing one-two *corps en cerise* per cell (20x).

[1] Image plates courtesy of Caitlynne Francis © 2014, University of Cape Town, South Africa

6.2 Results and Discussion

6.2.1 Extraction and isolation of metabolites from *L. complanata* (D1053, Port Edward)

The same extraction protocol was followed as in section **3.2.1** (chapter 3, page 54). Interestingly, the crude ^{1}H NMR spectrum of *L. complanata* showed prominent aromatic signals between δ_H 7.0-8.0 (Figure 6.2). From the spectral data of the step gradient silica gel column fractions (Figure 6.2) the majority of these resonances were sequestered within fraction B. A series of chromatographic purification techniques including normal phase HPLC and silica gel column chromatography permitted the isolation of compounds **6.1**, **6.2**, **6.3**, **6.4** and **6.5** from step gradient fraction B (Scheme 6.1).

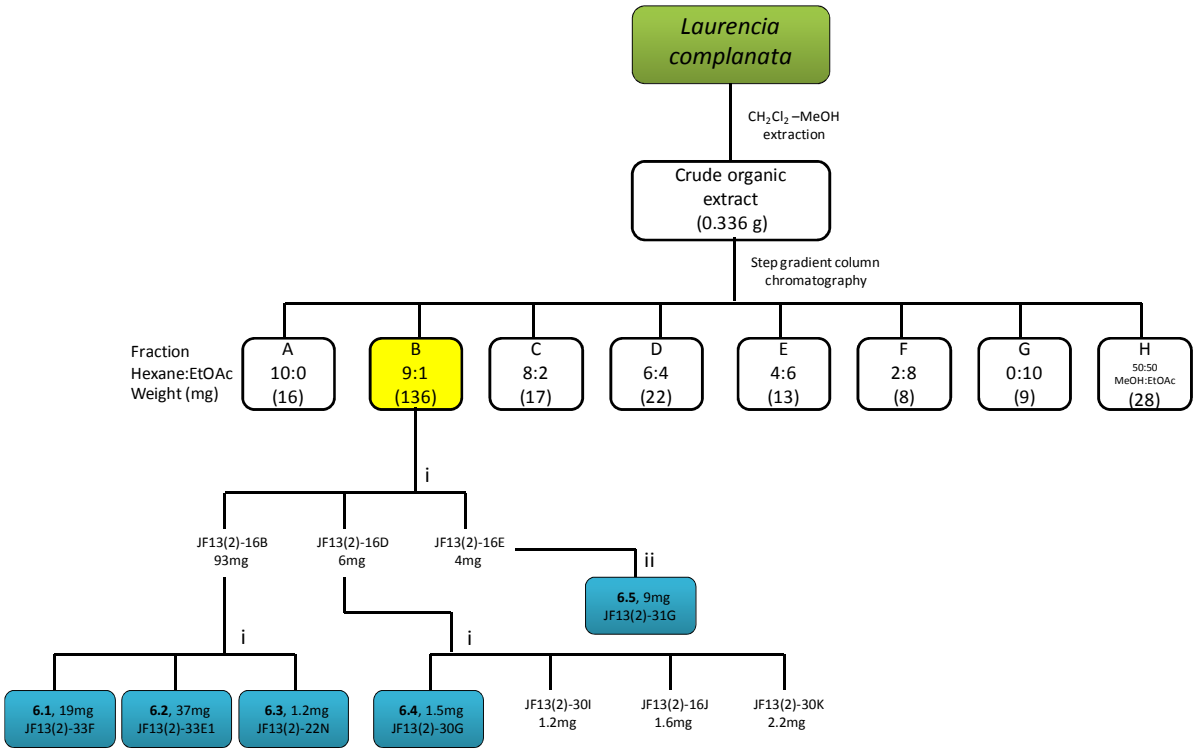

Scheme 6.1: Isolation scheme of metabolites from *L. complanata* (D1053)

Conditions: i) Silica gel column chromatography (9:1 hex:EtOAc); ii) Normal phase HPLC (9:1 hex:EtOAc)

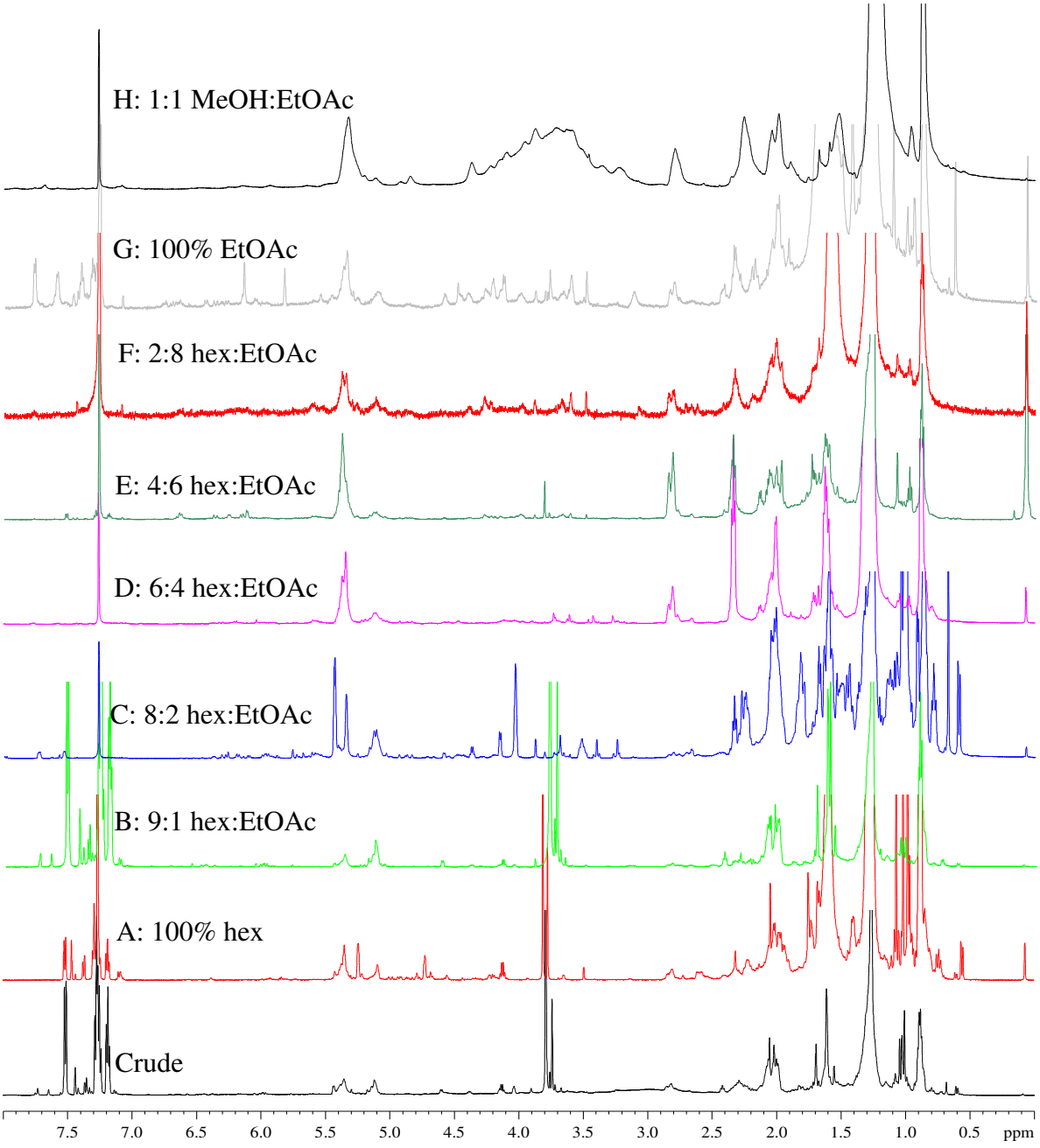

Figure 6.2: ^{1}H NMR spectra ($CDCl_3$, 600 MHz) of the crude organic extract of *L. complanata* (D1053) and step gradient column fractions A-H

6.2.2 Structure elucidation of metabolites

6.2.2.1 Compound 6.1

On close inspection of 1D and 2D NMR data, it was clear that compound **6.1** was isolated with a suspected analogue. Despite this, the structure of compound **6.1** was successfully elucidated as it was in much larger quantity.

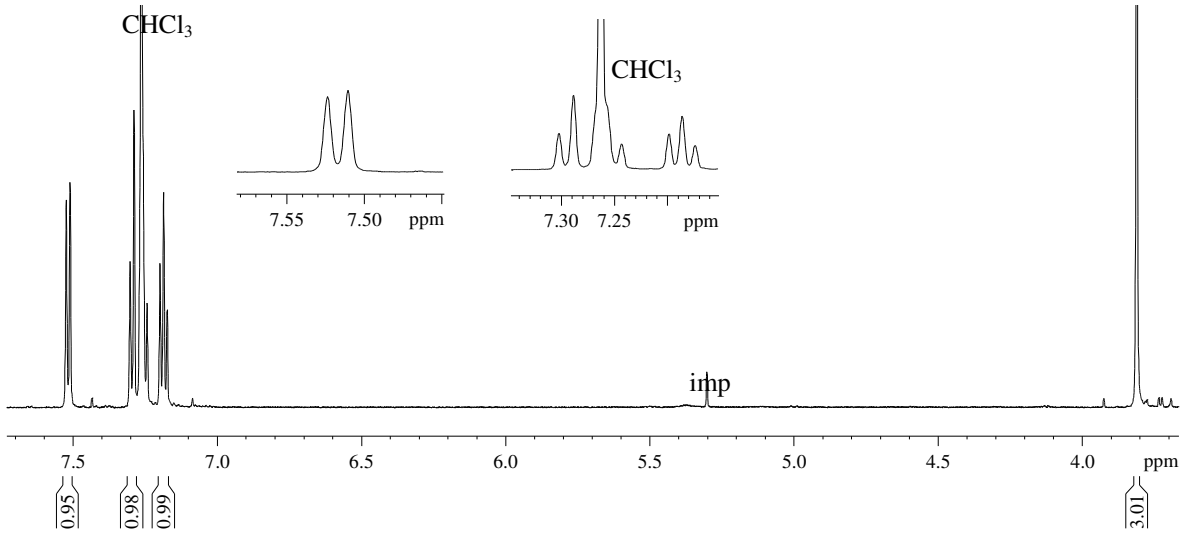

Figure 6.3: ^{1}H NMR spectrum ($CDCl_3$, 600 MHz) of compound **6.1**

The ^{1}H NMR spectrum of compound **6.1** (Figure 6.3) displayed a total of three coupled aromatic protons at δ_H 7.19 (t, J = 7.7 Hz), δ_H 7.29 (d, J = 7.7 Hz) and δ_H 7.52 (d, J = 7.7 Hz). A suspected fourth aromatic proton was thought to be concealed by the $CHCl_3$ solvent signal at δ_H 7.26. The validity of this suggestion was confirmed as both ^{13}C (Figure 6.4) and HSQC NMR spectra exposed four methine carbons (δ_C 109.6, 118.9, 120.9 and 122.8). The ^{1}H NMR spectrum further presented a deshielded methyl resonance at δ_H 3.81 typical of a methylated electronegative heteroatom.

Fortuitously, the HSQC and HMBC NMR spectra of compound **6.1** allowed for the assignment of nine carbon signals in the ^{13}C NMR spectrum of compound **6.1** (Figure 6.4), allowing for the disregard of peaks which did not belong to the compound.

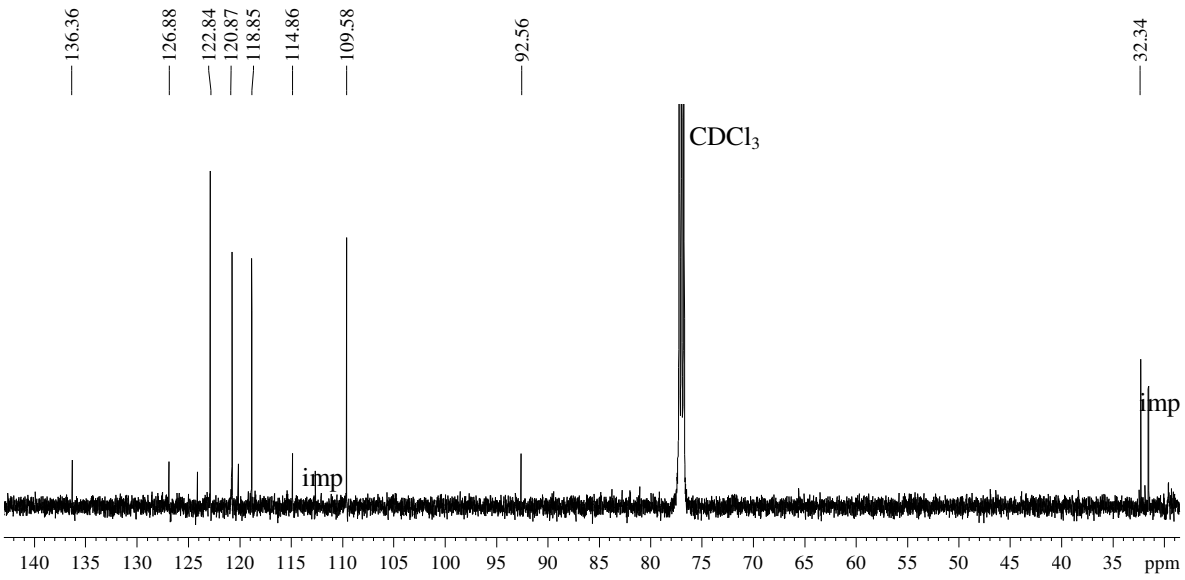

Figure 6.4: ^{13}C NMR spectrum ($CDCl_3$, 150 MHz) of compound **6.1**

A total of four quaternary (δ_C 92.6, 114.9, 126.9 and 136.4) and four methine (δ_C 109.6, 118.9, 120.9 and 122.8) carbon atoms were designated, including a deshielded methyl moiety at δ_C 32.3.

Since the HRAPCIMS[2] spectrum of compound **6.1** revealed a molecular ion cluster $[M+H]^+$ at *m/z* 287.9015 (calculated for 287.9024)/289.8996/291.8970, a molecular formula of $C_9H_7N^{79}Br_2$ was denoted. The isotopic abundance pattern was typical Br_2 system (Appendix 4).

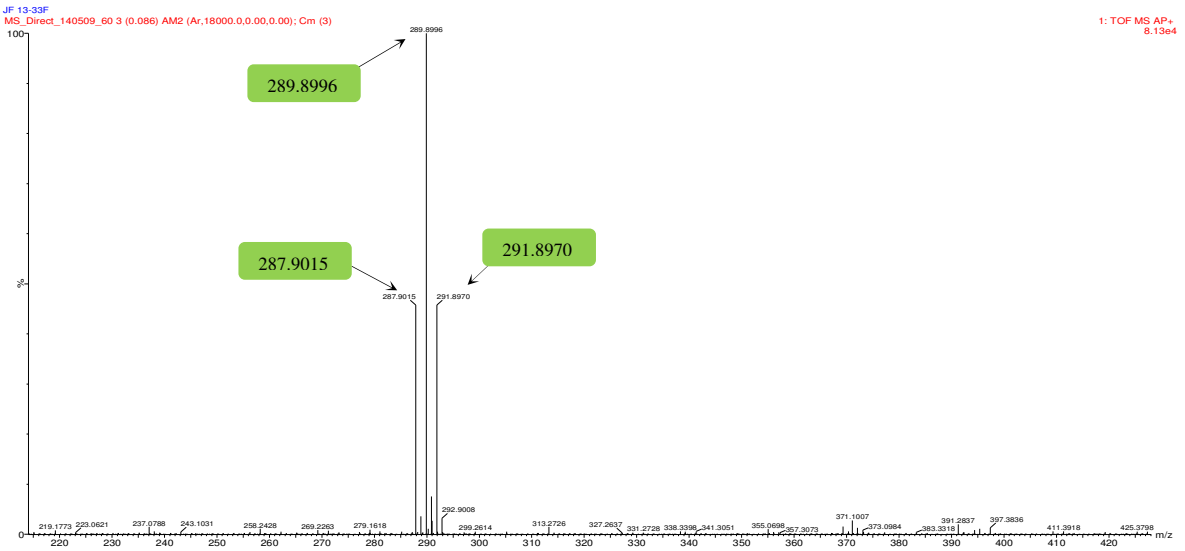

Figure 6.5: HRAPCIMS spectrum of compound **6.1**

[2] High resolution atmospheric pressure chemical ionisation mass spectrometry

With a calculated double bond equivalent of six, compound **6.1** was of the *N*-methyl indole class as shown below.

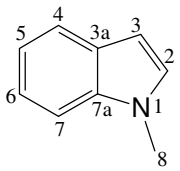

N-methyl indole

With two bromine atoms left to assign, it was evident that the benzene ring was not substituted due to the uninterrupted spin system (=CH-CH=CH-CH=) represented by signals at δ_H 7.52 (d, *J* = 8.1 Hz), δ_H 7.19 (t, *J* = 8.3 Hz), δ_H 7.26 (m) and δ_H 7.29 (d, *J* = 8.1 Hz) in the ^{1}H NMR spectrum (Figure 6.3). Quaternary carbons at positions C2 (δ_C 114.9) and C3 (δ_C 92.7) were believed to be the bromine bearing moieties. This was further confirmed by unambiguous HMBC correlations from the protons of the deshielded *N*-methyl functionality at C8 to C2 i.e. δ_H 3.81 to δ_C 114.9 (Figure 6.6). Compound **6.1** was thus *2,3-dibromo-methyl-indole*. Synthetic derivatives of this compound have been described by Liu and Gribble (2002), however, to the author's knowledge this is the first documented report of its isolation from marine algae.

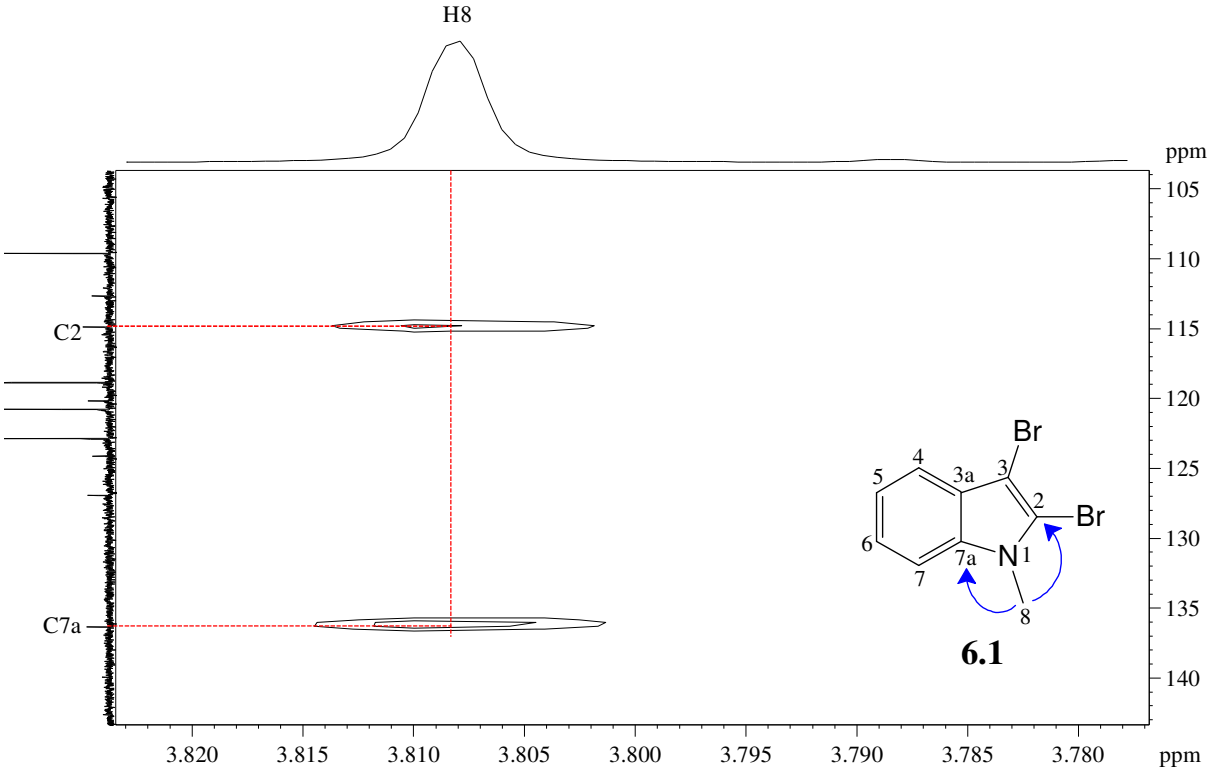

Figure 6.6: Partial HMBC spectrum of compound **6.1** showing key correlations

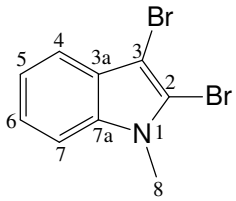

6.1

Table 6.1: NMR spectroscopic data of compound **6.1**[3]

Carbon No	δ_C	δ_C **mult**	δ_H, **mult, J (Hz)**
2	114.9	C	-
3	92.7	C	-
3a	127.0	C	-
4	118.9	CH	7.52, d, 8.2
5	120.8	CH	7.19, t, 8.2
6	122.9	CH	7.26, m
7	109.6	CH	7.29, d, 8.1
7a	136.4	C	-
8	32.3	CH_3	3.81, s

[3] The use of C_6D_6 to clarify the clustered aromatic proton signals was considered, however since adequate NMR data was obtained in $CDCl_3$ this was no longer necessary.

6.2.2.2 Compound 6.2

Compound **6.2** was identified as the "contaminating" analogue present in the fraction containing compound **6.1**. Compound **6.2** was also isolated with significant quantities of **6.1**. From integral values in the ^{1}H NMR spectrum (Figure 6.7), compound **6.2** appeared to be one sixth of the fraction. After several failed attempts at purifying this fraction, the structure of compound **6.2** was elucidated as a mixture.

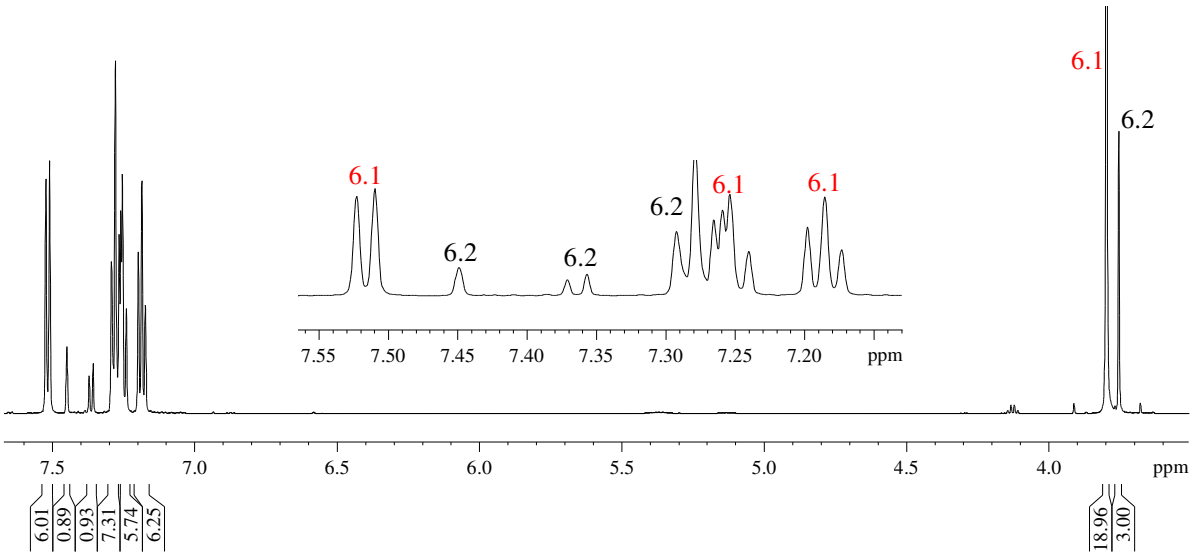

Figure 6.7: ^{1}H NMR spectrum ($CDCl_3$, 600 MHz) of compound **6.2/6.1**

The ^{1}H NMR spectrum (Figure 6.7) of the fraction containing compound **6.2** displayed a slightly more shielded hetero-atomic methyl at δ_H 3.76 *vs.* δ_H 3.81 as was seen in compound **6.1**. Further analysis of the ^{1}H NMR spectrum revealed a broad singlet at δ_H 7.45 as well as a doublet at δ_H 7.36 (J = 8.5 Hz). A methine signal, as confirmed by an edited HSQC experiment, was hidden in a cluster at δ_H 7.29. In total, the three methine resonances aforementioned were presumed to be the only aromatic signals belonging to compound **6.2**.

Since ^{13}C NMR peaks were now known for compound **6.1**, it was relatively simple to assign the ^{13}C resonances belonging to compound **6.2** (Figure 6.8), with validation of peaks performed by scrutiny of HSQC and HMBC NMR data. The replacement of a methine signal in compound **6.1** at δ_C 122.9 with a quaternary carbon at δ_C 116.7 in compound **6.2** was the only major difference between the ^{13}C NMR spectra of the two compounds suggesting that compound **6.2** was similar to compound **6.1** apart from additional substitution on the aromatic functionality.

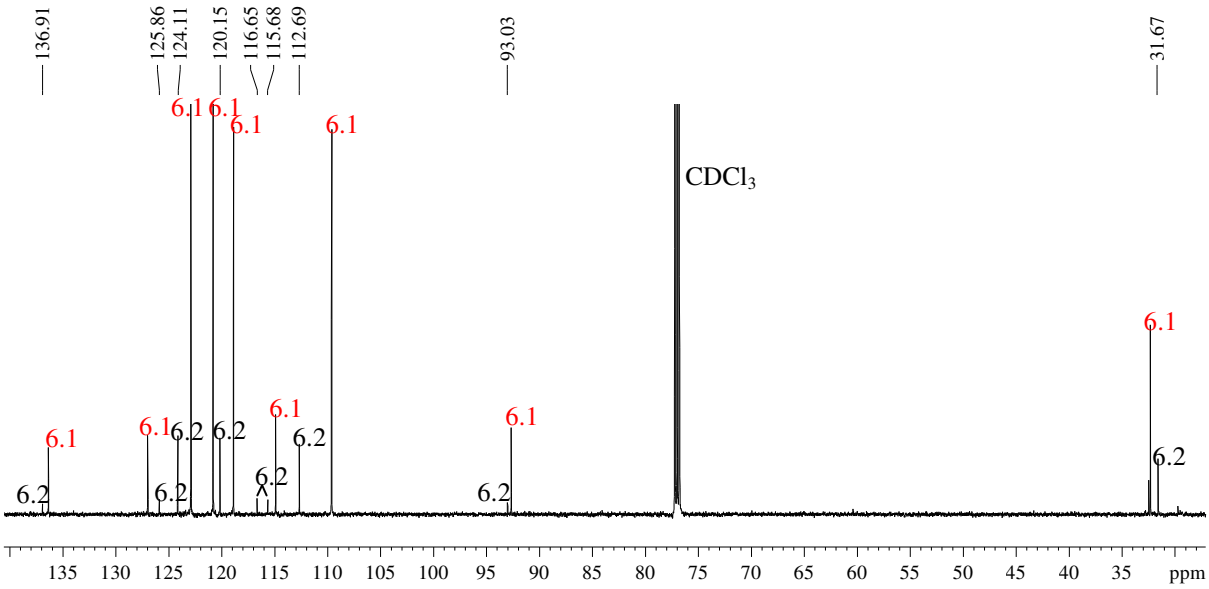

Figure 6.8: ^{13}C NMR spectrum ($CDCl_3$, 150 MHz) of compound **6.2/6.1**

After direct injection of compound **6.2** for HRAPCIMS analysis (Figure 6.9), and knowing to disregard the molecular cluster produced by the contaminating compound **6.1**, an array of peaks representing $[M+H]^+$ as well as isotopic signals were established at *m/z* 365.8109 (calculated for 365.8129)/367.8096/369.8079/371.8056. The isotopic abundance pattern displayed was consistent with a Br_3 system (Appendix 4) and a resultant molecular formula of $C_9H_6N^{79}Br_3$ was construed.

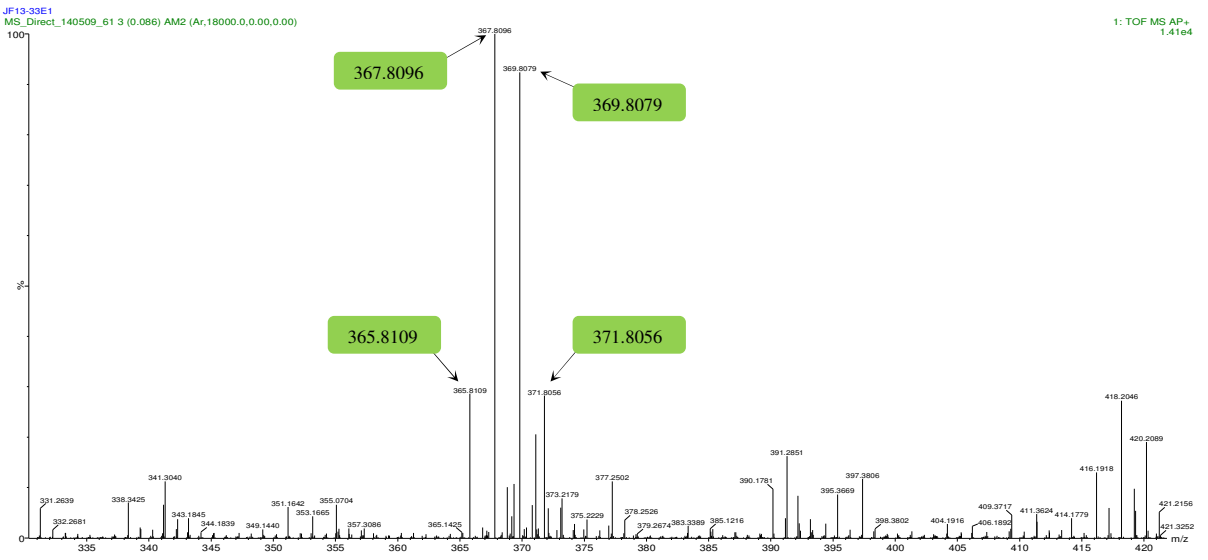

Figure 6.9: Expansion of the HRAPCIMS spectrum of compound **6.2/6.1**

Assigning the additional third bromine atom in compound **6.2** was based on a number of empirical hints. Firstly, a singlet in the ^1H NMR spectrum of compound **6.2** (Figure 6.7) at δ_H

7.45 suggested that methine singlet was flanked by two neighbouring quaternary carbons. This would then rule out any possibility of the bromine atom being at C4 or C7, inferring that positions C5 or C6 were more likely the substituted carbons.

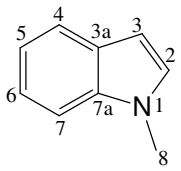

N-methyl-indole

HMBC correlations (H7 to C3a/C6) and NOESY correlations (H7 to H8) revealed that H7 was indeed the singlet at δ_H 7.45 and hence bromine substitution occurred at position C6. Compound **6.2** was identified as *2,3,6-tribromo-methyl-indole* previously reported by Carter *et al*., (1978) from *Laurencia brongniartii*.

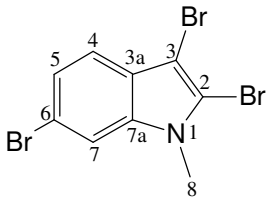

6.2

Table 6.2: NMR spectroscopic data of compound **6.2**

Carbon No	δ_C	δ_C mult	δ_H, mult, J (Hz)
2	115.7	C	-
3	93.0	C	-
3a	125.9	C	-
4	120.2	CH	7.36, d, 8.5
5	124.1	CH	7.29, m
6	116.7	C	-
7	112.7	CH	7.45, s
7a	136.9	C	-
8	31.7	CH_3	3.76, s

6.2.2.3 Compound 6.3

The ^{1}H NMR spectrum of compound **6.3** exhibited the same coupling pattern as in compound **6.2** with proton signals at δ_H 7.16 (d, J = 8.8 Hz), δ_H 7.33 (dd, J = 8.8, 2.1 Hz). *Meta*-coupling resulted in a doublet at δ_H 7.65, confirmed by a coupling constant of (J = 2 Hz).

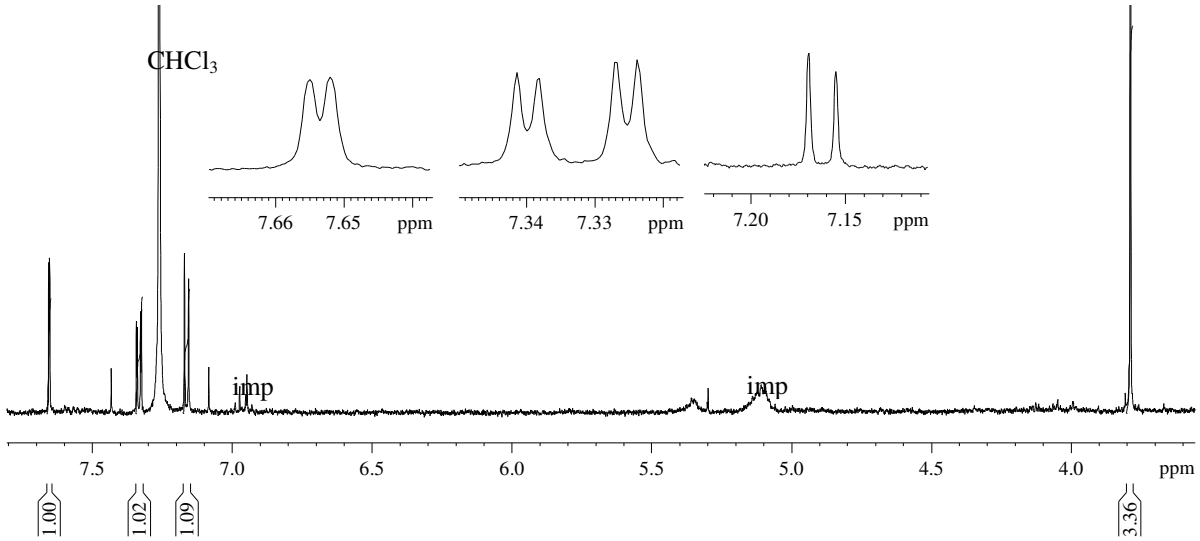

Figure 6.10: ^{1}H NMR spectrum ($CDCl_3$, 600 MHz) of compound **6.3**

The HRAPCIMS spectrum of compound **6.3** (Figure 6.11) was beneficial in confirming the structure as *2,3,5-tribromo-methyl-indole*. A similar molecular ion $[M+H]^+$ was observed as in compound **6.2**, at *m/z* 365.8130 (calculated for 365.8129). Isotopic signals were also observed at *m/z* 367.8104, 369.8085 and 371.8076, and the isotopic abundance pattern was again typical of a Br_3 system (Appendix 4) as in compound **6.2**. Compound **6.3** was amongst other indoles isolated by Carter *et al*., (1978) from *Laurencia brongniartii*.

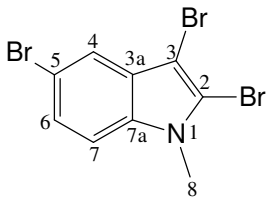

6.3

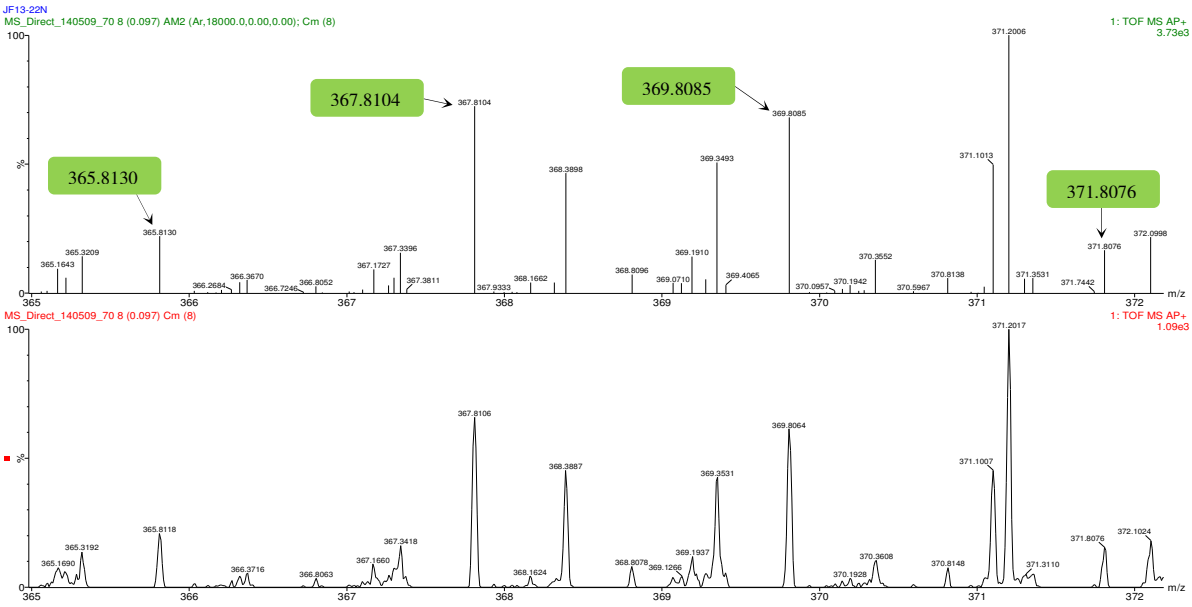

Figure 6.11: Expansion of the HRAPCIMS spectrum of compound **6.3**

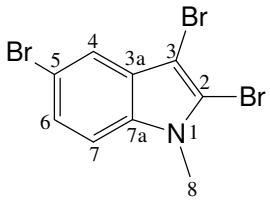

6.3

Table 6.3: NMR spectroscopic data of compound **6.3**[4]

Carbon No	δ_C	δ_C mult	δ_H, mult, J (Hz)
2	116.3	C	-
3	92.4	C	-
3a	128.6	C	-
4	121.5	CH	7.65, d, 2.1
5	114.3	C	-
6	126.0	CH	7.33, dd, 8.8, 2.1
7	111.2	CH	7.16, d, 8.8
7a	135.8	C	-
8	29.8	CH_3	3.79

[4] Carbon data deduced from HSQC and HMBC NMR spectra

6.2.2.4 Compound 6.4

The absence of a deshielded methyl moiety around δ_H 3.0 as well as the surfacing of a broad amino-proton at δ_H 8.31 were undoubtedly the most intriguing facets observed in the ^1H NMR spectrum of compound **6.4** (Figure 6.12). This immediately suggested loss of the amino-methyl entity, giving rise to a secondary amine.

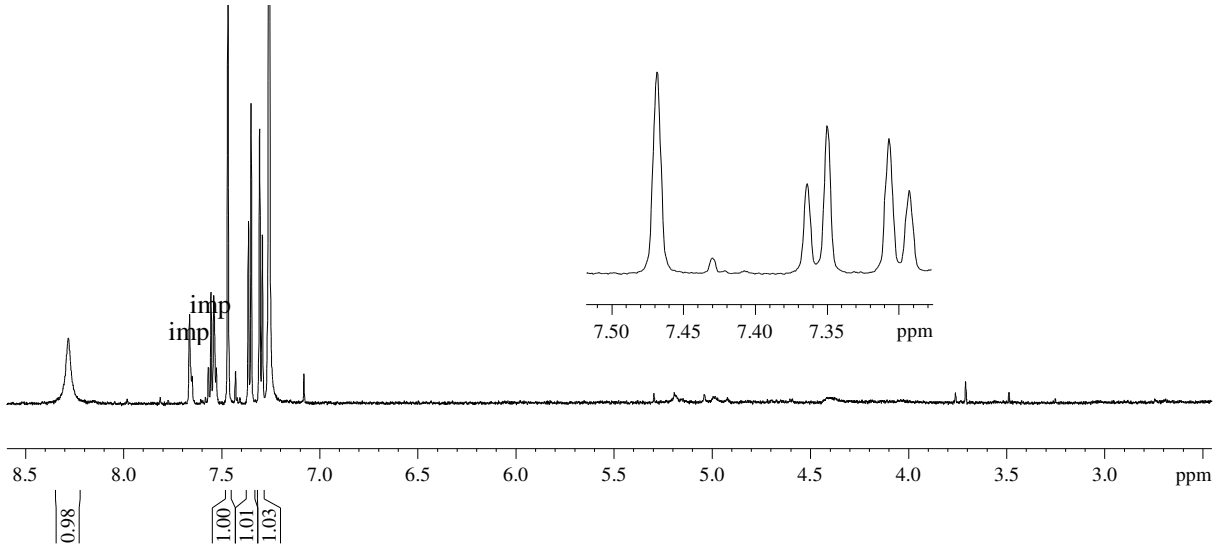

Figure 6.12: ^1H NMR ($CDCl_3$, 600 MHz) spectrum of compound **6.4**

The HRAPCIMS spectrum of compound **6.4** (Figure 6.13) supported a similar tribromo-indole system as seen in compound **6.2**, however in this particular case the loss of a CH_3 functionality was confirmed as a molecular ion cluster was observed at *m/*z 350.7884 (calculated for 350.7894/352.7851/354.7832/356.7813). This supported a molecular formula of $C_8H_4N^{79}Br_3$.

Compound **6.4** was identified as *2,3,6-tribromo-indole* previously documented by Wang *et al*., (2007) from a Chinese specimen of *Laurencia similis*.

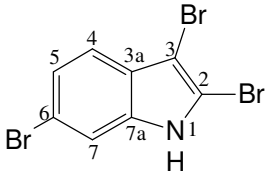

6.4

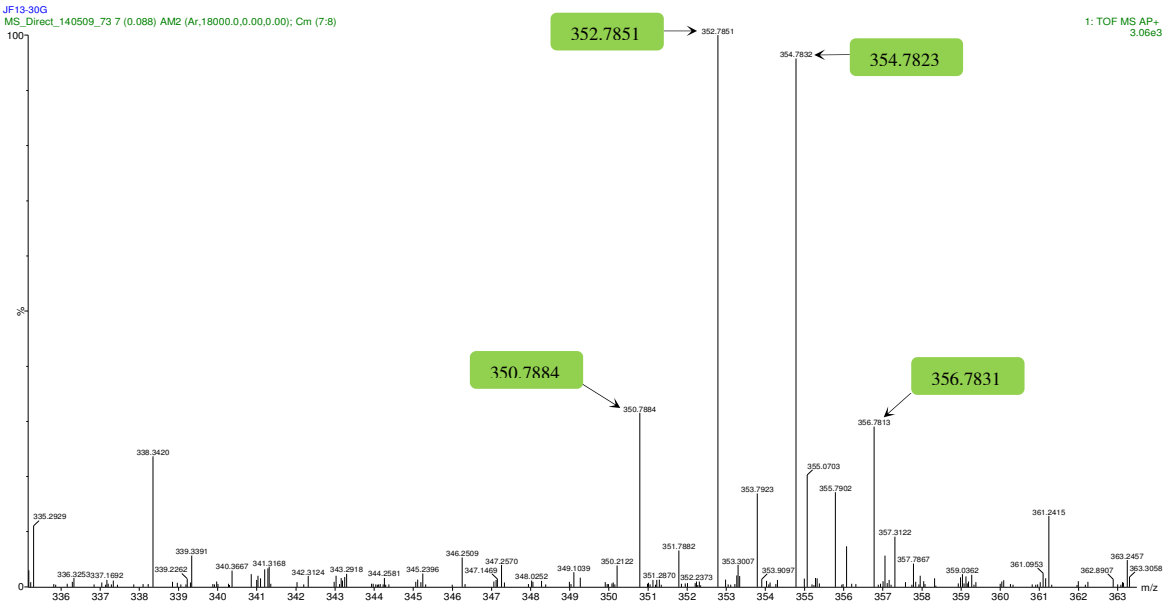

Figure 6.13: Expansion of the HRAPCIMS spectrum of compound **6.4**

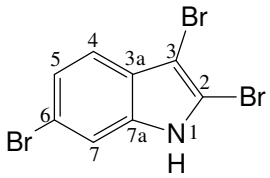

6.4

Table 6.4: NMR spectroscopic data of compound **6.4**[5]

Carbon No	δ_C	δ_C mult	δ_H, mult, J (Hz)
2	110.6[6]	C	-
3	93.8[6]	C	-
3a	126.7	C	-
4	120.2	CH	7.36, d, 8.6
5	124.7	CH	7.30, d, 8.6
6	117.1[6]	C	-
7	113.6	CH	7.47, s
7a	136.2	C	-

[5] Carbon data deduced from HSQC and HMBC NMR data
[6] Quaternary carbons not observed. Shifts as reported by Wang *et al*., (2007)

6.2.2.5 Compound 6.5

A seemingly simple ^{1}H NMR spectrum (Figure 6.14) belonging to compound **6.5** was again devoid of a deshielded amino-methyl function, as validated by the presence of a broad amino-proton at δ_H 8.34.

The highlight of the spectrum came in the form of two aromatic singlets at δ_H 7.61 and δ_H 7.77 suggesting that compound **6.5** harboured two aromatic protons which were secluded between quaternary carbons.

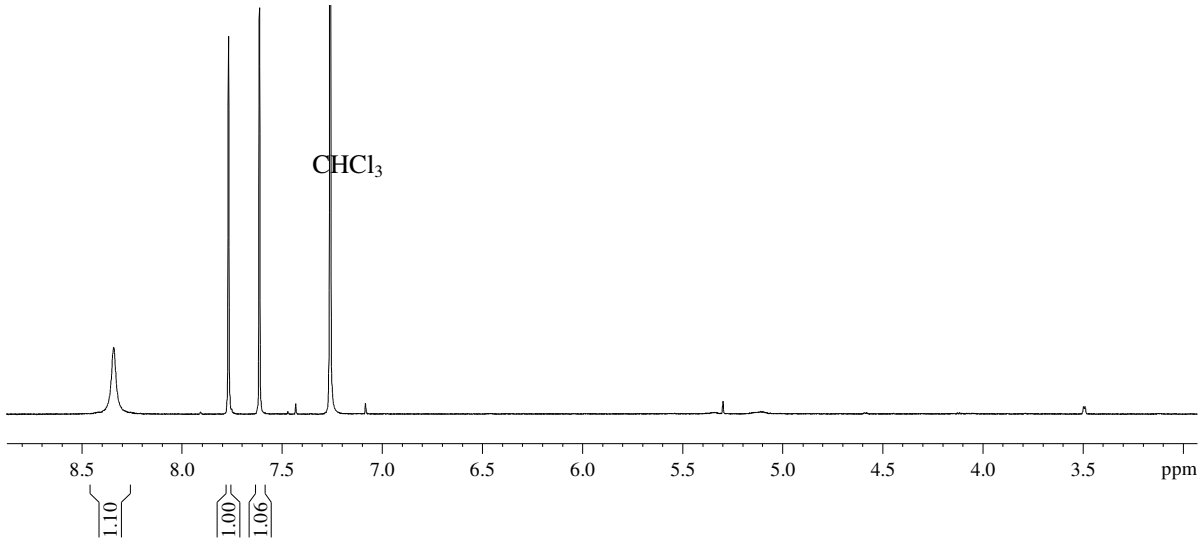

Figure 6.14: ^{1}H NMR spectrum ($CDCl_3$, 600 MHz) of compound **6.5**

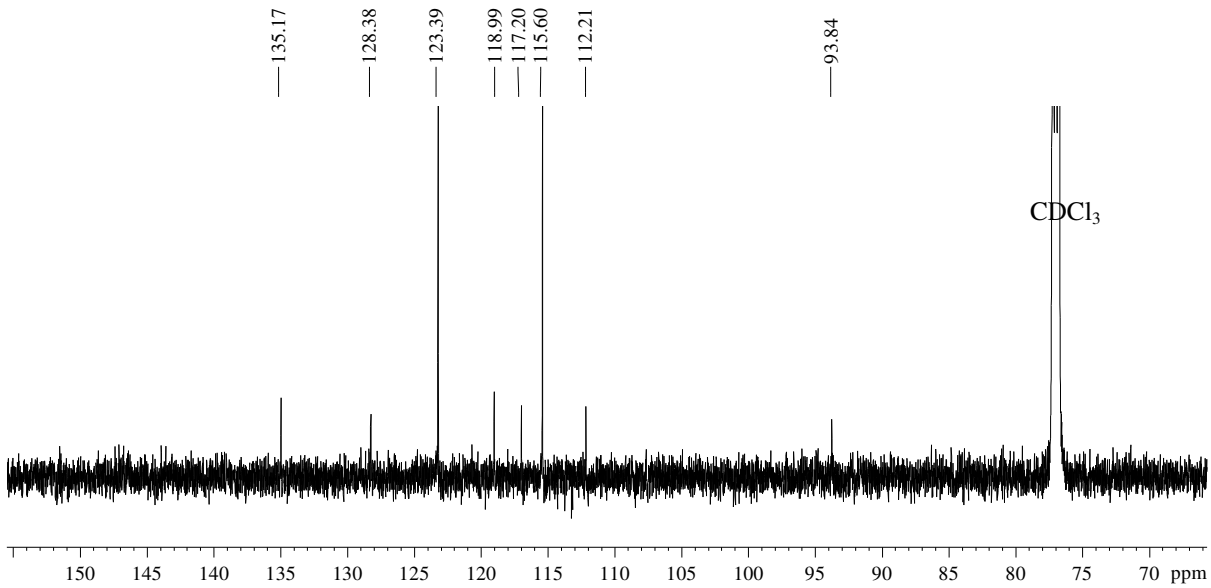

Figure 6.15: ^{13}C NMR spectrum ($CDCl_3$, 150 MHz) of compound **6.5**

The ^{13}C NMR spectrum (Figure 6.15) was fundamental in ascribing the two clearly visibly methine carbon signals at δ_C 115.6 and δ_C 123.4 amongst an assemblage of quaternary signals (δ_C 93.8, 112.2, 117.2, 128.4 and 135.2).

The HRAPCIMS spectrum (Figure 6.16) of compound **6.5** showed an undisputable molecular ion at *m/z* 428.7007 (calculated for 428.6999) as well as four other isotopic peaks at *m/z* 430.6942/432.6953/434.6936/436.6890 the abundance patterns of which were typical of a Br_4 system (Appendix 4). This implied a molecular formula of $C_8H_3N^{79}Br_4$.

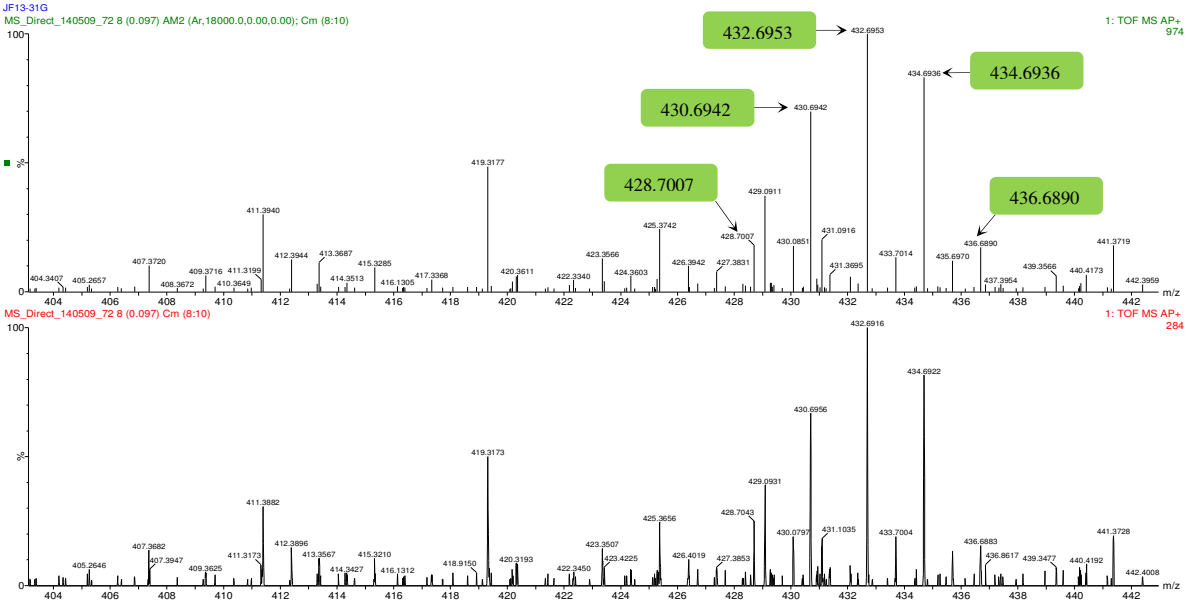

Figure 6.16: Expansion of the HRAPCIMS spectrum of compound **6.5**

Compound **6.5** was characterised as *2,3,5,6-tetrabromo-indole*, previously reported from the organic extract of *Laurencia brongniartii* by Carter *et al.*, (1978).

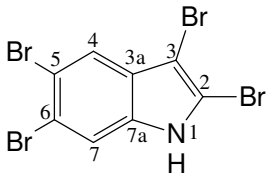

6.5

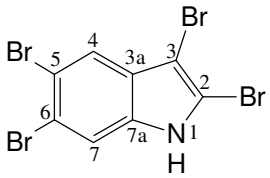

6.5

Table 6.5: ^{1}H NMR spectrum of compound **6.5**

Carbon No	δ_C	δ_C mult	δ_H, mult, J (Hz)
2	112.2	C	-
3	93.8	C	-
3a	128.4	C	-
4	123.4	CH	7.77, s
5	117.2	C	-
6	119.0	C	-
7	115.6	CH	7.61, s
7a	135.2	C	-

6.2.2.6 Other indoles

Tanaka *et al*., (1989) report the isolation of sulphur containing indoles amongst others from a specimen of *L. brongniartii* collected from the Japanese island Okinawa. The fact that similar indoles were not isolated from *L. complanata* should not rule out their non-existence in the species. This study in general was limited to small amounts of algal material thus compounds isolated herein are not absolute representatives of the species secondary metabolome.

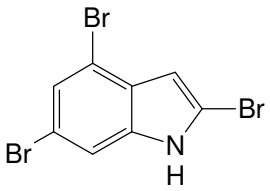

6.6

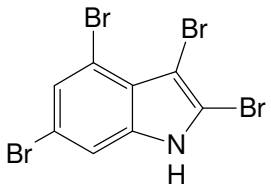

6.7

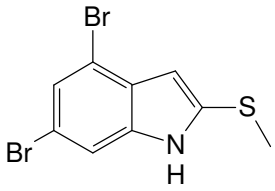

6.8

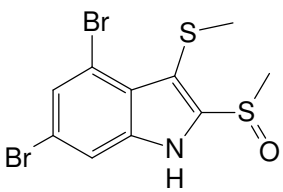

6.9

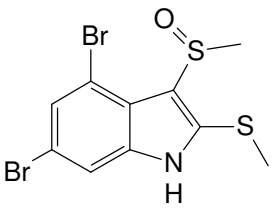

6.10

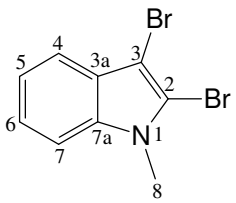

6.1

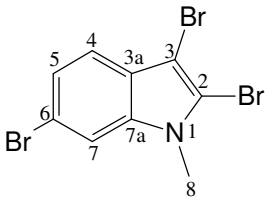

6.2

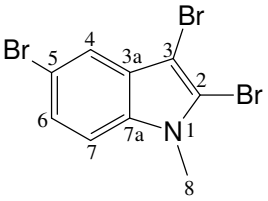

6.3

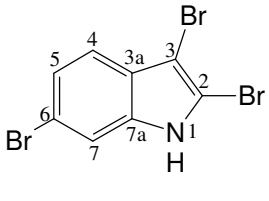

6.4

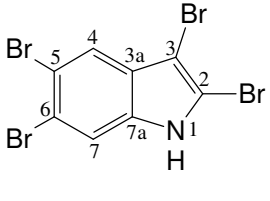

6.5

Table 6.6: ^{1}H NMR data ($CDCl_3$, 600 MHz) for compounds **6.1-6.5**

Proton No	6.1	6.2	6.3	6.4	6.5
4	7.52, d, 8.1	7.36, d, 8.5	7.65, d, 2.1	7.36, d, 8.6	7.77, s
5	7.19, t, 8.3	7.29, m	-	7.30, d, 8.6	-
6	7.26, m	-	7.33, dd, 8.8, 2.1	-	-
7	7.29, d, 8.1	7.45, s	7.16, d, 8.8	7.47, s	7.61, s
N-C**H$_3$**	3.81, s	3.76, s	3.79	-	-

Table 6.7: ^{13}C NMR data ($CDCl_3$, 150 MHz) for compounds **6.1-6.5**

Carbon No	6.1	6.2	6.3	6.4	6.5
2	114.9	115.7	116.3	110.6	112.2
3	92.7	93.0	92.4	93.8	93.8
3a	127.0	125.9	128.6	126.7	128.4
4	118.9	120.2	121.5	120.2	123.4
5	120.8	124.1	114.3	124.7	117.2
6	122.9	116.7	126.0	117.1	119.0
7	109.6	112.7	111.2	113.6	115.6
7a	136.4	136.9	135.8	136.2	135.2
N-**C**H$_3$	32.3	31.7	29.8	-	-

6.3 Experimental

6.3.1 General experimental

As per section **3.3.1** in chapter 3, page 54.

6.3.2 Plant material (*L. complanata*, D1053)

L. complanata was collected by hand at Port Edward on the east coast of South Africa in September 2011. A voucher specimen has been deposited in the Bolus Herbarium at the University of Cape Town. Identification of the alga was done by Professor John Bolton with the Department of Biological Sciences at the University of Cape Town, South Africa.

6.3.3 Extraction and isolation of metabolites

Same procedure as previously described in section **3.3.3**, chapter 3, page 54 (dry mass 3.5 g, crude extract 0.34 g, 8.9% yield).

Silica gel column chromatography (9:1 hex:EtOAc) as well as normal phase HPLC (9:1 hex:EtOAc) were critical in purifying *L. complanata* compounds from step gradient silica gel fraction B. Compounds **6.1** (19 mg, 0.51%) and **6.2** (37 mg, 1.0%) were elucidated in mixtures of one another, whereas compounds **6.3** (1.2 mg, 0.03%) **6.4** (1.5 mg, 0.04%) and **6.5** (9 mg, 0.23%) were isolated successfully.

6.3.4 Compounds isolated

6.3.4.1 Compound 6.1 (JF13(2)-33F)

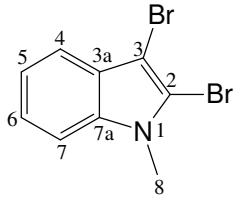

6.1

2,3-dibromo-methyl-indole (**6.1**): White amorphous solid; HRAPCIMS $[M+H]^+$ at *m/z* 287.9015 (calculated for 287.9024/289.8996/291.8970); $C_9H_7N^{79}Br_2$; ^1H and ^{13}C data available in Tables 6.6 and 6.7. As previously reported by Liu and Gribble (2002) as a synthetic analogue.

6.3.4.2 Compound 6.2 (JF13(2)-33E1)

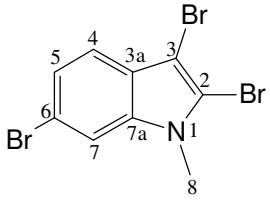

6.2

2,3,6-tribromo-methyl-indole (**6.2**): White amorphous solid; HRAPCIMS $[M+H]^+$ at *m/z* 365.8109 (calculated for 365.8129/367.8096/369.8079/371.8056); $C_9H_6N^{79}Br_3$; ^1H and ^{13}C data available in Tables 6.6 and 6.7. As previously reported by Carter *et al*., (1978).

6.3.4.3 Compound 6.3 (JF13(2)-22N)

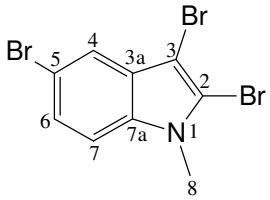

6.3

2,3,5-tribromo-methyl-indole (**6.3**): White amorphous solid; HRAPCIMS $[M+H]^+$ at *m/z* 365.8130 (calculated for 365.8129/367.8104/369.8085/371.8076); $C_9H_6N^{79}Br_3$; ^1H and ^{13}C data available in Tables 6.6 and 6.7. As previously reported by Carter *et al*., (1978).

6.3.4.4 Compound 6.4 (JF13(2)-30G)

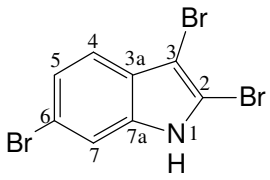

6.4

2,3,6-tribromo-indole (**6.4**): White amorphous solid; HRAPCIMS *m/z* 350.7884 (calculated for 350.7894/352.7851/354.7832/356.7813); $C_8H_4N^{79}Br_3$; ^1H and ^{13}C data available in Tables 6.6 and 6.7. As previously reported by Wang *et al*., (2007).

6.3.4.5 Compound 6.5 (JF13(2)-31G)

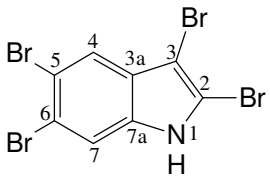

6.5

2,3,5,6-tetrabromo-indole (**6.5**): White amorphous solid; HRAPCIMS *m/z* 428.7007 (calculated for 428.6999/430.6942/432.6953/434.6936/436.6890); $C_8H_3N^{79}Br_4$; ^1H and ^{13}C data available in Tables 6.6 and 6.7. As previously reported by Carter *et al*., (1978).

6.4 References

Carter, G. T.; Rinehart, K. L.; Li, L. H.; Kuentzel, S. L.; Connor, J. L. Brominated indoles from *Laurencia brongniartii*. *Tetrahedron Letters* **1978**, *46*, 4479-4482.

De Clerck, O.; Bolton, J. J.; Anderson, R. J.; Coppejans, E. *Guide to the seaweeds of KwaZulu-Natal*. *Scripta Botanica Belgica 33*. National Botanic Garden of Belgium, VLIZ: Flanders Marine Institute and Flemish Community, **2005**, 1-294.

Francis, C. M. **2014**. Systematics of the *Laurencia* complex (Rhodomelaceae, Rhodophyta) in southern Africa. PhD Thesis. University of Cape Town, Cape Town, South Africa.

Liu, Y.; Gribble, G. W. Syntheses of polybrominated indoles from the red alga *Laurencia brongniartii* and the brittle star *Ophiocoma erinaceus*. *Journal of Natural Products* **2002**, *65*, 748-749.

Tanaka, J.; Higa, T.; Bernardinelli, G.; Jefford, C. W. Sulfur containing polybromoindoles from the red alga *Laurencia brongniartii*. *Tetrahedron* **1989**, *45*, 7301-7310.

Wang, B. G.; Ding, L. P.; Li, X. M.; Ji, N. Y. Aristolane sesquiterpenes and highly brominated indoles from the marine red alga *Laurencia similis* (Rhodomelaceae). *Helvetica Chimica Acta* **2007**, *90*, 385-391.

Chapter 7

Secondary metabolites from *Laurencia multiclavata*

Abstract

This chapter reports the first phycochemical investigation of *Laurencia multiclavata* which afforded three known acetylenic poly-cycles. The tri-cyclic acetogenin **7.1** was the major metabolite within the crude organic extract. Complex isomeric acetylenes **7.5** and **7.6** were also isolated.

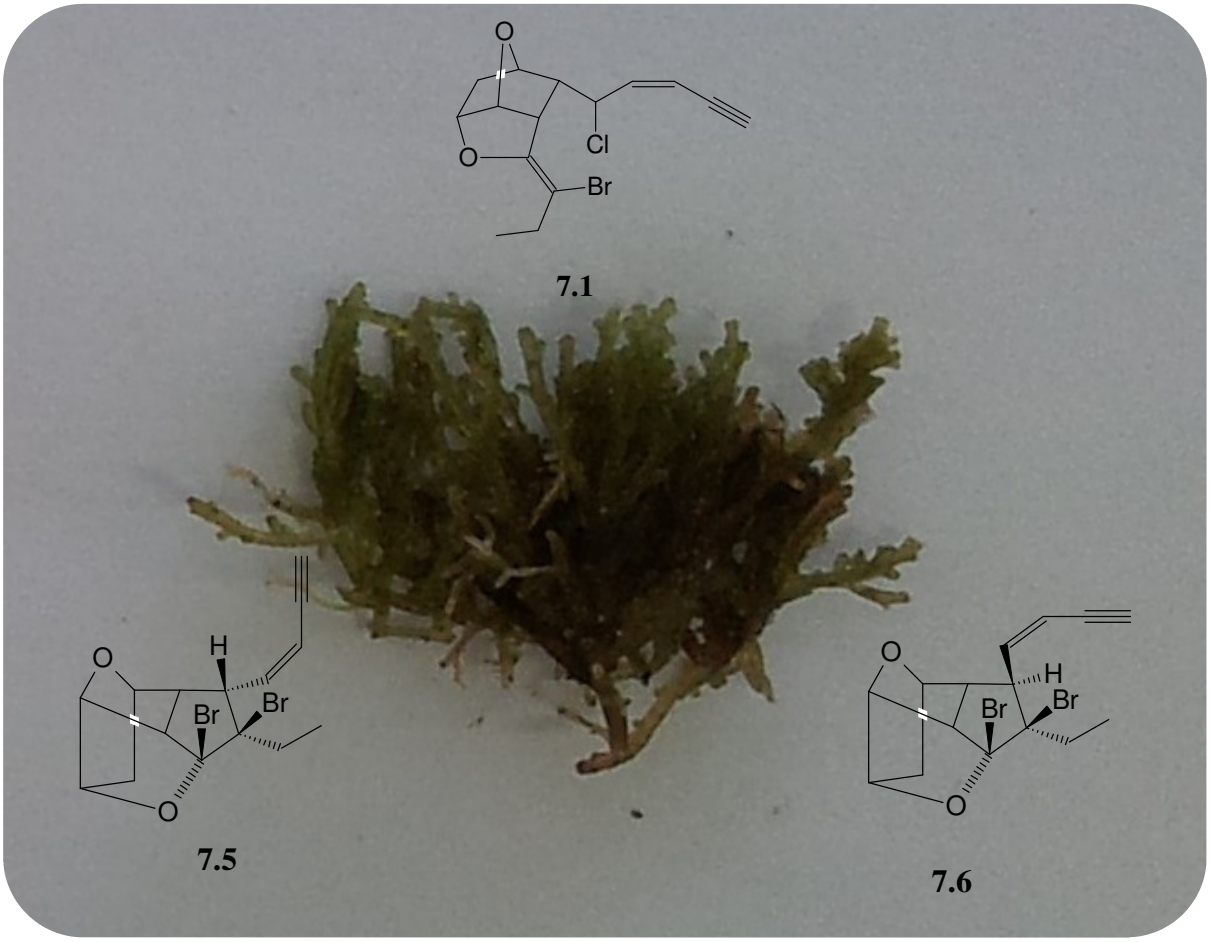

Chapter 7

Secondary metabolites from *Laurencia multiclavata*

7.1 Introduction

Laurencia multiclavata, a newly described species by Francis, (2014), is morphologically similar to *Laurencia natalensis*, however, the branching patterns within the two species are noted to be quite distinct. Furthermore *L. multiclavata* shows an average of three *corps en cerise* per cell whereas *L. natalensis* only contains one *corps en cerise* per cell (Francis, 2014). Plants of *L. multiclavata* are green with purple apices and usually grow 8 cm high. Branchlets possess many stud like projections as seen in (Figure 7.1, Plate A) (*multiclavata*: many studs). The species is epilithic and grows mainly on exposed ledges in the intertidal zone and is distributed along the south coast of South Africa extending eastward (Francis, 2014).

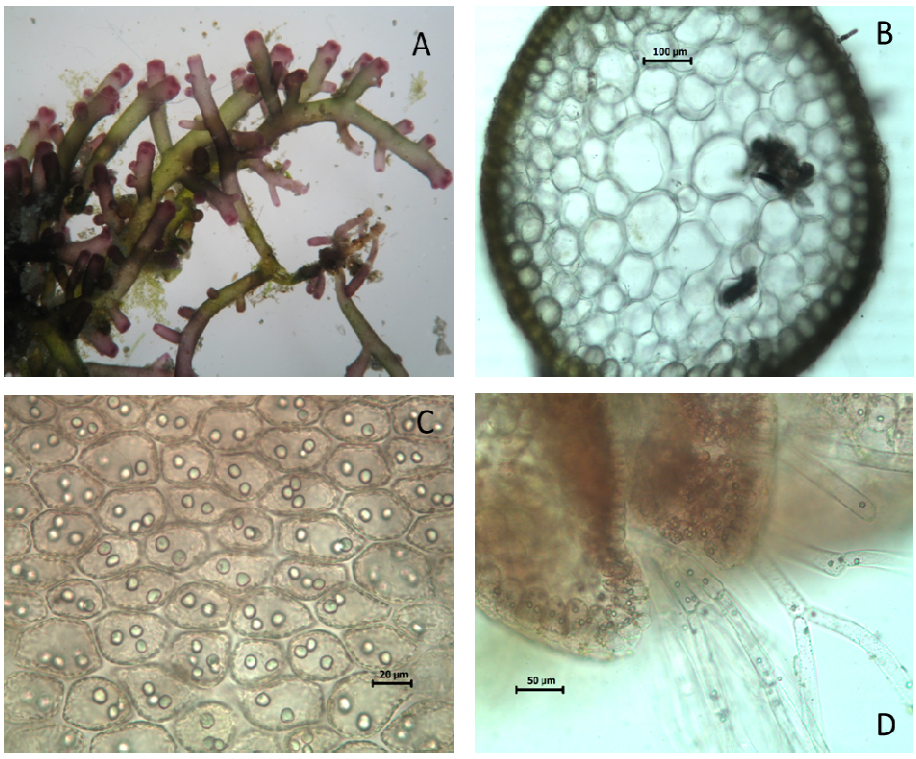

Figure 7.1: *Laurencia multiclavata*[1] (Caitlynne Francis © 2014)

A) Thallus with dark pink tips (8x).
B) Transverse thallus section (10x).
C) Outer cortical cells with two-three *corps en cerise* (40x).
D) Trichoblasts containing two *corps en cerise* per cell (20x).

[1] Image plates courtesy of Caitlynne Francis © 2014, University of Cape Town, South Africa

7.2 Results and Discussion

7.2.1 Extraction and isolation of metabolites from *L. multiclavata* (D969, Cape Vidal)

The extraction procedure followed that in section **3.2.1** (chapter 3, page 54). The ^{1}H NMR spectrum (Figure 7.2) of the crude *L. multiclavata* extract showed a wealth of methine resonances between δ_H 2.6-6.5. A series of purification attempts of the silica gel step gradient fraction C using normal phase HPLC led to the successful isolation of three major metabolites, compounds **7.1**, **7.5** and **7.6** (Scheme 7.1). This was despite a relatively small yield of organic extract i.e. 84 mg.

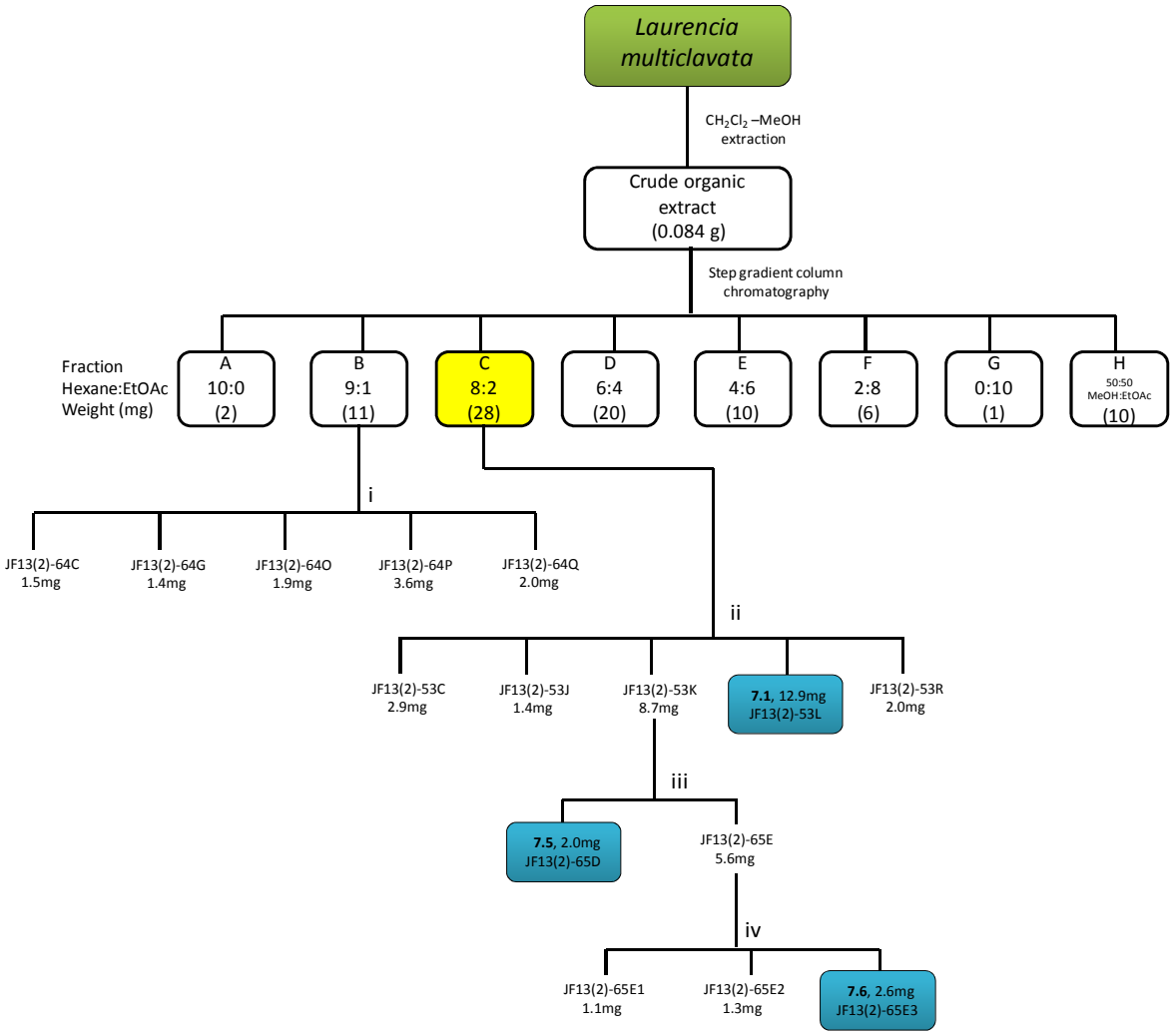

Scheme 7.1: Isolation scheme of metabolites from *L. multiclavata* (D969)

Conditions: i) Normal phase HPLC (9:1 hex:EtOAc); ii) Normal phase HPLC (4:1 hex:EtOAc); iii) Normal phase HPLC (19:1 hex:EtOAc); iv) Normal phase HPLC (49:1 hex:EtOAc)

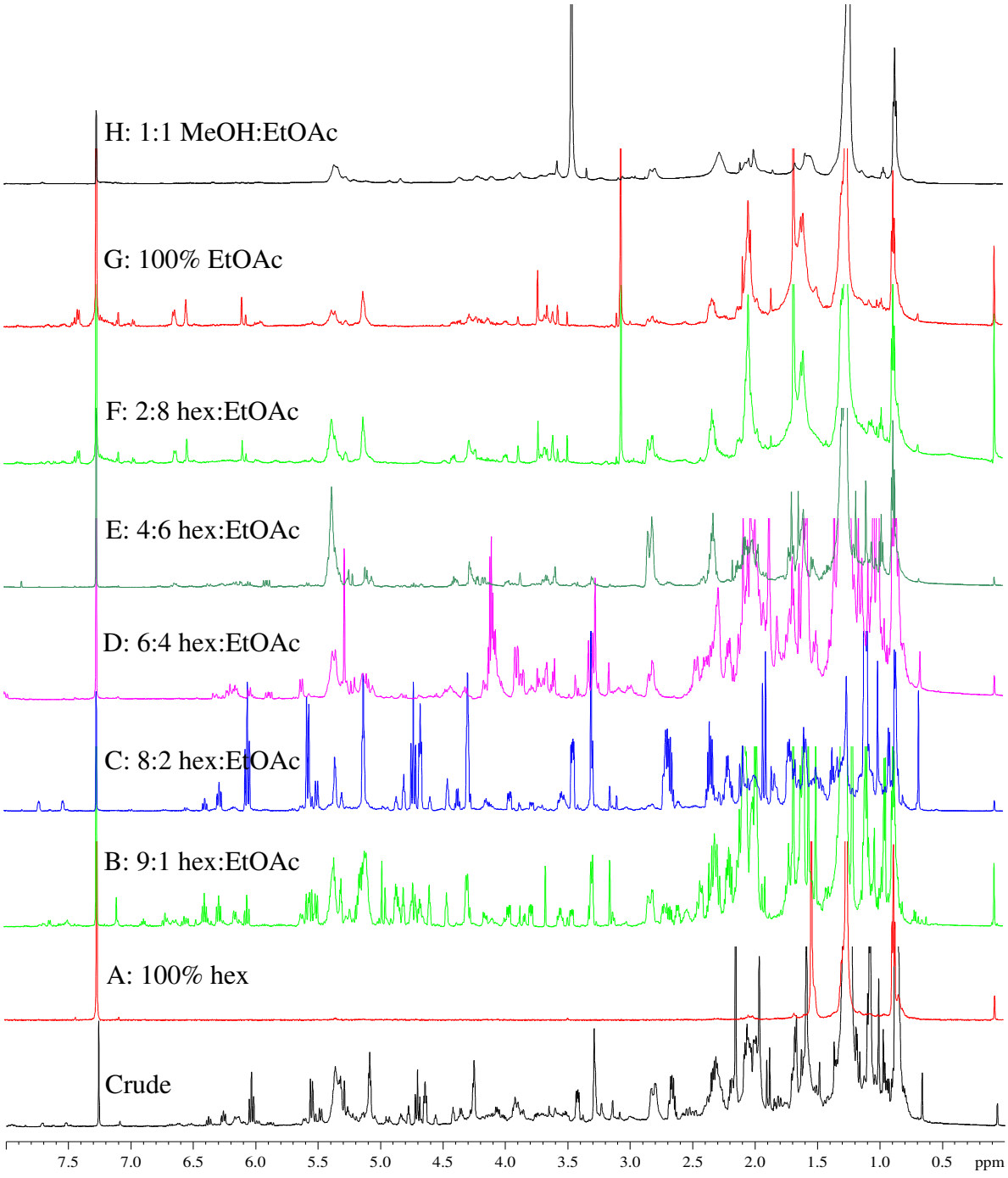

Figure 7.2: ^{1}H NMR spectra ($CDCl_3$, 600 MHz) of the crude organic extract of *L. multiclavata* (D969) and step gradient column fractions A-H

7.2.2 Structure elucidation of metabolites

7.2.2.1 Compound 7.1

A seemingly overwhelming ^{1}H NMR spectrum (Figure 7.3) belonging to compound **7.1**, a dense orange oil, displayed a surplus of methine moieties of varying splitting patterns. Of initial interest was a broad terminal alkyne singlet at δ_H 3.30 as well as an ABC spin system with an olefinic doublet at δ_H 5.57, an olefinic triplet at δ_H 6.05 and a halo-methine triplet at δ_H 4.72 (all three protons showing a coupling constant of J = 10.4 Hz).

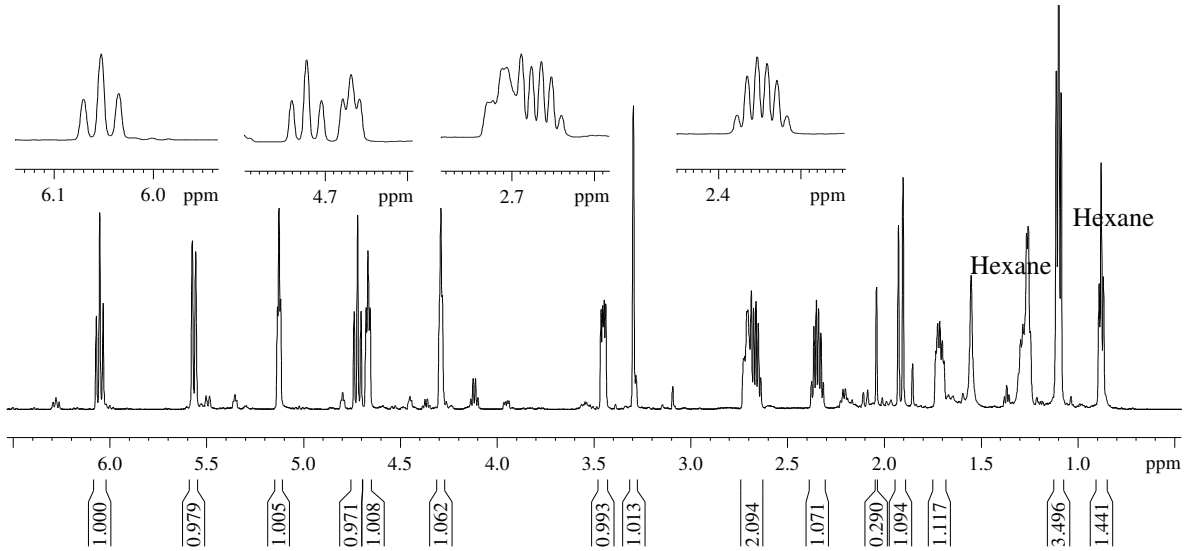

Figure 7.3: ^{1}H NMR spectrum ($CDCl_3$, 600 MHz) of compound **7.1**

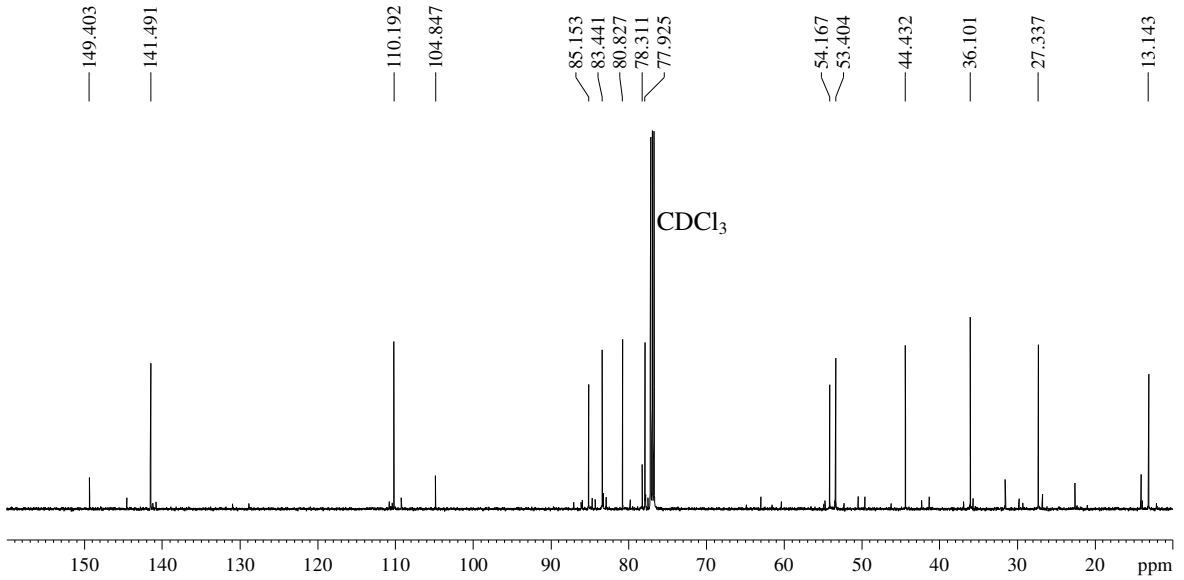

Figure 7.4: ^{13}C NMR spectrum ($CDCl_3$, 150 MHz) of compound **7.1**

After considering ^{13}C NMR resonances at (δ_C 85.2, 78.4, 110.6, 14.6 and 54.4) (Figure 7.4) it was clear that a *cis*-alkenyne side chain was present within compound **7.1** .This was further confirmed by a terminal acetylenic ≡C-H stretch at 3281 cm^{-1} in the IR spectrum of compound **7.1** (Figure 7.5).

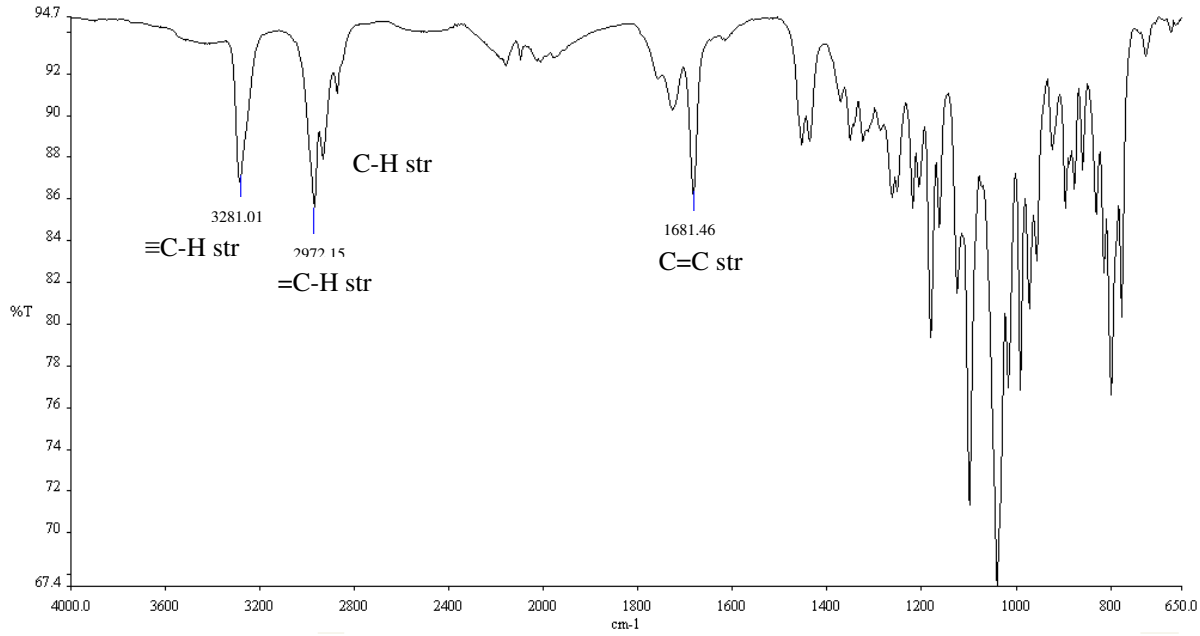

Figure 7.5: IR spectrum of compound **7.1**

Fragment **A** below shows the proposed alkenyne side chain in compound **7.1**. It was ascertained that the more deshielded proton resonance H5 (δ_H 4.72) implied possible halo-substitution. Conversely a markedly shielded ^1H NMR resonance at H6 (δ_H 2.71) suggested no heteroatom substitution at the tertiary carbon C6.

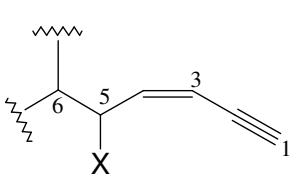

A

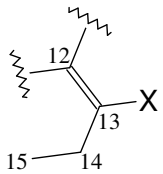

B

The ^1H NMR spectrum of compound **7.1** (Figure 7.3) additionally exposed an isolated ethyl moiety as confirmed by a methyl triplet at δ_H 1.10 as well as magnetically non-equivalent methylene protons appearing as sextets (J = 7.3 Hz) at δ_H 2.35 and δ_H 2.67. Scrutiny of HMBC correlations from both methyl and ethyl moieties at C14 and C15 revealed neighbouring quaternary carbons C12 and C13 (δ_C 149.4 and 104.9), confirming that the

butenyl functionality C12-C15 contained a tetra-substituted olefin as shown in fragment **B** above.

The ^{13}C NMR data (Figure 7.4) revealed one methyl (δ_C 13.14), two methylene (δ_C 27.3 and 36.1), nine methine (δ_C 44.4, 53.4, 54.2, 78.0, 80.8, 83.4, 85.2, 110.2 and 141.5) and three quaternary (δ_C 78.3, 104.9 and 149.4) resonances.

Of the nine methine resonances identified, it was evident that three carbon atoms (δ_C 78.0, 80.8 and 83.4) were oxygen bearing. The absence of hydroxyl and carbonyl stretches in the IR spectrum of compound **7.1,** in conjunction with sharp C-O bands at 1100 cm^{-1} (Figure 7.1), suggested that the three aforesaid carbon atoms were part of ether linkages.

Based on the above spectroscopic data, compound **7.1** was identified as *cis*-maneone C, a tri-cyclic C_{15} acetogenin previously described by Waraszkiewicz *et al*., (1978) from a Hawaiian sample of *Laurencia nidifica* in conjunction with isomers **7.2-7.4**.

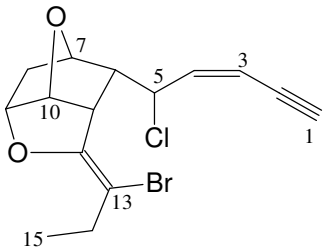

7.1

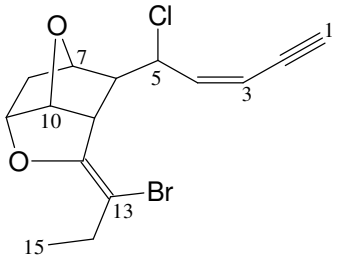

7.2

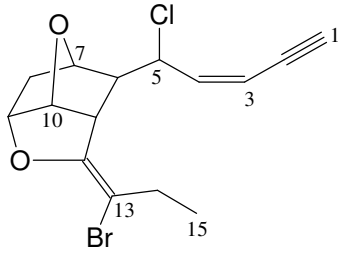

7.3

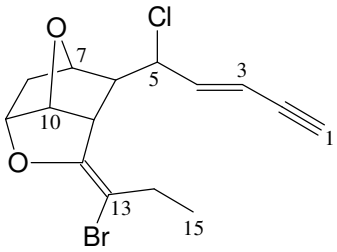

7.4

The relative configuration at C6 in compound **7.1** was clearly confirmed by NOESY correlations from the *exo* proton H6 (δ_H 2.71) to proton H7 (δ_H 4.29). Moreover, the coupling constants $J_{6,7}$ and $J_{6,11}$ are typical for an *exo* H6 (Waraszkiewicz *et al*., 1978).

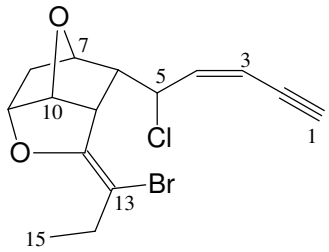

7.1

Table 7.1: NMR spectroscopic data of compound **7.1**

Carbon No	δ_C	δ_C **mult**	δ_H, **mult, J (Hz)**
1	85.2	CH	3.30, s
2	78.3	C	-
3	110.2	CH	5.57, d, 10.4
4	141.5	CH	6.05, t, 10.4
5	54.2	CH	4.72, t, 10.4
6	53.4	CH	2.71, dt, 10.4, 4.3, 4.3
7	77.9	CH	4.29, t, 4.3
8a	36.1	CH_2	1.72, m
8b			1.92, d, 14.5
9	80.8	CH	4.67, t, 5.9
10	83.4	CH	5.13, t, 5.9
11	44.4	CH	3.45, dd, 9.6, 5.9
12	149.4	C	-
13	104.9	C	-
14a	27.3	CH_2	2.35, sex, 7.3
14b			2.67, sex, 7.3
15	13.1	CH_3	1.10, t, 7.3

7.2.2.2 Compounds 7.5 and 7.6

A clear oil containing an isomeric mixture of compounds **7.5** and **7.6,** appearing in a 2:1 ratio, was successfully purified by normal phase HPLC (49:1 hex:EtOAc) as shown below (Figure 7.6). An assortment of methine signals in the region of δ_H 2.5-6.5 in the ^{1}H NMR spectra of both isomers **7.5** and **7.6** (Figure 7.6) was noticed.

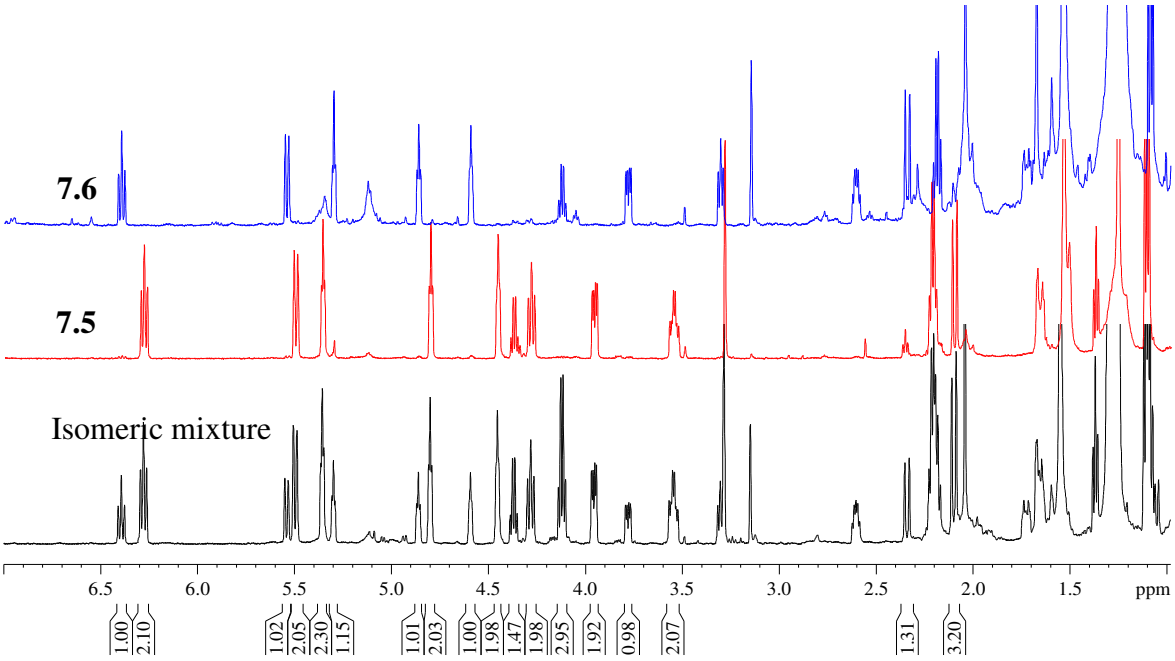

Figure 7.6: ^{1}H NMR spectra ($CDCl_3$, 600 MHz) of compounds **7.5** and **7.6**

The ^{1}H NMR spectrum of compound **7.5** (Figure 7.7) showed a similar acetylenic side chain to that observed in compound **7.1** i.e. δ_H 3.29 (s), δ_H 5.55 (d, J = 10.9 Hz), δ_H 6.28 (t, J = 9.6 Hz) and δ_H 4.29 (t, J = 9.6 Hz).

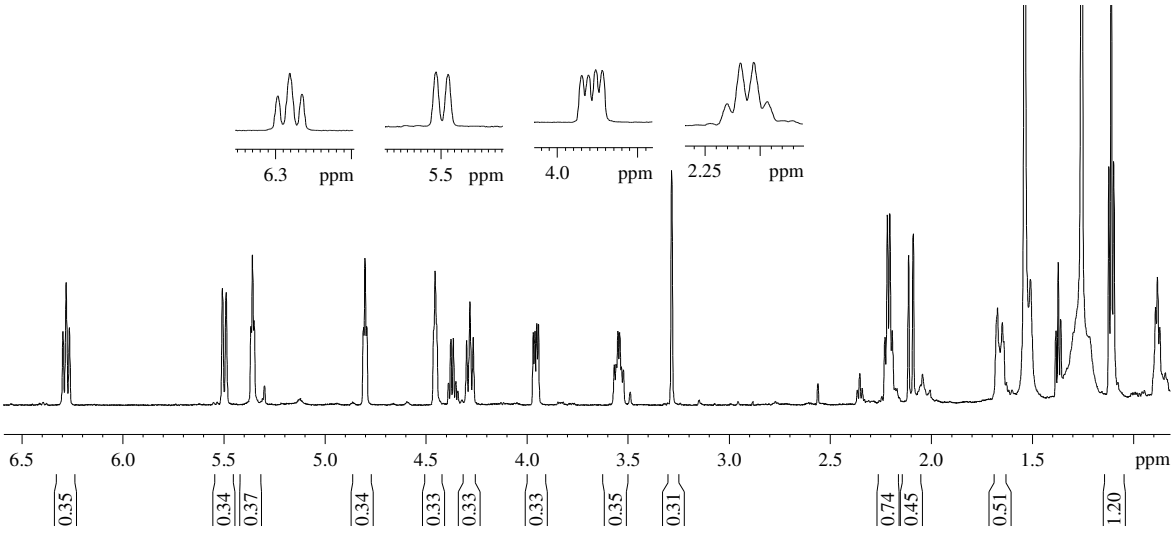

Figure 7.7: ^{1}H NMR spectrum ($CDCl_3$, 600 MHz) of compound **7.5**

On closer inspection, ^{13}C and COSY NMR data of compound **7.5** (Figure 7.8 and 7.9) revealed that the acetylenic side chain in compound **7.5** (fragment **C**) appeared to be truncated *vs*. that of compound **7.1** with C5 now assuming a tertiary alkyl methine function (δ_C 49.7) as opposed to a halo-methine moiety as seen in compound **7.1.**

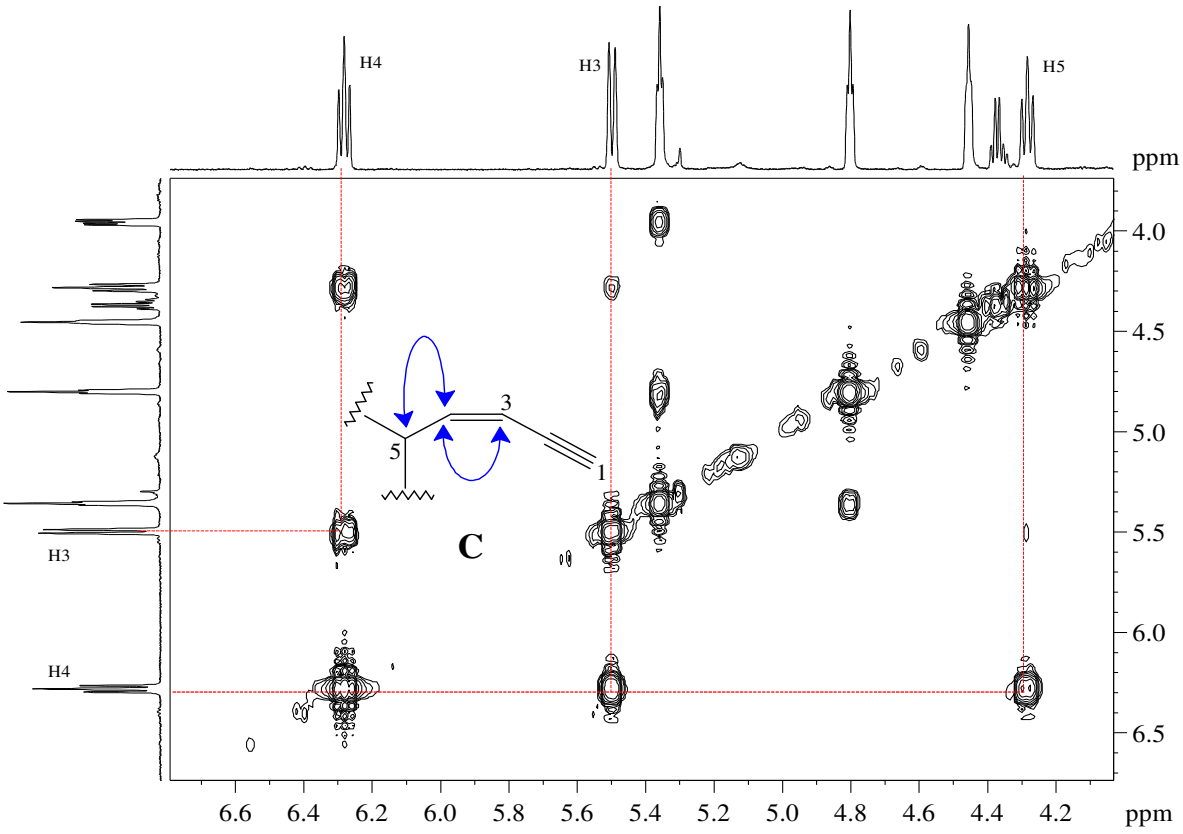

Figure 7.8: Partial COSY spectrum of compound **7.5** showing key correlations

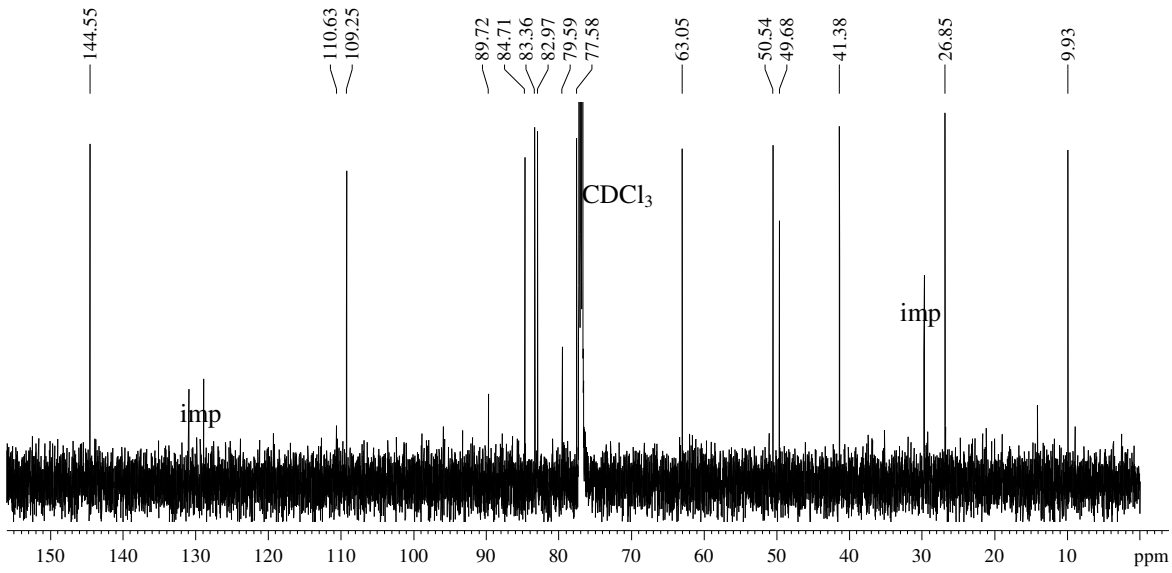

Figure 7.9: ^{13}C NMR spectrum ($CDCl_3$, 150 MHz) of compound **7.5**

A terminal ethyl moiety was assigned in compound **7.5** as the ^{1}H NMR spectrum (Figure 7.7) presented a triplet at δ_H 1.13 (J = 7.7 Hz) as well as a methylene quartet at δ_H 2.22 (J = 7.7 Hz). Considering a quaternary ^{13}C NMR chemical shift (Figure 7.9) at C13 (δ_C 89.7), the terminal ethyl moiety in compound **7.5** assumed part of a propanyl unit, as shown in fragment **D**, as opposed to a butenyl unit as in compound **7.1**.

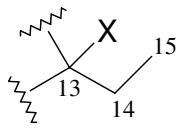

D

With the elucidation of the side chains (fragments **C** and **D**) in compound **7.5** it was evident that the remaining carbons C5-C13 formed part of a multi-cyclic entity. This was established as three oxygen bearing methine carbons (δ_C 77.6, 83.0 and 83.4), two alkyl methine carbons (δ_C 49.7 and 50.5), a further two quaternary carbons (δ_C 89.7 and 110.6) and one methylene carbon (δ_C 41.4) were identified from ^{13}C NMR as well as edited HSQC and HMBC NMR data.

Based on the above NMR spectroscopic data, compound **7.5** was elucidated as *iso*-maneonene A, a complex, caged, tetra-cyclic acetogenin isolated by Waraszkiewicz *et al*., (1978) from the same *Laurencia nidifica* sample whence compound **7.1** was isolated.

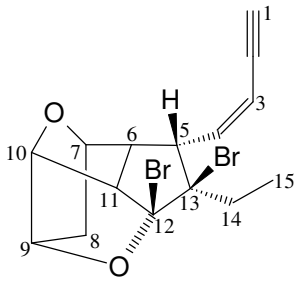

7.5

The stereochemistry at C5 was assigned by virtue of unambiguous NOESY correlations between H5 (δ_H 4.29, t, J = 11 Hz) and H6 (δ_H 3.54, m) as well as the consideration of coupling constants at both H5 and H11 (δ_H 3.96, dd, J =11, 5 Hz).

Compound **7.6** showed strikingly similar ^{1}H and ^{13}C NMR spectra (Figures 7.10 and 7.11) to that of the isomeric compound **7.5**

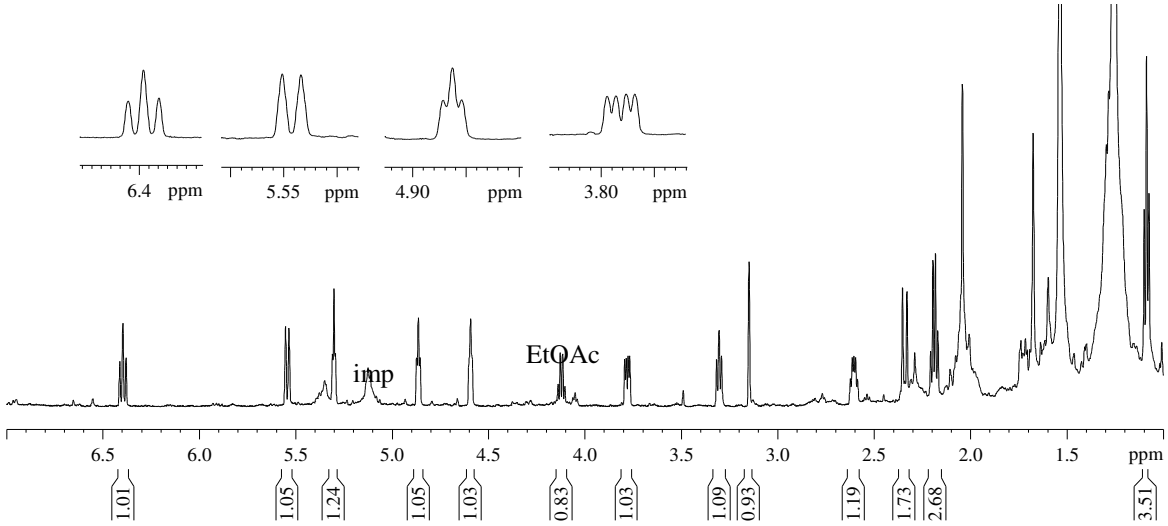

Figure 7.10: ^{1}H NMR spectrum ($CDCl_3$, 600 MHz) of compound **7.6**

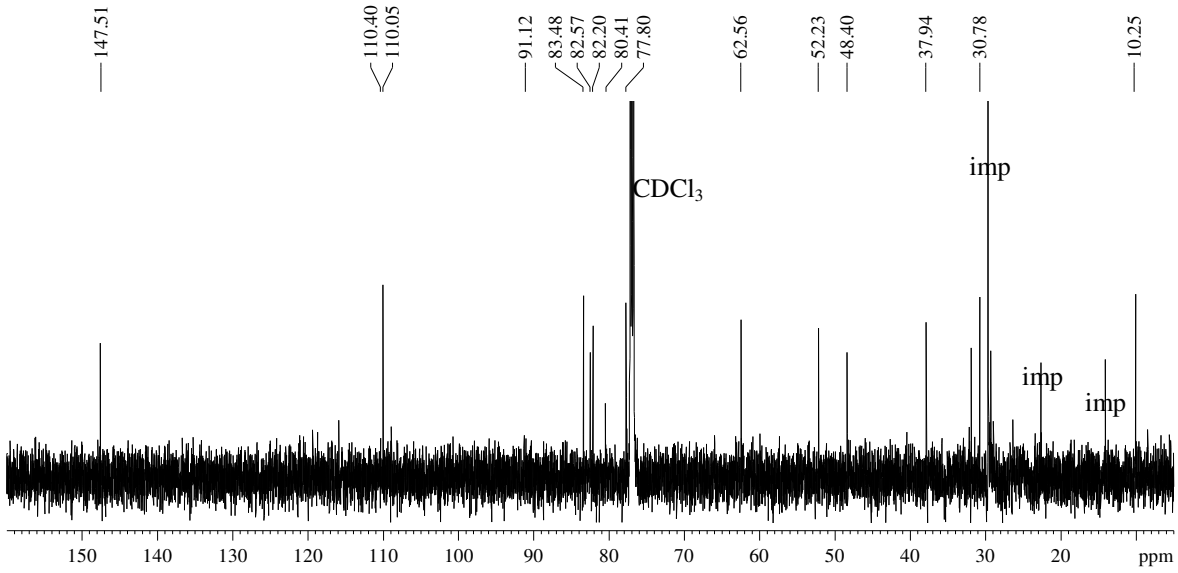

Figure 7.11: ^{13}C NMR spectrum ($CDCl_3$, 150 MHz) of compound **7.6**

The only fundamental spectral differences seen between compounds **7.5** and **7.6** were at positions C4, C5 and C6 as shown below in Table 7.2.

Table 7.2: Key differences in ^{1}H and ^{13}C chemical shifts of isomers **7.5** and **7.6**

	δ_H	
	7.5	**7.6**
H4	6.28	6.40
H5	4.29	3.31
H6	3.54	2.60

	δ_C	
	7.5	**7.6**
C4	144.6	147.5
C5	49.7	48.4
C6	50.5	52.2

To rule out the possibility of halogen variation in compound **7.6** its HREIMS spectrum was obtained (Figure 7.12). A molecular ion cluster was observed at *m/z* 385.9536 (calculated for 385.9517)/387.9524/389.9500 and the molecular formula was analogous to compound **7.5** i.e. $C_{15}H_{16}{}^{79}Br_2O_2$.

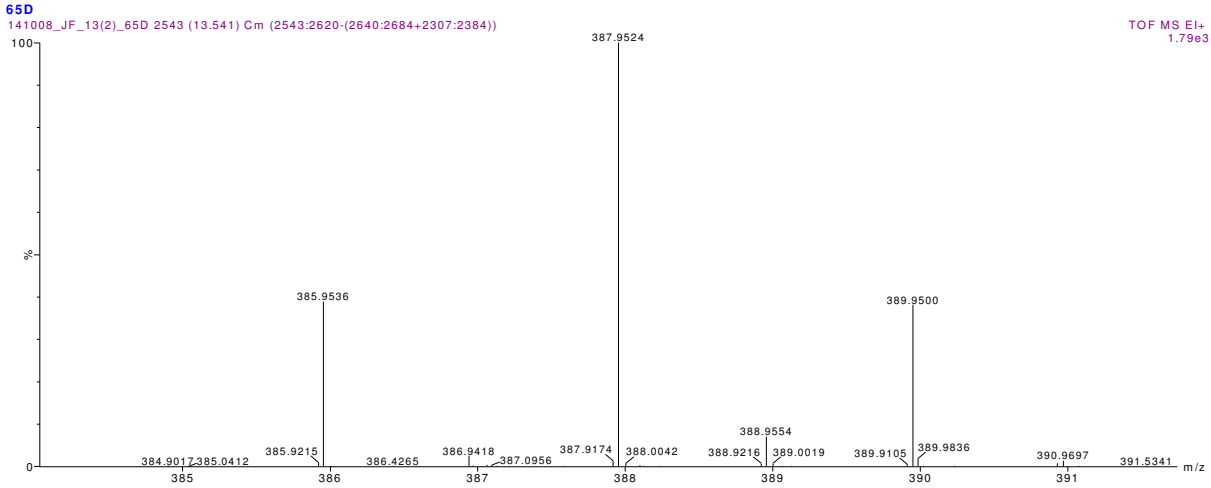

Figure 7.12: Expansion of the HRESIMS spectrum of compound **7.6**

Compounds **7.5** and **7.6** were consequently regarded as stereoisomers. NOESY correlations in compound **7.6** exposed the isomerism to be at position C5, wherein the acetylenic side chain now adopted a *cis*-configuration with respect to the bromine atom at C13 as opposed to a *trans*-configuration as in **7.5**.

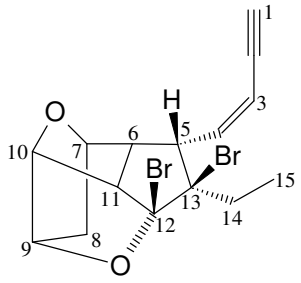

7.5

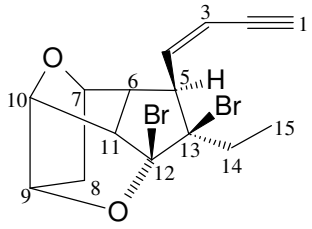

7.6

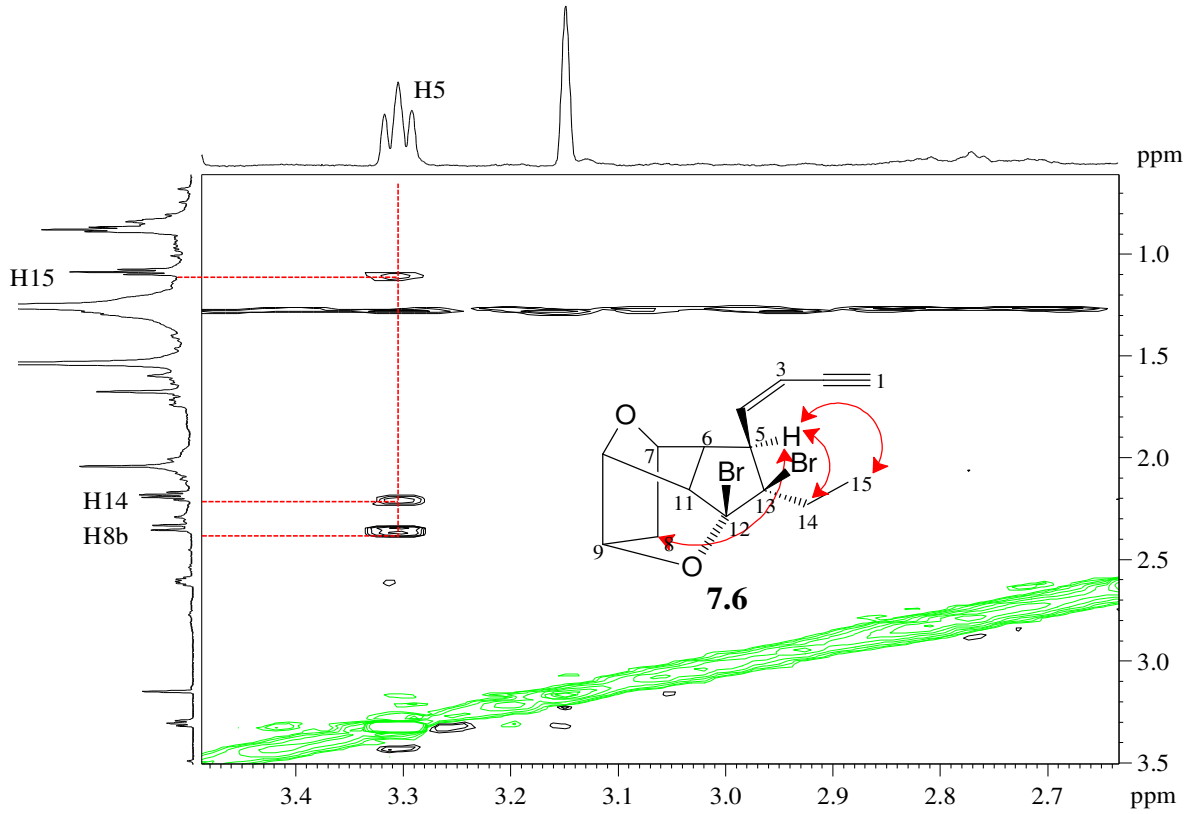

Figure 7.13: Partial NOESY spectrum of compound **7.6** showing key correlations

Compound **7.6** was identified as lembyne B, isolated by Vairappan *et al*., (2001) from an unidentified Malaysian *Laurencia* sp.

An epimer at position C13, *iso*-maneonene B (compound **7.7**) has also been reported by Waraszkiewicz *et al*., (1978) wherein stereo-assignments at C13 were made based on the effects of the C13-bromine substituent on proton chemical shifts, H5, H6 and H11. The complex carbon skeleton of **7.7** was deduced by X-ray analysis (Waraszkiewicz *et al*., 1978).

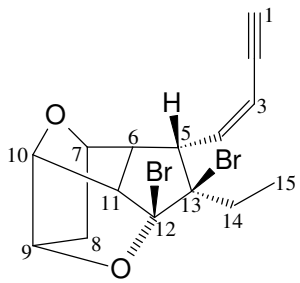

7.5
iso-maneonene A

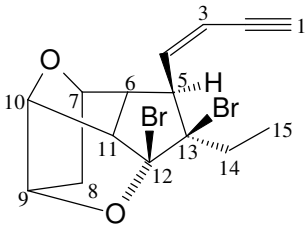

7.6
lembyne B

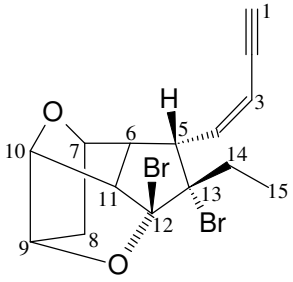

7.7
iso-maneonene B

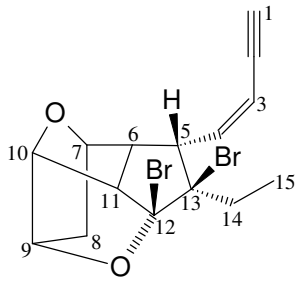

7.5

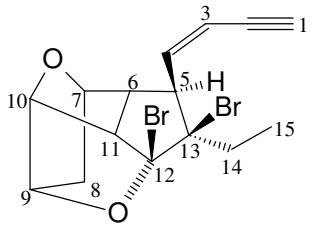

7.6

Table 7.3: NMR spectroscopic data of compounds **7.5** and **7.6**

			Compound **7.5**		Compound **7.6**
Carbon No	**δ_C mult**	**δ_C**	**δ_H, mult, J (Hz)**	**δ_C**	**δ_H, mult, J (Hz)**
1	CH	84.7	3.29, s	82.6	3.15, s
2	C	79.6	-	80.6	-
3	CH	109.3	5.55, d, 11.0	110.1	5.54, d, 11.0
4	CH	144.6	6.28, t, 10.5	147.5	6.40, t, 11.0
5	CH	49.7	4.29, t, 11.0	48.4	3.31, t, 6.8
6	CH	50.5	3.55, m	52.2	2.60, m
7	CH	77.6	4.45, t, 5.4	77.8	4.59, t, 5.4
8a	CH_2	41.4	1.67, d, 13.6	37.9	1.73, m
8b			2.10, d, 13.6		2.34, d, 13.6
9	CH	83.4	4.80, t, 5.4	83.5	4.86, t, 5.4
10	CH	83.0	5.37, t, 5.4	82.2	5.31, t, 5.4
11	CH	63.1	3.96, dd, 11.0, 5.4	62.6	3.78, dd, 10.8, 5.2
12	C	110.6	-	110.4	-
13	C	89.7	-	91.1	-
14	CH_2	26.9	2.22, q, 7.7	30.8	2.18, q, 7.9
15	CH_3	9.9	1.13, t, 7.7	10.3	1.09, t, 7.9

7.3 Experimental

7.3.1 General Experimental

As per section **3.3.1** in chapter 3, page 54.

HREIMS as per chapter section **4.3.2.2** in chapter 4, page 90.

7.3.2 Plant material (*L. multiclavata*, D969)

L. multiclavata was collected by hand at Cape Vidal on the east coast of South Africa in March 2011. A voucher specimen has been stowed away in the Bolus Herbarium at the University of Cape Town, South Africa. Identification of the alga was done by Professor John Bolton with the Department of Biological Sciences at the University of Cape Town, South Africa.

7.3.3 Extraction and isolation of metabolites

Same procedure as described in section **3.3.3**, page 54 (dry mass 7.07 g, crude extract 0.084 g, 1.2% yield).

Step gradient fraction C was subjected to normal phase HPLC using (9:1 hex:EtOAc) yielding compound **7.1** (12.9 mg, 0.180%). By decreasing the polarity of the HPLC solvent system to (19:1 hex:EtOAc) compound **7.5** eluted (2.0 mg, 0.028%). Finally an HPLC solvent system significantly less polar than preceding ones (49:1 hex:EtOAc) was instrumental in the purification of **7.6** (2.6 mg, 0.028%) from a mixture with **7.5**.

7.3.4 Compounds isolated

7.3.4.1 Compound 7.1 (JF13(2)-53L)

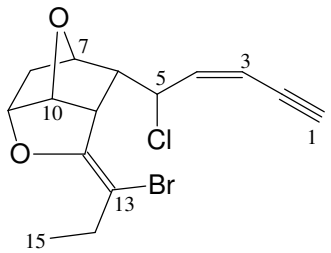

7.1

Cis-maneonene C (**7.1**): Orange oil; ^{1}H and ^{13}C NMR ($CDCl_3$) data available in Table 7.1. As previously reported by Waraszkiewicz *et al*., (1978).

7.3.4.2 Compound 7.5 (JF13(2)-65E3)

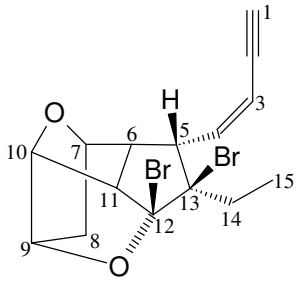

7.5

Iso-maneonene A (**7.5**): Clear oil; ^{1}H and ^{13}C NMR ($CDCl_3$) data available in Table 7.3. As previously reported by Waraszkiewicz *et al*., (1978).

7.3.4.3 Compound 7.6 (JF13(2)-65D)

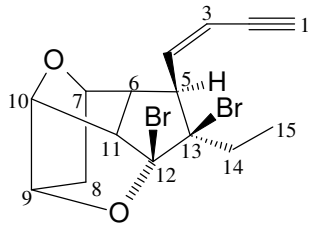

7.6

Lembyne B (**7.5**): Clear oil; ^{1}H and ^{13}C NMR ($CDCl_3$) data available in Table 7.3. As previously reported by Vairappan *et al*., (2001).

7.4 References

Francis, C. M. **2014**. Systematics of the *Laurencia* complex (Rhodomelaceae, Rhodophyta) in southern Africa. PhD Thesis. University of Cape Town, Cape Town, South Africa.

Vairappan, C. S; Daitoha, M.; Suzuki, M.; Abe, T.; Masuda, M. Antibacterial halogenated metabolites from the Malaysian *Laurencia* species. *Phytochemistry* **2001**, *58*, 291-297.

Waraszkiewicz, S. M.; Erickson, K. L.; Sun, H. H.; Clardy, J.; Finer, J. C_{15} halogenated compounds from the hawaiian marine alga *Laurencia nidifica*. Maneonenes and isomaneonenes. *Journal of Organic Chemistry* **1978**, *43*, 3194-3204.

Chapter 8

Secondary metabolites from *Laurencia flexuosa*

Abstract

Laurencia flexuosa has previously been investigated by Mann (2008) and Knott (2011). A re-investigation into the secondary metabolites of this species yielded previously isolated isomers 3*Z* and 3*E*-bromofucin (**8.1** and **8.2**). Compound **8.5**, previously isolated from *Laurencia obtusa*, was reported from *Laurencia flexuosa* herein for the first time.

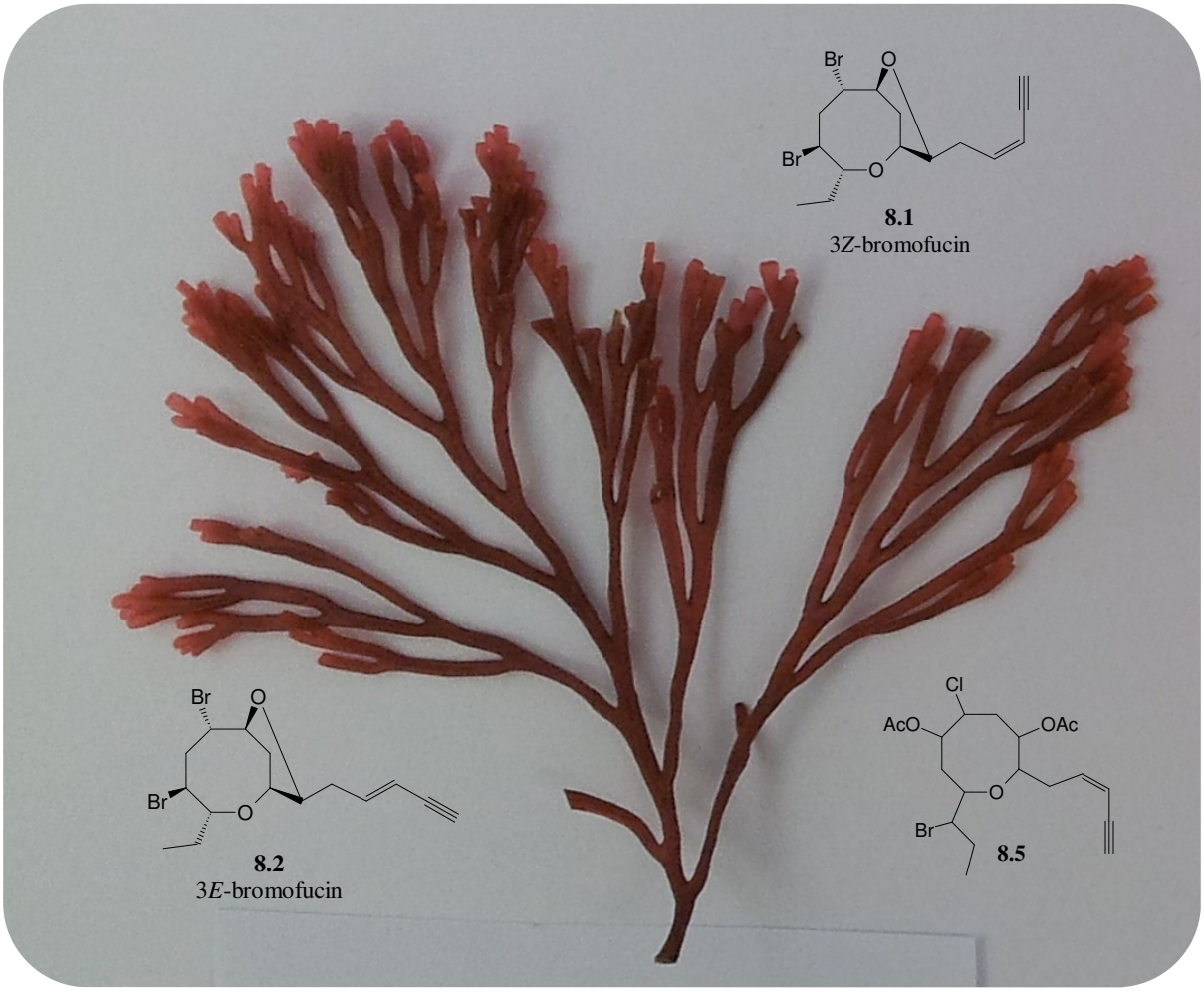

Chapter 8

Secondary metabolites from *Laurencia flexuosa*

8.1 Introduction

Laurencia flexuosa is South African endemic stretching from the south coast to the east coast. This particular species of *Laurencia* is known for its rose red hue and alternating branching pattern (*flexuosa*: bending branches) with plants growing up to 12 cm high (De Clerck *et al*., 2005; Francis, 2014). It is found commonly on wave exposed surfaces in the intertidal zone forming tufts. Cortical cells possess one-three *corps en cerise* (Figure 8.1) (De Clerck *et al*., 2005; Francis, 2014). There has been confusion distinguishing *L. flexuosa* from South African specimens of *L.* cf. *elata*, however, Francis (2014) shows significant *rbc*L sequence diversion, classifying both as separate species. Furthermore *L.* cf. *elata* possesses five-six *corps en cerise* per cortical cell (Francis, 2014).

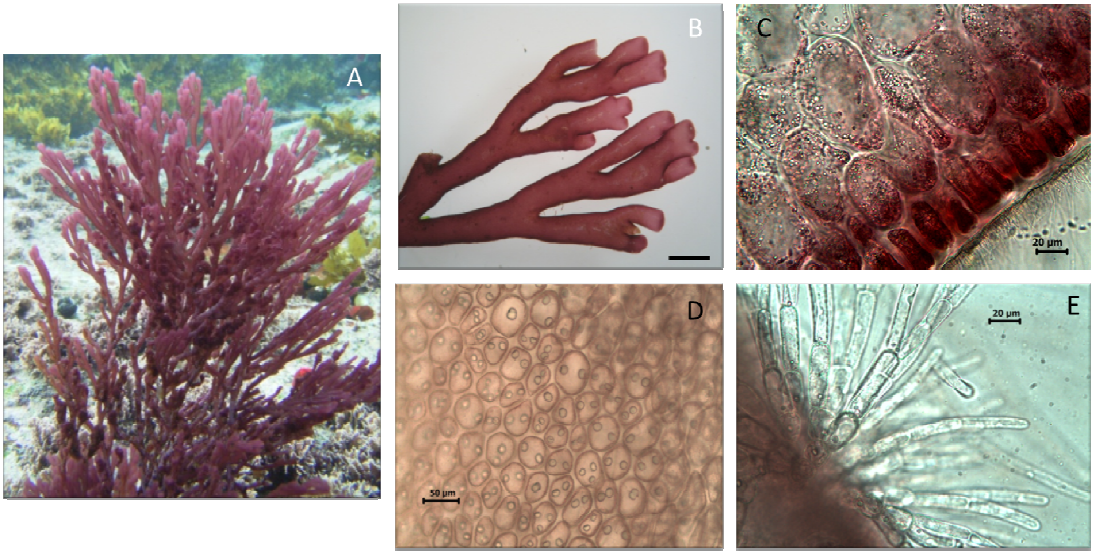

Figure 8.1: *Laurencia flexuosa*[1] (Caitlynne Francis © 2014)

A) Habit.

B) Branching pattern (higher order) (8x). Scale bar 1cm = 360µm

C) Thallus transverse section (40x).

D) Outermost cortical cells showing one-three *corps en cerise* per cell (20x).

E) Trichoblasts with one *corps en cerise* per cell (40x).

[1] Image plates courtesy of Caitlynne Francis © 2014, University of Cape Town, South Africa

8.2 Results and Discussion

8.2.1 Extraction and isolation of metabolites from *L. flexuosa* (D1013, Cape St. Francis)

After extraction and fractionation of the *L. flexuosa* crude as per section **3.2.1** (chapter 3, page 54), step gradient column fractions B and C (Figure 8.2) undoubtedly showed the most intriguing ^{1}H NMR resonances, with fraction D showing replicated resonances to fraction C. Numerous attempts at purifying a visible isomeric mixture in fraction B by way of silica gel column chromatography as well as normal phase HPLC proved ineffective. Although compound **8.1** was purified, the structure of compound **8.2** was elucidated in an isomeric mixture with **8.1**. Fraction C was purified by repeated silica gel column chromatography to afford compound **8.5**.

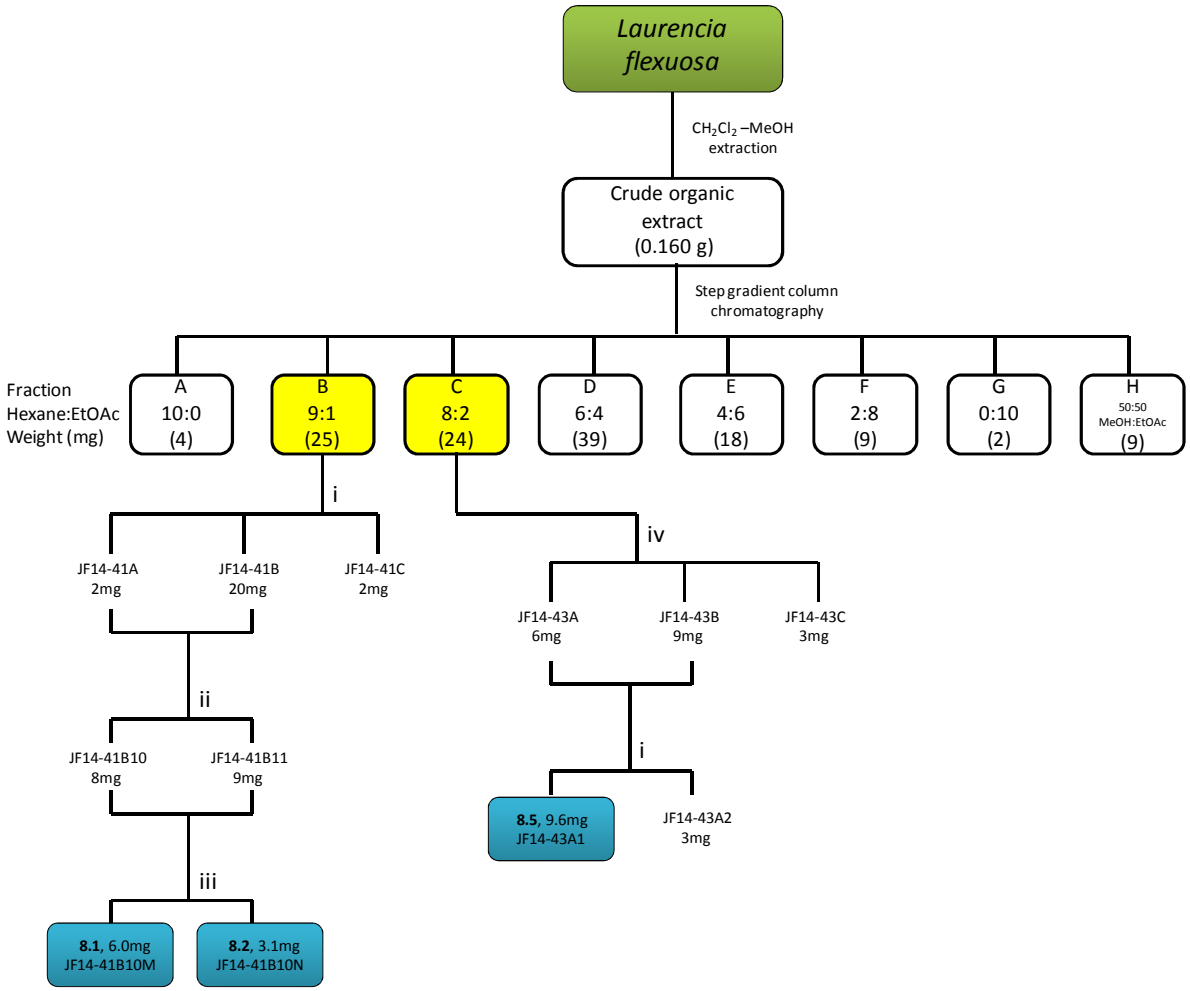

Scheme 8.1: Isolation scheme of metabolites from *L. flexuosa* (D1013)

Conditions: i) Silica gel column chromatography (9:1 hex:EtOAc); ii) Normal phase HPLC (19:1 hex:EtOAc); iii) Normal phase HPLC (49:1 hex:EtOAc); iv) Silica gel column chromatography (7:3 hex:EtOAc)

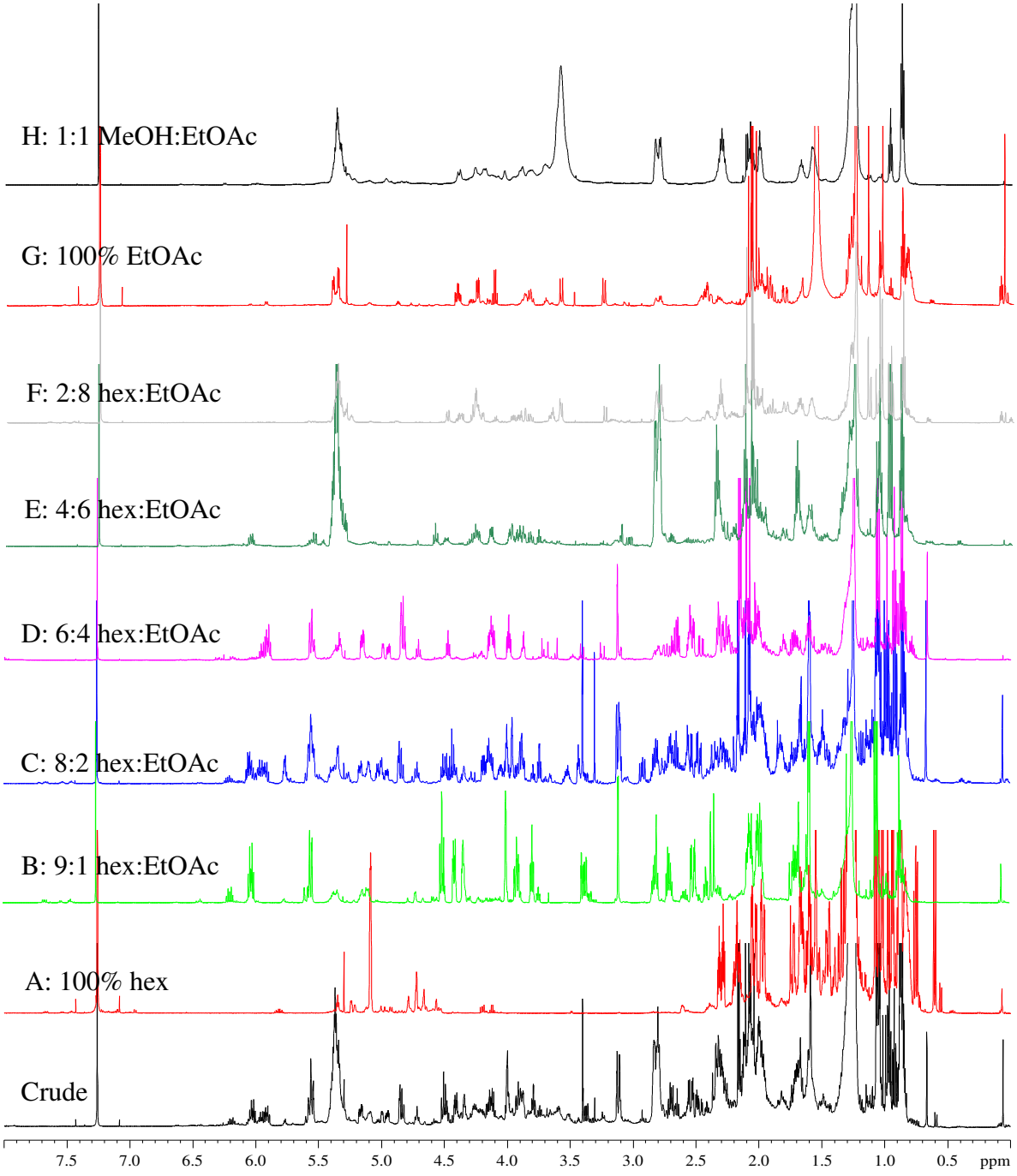

Figure 8.2: ^{1}H NMR spectra ($CDCl_3$, 600 MHz) of the crude organic extract of *L. flexuosa* (D1013) and step gradient column fractions A-H

8.2.2 Structure elucidation of metabolites

8.2.2.1 Compounds 8.1 and 8.2

Compound **8.1**, a dense orange oil, possessed a ^{1}H NMR spectrum (Figure 8.3) abundant in methine moieties between δ_H 2.5-6.5, the majority of which displayed unique splitting patterns. A *cis*-alkenyne terminus was deduced from ^{1}H NMR resonances at δ_H 3.11 (d, J = 1.8 Hz), δ_H 5.55 (m) and δ_H 6.03 (m).

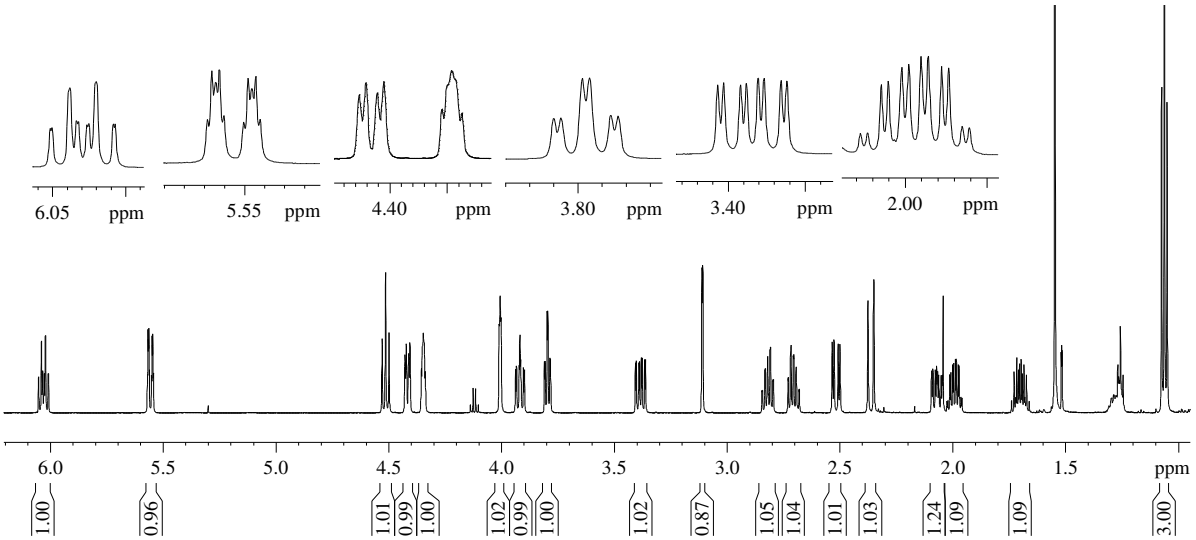

Figure 8.3: ^{1}H NMR spectrum ($CDCl_3$, 600 MHz) of compound **8.1**

The alkenyne was validated by ^{13}C NMR resonances (Figure 8.4) at δ_C 82.0. 80.1, 110.4 and δ_C 141.4. The IR spectrum (Figure 8.5) of compound **8.1** additionally bore testimony to the presence of alkyne functionality with a ≡C-H stretch at 3286 cm^{-1}.

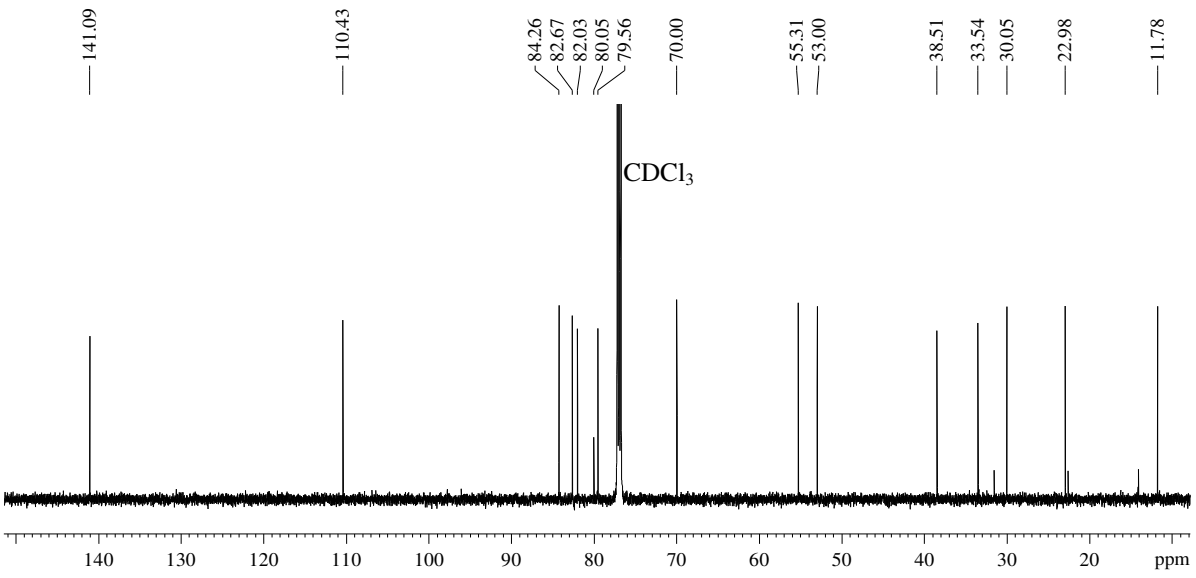

Figure 8.4: ^{13}C NMR spectrum ($CDCl_3$, 150 MHz) of compound **8.1**

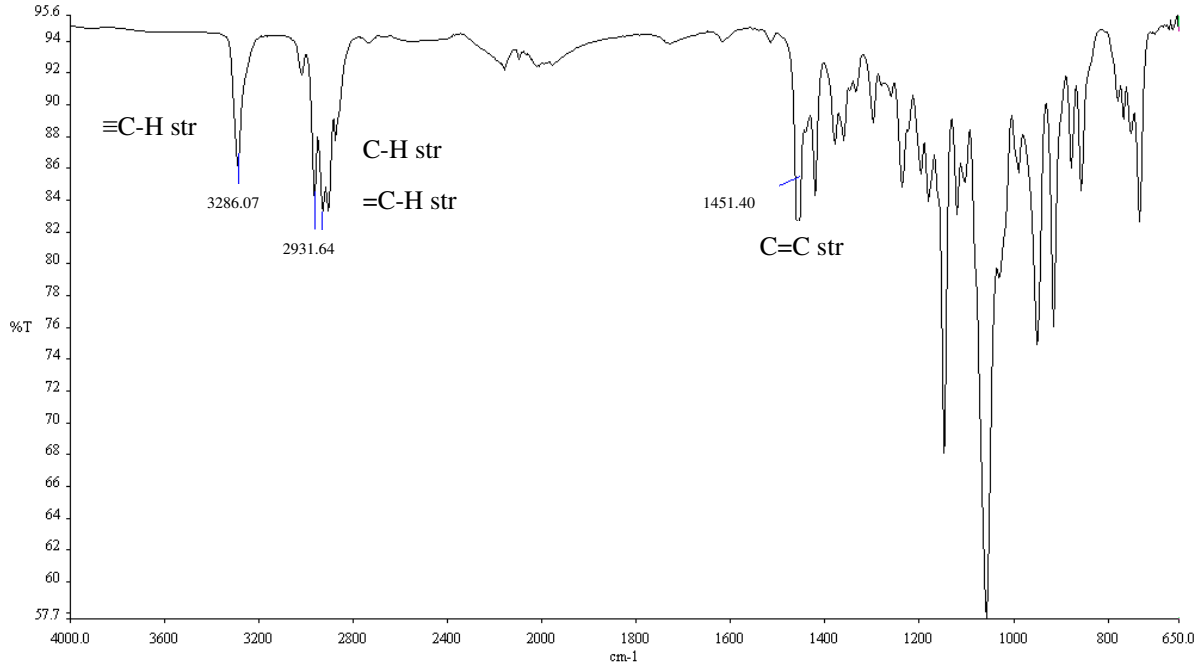

Figure 8.5: IR spectrum of compound **8.1**

The ^{13}C NMR spectrum (Figure 8.4) of compound **8.1** was also helpful in the assignment of two bromo-methine resonances at δ_C 53.0 and δ_C 55.3 as well as four oxy-methine carbons at δ_C 70.0, 79.6, 82.7 and δ_C 84.3 belonging to ether moieties.

The contiguous protonated nature of compound **8.1** enabled a relatively simple elucidation of the structure by analysis of NMR experiments, particularly the COSY spectrum.

Compound **8.1** was characterised as *cis*-bromofucin also known as 3*Z*-bromofucin. This eight membered heterocycle was previously isolated by McPhail *et al*., (2005) from a South African sea-hare.

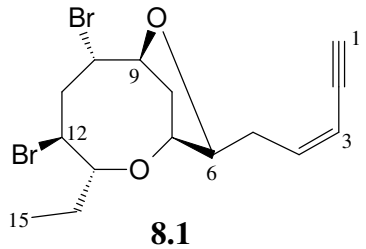

8.1
3*Z*-bromofucin

^1H and ^{13}C NMR data of compound **8.2** (Figures 8.6 and 8.7), isolated as a mixture with compound **8.1** (in five times less quantity) were strikingly similar to compound **8.1**. The only major spectral differences were viewed at the acetylenic terminus as shown below (Figure 8.8).

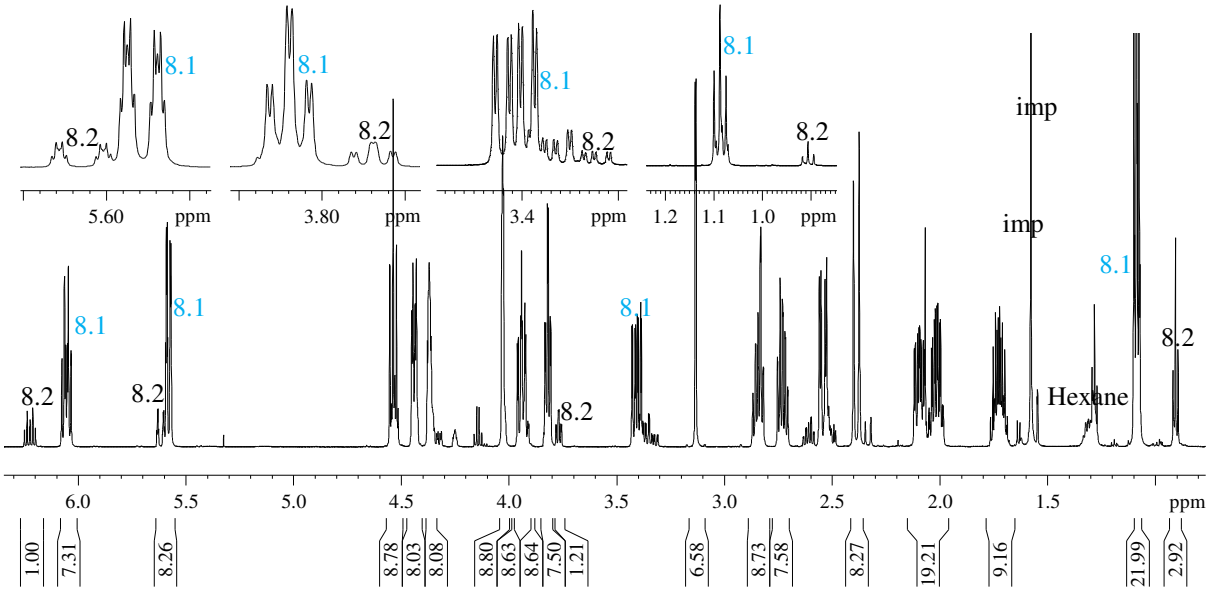

Figure 8.6: ^{1}H NMR spectrum ($CDCl_3$, 600 MHz) of compound **8.2** in a mixture with **8.1**

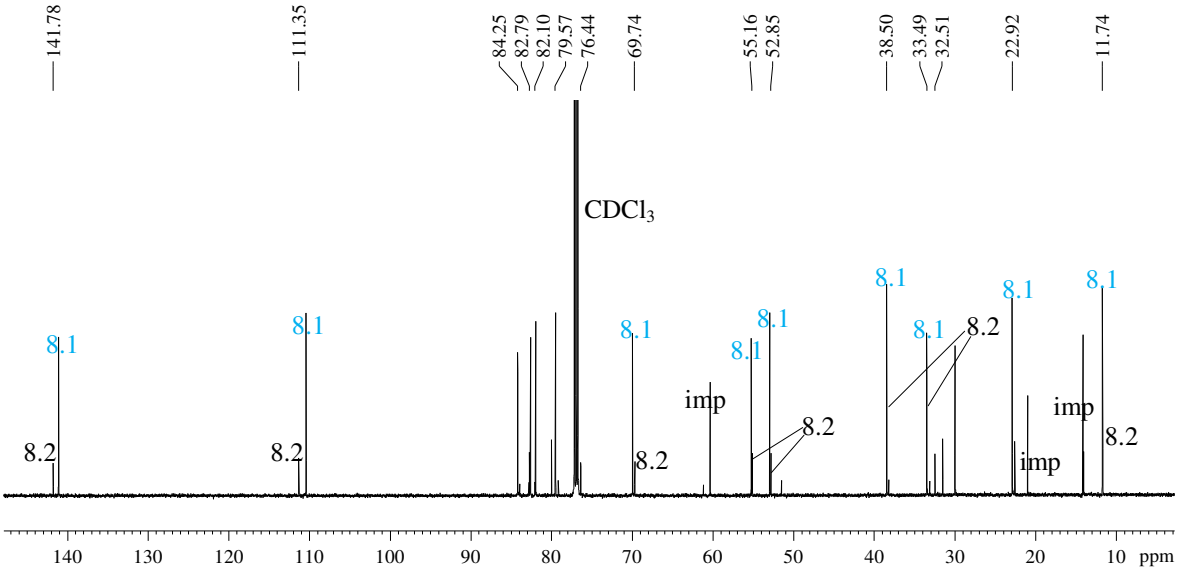

Figure 8.7: ^{13}C NMR spectrum ($CDCl_3$, 150 MHz) of compound **8.2** in a mixture with **8.1**

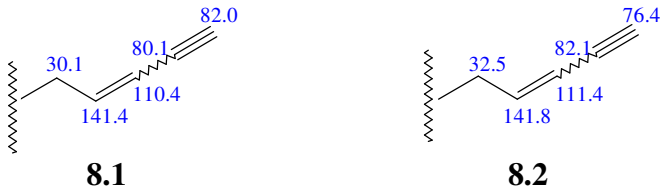

8.1 **8.2**

Figure 8.8: ^{13}C NMR ($CDCl_3$, 150 MHz) shifts of the terminal alkenyne moiety in compounds **8.1** and **8.2**

The differences in NMR spectral data depicted in compound **8.2** are consistent with geometrical isomerism at position C3 in compound **8.1** wherein compound **8.2** adopts a *trans* configuration at Δ^3.Compound **8.2** is 3*E*-bromofucin, initially reported by Coll *et al*., (1989) from *Laurencia intricata*. Similar eight membered acetogenins (**8.3** and **8.4**) to 3*Z* and 3*E*-bromofucin have been reported by Fukuzawa *et al*., (1972) and Howard *et al*., (1980).

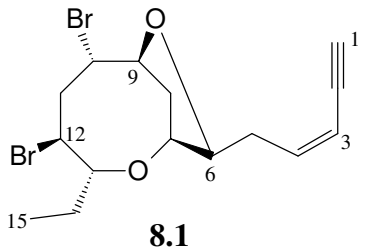

8.1
3*Z*-bromofucin

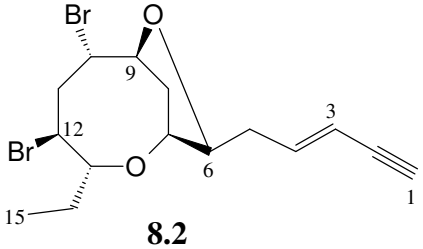

8.2
3*E*-bromofucin

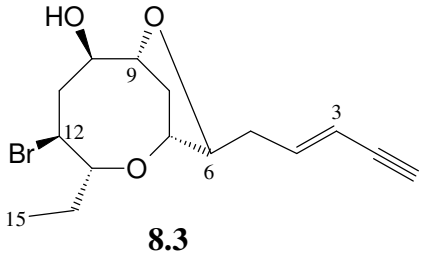

8.3
3*E*-laurefucin

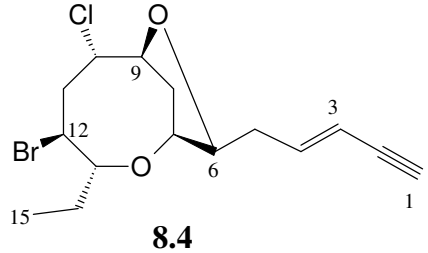

8.4
3*E*-chlorofucin

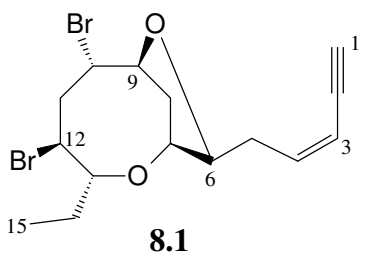

8.1

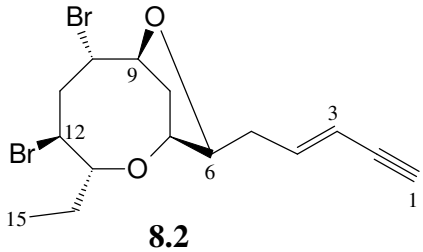

8.2

Table 8.1: NMR spectroscopic data of compounds **8.1** and **8.2**

		Compound **8.1**		Compound **8.2**	
Carbon No	δ_C **mult**	δ_C	δ_H, **mult, J (Hz)**	δ_C	δ_H, **mult, J (Hz)**
1	CH	82.0	3.11, d, 1.8	76.4	2.82, m
2	C	80.1	-	82.1	-
3	CH	110.4	5.55, m	111.4	5.59, m
4	CH	141.1	6.03, m	141.8	6.20, m
5a	CH_2	30.1	2.71, m	32.5	2.53, m
5b			2.82, m		2.58, m
6	CH	84.3	3.80, dt, 7.1, 1.9	84.3	3.74, dt, 7.2, 1.8
7	CH	70.0	4.01, m	69.7	4.01, m
8	CH_2	33.5	2.06, m	33.5	2.07, m
			2.36, d, 15.4		2.37, m
9	CH	79.6	4.41, m	79.6	4.41, m
10	CH	55.3	4.35, m	55.2	4.34, m
11a	CH_2	38.5	2.52, dd, 15.5, 4.3	38.5	2.53, m
11b			3.38, ddd, 15.5, 8.9, 2.4		3.34, m
12	CH	53.0	4.50, t, 9.5	52.9	4.51, m
13	CH	82.7	3.92, m	82.8	3.90, m
14a	CH_2	23.1	1.69, m	22.9	1.69, m
14b			2.00, m		2.00, m
15	CH_3	11.8	1.07, t, 7.4	11.7	1.07, t, 7.4

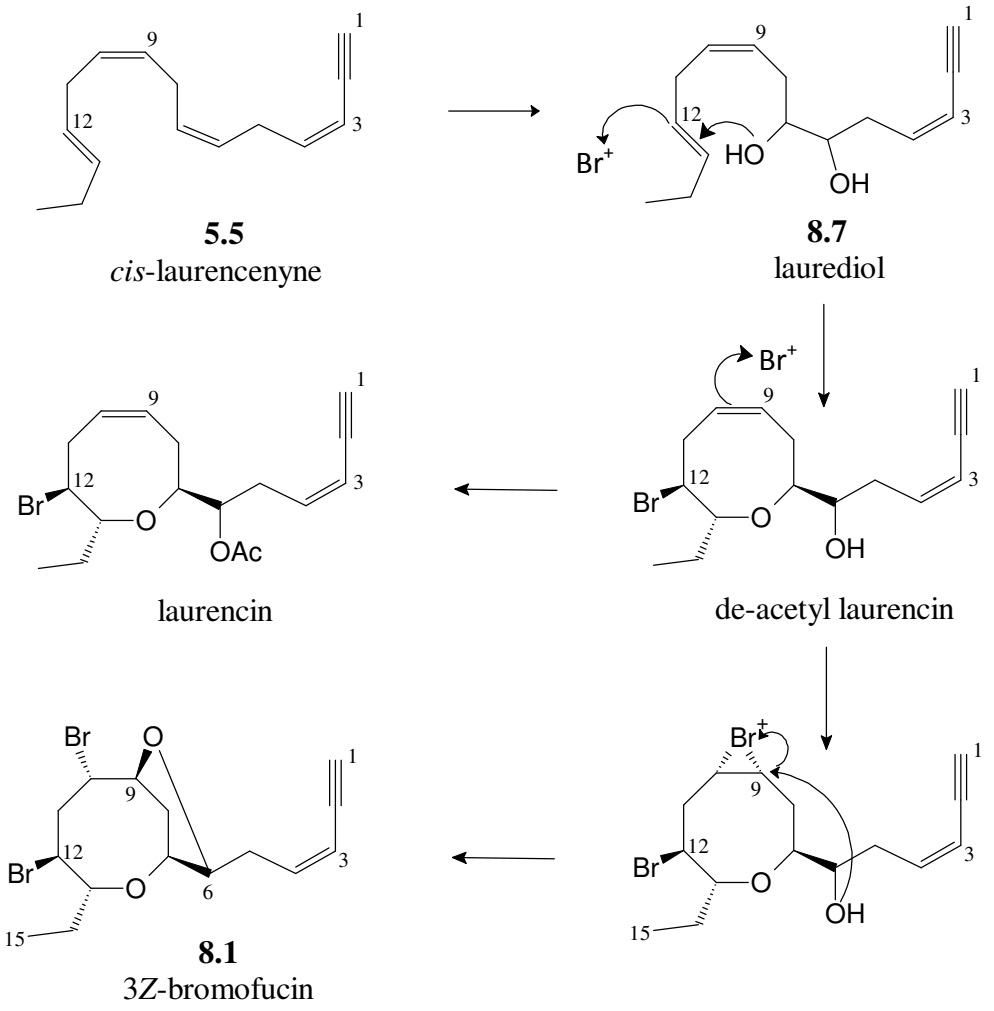

5.5
cis-laurencenyne

8.7
laurediol

laurencin

de-acetyl laurencin

8.1
3*Z*-bromofucin

Scheme 8.2: Proposed biosynthetic pathway for the formation of cyclic ether type compounds such as compound **8.1** from the linear acetogenin *cis*-laurencenyne, compound **5.5**[2]

[2] Despite the presence of compound **5.5** in *L. natalensis*, cyclic bromo-ethers were not isolated from the alga suggesting a probable lack of critical enzymes required for such transformation of the precursor, or merely no ecological rationale to do so. See Appendix 2 for proposed biosynthetic pathways of ALL isolated compounds

8.2.2.3 Compound 8.5

A COSY NMR experiment endorsed the presence of a truncated (C5) *cis*-acetylenic side in compound **8.5** *vs*. that of a (C6) chain previously observed in compound **8.1**.

Strong contiguous COSY correlations were seen amongst protons δ_H 3.16 (d, J = 7.6 Hz), δ_H 5.59 (m), δ_H 5.94 (m) and a methylene group δ_H 2.56 (m); δ_H 2.70 (m) all belonging to the alkyl side chain. A trio of methyl signals were observed in the ^{1}H NMR spectrum of compound **8.5** (Figure 8.9), two of which were singlets at δ_H 2.11 and δ_H 2.16, and a triplet at δ_H 1.06 (J = 7.6 Hz).

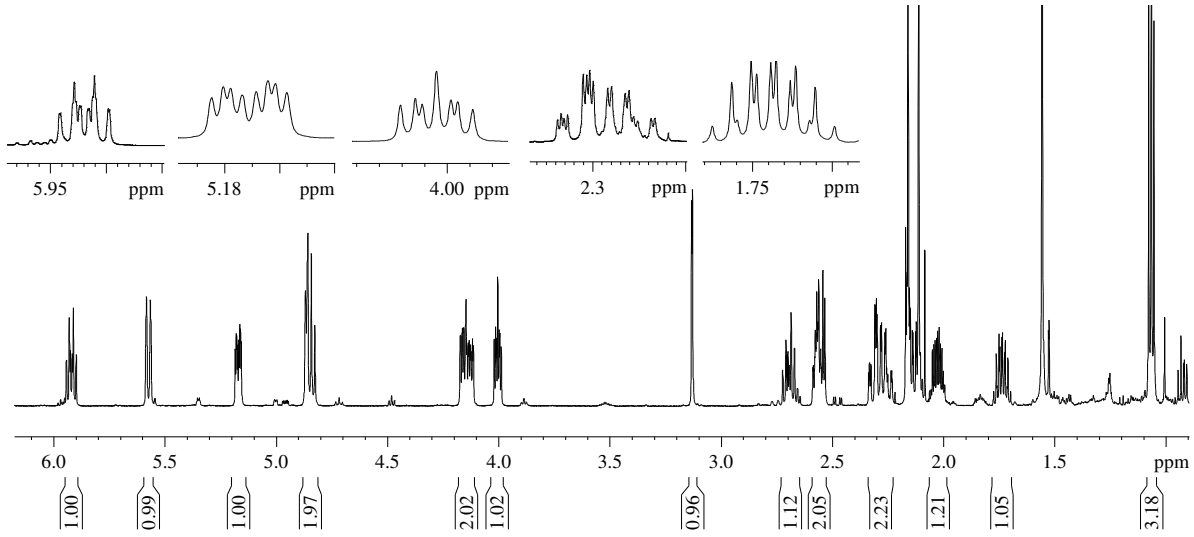

Figure 8.9: ^{1}H NMR spectrum ($CDCl_3$, 600 MHz) of compound **8.5**

Despite a truncated alkenyne chain, the sesquiterpenoid nature of compound **8.5** was retained by the extension of the terminal ethyl moiety seen in bromofucin, to a propyl unit with ^{13}C NMR shifts at δ_C 12.2, 29.2 and 60.4.

The ^{13}C NMR spectrum (Figure 8.10) also revealed recognisable ether bearing carbon atoms with resonances at δ_C 71.6 and δ_C 74.2. Inspection of the IR spectrum (Figure 8.11) of compound **8.5** surprisingly exposed a carbonyl stretch at 1734 cm^{-1} suggesting that the compound exhibited further oxygenation other than the ether functionality.

Two acetyl groups within compound **8.5** were confirmed. The evidence for this came in the form of the sharp methyl singlets in the ^{1}H NMR spectrum δ_H 2.11 and δ_H 2.16 previously discussed, as well as unambiguous carbonyl signals detected in the HMBC spectrum of compound **8.5** at δ_C 169.9 and δ_C 170.1.

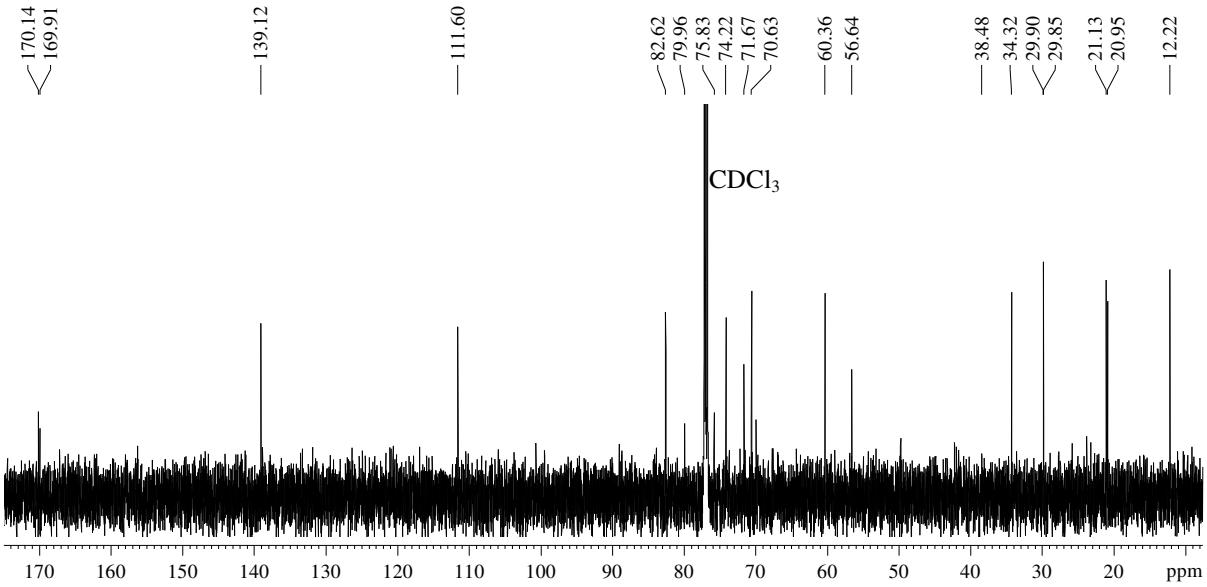

Figure 8.10: ^{13}C NMR spectrum ($CDCl_3$, 150 MHz) of compound **8.5**

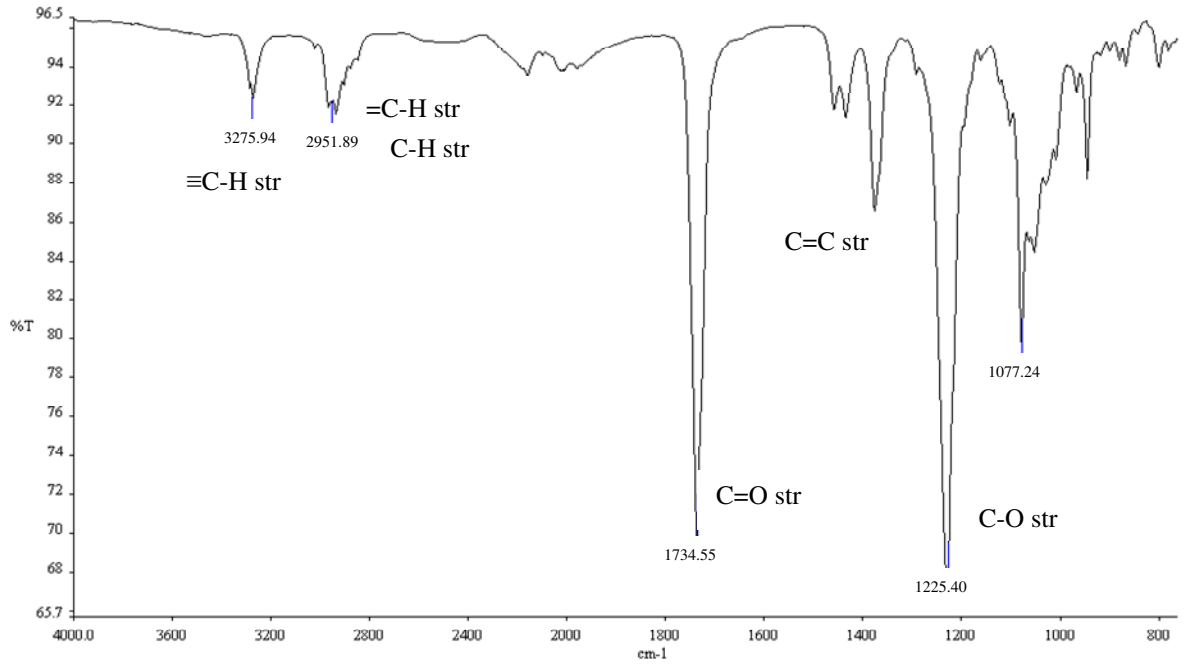

Figure 8.11: IR spectrum of compound **8.5**

Compound **8.5** was found to be identical to a di-acetyl, halogen bearing acetogenin as previously isolated by Iliopoulou *et al*., (2012) from a Greek specimen of *Laurencia obtusa*. This is the first record of the isolation of this compound from *Laurencia flexuosa*.

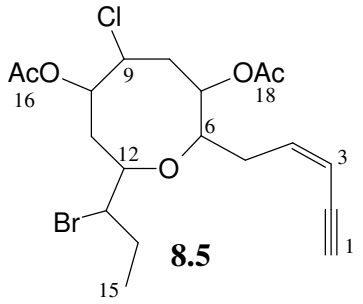

8.5

Table 8.2: NMR spectroscopic data of compound **8.5**

Carbon No	δ_C	δ_C **mult**	δ_H, **mult, J (Hz)**
1	82.6	CH	3.16, d, 2.3
2	80.0	C	-
3	111.6	CH	5.59, d, 10.4
4	139.1	CH	5.94, m
5a	34.3	CH_2	2.56, m
5b			2.70, m
6	71.7	CH	4.16, m
7	70.6	CH	4.86, m
8a	38.5	CH_2	2.56, m
8b			2.16, m
9	56.6	CH	4.84, m
10	75.8	CH	5.19, dq, 9.9, 2.7
11a	29.8	CH_2	2.28, m
11b			-
12	74.2	CH	4.14, m
13	60.4	CH	4.00, m
14a	29.9	CH_2	1.74, m
14b			2.03, m
15	12.2	CH_3	1.06, t, 7.6
16	169.0	$CH_3\underline{\mathbf{C}}O$	-
17	21.0	$\underline{\mathbf{C}}H_3CO$	2.11, s
18	170.01	$CH_3\underline{\mathbf{C}}O$	-
19	21.1	$\underline{\mathbf{C}}H_3CO$	2.16, s

8.3 Experimental

8.3.1 General experimental

As per section **3.3.1** in chapter 3, page 54.

8.3.2 Plant material (*L. flexuosa*, D1013)

L. flexuosa was collected by hand at Cape St. Francis on the south coast of South Africa in May 2011. A voucher specimen has been stowed away in the Bolus Herbarium at the University of Cape Town, South Africa. Identification of the alga was done by Professor John Bolton with the Department of Biological Sciences at the University of Cape Town, South Africa.

8.3.3 Extraction and isolation of metabolites

Same procedure as per section **3.3.3** as in chapter 3, page 54 (dry mass 16.1 g, crude extract 0.16 g, 0.98% yield).

Column chromatography step gradient fraction B was repeatedly purified by normal phase HPLC in an attempt to purify evident isomers. Compound **8.1** (6.0 mg, 0.037%) was successfully purified however compound **8.2** (3.1 mg, 0.019%) was isolated and elucidated in combination with compound **8.1**.

Compound **8.5** (9.6 mg, 0.059%) was isolated as a white solid from step gradient fraction C by means of silica gel column chromatography.

8.3.4 Compounds isolated

8.3.4.1 Compound 8.1 (JF14-41B10M)

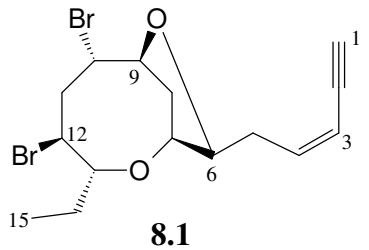

8.1

3Z-bromofucin (**8.1**): Orange oil; ^{1}H and ^{13}C data available in Table 8.1. As previously reported by McPhail *et al*., (2005).

8.3.4.2 Compound 8.2 (JF14-41B10N)

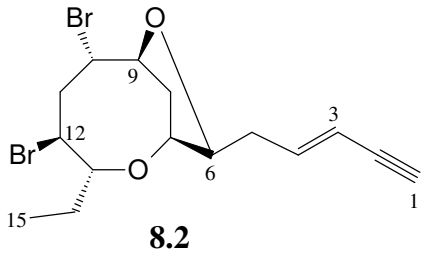

8.2

3E-bromofucin (**8.2**): Orange oil; ^{1}H and ^{13}C data available in Table 8.1. As previously reported by Coll *et al*., (1989).

8.3.4.3 Compound 8.5 (JF14-43A1)

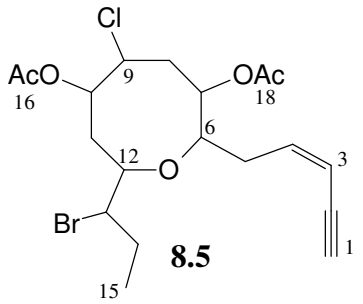

8.5

9-chloro-13-bromo-6:12-epoxy-7,10-diacetoxy-pentadec-3-en-1-yne (**8.5**): White solid; ^{1}H and ^{13}C data available in Table 8.2. As previously reported by Iliopoulou *et al*., (2002).

8.4 References

Coll, J. C.; Wright, A. D. Tropical Marine Algae. IV. Novel metabolites from the red alga *Laurencia implicata* (Rhodophyta, Rhodophyceae, Ceramiales, Rhodomelaceae). *Australian Journal of Chemistry* **1989**, *42*, 1685-1693.

De Clerck, O.; Bolton, J. J.; Anderson, R. J.; Coppejans, E. *Guide to the seaweeds of KwaZulu-Natal*. *Scripta Botanica Belgica 33*. National Botanic Garden of Belgium, VLIZ: Flanders Marine Institute and Flemish Community, **2005**, 1-294.

Francis, C. M. **2014**. Systematics of the *Laurencia* complex (Rhodomelaceae, Rhodophyta) in southern Africa. PhD Thesis. University of Cape Town, Cape Town, South Africa.

Fukuzawa, A.; Kurosawa, E.; Irie, T. Laurefucin and acetyl-laurefucin. New bromo compounds from *Laurencia nipponica* Yamada. *Tetrahedron Letters* **1972**, *1*, 3-6.

Howard, B. M.; Schulte, G. R.; Fenical, W.; Solheim, B.; Clardy, J. Three new vinyl acetylenes from the marine alga *Laurencia*. *Tetrahedron* **1980**, *36*, 1747-1751.

Iliopoulou, D.; Vagias, C.; Harvala, C.: Roussis, V. C_{15} acetogenins from the red alga *Laurencia obtusa*. *Phytochemistry* **2002**, *59*, 111-116.

Knott, M. G. **2011** Isolation, structural characterisation and anti-cancer activity of natural products from selected South African marine algae. Ph.D thesis. Rhodes University, Grahamstown.

Mann, M. G. A. **2008**. An investigation of the antimicrobial and antifouling properties of marine algal metabolites. M.Sc thesis. Rhodes University, Grahamstown.

McPhail, K. L.; Davies-Coleman, M. T. (3*Z*)-bromofucin from a South African sea hare. *Natural Product Research* **2005**, *19*, 449-452.

Chapter 9

Secondary metabolites from *Laurencia sodwaniensis*

Abstract

The newly described algal species *Laurencia sodwaniensis*, whose chemistry was previously unknown, afforded two known halogenated chamigranes as the main constituents, (**9.1** and **9.3**). Compound **9.1**, also known as cartilagineol, was clearly the major metabolite within the crude organic extract of the alga.

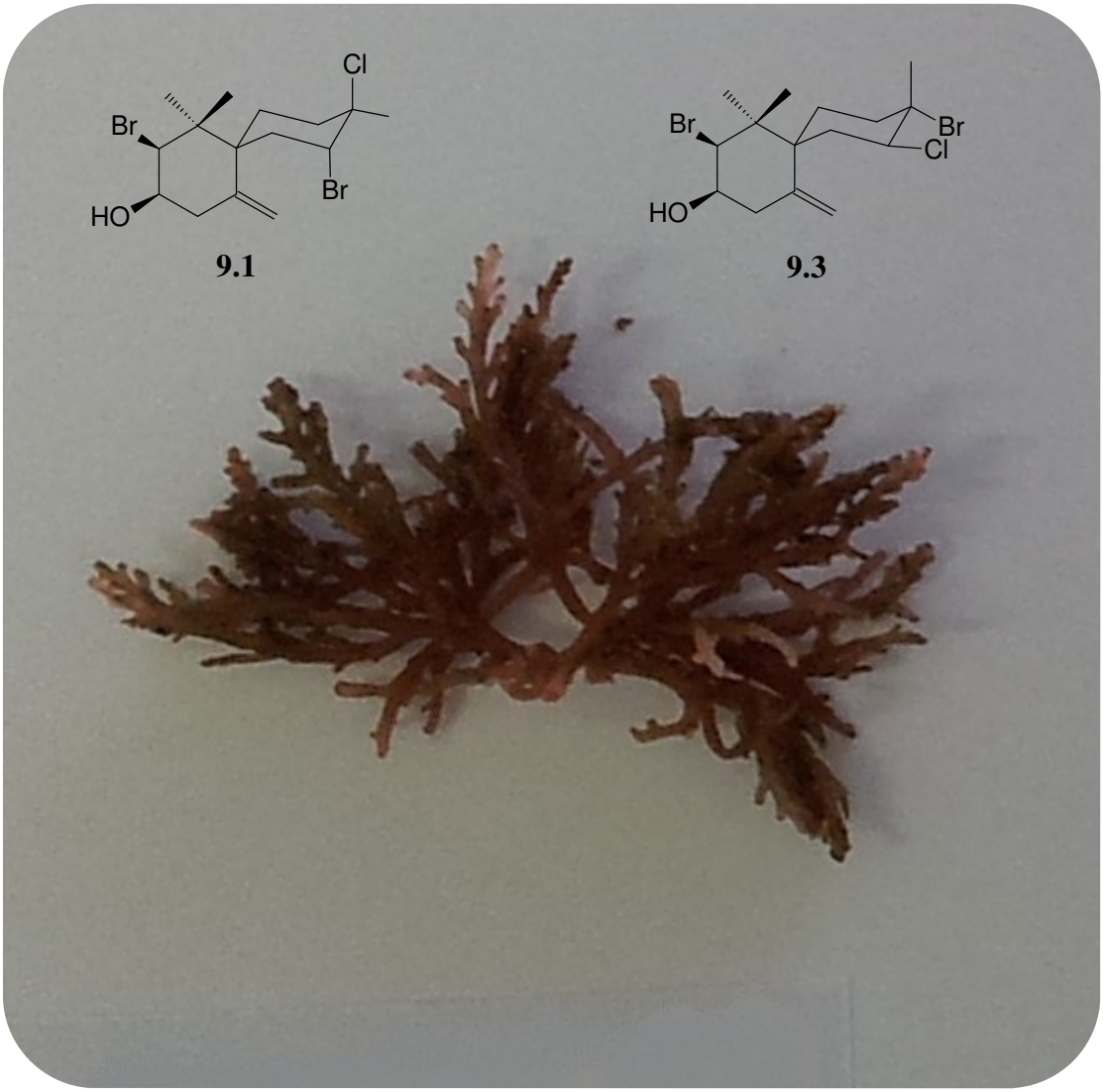

9.1 **9.3**

Chapter 9

Secondary metabolites from *Laurencia sodwaniensis*

9.1 Introduction

The newly described epilithic species, *Laurencia sodwaniensis* (Francis, 2014) is endemic to South Africa with the type specimen obtained on the east coast in Sodwana bay (*Sodwaniensis*: from Sodwana bay). Plants grow to 5 cm high and possess a light pink thallus. Cortical cells show an average of three *corps en cerise* per cell (Francis, 2014).

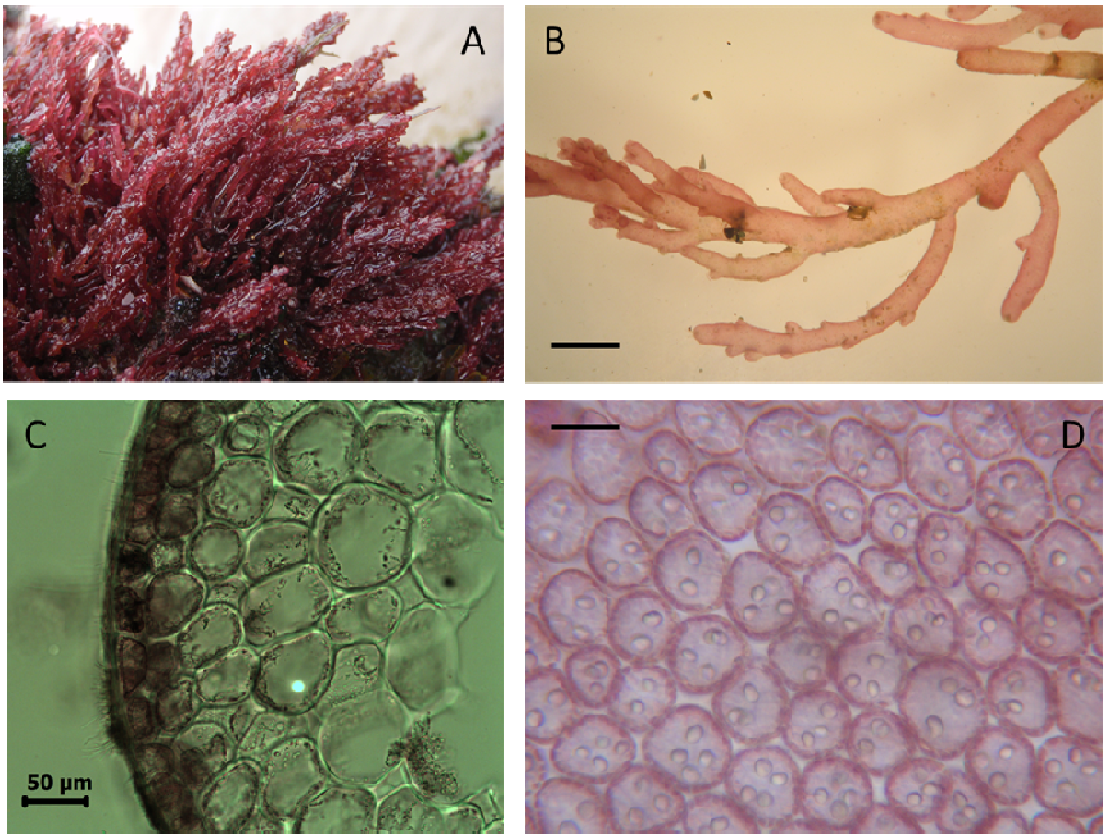

Figure 9.1: *Laurencia sodwaniensis*[1] (Caitlynne Francis © 2014)

A) Habit.

B) Branching pattern (8x). Scale 1cm: 240µm

C) Cortical cells (20x).

D) Two-Four *corps en cerise* per cell (40x). Scale 1cm: 20µm

[1] Image plates courtesy of Caitlynne Francis © 2014, University of Cape Town, South Africa

9.2 Results and Discussion

9.2.1 Extraction and isolation of metabolites from *L. sodwaniensis* (D968, Cape Vidal)

The quantity of fresh *L. sodwaniensis* obtained was diminutive, with the dry algal material weighing a mere 0.75 g. Despite this after standard extraction and fractionation procedures (section **3.2.1,** page 54) the crude ^{1}H NMR spectrum (Figure 9.2) showed fascinating broad related peaks in the deshielded region, belonging to a possible major metabolite. When superimposed, the ^{1}H NMR spectra (Figure 9.2) of silica gel step gradient column fractions B and C were analogous and hence were combined and further purified. Normal phase HPLC (19:1 hex:EtOAc) of the resultant column fraction yielded compounds **9.1** and **9.3**.

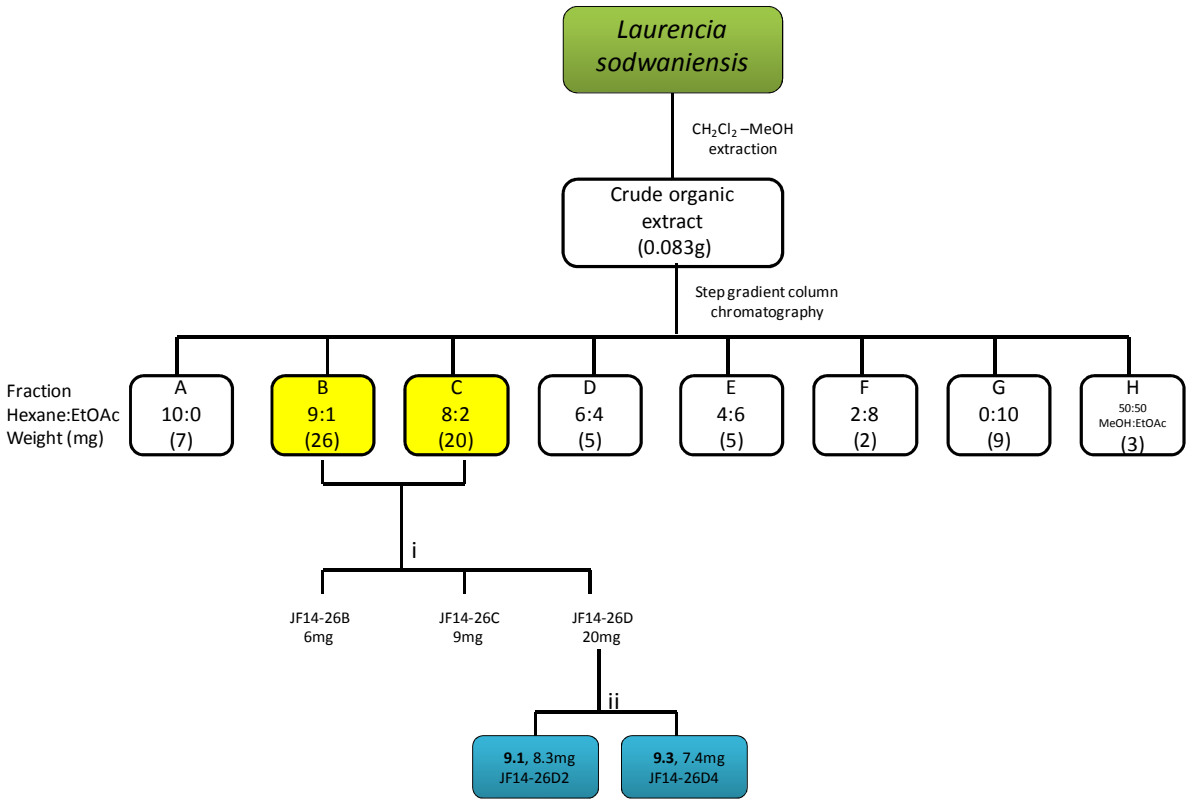

Scheme 9.1: Isolation scheme of metabolites from *L. sodwaniensis* (D968)

Conditions: i) Silica gel column chromatography (9:1 hex:EtOAc); ii) Normal phase HPLC (19:1 hex:EtOAc)

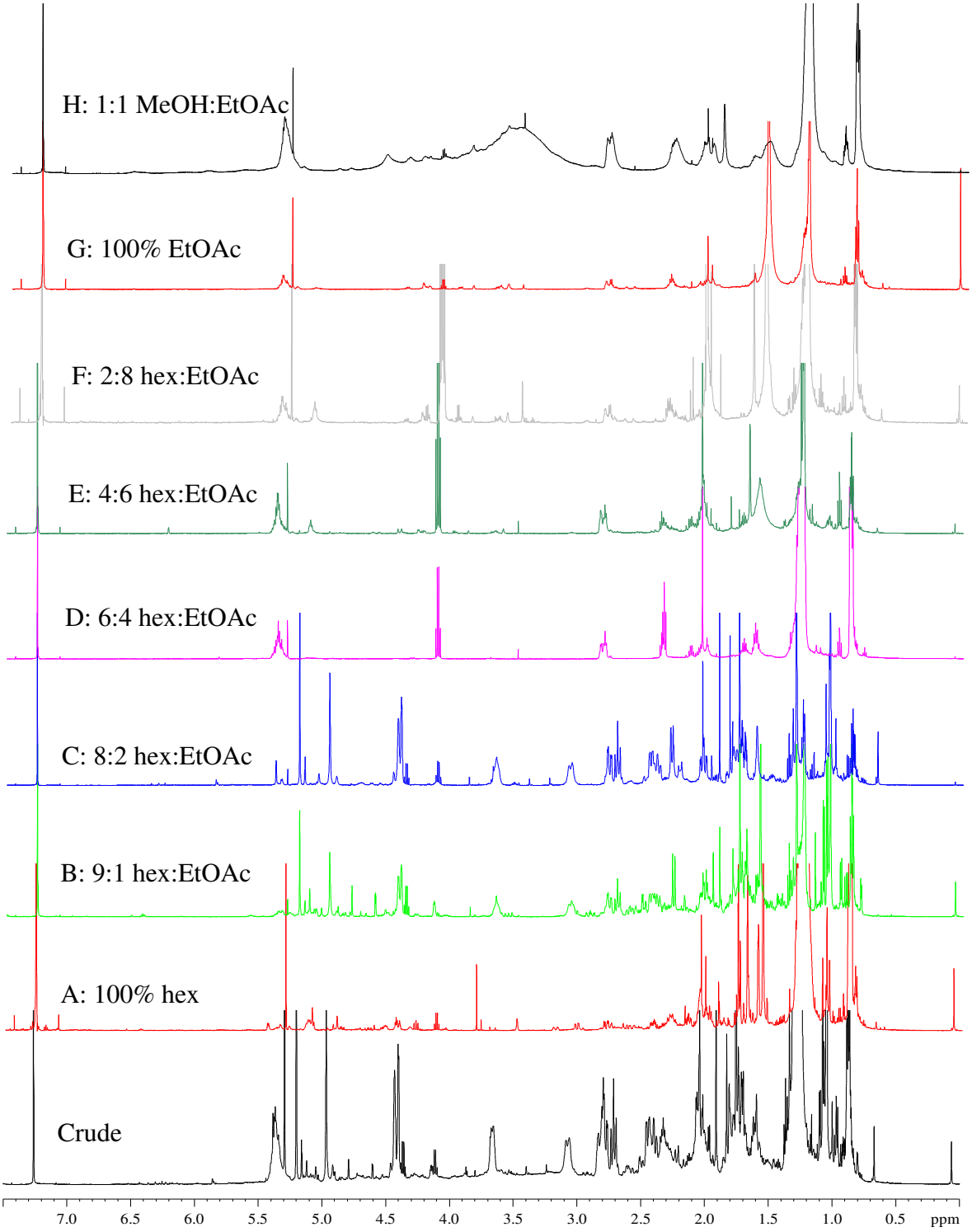

Figure 9.2: ^{1}H NMR spectra ($CDCl_3$, 600 MHz) of the crude organic extract of *L. sodwaniensis* (D968) and step gradient column fractions A-H

9.2.2 Structure elucidation of metabolites

9.2.2.1 Compound 9.1

The ^{1}H NMR spectrum (Figure 9.3) of compound **9.1** was similar to that of compound **5.8** (Figure 5.7, page 106) in that two deshielded methylidene protons were observed as singlets at δ_H 4.96 and δ_H 5.20, as well as three methyl singlet resonances at δ_H 0.99, δ_H 1.31 and δ_H 1.75.

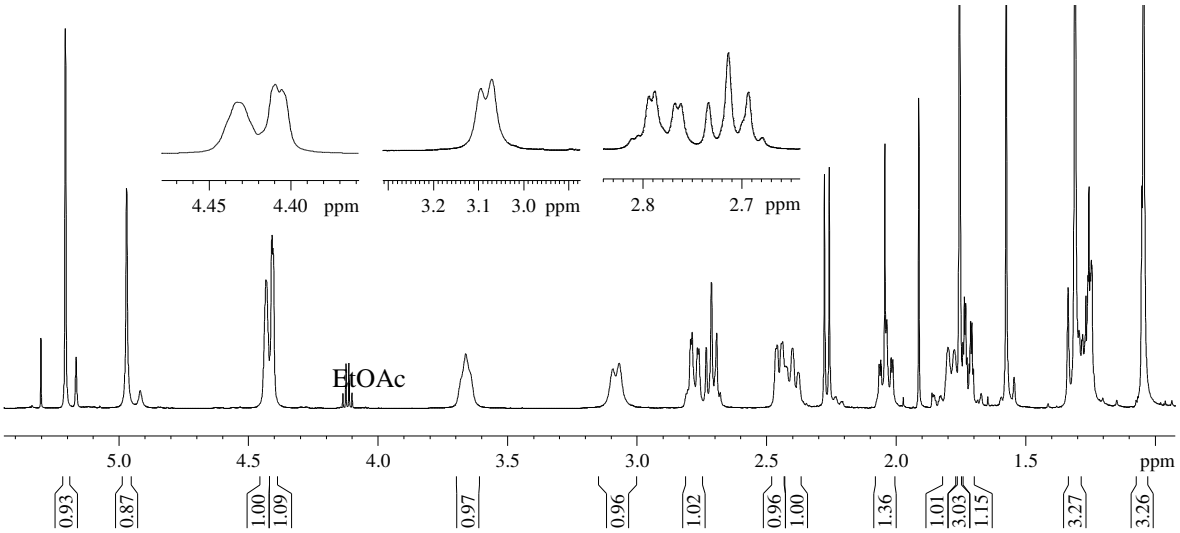

Figure 9.3: ^{1}H NMR spectrum ($CDCl_3$, 600 MHz) of compound **9.1**

The ^{13}C NMR spectrum (Figure 9.4) aided in confirming the chamigrane nature of compound **9.1** as a spiro quaternary carbon was detected at δ_C 43.7, including three additional quaternary (δ_C 44.0, 73.4 and 147.3), three methine (δ_C 57.1, 69.6 and 76.4), five methylene (δ_C 24.3, 32.4, 33.8, 39.4 and 114.7) and three methyl (δ_C 24.9, 25.4 and 33.2) carbons.

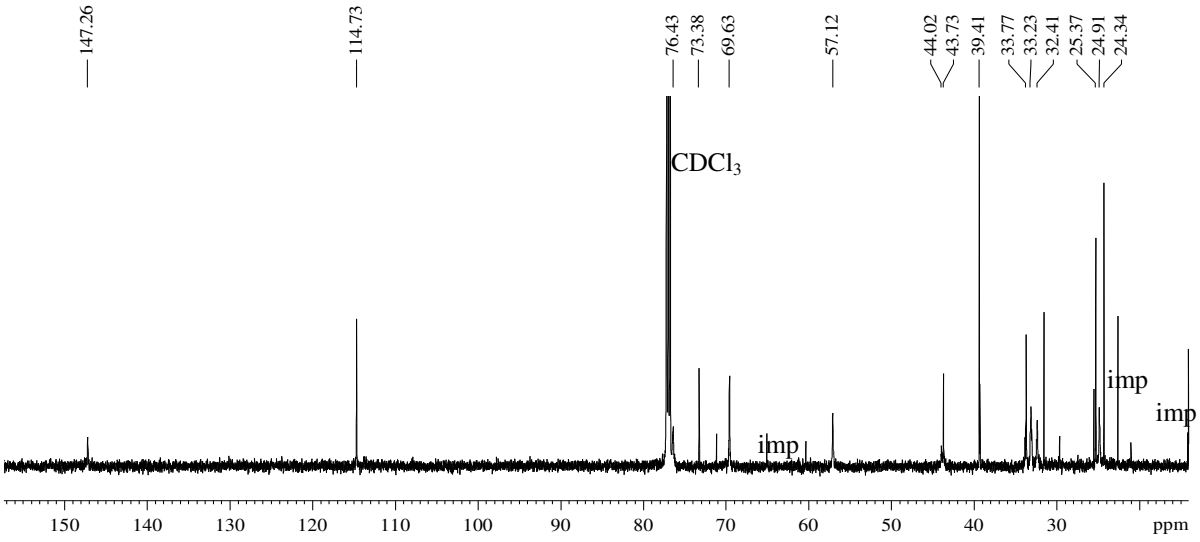

Figure 9.4: ^{13}C NMR spectrum ($CDCl_3$, 150 MHz) of compound **9.1**

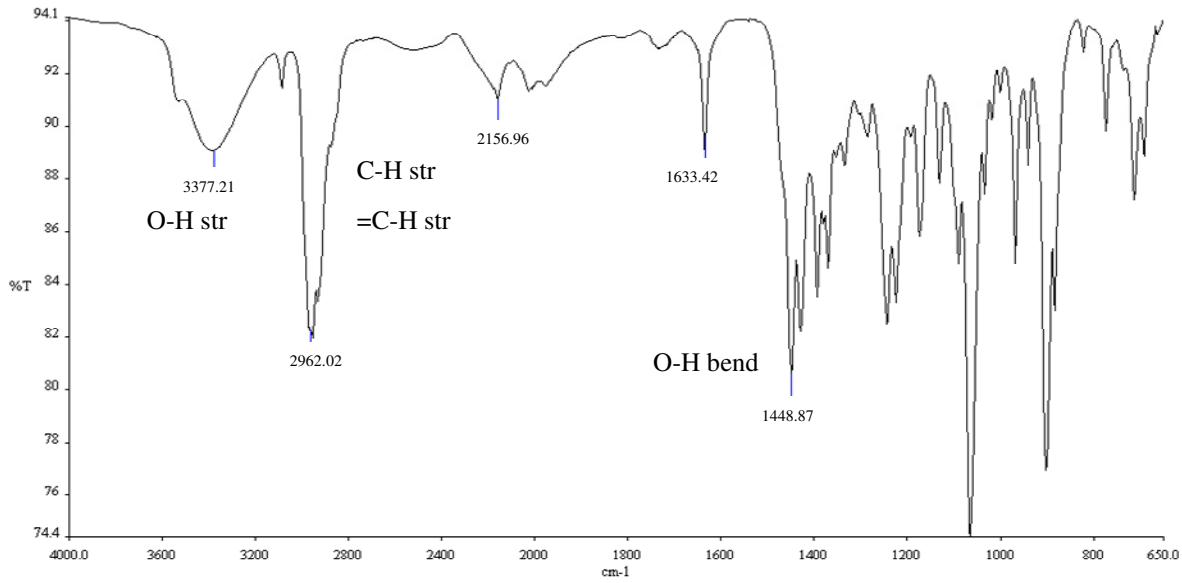

Figure 9.5: IR spectrum of compound **9.1**

A hydroxyl moiety within compound **9.1** was confirmed by a broad stretch in the IR spectrum (Figure 9.5) at 3377 cm^{-1}.

Compound **9.1** presented spectroscopic data akin to cartilagineol, a C_{15} halo-chamigrane with unprecedented stereochemical features at C3 and C4 i.e. diaxial halides.

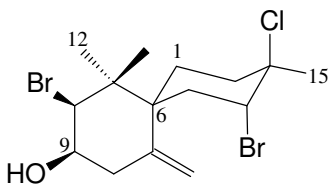

9.1
Cartilagineol

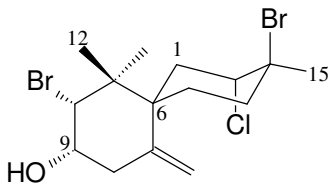

9.2
allo-isoobtusol

Initially, Juagdan *et al*., (1997) had named compound **9.1** *allo*-isoobtusol (**9.2**), however Guella *et al*., (1997) and Francisco *et al*., (1998) revised the structure proposed by Juagdan *et al*., (1997) to cartilagineol (compound **9.1**). This was confirmed by Francisco *et al*., (1998) after securing an X-ray crystal structure from crystals of cartilagineol obtained from a specimen of *Laurencia* sp. from the Philippines.

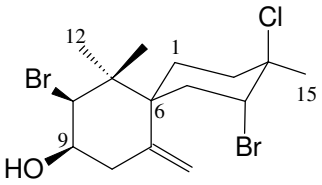

9.1

Table 9.1: NMR spectroscopic data of compound **9.1**[2]

Carbon No	δ_C	δ_C mult	δ_H, mult, J (Hz)
1a	24.3	CH_2	1.72, dq, 13.3, 3.5
1b			2.04, dt, 13.3, 3.5
2a	32.4	CH_2	1.80, d, 14.8
2b			2.40, t, 14.8
3	73.4	C	-
4	57.1	CH	4.43, br s
5a	33.8	CH_2	2.78, dd, 15.1, 4.1
5b			3.08, br d, 15.1
6	44.0	C	-
7	147.3	C	-
8a	39.4	CH_2	2.45, dd, 12.7, 3.4
8b			2.72, t, 12.7
9	69.6	CH	3.67, t, 10.4
10	76.4	CH	4.41, br d, 2.3
11	43.7	C	-
12	24.9	CH_3	1.31
13	25.4	CH_3	0.99
14a	114.7	CH_2	4.96
14b			5.20
15	33.2	CH_3	1.75

[2] Stereochemistry assigned by analysis of coupling constants

9.2.2.2 Compound 9.3

The ^{1}H NMR spectrum (Figure 9.6) of compound **9.3** was comparable in many ways to that observed for compound **9.1** (Figure 9.3). Broad methine moieties were observed at δ_H 4.12 and δ_H 4.72 as well as a doublet at δ_H 4.47 (J = 2.6 Hz). Sharp exocyclic vinyl protons peaked at δ_H 5.06 and δ_H 5.40 amongst other methylene groups between δ_H 1.7-2.5

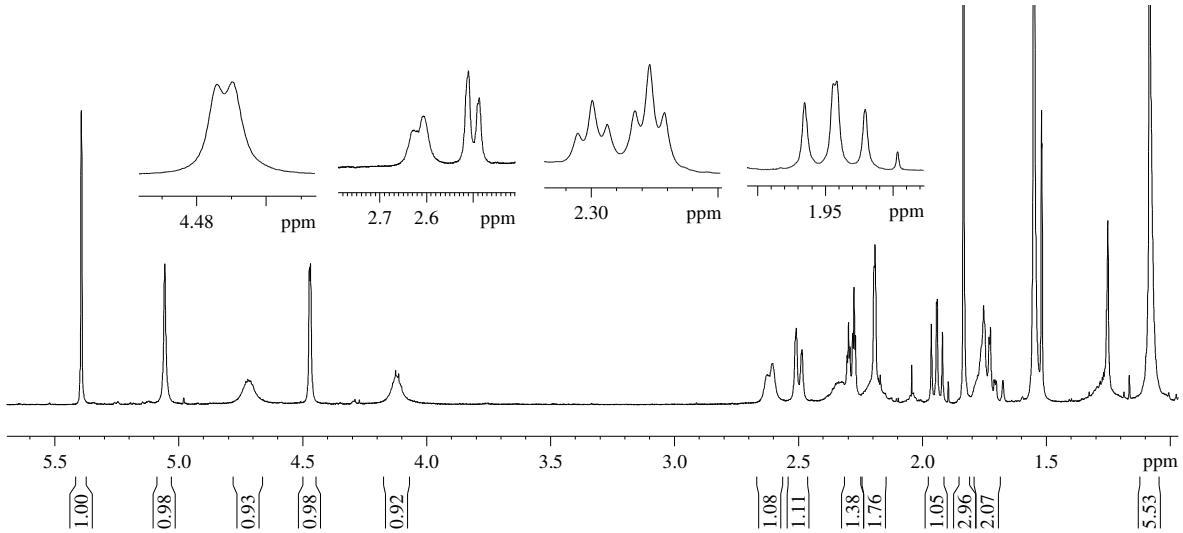

Figure 9.6: ^{1}H NMR spectrum ($CDCl_3$, 600 MHz) of compound **9.3**

The similarity in spectroscopic data between compound **9.3** and **9.1** continued as the IR spectra were almost identical (Figure 9.7).

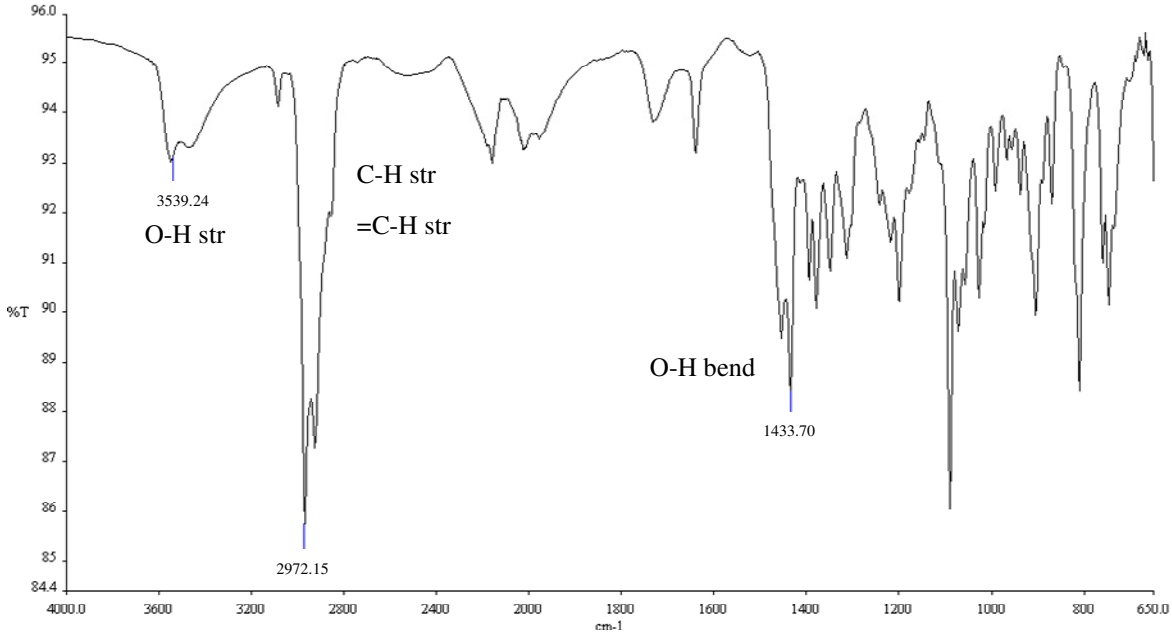

Figure 9.7: IR spectrum of compound **9.3**

HSQC and HMBC analysis allowed for identification of compound **9.3** as obtusol, a regio-isomer of compound **9.1**, with evident differences in ^{13}C NMR shifts at positions C3, C4 and C15 i.e. (δ_C 68.0, 67.6 and 23.6 for compound **9.3**) and (δ_C 73.4, 57.1 and 33.2 for compound **9.1**). Obtusol was initially isolated by Gonzalez *et al*, (1976) from *Laurencia obtusa* after which a revised X-ray crystal structure was documented by Gonzalez *et al*., (1979a).

Additional isomers, compound **9.4** (Gonzalez *et al*, 1976) and the C2/C3 trans-equatorial halo-compound **9.5** (Guella *et al*., 1990), in conjunction with isolated compounds **9.1** and **9.3**, furnish a fascinating stereochemical series particularly at carbons C2, C3 and C4[3].

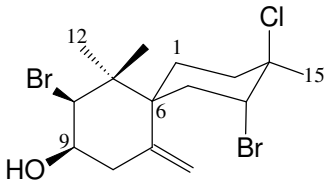

9.1
Cartilagineol

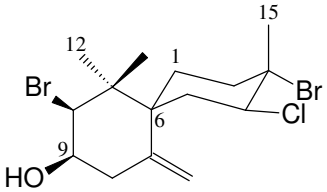

9.3
Obtusol

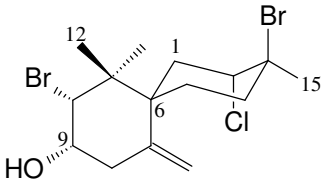

9.4
iso-obtusol

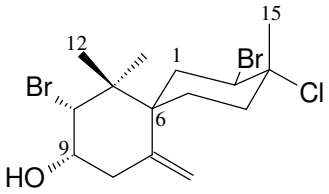

9.5
Rogiolol

[3] ^{13}C NMR assignments of various isomers about these positions are shown in Appendix 3

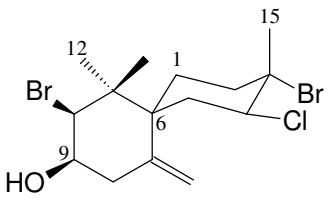

9.3

Table 9.2: NMR spectroscopic data of compound **9.3**[4]

Carbon No	δ_C	δ_C **mult**	δ_H**, mult, J (Hz)**
1	26.0	CH_2	1.75, m
2a	41.3	CH_2	2.27, td, 13.1, 3.1
2b			2.19, m
3	68.5	C	-
4	67.3	CH	4.72, br m
5a	39.0	CH_2	2.50, m
5b			2.61, m
6	50.3	C	-
7	140.9	C	-
8a	37.9	CH_2	1.94, t, 12.6
8b			2.33, m
9	72.3	CH	4.12, br m
10	70.7	CH	4.47, d, 2.8
11	44.0	C	-
12	24.0	CH_3	1.09, s
13	21.2	CH_3	1.08, s
14a	118.7	CH_2	5.06, s
14b			5.40, s
15	23.6	CH_3	1.84, s

[4] ^{13}C NMR shifts assigned using HSQC and HMBC NMR experiments

9.2.3 Molecular dynamics of compounds 9.1 and 9.3

The ^{1}H NMR spectra of both compounds **9.1** and **9.3** (Figures 9.3 and 9.6) showed characteristic broadening of methine resonances especially at H4. Initially, Guella *et al*., (1990) reported similar broadening of signals in both ^{1}H NMR and ^{13}C NMR spectra of rogiolol acetate (compound **9.6a**).

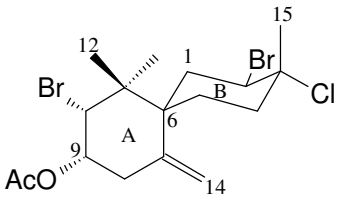

9.6a
Rogiolol acetate

During preliminary studies, Guella *et al*., (1990) discussed that the broadening of the signals was proved to be temperature dependant as probe temperatures of +50 ^{o}C and -30 ^{o}C yielded sharper NMR signals, particularly ^{1}H NMR (300 MHz) resonances.

Since broadening of ^{13}C NMR resonances was only viewed on ring **A** of compound **9.6a**, Guella *et al*., (1991) then proposed a possible chair-chair inversion in ring A, while ring **B** retained its conformation by virtue of it being a rigid chair. The major conformer (compound **9.6a)** possessed a vinylic methylene moiety (C14) which directed toward the bromo-methine group at C2. Upon ring **A** inversion, the minor conformer (compound **8.6b**) would conversely possess a vinylic methylene (C14) directing toward the methylene protons at C5 (Guella *et al*., (1991).

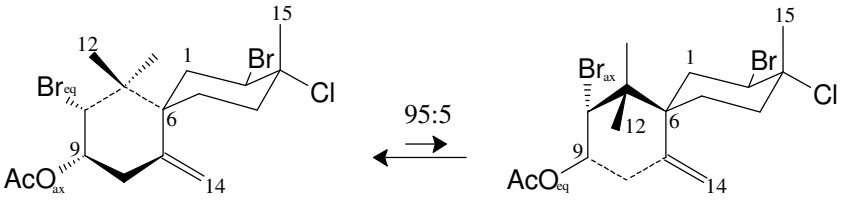

9.6a
Rogiolol acetate

9.6b
Rogiolol acetate

The minor conformer is less favoured due to possible repulsive hindrances between the axial bromine at C10 and the equatorial hydrogen at C1. The resultant low concentration of compound **9.6b** would consequently fail to display distinct ^{1}H NMR signals of its own, but rather affect the spectral width of ^{1}H NMR signals belonging to the major conformer **9.6a**. This then causes the broadening of the spectral signals.

When compound **9.6a** was analysed at a lower NMR field strength (80 MHz), the need for extreme probe temperatures vanished, as sharpened ^{1}H NMR peaks were observed at room temperature. Guella *et al*., (1991) then concluded that exposing compounds such as rogiolol acetate (**9.6**) to greater NMR field strengths, allowed for chemical exchange to occur within the molecule among non-equivalent sites hence favouring the production of conformers. These are subsequently detected by witnessing broadened spectral signals, especially within ^{1}H NMR spectra.

9.3 Experimental

9.3.1 General experimental

As per section **3.3.1** in chapter 3, page 54.

9.3.2 Plant material (*L.sodwaniensis*, D968)

L. sodwaniensis was collected by hand at Cape Vidal on the east coast of South Africa in March 2011. A voucher specimen has been stowed away in the Bolus Herbarium at the University of Cape Town. Identification of the alga was done by Professor John Bolton with the Department of Biological Sciences at the University of Cape Town, South Africa.

9.3.3 Extraction and isolation of metabolites

Same procedure as in section **3.3.3**, page 54 (dry mass 0.75 g, crude extract 0.083 g, 10.0% yield).

Compound **9.1** (8.3 mg, 1.0%) as well as compound **9.2** (7.4 mg, 0.9%) were isolated after purifying combined silica gel column fractions B and C *via* silica gel column chromatography (9:1 hex:EtOAc) and subsequently normal phase HPLC (19:1 hex:EtOAc).

9.3.4 Compounds isolated

9.3.4.1 Compound 9.1 (JF14-26D2)

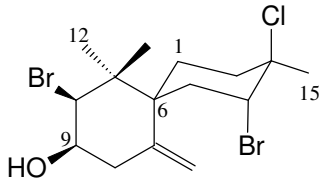

9.1

Cartilagineol OR *(2S*,3R*)-2,8-dibromo-9-chloro-1,1,9-trimethyl-5-methylidenespiro [5.5] undecan-3-ol* (**9.1**): White amorphous solid; ^{1}H and ^{13}C data available in Table 9.1. As previously reported by Francisco *et al*., (1998).

9.3.4.2 Compound 9.3 (JF14-26D4)

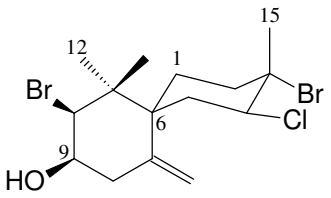

9.3

Obtusol OR (*2S*,3R*) - 2,9 - dibromo-8-chloro-1,1,9-trimethyl-5-methylidenespiro[5.5] undecane -3- ol* (**9.3**): White amorphous solid; ^{1}H and ^{13}C data available in Table 9.2. As previously reported by Gonzalez *et al*., (1976).

9.4 References

Francis, C. M. **2014**. Systematics of the *Laurencia* complex (Rhodomelaceae, Rhodophyta) in southern Africa. PhD Thesis. University of Cape Town, Cape Town, South Africa.

Francisco, M. E. Y.; Turnbull, M. M.; Erickson, K. L. Cartilagineol, the fourth lineage of *Laurencia* derived polyhalogenated chamigrene. *Tetrahedron Letters* **1998**, *39*, 5289-5292.

Gonzalez, A. G.; Darias, J.; Diaz, A.; Fourneron, J. D.; Martin, J. D.; Perez, C. Evidence for the biogenesis of halogenated chamigrenes from the red alga *Laurencia obtusa*. *Tetrahedron Letters* **1976**, *35*, 3051-3054.

Gonzalez, A. G.; Martin, J. D.; Martin, V. S. X-Ray study of sesquiterpene constituents of the alga L. obtusa leads to structure revision. *Tetrahedron Letters* **1979**, *20*, 2717-2718.

Guella, G.; Mancini, I.; Chiasera, G.; Pietra, F. Rogiolol acetate: a novel *β*-chamigrene type sesquiterpene isolated from a marine sponge. *Helvetica Chimica Acta* **1990**, *73*, 1612-1620.

Guella, G.; Mancini, I.; Chiasera, G.; Pietra, F. Conformational analysis of marine polyhalogenated *β*-chamigrenes through temperature dependent NMR spectra. *Helvetic Chimica Acta* **1991**, *74*, 774-786.

Guella, G.; Mancini, I.; Chiasera, G.; Pietra, F. Stereochemical features of sesquiterpene metabolites as a distinctive trait or red seaweeds of the genus *Laurencia*. *Tetrahedron Letters* **1997**, *38*, 8261-8264.

Juagdan, E. G.; Kaldindi, R.; Scheuer, P. Two new chamigranes from an Hawaiian red alga, *Laurencia cartilaginea. Tetrahedron* **1997**, *53*, 521-528.

Chapter 10

Chemotaxonomic significance of isolated metabolites

Abstract

Given that a secondary metabolite is the end result of enzyme dependent metabolic pathways within an organism, these molecules can be considered as phenotypic. Intrinsic genetic sequences will dictate the nature of the enzyme produced, and hence the characteristics of the final metabolite.

This chapter reveals the possible role secondary metabolites could play in predicting phylogeny of *Laurencia* spp. by determining whether closely related species produce comparable chemistry. For this to occur, an exhaustive analysis of additional *Laurencia* spp. which also produce the metabolites isolated from species in this study was performed.

The simpler chamigrane type compounds isolated within this study were shown to be biosynthesised by a wider variety of *Laurencia* spp. *vs.* that of the more complex molecules such as the multi-cyclic acetogenins, compounds **7.5** and **7.6**, prevalent in much fewer *Laurencia* spp.

Investigation of an *rbc*L based *Laurencia* spp. phylogeny tree revealed that the secondary metabolites isolated from *L. complanata*, *L. multiclavata and L. sodwaniensis* within this study, were produced almost exclusively by their sister species, allowing for a general inference to be made on the chemotaxonomic significance of the isolated structures.

Chapter 10

Chemotaxonomic significance of isolated metabolites

10.1 Introduction

As shown by Wang *et al*., (2013), the most common classes of secondary metabolites isolated from *Laurencia* spp. include sesquiterpenes, diterpenes, C_{15} acetogenins, and indole alkaloids, as has been mentioned in more detail in chapter 2. These secondary metabolites may play critical roles in the species delineation process as specialist enzymes, produced by the expression of inherent gene sequences, are required for their biosynthesis as shown below (Butler and Carter-Franklin, 2004).

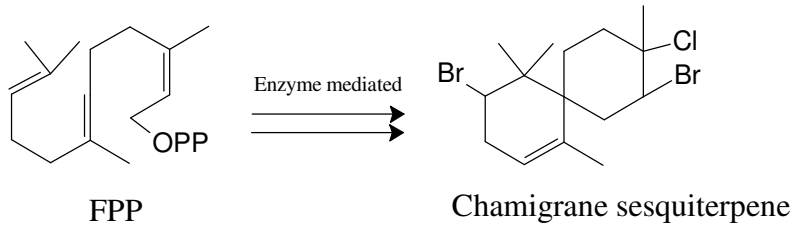

FPP Chamigrane sesquiterpene

Figure 10.1: Example of an enzyme mediated biosynthesis in *Laurencia* spp.

The chapters hitherto have exposed the natural product chemistry, as far as possible, of various South African *Laurencia* spp. A detailed *rbc*L based *Laurencia* spp. phylogeny tree produced in parallel by Francis (2014), allowed for a visual representation of the genetic relationship amongst the study species and other *Laurencia* spp. To expose the chemotaxonomic significance of the metabolites isolated herein, an exhaustive documentation of additional *Laurencia* spp. possessing identical phycochemistry was compiled. If the study metabolites were simultaneously produced within other closely related *Laurencia* spp. i.e. those within the monophyletic group, then a general implication can be made regarding the additional use of secondary metabolites as chemotaxonomic markers.

10.2 Results and discussion

10.2.1 Phylogeny of the *Laurencia* complex

The plastid *rbc*L phylogeny tree obtained by Francis (2014) (Scheme 10.1) reflects the relative placements of the seven *Laurencia* species analysed in this study, including *Laurenciella marilzae*, based on a 50% majority rule Bayesian inference. Ideally, to prove the feasibility of the chemotaxonomic approach with respect to *Laurencia* spp., the natural product chemistry exposed from *Laurencia* spp. within the scope of this study should be comparable to other *Laurencia* spp. to which close phylogenetic relationships exist.

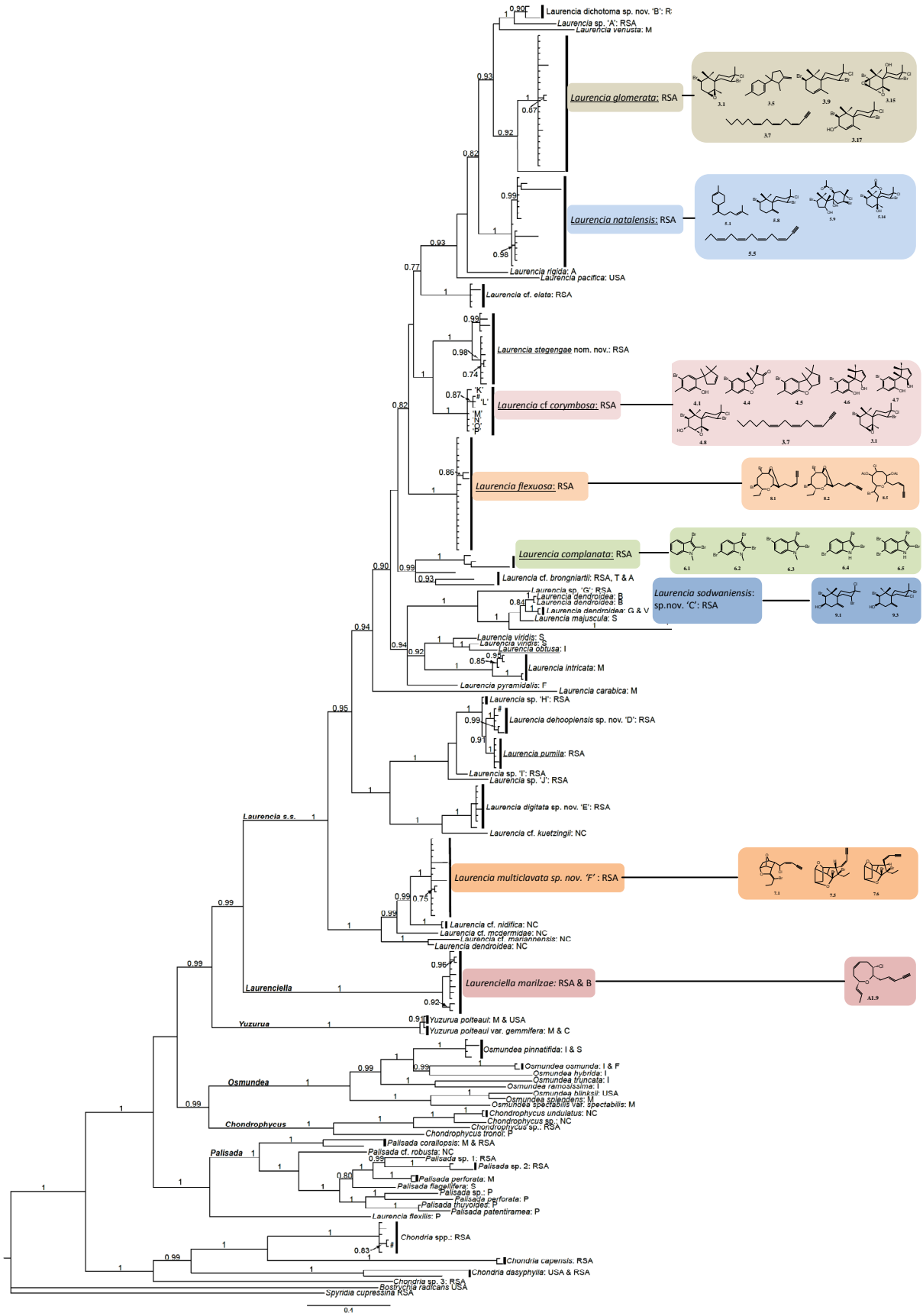

Scheme 10.1: Plastid *rbc*L phylogeny tree of the South African *Laurencia* complex including species utilised within this study

(Adapted from: Caitlynne Francis © 2014, University of Cape Town, South Africa)

See supplementary data for further information on the phylogeny tree. A clearer image may be obtained by viewing the electronic thesis (eCopy) on the CD provided.

10.2.2 Incidence of isolated metabolites in other *Laurencia* spp.

Preceding any analyses or inferences based on the phylogeny tree above, a detailed account of additional *Laurencia* spp.[1], which also produce the compounds isolated in this study, was documented (Table 10.1). Subsequent assessment of how closely related these species are can then occur by analysis of the phylogeny tree (Scheme 10.1).

[1] Obtained by searching the structures in Scifinder® https://scifinder.cas.org; Accessed: 25/12/2014

Table 10.1: Listings of *Laurencia* spp. and other organisms containing the compounds isolated in this study[2]

Organism		*L. brongniartii*	*A. californica*	*L. cartilaginea*	*L. clavifromis*	***L. complanata***	*L. composita*	***L. cf. corymbosa***	*A. dactylomela*	*L. dendroidea*	*L. filiformis*	***L. flexuosa***	*L. glandulifera*	***L. glomerata***	*L. gracilis*	*L. implicata*	*L. intricata*	*L. japonensis*	*L. majuscula*	*L. mariannensis*	*L. microcladia*	***L. multiclavata***	***L. natalensis***	*L. nidifica*	*L. nipponica*	*L. obtusa*	*L. okamurai*	*L. pacifica*	*L. papillosa*	*A. parvula*	*L. pinnatifida*	*L. saitoi*	*L. scoparia*	*L. similis*	***L. sodwaniensis***	*Laurencia sp.*
Compound																																				
L. glomerata	**3.1**						1	*						*											2		3				4		5			6
	3.5													*											7											
	3.7							*						*													8									
	3.9				9		10				11		12	*	13			14						15	16	17			18	19						20
	3.15		21				22		23					*										24			25									
	3.17				26		27							*											28		29	30				31				
L. corymbosa	**4.1**							*																											
	4.4							*																											
	4.5							*				32																							
	4.6							*																											
	4.7							*				33																							
	4.8							*						34																					
L. natalensis	**5.1**																						*												
	5.5						35																*				36									
	5.8						37		38											39			*	40	41		42									
	5.9								43														*													
	5.14																44						*													
L. complanata	**6.1**					*																														
	6.2	45				*															46															
	6.3	47				*																														
	6.4					*																												48		
	6.5	49				*																														
L. multiclavata	**7.1**																					*		50		51										52
	7.5																					*		53												
	7.6																					*														54
L. flexuosa	**8.1**											*																		55						
	8.2											*				56																				
	8.5											*														57										
L. sodwaniensis	**9.1**			58					59	60																									*	61
	9.3								62	63									64							65									*	

[2] -Refer to Appendix 5 for structures of ALL compounds isolated.
-Each number designating a compound to a particular organism (correlation number) is representative of a reference shown in (Table 10.2) overleaf.
-Species analysed in this study are highlighted yellow, and an asterisk (*) represents isolation of the compound in this study.
- Although every effort was made to be thorough, the above table may not represent an absolute account of all species containing the isolated compounds.

Table 10.2: References of correlation numbers depicted in Table 10.1

Correlation number	Reference	Correlation number	Reference
1	Ji *et al*., 2009a[3]	44	McMillan *et al*.,1974[3]
2	Suzuki *et al*., 1982[3]	45	Carter *et al*., 1978
3	Ojika *et al*., 1982[3]		Tanaka *et al*., 1989
4	Bano *et al*., 1987	46	Combaut *et al*., 1984
5	Combaut *et al*., 1984	47	Carter *et al*., 1978
	Kennedy *et al*., 1988		Tanaka *et al*., 1989
6	Howard and Fenical, 1975	48	Ji *et al*., 2007
7	Suzuki *et al*., 1982	49	Carter *et al*., 1978
8	Kigoshi *et al*., 1981		Tanaka *et al*., 1989
9	Rovirosa *et al.,* 1999	50	Waraszkiewicz *et al*., 1978
10	Ji *et al.*, 2009a	51	Ayyad *et al*., 2011
11	Jongaramruong *et al*., 2002	52	Vairappan *et al*., 2001
12	Suzuki *et al*., 1979	53	Waraszkiewicz *et al*., 1978
13	König and Wright, 1994	54	Waraszkiewicz *et al*., 1978
14	Takahashi *et al*., 1998	55	McPhail and Davies-Coleman, 2005
15	Kimura *et al*., 1999	56	Coll and Wright, 1989
16	Abe *et al*., 1997	57	Iliopoulou *et al*., 2002
17	Alarif *et al*., 2012	58	Juagdan *et al*., 2007
18	Abou-Elnaga *et al*., 2011	59	Wessels *et al*., 2000
19	Jongaramruong *et al*., 2002	60	Machado *et al*., 2011
20	Howard and Fenical, 1975	61	Francisco *et al*., 1998
21	Faulkner *et al*., 1974	62	Wessels *et al*., 2000
	Ireland *et al*., 1976	63	Machado *et al*., 2011
22	Masuda *et al*., 2002	64	Diaz-Marrero *et al*., 2009
23	McPhail *et al*., 1999	65	Gonzalez *et al*., 1976
	Pitombo *et al*., 1996		
24	Kimura *et al*., 1999		
25	Ojika *et al*., 1982		
26	Rovirosa *et al*., 1999		
27	Suzuki *et al*., 1988		
28	Ji *et al*., 2009a		
29	Ojika *et al*., 1982		
30	Fenical, 1976		
31	Ji *et al*., 2009b		
32	Mann, 2008		
33	Mann, 2008		
34	Elsworth and Thomson, 1989		
35	Ji *et al*., 2009a		
36	Kigoshi *et al*., 1981		
37	Ji *et al*., 2009a		
38	McPhail *et al*., 1999		
39	Ji *et al*., 2007		
40	Waraszkiewicz and Erickson, 1974		
41	Suzuki *et al*., 1983		
42	Ojika *et al*., 1982		
43	McPhail *et al*., 1999		

[3] Stereoisomer isolated

10.2.3 Chemotaxonomic significance of isolated metabolites

10.2.3.1 *Laurencia glomerata*

From (Table 10.1), it is evident that most of the compounds isolated from *L. glomerata* have been isolated from a reasonable number of other *Laurencia* spp.

A pronounced example is the halo-chamigrane (**3.9**) which has been isolated from a total of 11 other *Laurencia* spp. as well as from the sea-hare *Aplysia parvula*[4] indicating the herbivorous nature of the mollusc on *Laurencia* spp. containing compound **3.9**.

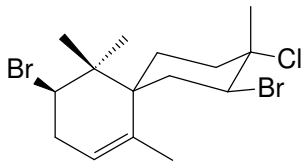

3.9

Certainly from a chemotaxonomic perspective, the ubiquitous nature reflected by the halo-chamigrane (**3.9**) amongst other *Laurencia* spp. renders it as an ineffective chemical marker of phylogeny as it prevents placement of *L. glomerata* to a particular monophyletic group.

10.2.3.2 *Laurencia* cf. *corymbosa*

A contrasting situation exists for the compounds isolated from *L.* cf. *corymbosa*. From (Table 10.1) it is clear that the compounds isolated from *L.* cf. *corymbosa* are predominantly exclusive to the alga (especially the new cyclic keto-cuparane **4.4**) with the exception of cuparanes **4.5**, **4.7** and chamigrane **4.8** which were all previously isolated from only one other *Laurencia* spp.

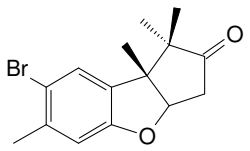

4.4

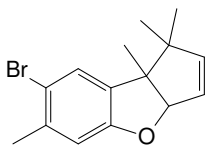

4.5

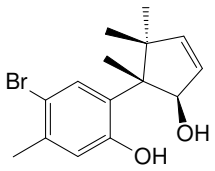

4.7

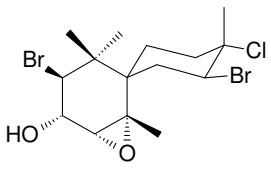

4.8

[4] Sea-hares sequester metabolites from dietary algae, releasing them in a purple ink when attacked by predators. The ink has been shown to affect chemosensory apparatus of predators (Hay and Fenical, 1988).

In instances where the natural product chemistry is found to be exclusive to a single taxon, predicting the phylogeny of an unknown species can be precarious as there are no reference points employable on the phylogeny tree (as no other *Laurencia* spp. possess comparable chemistry). Despite this, such species can subsequently be successfully characterised based on their unique natural product chemistry.

10.2.3.3 *Laurencia natalensis*

Gamma-bisabolene (**5.1**) and *cis*-laurencenyne (**5.5**) are shown to be likely precursors to the formation of other complex metabolites contained in *Laurencia* spp. (Appendix 2). Considering the lack of documented evidence for the isolation of compound **5.1** in other species of *Laurencia*, including the scarce number of *Laurencia* spp. in which compound **5.5** is found (Table 10.1), these metabolites are less favoured for inferring phylogenetic relationships, and would be more useful in identifying the few species which do produce them.

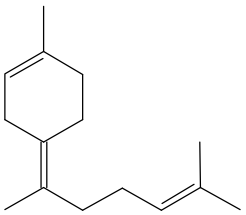

5.1

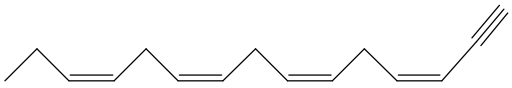

5.5

The halo-chamigrane, nidificene (**5.8**), as with chamigrane (**3.9**), displays a widespread presence amongst other *Laurencia* spp. (Table 10.1) which are scattered all over the phylogeny tree (Scheme 10.1). A possible explanation for such a trend could be the relative structural simplicity of the molecule. Enzymatic systems required for such straightforward biosyntheses need not be specialised and as a result, the "primitive" enzymes required for the production of compounds such as chamigrane (**5.8**) could have been introduced by a distant common ancestor at a much earlier stage within the phylogeny tree. This results in the widespread presence of such simple metabolites amongst numerous *Laurencia* spp.

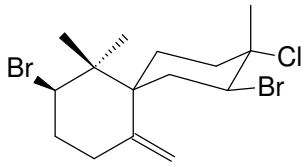

5.8

As the first documented isolation from *Laurencia* spp., *viz. L. natalensis,* the use of the sesquiterpene (**5.9**) as a chemical marker for the identification of *L. natalensis* is indispensable. Compound **5.9** (algoane) was initially isolated from a sea-hare, *Aplysia dactylomela* (Table 10.1), reaffirming the herbivorous nature these molluscs display toward red algae.

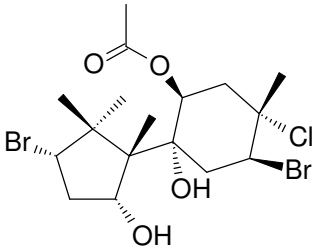

5.9

10.2.3.4 *Laurencia complanata*

From (Table 10.1) it is clear that the majority of the indole alkaloids isolated from *L. complanata* in this study have been isolated before mainly from *L. brongniartii.* On inspection of the phylogeny tree (Scheme 10.1, expansion shown below) an intriguingly close phylogenetic relationship was noticed between the two species i.e. sister species, and hence each other's closest relatives.

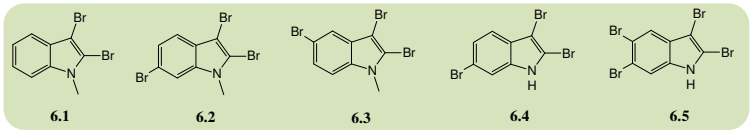

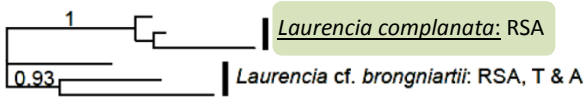

Among the morphological and genetic similarities that currently exist between *L. complanata* and *L. brongniartii*, the disclosure of their congruency in natural product chemistry adds fidelity to the chemotaxonomic principle.

No sequences are available for the other two *Laurencia* spp. wherein *L. complanata* indoles were also found (*L. microcladia* and *L. similis*) resulting in their absence from the tree (Scheme 10.1).

10.2.3.5 *Laurencia multiclavata*

The acetylenic acetogenin, compound **7.1**, was isolated from of *L. obtusa*, *L. nidifica* and an unidentified Malaysian *Laurencia* sp. (Table 10.1). Interestingly, from (Scheme 10.1, expansion shown below), *L. nidifica* displays a strikingly close phylogenetic relationship to *L. multiclavata* i.e. sister species, again increasing the perceived dependability of chemotaxonomy as an aid to classification.

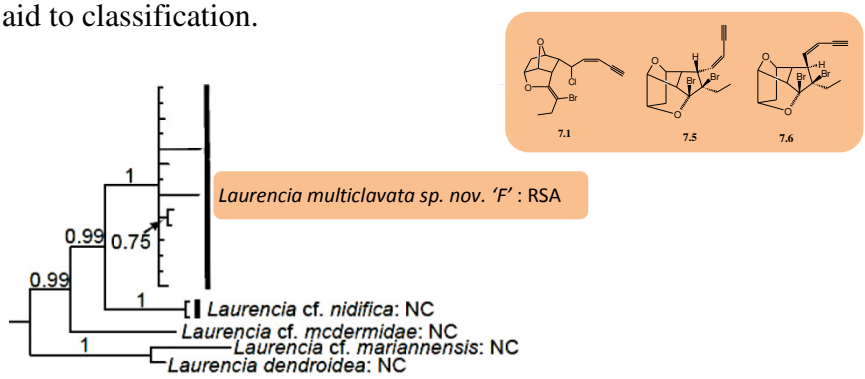

The presence of compound **7.1** in *L. obtusa*, which can occupy various regions on the phylogeny tree, cannot be ignored. Francis (2014) mentions the deficiency of clear species boundaries in the delineation of *Laurencia obtusa* while Stegenga et al., (2007) note its dubious global taxonomic status. Rampant misidentification of *L. obtusa* over the years (Francis, 2014) necessitates investigators to include intricate details which shed light on techniques used in identifying the specimen used i.e. based on morphology alone, or backed up by genetic sequences. Such details were not provided in this particular record by Ayyad *et al*., (2011). This leads to scepticism as to the true identity of the species used in past studies.

L. multiclavata also produced compound **7.5**, a unique poly-cyclic acetylenic acetogenin previously exclusive to *L. nidifica*.

The complex acetogenin **7.6**, an epimer of compound **7.5** was isolated in the same unidentified Malaysian *Laurencia* sp. in which compound **7.1** was isolated. Since *L. multiclavata* is South African endemic it would be reasonable to broadly predict that the identity of the unknown Malaysian *Laurencia* sp. could possibly have been *L. nidifica* based on the strong chemical congruency displayed.

10.2.3.6 *Laurencia flexuosa*

Both bromofucin isomers, compound **8.1** and **8.2**, were isolated previously from *L. flexuosa* (Table 10.1) and are considered as the major metabolites within this particular species. Since their isolation seems to be reproducible they can be considered as possible marker compounds, assisting in the chemical identification of *L. flexuosa* specimens.

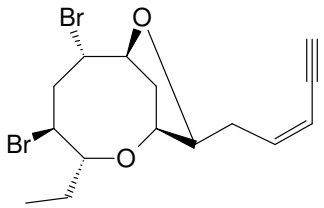

8.1

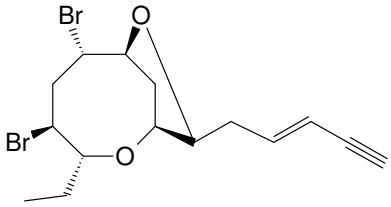

8.2

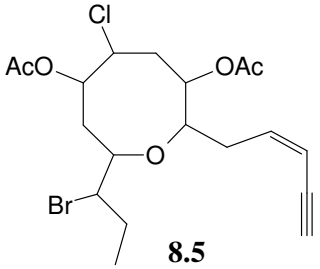

8.5

This is the first record of the cyclic acetylenic ether **8.5** from *L. flexuosa*. It was first isolated from a Greek specimen of *L. obtusa*. Phylogenetically, *L. flexuosa* and *L. obtusa*, although not sister species, do exist in the same clade with a common ancestor, however a considerable amount of speciation can be seen to have occurred since then (Scheme 10.1).

10.2.3.7 *Laurencia sodwaniensis*

The organic extract of *Laurencia sodwaniensis* afforded compounds **9.1** (cartilagineol) and compound **9.3** (obtusol). Halo-chamigrane **9.1** was originally isolated from *L. cartilagineol* (Table 10.1) for which no sequencing data is available. *L. dendroidea* also produces compound **9.1** (Table 10.1) and interestingly, *L. dendroidea* shows a close phylogenetic relationship to *L. sodwaniensis* (Scheme 10.1; expansion shown below).

Similarly, chamigrane **9.3** was produced by *L. dendroidea* and *L. majuscula* (Table 10.1) both of which share close phylogenetic relationships to *L. sodwaniensis* (Scheme 10.1).

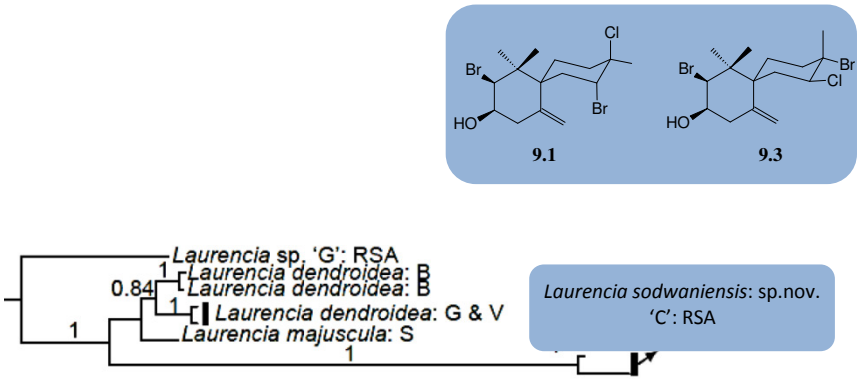

10.2.4 The usefulness of chemotaxonomy in *Laurencia* spp.

Considering the above analyses, it is clear that the chamigrane type sesquiterpenoids such as compound **3.9** are generally observed as being widespread amongst the *Laurencia* spp. As a result the chemotaxonomic reliability of such compounds is questionable.

Despite this there are instances wherein more exclusive chamigranes such as those which display both regio and stereoisomerism of their halogen moieties, can be successfully used for making chemotaxonomic inferences e.g. cartilagineol (**9.1**) and obtusol (**9.3**) appear exclusively in *L. sodwaniensis* and other closely related *Laurencia* spp.

The indole alkaloids isolated from *L. complanata* displayed a striking resemblance to those isolated from its sister species, *L. brongniartii.* This particular structural class was seen to be almost exclusive within both algae.

L. multiclavata and *L. nidifica*, which are sister species, also displayed prominent similarities in their natural product chemistry in the form of compounds **7.1**, **7.5** and **7.6**.

The value of the chemotaxonomic approach is reiterated as two morphologically similar *Laurencia* spp. viz. *L.* cf. *corymbosa* and *L. glomerata*, which are often confused with one another, have shown to produce distinctive chemical profiles, now allowing for easier distinction.

Furthermore, when analysing chemically unexplored species of *Laurencia*, the emergence of new chemistry exclusive to a particular species introduces the concept of molecular markers. Such compounds make it easier to identify a particular species in subsequent investigations. e.g. algoane (**5.9**) is seen to be exclusively found in *L. natalensis* and hence can act as a marker compound for the identification of this particular species.

Despite the potentially useful role the chemotaxonomic approach may display, a few factors must be considered. It is imperative to realise that, as a classification tool, chemotaxonomy should not be used alone, but rather as a complementary method amongst other more robust methods such as gene sequencing and histological analyses[5].

Secondly, a phylogeny tree depicts genetic relationships between predefined sequences, in this case the *rbc*L sequence. The sequences coding for the enzymes responsible for secondary metabolites synthesis are not considered in the tree. This could then suggest that two sister species on the phylogeny tree, related solely by similarity of *rbc*L sequences, could in fact possess greatly varied sequences coding for enzymes systems involved secondary metabolite synthesis. This implies the possibility of contrasting metabolite chemistry amongst two closely related sister species.

Finally, the chemistry from an individual species analysed during different seasons and from different geographical locations may not always be analogous. Environmental conditions such as temperature, salinity of the water, predation and pH are all capable of influencing the chemical profile of an alga. This should always be taken into account during chemotaxonomic analyses.

[5] Reassignment of *Laurencia* spp. which were incorrectly classified is occurring as a result of these emerging methods of species delineation. See Appendix 1 for the natural product chemistry of the recently re-assigned species *Laurenciella marilzae* (Basionym: *Laurencia marilzae*)

10.3 References

Abe, T.; Masuda, M.; Kawaguchi, S.; Itoh, T.; Suzuki, M. Additional analysis of the chemical diversity in *Laurencia nipponica* (Ceramiales, Rhodophyta). *Phycological Research* **1997**, *45*, 173-176.

Abou-Elnaga, Z. S.; Alarif, W. M.; Al-lihaibi, S. S. New larvicidal acetogenin from the eed alga *Laurencia papillosa*. *Clean: Soil, Air, Water* **2011**, *39*, 787-794.

Alarif, W. M.; Al-lihaibi, S. S.; Ayyad, S. N.; Abdel-Rahman, M. H.; Badria, F. A. Laurene-type sesquiterpenes from the Red Sea red alga *Laurencia obtusa* as potential antitumor-antimicrobial agents. *European Journal of Medicinal Chemistry* **2012**, *55*, 462-466.

Ayyad, S. E. N.; Al-Footy, K. O.; Alarif, W. M.; Sobahi, T. R.; Bassaif, S. A.; Makki, M. S.; Asiri, A. M.; Al-Halwani, A. Y.; Badria, A. F.; Badria, F. A. A. Bioactive C15 acetogenins from the red alga *Laurencia obtusa*. *Chemical and Pharmaceutical Bulletin* **2011**, *59*, 1294-1298.

Bano, S.; Ali, M. S.; Ahmad, V. U. Marine Natural Products Vl.A halogenated chamigrene epoxide fromthe red alga *Laurencia pinnatifida*. *Planta Medica* **1987**, *53*, 508.

Butler, A.; Carter-Franklin, J. N. The role of vanadium bromoperoxidase in the biosynthesis of halogenated marine natural products. *Natural Product Reports* **2004**, *21*, 180-188.

Carter, G. T.; Rinehart, K. L.; Li, L. H.; Kuentzel, S. L.; Connor, J. L. Brominated indoles from *Laurencia brongniartii*. *Tetrahedron letters* **1978**, *46*, 4479-4482.

Coll, J. C.; Wright, A. D. Tropical marina algae. IV. Novel metabolites from the red alga *Laurencia implicata* (Rhodophyta, Rhodophycaeae, Ceramiales, Rhodomelaceae). *Australian Journal of Chemistry* **1989**, *42*, 1685-1693.

Combaut, G.; Piovetti, L.; Kornprobst, J. M. Study of some red algae from the Senegalese coast. *Comptes Rendus de l'Academie des Sciences, Serie II: Mecanique, Physique, Chimie, Sciences de la Terre et de l'Uinvers* **1984**, *299*, 433-435.

da Silva Machado, F. L. D. Pacienza-Lima, W. Rossi-Bergman, B.; Gestinari, L. M. D.; Fujii, M .T.; de Paula, J. C.; Costa, S. S.; Lopes, N. P.; Kaiser, C, R.; Soares, A. R. Antileishmanial sesquiterpenes from the Brazilian red alga *Laurencia dendroidea*. *Planta Medica* **2011**, *77*, 733-735.

Diaz-Marrero, A. R.; Brito, I.; de la Rosa, J. M.; D'Croz, L.; Fabelo, O.; Ruiz-Perez, C.; Darias, J.; Cueto, M. Novel lactone chamigrene-derived metabolites from Laurencia majuscula. *European Journal of Organic Chemistry* **2009**, *9*, 1407-1411.

Elsworth, J. F.; Thomson, R. H. A new chamigrane from *Laurencia glomerata. Journal of Natural Products* **1989**, *52*, 893-895.

Faulkner, J. D.; Stallard, M. O.; Ireland, C. Prepacifenol epoxide, a halogenated sesquiterpene diepoxide. *Tetrahedron Letters* **1974**, *40*, 3571-3574.

Fenical, W. Chemical variation in a new bromochamigrene derivative from the red seaweed *Laurencia pacficia*. *Phytochemistry* **1976**, *15*, 511-512.

Francis, C. M. **2014**. Systematics of the *Laurencia* complex (Rhodomelaceae, Rhodophyta) in southern Africa. PhD Thesis. University of Cape Town, Cape Town, South Africa.

Francisco, M. E. Y.; Turnbull, M. M.; Erickson, K. L. Cartilagineol, the fourth lineage of *Laurencia* derived polyhalogenated chamigrene. *Tetrahedron Letters* **1998**, *39*, 5289-5292.

Gonzalez, A. G.; Darias, J.; Diaz, A.; Fourneron, J. D.; Martin, J. D.; Perez, C. Evidence for the biogenesis of halogenated chamigrenes from the red alga *Laurencia obtusa*. *Tetrahedron Letters* **1976**, *35*, 3051-3054.

Howard, B. M.; Fenical, W. Structures and chemistry of two new halogen-containing chamigrene derivatives from *Laurencia*. *Tetrahedron Letters* **1975**, 21, 1687-1690.

Iliopoulou, D.; Vagias, C.; Harvala, C.: Roussis, V. C_{15} acetogenins from the red alga *Laurencia obtusa*. *Phytochemistry* **2002**, *59*, 111-116.

Ireland, C.; Stallard, M. O.; Faulkner, J. D.; Finer, J.; Clardy, J. Some chemical constituents of the digestive gland of the sea hare *Aplysia californica. Journal of Organic Chemistry* **1976**, *41*, 2461-2465.

Ji, N. Y.; Li, X, M.; Li. K.; Ding, L. P.; Gloer, J. B.; Wang, B. G. Diterpenes, sesquiterpenes, and a C_{15}-acetogenin from the red alga *Laurencia mariannensis*. *Journal of Natural Products* **2007**, *70*, 1901-1905.

Ji, N. Y.; Li, X. M.; Li, K.; Gloer, J. B.; Wang, B. G. Halogenated sesquiterpenes and non-halogenated linear C_{15}-acetogenins from the marine red alga *Laurencia composita* and their chemotaxonomic significance. *Biochemical Systematics and Ecology*, **2009a**, *36*, 938-941.

Ji, N. Y.; Li, X. M.; Li. K.; Wang, B. G. Halogenated sesquiterpenes from the red alga *Laurencia saitoi*. *Helvetica Chimica Acta* **2009b**, *92*, 1873-1879.

Jongaramruong, J.; Blackman, A. J.; Skelton, B. W.; White, A. H. Chemical relationships between the sea hare *Aplysia parvula* and the red seaweed *Laurencia filiformis* from Tasmania. *Australian Journal of Chemistry* **2002**, *55*, 275-280.

Juagdan, E. G.; Kaldindi, R.; Scheuer, P. Two new chamigranes from an Hawaiian red alga, *Laurencia cartilaginea. Tetrahedron* **1997**, *53*, 521-528.

Kennedy, D. J.; Selby, I. A.; Thomson, R. H. *Chamigrane metabolites* from *Laurencia obtusa* and *L. scoparia*. *Phytochemistry* **1988**, *27*, 1761.

Kigoshi, H.; Shizuri, Y.; Niwa, H.; Yamada, K.. Laurencenyne, a plausible precursor of various nonterpenoid C_{15}-compounds, and neolaurencenyne from the red alga *Laurencia okamurai*. *Tetrahedron Letters* **1981**, *2,* 4729-4732.

Kimura, J.; Kamada, N.; Tsujimoto, Y. Fourteen chamigrane derivatives from a red alga, *Laurencia nidifica*. *Bulletin of the Chemical Society of Japan* **1999**, *72*, 289-292.

König, G. M.; Wright, A. D. New C_{15} acetogenins and sesquiterpenes from the red alga *Laurencia* sp. cf. *L. gracilis*. *Journal of Natural Products* **1994**, *57*, 477-485.

Mann, M. G. A. **2008**. An investigation of the antimicrobial and antifouling properties of marine algal metabolites. M.Sc thesis. Rhodes University, Grahamstown.

Masuda, M.; Kawaguchi, S.; Abe, T.; Kawamoto, T.; Suzuki, M. Additional analysis of the chemical diversity of *Laurencia* (Rhodomelaceae) from Japan. *Phycological Research* **2002**, *50*, 135-144.

McMillan, J.; Paul, I. C.; White, R. H.; Hager, L. P. Molecular structure of acetoxyintricatol: a new bromo compound from *Laurencia intricata*. *Tetrahedron* **1974**, *23*, 2039-2042.

McPhail K. L.; Davies-Coleman M. T.; Copley R. C. B.; Eggleston D. S. New halogenated sesquiterpenes from South African specimens of the circumtropical sea hare *Aplysia dactylomela. Journal of Natural Products* **1999**, *62*, 1618-1623.

McPhail, K. L.; Davies-Coleman, M. T. (3*Z*)-bromofucin from a South African sea hare. *Natural Product Research* **2005**, *19*, 449-452.

Ojika, M.; Shizuri, Y.; Yamda, K. A halogenated chamigrane epoxide and six related halogen-containing sesquiterpenes from the red alga *Laurencia okamurai*. *Phytochemistry* **1982**, *21*, 2410-2411.

Pitombo, L. F.; Kaiser, C. R.; Pinto, A. C.; Occurence of chamigrenes in *Aplysia dactylomela* from Brazilian waters. *Boletin de la Sociedad Chilena de Quimica* **1996**, *41*, 433-436.

Rovirosa, J.; Soto, H.; Cueto, M.; Dárias, J.; Herrera, J.; San-Martín, A. Sesquiterpenes from *Laurencia claviformis*. *Phytochemistry* **1999**, *50*, 745-748.

Stegenga, H.; Bolton, J. J.; Anderson, R. J. Seaweeds of the South African west coast; *Contributions from the Bolus herbarium* **1997**, *18*, 1-655.

Suzuki, M.; Furusaki, A.; Kurosawa, E. The absolute configurations of halogenated chamigrane derivatives from the marine alga, *Laurencia glandulifera* Kützing. *Tetrahedron* **1979**, *35*, 823-831.

Suzuki, T.; Kikuchi, H.; Kurosawa, E. Six new sesquiterpenoids from the red alga *Laurencia nipponica* Yamada. *Bulletin of the Chemical Society of Japan* **1982**, *55*, 1561-1563.

Suzuki, M.; Segawa, M.; Suzuki, T.; Kurosawa, E. Structures of halogenated chamigrene derivatives, minor constituents from the red alga *Laurencia nipponica* Yamada. *Bulletin of the Chemical Society of Japan* **1983**, *56*, 3824-3826.

Takahashi, Y.; Suzuki, M.; Abe, T.; Masuda, M. Anhydroaplysiadiol from *Laurencia japonensis*. *Phytochemistry* **1998**, *48*, 987-990.

Tanaka, J.; Higa, T.; Bernardinelli, G.; Jefford, C. W. Sulfur containing polybromoindoles from the red alga *Laurencia brongniartii* . *Tetrahedron* **1989**, *45*, 7301-7310.

Vairappan, C. S; Daitoha, M.; Suzuki, M.; Abe, T.; Masuda, M. Antibacterial halogenated metabolites from the Malaysian *Laurencia* species. *Phytochemistry* **2001**, *58*, 291-297.

Wang, B. G.; Gloer, J. B.; Ji, N, Y.; Zhao, J. C.; Halogenated organic molecules of Rhodomelaceae origin: Chemistry and Biology. *Chemical Reviews* **2013**, *113*, 3632-3685.

Waraszkiewicz, S. M.; Erickson, K. L. Halogenated sesquiterpenoids from the Hawaiian marine alga *Laurencia nidifica*: Nidificene and Nidifidiene. *Tetrahedron Letters* **1974**, *23*, 2003-2006.

Waraszkiewicz, S. M.; Erickson, K. L.; Sun, H. H.; Clardy, J.; Finer, J. C_{15} halogenated compounds from the hawaiian marine alga *laurencia nidifica*. Maneonenes and isomaneonenes. *Journal of Organic Chemistry* **1978**, 43, 3194-3204.

Wessels, M.; König, G. M. Wright, A. D. New natural product isolation and comparison of the secondary metabolite content of three distinct samples of the sea hare *Aplysia dactylomela* from Tenerife. *Journal of Natural Products* **2000**, *63*, 920-928.

Chapter 11

^{1}H NMR profiling of crude organic extracts as a discriminatory tool for the identification of selected *Laurencia* spp.

Abstract

^{1}H NMR profiling of crude algal extracts allows for a visual assessment of the sample's "metabolite fingerprint". Discrimination between algal species can occur provided ^{1}H NMR spectra are reproducible and exclusive to each individual species. Moreover, there is a possibility of identifying major metabolites attributed to a particular species, further assisting the process of species identification.

This chapter investigates the crude organic ^{1}H NMR profiles of nine selected South African *Laurencia* spp. Profiling was conducted on the seven *Laurencia* spp. explored earlier in this study including *Laurencia* cf. *elata* and *Laurencia peninsularis*.

Where possible, an individual species was collected from more than one location to assess the effect of geographical location on ^{1}H NMR profiles (i.e. will the metabolites produced be different). Moreover, spectral reproducibility was assessed by analysing three separate plants per specimen.

For the most part, the crude ^{1}H NMR spectra obtained were reproducible and exclusive to individual *Laurencia* spp. Samples of *L. glomerata* collected from Kenton-on-Sea showed differing metabolite profiles to those collected from Noordhoek, while morphologically varying samples of *L. flexuosa* from four different locations produced comparable profiles. Major metabolites were identified within the majority of the ^{1}H NMR profiles generated.

Chapter 11

^{1}H NMR profiling of crude organic extracts as a discriminatory tool for the identification of selected *Laurencia* spp.

11.1 Introduction

11.1.1 Plant taxonomy

Plant taxonomy or classification is described as the confinement, description and naming of any grouping of plants considered to embody a single entity or taxa which are reproductively isolated from any other similar groups (Hegnauer, 1986).

The earliest evidence of classifying plants (370-250 BC) was undertaken by Theophrastus, a Greek naturalist who is regarded as the father of botany. His findings were recorded in his manuscript entitled "*Enquiries into Plants and the Causes of Plants*" (Levetin and McMahon, 2008).

In South Africa, evidence of seaweed systematics extends from as early as the 18th century when colonial European phycologists took an interest in local samples. Two pioneering taxonomists, George Papenfuss and Herre Stegenga are responsible for vast contributions to seaweed systematics along the South African coastline (Bolton, 1999).

11.1.2 Conventional algal classification tools

There has been much debate in recent years as to the approaches that should be employed during the delimitation of a species. Experts argue that features such as geographical, ultra-structural, biochemical, morphological, ecological and breeding data are vital aspects which should be considered during the classification process (Leliaert *et al*., 2014).

11.1.2.1 Morphology

Undoubtedly the most common approach used to classify algae is through morphological assessment. Structures such as female reproductive systems or ultra-structural entities such as pit-plugs are intricately scrutinised to assist in species delimitation. If two species are regularly differentiated by one or more indicative morphological differences, then it would be safe to argue that there is no gene flow between them (Wiens, 2007).

Morphological classification faces a variety of challenges including:

- Phenotypic plasticity wherein phenotypes change under varying environments
- Morphological convergence of different species
- Polymorphism of a single species
- Morphological stasis

This reduces the reliability of the method and necessitates the need for other classification tools to be used concomitantly during the taxonomic process (Maggs *et al*., 2007; Leliaert *et al*., 2014).

11.1.2.2 Molecular systematics (DNA based)

According to Wiens (2007) DNA sequencing is emerging as an increasingly accepted approach in either identifying species (DNA bar-coding) or during discovery of new species (DNA taxonomy). Analyses of single or multiple genetic loci are made as various ideologies exist as to which gene clusters are representative of species phylogeny (Davis and Nixon, 1992).

The most common DNA-based phylogenetic markers in red algae are shown below in (Table 11.1) with the plastid ribulose bisphosphate carboxylase large chain (*rbc*L) sequence being one of the most commonly used markers. This gene sequence possesses a vast amount of phylogenetically relevant sites owing to its high mutation rate *vs*. the small subunit ribosomal marker (SSU) (Freshwater and Bailey, 1998).

Table 11.1: DNA based phylogenetic markers used in Rhodophyta (Maggs *et al*., 2007)

DNA marker		
Plastid	**Mitochondrial**	**Nuclear**
*rbc*L	*cox*1	Phycoerythrin
*rbc*S	*cox*2-3 spacer	Elongation factor
RuBisCo spacer		ITS region
URP		Actin
16S		LSU rDNA

A major advantage of DNA based taxonomy is the ability to cladistically monitor the speciation process as descriptive phylogenetic trees can be constructed depicting possible species ancestry (Hey and Pinho, 2012).

11.1.3 Chemotaxonomy

Chemotaxonomy can be regarded as a molecular systematics tool reflective of the secondary metabolite profile of an organism. This is a relatively foreign classification tool relying on the notion that an organism's secondary metabolite profile may possess phylogenetic inferences. Secondary metabolites are fashioned by enzymes which are a direct expression of an organism's genetic code and hence phenotypic (Carreno-Quintero, 2013).

The sheer diversity of secondary metabolites produced by organisms such as marine macroalgae allows for greater opportunity for chemotaxonomy to flourish as a large chemical space favours the probability of chemical exclusivity between species i.e. the chances of different species producing different metabolites increases. Considering that the genes coding for the production of these compounds are limited, the immense structural diversity of these metabolites can thus be attributed to the presence of multifunctional enzymes to which there is poor enzyme specifity (Schwab, 2003).

There are several literary reports which document the usefulness of chemotaxonomy in species identification and or delineation.

Morphologically similar species within the genera *Gelidium* and *Gracilaria* were successfully differentiated by chemo-analysis of structurally varied agars they produced (Nelson *et al*., 1994; Falshaw *et al*., 1999).

Dussert *et al*., (2008) showed the value of seed lipids in determining phylogenetic relationships within various species of the coffee producing plant of the genus *Coffea.*

The eukaryotic *Oomycetes,* originally thought to be fungi, were later classed as Protista. Since fungi such as *Blastocladiella emersonii* are known to produce secondary metabolites including polyols, the deficiency of similar molecules in *Oomycota* was in phylogenetic agreement with their removal from the Fungi kingdom (Pfyffer, 1998).

The secondary metabolite profiles of various species of Phillipino samples of the red marine algae *Portieria hornemannii* were analysed *via* GC-MS (gas chromatography-mass spectrometry) wherein inter and intra-specific metabolite variation was observed, attributable to factors such as cryptic species, life-stage history as well as environmental factors (Payo *et al*., 2011).

The chemotaxonomic classification approach is not without drawbacks. The fungus *Rhizopus microsporus* was shown to possess secondary metabolites which were later discovered as being produced by endosymbiotic bacteria of the genus *Burkholderia* (Partida-Martinez *et al*., 2007).

Instances have occurred wherein the secondary metabolite profile of an individual species of marine algae, *Laurencia microcladia*, found in different geographical settings, produced varying compound profiles (Pietra, 2002). This phenomenon could possibly be ascribed to phenotypic plasticity wherein environmental fluctuations trigger a phenotypic change (Leliaert *et al*., 2014). Such occurrences need to be considered if the chemotaxonomic approach is to be successful.

In direct contrast to the above Howard *et al*., (1980) and Masuda *et al*., (1997) have shown that *Laurencia snyderae and Laurencia nipponica* produce unaltered metabolite profiles under varying environmental conditions.

The success of chemotaxonomy as a robust classification tool relies on factors such as the quantitative constancy of metabolites as well as a distinct independence of fluctuating environmental conditions when produced (Howard *et al*., 1980).

Having considered the aforementioned it is critical that chemotaxonomic assignments should always be made in conjunction with other classification tools such as gene sequencing and or morphological assessment. This reduces the chances of misassignment of a species and also allows for an inspection of conformity between classification methods i.e. will all methods identify the organism as the same species?

11.1.4 Challenges in algal taxonomy

Despite the expansive efforts made by phycologists in describing marine algal species, with over 20 000 accepted species recorded over the last 200 years, there are many challenges which are faced in the field of algal systematics and could translate into major causes for concern if not addressed in a well structured manner (de Clerck, 2013).

Payo *et al*., (2013) identified 21 cryptic species of *Portieria hornemanii* in the Philippines archipelago. This species was thought to be the only kind within the genus. The possibility of such diversity amongst a single species needs to be acknowledged and DNA sequencing

among other classification tools should become mandatory upon species delimitation so as to establish such discrepancies.

De Clerk *et al*., (2013) further discuss the abundance of synonymous algal species wherein a single species has been described under various names. Furthermore, with the advent of simpler, rapid DNA sequencing kits, the volumes of algal genetic information being produced is merely being used to cladistically classify species instead of providing full descriptions with binomial names. These specimens are commonly referred to as "dark taxa".

Moreover, the DNA molecular confirmation of species reported in the distant past is increasingly difficult as type specimens are either missing or difficult to obtain from cited sources.

The role of phycologists has consequently expanded wherein a strict presentation of a greater number of sample details is required during its delimitation. This includes mandatory data such as DNA molecular sequences of specific gene clusters, detailed morpho-anatomical analyses, as well as careful preservation of type specimens for future reference.

11.1.5 Spectroscopic techniques in natural product profiling

11.1.5.1 Hyphenated techniques

There is an increasing use of hyphenated spectroscopic techniques for natural product profiling following miniaturisation and increased sensitivity of instruments. Brkljača and Urban (2011) reveal the common use of HPLC-NMR (high performance liquid chromatography-nuclear magnetic resonance) for metabolite profiling of marine organisms.

HPLC-NMR was also the spectroscopic profiling technique of choice for Dias *et al*., (2009a) who report the isolation of the new metabolites cyclo-*iso*-allolaurinterol as well as *iso*-allolaurinterol from an Australian specimen of *Laurencia filiformis*. The same technique was employed to successfully profile the metabolites of the red algae *Plocamium mertensii* and a marine sponge of the genus *Dactylospongia* (Dias *et al*., 2008, 2009b).

Extracts of *Laurencia chondrioides* were subjected to UHPLC-PDA-HRMS (ultra high performance liquid chromatographic-photodiode array-high resolution mass spectrometry) analysis which led to rapid identification of known metabolites as well as the identification of two new C_{15} bromo-allenes (Kokkotou *et al*., 2014).

Machín-Sánchez *et al*., (2014) investigated the use of CE-MS (capillary electrophoresis-mass spectrometry) metabolite profiling on Tenerife algal specimens within the *Laurencia* complex. A viable discernment of species and genera of the collected samples was possible as CE-MS fingerprints were shown to be exclusive and reproducible.

A GC-MS geographical and seasonal variation study of the secondary metabolites from *Laurencia decidua* samples collected in Baja, California showed little profile variation (Caccamese *et al*., 1979).

11.1.5.2 ^{1}H NMR profiling

NMR spectroscopy has played a vital role in better understanding various metabolic pathways within organisms. A classic example of this was the use of isotope-tracer analysis to deduce the metabolic route of ethanol (Wilson and Burlingame, 1974).

Literary evidence of ^{1}H NMR profiling for the classification and or identification of plants and derived products thereof exists.

Examples include the distinction of *Cannabis sativa* cultivars (Choi *et al*., 2004) as well as the classification of *Ephedra* species including its commercial herbs (Kim *et al*., 2005).In addition, Craigie *et al*., (2008) document the successful use of ^{1}H NMR profiles of aqueous extracts of the brown alga *Ascophyllum nodosum* to identify a seasonal variation of secondary metabolites produced.

As a spectroscopic technique, ^{1}H NMR profiling is considered to be universal as only minor fluctuations are viewed in spectra obtained on different NMR instruments. It is shown to best suited for the qualitative as well as the quantitative analyses of complex crude fractions containing a vast array of metabolites. The none-destructive nature allows for full retrieval of the analyte and with modern day advances such as larger electromagnetic field strengths and cryogenic probes, issues of instrument sensitivity are fast dissipating (Wishart, 2008). NMR sample preparation is relatively quick and a high throughput capacity is possible with spectra developing in a minimal number of scans (Verpoorte, 2010). The nature of a ^{1}H NMR spectrum is such that it depicts a comprehensive visualisation of the protonated metabolite profile within the crude sample (dependant on the polarity of the solvent used). NMR consequently provides comprehensive structural information *via* analysis of coupling constants, chemical shifts and signal intensities within spectra obtained as opposed to other

spectroscopic techniques such as HPLC or MS (Wolfender *et al*., 2014). The resultant profile may also serve as a unique molecular fingerprint which, if consistent, could be used as a constructive template for identifying species provided that inter-species profiles are distinct. Cross references can be made to compounds whose spectra already exist in well defined databases, such as the flavonoid class (Mihaleva *et al*., 2013).

11.1.6 Chapter aims

^{1}H NMR profiling of crude algal extracts has the potential to be a rapid tool for discerning the identity of *Laurencia* spp. species provided that the profiles are reproducible and unique between species.

This part of the study seeks to consider the feasibility of implementing such an approach when applied to South African *Laurencia* spp. and contributions toward the efficacy and practicality of this method are presented.

The main objectives were to:

1) Develop a simple yet reliable ^{1}H NMR profiling study protocol.

2) Generate ^{1}H NMR profiles of nine selected *Laurencia* spp.

3) Analyse the profiles for exclusivity so as to allow for species differentiation.

4) Where possible, explore intra and inter-site variation of metabolites produced.

5)Where possible, assess metabolite profiles of various morphotypes.

6) Identify major metabolites in generated profiles.

11.2 Results and Discussion

11.2.1 *Laurencia* spp. selected for profiling

A total of nine *Laurencia* spp. (Table 11.2) were selected for ^{1}H NMR profiling of which the phytochemistry of seven has been revealed within this study (Chapters 3-9) with the exception of *Laurencia* cf. *elata* and *Laurencia peninsularis*. Geographical and morphological variants of species were collected and analysed where possible e.g. ^{1}H NMR profiles of *L. flexuosa* specimens from four different geographical settings were investigated including five morphotypes from Kenton-on-Sea (Table 11.2). As a result a grand total of 22 samples were profiled *via* ^{1}H NMR spectroscopy.

Table 11.2: *Laurencia* spp. selected for ^{1}H NMR profiling

	Algae	Collection Code	Collection site	Collection Date
1.	*L. flexuosa*	KOS130823-1	Kenton-on-Sea	August, 2013
2.		KOS130823-2	Kenton-on-Sea	August, 2013
3.		KOS130823-4	Kenton-on-Sea	August, 2013
4.		KOS130823-5	Kenton-on-Sea	August, 2013
5.		KOS130823-6	Kenton-on-Sea	August, 2013
6.		NDK130821-12	Noordhoek	August, 2013
7.		D1013	Cape St. Francis	May, 2011
8.		D904	De Hoop	February, 2011
9.	*L. glomerata*	KOS130823-3	Kenton-on-Sea	August, 2013
10.		NDK130821-10	Noordhoek	August, 2013
11.	*L.natalensis*	KOS130823-8	Kenton-on-Sea	August, 2013
12.		D930	De Hoop	February, 2011
13.		D1022	Cape Vidal	September, 2011
14.	*L.* cf. *corymbosa*	NDK130821-11	Noordhoek	August, 2013
15.	*L.* cf. *elata*	TS090311	Port Alfred	March, 2009
16.	*L. peninsularis*	KB101108	Kalk Bay	November, 2010
17.		D900	De Hoop	February, 2011
18.		GC120901	Glencairn	September, 2012
19.	*L. complanata*	D1053	Port Edward	September, 2011
20.	*L. sodwaniensis*	D968	Cape Vidal	March, 2011
21.	*L. multiclavata*	D1024	Cape Vidal	September, 2011
22.		D969	Cape Vidal	March, 2011

11.2.2 Study design

In order to generate reliable ^{1}H NMR profiles, a simple yet robust study design was developed and strictly adhered to so as to ensure that consistency was maintained throughout the investigation.

The reproducibility of the profiling method was assessed by separately analysing three different plants from each of the 22 specimens.

Constancy of certain variables such as $CDCl_3$ volume (0.5 mL), NMR parameters and sonication times during extraction were maintained, however other variables such as the weight of the plant analysed were more difficult to control as individual plant sizes varied considerably between the various algal species.

A brief description of the general method employed in the study is shown (Scheme 11.1). The weights of the wet algae pre-extraction, dry algae post-extraction and the crude organic extract were all obtained.

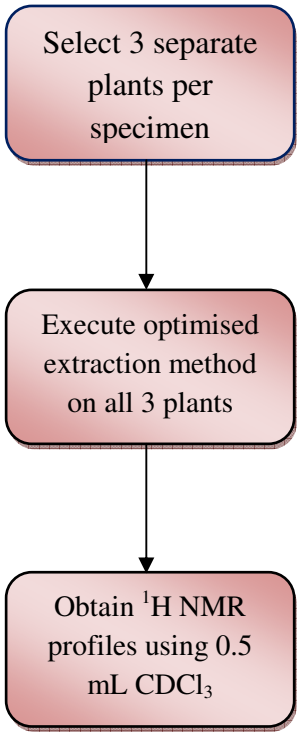

Scheme 11.1: Brief overview of ^{1}H NMR profiling study design

11.2.2.1 Optimisation of small scale extractions

The majority of *Laurencia* spp. secondary metabolites fall within the non-polar to intermediate polarity range. We therefore focused our attention on procedures that would extract a high concentration of these types of compounds. It was thus essential to standardise an extraction procedure that would not only display a rudimentary selectivity toward these lipophilic metabolites but also allow for their isolation in reasonable quantity.

The most common extraction solvent used in the study of *Laurencia* spp. metabolites is a mixture of dichloromethane and methanol (CH_2Cl_2-MeOH). In a preliminary study we compared the ^{1}H NMR spectra of CH_2Cl_2-MeOH (1:1 and 2:1) (Figure 11.1). There was very little difference between the two solvent extracts except for more pronounced signals due to unwanted, polar, sugar type moieties in the CH_2Cl_2-MeOH (1:1) extract.

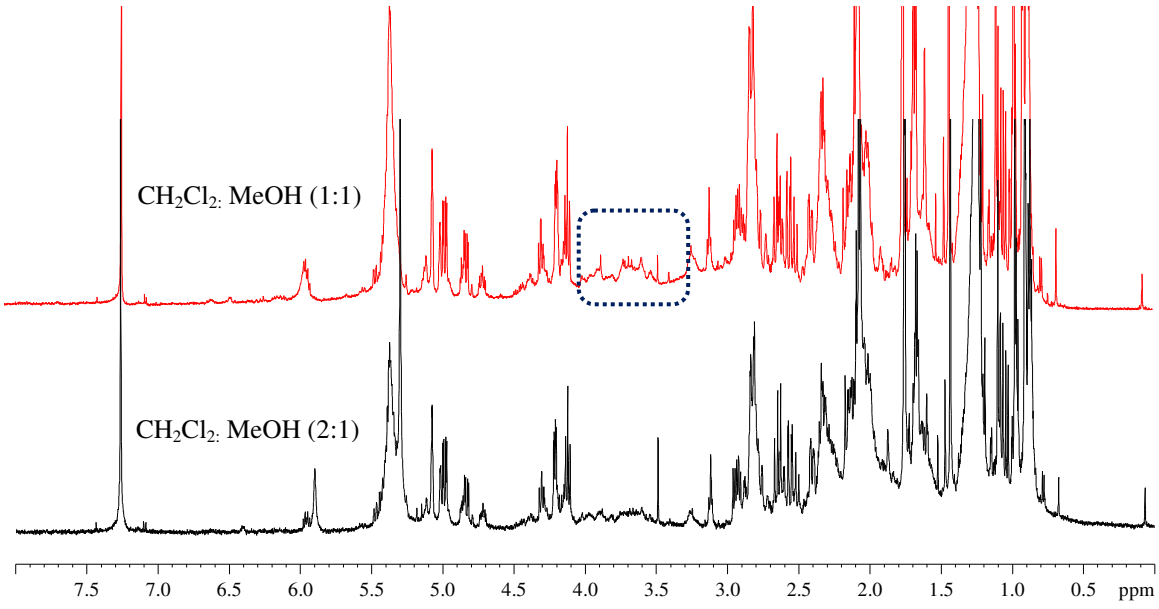

Figure 11.1: A comparison of the ^{1}H NMR ($CDCl_3$, 600 MHz) spectra of crude CH_2Cl_2-MeOH (2:1 and 1:1) extracts of *Laurencia natalensis* (KOS130823-8)

After obtaining an ideal solvent system the next challenge was to maximise the quantity of crude extract obtained. Flash freezing the algae with liquid N_2 and subsequent size reduction afforded a more substantial organic extract with the emergence of some resonances that were not noticed in samples which had not been size reduced (Figure 11.2).

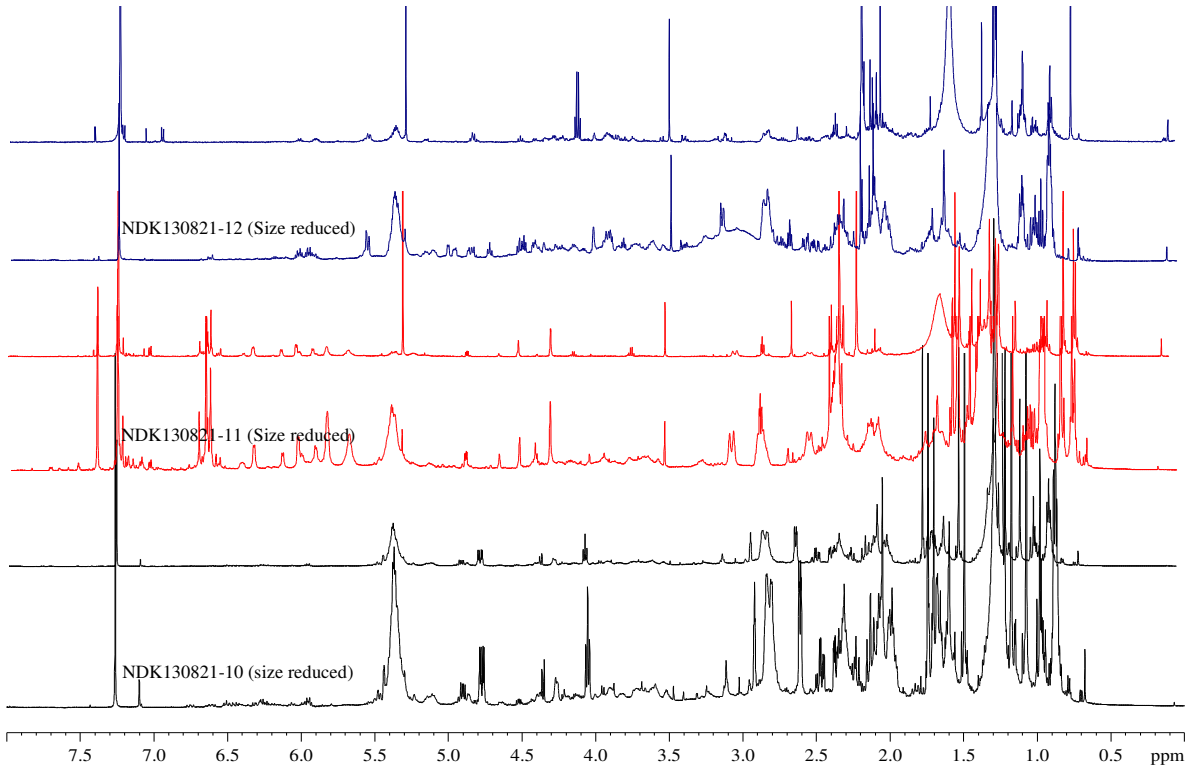

Figure 11.2: A comparison of the ^{1}H NMR ($CDCl_3$, 600 MHz) spectra of crude CH_2Cl_2-MeOH (2:1) extracts of various *Laurencia spp.* with and without flash freeze size reduction.

11.2.2.2 Optimised study procedure

After considering the ideal solvent system as well as the need for size reduction the final method employed for the small scale extraction procedure was as shown below in (Scheme 11.2). It is important to mention that the optimisation of the study procedure was abbreviated as a simple yet reproducible method was merely required.

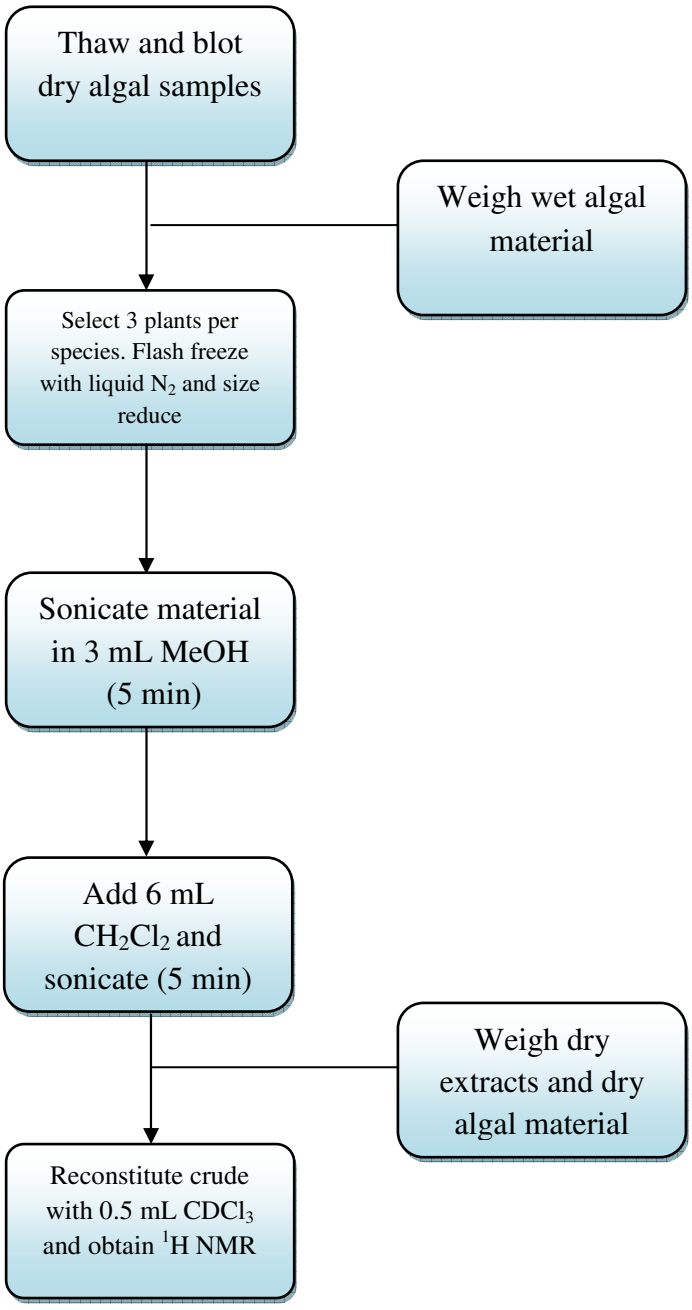

Scheme 11.2: Optimised study protocol for the ^{1}H NMR profiling of *Laurencia* spp. crude extracts

11.2.2.4 NMR parameters

It was observed that 32 scans were sufficient to produce well defined ^{1}H NMR profiles. All NMR experiments were executed on the same day so as to prevent any experimental bias.

Table 11.3: ^{1}H NMR parameters used for profiling

Acquisition mode	DQD
NS	32
PROBHD	5mm BBI
PulseProg	zg30
TD	65536
Solvent	$CDCl_3$
TE	298K
DS	2
D1	1s

11.2.3 ^{1}H NMR profiles of selected *Laurencia* spp

The corresponding masses of all the samples profiled are as shown overleaf in (Table 11.4) wherein three separate plants per individual algal sample were extracted. This is as depicted by the lettering (a-c) per sample.

The ^{1}H NMR profiles reported shortly after are shown in triplicate and major metabolites are identified within the crude spectrum. NMR profiles of morphological or geographical variants that were identical were placed in the supplementary data.

Table 11.4: Wet and dry masses of algal material

Algae Sample			Wet mass (g)	Dry mass (g)	Mass of extract (g)	% Extract (Dry mass)
L. flexuosa	1.	KOS130823-1a	1.5412	0.3156	0.0142	4.3
		KOS130823-1b	0.7316	0.1708	0.0101	5.6
		KOS130823-1c	1.5661	0.2308	0.0131	5.4
	2.	KOS130823-2a	2.8167	0.3246	0.0232	6.7
		KOS130823-2b	0.9582	0.1350	0.0201	13.0
		KOS130823-2c	0.6646	0.0731	0.0227	23.7
	3.	KOS130823-4a	3.0882	0.3063	0.0290	8.6
		KOS130823-4b	3.3780	0.3411	0.0147	4.1
		KOS130823-4c	2.5290	0.1919	0.0097	4.8
	4.	KOS130823-5a	2.8161	0.2599	0.0160	5.8
		KOS130823-5b	1.7682	0.1149	0.0077	6.3
		KOS130823-5c	1.5815	0.1044	0.0121	10.4
	5.	KOS130823-6a	1.2429	0.1848	0.0251	12.0
		KOS130823-6b	0.9816	0.1810	0.0183	9.2
		KOS130823-6c	0.7915	0.1556	0.0219	12.3
	6.	NDK130821-12a	1.3683	0.1300	0.0279	17.7
		NDK130821-12b	0.8942	0.0910	0.0079	8.0
		NDK130821-12c	0.9568	0.0631	0.0068	9.7
	7.	D1013a	1.2735	0.0597	0.0082	12.1
		D1013b	0.7342	0.0356	0.0251	41.4
		D1013c	1.2200	0.0687	0.0073	9.6
	8.	D904a	1.3158	0.0685	0.0076	10.0
		D904b	0.5886	0.0288	0.0078	21.3
		D904c	0.6221	0.0456	0.0089	16.3
L.glomerata	*9.*	KOS130823-3a	3.1888	0.3219	0.0741	18.7
		KOS130823-3b	2.7026	0.2919	0.0313	9.7
		KOS130823-3c	3.3269	0.3661	0.0451	11.0
	10.	NDK130821-10a	2.4040	0.1953	0.0158	7.5
		NDK130821-10b	3.0118	0.2848	0.0293	9.3
		NDK130821-10c	2.5190	0.2100	0.0191	8.3
L. natalensis	11.	KOS130823-8a	1.0258	0.1203	0.0253	17.4

Table 11.4: Continued

Algae Sample			Wet mass (g)	Dry mass (g)	Mass of extract (g)	% Extract (Dry mass)
		KOS130823-8b	1.0116	0.1231	0.0139	10.1
		KOS130823-8c	2.2480	0.2270	0.0403	15.1
	12.	D930a	0.7107	0.2851	0.0180	5.9
		D930b	0.9626	0.3813	0.0121	3.1
		D930c	0.9802	0.3978	0.0129	3.1
	13.	D1022a	0.2943	0.0792	0.0087	9.9
		D1022b	0.5296	0.0716	0.0082	10.3
		D1022c	0.4347	0.1161	0.0068	5.5
L. corymbosa	14.	NDK130821-11a	2.6562	0.2961	0.0160	5.1
		NDK130821-11b	1.5874	0.1464	0.0184	11.2
		NDK130821-11c	2.5867	0.3333	0.0590	15.0
L. cf. *elata*	15.	TS090311-1a	2.5530	0.3173	0.0594	15.8
		TS090311-1b	1.2600	0.1161	0.0080	6.4
		TS090311-1c	1.3873	0.1174	0.0066	5.3
L. peninsularis	16.	KB101108a	1.8329	0.2904	0.0350	10.8
		KB101108b	1.6510	0.1652	0.0211	11.3
		KB101108c	3.0031	0.3620	0.0158	4.2
	17.	D900a	2.1720	0.1738	0.0128	6.9
		D900b	4.4876	0.6399	0.0142	2.2
		D900c	1.4880	0.1663	0.0102	5.8
	18.	GC120901a	2.5312	0.2861	0.0189	6.2
		GC120901a	1.8178	0.1612	0.0110	6.4
		GC120901a	2.3611	0.6105	0.0497	7.5
L. complanata	19.	D1053a	1.4705	0.1047	0.0618	37.1
		D1053b	2.1315	0.1059	0.0245	18.8
		D1053c	1.2113	0.0613	0.0491	44.5
L. sodwanienses	20.	D968a	0.3513	0.1355	0.0181	11.8
		D968b	0.3311	0.1504	0.0150	9.1
		D968c	0.3534	0.1270	0.0135	9.6
L. multiclavata	21.	D1024a	1.2390	0.4312	0.0035	0.8
		D1024b	1.1049	0.6485	0.0065	1.0
		D1024c	0.6102	0.1983	0.0100	4.8
	22.	D969a	1.8262	0.2010	0.0105	5.0
		D969b	1.7536	0.2096	0.0044	2.1
		D969c	1.5329	0.0199	0.0060	23.2

11.2.3.1 *L. flexuosa* (KOS130823-1)

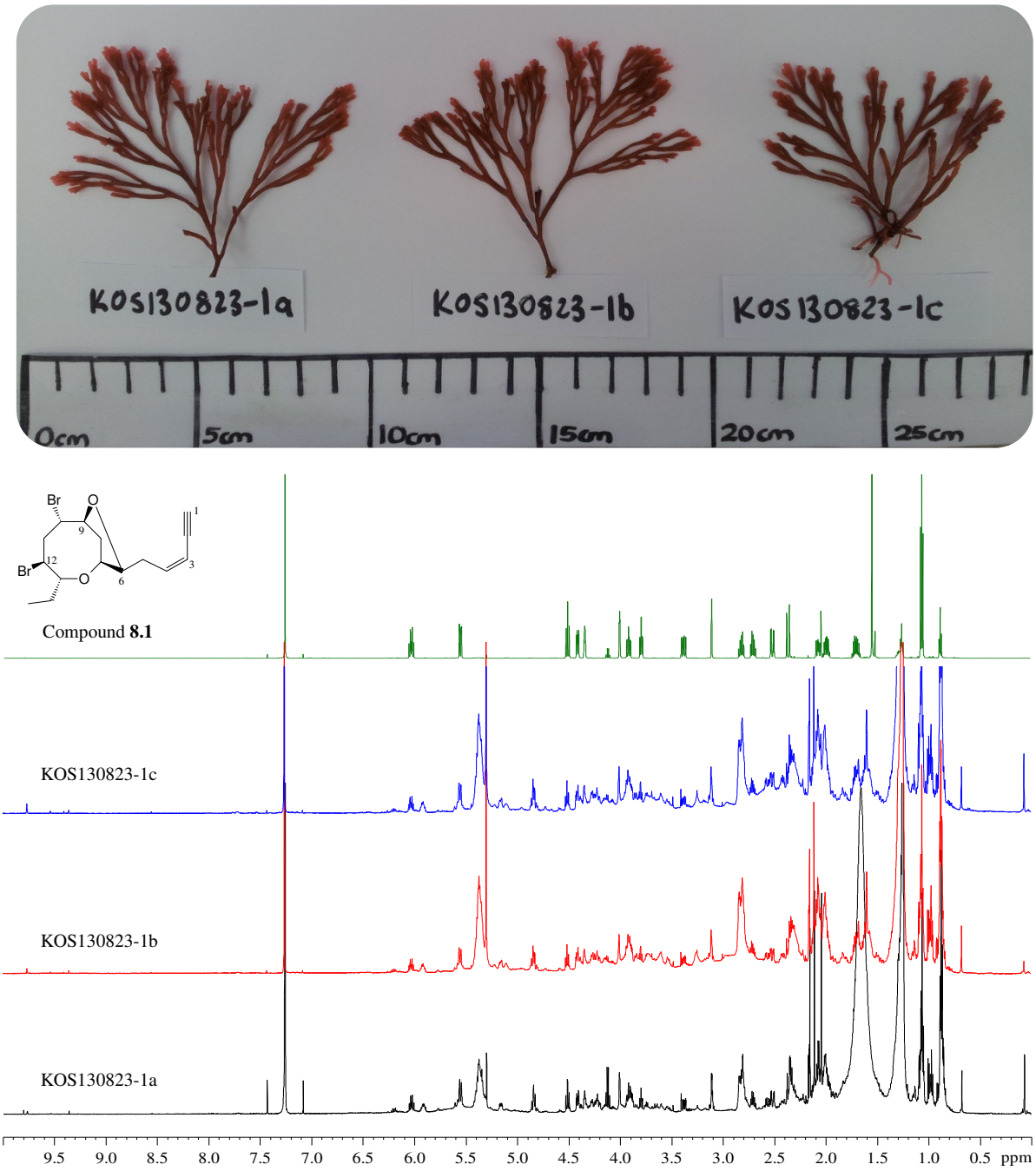

Figure 11.3: [1]H NMR ($CDCl_3$, 600 MHz) profiles of *L. flexuosa* (KOS130823-1)

Specimens of *L. flexuosa* showed reproducible intra and inter-site [1]H NMR profiles. Morphological variants were also observed as possessing the same profiles[1] with compound **8.1**, *cis*-bromofucin, clearly standing out as a major metabolite within this species (Figure 11.3)

[1] [1]H NMR profiles of remaining morphological and geographical variants of *L. flexuosa* are placed in the supplementary data

11.2.3.2 *L. glomerata* (KOS130823-3)

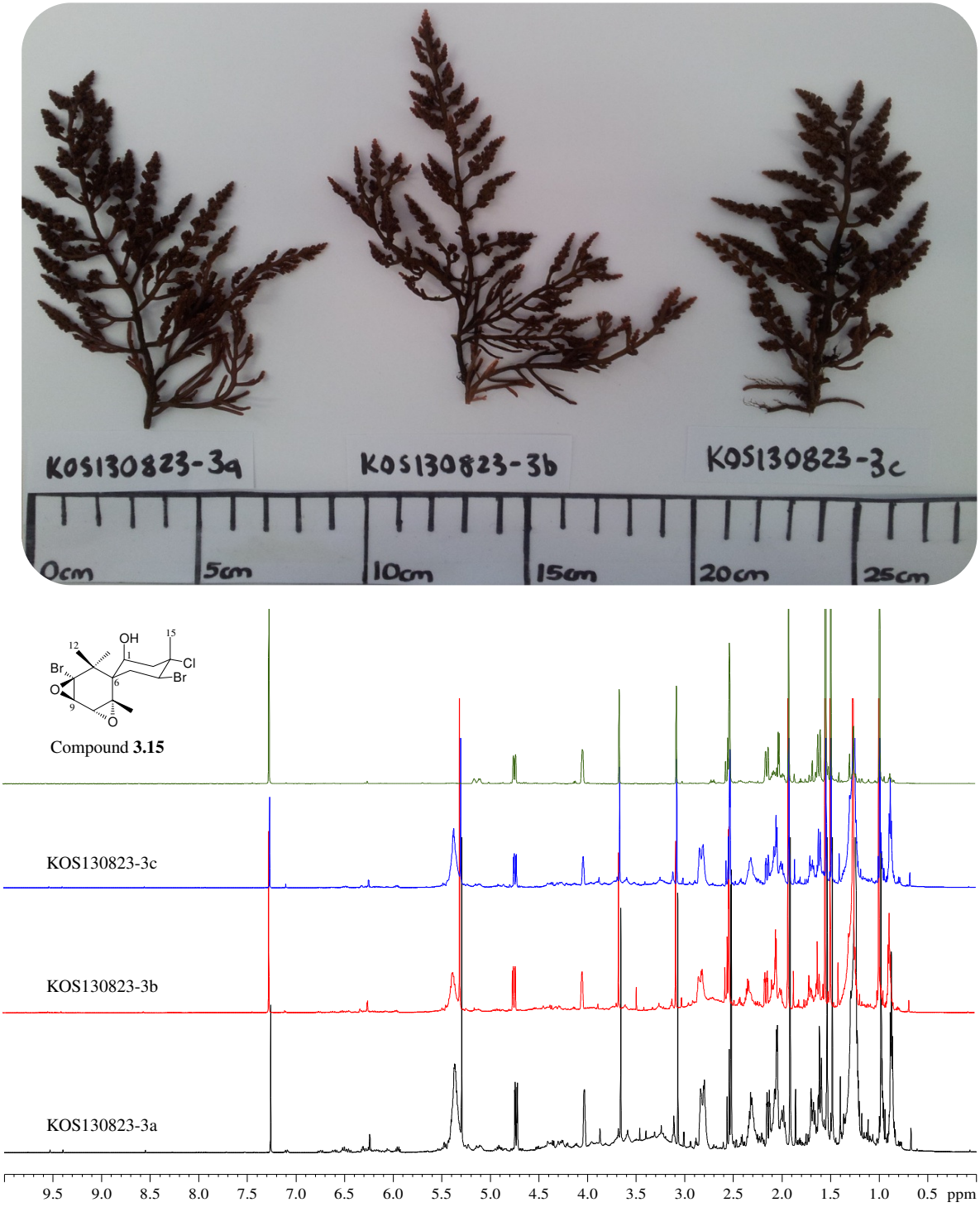

Figure 11.4: [1]H NMR ($CDCl_3$, 600 MHz) profiles of *L. glomerata* (KOS130823-3)

L. glomerata collected from Kenton-on-Sea displayed distinct terpenoid type shielded methyl singlets in the range of δ_H 0.9-2.0 as well as a distinct double doublet at ~ δ_H 4.7 characteristic of compound **3.15** (Figure 11.4).

A geographical variant of *L. glomerata* from Noordhoek (Figure 11.5) surprisingly showed attenuation of the major resonances in (Figure 11.4) with peaks emerging at δ_H 2.0-2.5 including a distinct triplet at δ_H 4.03. These peaks were clearly attributable to compound **3.1**.

11.2.3.3 *L. glomerata* (NDK130821-10)

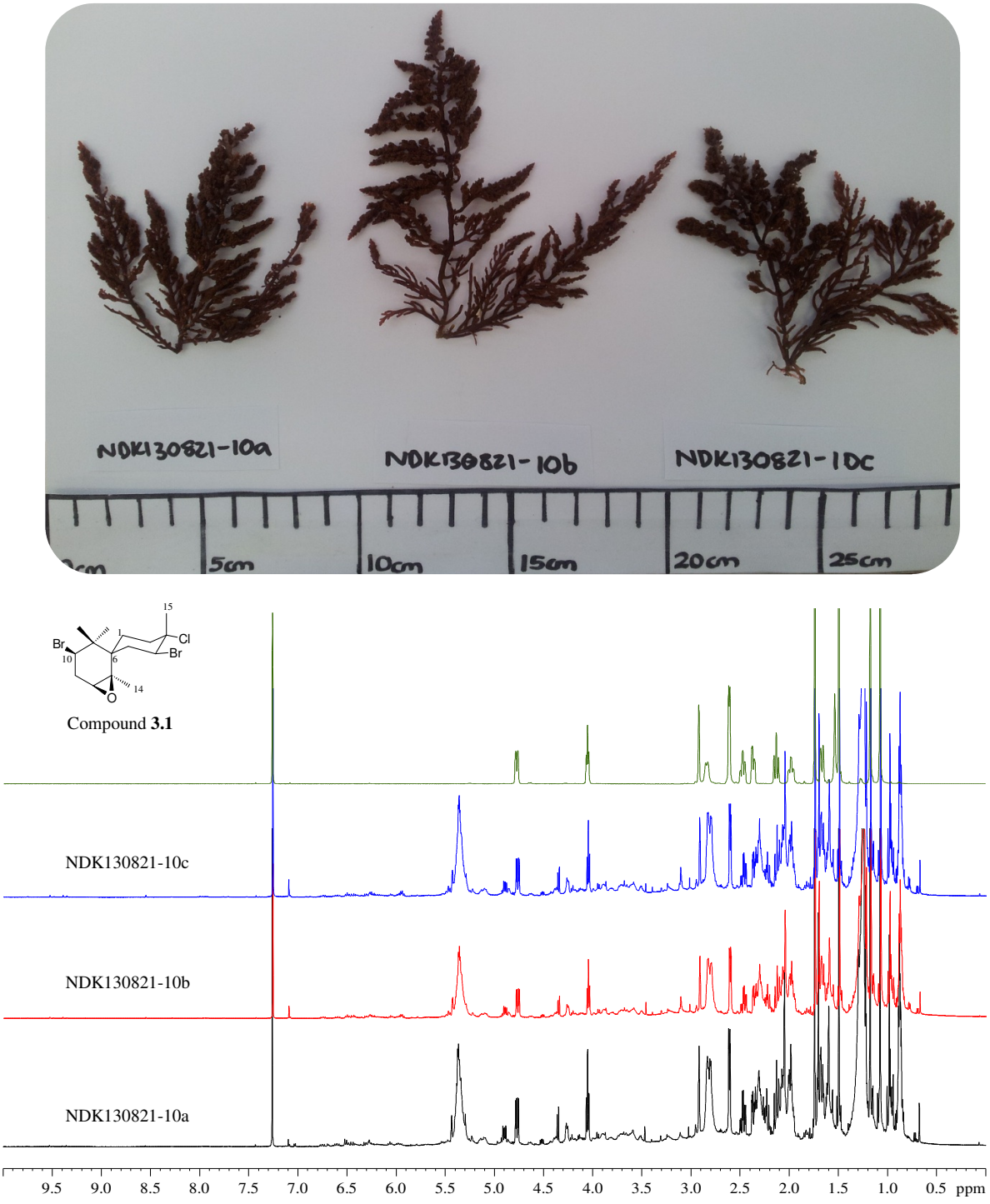

Figure 11.5: ^{1}H NMR ($CDCl_3$, 600 MHz) profiles of *L. glomerata* (NDK130821-10)

11.2.3.4 *L. natalensis* (KOS130823-8)

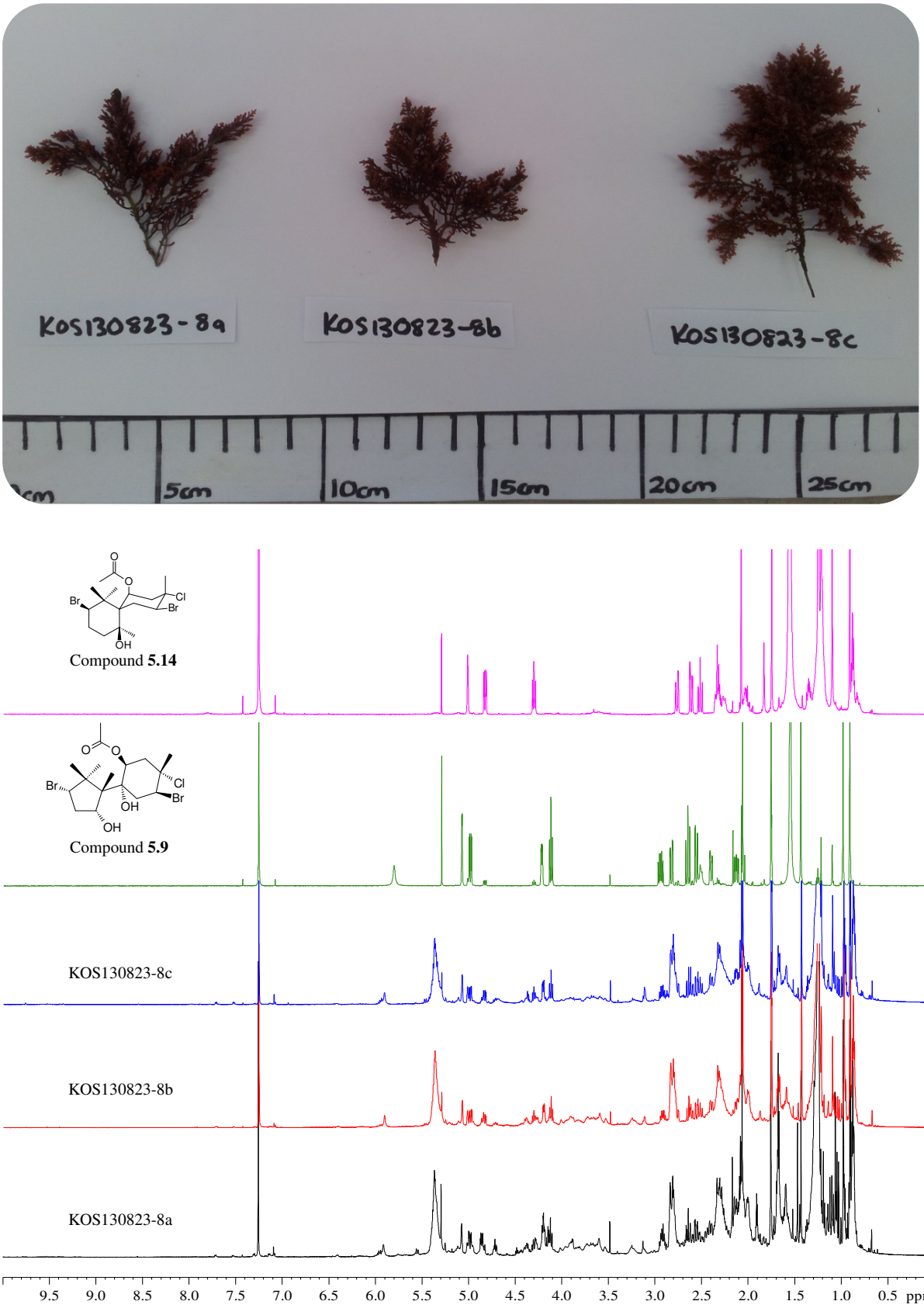

Figure 11.6: [1]H NMR ($CDCl_3$, 600 MHz) profiles of *L. natalensis* (KOS130823-8)

Reproducible ^{1}H NMR profiles were observed in *L. natalensis* from Kenton-on-Sea with compounds **5.9** and **5.14** clearly representing the major metabolites within the profiles (Figure 11.6). A collection of *L. natalensis* from Cape Vidal[2] showed similar ^{1}H NMR profiles to the Kenton-on-Sea specimens.

11.2.3.5 *L. natalensis* (D930)

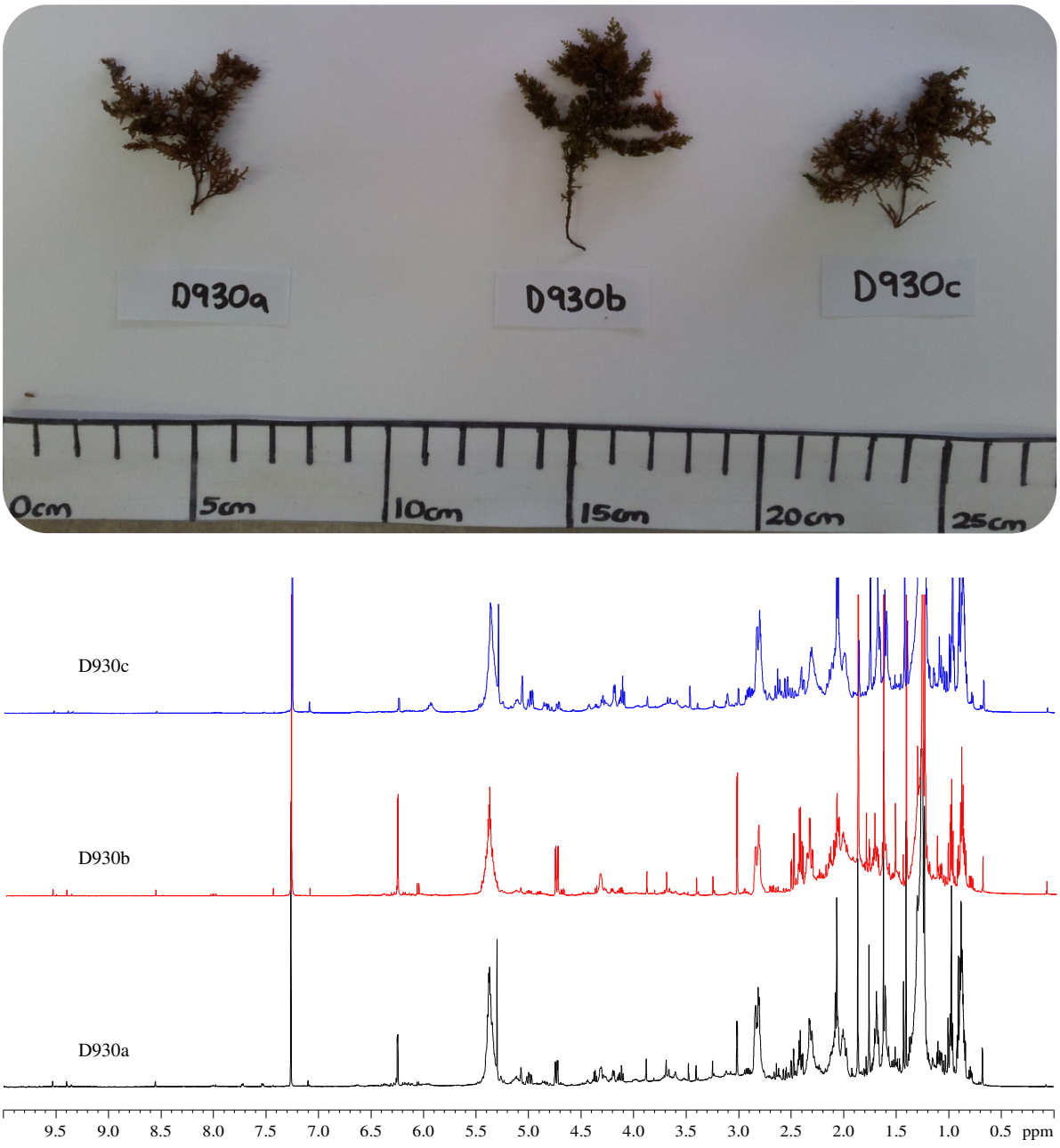

Figure 11.7: ^{1}H NMR ($CDCl_3$, 600 MHz) profiles of *L. natalensis* (D930)

[2] Supplementary data

The profiles of De Hoop specimens of *L. natalensis* were slightly different. ^{1}H NMR profile D930c proved to be similar to those obtained from the Kenton-on-Sea *L. natalensis* samples (Figure 11.7) however profiles D930a and D930b, although similar to each other, showed a visible attenuation of resonances displayed in profile D930c with a prominent double doublet emerging at δ_H 4.70.

11.2.3.6 *L. corymbosa* (NDK130821-11)

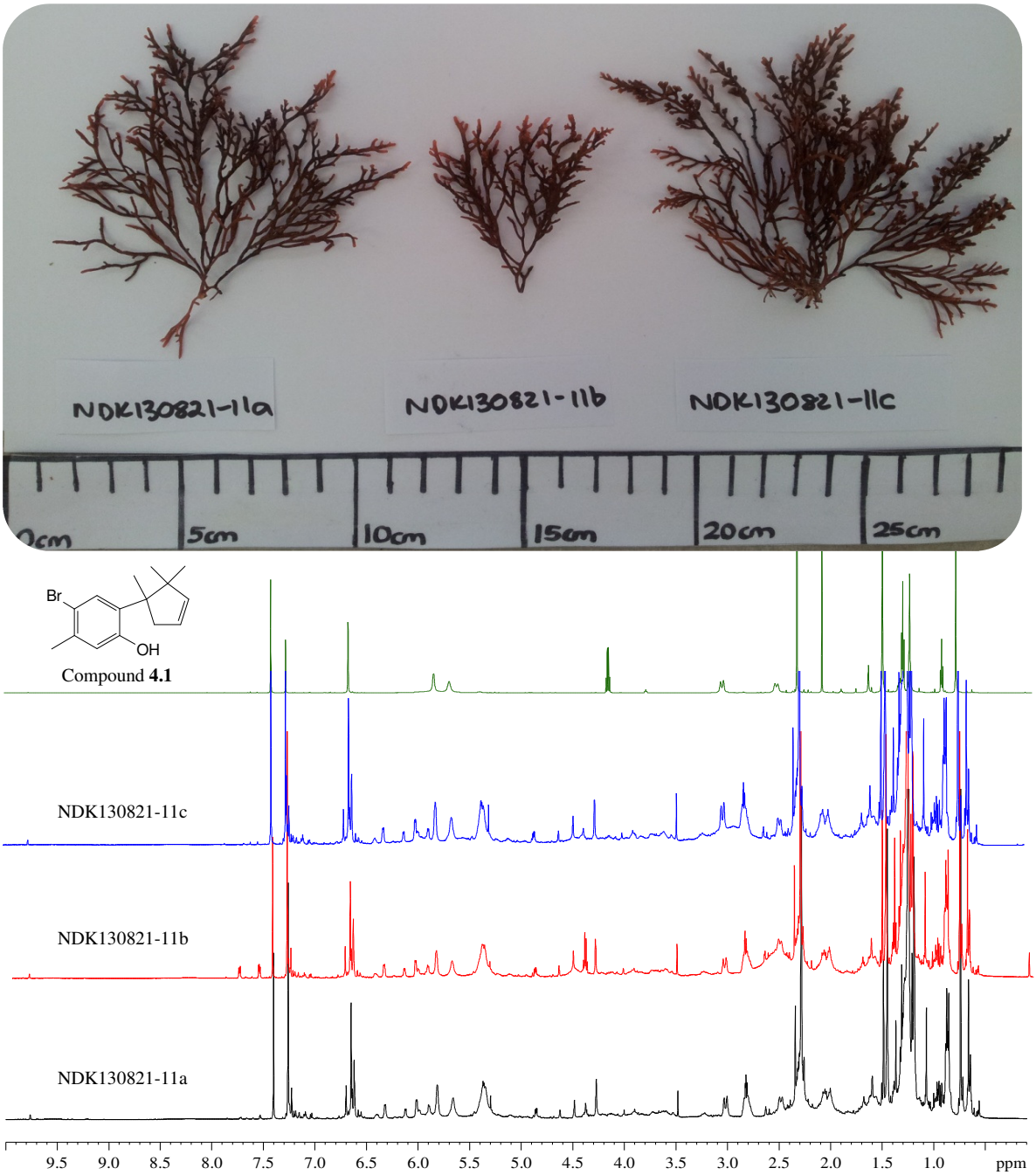

Figure 11.8: ^{1}H NMR ($CDCl_3$, 600 MHz) profiles of *L. corymbosa* (NDK130821-11)

The most distinguishing features of the ^{1}H NMR profiles generated by a sample of *L. corymbosa* collected from Noordhoek were undoubtedly the cluster of aromatic singlets between δ_H 7.0-7.5 as well as a considerable collection of deshielded methine signals in the range of δ_H 5.5-6.5. Compound **4.1** was visibly a major metabolite within the crude extract, with the isomers, compounds **5.6** and **5.7**, also clearly distinguishable.

11.2.3.7 *L.* cf. *elata* (TS090311-1)

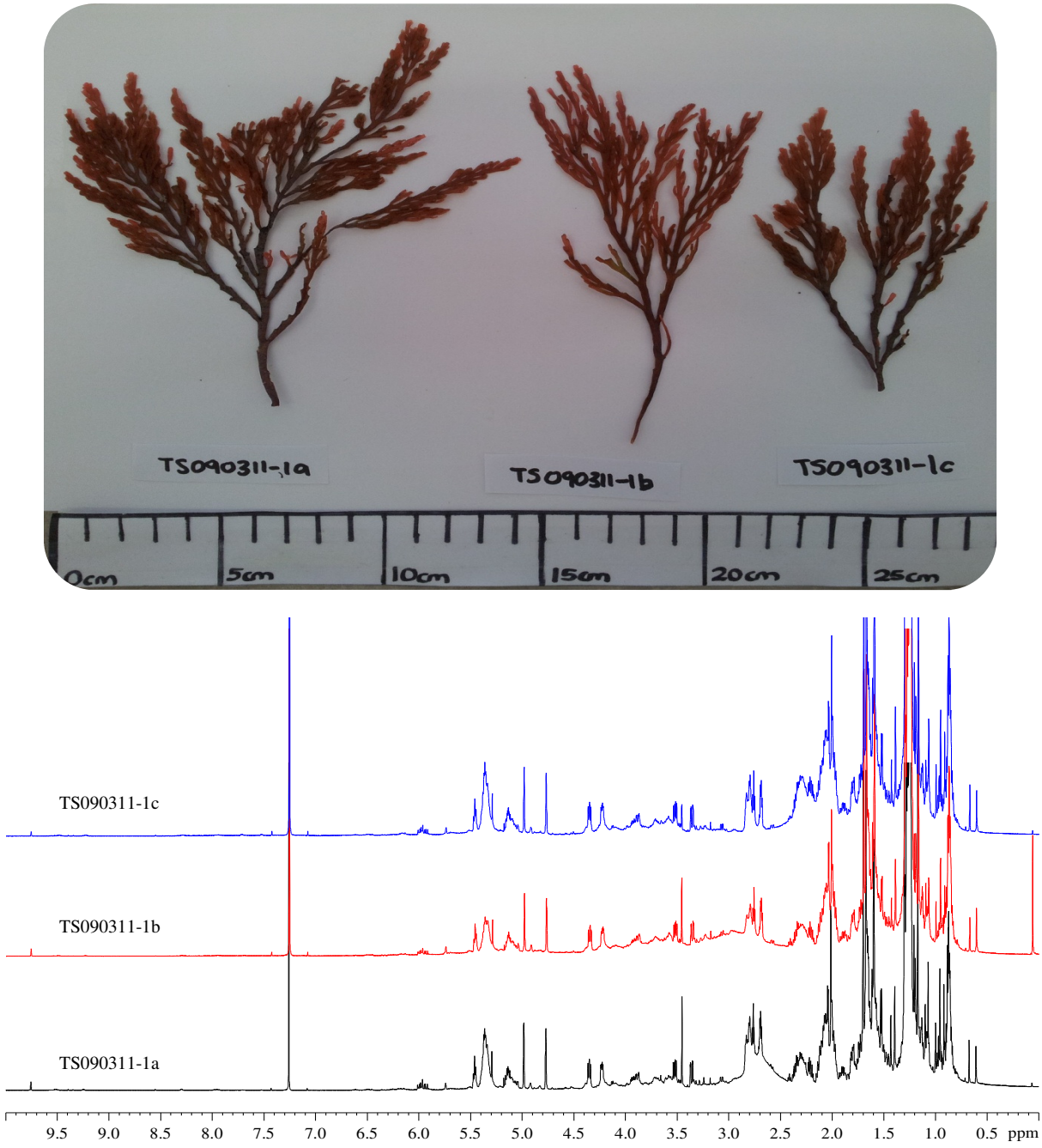

Figure 11.9: ^{1}H NMR ($CDCl_3$, 600 MHz) profiles of *L.* cf. *elata* (TS090311-1)

L. cf. *elata* samples afforded reproducible ^{1}H NMR profiles with an abundance of resonances within the shielded methyl moiety of δ_H 0.5-2.0. Interesting singlets and multiplets were also observed between δ_H 3.5-5.5.

11.2.3.8 *L. peninsularis* (KB101108)

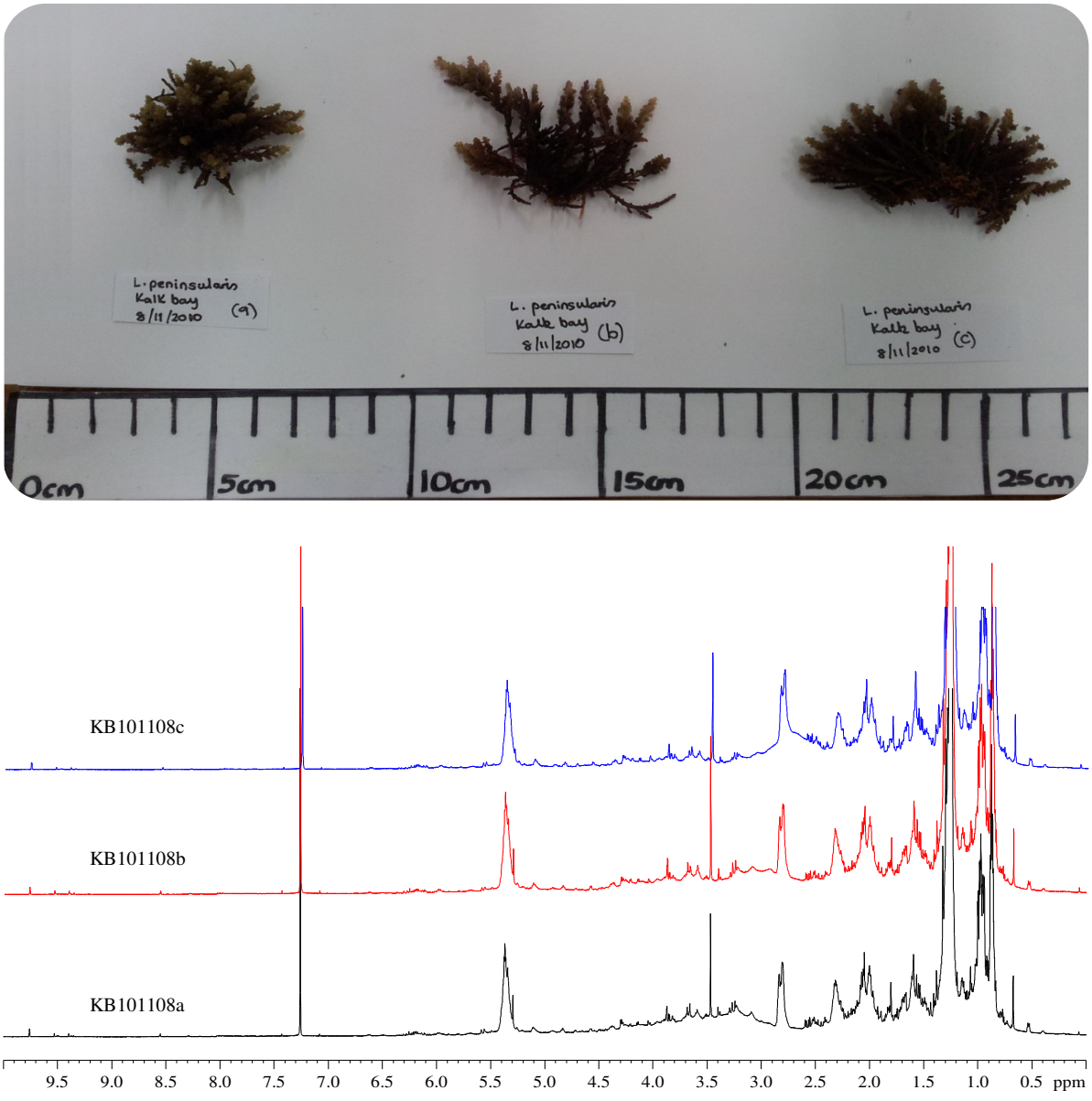

Figure 11.10: ^{1}H NMR ($CDCl_3$, 600 MHz) profiles of *L. peninsularis* (KB101108)

In a *L. peninsularis* sample collected from Kalk Bay, major resonances were identified at δ_H 1.5, 2.0, 2.3, 2.8 and δ_H 5.4. The region between δ_H 3.0-4.0 illustrated a multitude of overlapping signals consequently making individual resonances difficult to examine. Two

additional samples of *L. peninsularis*[3] collected in Glencairn (GC120901) and De Hoop (D900) produced identical [1]H NMR profiles to the sample from Kalk Bay.

11.2.3.9 *L. complanata* (D1053)

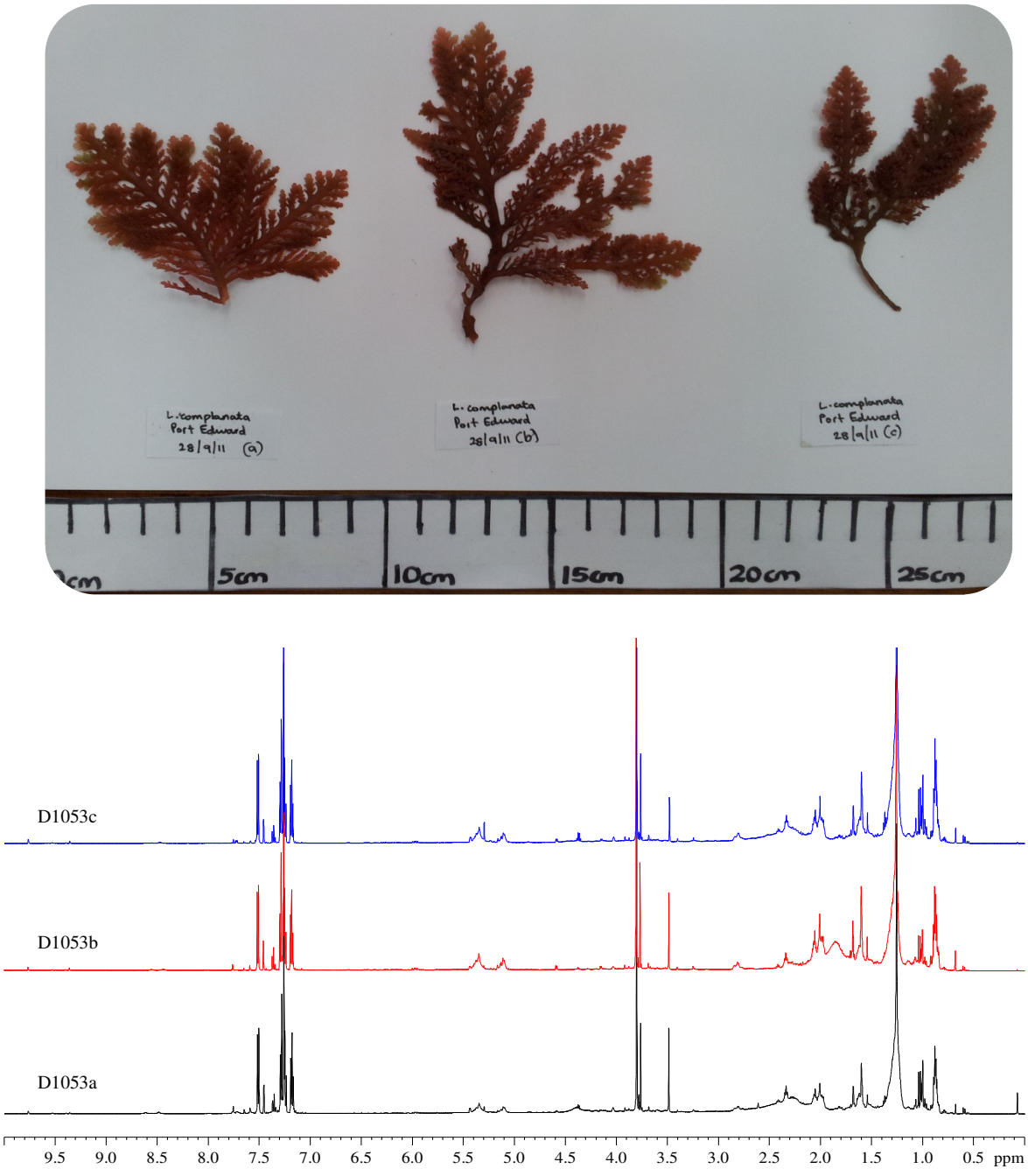

Figure 11.11: [1]H NMR ($CDCl_3$, 600 MHz) profiles of *L. complanata* (D1053)

[3] See supplementary data

An abundance of aromatic signals between δ_H 7.0-7.6 were outstanding in the NMR profiles of *L. complanata*. Similarly, large singlets were also observed at ~ δ_H 3.7. These resonances correspond to *N*-methylindole type compounds shown to be present within this particular *Laurencia* sp. (Chapter 6).

Since there are numerous overlapping signals within the ^{1}H NMR profiles of *L. complanata*, determining a particular major metabolite is difficult, however it is quite clear that the majority of the metabolites are aromatic indole type.

11.2.3.10 *L. sodwaniensis* (D968)

Distinct methyl singlets between δ_H 1.0-1.8 as well as broad methine resonances at δ_H 3.1 and δ_H 3.7 were of main interest in the ^{1}H NMR profiles displayed by *L. sodwaniensis* (Figure 11.12). Also noted were various deshielded singlets in the spectral range of δ_H 4.4-5.2. These signals were ditto to those displaced by the ^{1}H NMR spectrum of compound **9.1** also known as cartilagineol.

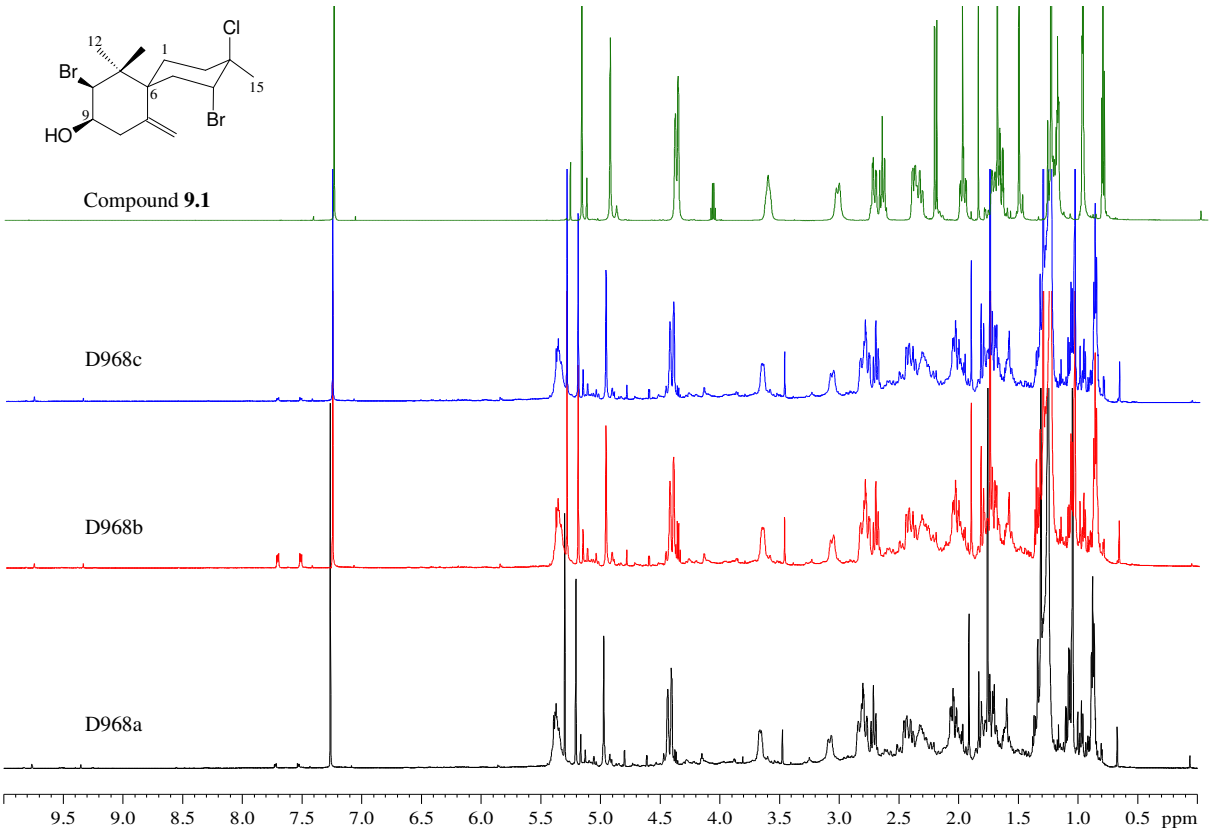

Figure 11.12: [1]H NMR ($CDCl_3$, 600 MHz) profiles of *L. sodwaniensis* (D968)

11.2.3.11 *L. multiclavata* (D1024)

Two specimens of *L. multiclavata* (basionym: *L. natalensoid*) D1024 and D969[4] collected from Cape Vidal furnished identical [1]H NMR profiles with a multitude of various methine signals observed between δ_H 3.5-6.5 showing diverse splitting patterns.

It was immediately apparent that compound **7.1** was the major metabolite within the extract. The two poly-cyclic C_{15} acetogenic isomers, compounds **7.5** and **7.6** were also detectable within the profiles (Figure 11.13).

[4] See supplementary data

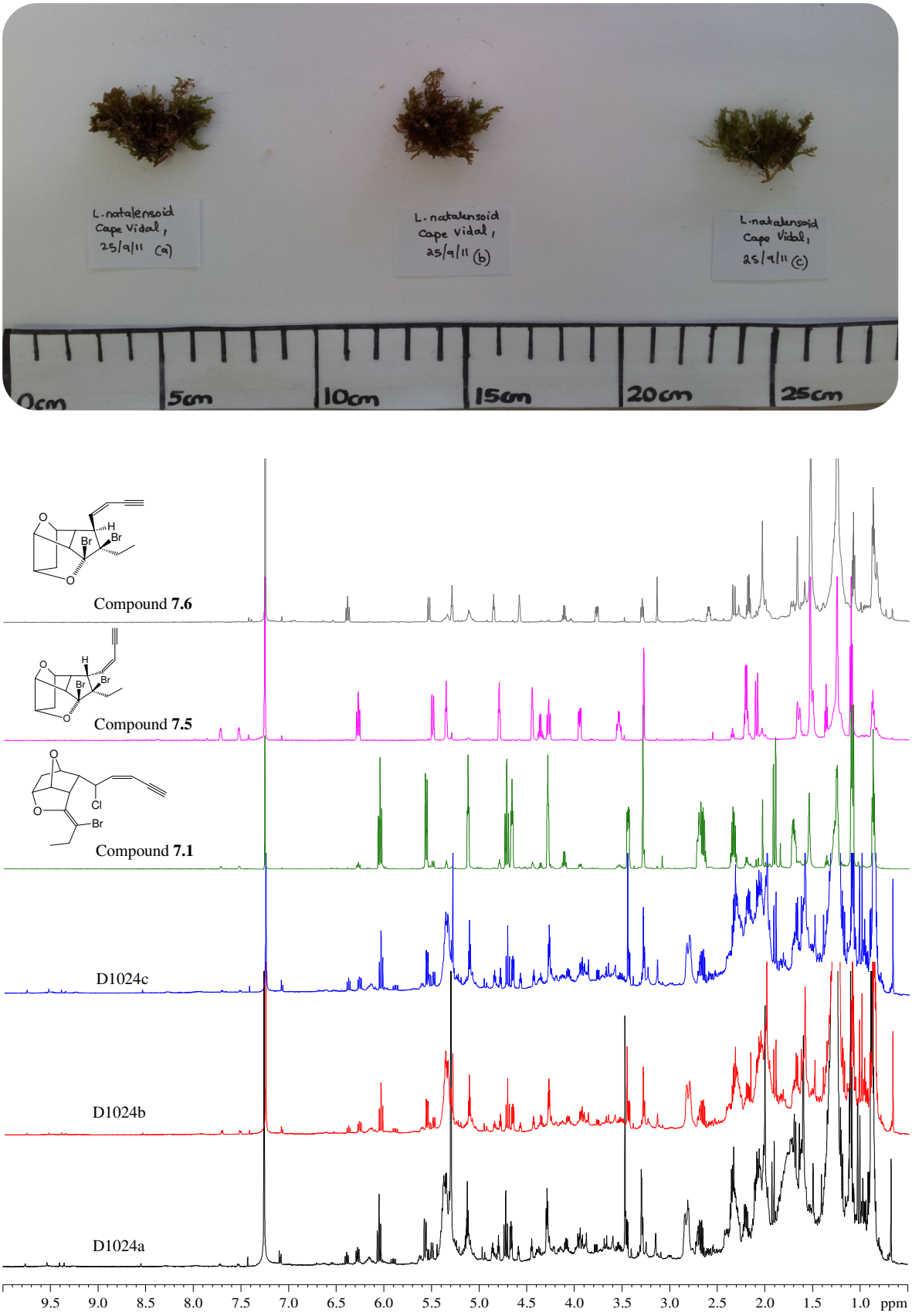

Figure 11.13: [1]H NMR ($CDCl_3$, 600 MHz) profiles of *L. multiclavata* (D1024)

It was clear that some profiles e.g. NDK130821-11b, possessed a minute quantity of re-emerging multiplets between δ_H 7.5-8.0. These signals were identified as minor phthalate contaminants originating from arbitrary solvent removal of rubber from Pasteur pipette teats. The ^{1}H NMR profile of the contaminant was ascertained as below (Figure 11.14).

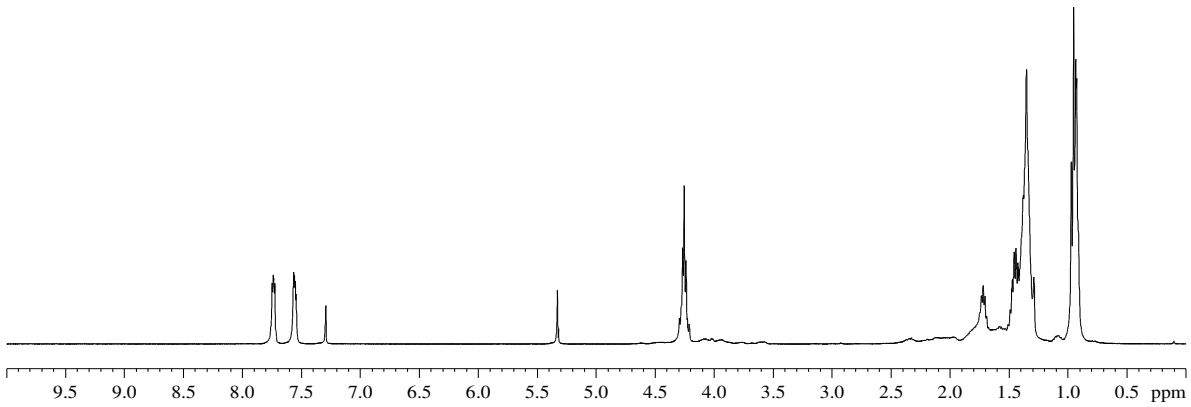

Figure 11.14: ^{1}H NMR spectrum ($CDCl_3$, 600 MHz) of phthalates originating from rubber teat

11.3 Conclusion

In the context of the aims of this element of the study it was seen that a simple yet reliable protocol was designed for the effective ^{1}H NMR crude extract profiling of the various *Laurencia* spp. Major contributors to the success of the profiles included the size reduction of samples after flash freezing with N_2 (liq) as well as the use of a suitable extraction solvent system of CH_2Cl_2:MeOH (2:1).

It was evident that the majority of *Laurencia* spp. species screened produced unique ^{1}H NMR profiles which were seen to be reproducible on three distinct plants from the same species, implying the feasibility of using ^{1}H NMR profiling of crude *Laurencia* spp. extracts for species discrimination. In addition major metabolites were identified within ^{1}H NMR profiles, introducing the possibility of using single molecular markers to identify species.

As shown by *L. flexuosa*, morphological variants produced similar chemistry consequently increasing the reliability of the chemotaxonomic approach i.e. the classification/identification of morphologically distinct plants of an individual species can be assisted by assessing metabolite profiles provided they are constant.

This chapter has successfully exposed the usefulness of ^{1}H NMR as a discriminatory tool in distinguishing *Laurencia* spp. based on their crude, organic secondary metabolite profile.

11.4 Experimental

11.4.1 General experimental

All NMR experiments were performed using a Bruker® Avance 600 MHz spectrometer using $CDCl_3$ and standard pulse sequences. All spectra were referenced according to residual proton residues in deuterated solvent ($CHCl_3$ δ_H 7.26).

Extraction solvents used were chromatography grade (LiChrosolv®), obtained from Merck®, Darmstadt, Germany.

11.4.2 Plant material

See (Table 11.2). Samples were collected by hand and species identity was obtained by South African phycologists Prof John Bolton and Dr. Caitlynne Francis from the University of Cape Town. Specimens were assigned unique collection codes and stored at -4 ^{o}C.

11.4.3 Optimised procedure for ^{1}H NMR screening

Thawed algal samples were rinsed with de-ionised water and blot dried with absorbent paper towel. Each collection bag containing individual species was sifted for three separate plants to be used in the analysis. These triplicate samples were photographed, weighed and size reduced in a mortar after flash freezing with N_2 (liq).

The crushed algal material was placed into test tubes and sonicated (UMC® sonicator, South Africa) for 5 min in 3 mL MeOH followed by another 5 min sonication upon addition of 6 mL CH_2Cl_2. The resultant extract was dried in vacuo using a Buchi® R215 rotavapor and both extract as well as algal dry weight were recorded.

The filtered crude extract was reconstituted in 0.5 mL $CDCl_3$ and the ^{1}H NMR profiles were obtained.

11.5 References

Bolton, J. Seaweed systematics and diversity in South Africa: an historical account. *Transactions of the Royal Society of South Africa* **1999**, *54*, 167-177.

Brkljača, R.; Urban, S. Recent advancements in HPLC-NMR and applications for natural product profiling and identification. *Journal of Liquid Chromatography & Related Technologies* **2011**, *34*, 1063-1076.

Caccamese, S.; Hager, L. P.; Rinehart Jr, K. L.; Setzer, R. B. Characterisation of *Laurencia* species by gas chromatography-mass spectrometry. *Botanica marina* **1979**, *22*, 41-46.

Carreno-Quintero, N.; Bouwmeester, H. J.; Keurentjes, J. J. B. Genetic analysis of metabolome-phenotype interactions: from model to crop species. *Trends in Genetics* **2013**, *29*, 41-50.

Choi, Y. H.; Kim, H. K.; Hazekamp, A.; Erkelens, C.; Lefeber, A. W. M.; Verpoorte, R. Metabolomic differentiation of *Cannabis sativa* cultivars using ^{1}H NMR spectroscopy and principal component analysis. *Journal of Natural Products* **2004**, *67*, 953–957.

Davis, J. I.; Nixon, K. C. Populations, genetic variation, and the delimitation of phylogenetic species. *Systematic Biology* **1992**, *41*, 421-435.

de Clerck, O.; Guiry, M. D.; Leliaert, F.; Samyn, Y.; Verbruggen, H. Algal taxonomy: a road to nowhere? *Journal of Phycology* **2013**, *49*, 215-225.

Dias, D. A.; Urban, S. Phytochemical analysis of the southern Australian marine alga, *Plocamium mertensii* using HPLC-NMR. *Phytochemical Analysis* **2008**, *19*, 453-470.

Dias, D. A.; White, J. M.; Urban, S. *Laurencia filiformis*: Phytochemical profiling by conventional and HPLC-NMR approaches. *Natural Product Communications* **2009a**, *4*, 157-172.

Dias, D. A.; Urban, S. Application of HPLC-NMR for the rapid chemical profiling of a southern Australian sponge, *Dactylospongia* sp. *Journal of Separation Science* **2009b**, *32*, 542-548.

Dussert, S.; Laffargue, A.; de Kochko, A.; Joët, T. Effectiveness of the fatty acid and sterol composition of seeds for the chemotaxonomy of *Coffea* subgenus *Coffea*. *Phytochemistry* **2008**, *69*, 2950-2960.

Falshaw, R.; Furneaux, R. H.; Pickering, T. D.; Stevenson, D. E. Agars from three Fijian *Gracilaria* species. *Botanica Marina* **1999**, *42*, 51-59.

Freshwater, D. W.; Bailey, J. C. A multigene phylogeny of the Gelidiales including nuclear large-subunit rRNA sequence data. *Journal of Applied Phycology* **1998**, *10*, 229-236.

Hegnauer, R. Phytochemistry and plant taxonomy-An essay on the chemotaxonomy of higher plants. *Phytochemistry* **1986**, *25*, 1519-1535.

Hey, J.; Pinho, C. Population genetics and objectivity in species diagnosis. *Evolution* **2012**, *66*, 1413-1429.

Howard, B. M.; Nonomura. A. M.; Fenical, W. Chemotaxonomy in Marine Algae: Secondary Metabolite Synthesis by *Laurencia* in Unialgal Culture. *Biochemical Systematics and Ecology* **1980**, *8*, 329-336.

Kim, H. K.; Choi, Y. H.; Erkelens, C.; Lefeber, A. W. M.; Verpoorte, R. Metabolic fingerprinting of *Ephedra* species using ^{1}H-NMR spectroscopy and principal component analysis. *Chemical and Pharmaceutical Bulletin* **2005**, *53*, 105-109.

Kokkotou, K.; Ioannou, E.; Nomikou, M.; Pitterl, F.; Vonaparti, A.; Siapi, E.; Zervou, M.; Roussis, V. An integrated approach using UHPLC-PDA-HRMS and 2D HSQC NMR for the metabolic profiling of the red alga *Laurencia*: dereplication and tracing of natural products. *Phytochemistry* **2014**, *108*, 208-219.

Leliaert, F.; Verbruggen, H.; Vanormelingen, P.; Steen, F.; López-Bautista, J. M.; Zuccarello, G. C.; De Clerk, O. DNA-based species delimitation in algae. *European Journal of Phycology* **2014**, *49*, 179-196.

Levetin, E.; McMahon, K. *Plants and Society*, 6th ed.; McGraw-Hill higher Education: New York, **2011**, 123-138.

Machín-Sánchez, M.; Asensio-Ramos, M.; Hernández-Borges, J.; Gil-Rodríguez, M. C. CE–MS fingerprinting of *Laurencia* complex algae (Rhodophyta). *Journal of separation science* **2014**, *37*, 711-716.

Maggs, C. A.; Verbruggen, H.; De Clerk, O. Molecular systematics of red algae: building future structures on firm foundations. In *Unraveling the algae: the past, present, and future of algal systematics*; Brodie, J.; Lewis, J., Ed.; Taylor and Francis Group: Florida, U.S.A., **2007**, 103-121.

Masuda, M.; Abe, T.; Sato, S.; Suzuki, T.; Suzuki, M. Diversity of halogenated secondary metabolites in the red alga *Laurencia nipponica* (Rhodomelaceae, Ceramiales). *Journal of Phycology* **1997**, *33*, 196-208.

Mihaleva, V. V.; te Beek, T. A.; van Zimmeren, F.; Moco, S.; Laatikainen, R.; Niemitz, M.; Korhonen, S. P.; van Driel, M. A.; Vervoort, J. MetIDB: a publically accessible database of predicted and experimental ^{1}H NMR spectra of flavonoids. *Analytical Chemistry* **2013**, *85*, 8700-8707.

Nelson, W. A.; Knight, G. A.; Falshaw, R.; Furneaux, R. H.; Falshaw, A.; Lynds, S. M. Characterisation of the enigmatic, endemic red alga *Gelidium allanii* (Gelidiales) from northern New Zealand - morphology, distribution, agar chemistry. *Journal of Applied Phycology* **1994**, *6*, 497-507.

Partida-Martinez, L. P.; de Loss, C. F.; Ishida, K.; Ishida, M.; Roth, M.; Buder, K.; Hertweck, C. Rhizonin, the first mycotoxin isolated from the *Zygomycota*, is not a fungal metabolite but is produced by bacterial endosymbionts. *Applied and Environmental Microbiology* **2007**, *73*, 793-797.

Payo, D. A.; Colo, J.; Calumpong, H.; de Clerck, O. Variability of non-polar secondary metabolites in the red alga *Portieria. Marine Drugs* **2011**, *9*, 2438-2468.

Payo, D. A.; Leliaert, F.; Verbruggen, H.; d'hondt, S.; Calumpong, H. P.; de Clerck, O. Extensive cryptic species diversity and fine-scale endemism in the marine red alga

Portieria in the Philippines. *Proceedings of the Royal Society B: Biological Sciences* **2013**, *280.*

Pfyffer G. E. *Carbohydrates and their impact on fungal taxonomy*. In: *Chemical Fungal Taxonomy*; Frisvad J. C.; Bridge, P. D.; Arora, D. K. Ed,; Marcel Dekker: New York., **1998**, 247-261.

Pietra, F. Evolution of the secondary metabolite versus evolution of the species. *Pure and Applied Chemistry* **2002**, 74, 2207-2211.

Schwab, W. Metabolome diversity: too few genes, too many metabolites? *Phytochemistry* **2003**, *62*, 837-849.

Verpoorte, R.; Choi Y. H.; Kim H. K. Metabolomics: what's new? *Flavour and Fragrance Journal* **2010**, *25*, 128-131.

Wiens, J. Species delimitation: New approaches for discovering diversity. *Systematic Biology* **2007**, *56*, 875-878.

Wilson, D. M.; Burlingame, A. L. Deuterium and carbon-13 tracer studies of ethanol metabolism in the rat by ^{2}H, ^{1}H-decoupled ^{13}C nuclear magnetic resonance. *Biochemical and Biophysical Research communications* **1974**, *56*, 828-835.

Wishart, D. S. Quantitative metabolomics using NMR. *Trends in Analytical Chemistry* **2008**, *27*, 228-237.

Wolfender, J. L.; Marti, G.; Thomas, A.; Bertrand, S. Current approaches and challenges for the metabolite profiling of complex natural extracts. *Journal of Chromatography* **2014**, In press.

Chapter 12

Conclusion

Rhodophyta of the *Laurencia* genus are reputable for producing a plethora of captivating, structurally diverse secondary metabolites. Consequently, the continual pursuit of novel molecules from this genus in search of potential drug leads continues. The number of new species being discovered by phycologists is growing; most of which afford at least one novel secondary metabolite.

Owing to ideal ecological conditions, the South African coastline boasts a significant number of *Laurencia* spp. possessing high levels of endemism. This study has reported, for the first time, the secondary metabolite chemistry of the majority of these species.

A key research objective included the isolation and structure elucidation of as many secondary metabolites as was possible from a select group of South African *Laurencia* spp. including *Laurencia natalensis*, *Laurencia* cf. *corymbosa, Laurencia complanata, Laurencia sodwaniensis, Laurencia multiclavata* as well as a South African specimen of *Laurenciella marilzae* (basionym: *Laurencia marilzae*).

An enthralling assortment of metabolites including chamigrane sesquiterpenes, C_{15} acetogenins, indole alkaloids and cuparanes were isolated, including the new tricyclic cuparane *(3aS*,8bR*)-7-bromo-1,1,6,8b-tetramethyl-1,3,3a,8b- tetrahydro- 2H -benzo [b] cyclopenta [d] furan-2-one* (**4.4**) from *L.* cf. *corymbosa*.

A re-analysis of *Laurencia flexuosa* and *Laurencia glomerata* afforded metabolites which the algae were known to produce (**3.1**, **3.9**, **3.7**, **3.17**, **8.1** and **8.2**) including known metabolites previously unobserved i.e. **3.5** and **3.15** from *L. glomerata* and **8.5** from *L. flexuosa.*

In general, relatively small samples of algae were available for this study and as a result the metabolites isolated herein do not represent the absolute secondary metabolome of the species. Furthermore, difficulty in purifying metabolites from interesting step gradient column chromatography fractions undoubtedly suggests that the species analysed herein possess metabolites yet to be successfully purified and characterised.

The application of ^{1}H NMR profiling on the organic crude extracts of *Laurencia* spp. was effectively explored affording unique, reproducible spectra synonymous to the organisms

'molecular fingerprint'. Major metabolites, such as **5.9** (algoane) from *L. natalensis*, were also identified. Such profiles could later assist in chemical means of species identification.

A detailed chemotaxonomic analysis of the metabolites isolated herein was performed using a *Laurencia* spp. phylogeny tree inferred by plastid *rbc*L sequences, constructed in a parallel study.

The chemotaxonomic value of simple chamigranes with modest substitution e.g. compound **3.9** isolated from *L. glomerata*, proved feeble as their presence was prevalent amongst various other *Laurencia* spp. possibly due to the ease at which they can be biosynthesised.

L. cf. *corymbosa*, often morphologically confused with *L. glomerata*, displayed a markedly different chemical profile consisting of mainly cuparane type entities. The new structures, **4.1**, **4.4** and **4.6** displayed noteworthy chemotaxonomic value as they were exclusively found in *L.* cf. *corymbosa*.

The marker compound **5.9** (algoane) from *L. natalensis* was exclusive to the sea-hare *Aplysia dactylomela*, proving the herbivorous nature of the mollusc on the alga, and inferring chemical uniqueness to *L. natalensis* organic extracts as this is its first documented isolation from marine algae.

Predicting the phylogeny of *L. complanata* from its secondary metabolite profile proved viable as most of the indole alkaloids isolated therein (**6.2**, **6.3** and **6.5**) were also exclusively present within its sister species, *L. brongniartii*.

The same applied for *L. multiclavata* as the complex poly-cyclic acetogenins (**7.1** and **7.5**) were also produced almost exclusively in the sister species *L. nidifica.* Compound **7.6**, isomeric to **7.5**, was previously isolated from an unknown Malaysian *Laurencia* sp., and given the exclusive nature of **7.5** to *L. nidifica*, the identity of the unknown species could possibly have been *L. nidifica*.

Compound **9.1** (cartilagineol) and **9.3** (obtusol) isolated from *L. sodwaniensis* further endorsed the use of chemotaxonomy, as the closely related species *L. dendroidea* and *L. majuscula* afforded identical compounds.

Considering the above, it is evident that the more complex molecules, such as compound **7.5**, are more exclusive amongst individual *Laurencia* spp. perhaps attributable to a lack of

specialist enzymes required for their biosynthesis. Consequently the chemotaxonomic value of such compounds cannot be overemphasised.

It is crucial to re-iterate that chemotaxonomy as a classification tool should never be used alone but rather in conjunction with other accepted means of delimiting an organism to a particular taxon, the most common being the identification of targeted gene sequences and the analysis of morpho-anatomical features.

This study has shed new insight into the chemotaxonomic value secondary metabolites from *Laurencia* spp. display. The need for intimate collaboration between natural product chemists and phycologists has arisen as classification of marine algae could be more effective if additional traits such as chemical profiles are also considered.

Appendix 1

Isolation of laurenyne from *Laurenciella marilzae*

A1.1 Introduction

Following the delineation of the marine alga *Laurencia marilzae* by Gil-Rodríguez *et al*., (2009) from the Spanish Canary islands, Gutiérrez Cepeda *et al*., (2011) went on to report its natural product chemistry, isolating compounds **A1.1-A1.8** (Figure A1.1).

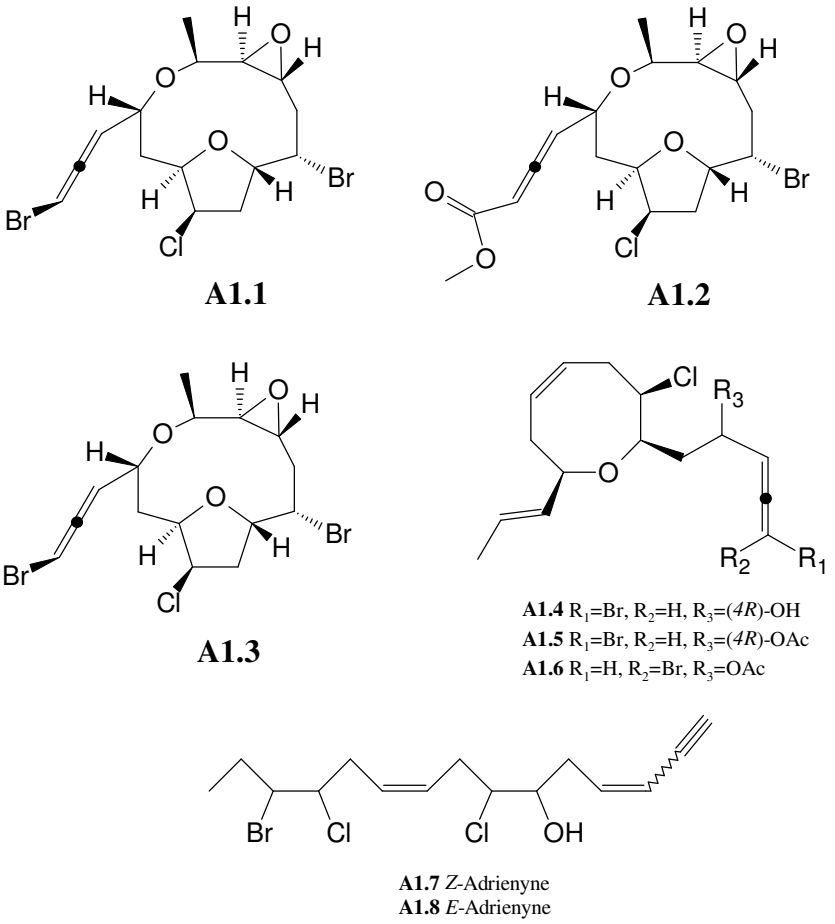

Figure A1.1: Compounds isolated from *Laurencia marilzae* (Gutiérrez Cepeda *et al*., 2011)

Following a comprehensive molecular phylogenetic study on this species based on the plastid encoded gene *rbc*L, Cassano *et al*., (2012) presented a strong substantiation that *Laurencia marilzae* (including the Canary island specimen) possessed too significant a genetic variation to be classified amongst conventional *Laurencia* spp.

Instead, the specimen represents a sixth genus of the *Laurencia* complex (*Laurencia* s.s.; *Chondrophycus*; *Osmundea*; *Palisada and Yuzura*) and was given the name *Laurenciella* gen. nov.

The plants of this species are red with orange tips, and despite the presence of only one *corps en cerise* per cell, their distribution is not limited to cortical cells as seen in *Laurencia sensu stricto*, as they also exist within all cells of the thallus (Figure A1.2) (Francis, 2014).

This section of the study reports the first phycochemical analysis of a South African specimen of *Laurenciella marilzae* formerly known as *Laurencia marilzae*.

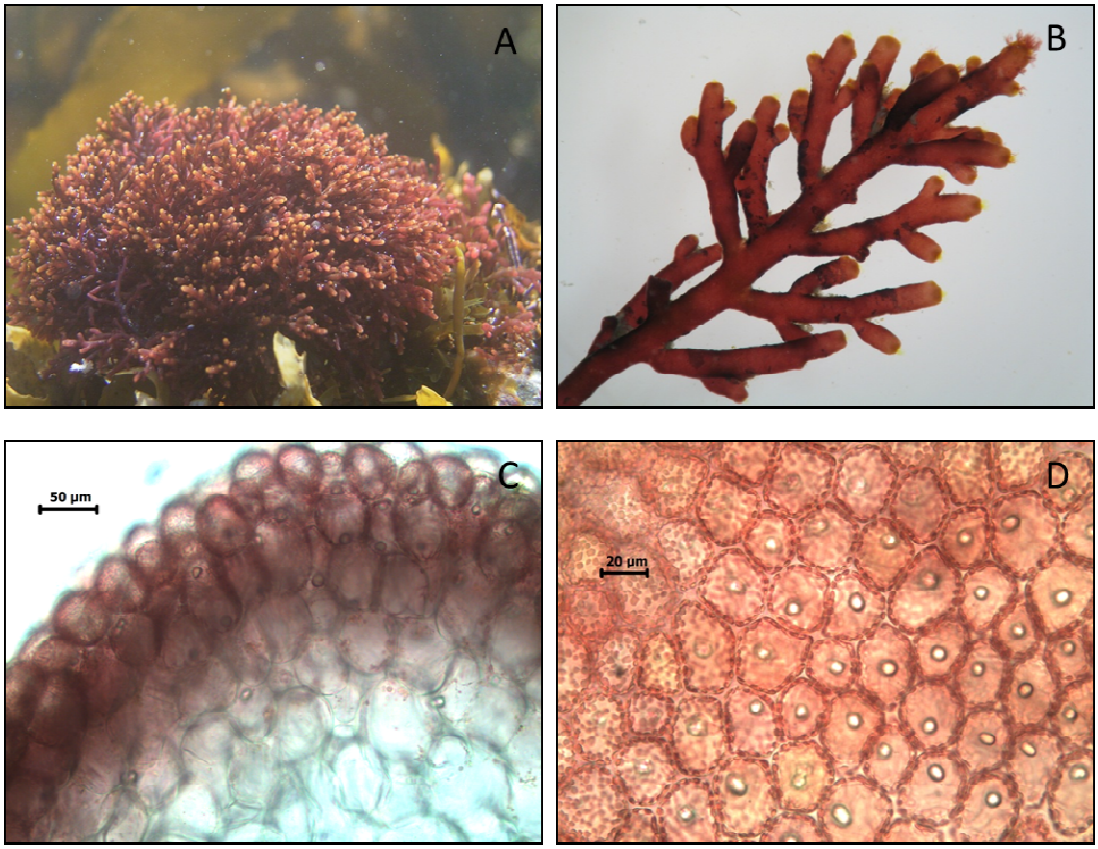

Figure A1.2: *Laurenciella marilzae*[1] (Caitlynne Francis © 2014)

A) Habit.

B) Branching pattern.

C) Cross section of thallus showing corps en cerise in cortical and medullary cells (20x).

D) Outermost cortical cells and thallus showing one *corps en cerise* per cell (40x).

[1] Image plates courtesy of Caitlynne Francis © 2014, University of Cape Town, South Africa

A1.2 Results and discussion

A1.2.1 Extraction and isolation of metabolites from *Laurenciella marilzae* (DH110219-5, De Hoop)

Following our normal extraction procedure (section **3.2.1,** page 54), the majority of the silica gel step gradient column fractions of *Laurenciella marilzae* were deficient of notable ^{1}H NMR secondary metabolite signals, except for fraction B (9:1 hex:EtOAc). After purification of this fraction *via* further silica gel chromatography using (19:1 hex:EtOAc) followed by (3:2 CH_2Cl_2:hex), compound **A1.9** was isolated.

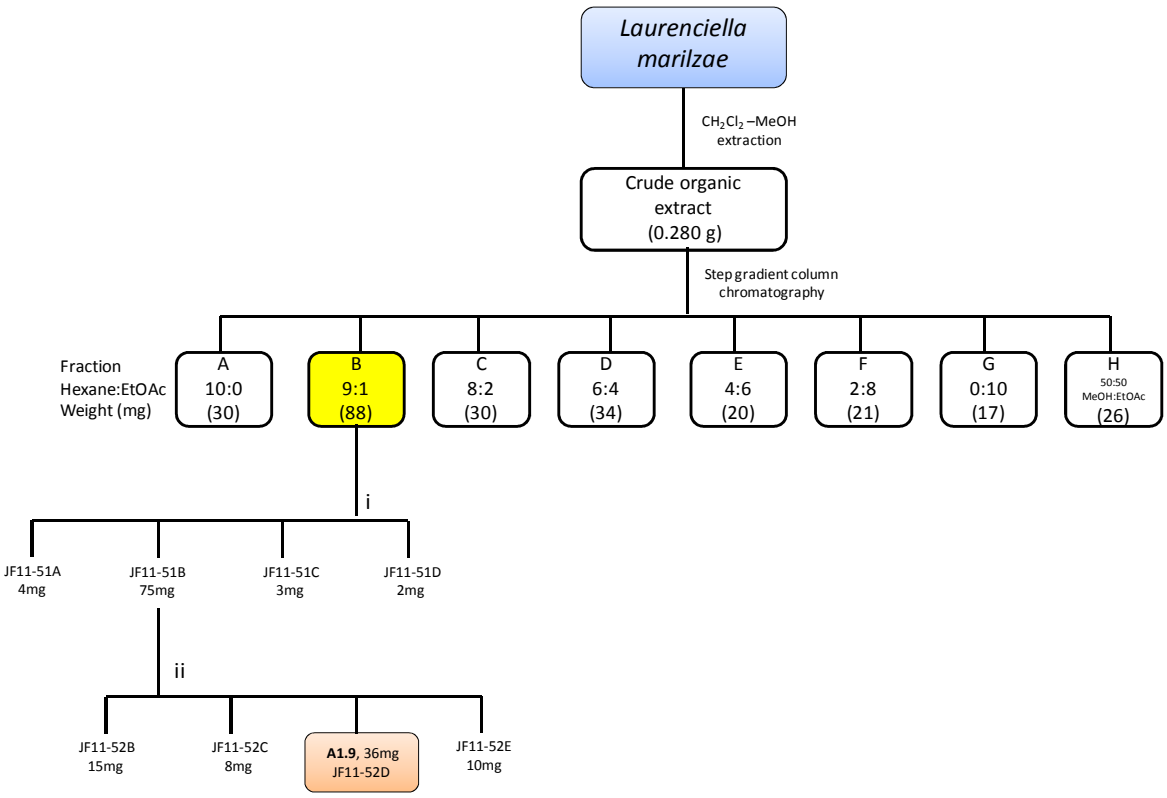

Scheme A1.1: Isolation scheme of metabolites from *Laurenciella marilzae* (DH110219-5)

Conditions: i) Silica gel column chromatography (19:1 hex:EtOAc); ii) Silica gel column chromatography (3:2 CH_2Cl_2:hex)

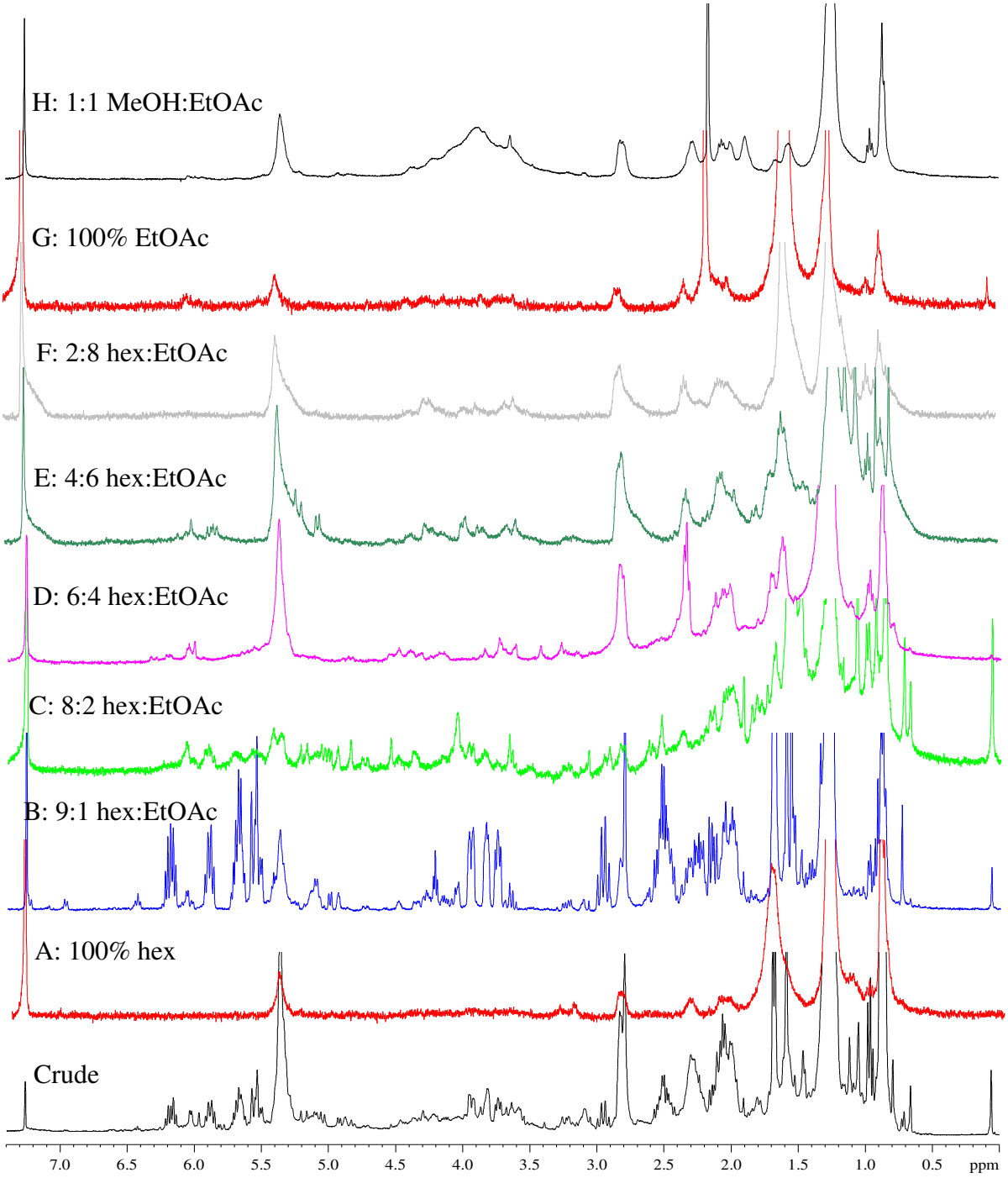

Figure A1.3: ^{1}H NMR spectra ($CDCl_3$, 400 MHz) of the crude organic extract of *Laurenciella marilzae* (DH110219-5) and step gradient column fractions A-H

A1.2.2 Structure elucidation of metabolites

Compound A1.9

Increasing the NMR field strength (600 MHz *vs*. 400 MHz) enabled the acquisition of a well resolved ^{1}H NMR spectrum (Figure A1.4) with more distinctive splitting for compound **A1.9**.

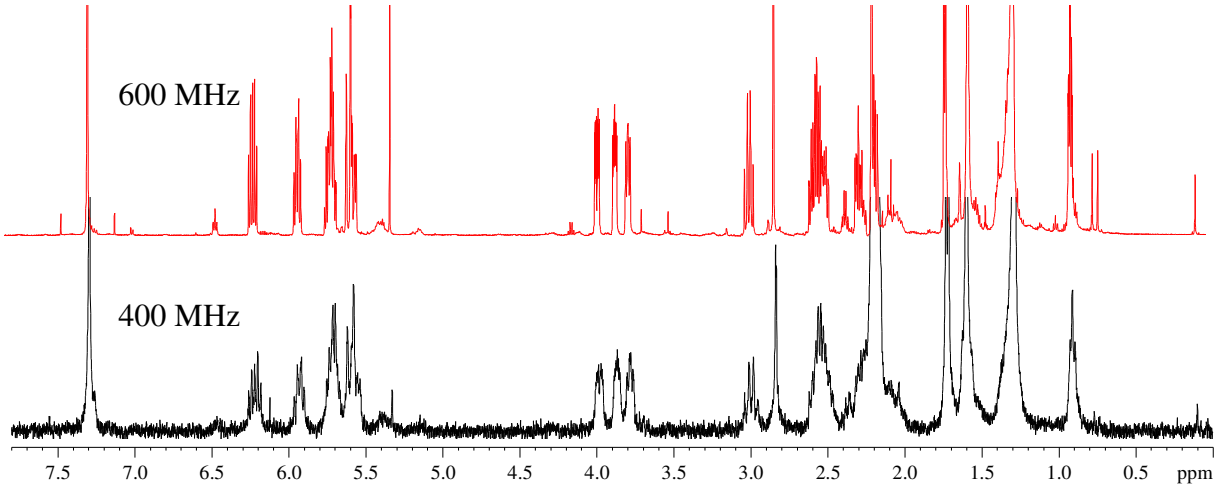

Figure A1.4: ^{1}H NMR spectra of compound **A1.9** at 400 MHz and 600 MHz ($CDCl_3$)

Compound **A1.9** showed a *trans*-acetylenic side chain with ^{1}H NMR (Figure A1.5) signals at δ_H 2.81 (s), δ_H 5.57 (m), δ_H 6.19 (quin, J = 7.9 Hz) and methylene resonances at δ_H 2.25 (m); δ_H 2.55 (m). An olefin containing terminal propyl functionality was deduced after considering a methyl resonance at δ_H 1.67 (d, J = 6.8 Hz) as well as two olefinic signals at δ_H 5.68 (m) and δ_H 5.53 (m).

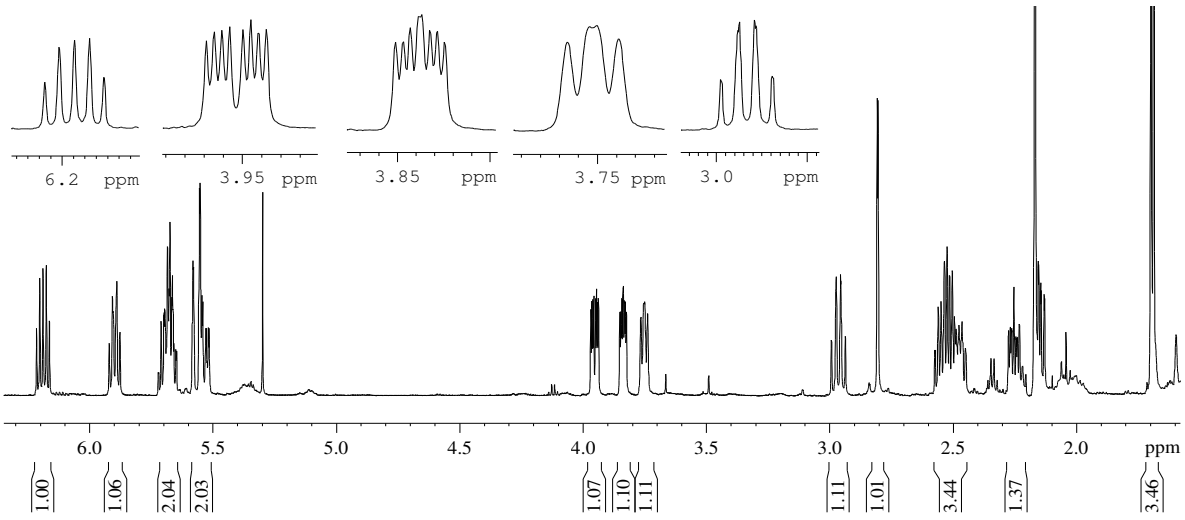

Figure A1.5: ^{1}H NMR spectrum ($CDCl_3$, 600 MHz) of compound **A1.9**

The ^{13}C NMR spectrum (Figure A1.6) of compound **A1.9** provided evidence for a chloro-methine and two oxy-methine moieties at δ_C 65.0, 79.1 and 81.7 corresponding to protons δ_H 3.95 (m), δ_H 3.83(m) and δ_H 3.76(m) respectively.

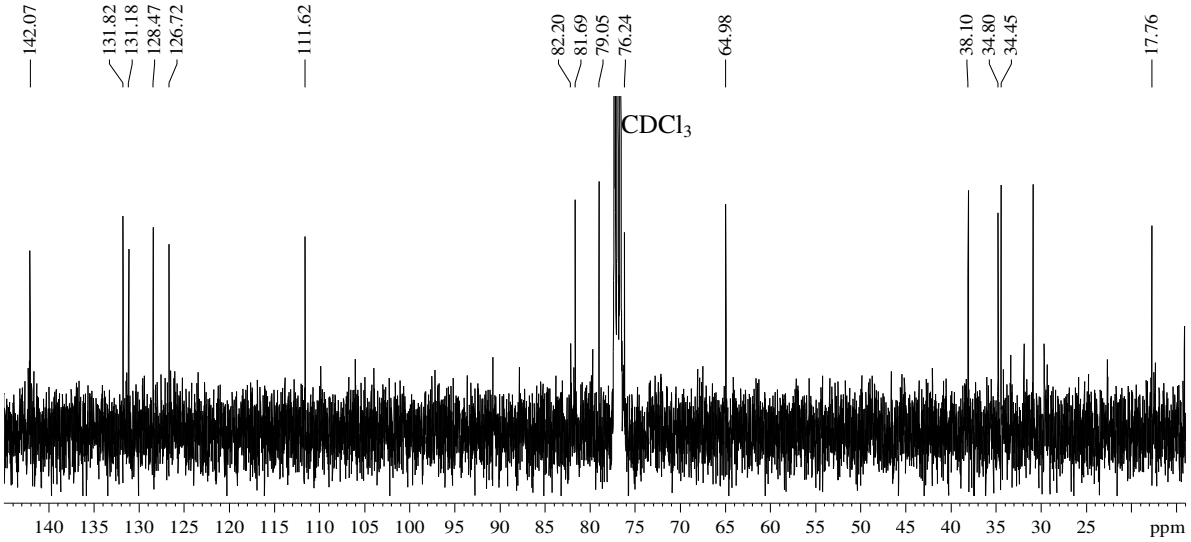

Figure A1.6: ^{13}C NMR spectrum ($CDCl_3$, 150 MHz) of compound **A1.9**

After analysis of 2D NMR experiments including COSY and HSQC-TOCSY (ideal for systems with contiguous protonation), compound **A1.9** was elucidated as 3*E*-laurenyne, a cyclic acetylenic ether previously reported from *Laurencia obtusa* (Falshaw *et al*., 1980).

The relative configuration of compound **A1.9** was confirmed by NOESY and ROESY spectroscopic data.

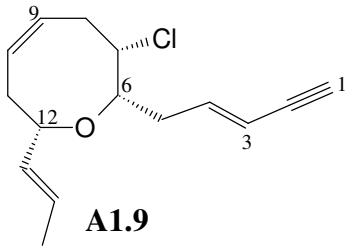

A1.9

Compound **A1.9** is similar in many ways to a brominated analogue compound **A1.10** isolated by Iliopoulou *et al*., (2002) from a Greek specimen of *Laurencia obtusa*.

Furthermore, it is evident that a stereoisomer of compound **A1.9** could serve as a plausible precursor to the allenic compounds **A1.4**, **A1.5** and **A1.6** isolated by Gutiérrez Cepeda *et al*., (2011) from what was then *Laurencia marilzae*.

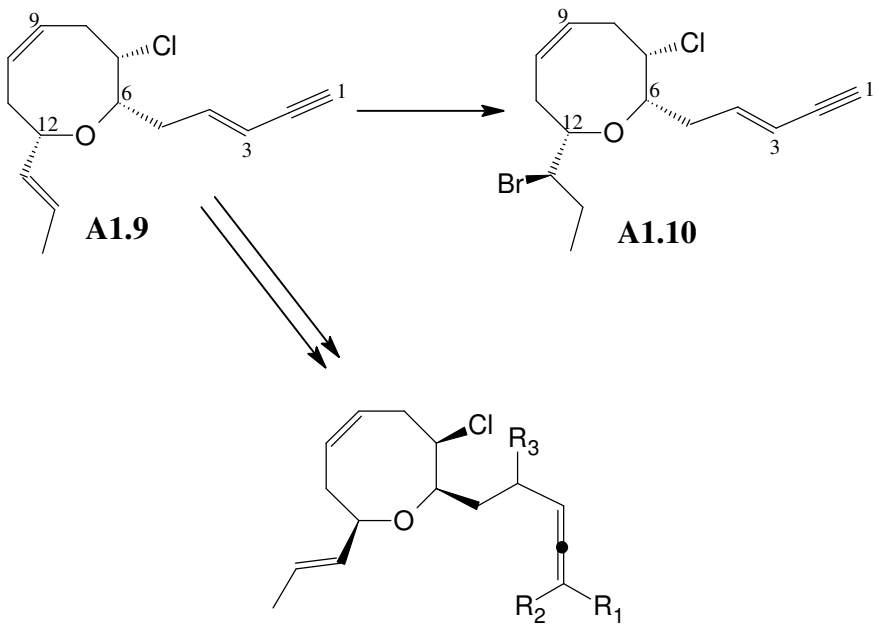

A1.9 **A1.10**

A1.4 R_1=Br, R_2=H, R_3=(*4R*)-OH
A1.5 R_1=Br, R_2=H, R_3=(*4R*)-OAc
A1.6 R_1=H, R_2=Br, R_3=OAc

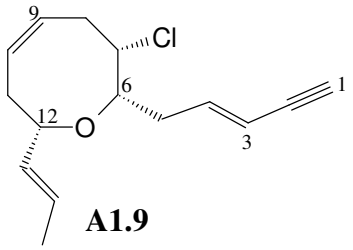

A1.9

Table A1.1: NMR spectroscopic data for compound **A1.9**

Carbon No	δ_C	δ_C **mult**	δ_H, **mult, J (Hz)**
1	82.2	CH	2.81, s
2	76.2	C	-
3	111.6	CH	5.57, m
4	142.1	CH	6.19, quin, 7.9
5a	38.1	CH_2	2.25, m
5b			2.55, m
6	79.1	CH	3.83, m
7	65.0	CH	3.95, m
8a	34.5	CH_2	2.51, m
8b			2.97, q, 12.5
9	128.5	CH	5.68, m
10	131.2	CH	5.89, q, 8.4
11a	34.8	CH_2	2.14, m
11b			2.51, m
12	81.7	CH	3.76, m
13	131.8	CH	5.53, m
14	126.7	CH	5.68, m
15	17.8	CH_3	1.67, d, 6.8

A1.3 Experimental

A1.3.1 General experimental

As per section **3.3.1** in chapter 3, page 54.

NMR spectra were obtained on a Bruker® Avance 600 MHz instrument as well as a Bruker® Avance 400 MHz instrument using standard pulse sequences.

A1.3.2 Plant material (*Laurenciella marilzae*, DH110219-5)

Laurenciella marilzae was collected by hand at De Hoop on the south coast of South Africa in February 2011. A voucher specimen has been stowed away in the seaweed sample repository at the School of Pharmacy, University of the Western Cape. Identification of the alga was done by Professor John Bolton with the Department of Biological Sciences at the University of Cape Town, South Africa.

A1.3.3 Extraction and isolation of metabolites

Same procedure as in section **3.3.3**, page 54 (dry mass 2.6 g, crude extract 0.28 g, 9.7% yield).

Repeated silica gel column chromatography (19:1 hex:EtOAc; 3:2 CH_2Cl_2:hex) of step gradient fraction B (9:1 hex:EtOAc) afforded compound **A1.9** (36 mg, 1.3%).

A1.3.4 Compound isolated

Compound A1.9 (JF11-52D)

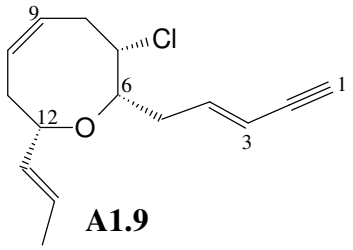

A1.9

*3E-laurenyne (***A1.9**): White solid; ^{1}H and ^{13}C NMR data available in Table A1.1. As previously reported by Falshaw *et al*., (2002).

A1.4 References

Cassano, V.; Gil-Rodríguez, M. C.; Sentíes, A.; Díaz-Larrea, J.; Fujii, M. T. Molecular support for the establishment of the new genus *Laurenciella* within the *Laurencia* complex (Ceramiales, Rhodophyta). *Botanica Marina* **2012**, *55*, 349-357.

Falshaw, C. P.; King, T. J.; Imre, S.; Islimyeli, S.; Thomson, R. H. Laurenyne, a new acetylene from *Laurencia obtusa*: crystal structure and absolute configuration. *Tetrahedron Letters* **1980**, *21*, 4951-4954.

Gil-Rodríguez, M. C.; Sentíes, A.; Díaz-Larrea, J.; Cassano, V.; Fujii, M. T. *Laurencia marilzae* sp. nov. (Ceramiales, Rhodophyta) from the Canary islands, Spain, based on morphological and molecular evidence. *Journal of Phycology* **2009**, *45*, 264-271.

Gutiérrez-Cepeda, A.; Fernández, J. J.; Gil, L.V.; López-Rodríguez, M.; Norte, M.; Souto, M. L. Nonterpenoid C_{15} Acetogenins from *Laurencia marilzae*. *Journal of Natural Products* **2011**, *74*, 441-448.

Iliopoulou, D.; Vagias, C.; Harvala, C.: Roussis, V. C_{15} acetogenins from the red alga *Laurencia obtusa*. *Phytochemistry* **2002**, *59*, 111-116.

Appendix 2 –Proposed biosynthetic pathways of the majority of the isolated metabolites

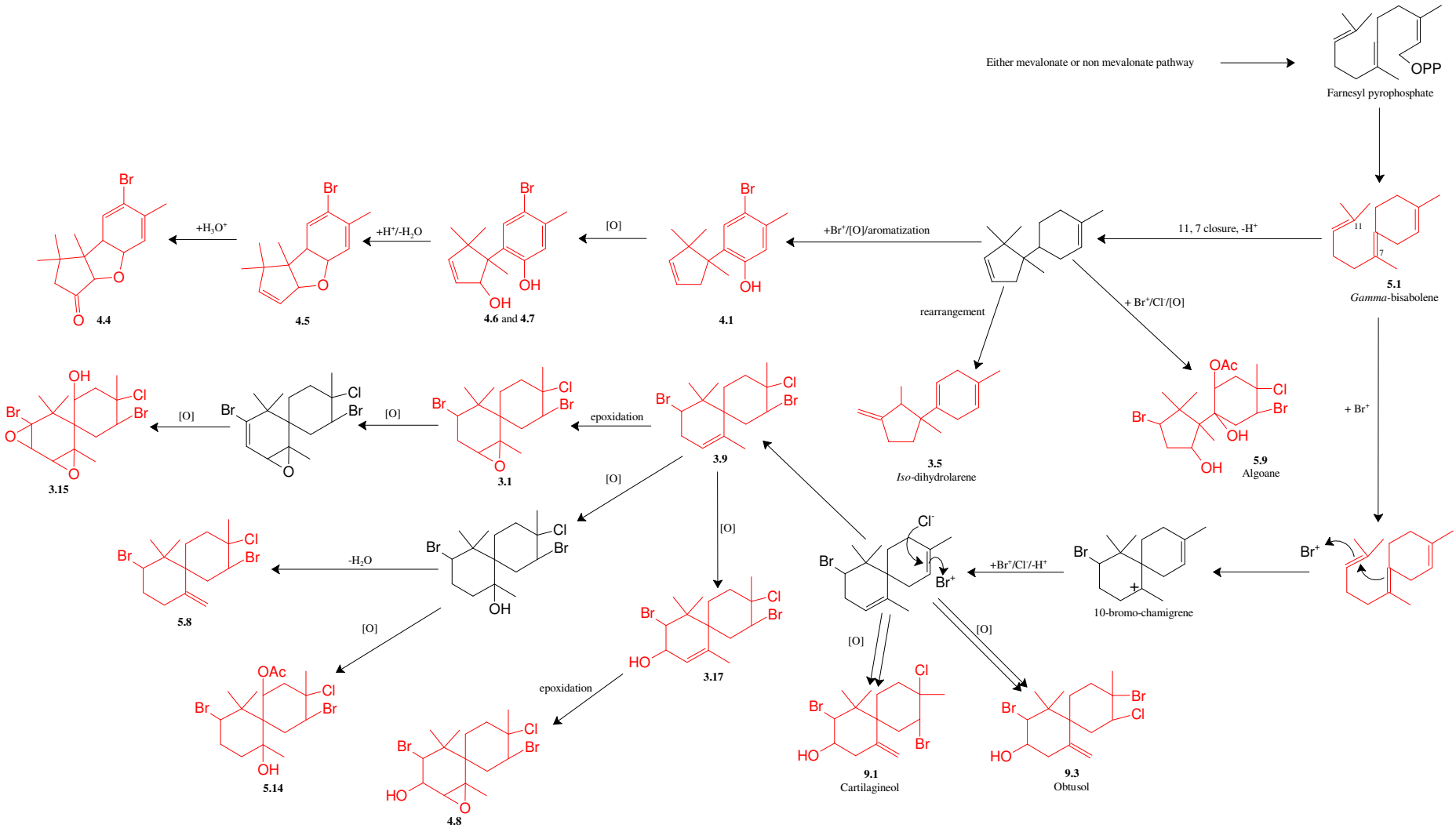

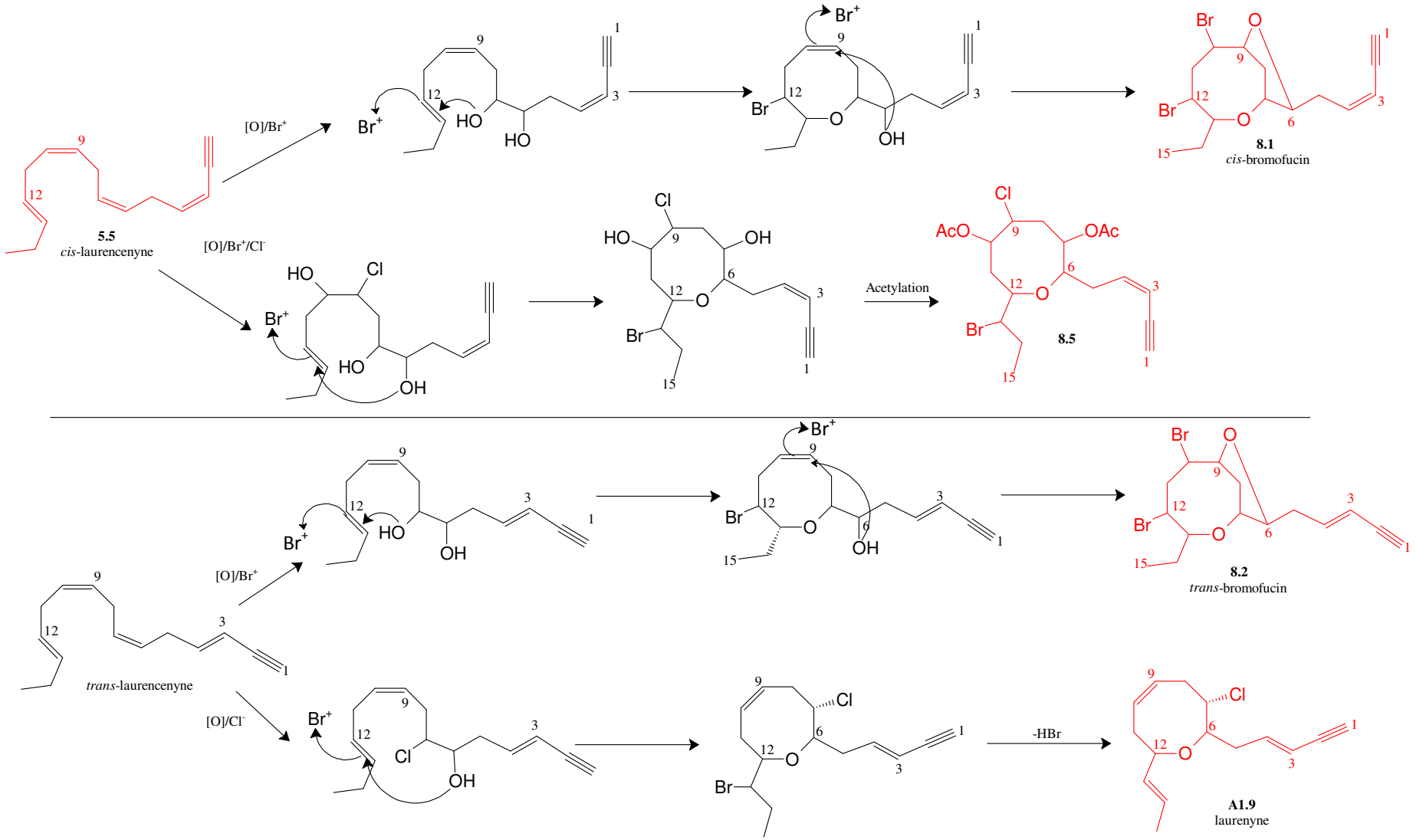
5.5
cis-laurencenyne
[O]/Br+
[O]/Br+/Cl-
Acetylation
8.1
cis-bromofucin
8.5
trans-laurencenyne
[O]/Br+
[O]/Cl-
8.2
trans-bromofucin
-HBr
A1.9
laurenyne

Appendix 3 –A ^{13}C NMR guide relating to ring B chemical shifts of various halogenated chamigrane sesquiterpenes[1]

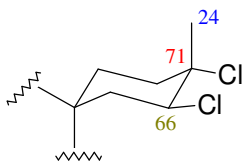

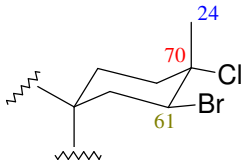

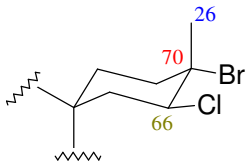

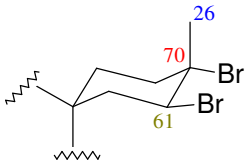

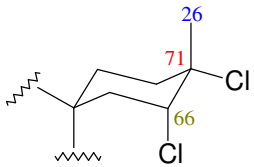

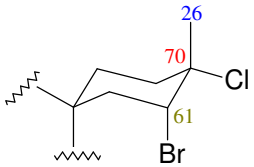

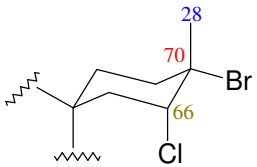

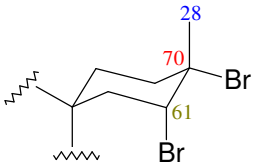

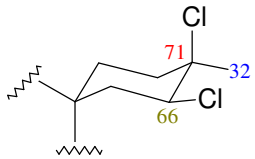

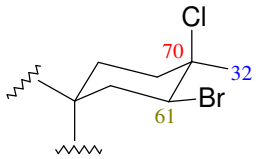

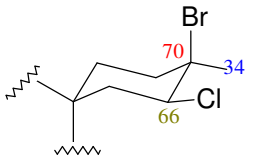

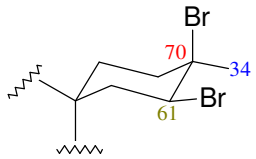

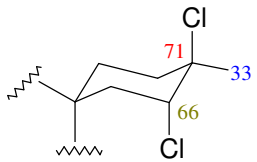

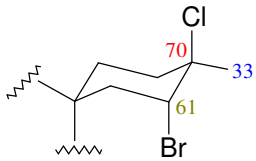

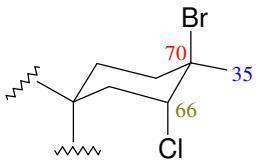

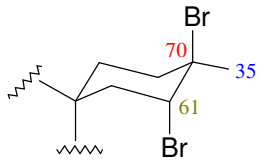

[1] (Crews, P.; Kho-Wiseman, E. Stereochemical assignments in marine natural products by ^{13}C NMR γ effects. *Tetrahedron Letters* **1978**, *28*, 2483-2486); (Gonzalez, A. G.; Martin J. D.; Martin, V. S.; Norte, M. Carbon- 13 NMR applications to *Laurencia* polyhalogenated sesquiterpenes. *Ibid,* **1979,** *23*, 2719 – 2722). (Crews, P.; Naylor, S.; Hanke, J. F.; Hogue, E. R.; Kho, E.; Braslaw, R. Halogen regiochemistry and substituent stereochemistry determination in marine monoterpenes by ^{13}C NMR. *Journal of Organic Chemistry* **1984**, *49*, 1371-1377).

Appendix 4 – Halogen abundance patterns in mass spectrometry[1]

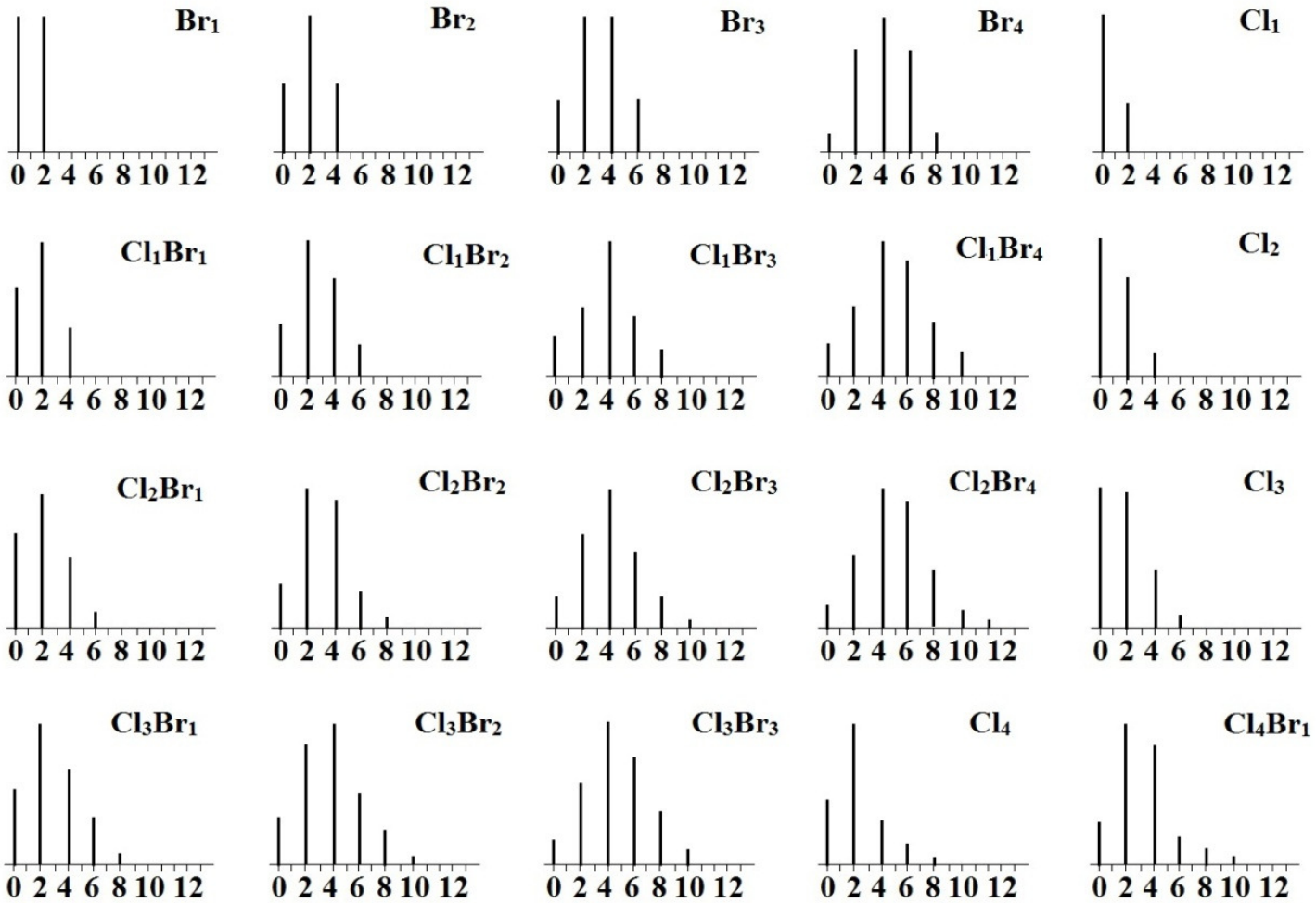

[1] Adapted from: Gross, J. H. *Mass Spectrometry. A Textbook*, 2nd ed.; Springer, Berlin, Heidelberg, New York, 2011; 78.

Appendix 5 –Summary of metabolites isolated/derivatised from this study

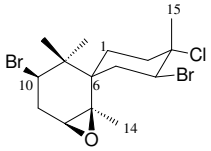

3.1

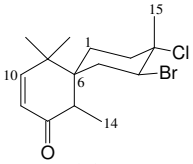

3.3

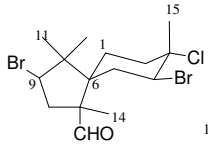

3.4

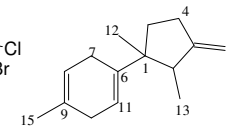

3.5

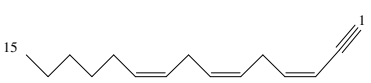

3.7

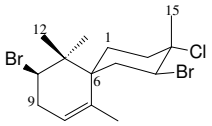

3.9

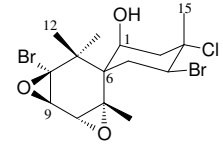

3.15

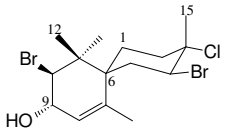

3.17

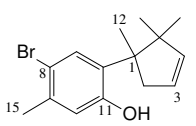

4.1

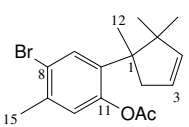

4.3

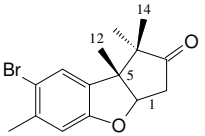

4.4

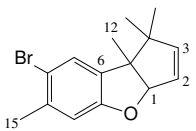

4.5

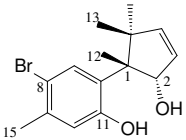

4.6

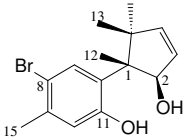

4.7

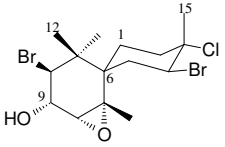

4.8

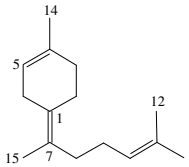

5.1

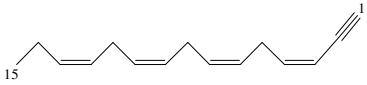

5.5

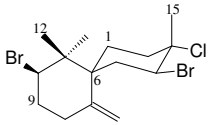

5.8

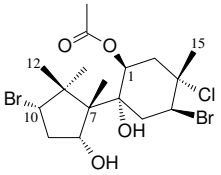

5.9

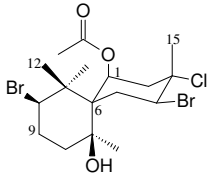

5.14

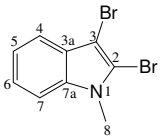

6.1

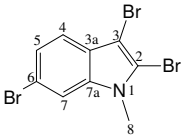

6.2

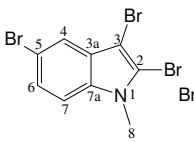

6.3

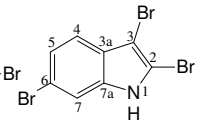

6.4

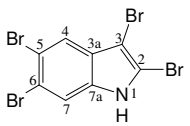

6.5

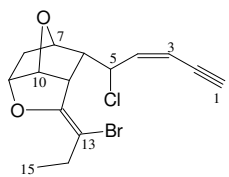

7.1

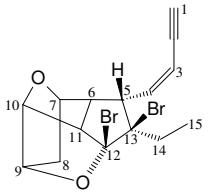

7.5

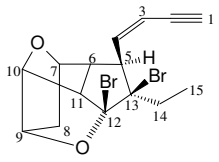

7.6

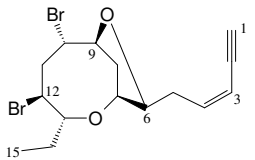

8.1

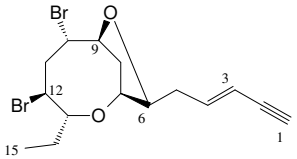

8.2

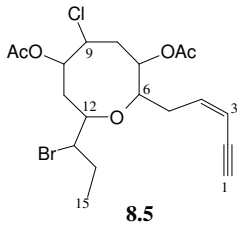

8.5

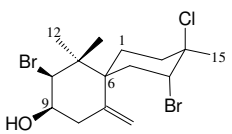

9.1

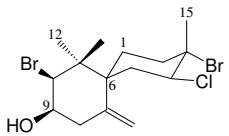

9.3

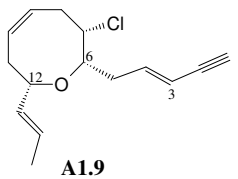

A1.9

The Isolation, Characterisation and Chemotaxonomic Significance of Secondary Metabolites from Selected South African *Laurencia* spp. Rhodophyta

A Thesis Submitted in Fulfillment of the Requirements for the Degree of

DOCTOR OF PHILOSOPHY (PHARMACY)

of

RHODES UNIVERSITY

By

Jameel Fakee

February 2015

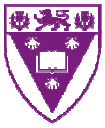

RHODES UNIVERSITY

Where leaders learn

Supplementary Data

Chapter 3 - Secondary metabolites from *Laurencia glomerata*

S3.1 Compound 3.1

Figure S3.1 ^{1}H NMR spectrum ($CDCl_3$, 600 MHz) of compound **3.1**

Figure S3.2 ^{13}C NMR spectrum ($CDCl_3$, 150 MHz) of compound **3.1**

Figure S3.3 COSY NMR spectrum of compound **3.1**

Figure S3.4 HSQC NMR spectrum of compound **3.1**

Figure S3.5 HMBC NMR spectrum of compound **3.1**

Figure S3.6 NOESYSY NMR spectrum of compound **3.1**

Figure S3.7 DEPT-135 NMR spectrum of compound **3.1**

Figure S3.8 IR spectrum of compound **3.1**

Figure S3.9 Coupled ^{13}C NMR spectrum ($CDCl_3$, 150 MHz) of compound **3.1**

S3.2 Compound 3.3

Table S3.1 NMR spectroscopic data of compound **3.3**

Figure S3.10 ^{1}H NMR spectrum ($CDCl_3$, 600 MHz) of compound **3.3**

Figure S3.11 COSY NMR spectrum of compound **3.3**

Figure S3.12 HSQC NMR spectrum of compound **3.3**

Figure S3.13 HMBC NMR spectrum of compound **3.3**

Figure S3.14 IR spectrum of compound **3.3**

S3.3 Compound 3.4

Table S3.2 NMR spectroscopic data of compound **3.4**

Figure S3.15 ^{1}H NMR spectrum ($CDCl_3$, 600 MHz) of compound **3.4**

Figure S3.16 ^{13}C NMR spectrum ($CDCl_3$, 150 MHz) of compound **3.4**

S4.2 Compound 4.3

Figure S4.9 ^{1}H NMR spectrum ($CDCl_3$, 600 MHz) of compound **4.3**

Figure S4.10 ^{13}C NMR spectrum ($CDCl_3$, 150 MHz) of compound **4.3**

Figure S4.11 COSY NMR spectrum of compound **4.3**

Figure S4.12 HSQC NMR spectrum of compound **4.3**

Figure S4.13 HMBC NMR spectrum of compound **4.3**

Figure S4.14 IR spectrum of compound **4.3**

S4.3 Compound 4.4

Figure S4.15 ^{1}H NMR spectrum ($CDCl_3$, 600 MHz) of compound **4.4**

Figure S4.16 ^{13}C NMR spectrum ($CDCl_3$, 150 MHz) of compound **4.4**

Figure S4.17 COSY NMR spectrum of compound **4.4**

Figure S4.18 HSQC NMR spectrum of compound **4.4**

Figure S4.19 HMBC NMR spectrum of compound **4.4**

Figure S4.20 NOESY NMR spectrum of compound **4.4**

Figure S4.21 HRGCEIMS spectrum of compound **4.4**

Figure S4.22 IR spectrum of compound **4.4**

S4.4 Compound 4.5

Figure S4.23 ^{1}H NMR spectrum ($CDCl_3$, 600 MHz) of compound **4.5**

Figure S4.24 COSY NMR spectrum of compound **4.5**

Figure S4.25 HSQC NMR spectrum of compound **4.5**

Figure S4.26 HMBC NMR spectrum of compound **4.5**

S4.5 Compound 4.6

Figure S4.27 ^{1}H NMR spectrum ($CDCl_3$, 600 MHz) of compound **4.6**

Figure S11.7 ^{1}H NMR ($CDCl_3$, 600 MHz) profiles of *L. flexuosa* (D904)

S11.1.8 L. natalensis (D1022)

Figure 11.8: ^{1}H NMR ($CDCl_3$, 600 MHz) profiles of *L. natalensis* (D1022)

S11.1.9 L. peninsularis (D900)

Figure S11.9 ^{1}H NMR ($CDCl_3$, 600 MHz) profiles of *L. peninsularis* (D900)

S11.1.10 L. peninsularis (GC120901)

Figure S11.10 ^{1}H NMR ($CDCl_3$, 600 MHz) profiles of *L. peninsularis* (GC120901)

S11.1.11 L. multiclavata (D969)

Figure S11.11 ^{1}H NMR ($CDCl_3$, 600 MHz) profiles of *L. multiclavata* (D969)

Appendix 1 – Isolation of laurenyne from *Laurenciella marilzae*

S.A1.1 Compound A1.9

Figure S.A1.1.1: ^{1}H NMR spectrum ($CDCl_3$, 600 MHz) of compound **A1.9**

Figure S.A1.1.2: ^{13}C NMR spectrum ($CDCl_3$, 150 MHz) of compound **A1.9**

Figure S.A1.1.3: COSY spectrum of compound **A1.9**

Figure S.A1.1.4: HSQC spectrum of compound **A1.9**

Figure S.A1.1.5: HMBC spectrum of compound **A1.9**

Figure S.A1.1.6: HSQC-TOCSY spectrum of compound **A1.9**

Figure S.A1.1.7: NOESY spectrum of compound **A1.9**

Figure S.A1.1.8: ROESY spectrum of compound **A1.9**

Figure S.A1.1.9: IR spectrum of compound **A1.9**

Chapter 3

Secondary metabolites from *Laurencia glomerata*

S3.1 Compound 3.1

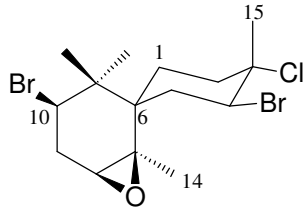

3.1

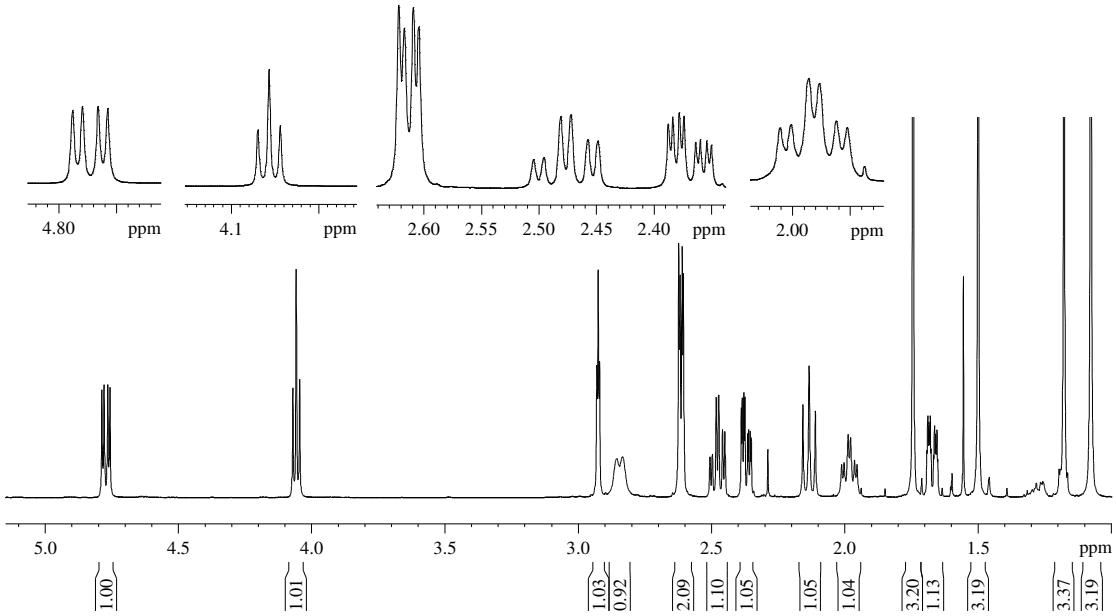

Figure S3.1 ^{1}H NMR spectrum ($CDCl_3$, 600 MHz) of compound **3.1**

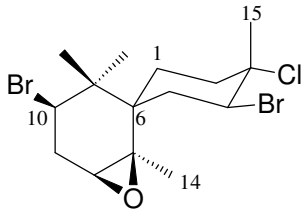

3.1

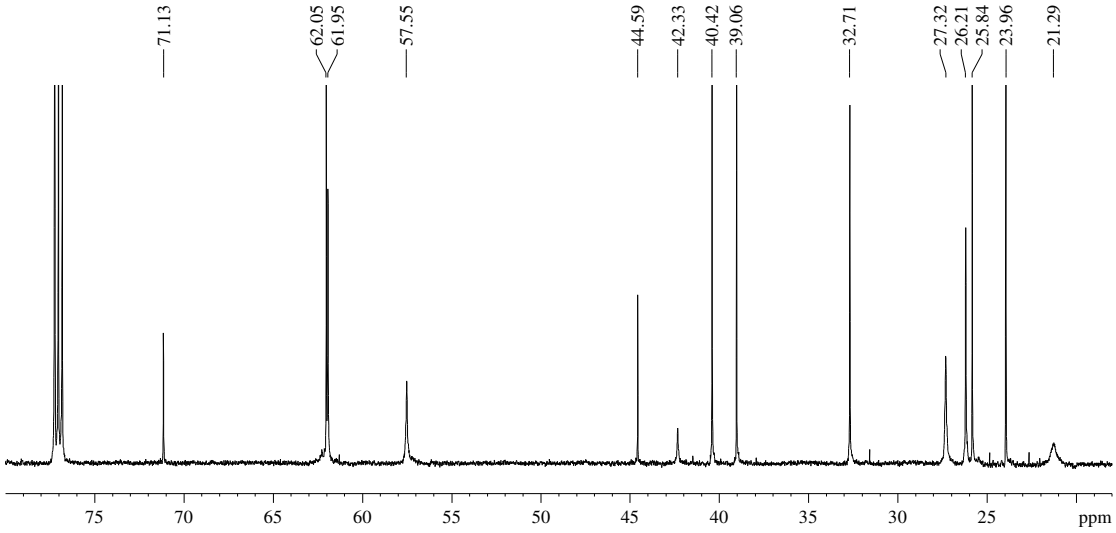

Figure S3.2 ^{13}C NMR spectrum ($CDCl_3$, 150 MHz) of compound **3.1**

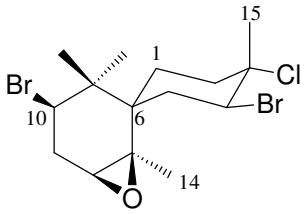

3.1

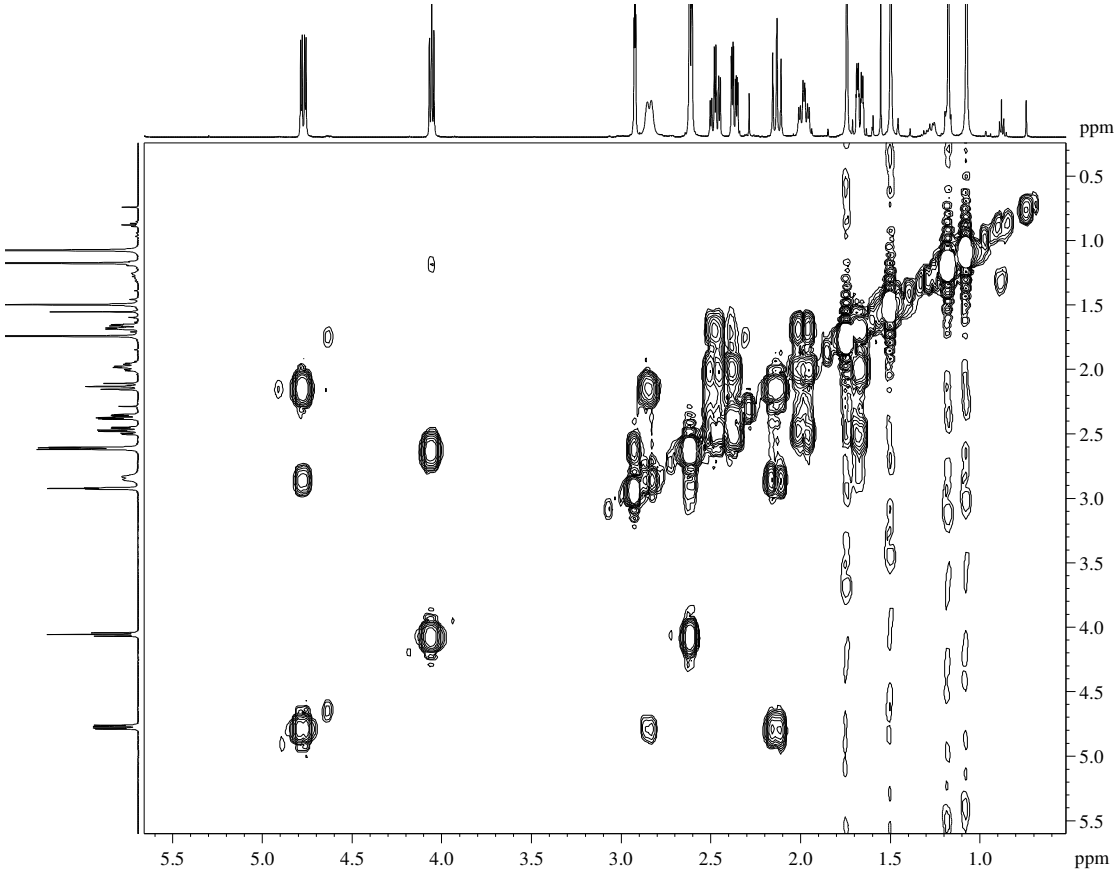

Figure S3.3 COSY NMR spectrum of compound **3.1**

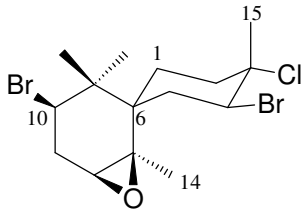

3.1

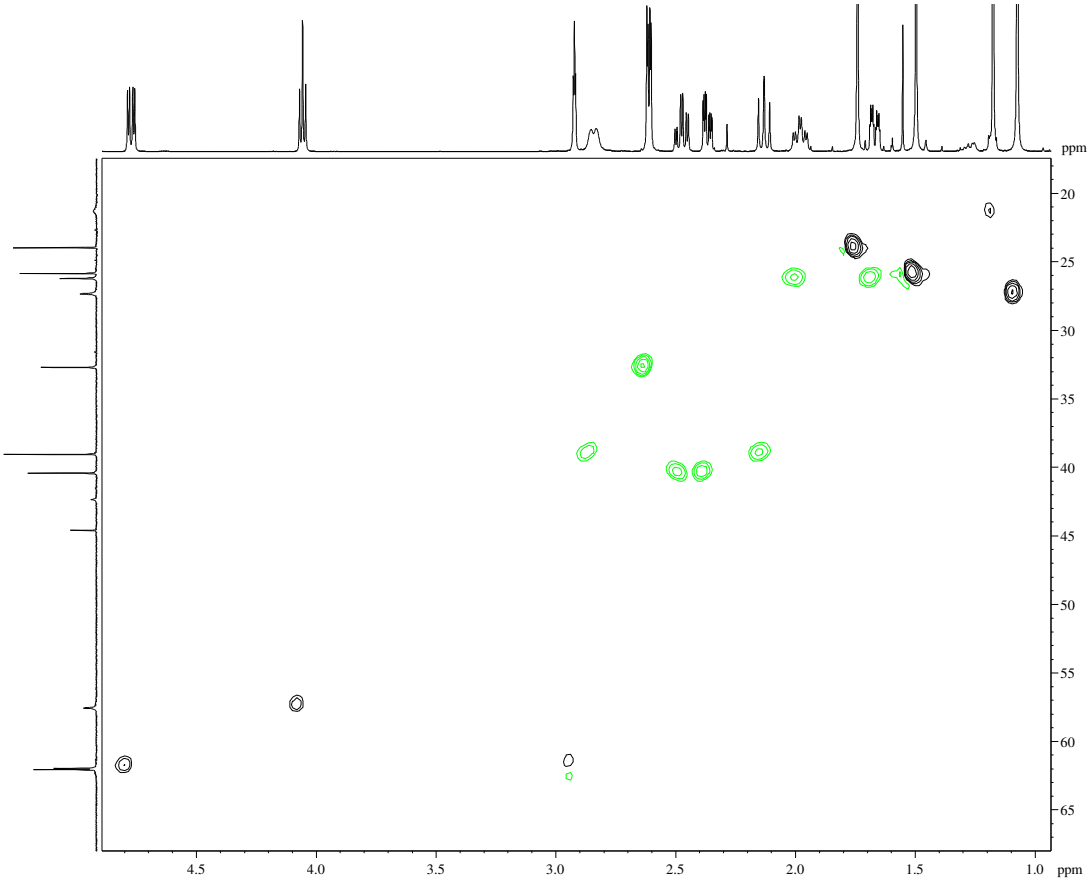

Figure S3.4 HSQC NMR spectrum of compound **3.1**

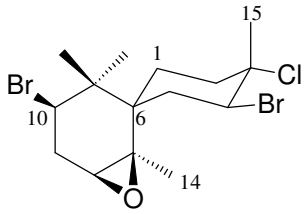

3.1

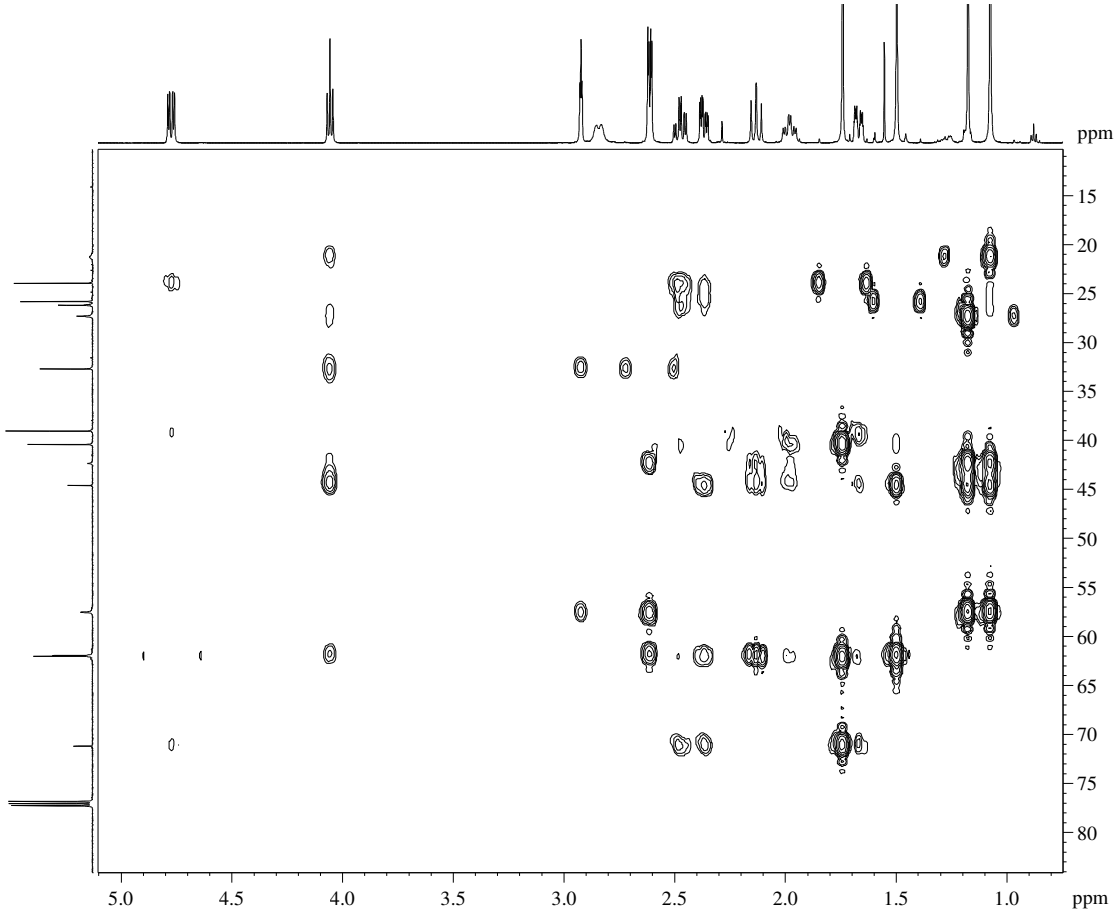

Figure S3.5 HMBC NMR spectrum of compound **3.1**

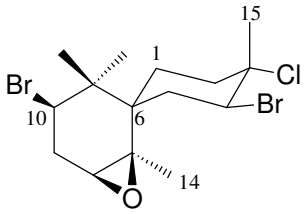

3.1

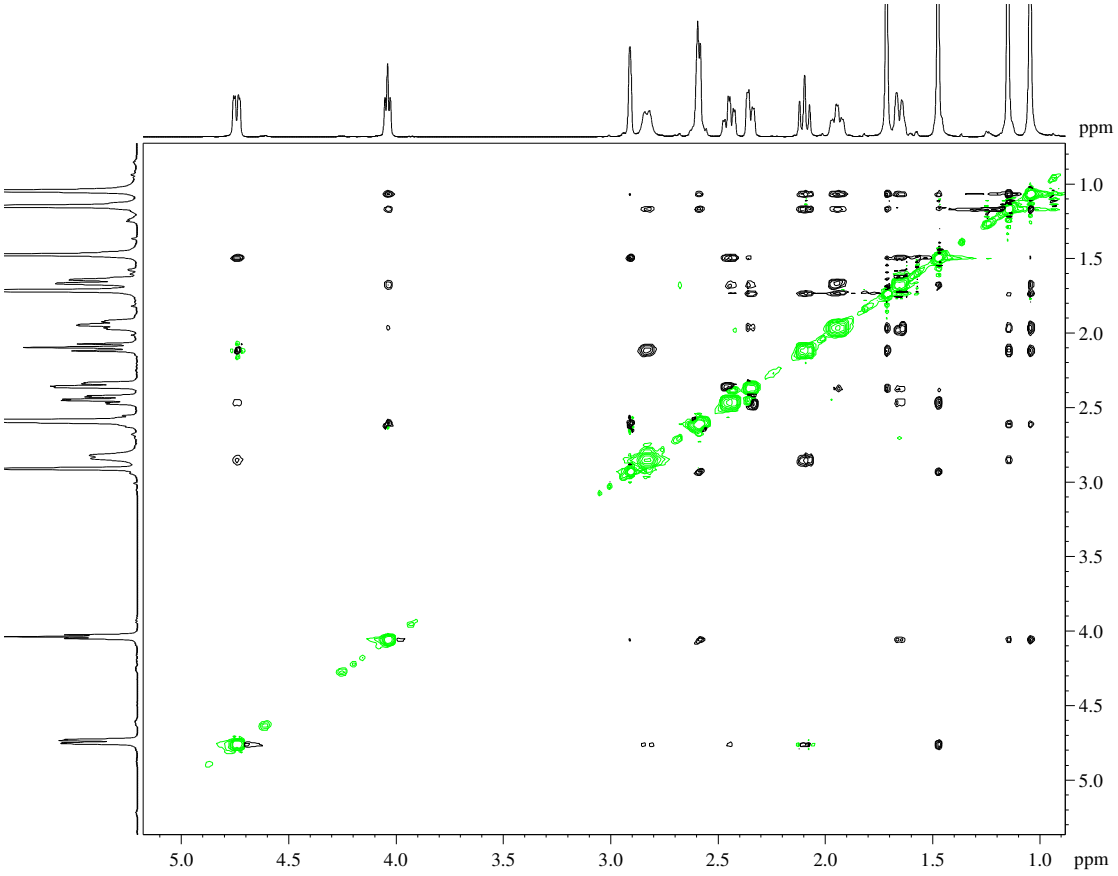

Figure S3.6 NOESY NMR spectrum of compound **3.1**

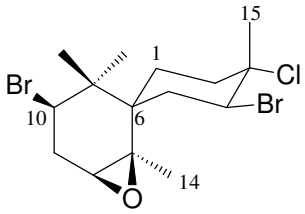

3.1

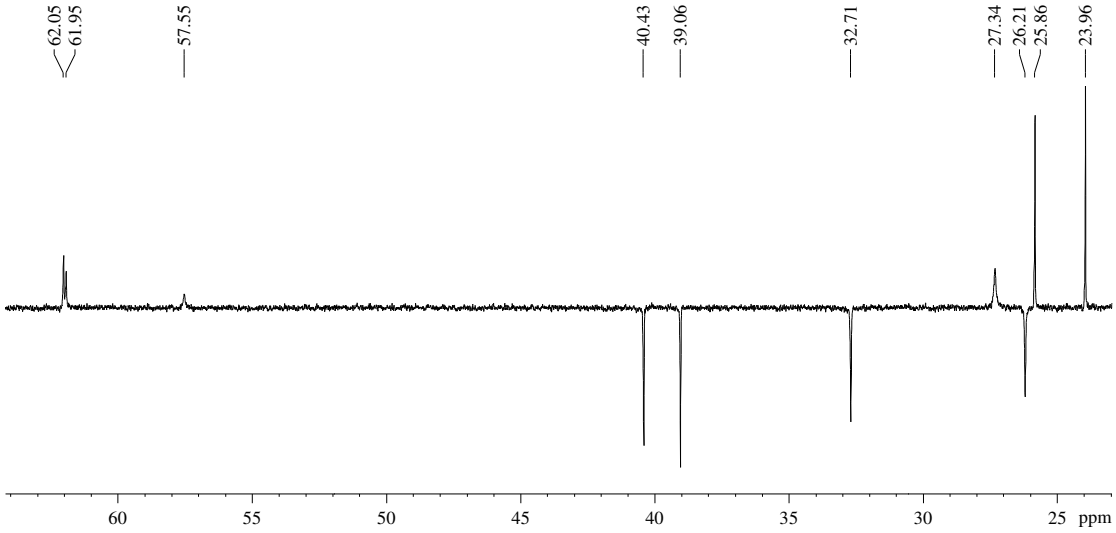

Figure S3.7 DEPT-135 NMR spectrum of compound **3.1**

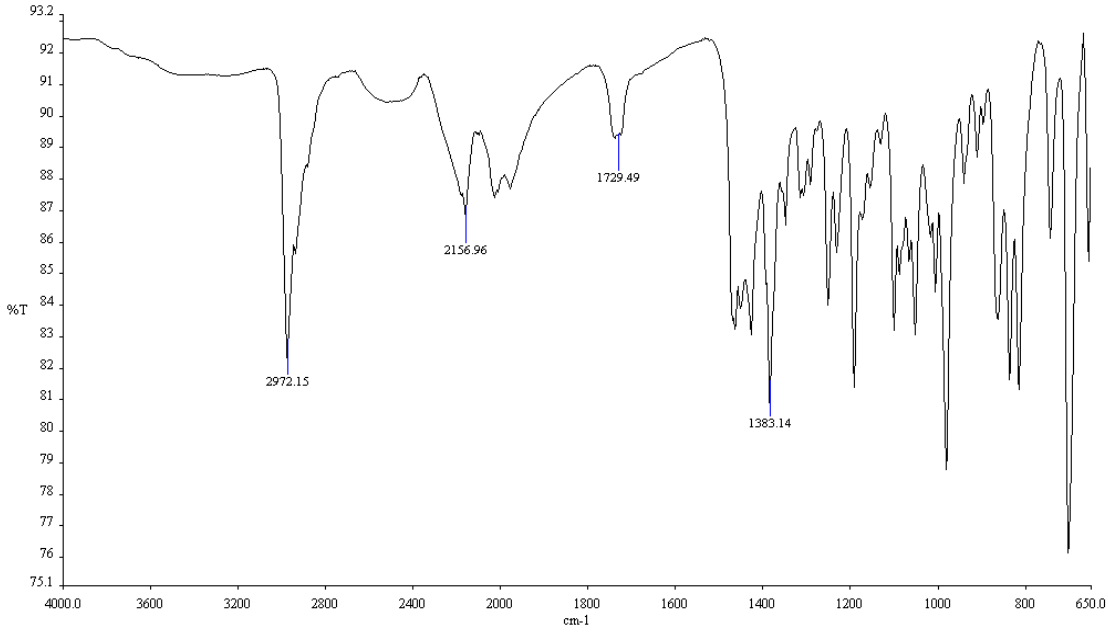

Figure S3.8 IR spectrum of compound **3.1**

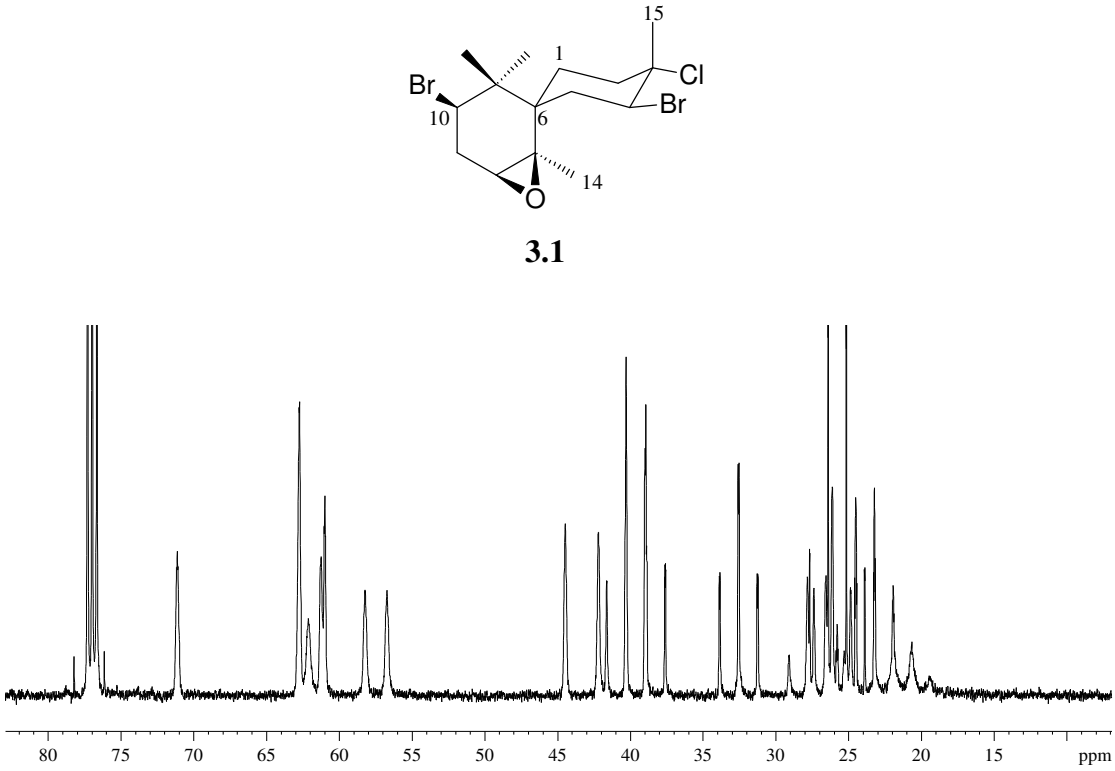

3.1

Figure S3.9 Proton coupled ^{13}C NMR spectrum ($CDCl_3$, 150 MHz) of compound **3.1**

S3.2 Compound 3.3

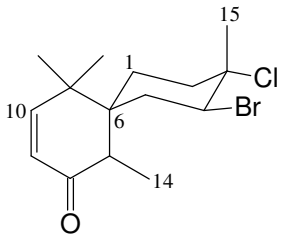

3.3

Table S3.1 NMR spectroscopic data of compound **3.3**

Carbon No	δ_C*	δ_C mult	δ_H, mult, J (Hz)	COSY	HMBC
1a	28.3	CH_2	1.43, dq, 15.0, 2.9	H2b	-
1b			1.71, m	H2a	-
2a	37.7	CH_2	2.19, td, 14.8, 4.1	H1b	-
2b			2.35, dt, 14.8, 4.1	H1a	-
3	71.8	C	-	-	-
4	59.7	CH	4.45, dd, 13.3, 4.5	H5a, H5b	-
5a	37.1	CH_2	1.98, t, 13.3	H4	-
5b			2.40, td, 13.3, 4.5	H4	-
6	43.1	C	-	-	-
7	44.1	CH	2.90, q, 7.8	H14	C6, C8, C11, C14
8	201.5	C	-	-	-
9	123.8	CH	5.82, d, 10.2	H10	-
10	156	CH	6.43, d, 10.2	H9	C8
11	39.1	C	-	-	-
12	25.4	CH_3	1.09, s	-	C6, C10, C11, C13
13	25.2	CH_3	1.21, s	-	C6, C10, C11, C12
14	15.4	CH_3	1.30, d, 8.1	H7	C7, C8
15	23.7	CH_3	1.70, s	-	C2, C3, C4

*Carbons assigned via HMBC

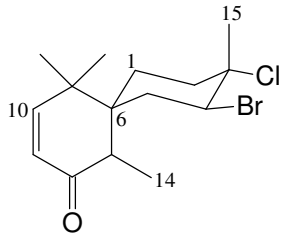

3.3

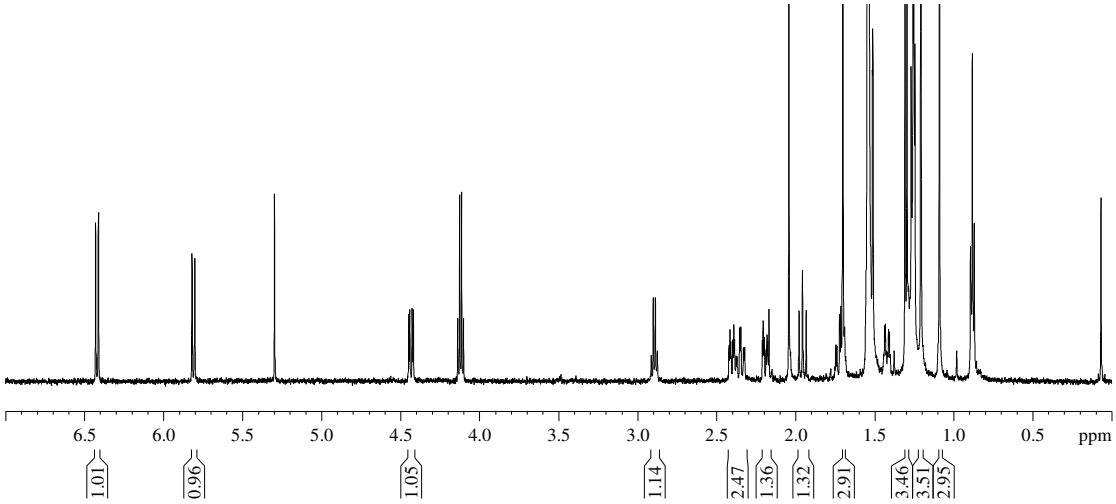

Figure S3.10 ^{1}H NMR spectrum ($CDCl_3$, 600 MHz) of compound **3.3**

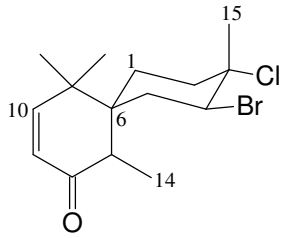

3.3

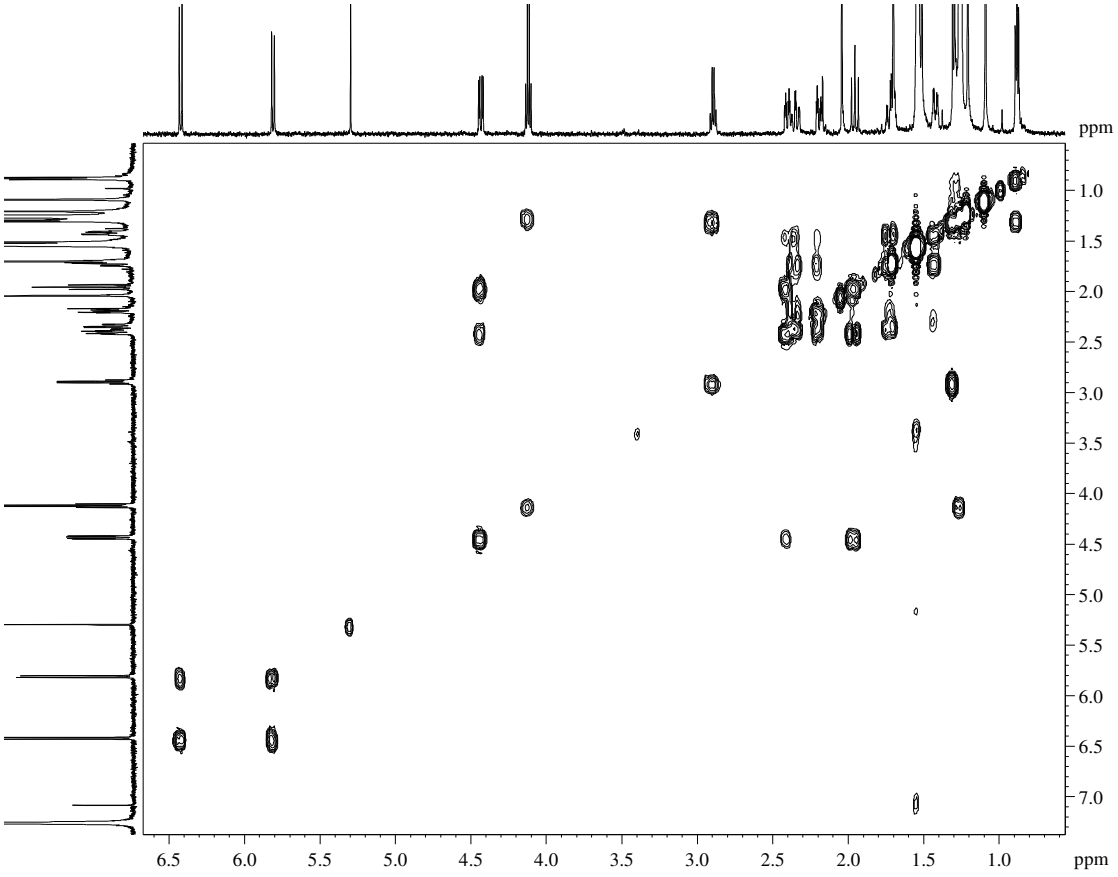

Figure S3.11 COSY NMR **s**pectrum of compound **3.3**

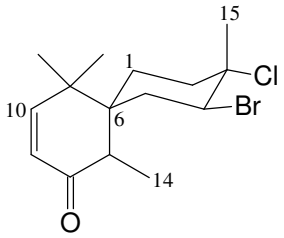

3.3

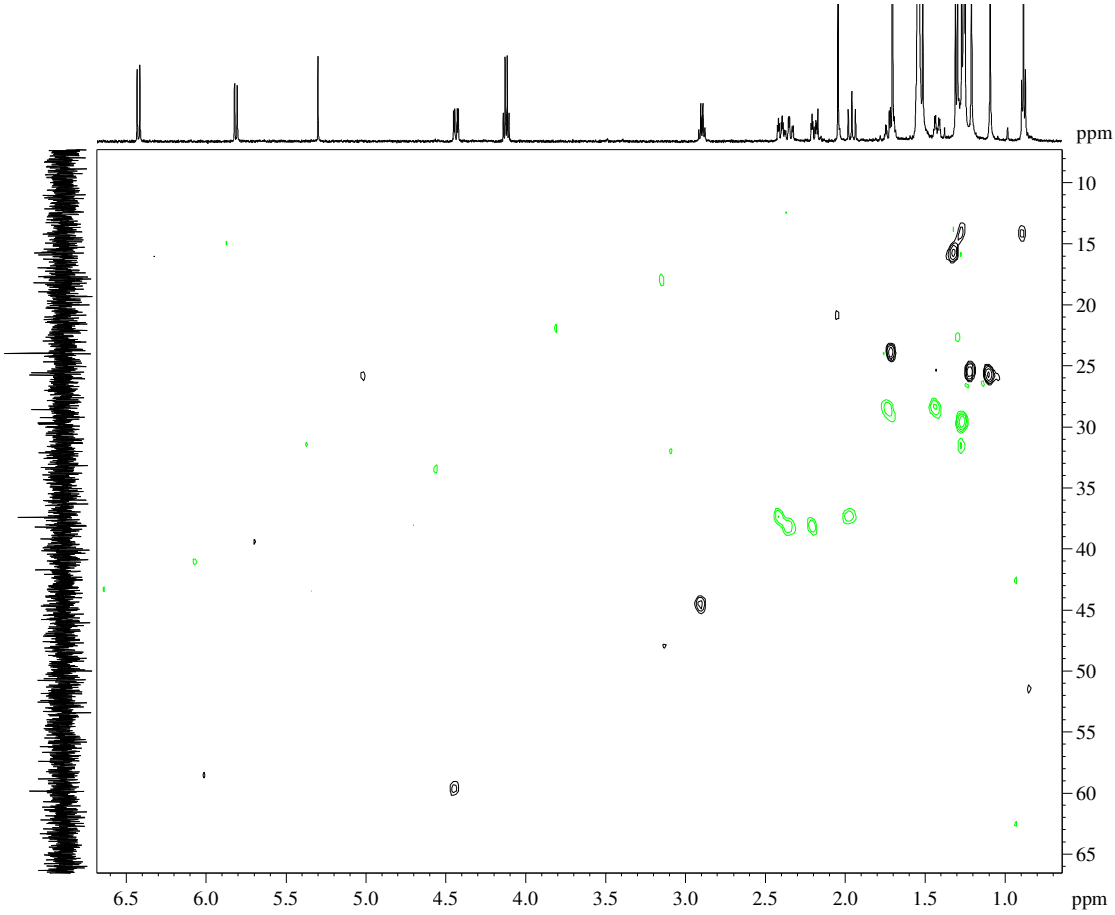

Figure S3.12 HSQC NMR spectrum of compound **3.3**

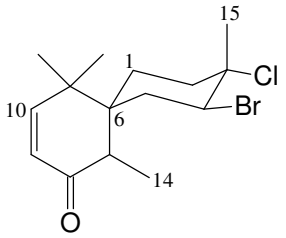

3.3

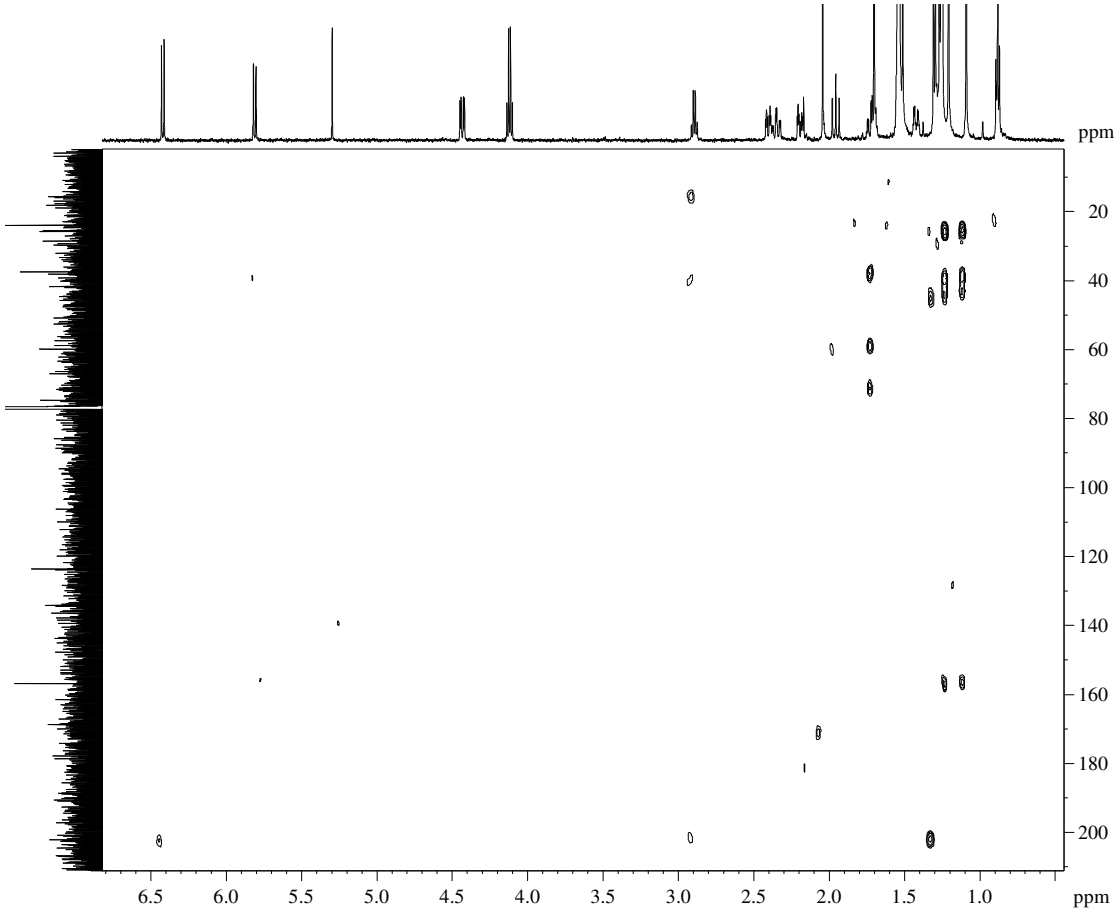

Figure S3.13 HMBC NMR spectrum of compound **3.3**

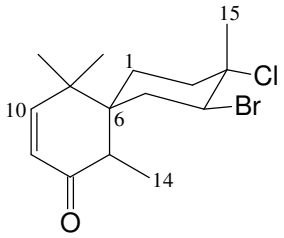

3.3

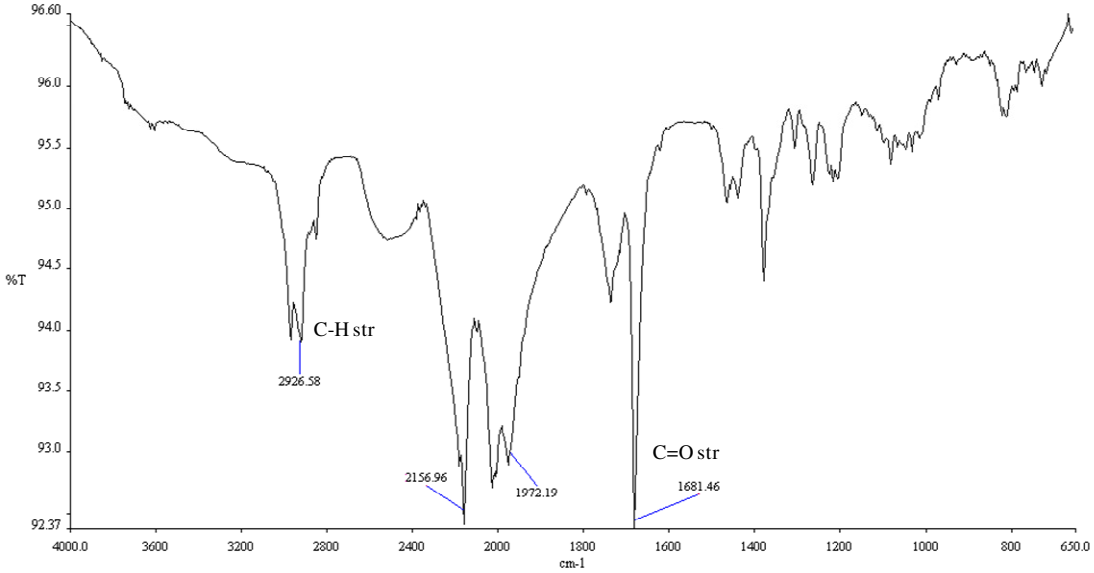

Figure S3.14 IR spectrum of compound **3.3**

S3.3 Compound 3.4

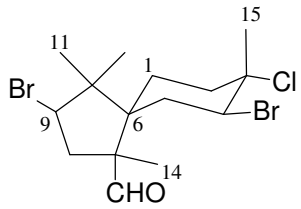

3.4

Table S3.2 NMR spectroscopic data of compound **3.4**

Carbon No	δ_C	δ_C mult	δ_H, mult, J (Hz)	COSY	HMBC
1	CH_2	27.3	1.70, m	H2a, H2b	-
2a	CH_2	40.5	2.32, td, 14.1, 4.0	H1	-
2b			2.42, dt, 14.1, 4.0	H1	-
3	C	71.0	-	-	-
4	CH	60.5	4.56, dd, 13.4, 3.6	H5a, H5b	-
5a	CH_2	39.4	1.92, t, 14.6	H4	-
5b			2.26, td, 14.6, 3.1	-	-
6	C	56.0	-	-	-
7	C	52.0	-	-	-
8a	CH_2	43.4	1.97, dd, 14.1, 8.4	H9	C7, C14
8b			2.88, dd, 14.1, 8.4	H8a, H9	C9, C13
9	CH	58.4	4.15, dd, 11.3, 8.4	H8a, H8b	C11
10	C	51.2	-	-	-
11	CH_3	20.4	0.88, s	-	C6, C9, C12
12	CH_3	22.6	0.98, s	-	C6, C9, C11
13	C**H**O	203.5	9.79, s	-	C6, C8, C14
14	CH_3	23.2	1.38, s	-	C6, C7, C8, C13
15	CH_3	23.7	1.71, s	-	C2, C3, C4

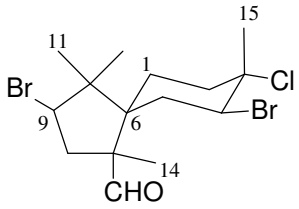

3.4

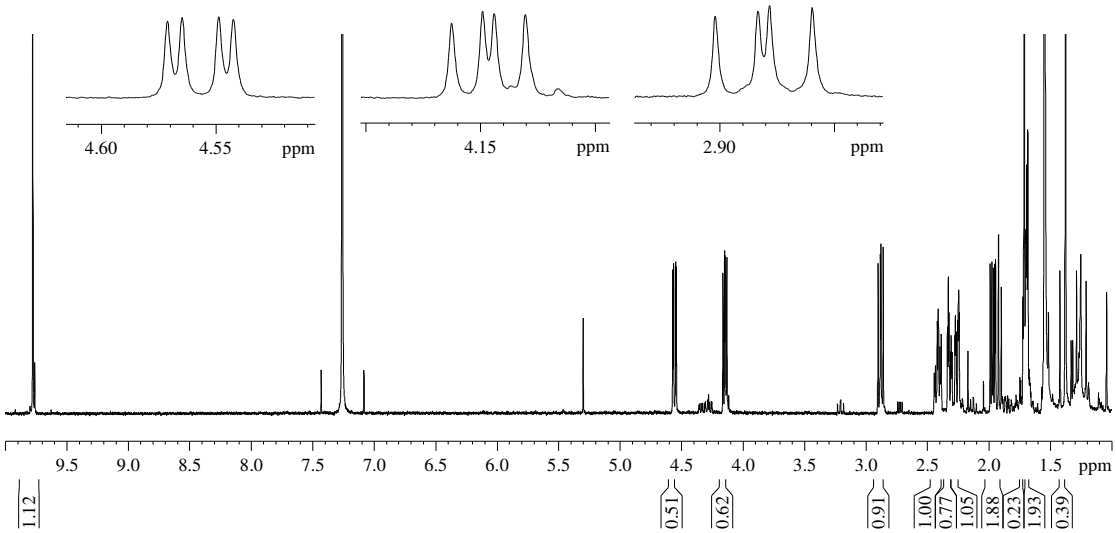

Figure S3.15 ^{1}H NMR spectrum ($CDCl_3$, 600 MHz) of compound **3.4**

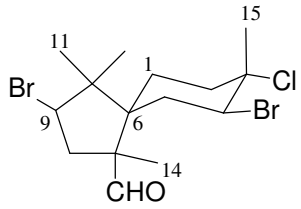

3.4

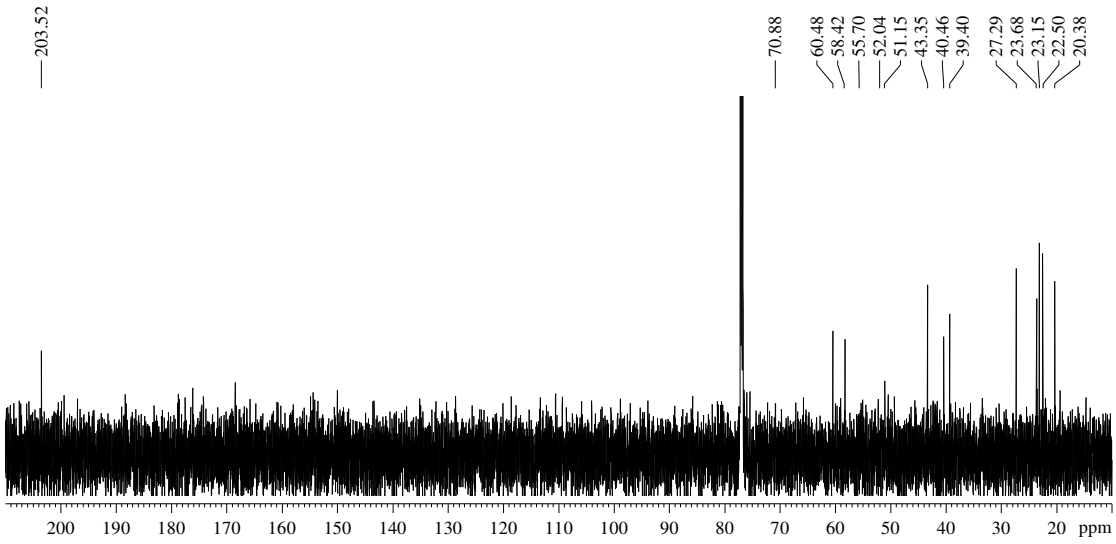

Figure S3.16 ^{13}C NMR spectrum ($CDCl_3$, 150 MHz) of compound **3.4**

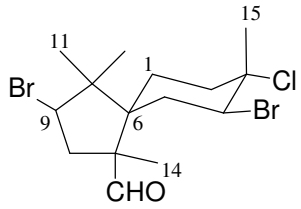

3.4

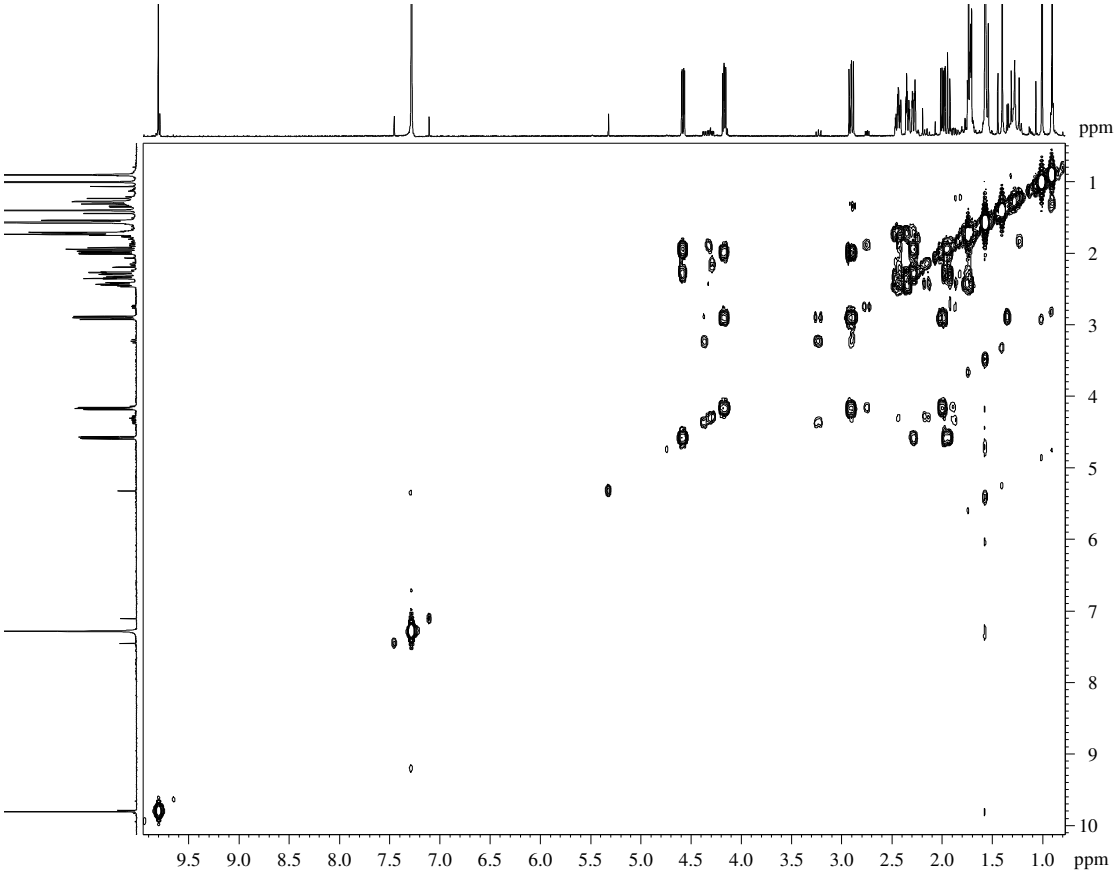

Figure S3.17 COSY NMR spectrum of compound **3.4**

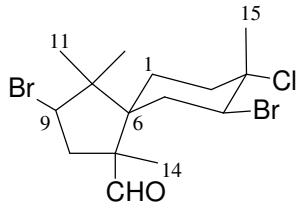

3.4

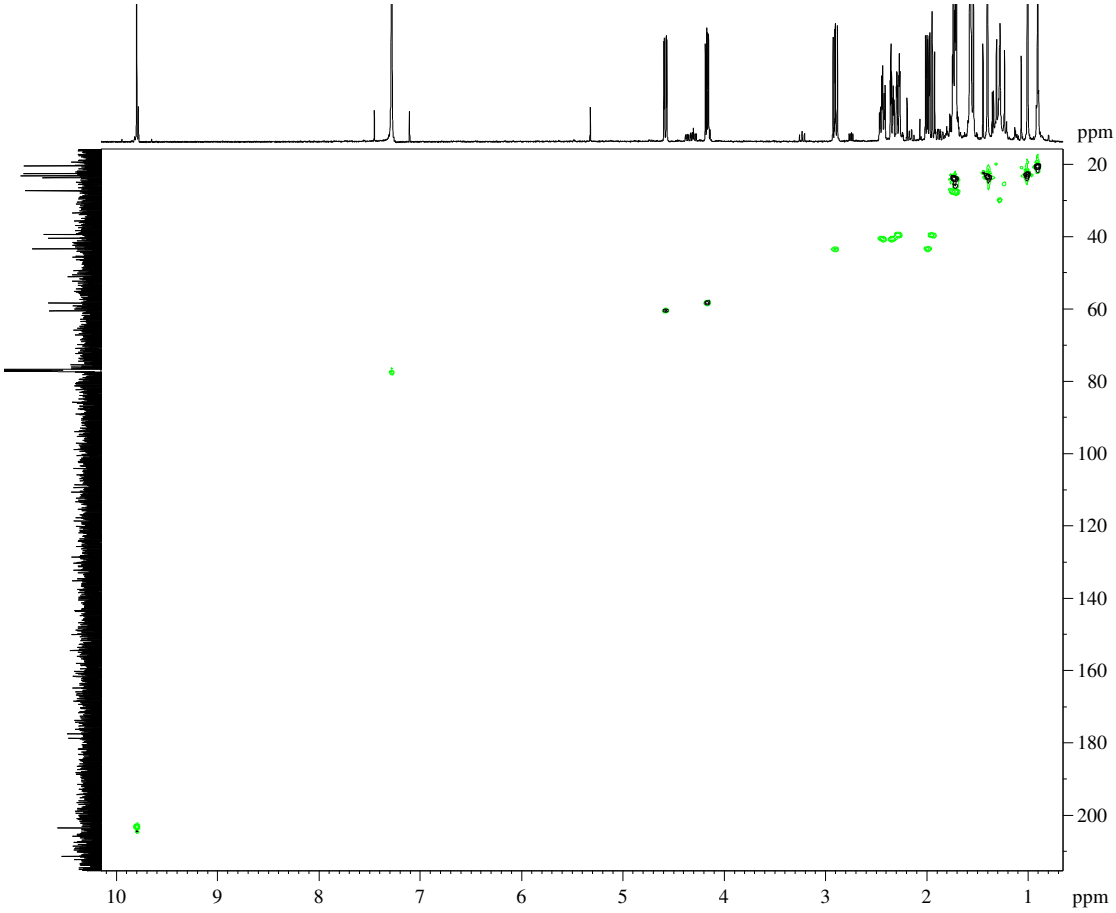

Figure S3.18 HSQC NMR spectrum of compound **3.4**

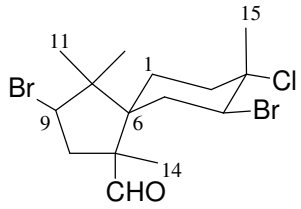

3.4

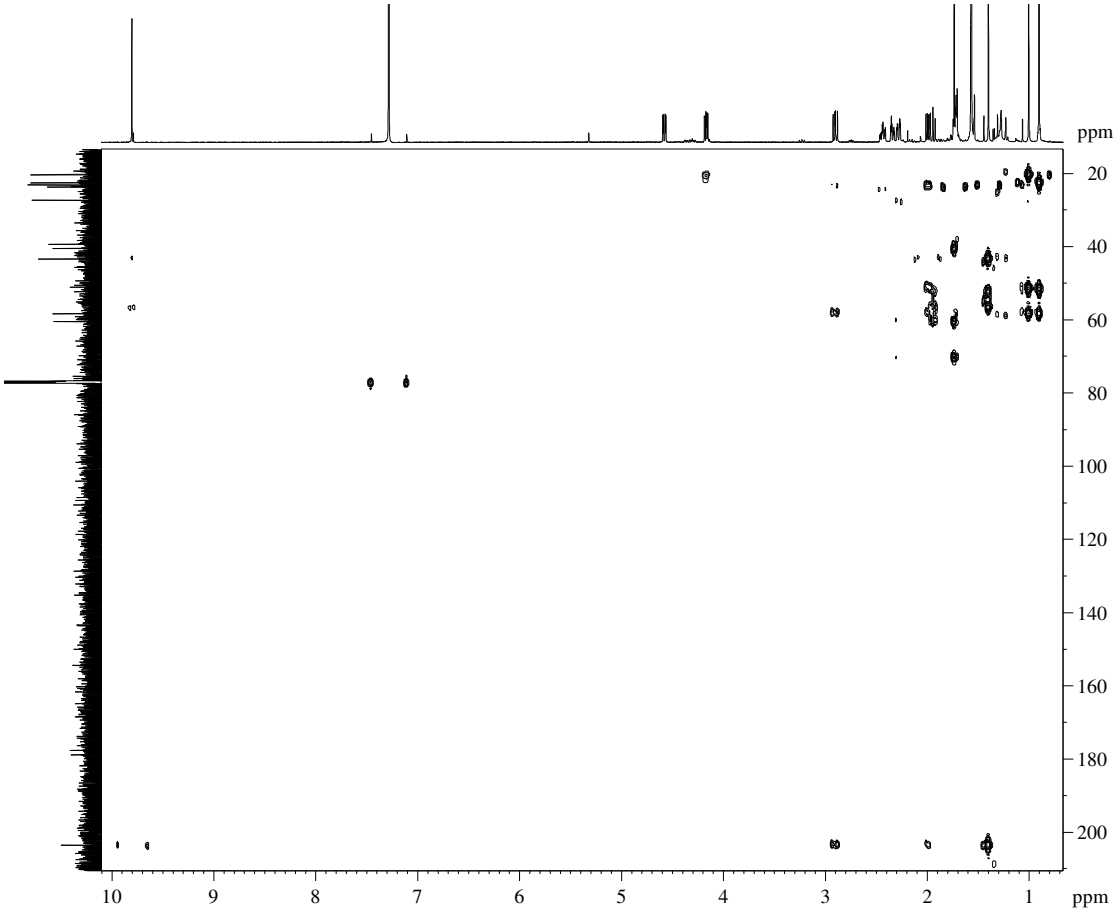

Figure S3.19 HMBC NMR spectrum of compound **3.4**

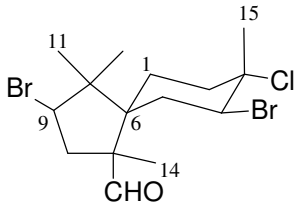

3.4

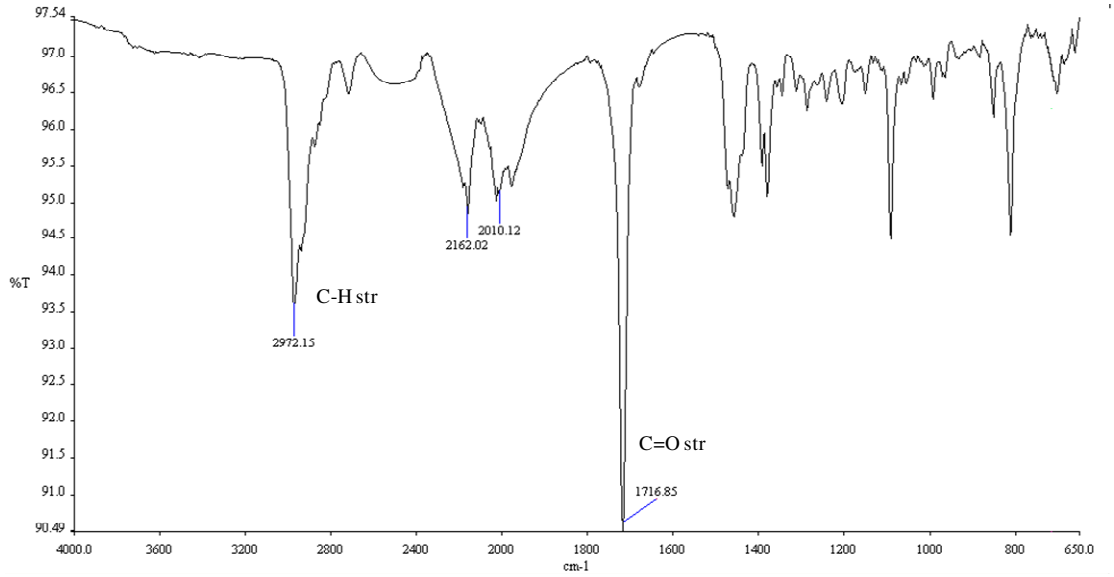

Figure S3.20 IR spectrum of compound **3.4**

S3.4 Compound 3.5

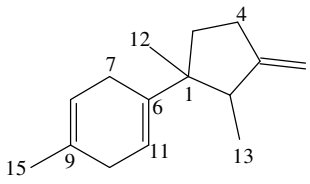

3.5

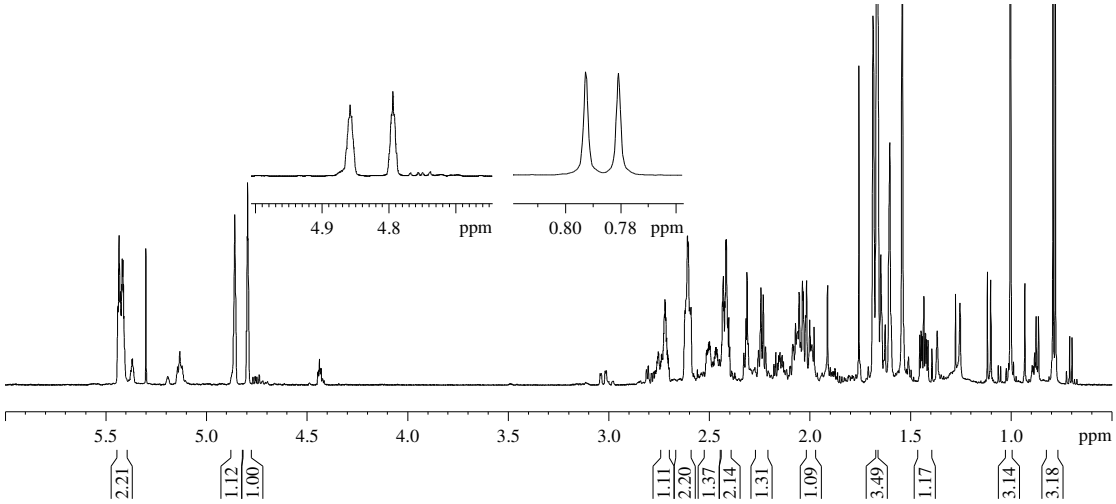

Figure S3.21 ^{1}H NMR spectrum ($CDCl_3$, 600 MHz) of compound **3.5**

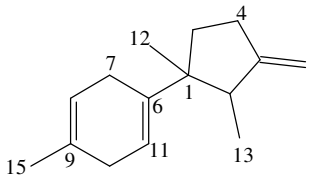

3.5

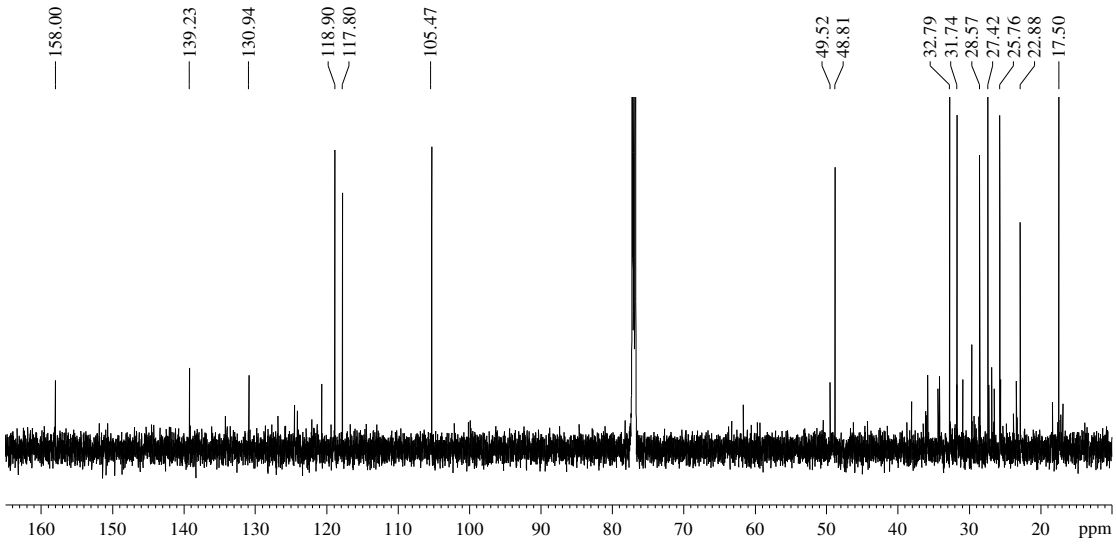

Figure S3.22 ^{13}C NMR spectrum ($CDCl_3$, 150 MHz) of compound **3.5**

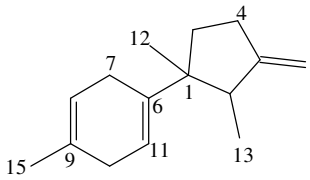

3.5

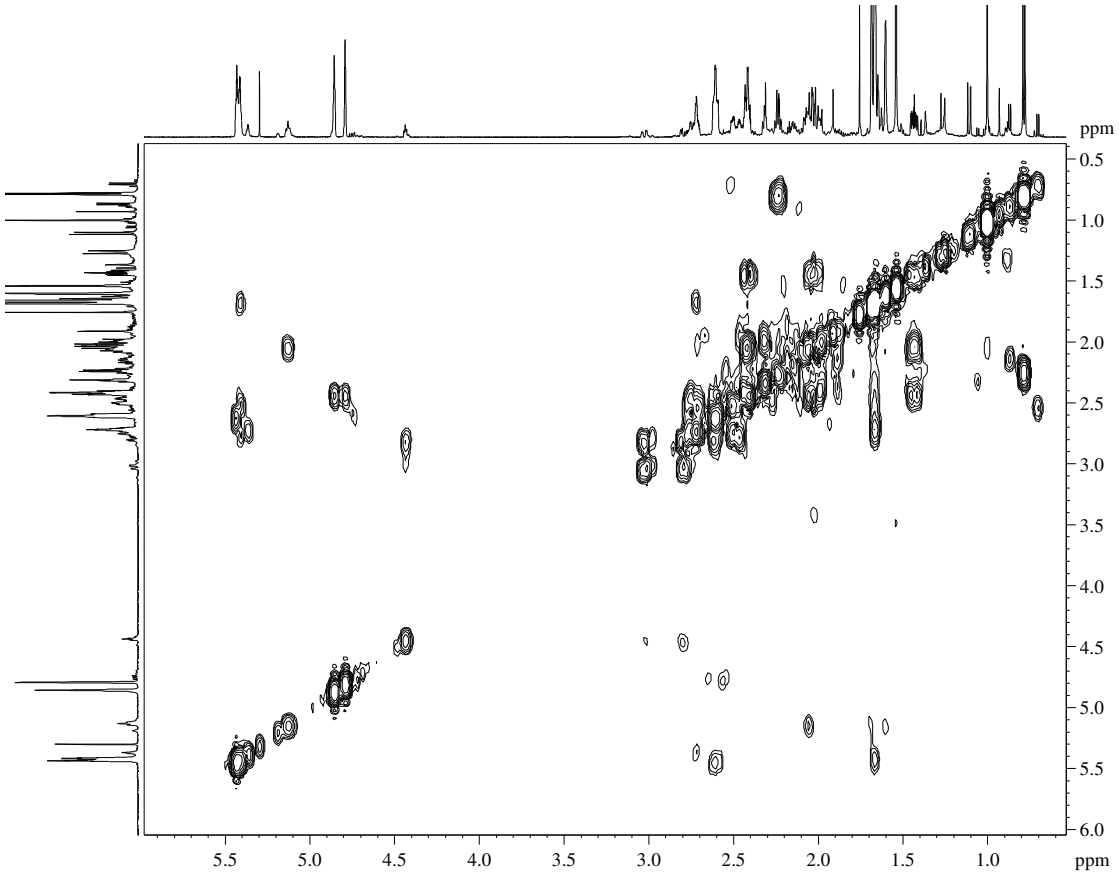

Figure S3.23 COSY NMR spectrum of compound **3.5**

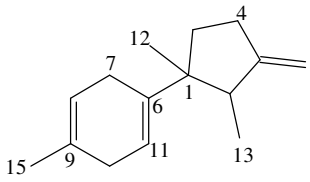

3.5

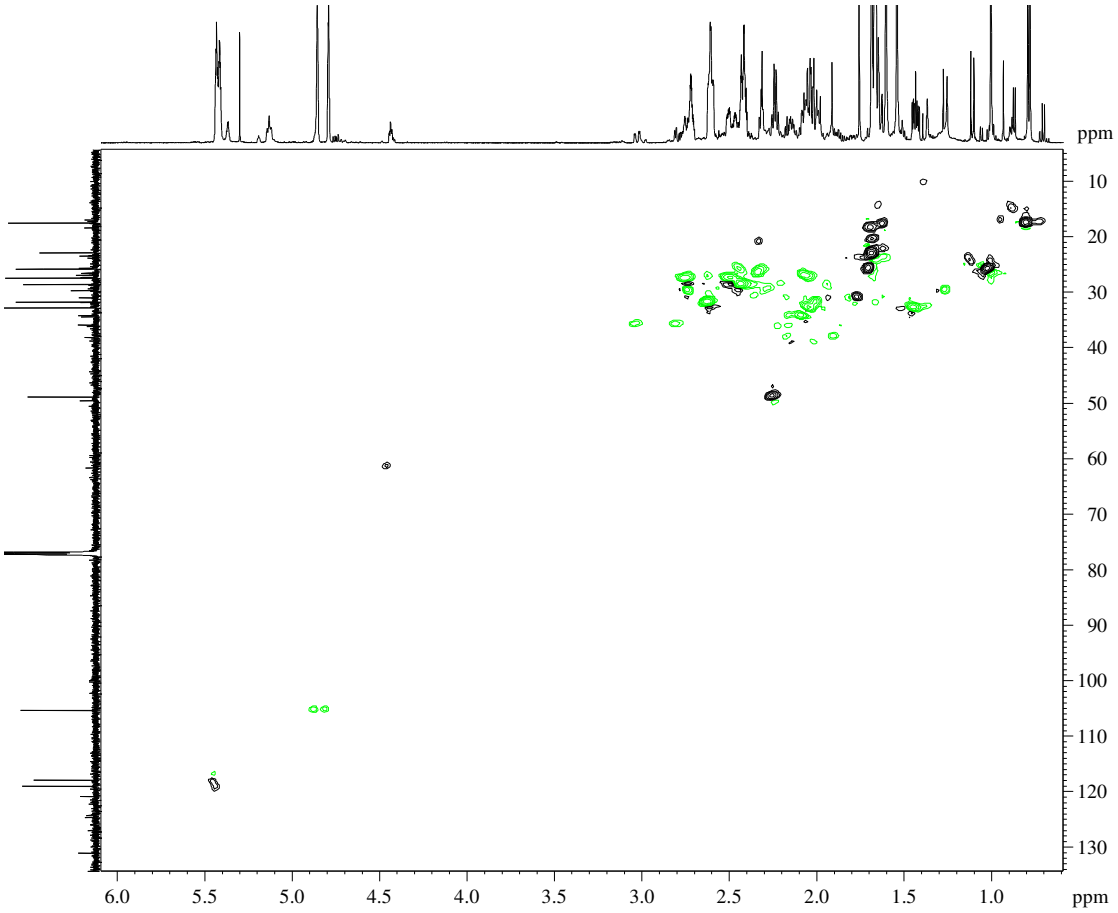

Figure S3.24 HSQC NMR spectrum of compound **3.5**

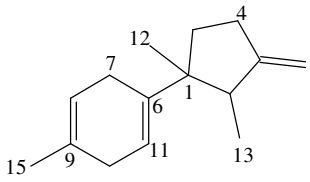

3.5

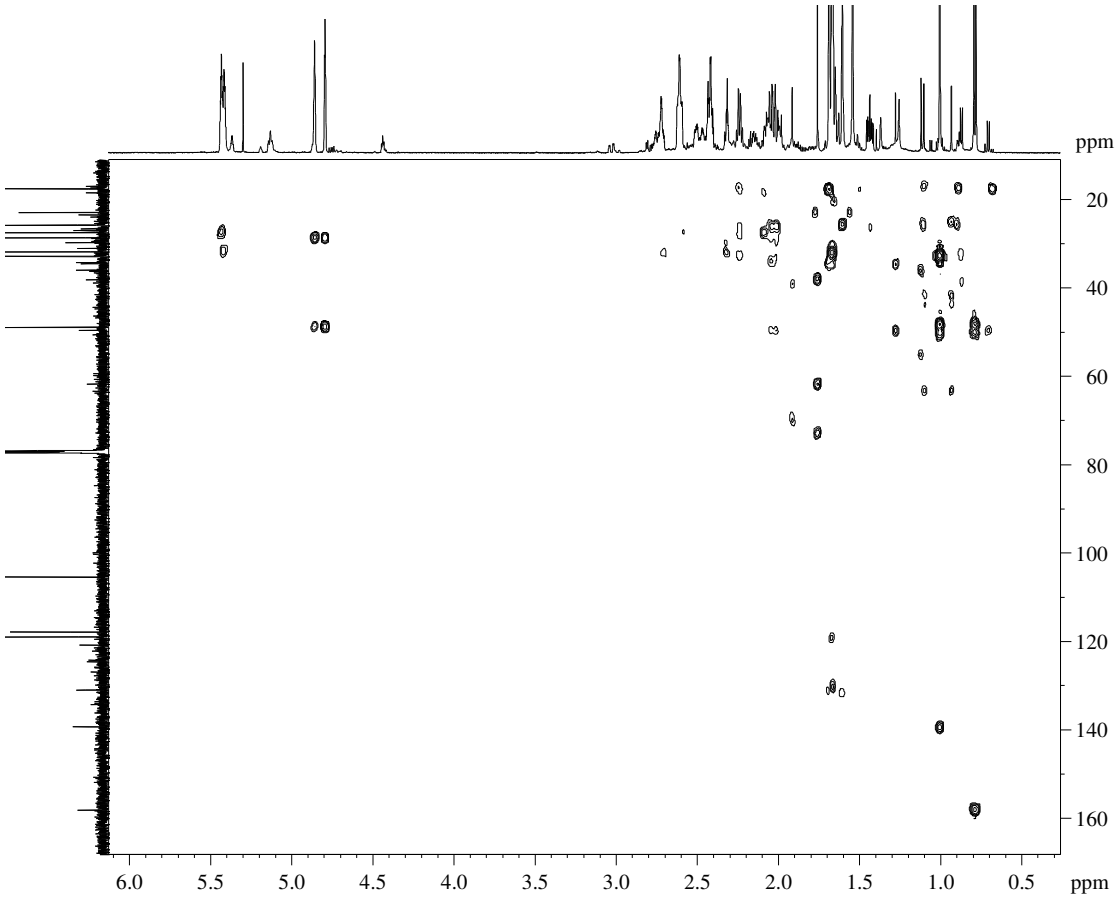

Figure S3.25 HMBC NMR spectrum of compound **3.5**

S3.5 Compound 3.7

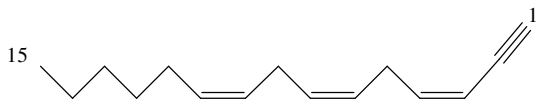

3.7

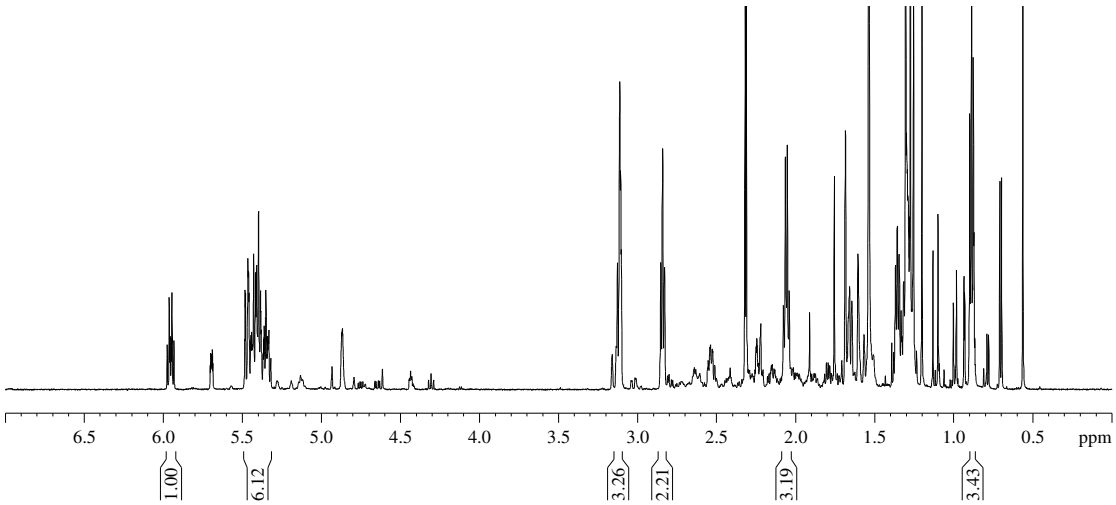

Figure S3.26 ^{1}H NMR spectrum ($CDCl_3$, 600 MHz) of compound **3.7**

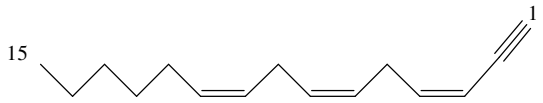

3.7

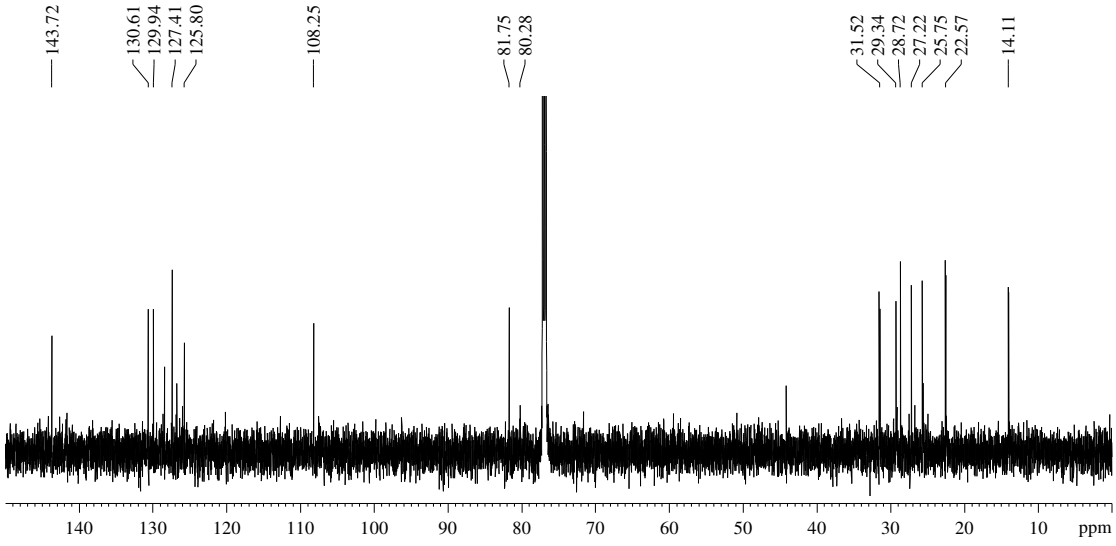

Figure S3.27 ^{13}C NMR spectrum ($CDCl_3$, 150 MHz) of compound **3.7**

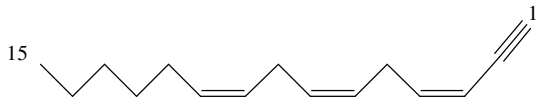

3.7

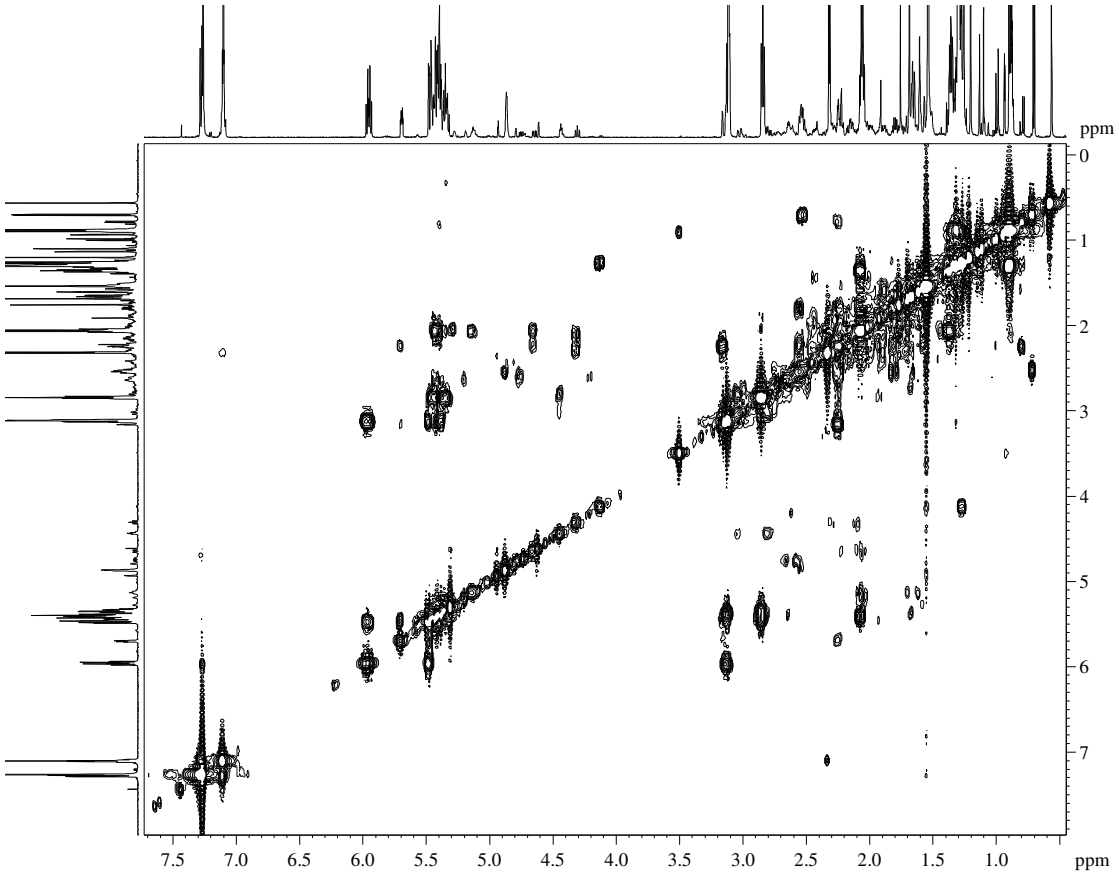

Figure S3.28 COSY NMR spectrum of compound **3.7**

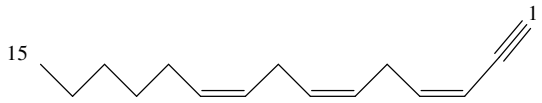

3.7

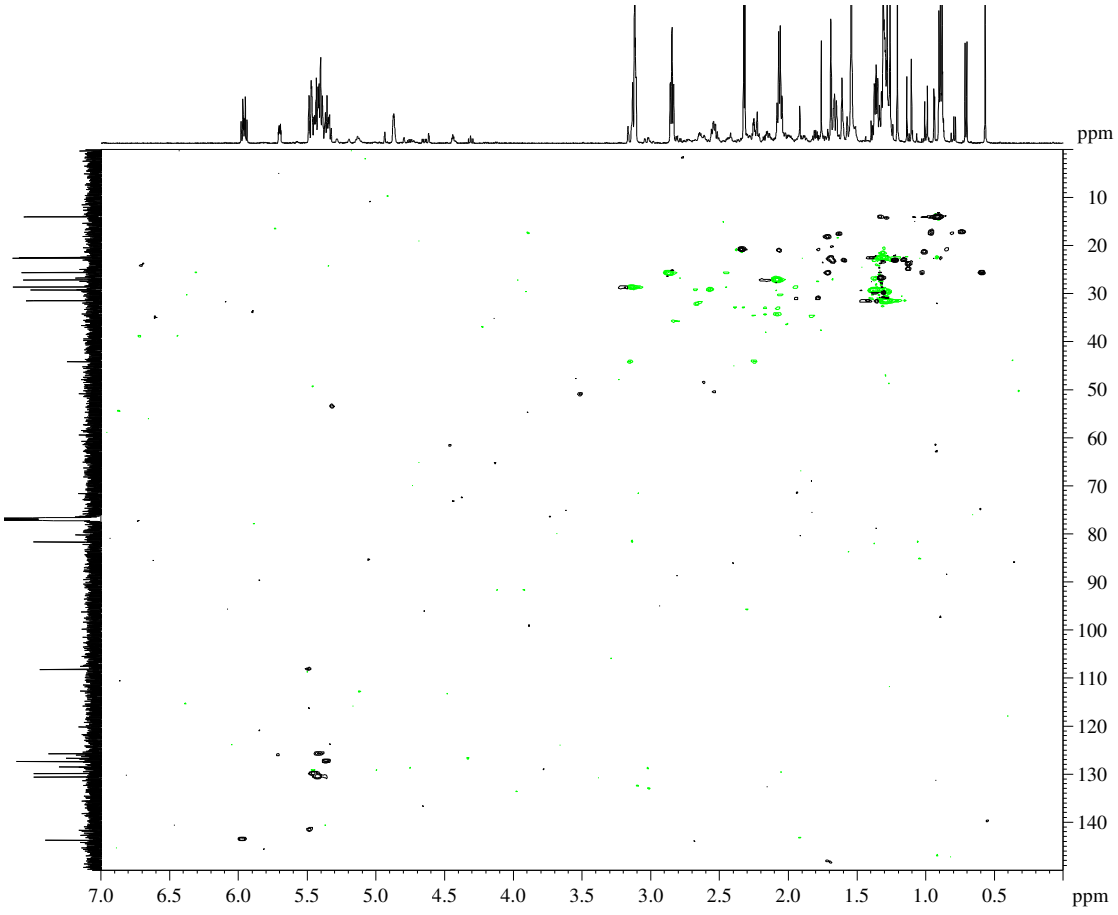

Figure S3.29 HSQC NMR spectrum of compound **3.7**

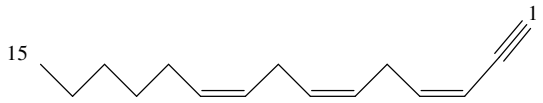

3.7

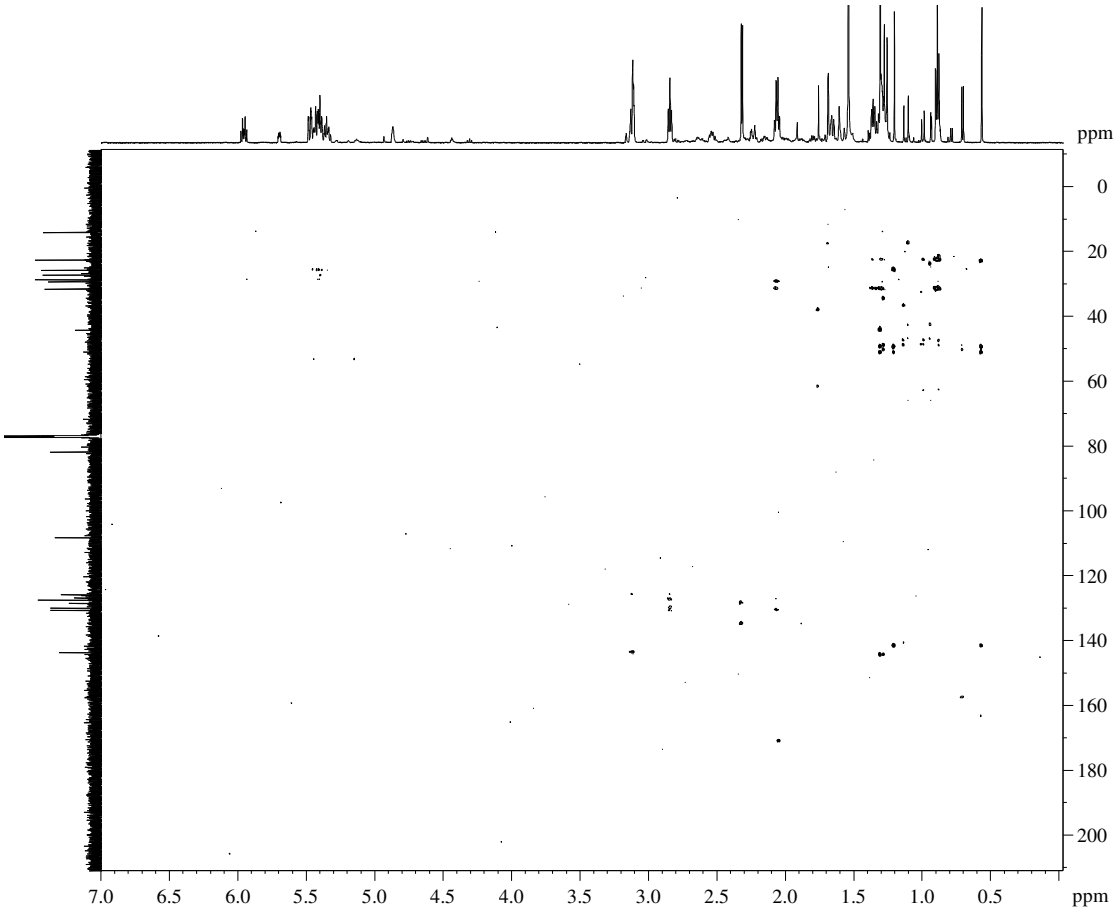

Figure S3.30 HMBC NMR spectrum of compound **3.7**

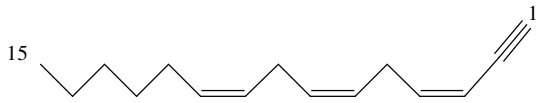

3.7

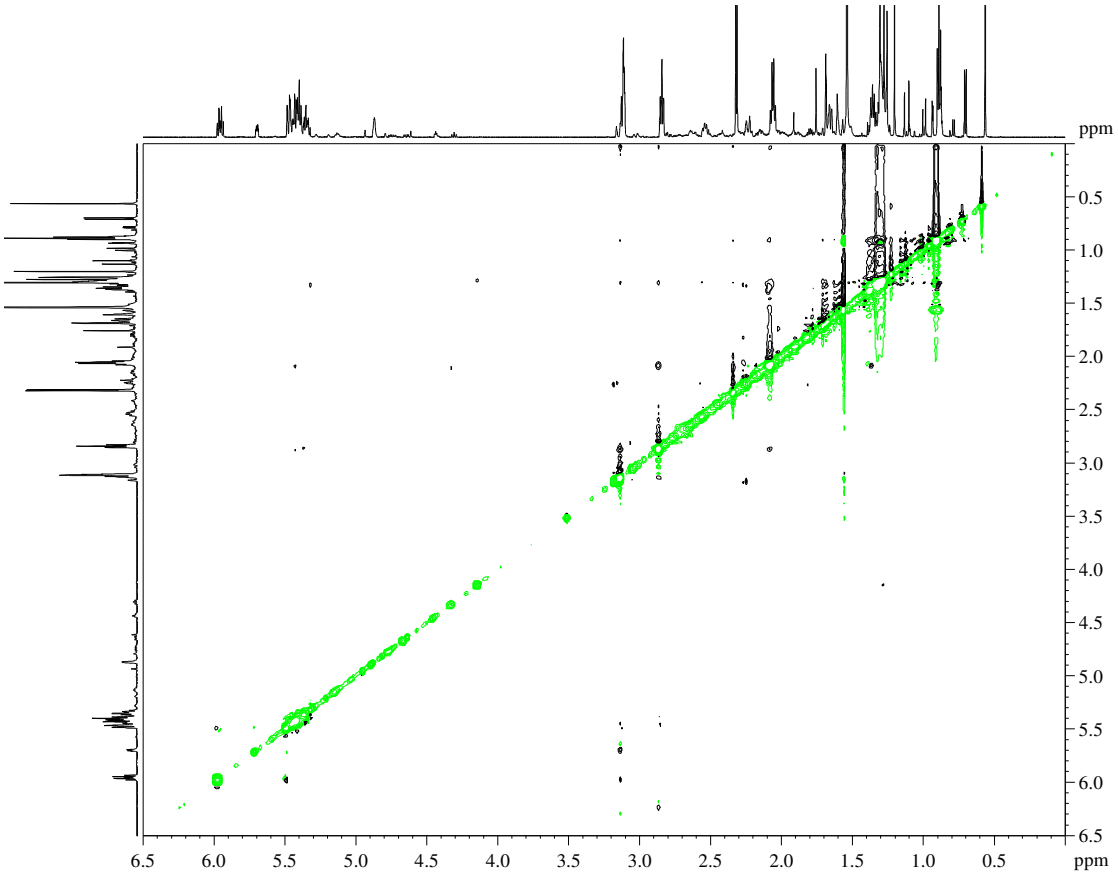

Figure S3.31 NOESY NMR spectrum of compound **3.7**

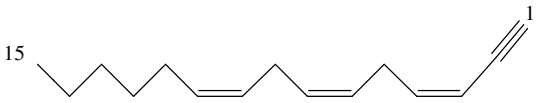

3.7

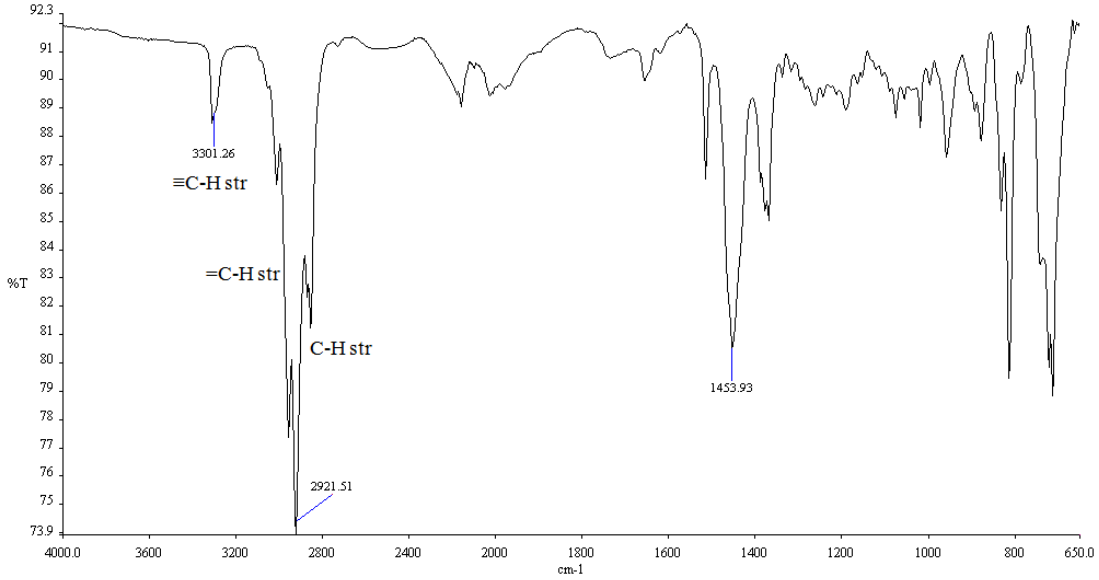

Figure S3.32 IR spectrum of compound **3.7**

S3.6 Compound 3.9

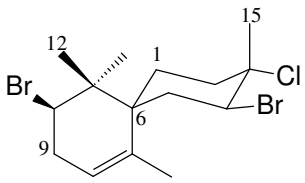

3.9

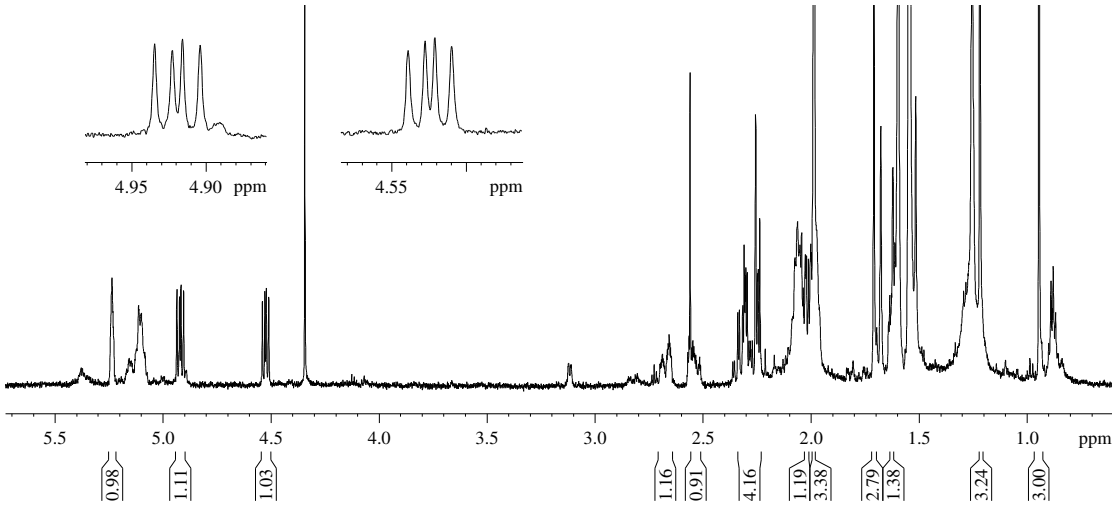

Figure S3.33 ^{1}H NMR spectrum ($CDCl_3$, 600 MHz) of compound **3.9**

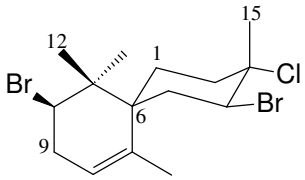

3.9

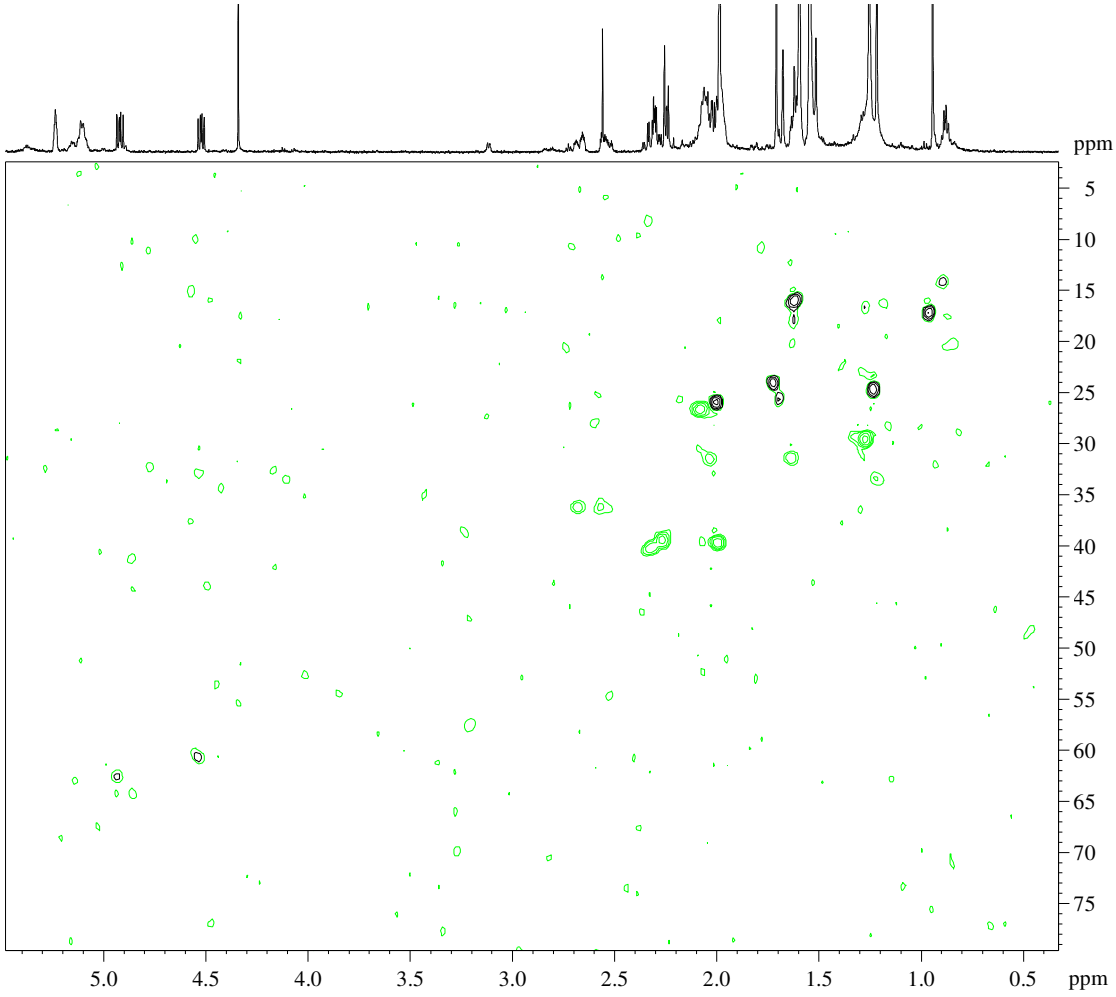

Figure S3.34 HSQC NMR spectrum of compound **3.9**

(No ^{13}C NMR data obtained)

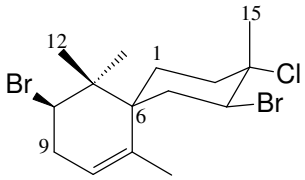

3.9

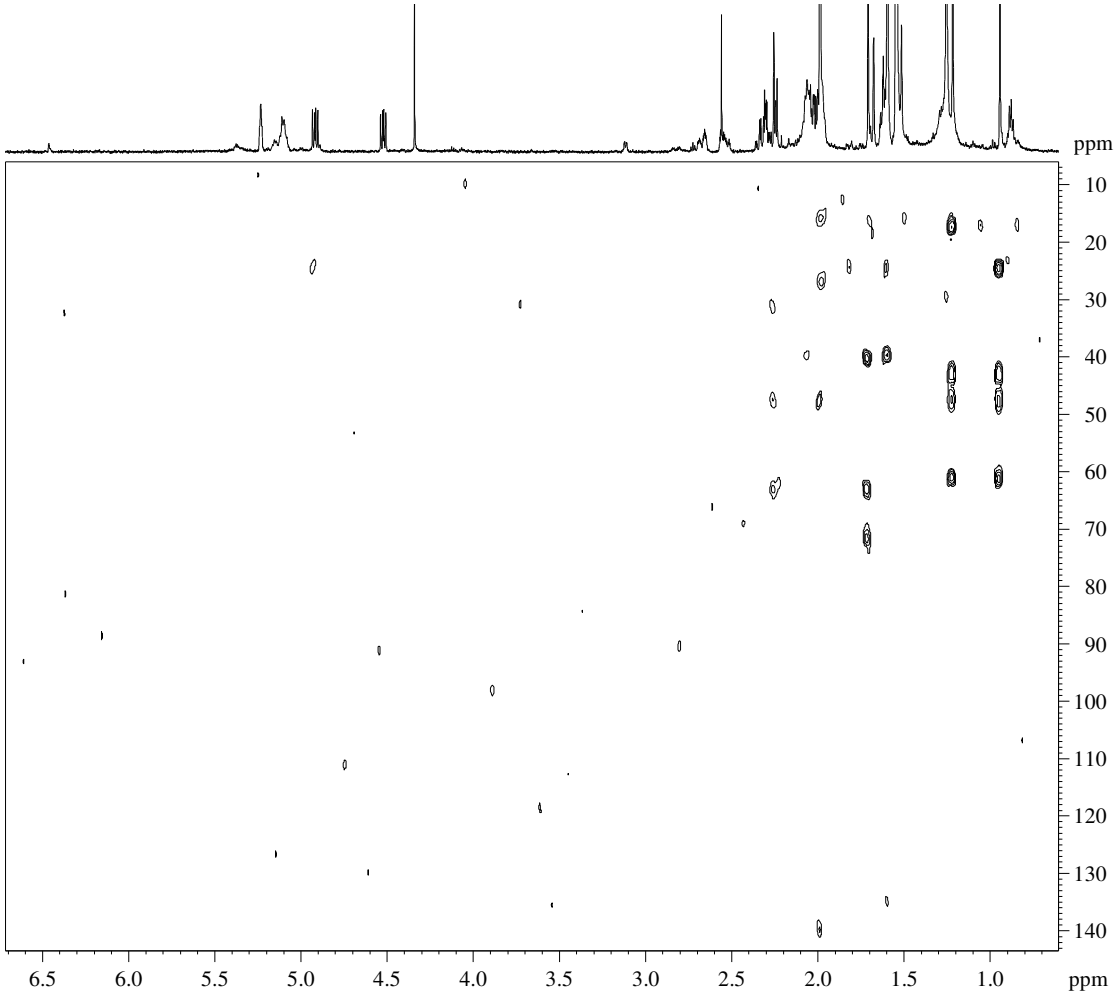

Figure S3.35 HMBC NMR spectrum of compound **3.9**

S3.7 Compound 3.15

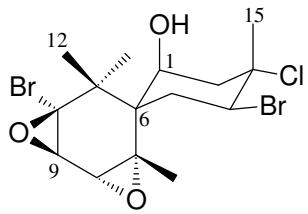

3.15

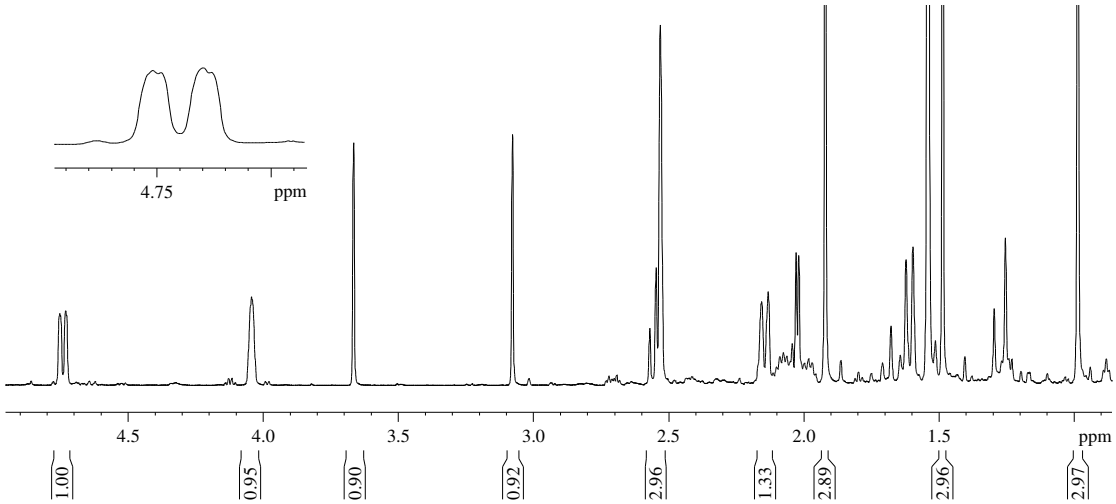

Figure S3.36 ^{1}H NMR spectrum ($CDCl_3$, 600 MHz) of compound **3.15**

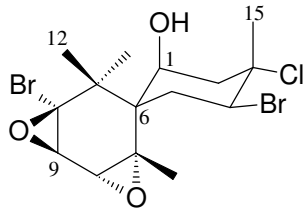

3.15

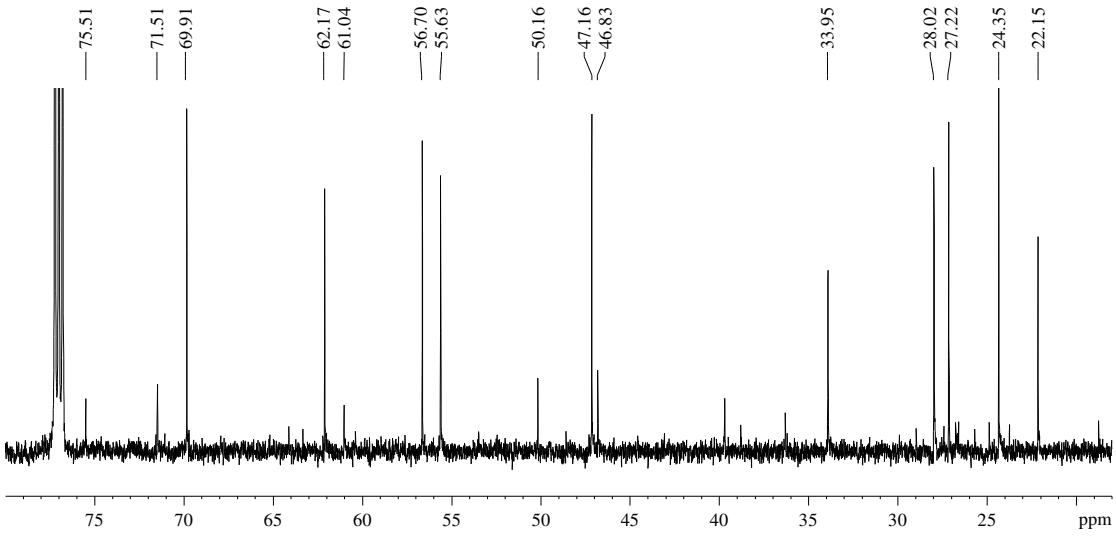

Figure S3.37 ^{13}C NMR spectrum ($CDCl_3$, 150 MHz) of compound **3.15**

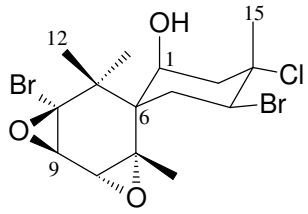

3.15

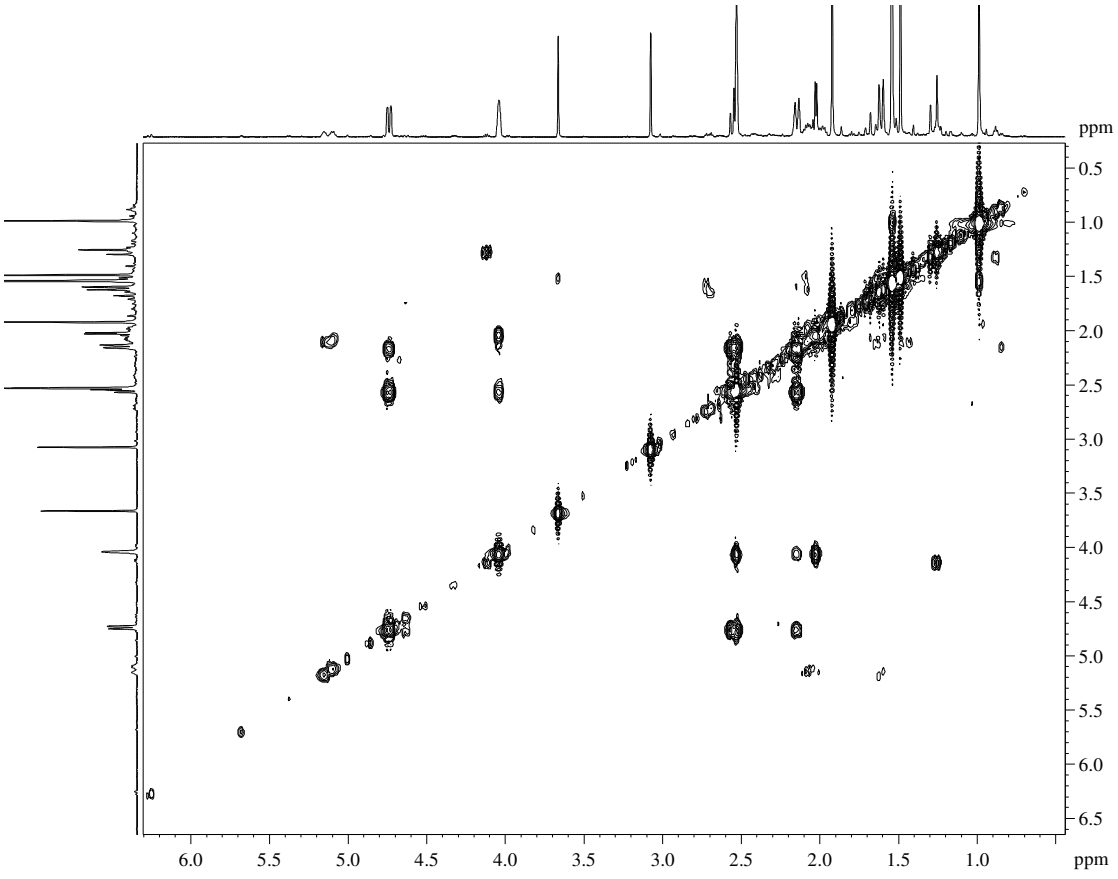

Figure S3.38 COSY NMR spectrum of compound **3.15**

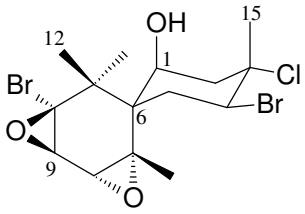

3.15

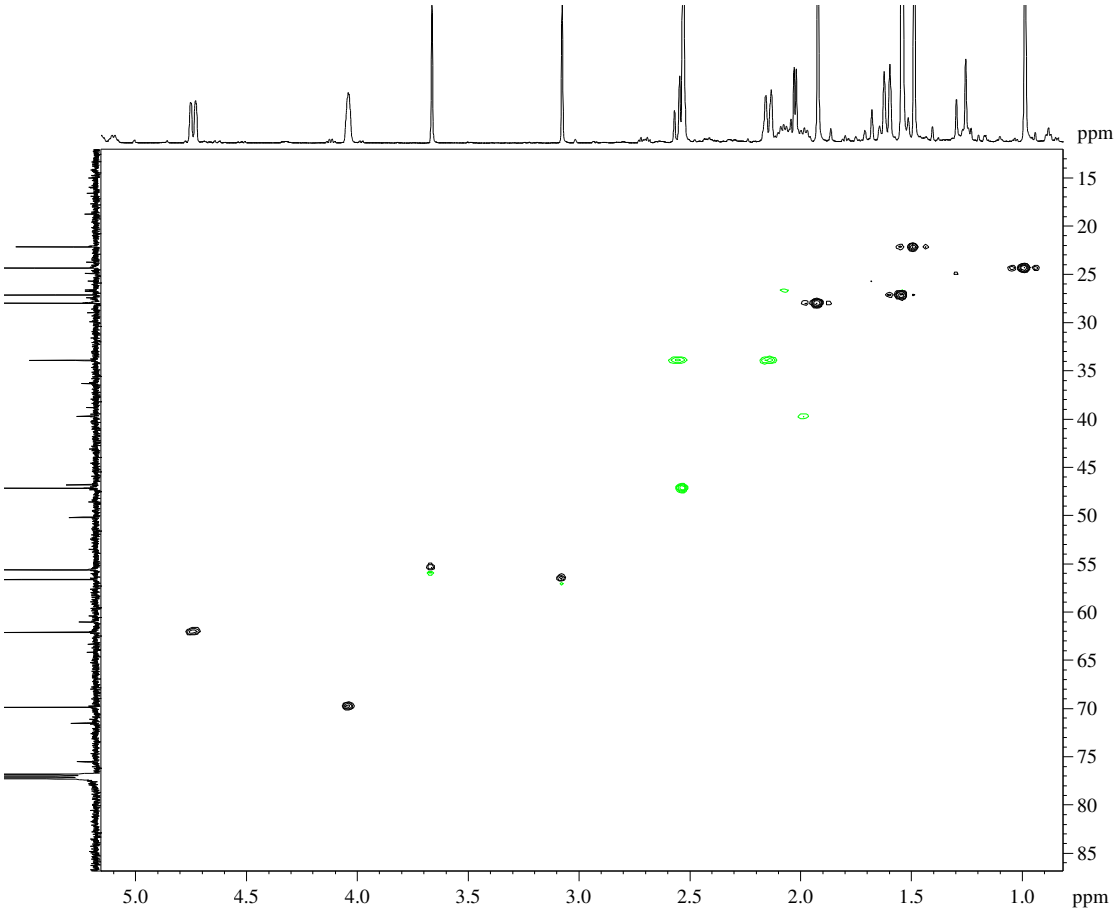

Figure S3.39 HSQC NMR spectrum of compound **3.15**

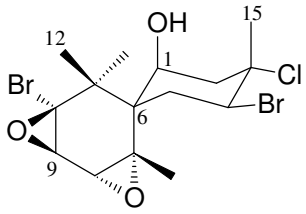

3.15

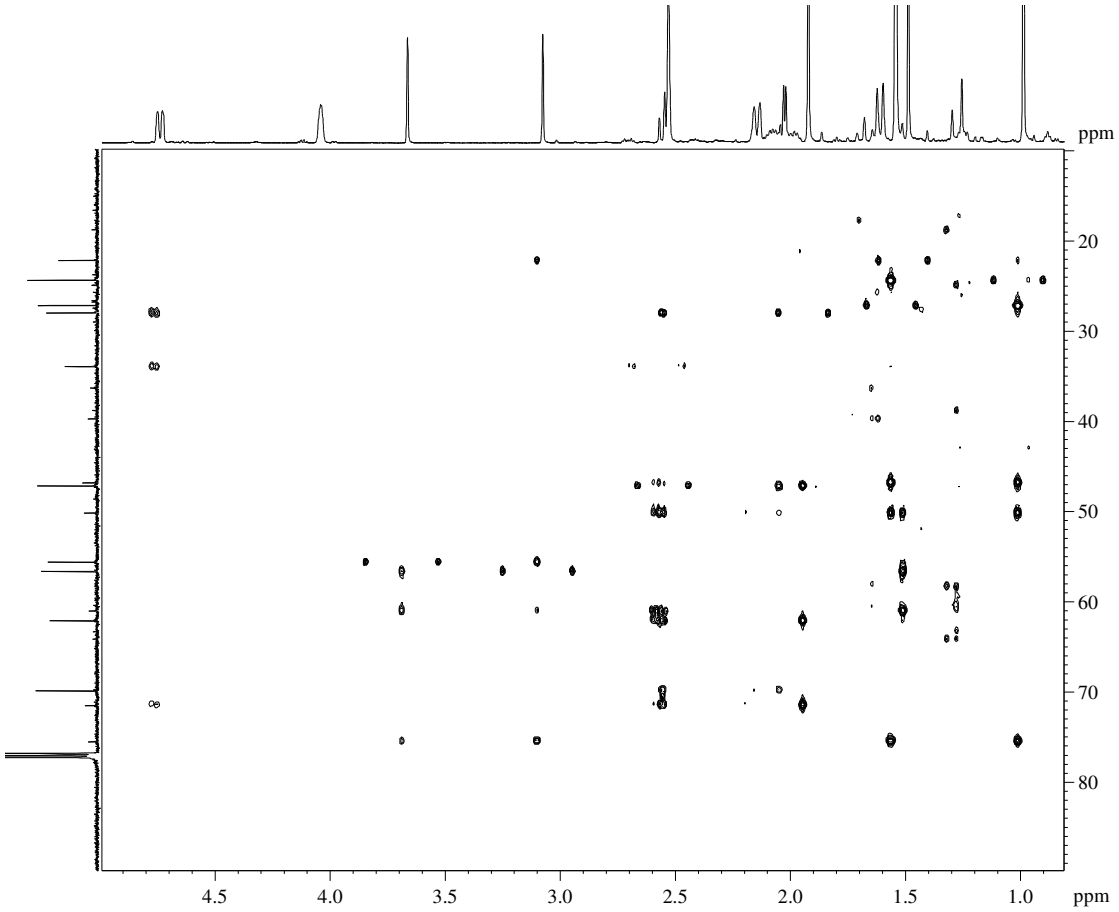

Figure S3.40 HMBC NMR spectrum of compound **3.15**

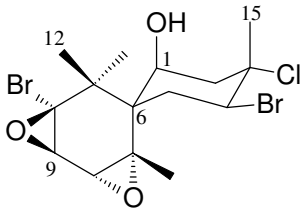

3.15

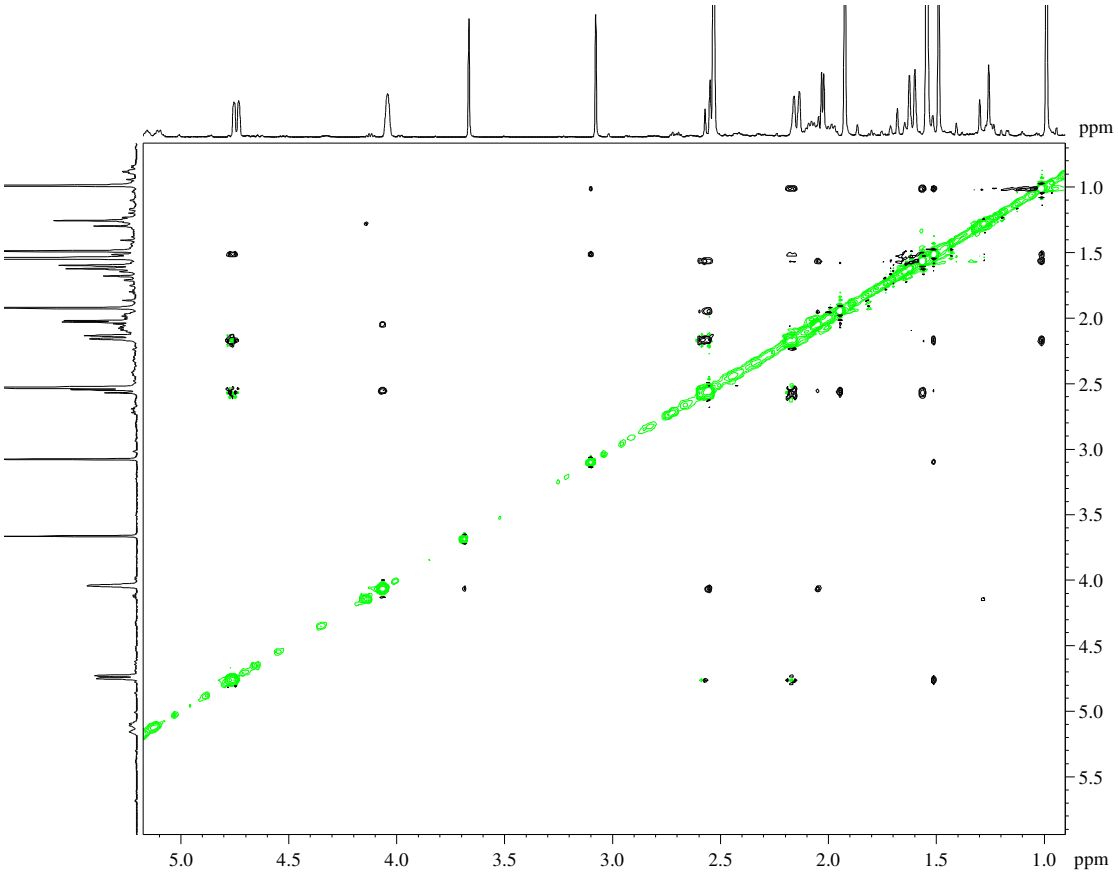

Figure S3.41 NOESY NMR spectrum of compound **3.15**

S3.8 Compound 3.17

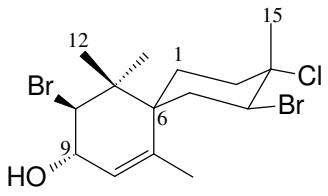

3.17

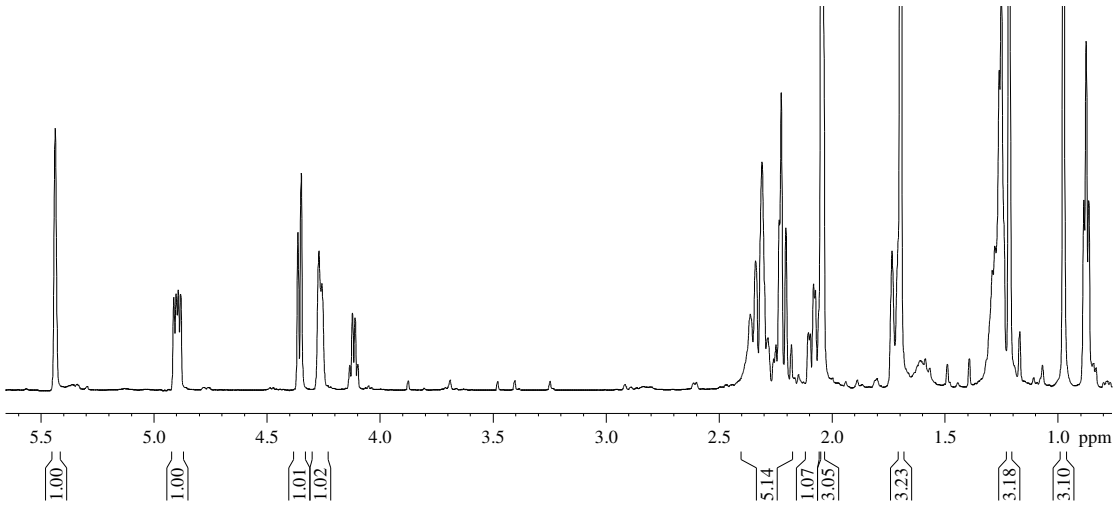

Figure S3.42 ^{1}H NMR spectrum ($CDCl_3$, 600 MHz) of compound **3.17**

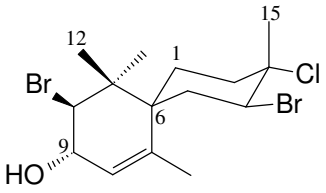

3.17

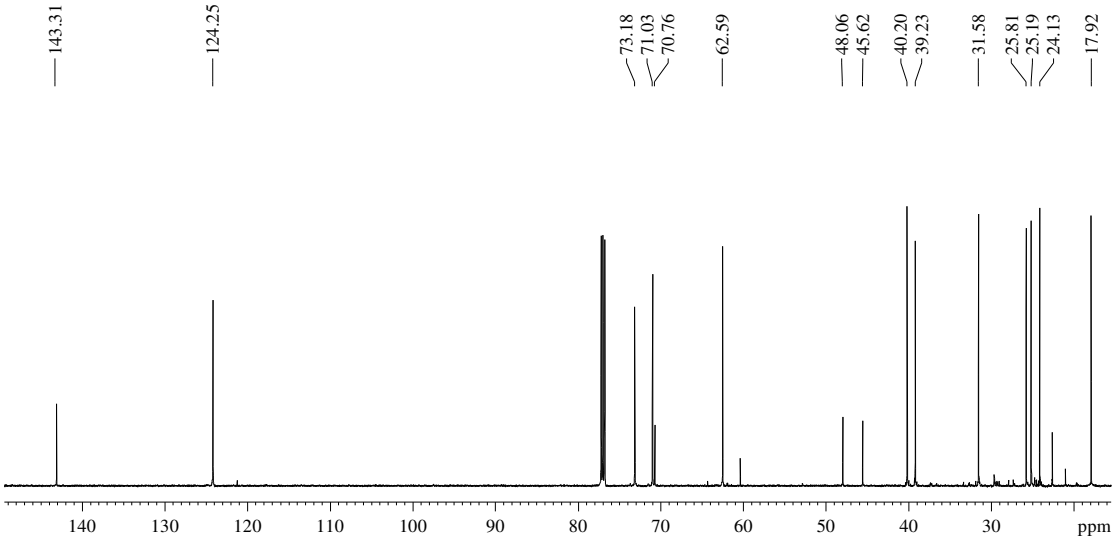

Figure S3.43 ^{13}C NMR spectrum ($CDCl_3$, 150 MHz) of compound **3.17**

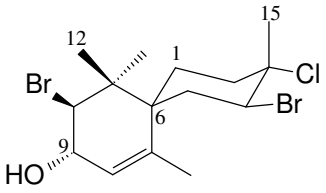

3.17

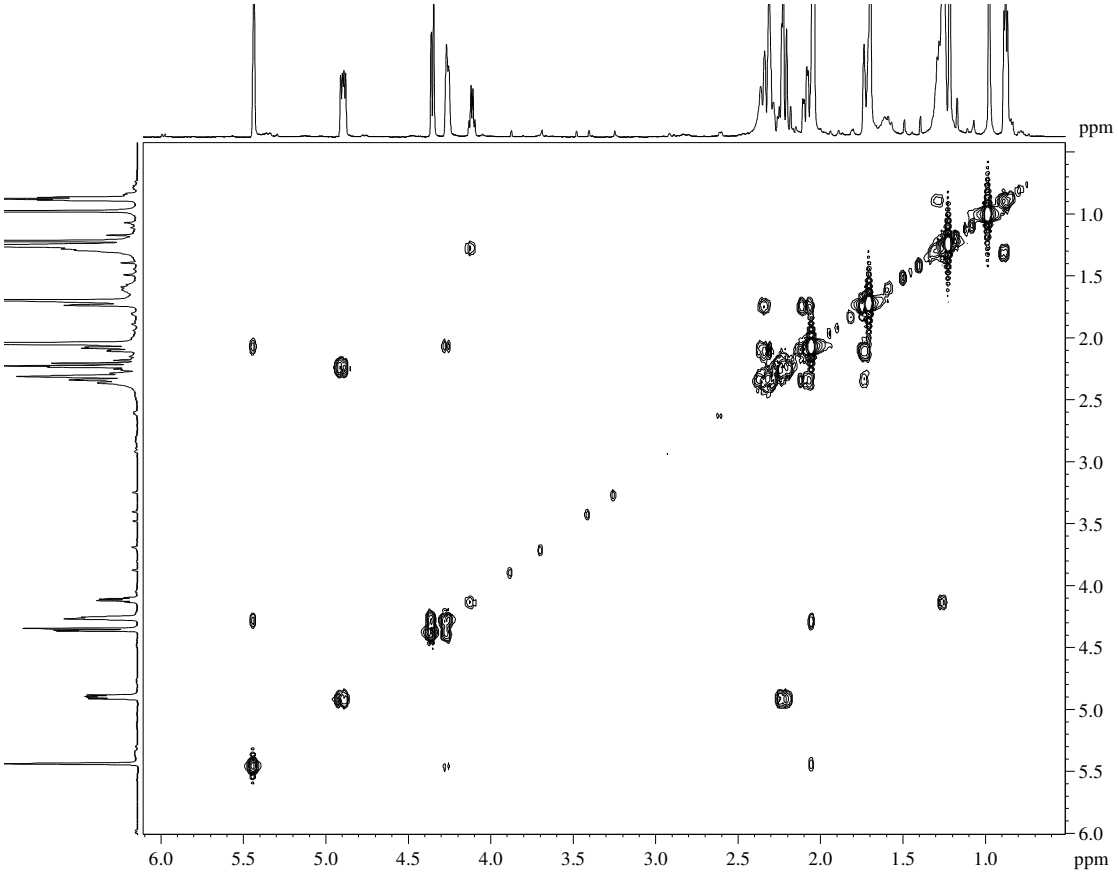

Figure S3.44 COSY NMR spectrum of compound **3.17**

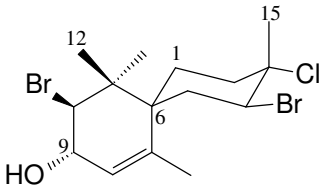

3.17

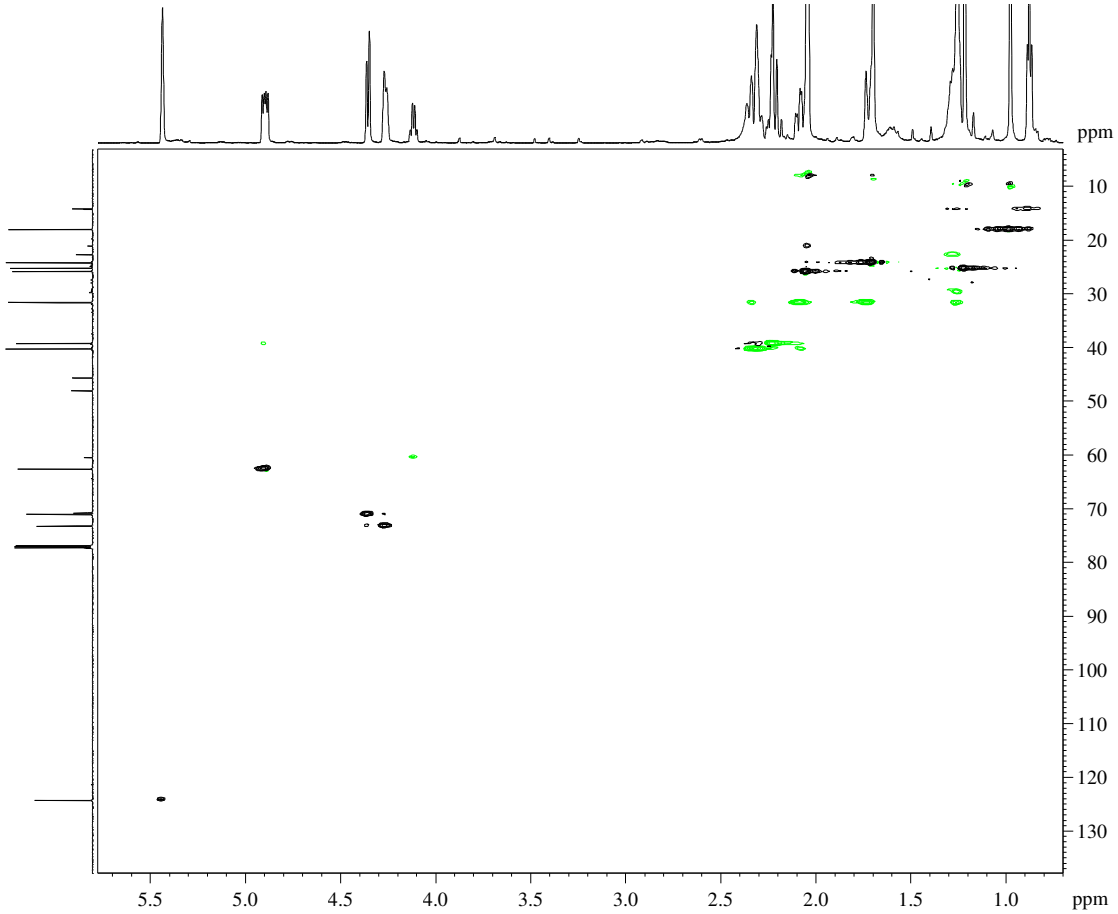

Figure S3.45 HSQC NMR spectrum of compound **3.17**

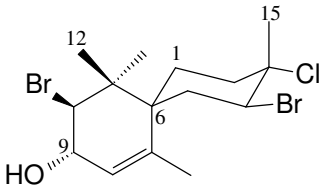

3.17

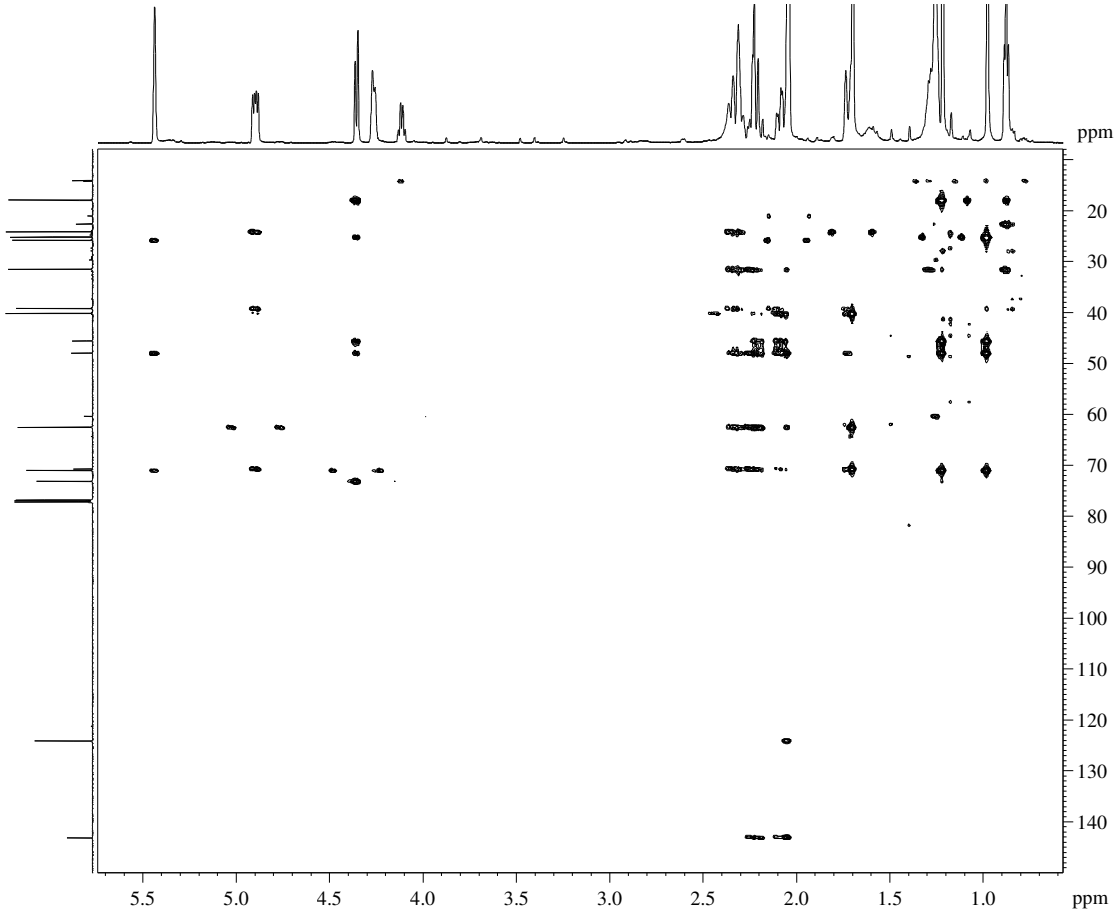

Figure S3.46 HMBC NMR spectrum of compound **3.17**

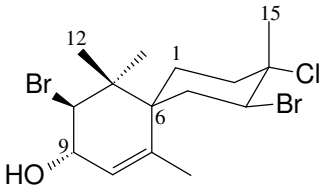

3.17

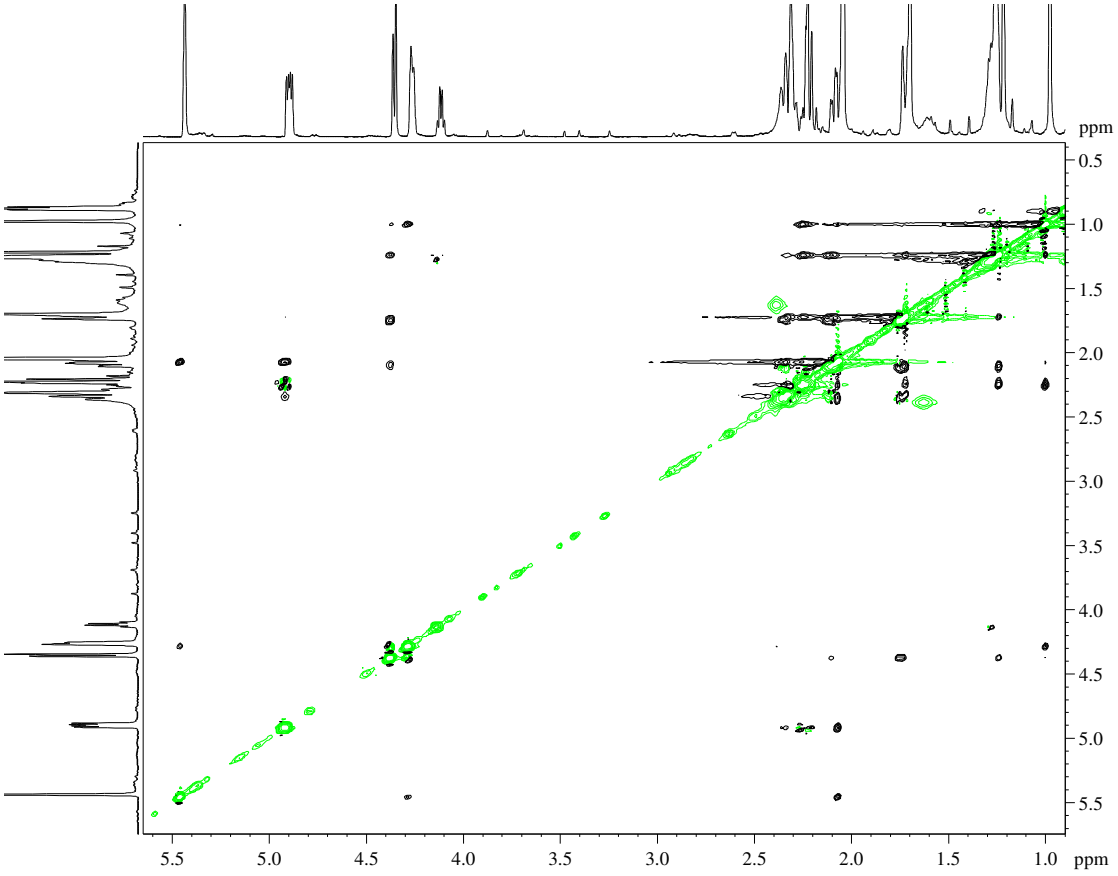

Figure S3.47 NOESY NMR spectrum of compound **3.17**

Chapter 4

Secondary metabolites from *Laurencia* cf. *corymbosa*

S4.1 Compound 4.1

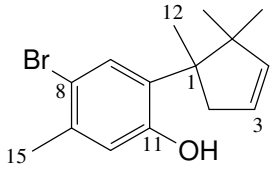

4.1

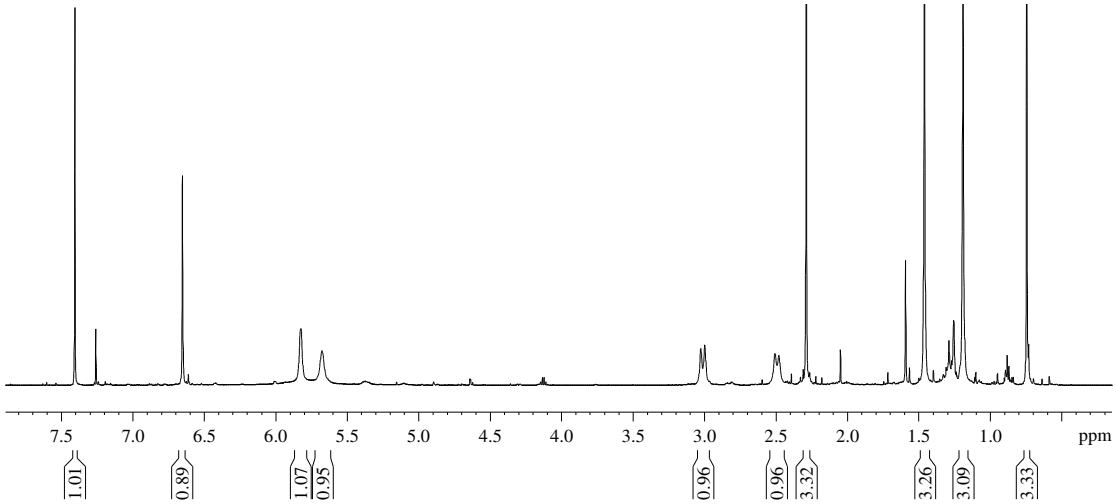

Figure S4.1 ^{1}H NMR spectrum ($CDCl_3$, 600 MHz) of compound **4.1**

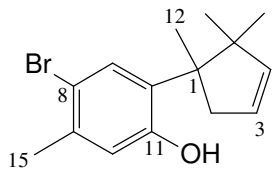

4.1

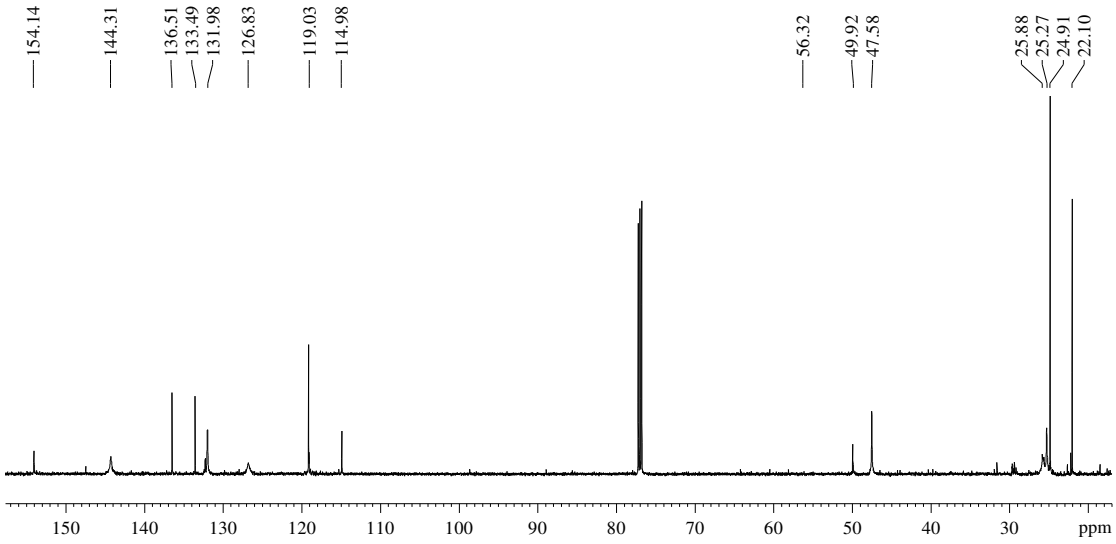

Figure S4.2 ^{13}C NMR spectrum ($CDCl_3$, 150 MHz) of compound **4.1**

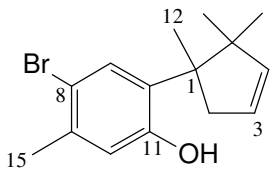

4.1

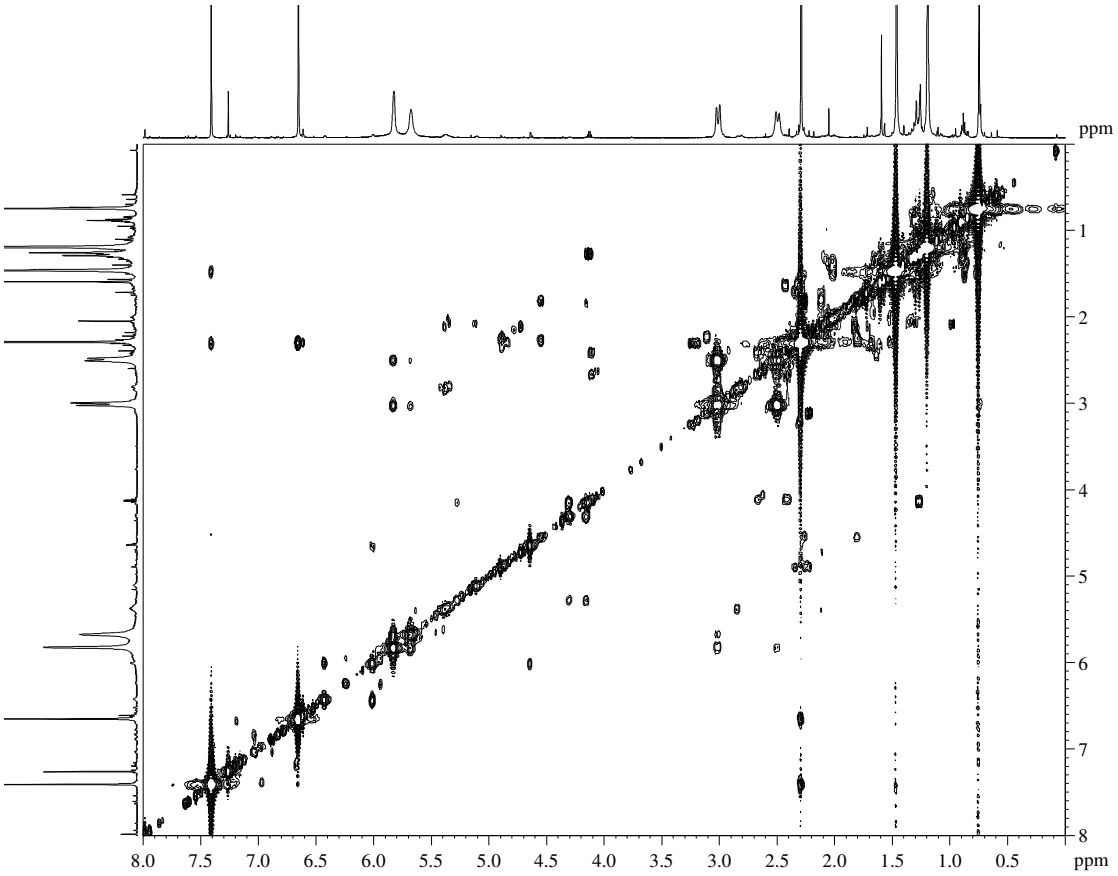

Figure S4.3 COSY NMR spectrum of compound **4.1**

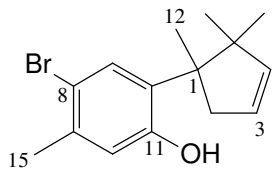

4.1

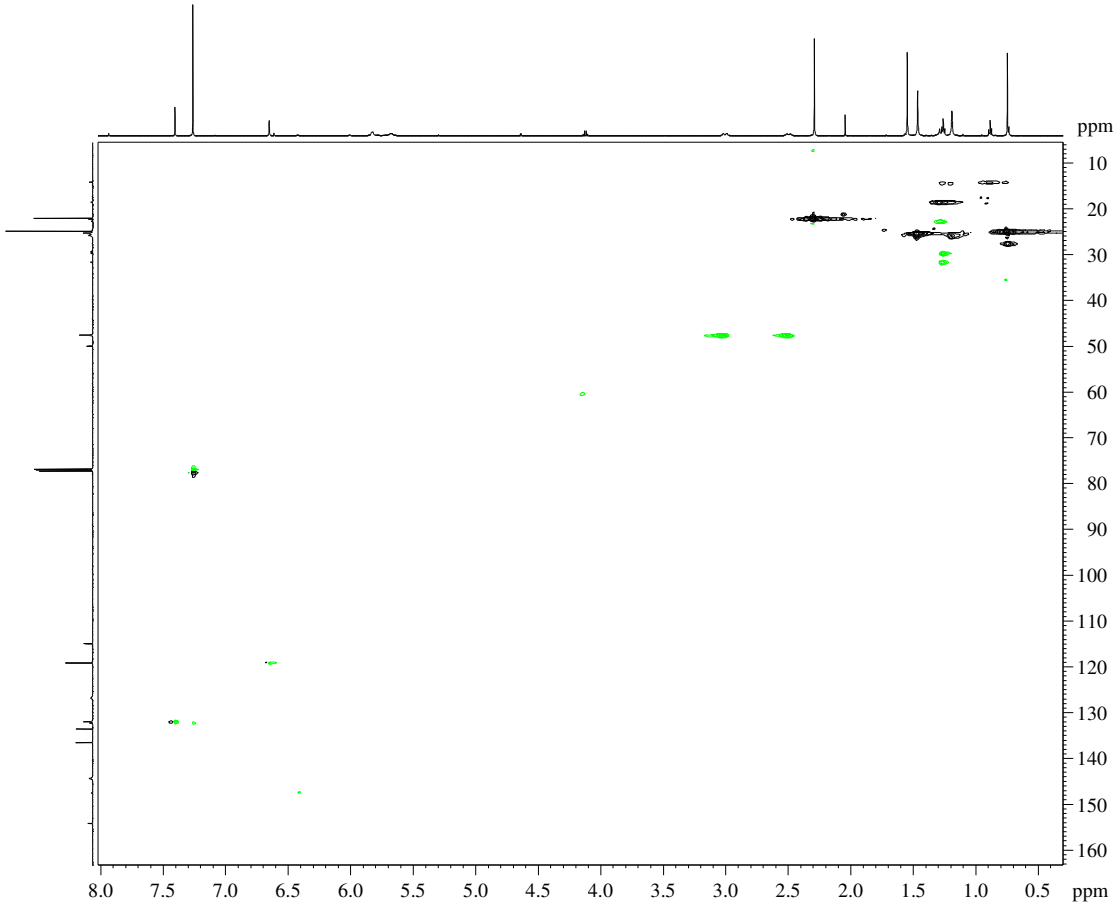

Figure S4.4 HSQC NMR spectrum of compound **4.1**

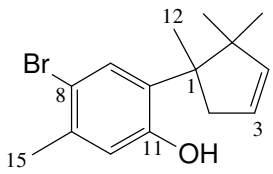

4.1

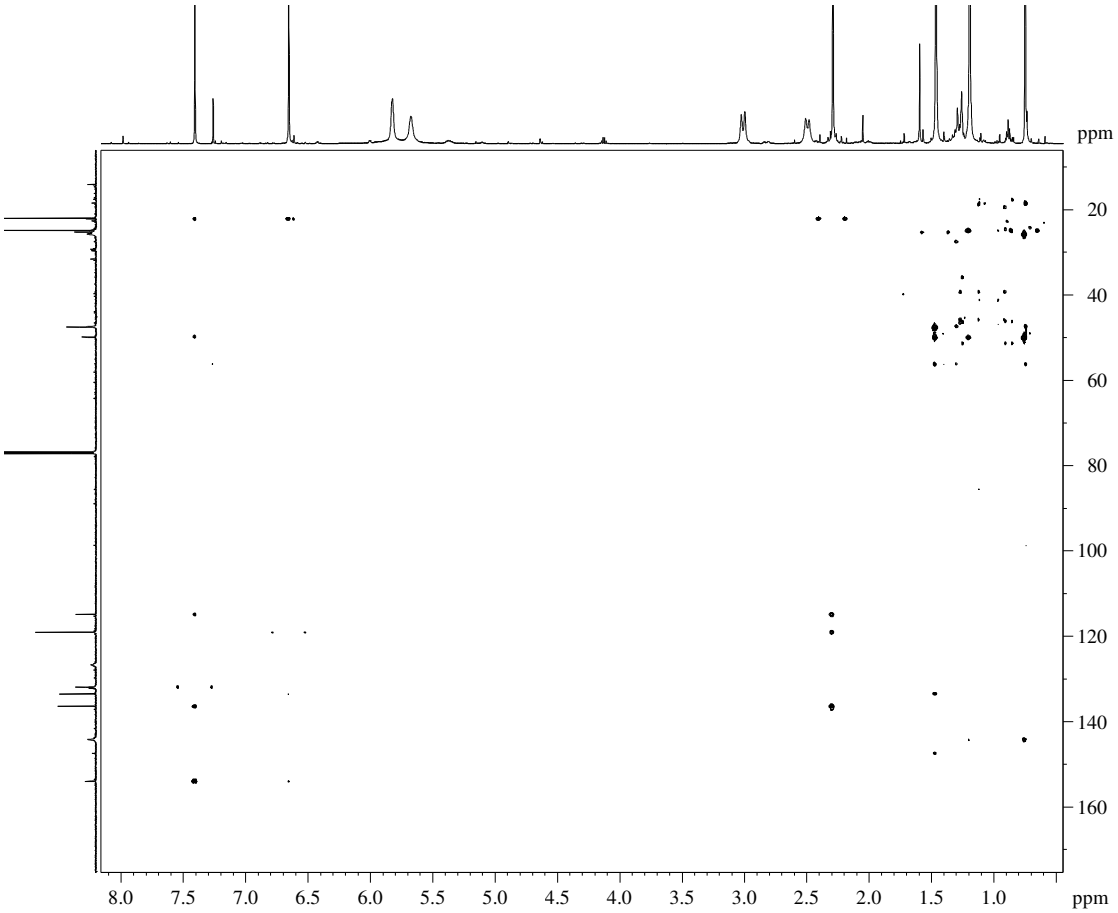

Figure S4.5 HMBC NMR spectrum of compound **4.1**

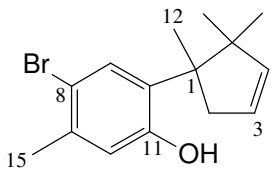

4.1

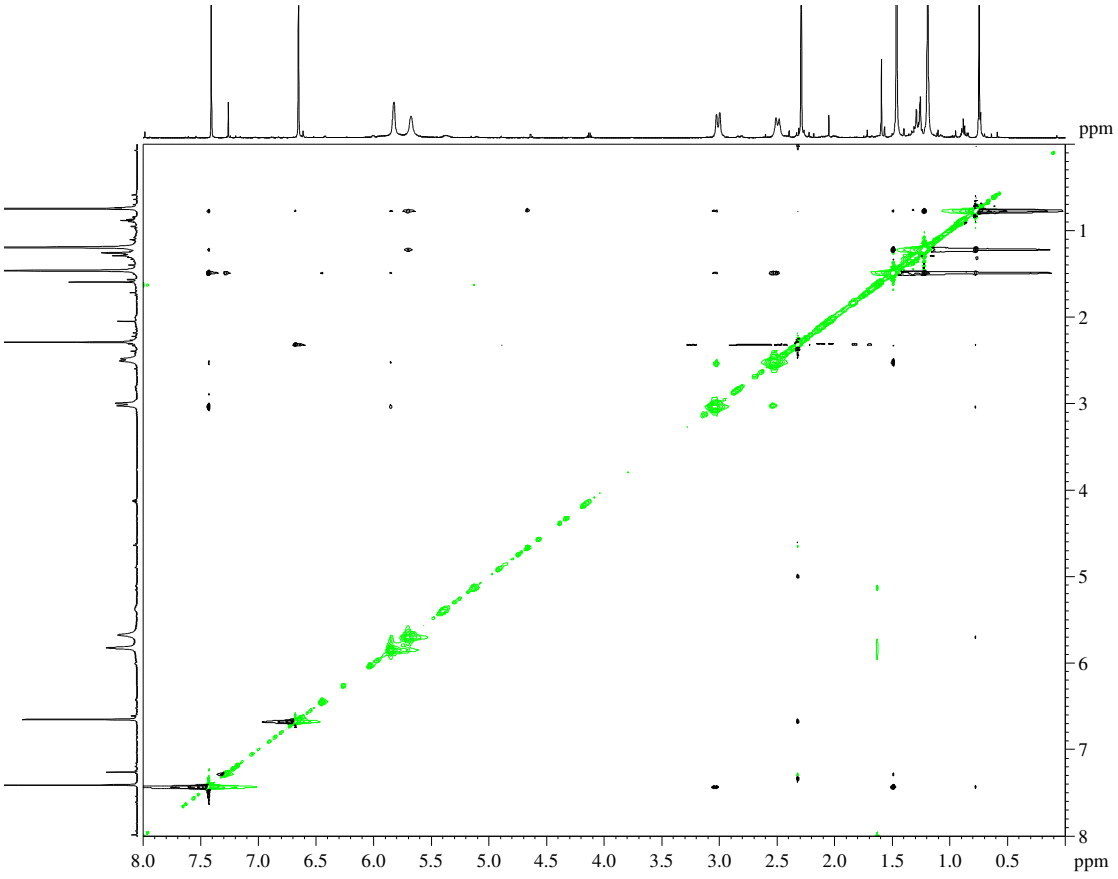

Figure S4.6 NOESY NMR spectrum of compound **4.1**

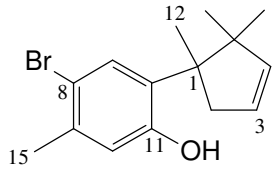

4.1

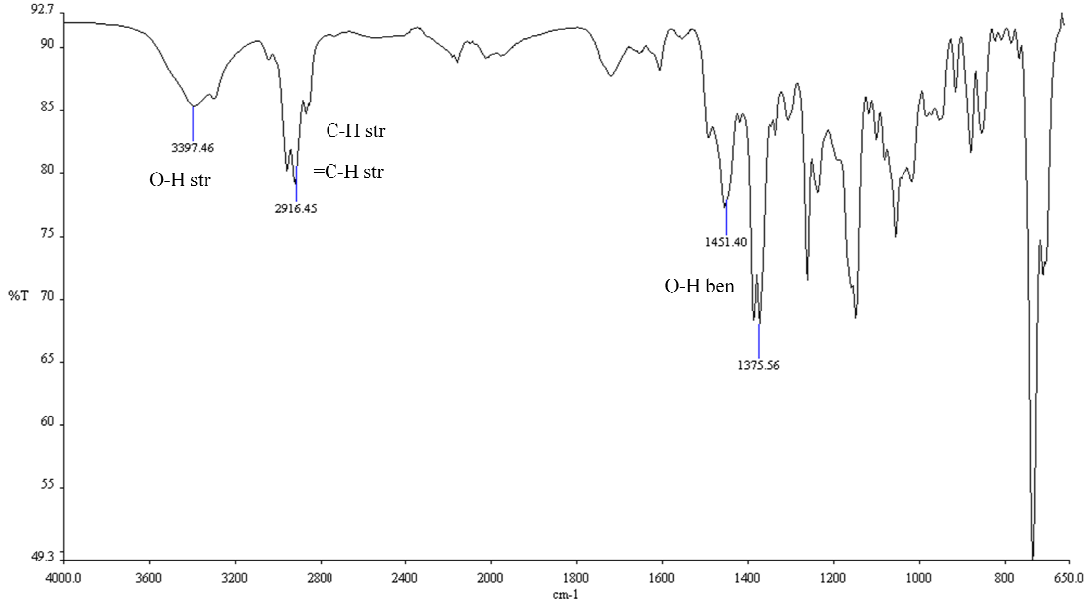

Figure S4.7 IR spectrum of compound **4.1**

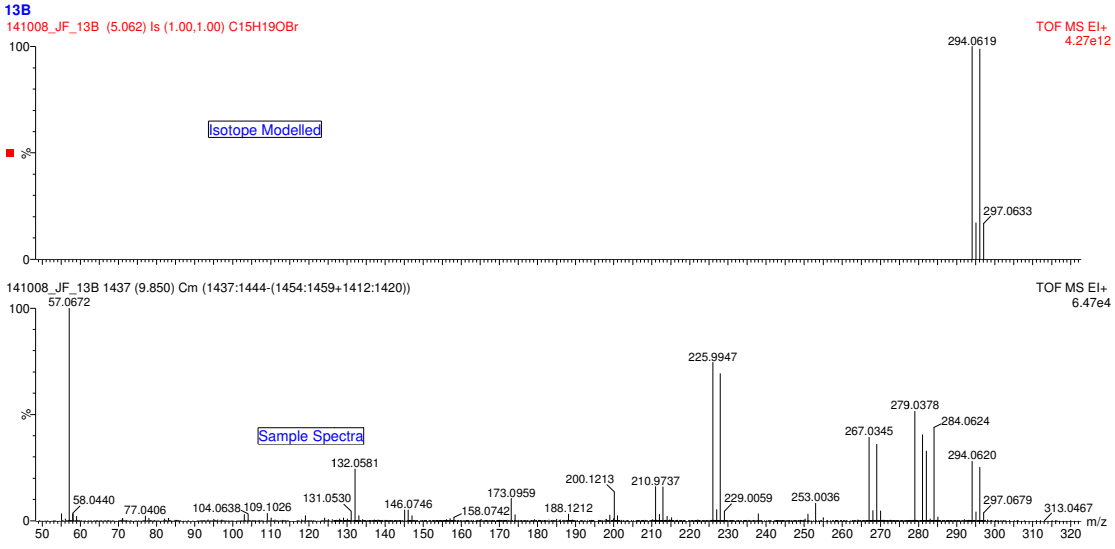

Figure S4.8 HREIMS spectrum of compound **4.1**

S4.2 Compound 4.3

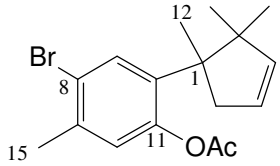

4.3

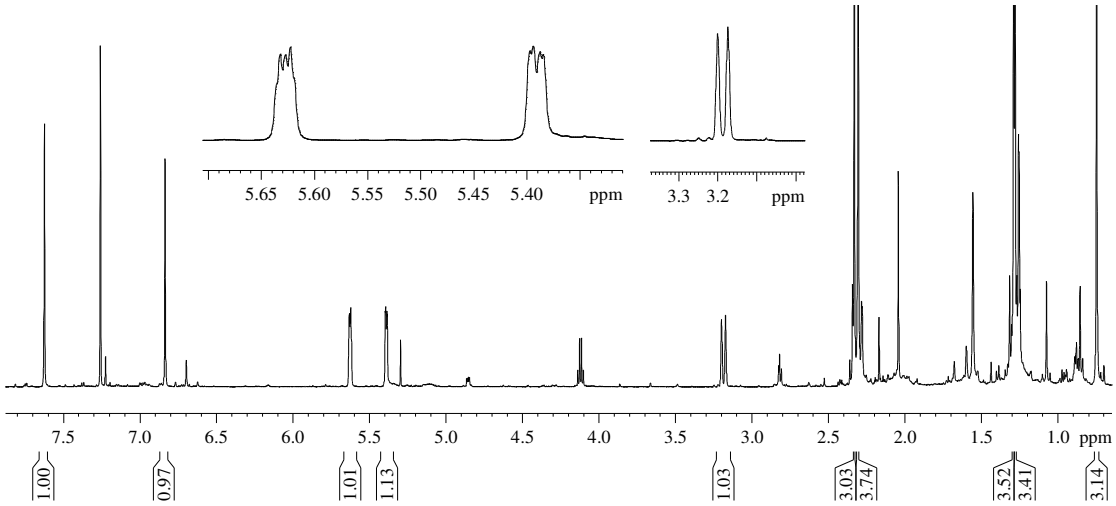

Figure S4.9 ^{1}H NMR spectrum ($CDCl_3$, 600 MHz) of compound **4.3**

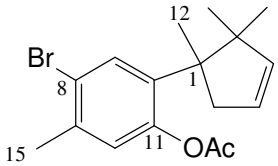

4.3

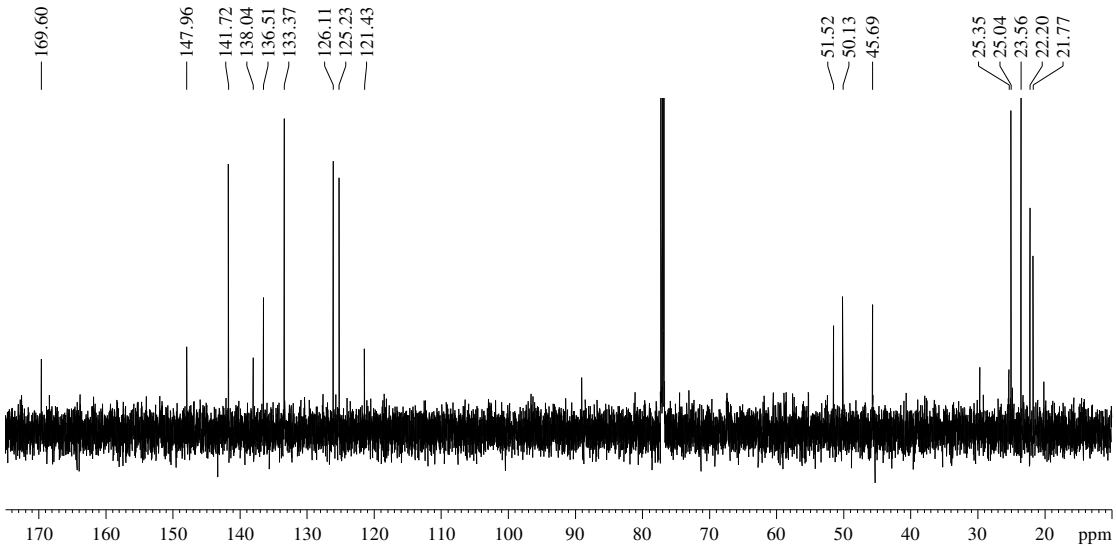

Figure S4.10 ^{13}C NMR spectrum ($CDCl_3$, 150 MHz) of compound **4.3**

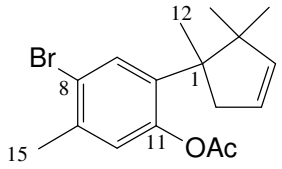

4.3

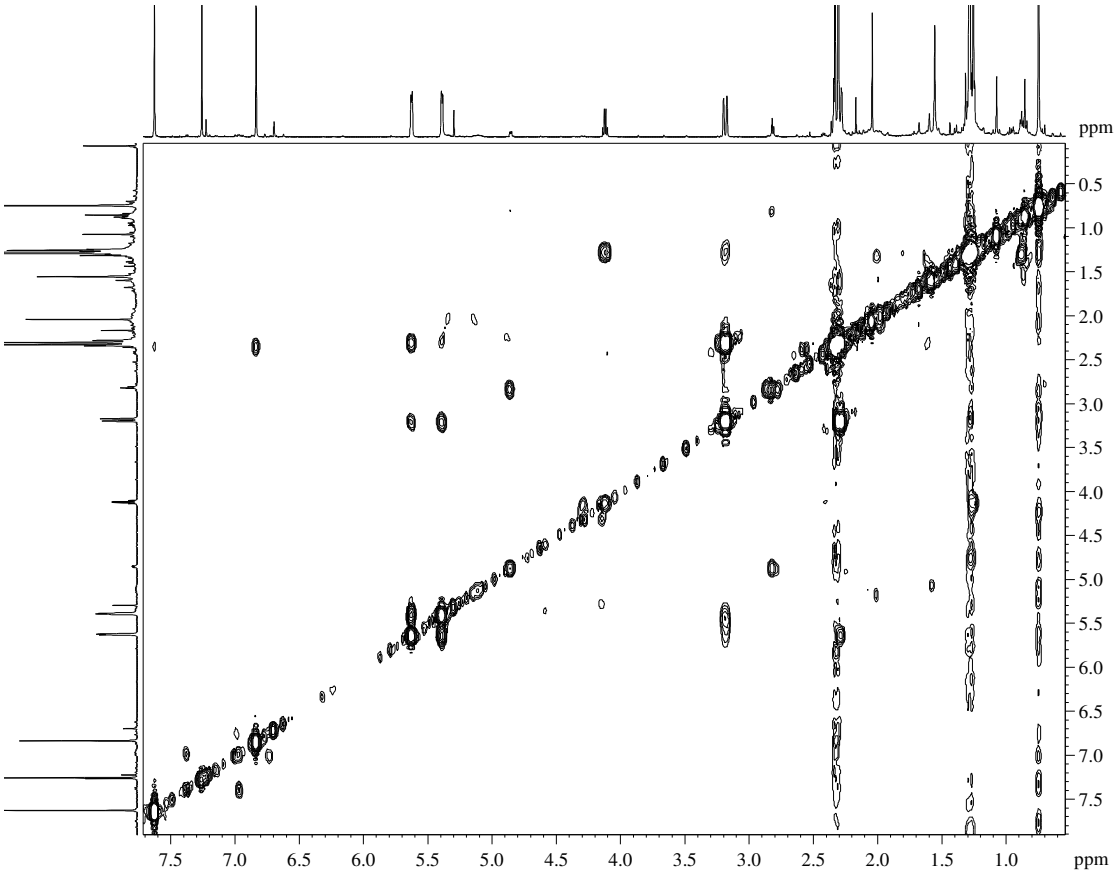

Figure S4.11 COSY NMR spectrum of compound **4.3**

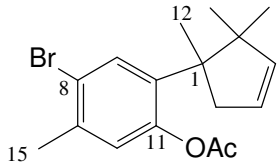

4.3

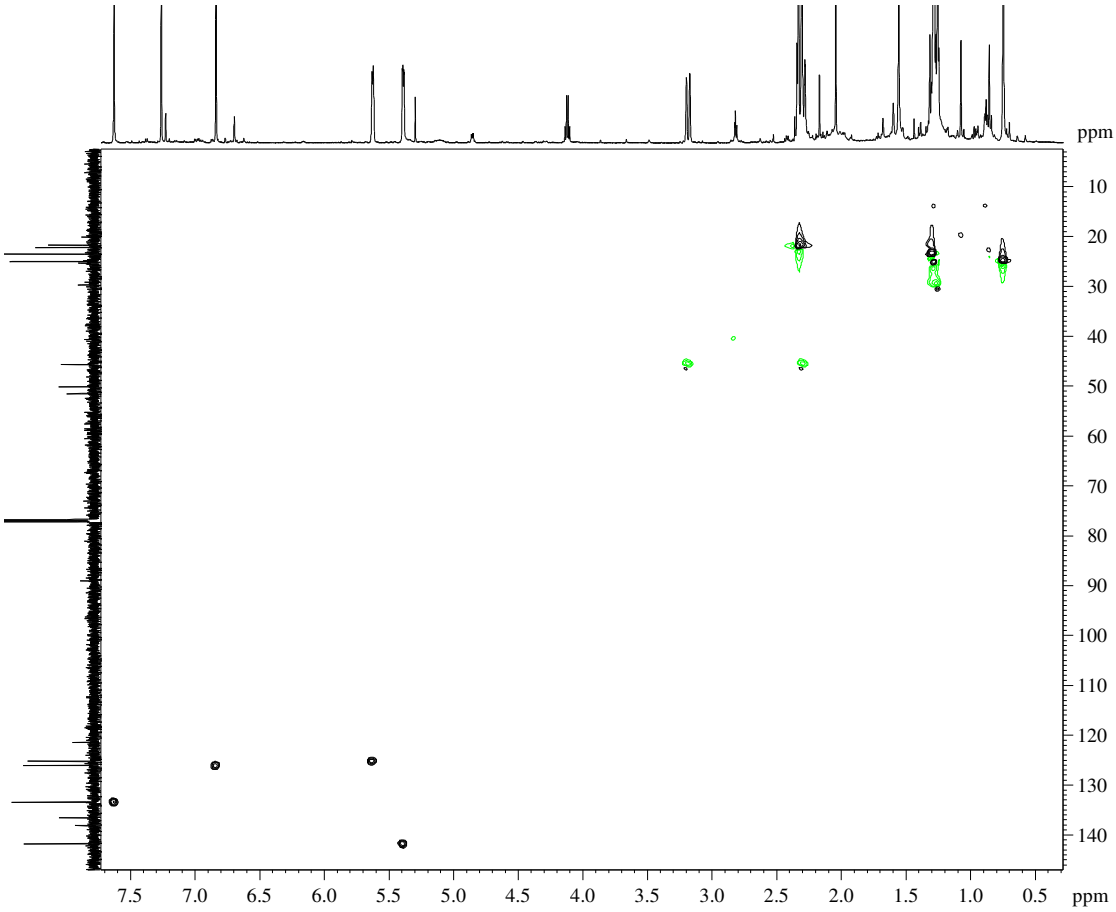

Figure S4.12 HSQC NMR spectrum of compound **4.3**

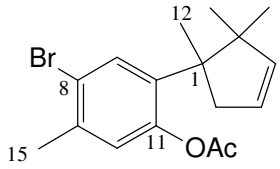

4.3

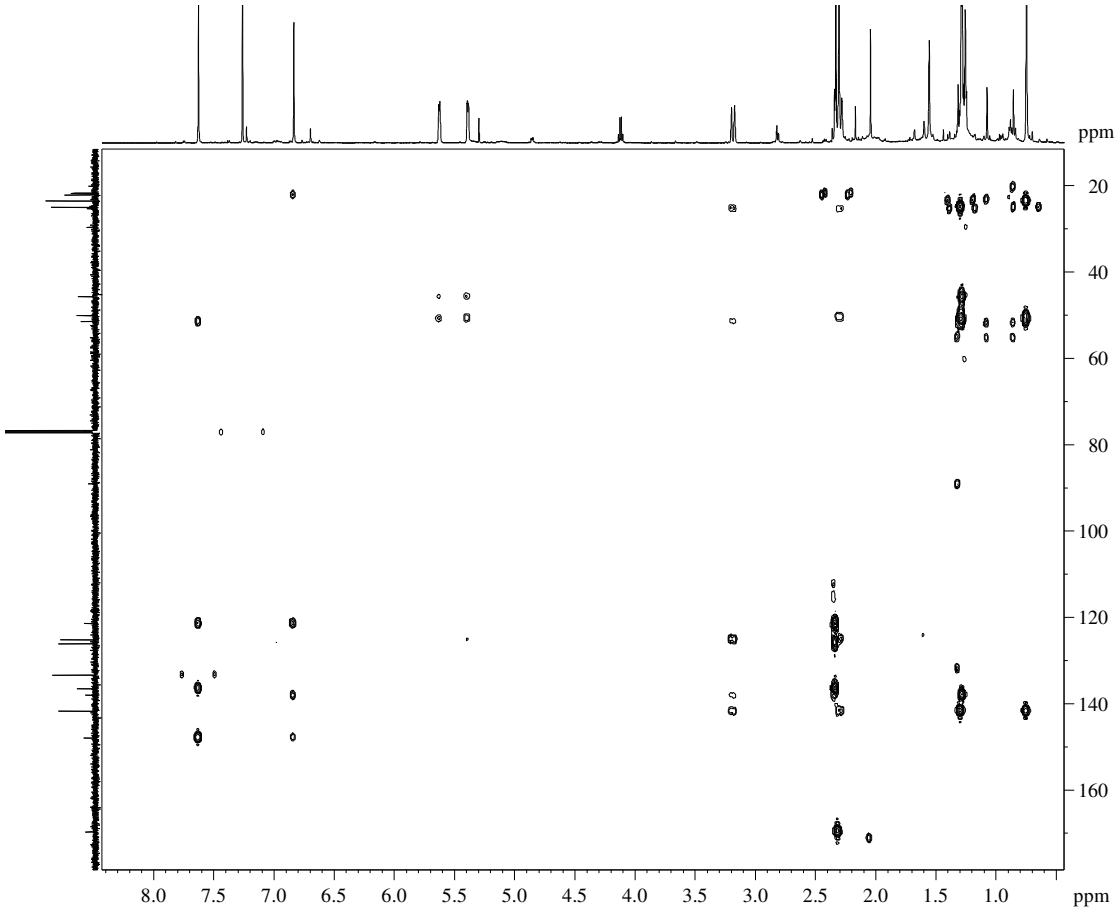

Figure S4.13 HMBC NMR spectrum of compound **4.3**

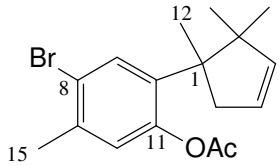

4.3

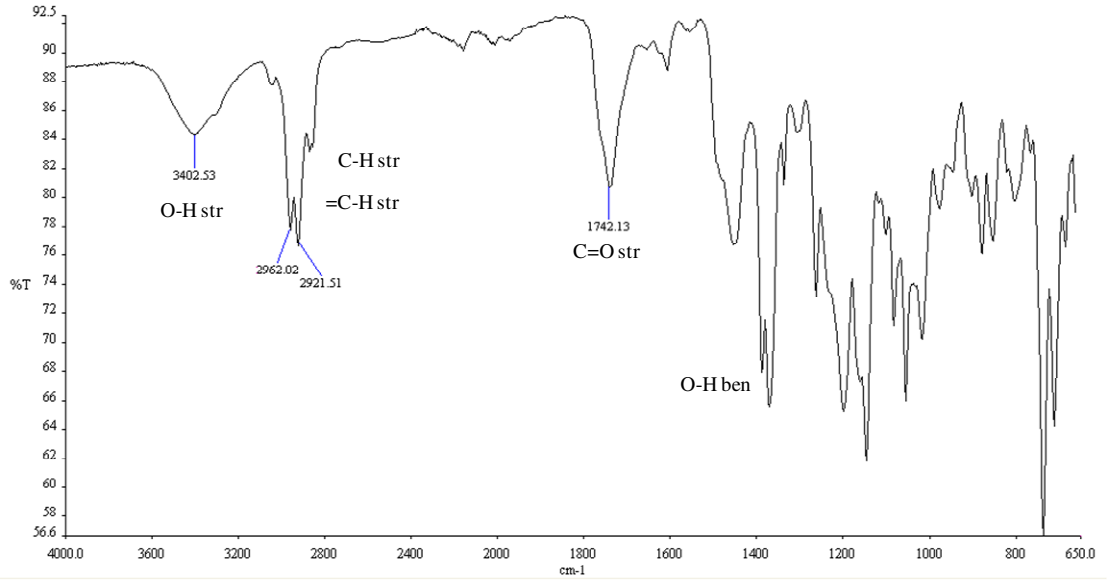

Figure S4.14 IR spectrum of compound **4.3**

Infra red showed the emergence of a carbonyl stretch confirming acetyl substitution however OH stretches still present possibly due to unreacted material

S4.3 Compound 4.4

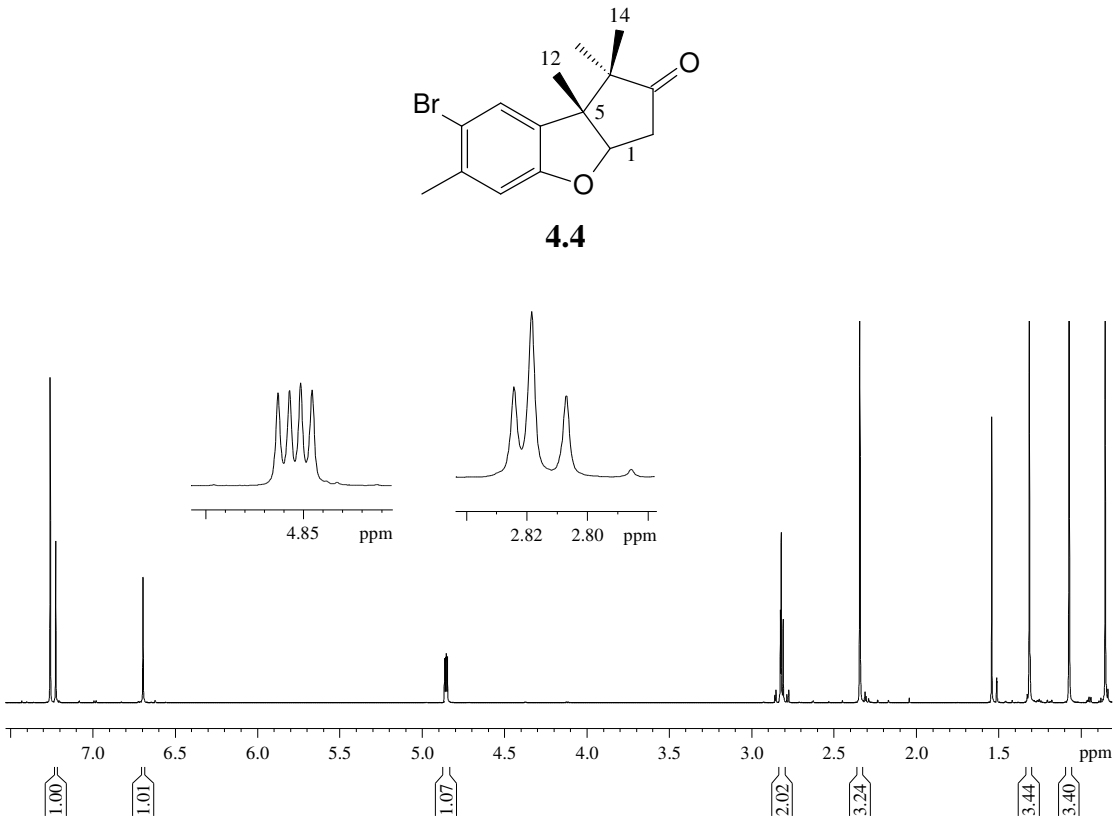

4.4

Figure S4.15 ^{1}H NMR spectrum ($CDCl_3$, 600 MHz) of compound **4.4**

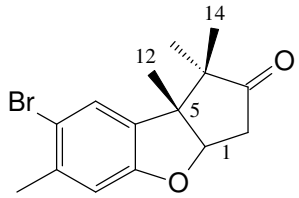

4.4

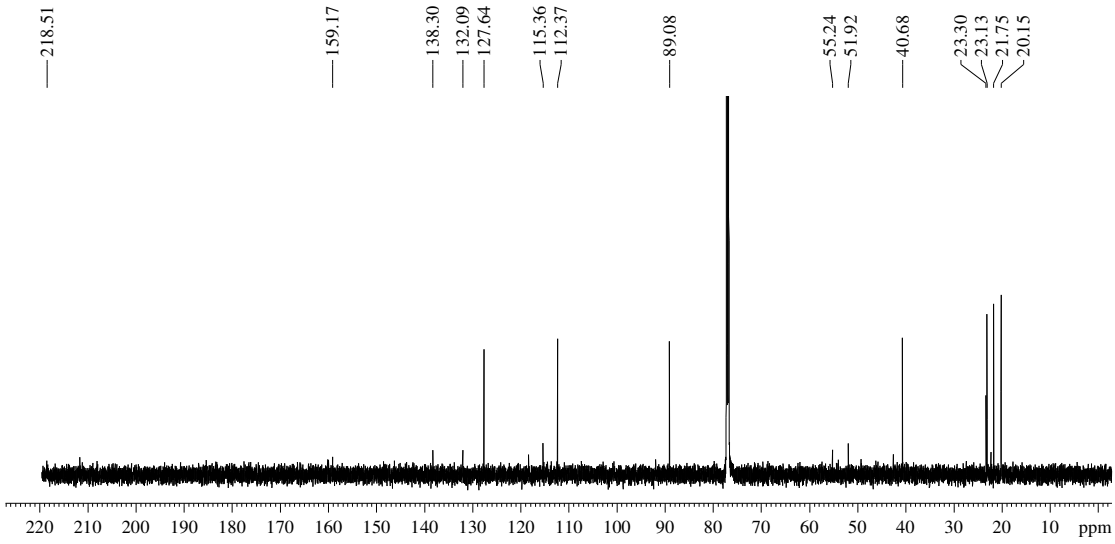

Figure S4.16 ^{13}C NMR spectrum ($CDCl_3$, 150 MHz) of compound **4.4**

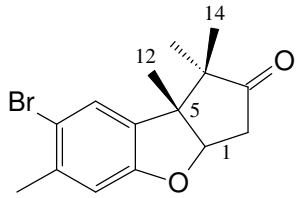

4.4

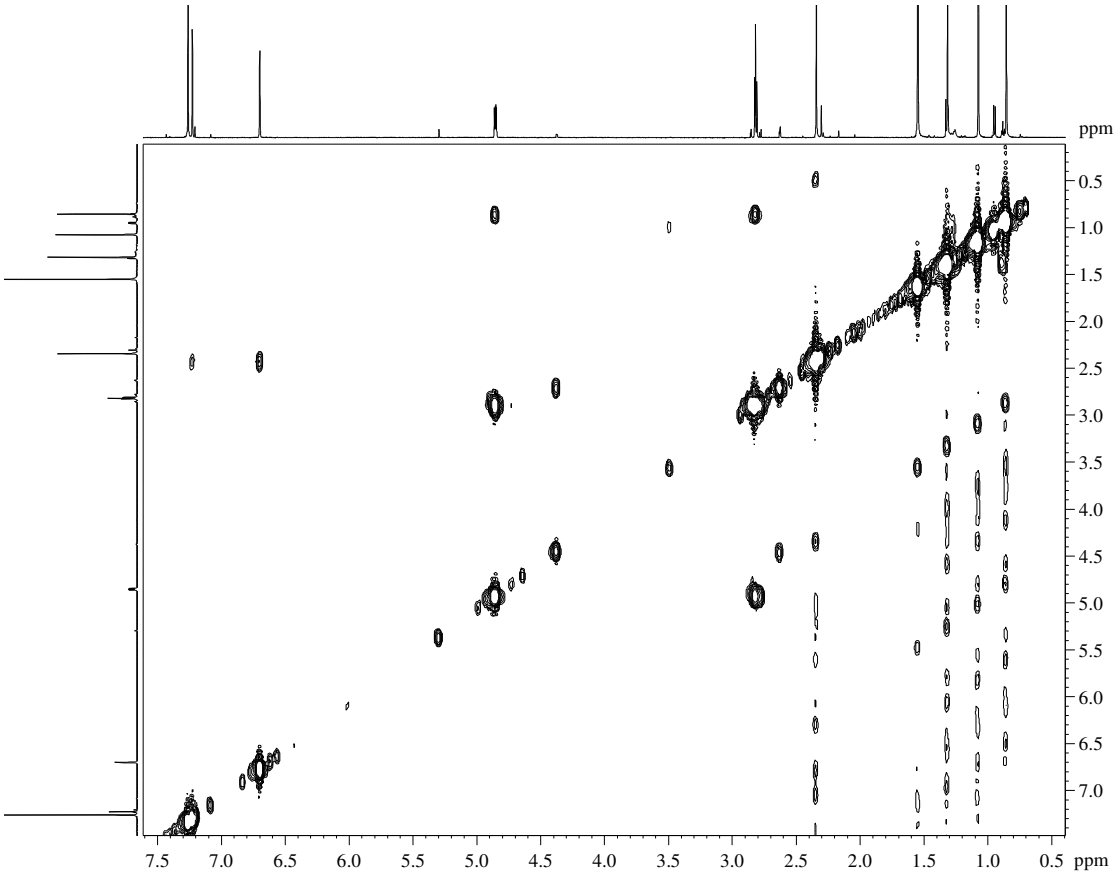

Figure S4.17 COSY NMR spectrum of compound **4.4**

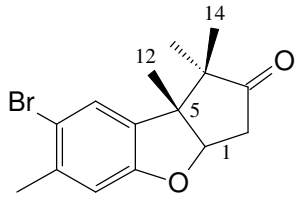

4.4

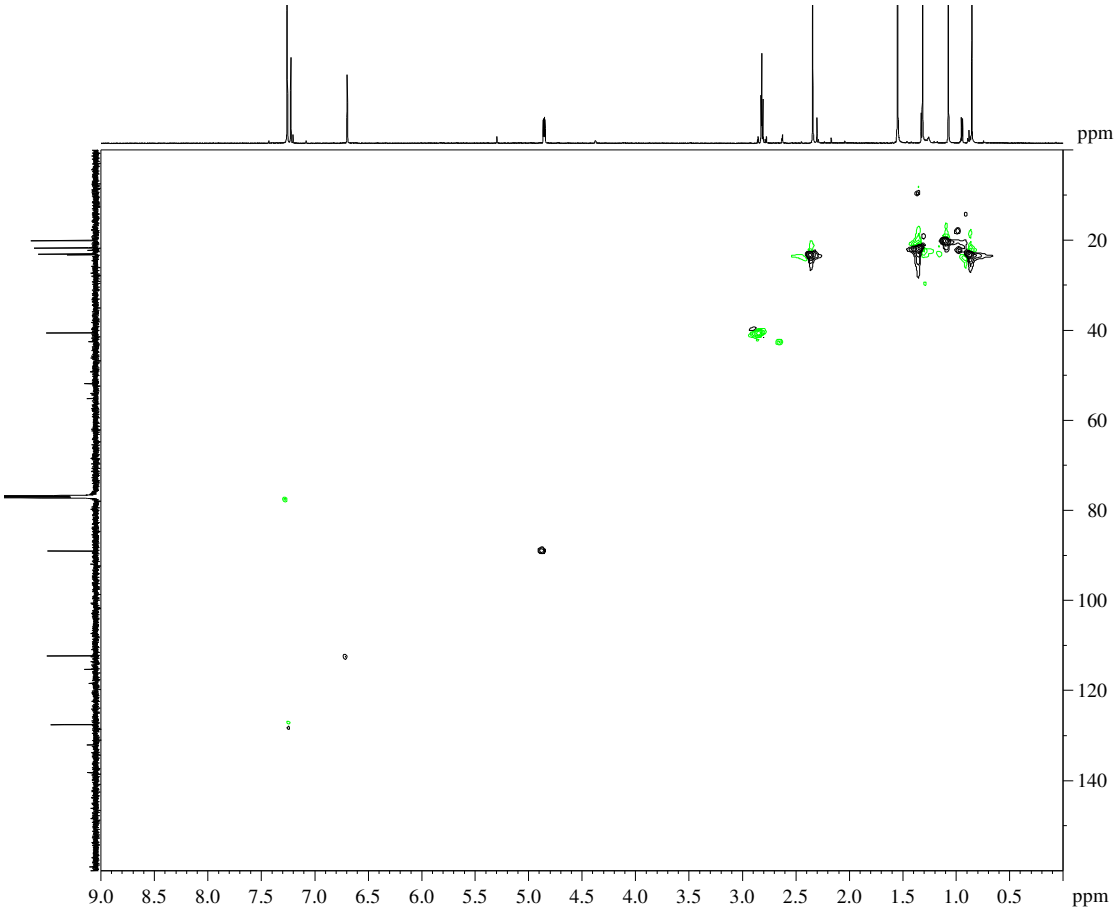

Figure S4.18 HSQC NMR spectrum of compound **4.4**

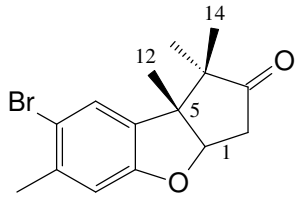

4.4

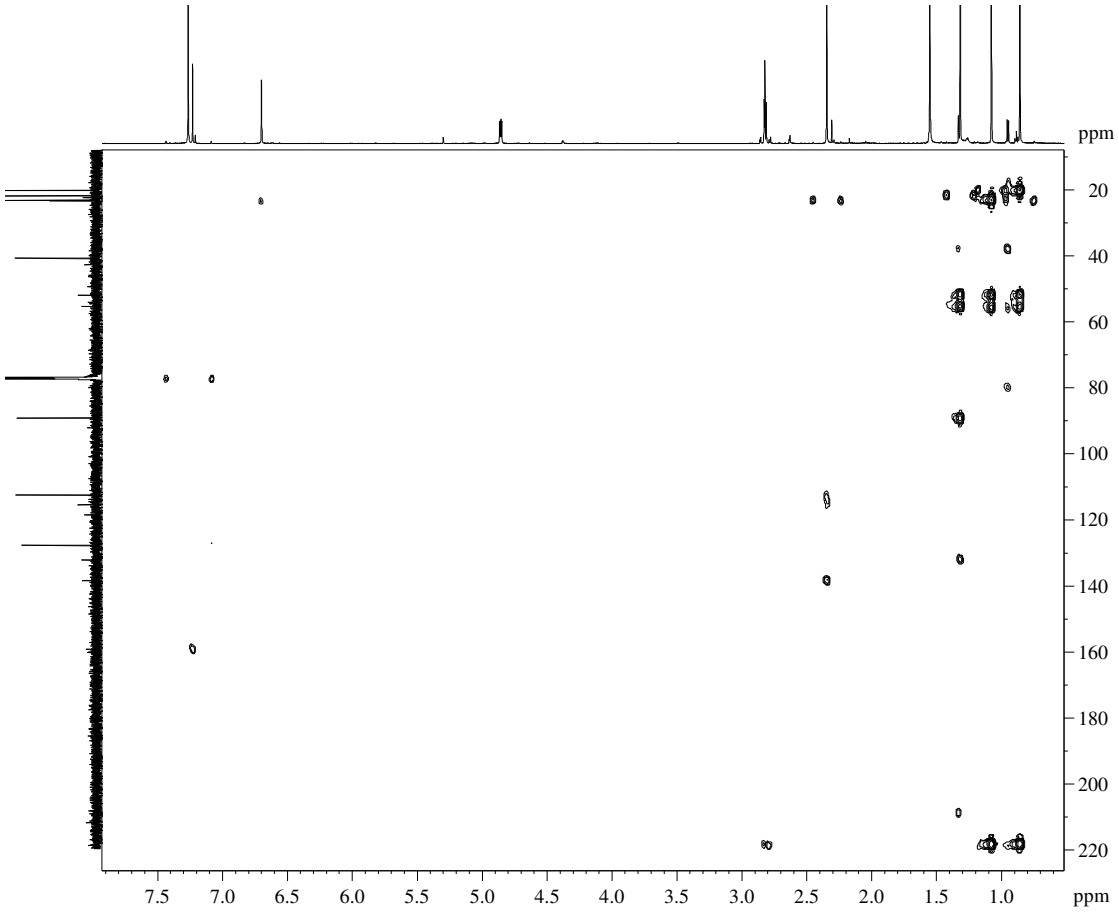

Figure S4.19 HMBC NMR spectrum of compound **4.4**

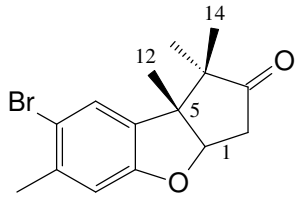

4.4

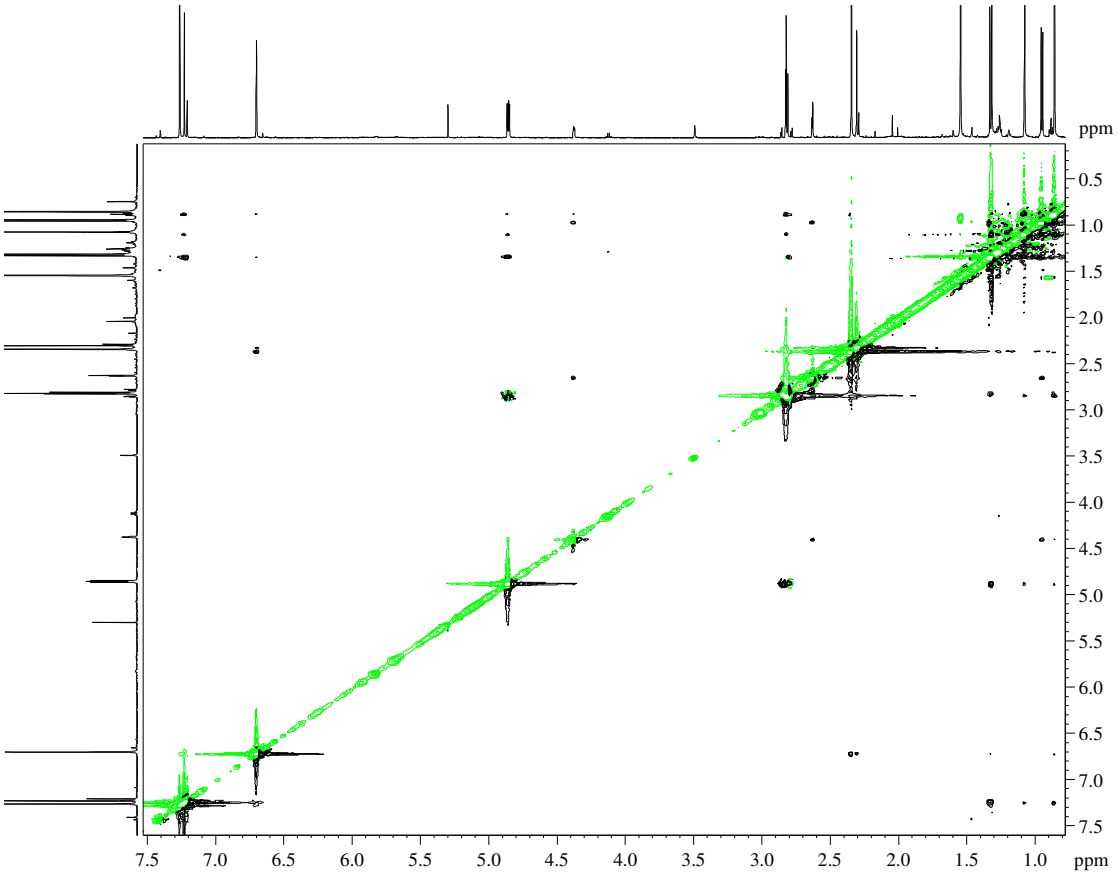

Figure S4.20 NOESY NMR spectrum of compound **4.4**

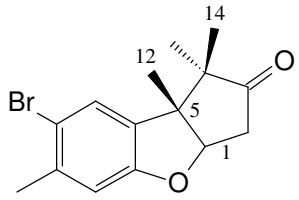

4.4

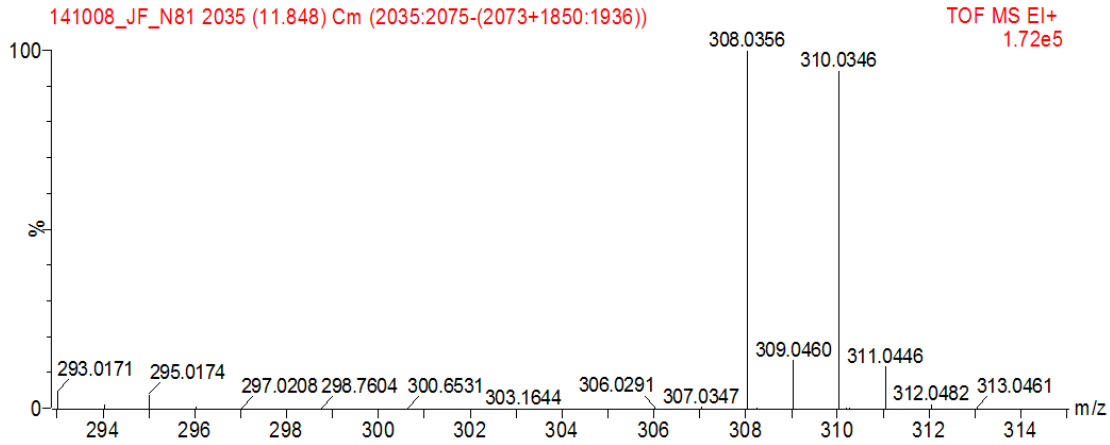

Figure S4.21 HRGCEIMS spectrum of compound **4.4**

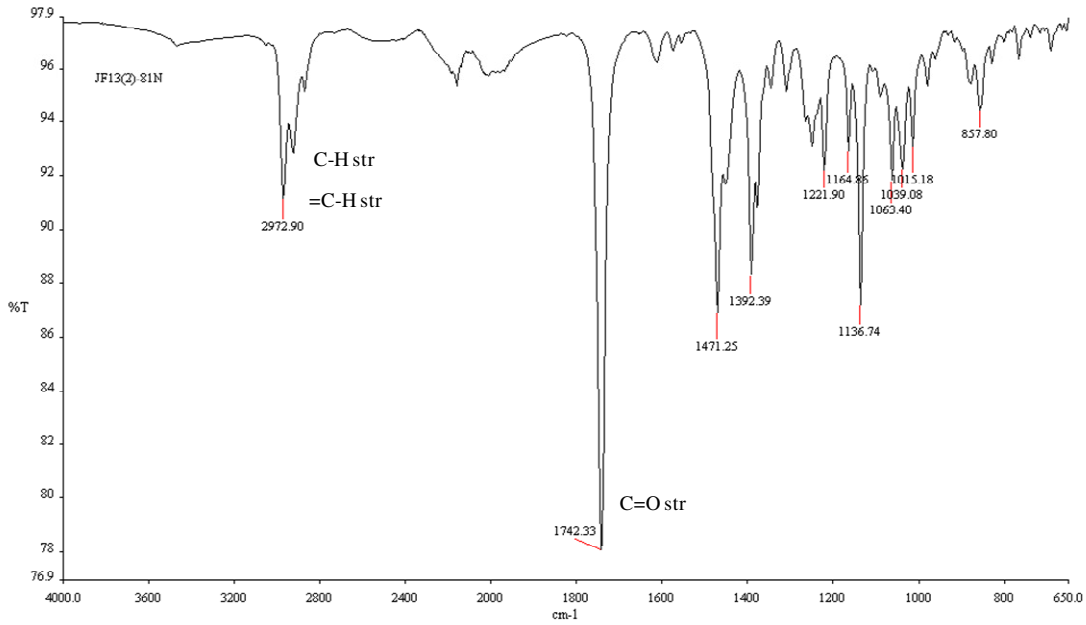

Figure S4.22 IR spectrum of compound **4.4**

S4.4 Compound 4.5

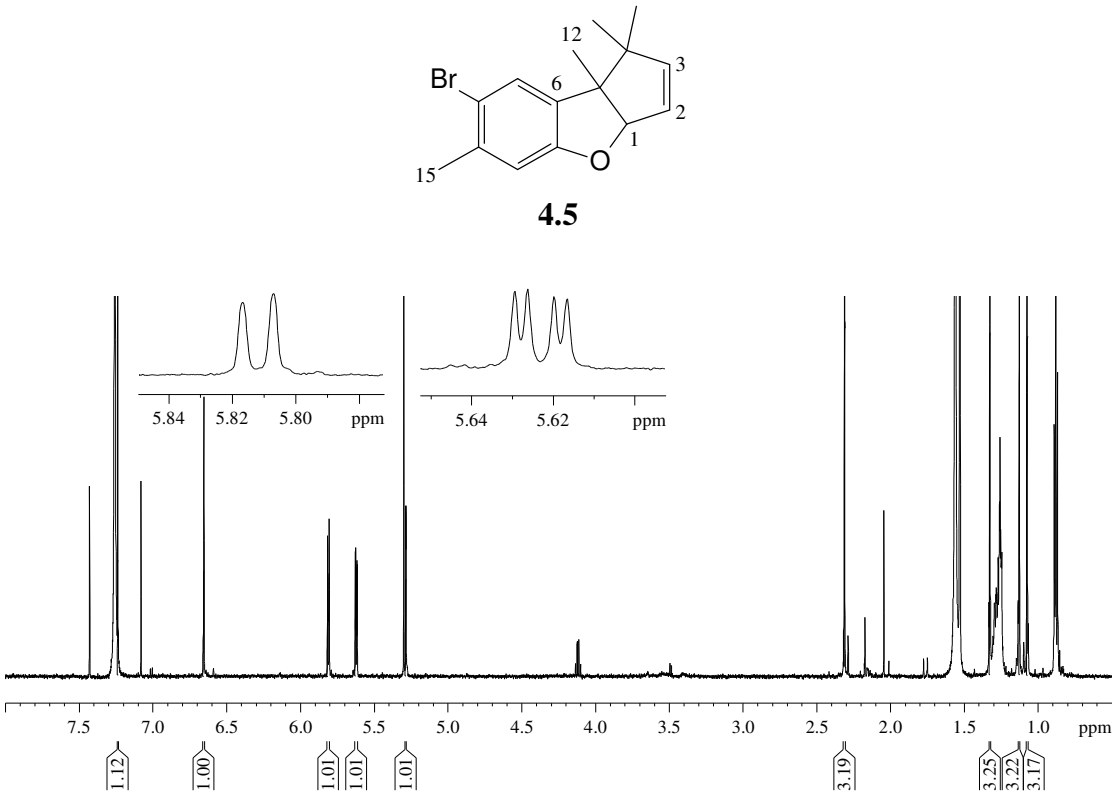

Figure S4.23 ^{1}H NMR spectrum ($CDCl_3$, 600 MHz) of compound **4.5**

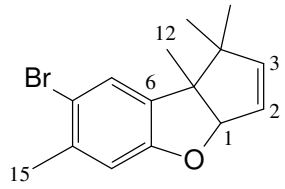

4.5

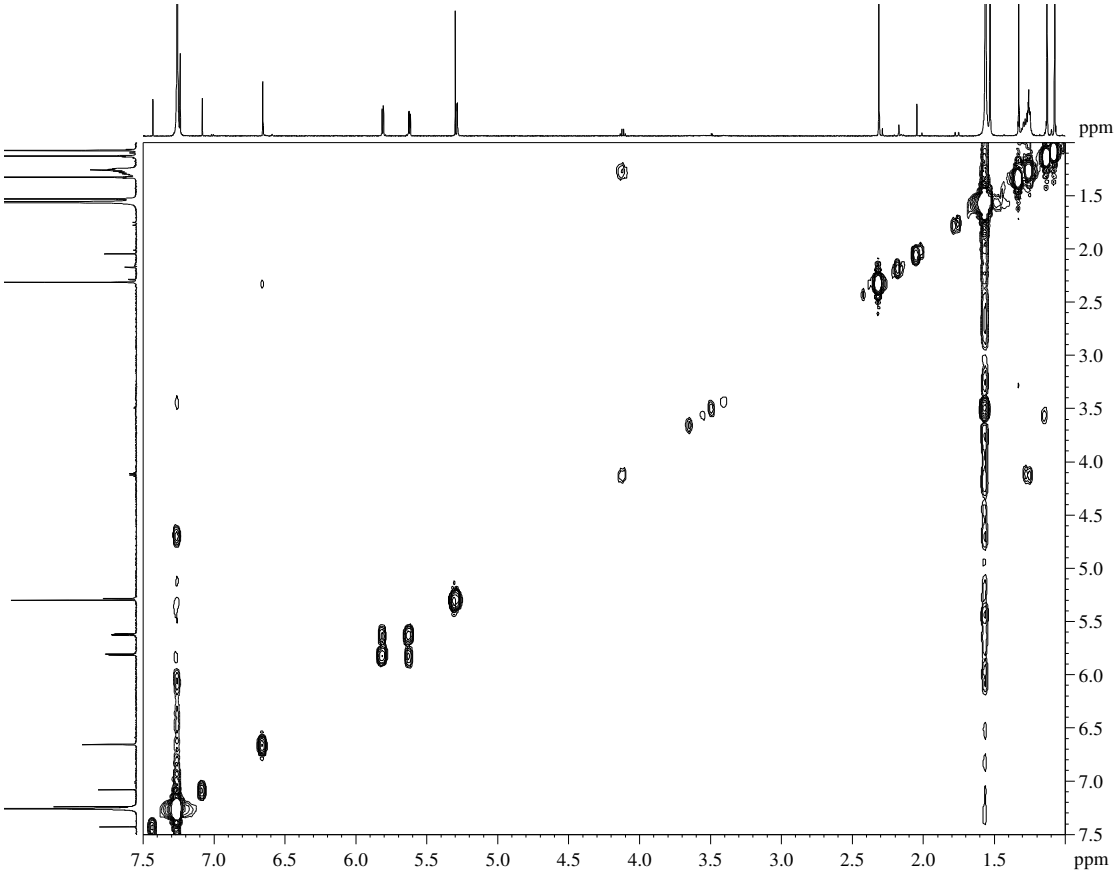

Figure S4.24 COSY NMR spectrum of compound **4.5**

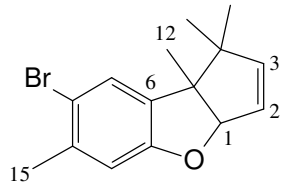

4.5

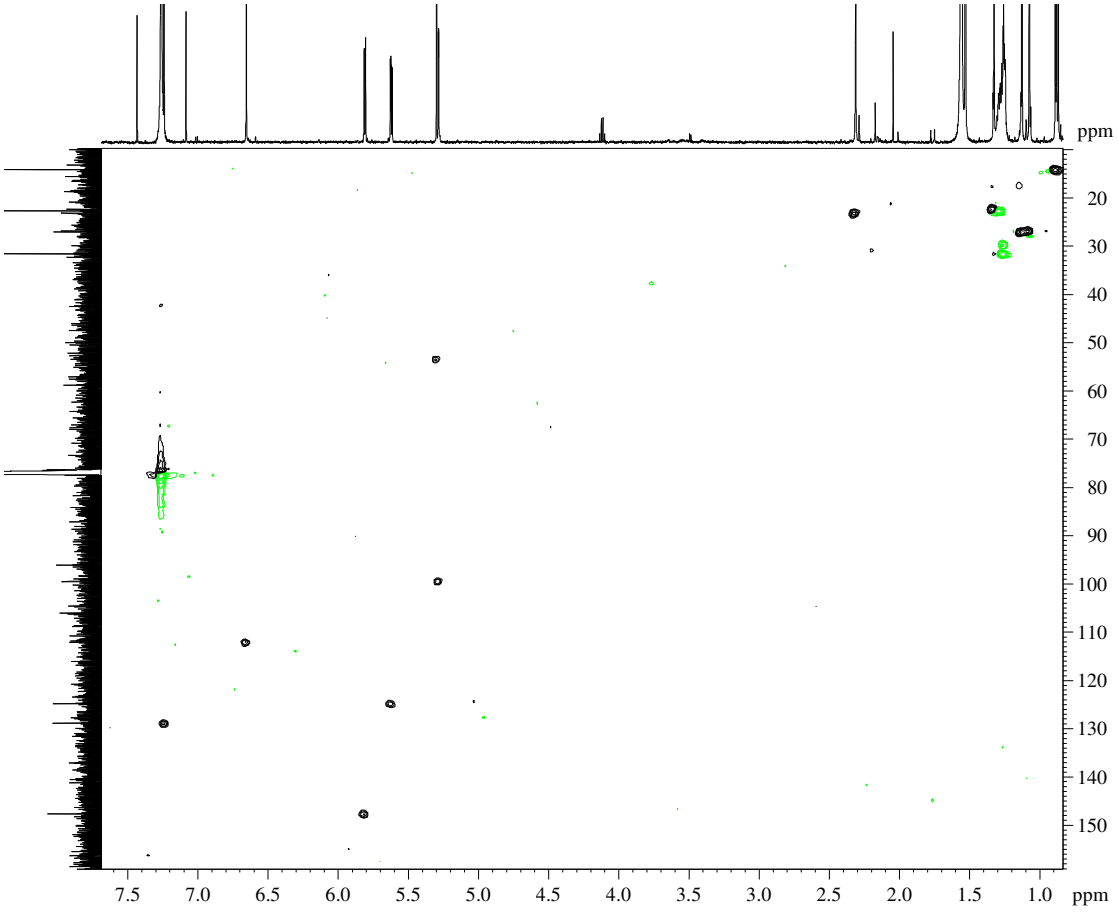

Figure S4.25 HSQC NMR spectrum of compound **4.5**

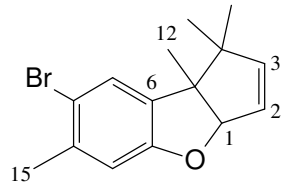

4.5

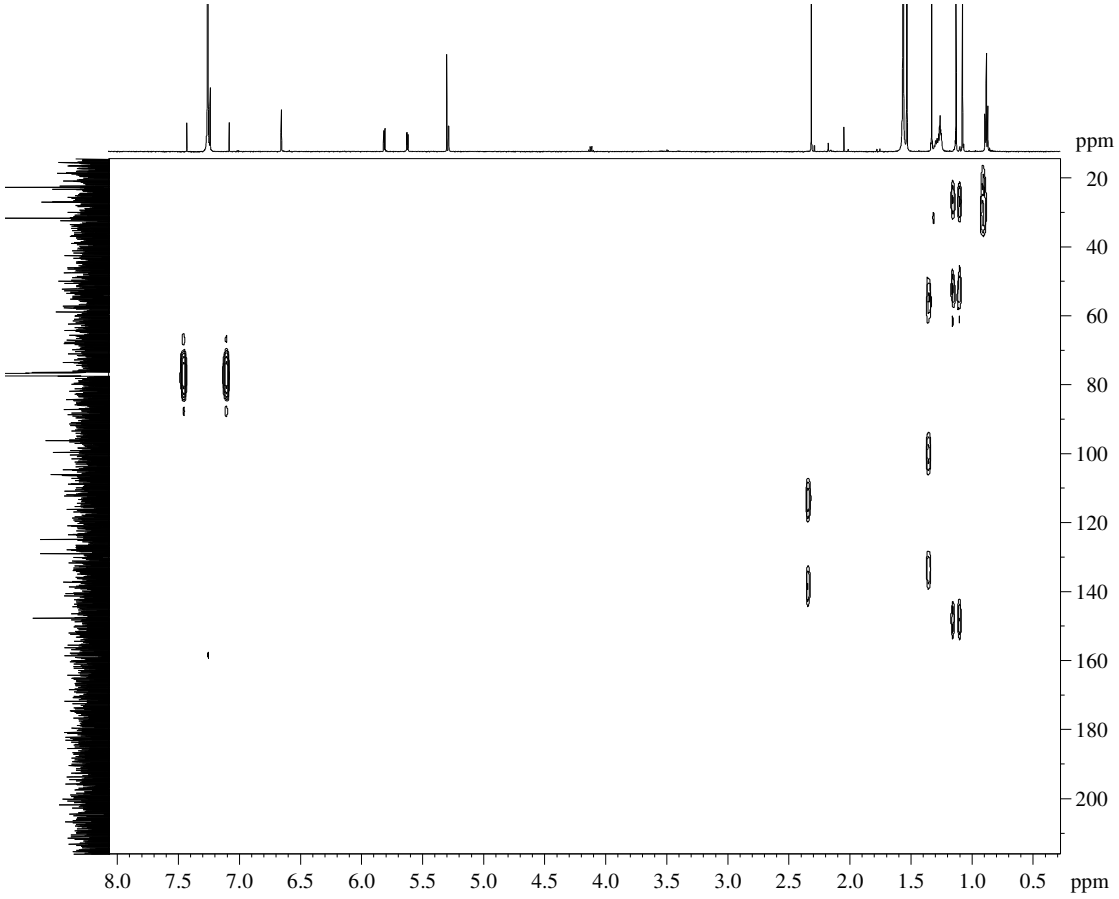

Figure S4.26 HMBC NMR spectrum of compound **4.5**

S4.5 Compound 4.6

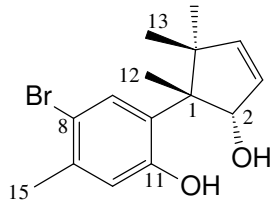

4.6

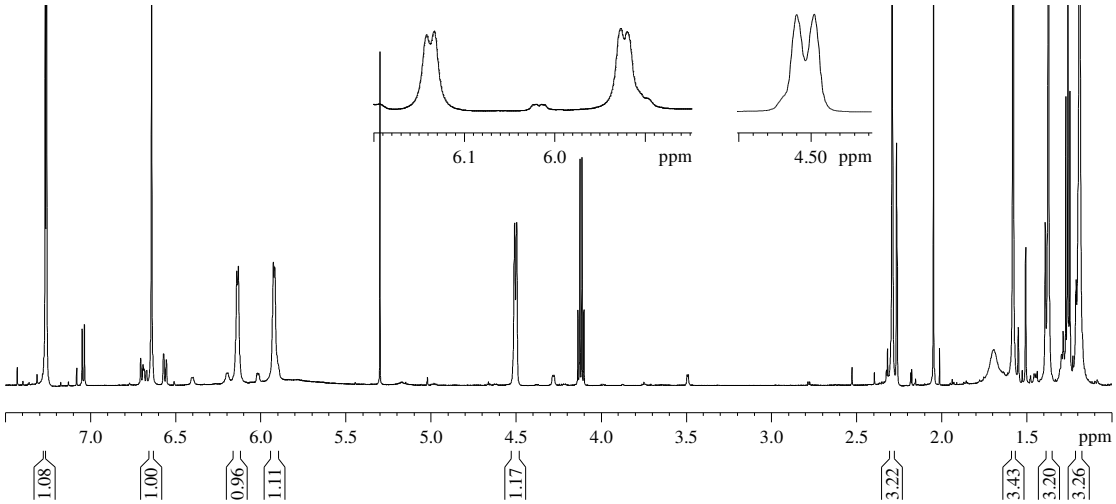

Figure S4.27 ^{1}H NMR spectrum ($CDCl_3$, 600 MHz) of compound **4.6**

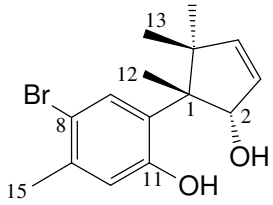

4.6

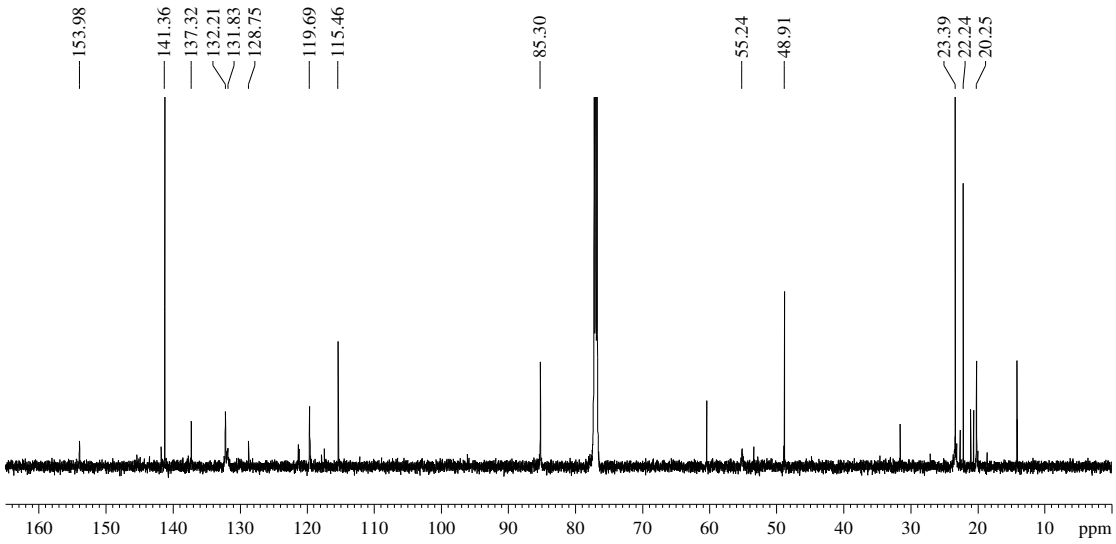

Figure S4.28 ^{13}C NMR spectrum ($CDCl_3$, 150 MHz) of compound **4.6**

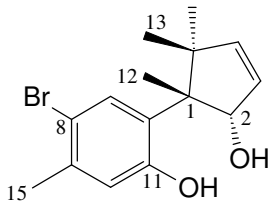

4.6

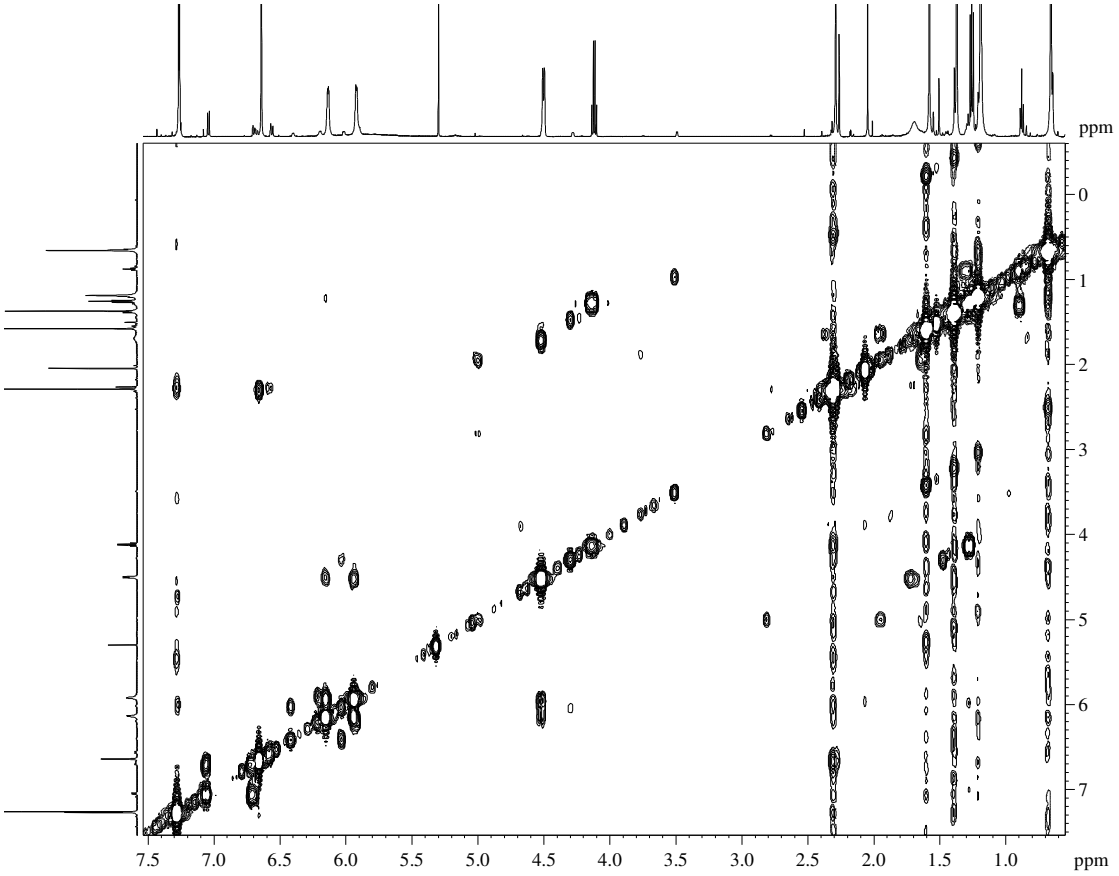

Figure S4.29 COSY NMR spectrum of compound **4.6**

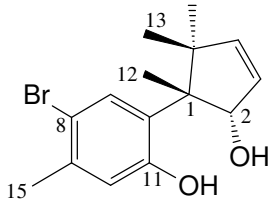

4.6

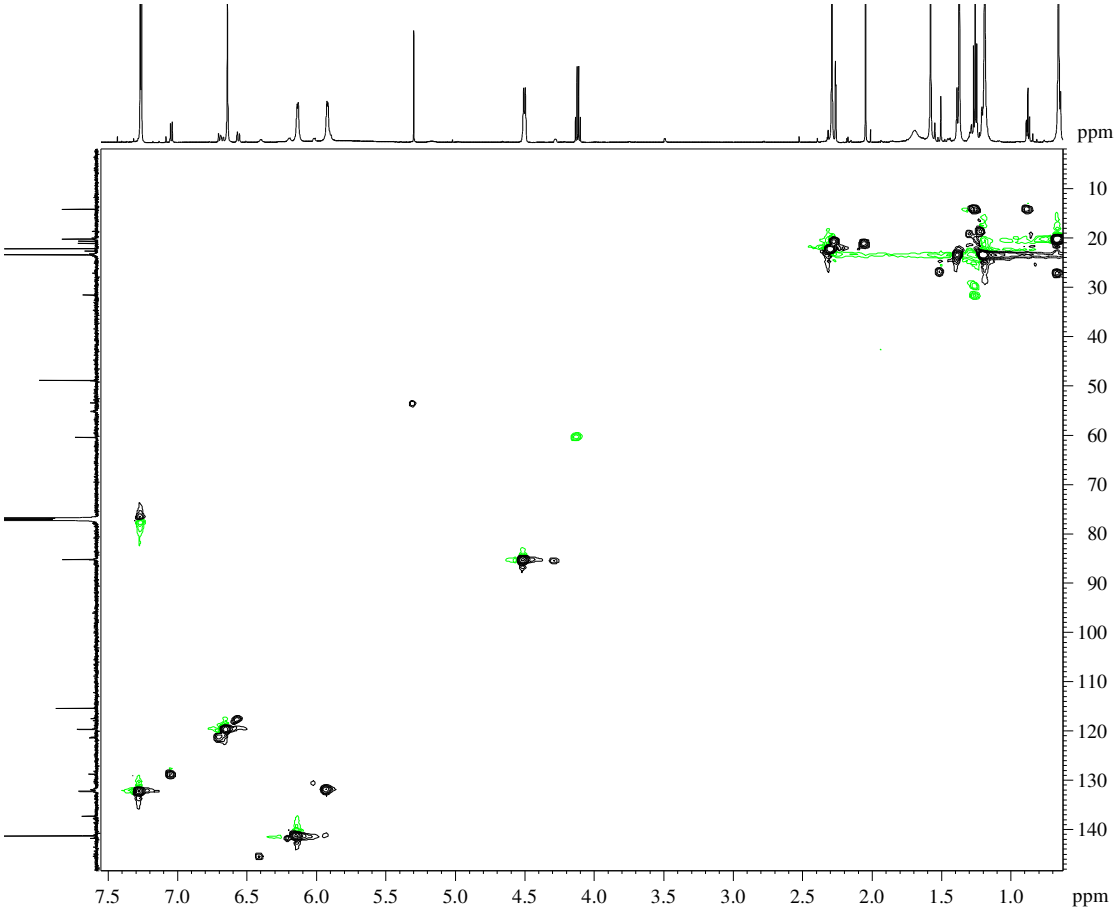

Figure S4.30 HSQC NMR spectrum of compound **4.6**

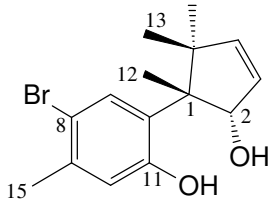

4.6

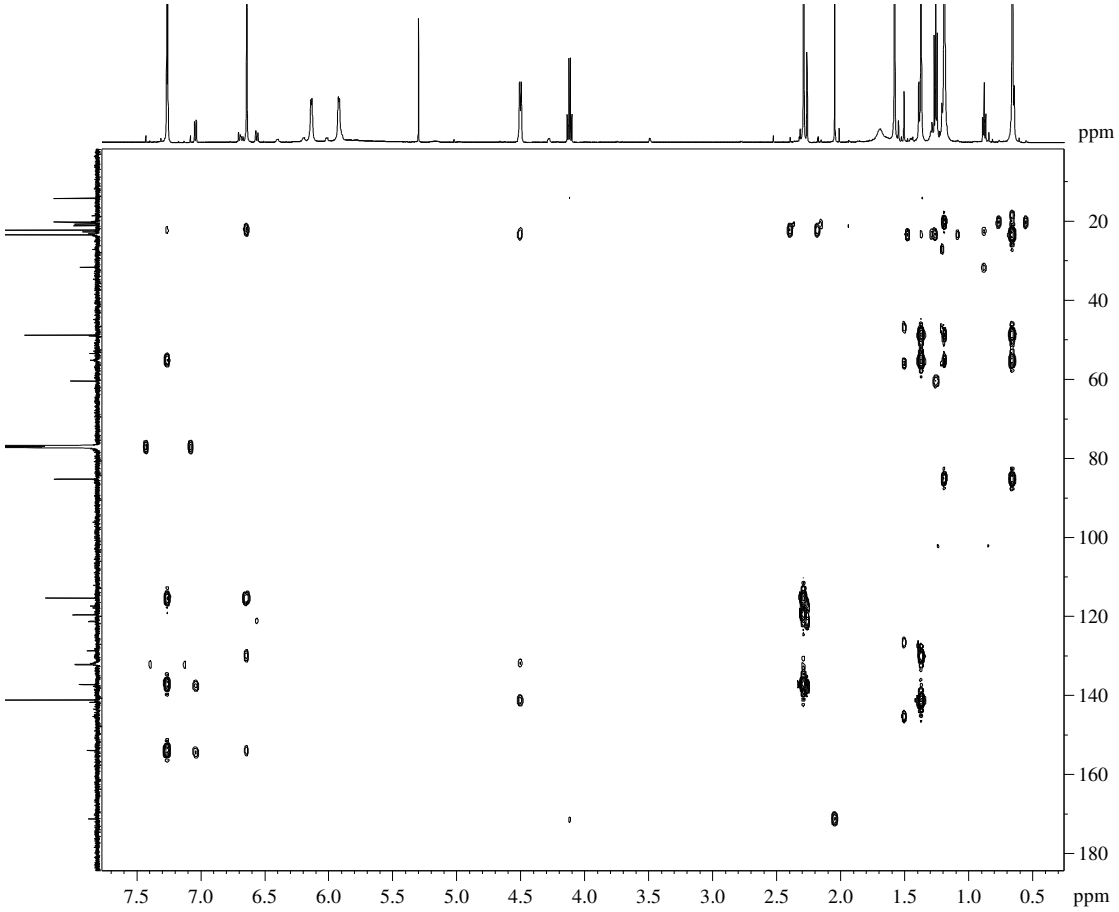

Figure S4.31 HMBC NMR spectrum of compound **4.6**

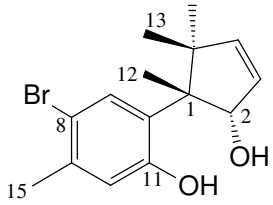

4.6

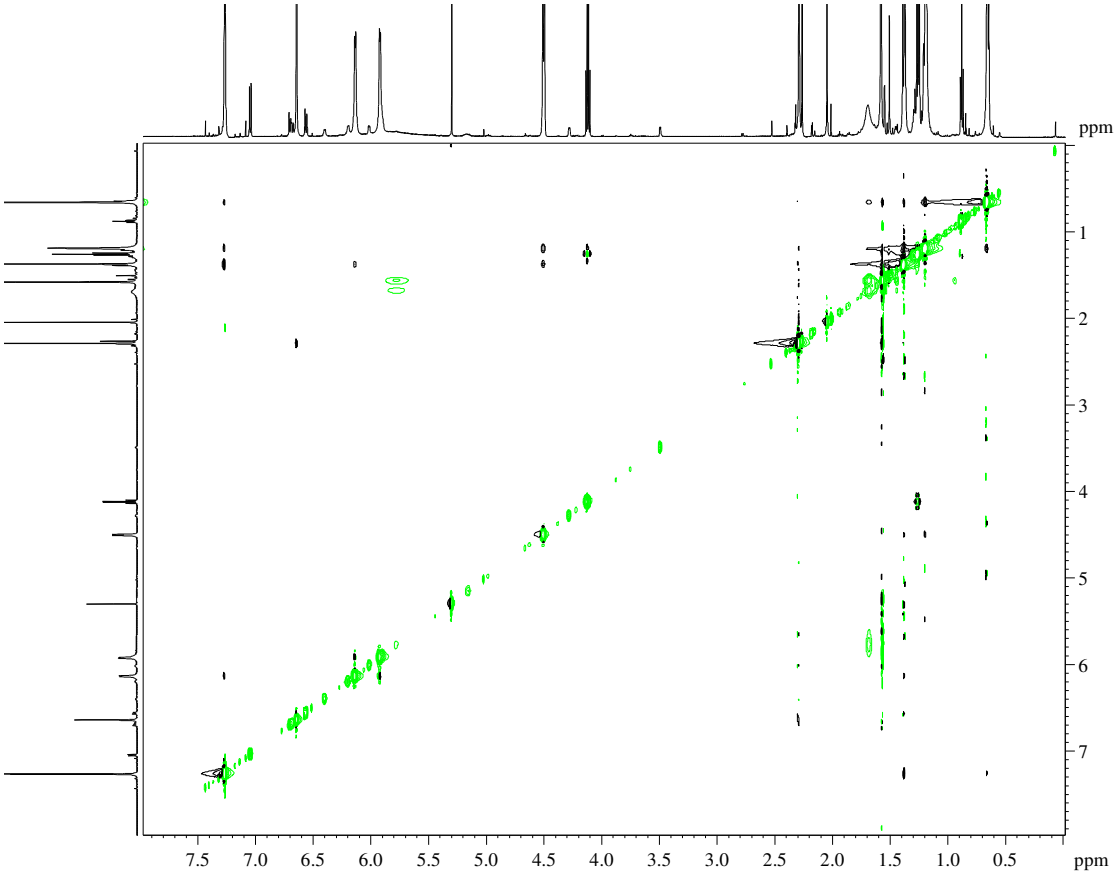

Figure S4.32 NOESY NMR spectrum of compound **4.6**

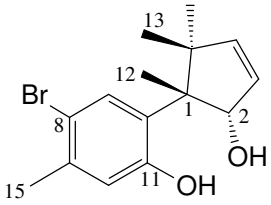

4.6

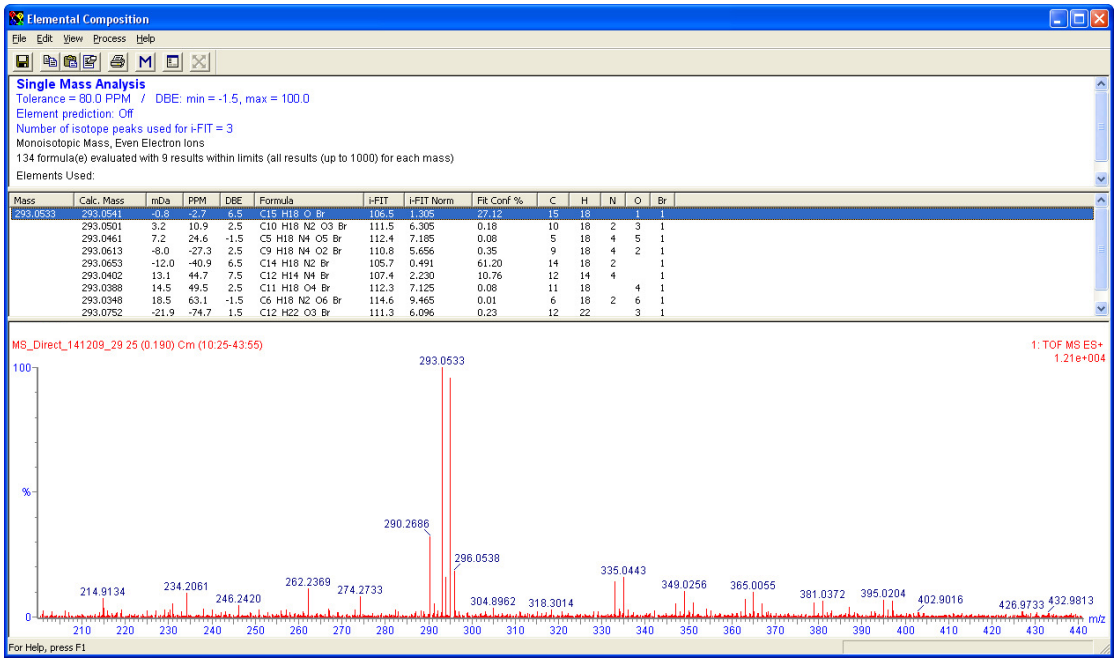

Figure S4.33 HRESIMS spectrum of compound **4.6**

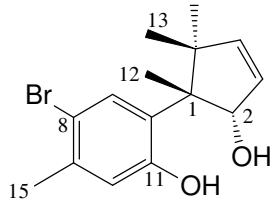

4.6

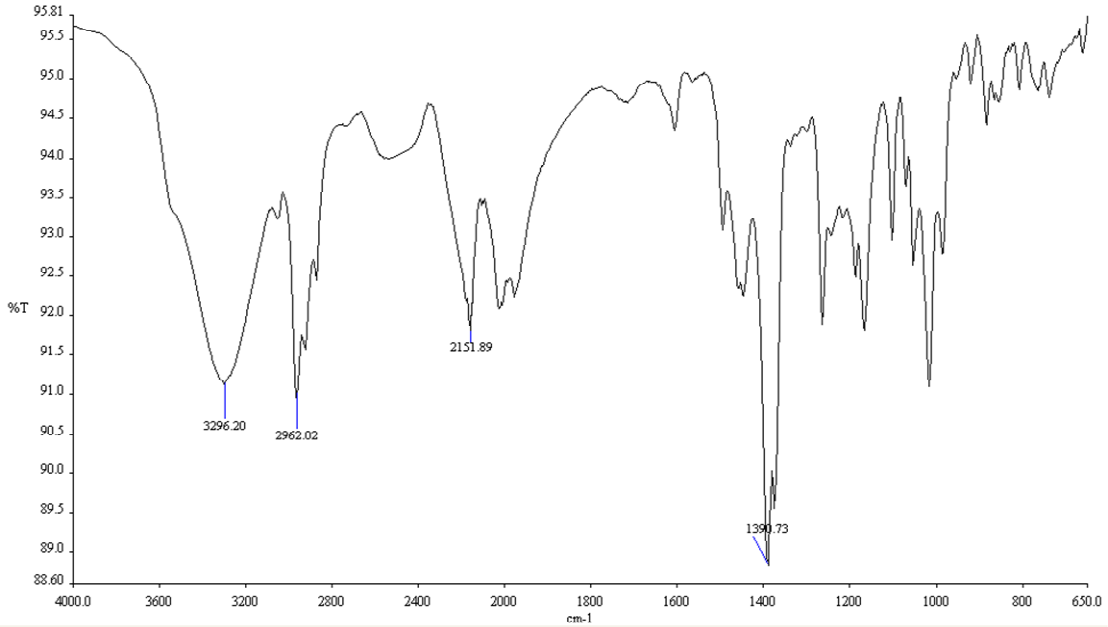

Figure S4.34 IR spectrum of compound **4.6**

S4.6 Compound 4.7

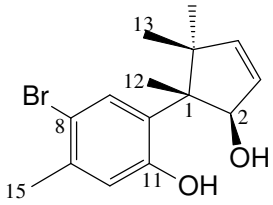

4.7

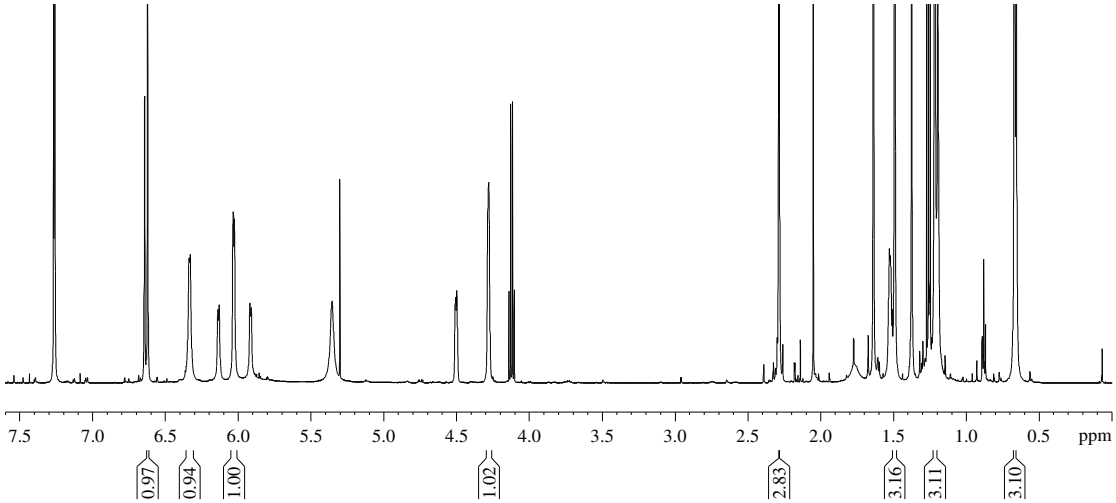

Figure S4.34 ^{1}H NMR spectrum ($CDCl_3$, 600 MHz) of compound **4.7**

Compound **4.7** was isolated and elucidated in a mixture with compound **4.6**

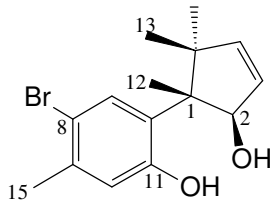

4.7

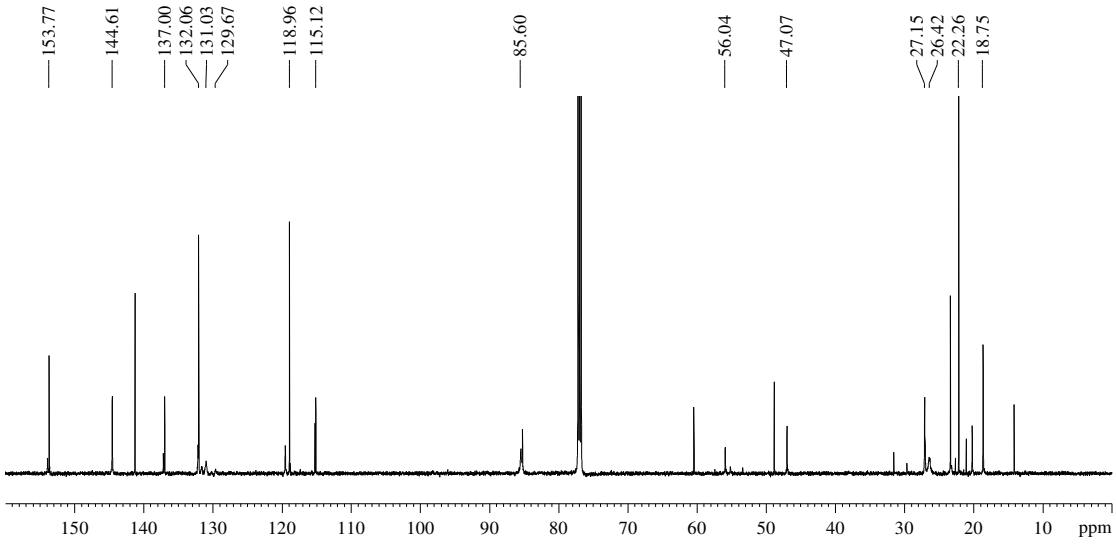

Figure S4.35 ^{13}C NMR spectrum ($CDCl_3$, 150 MHz) of compound **4.7**

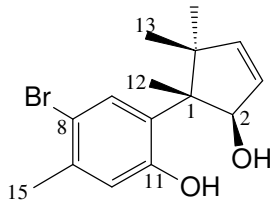

4.7

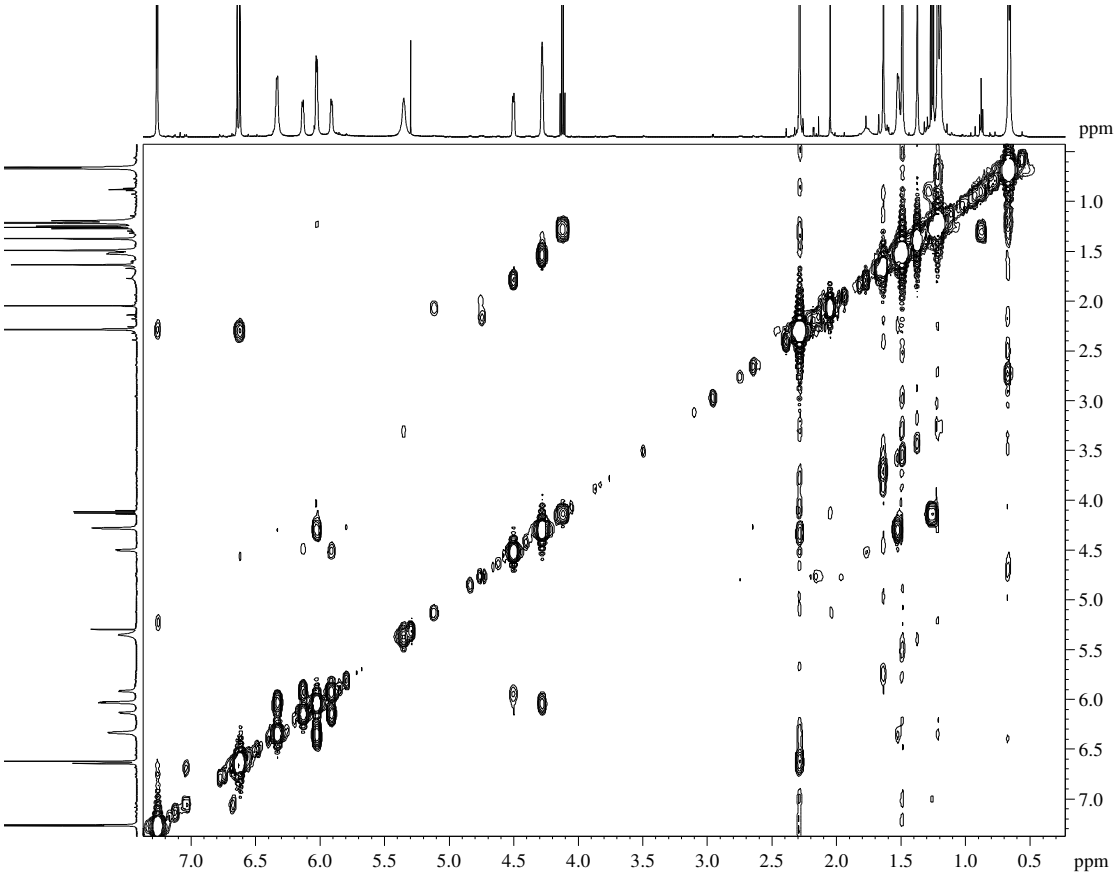

Figure S4.36 COSY NMR spectrum of compound **4.7**

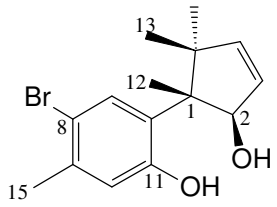

4.7

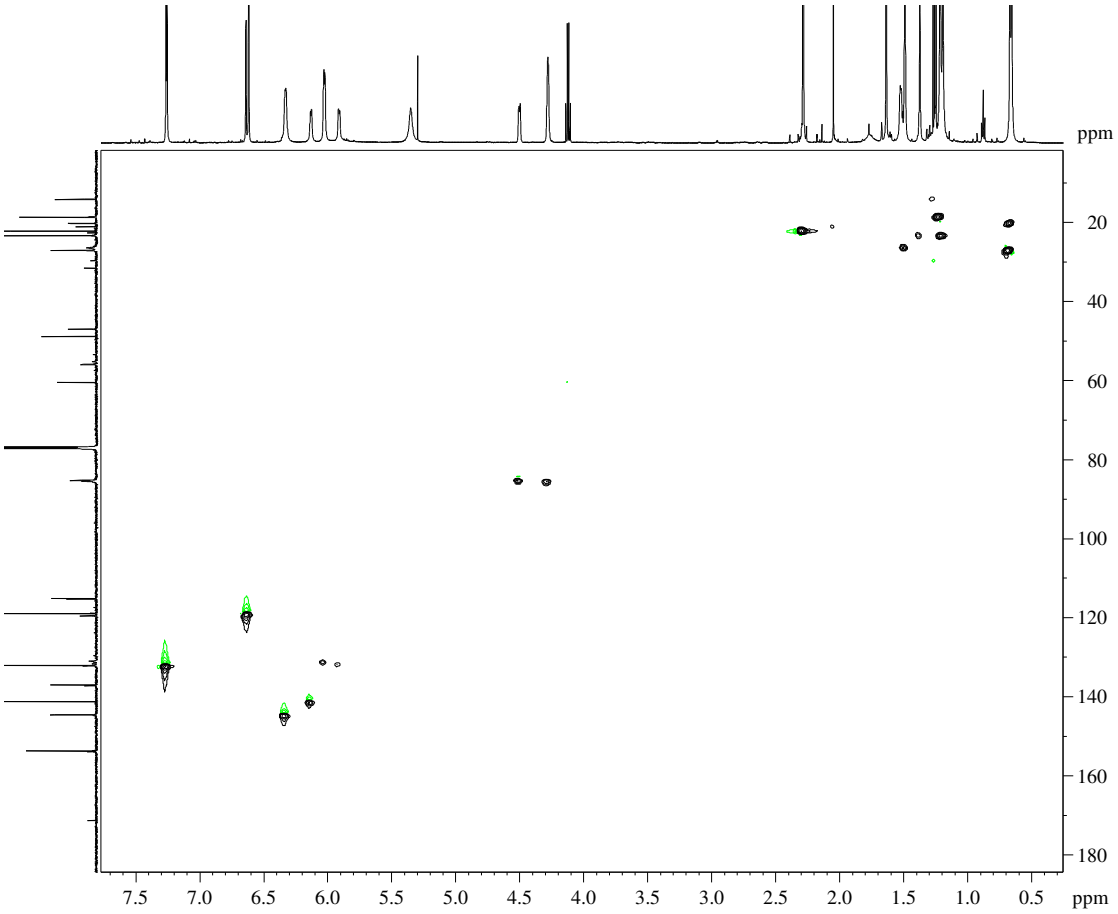

Figure S4.37 HSQC NMR spectrum of compound **4.7**

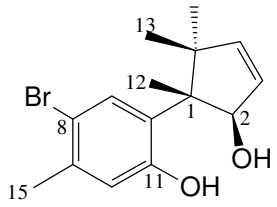

4.7

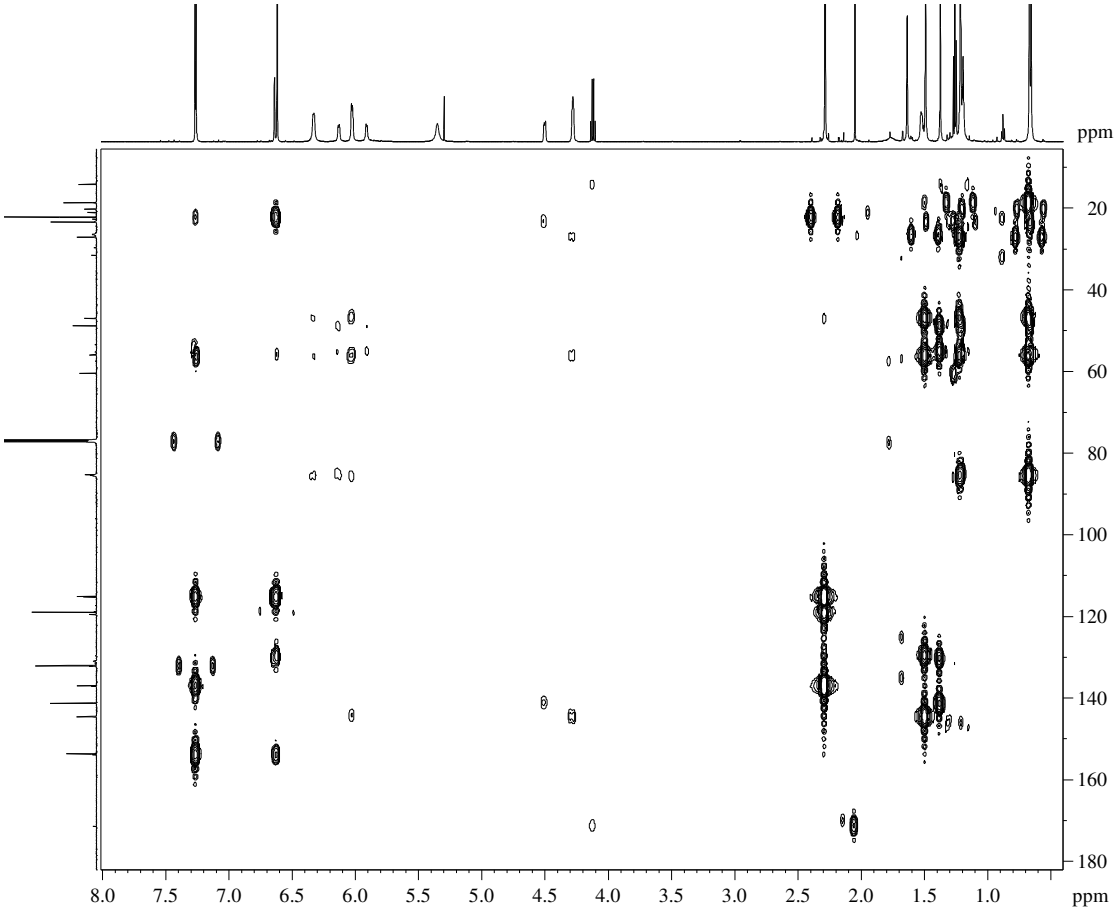

Figure S4.38 HMBC NMR spectrum of compound **4.7**

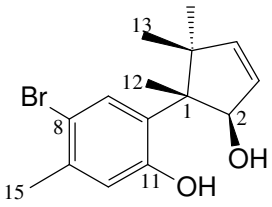

4.7

-

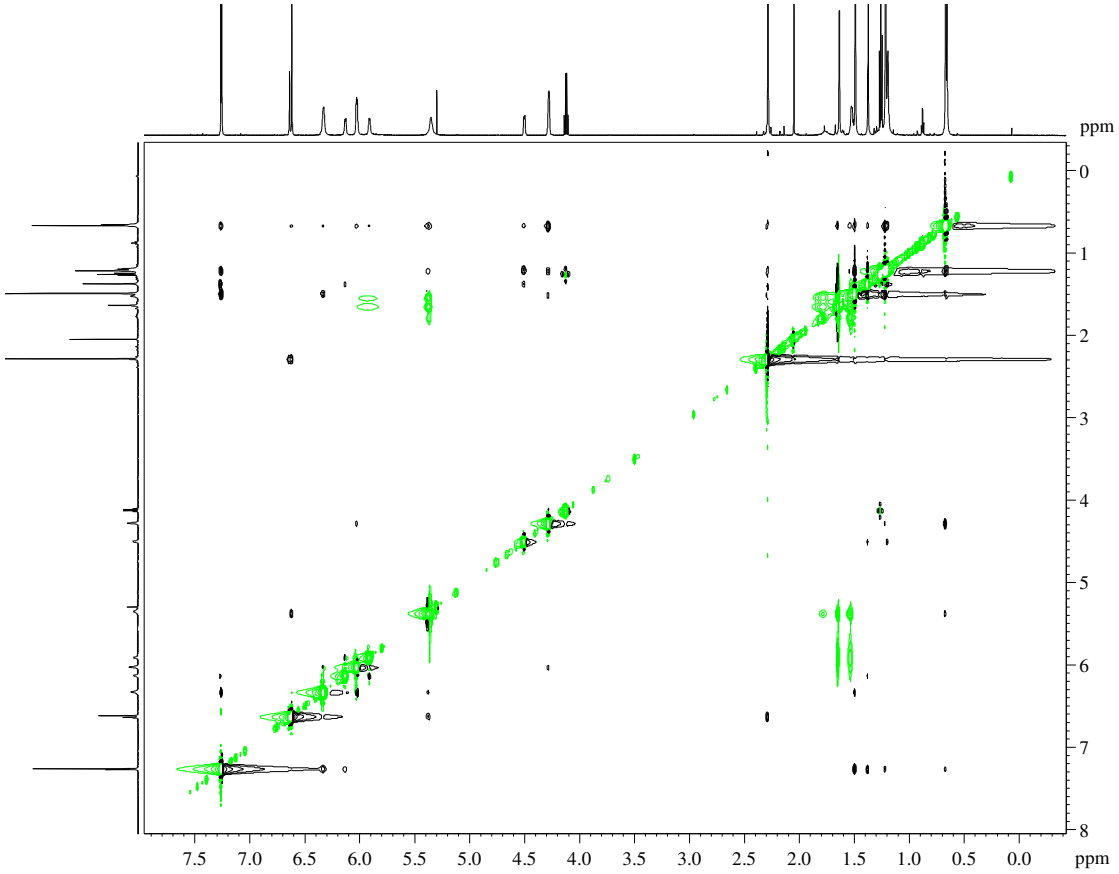

Figure S4.39NOESY NMR spectrum of compound **4.7**

S.7 Compound 4.8

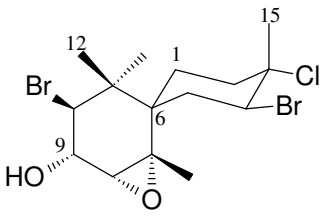

4.8

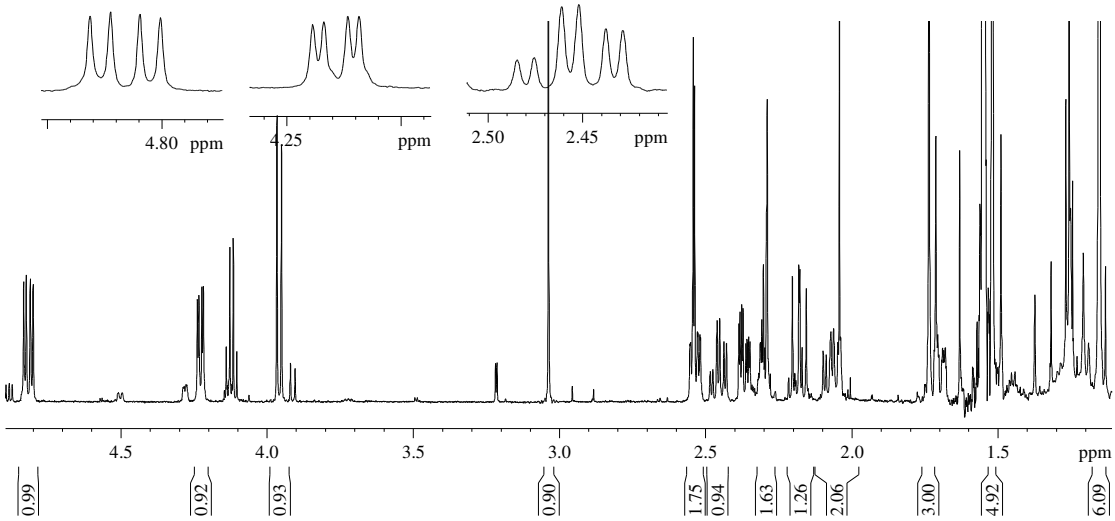

Figure S4.41 ^{1}H NMR spectrum ($CDCl_3$, 600 MHz) of compound **4.8**

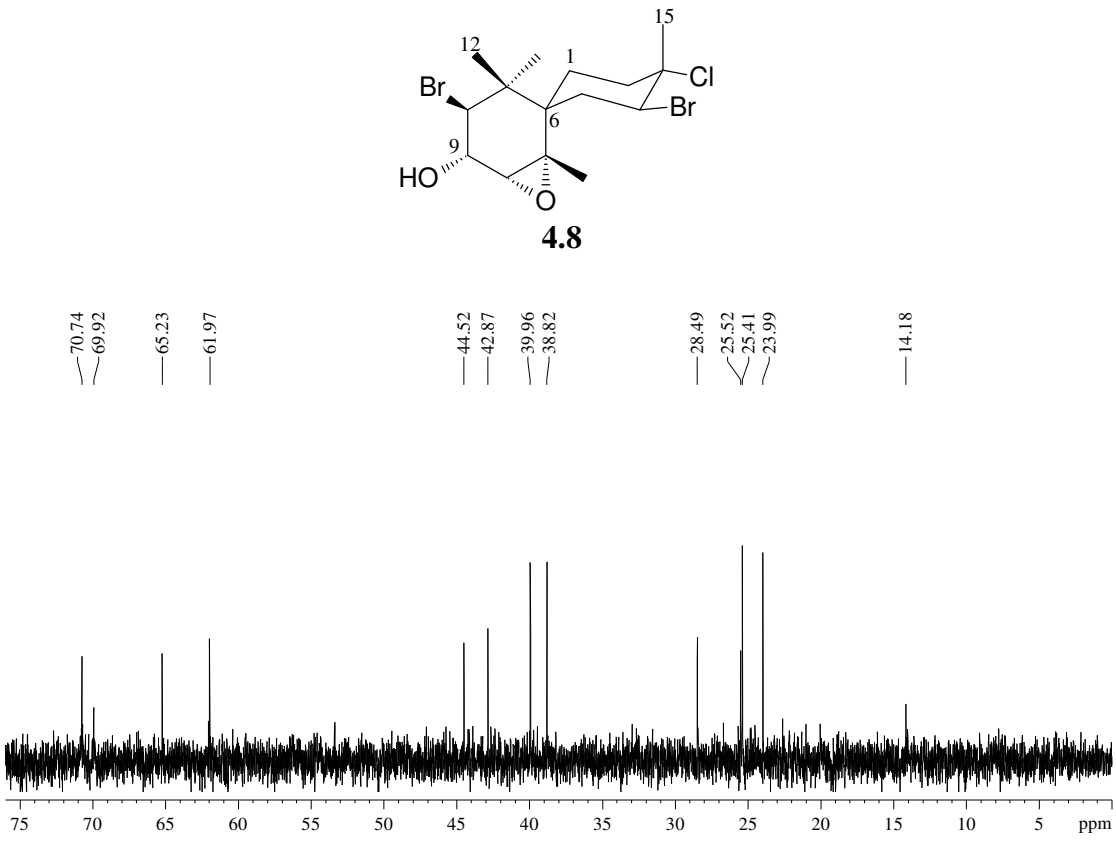

Figure S4.42 ^{13}C NMR spectrum ($CDCl_3$, 150 MHz) of compound **4.8**

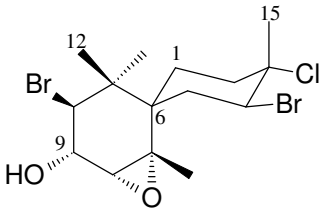

4.8

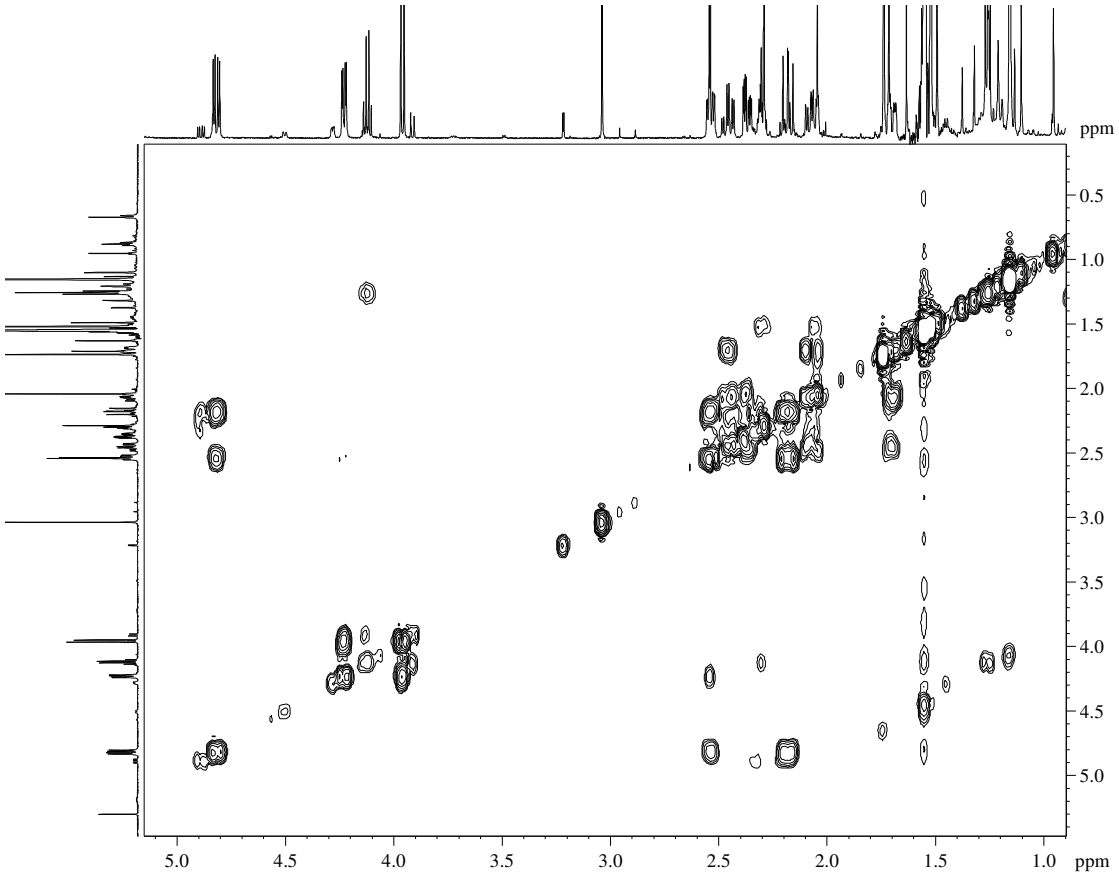

Figure S4.43 COSY NMR spectrum of compound **4.8**

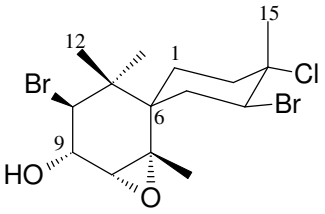

4.8

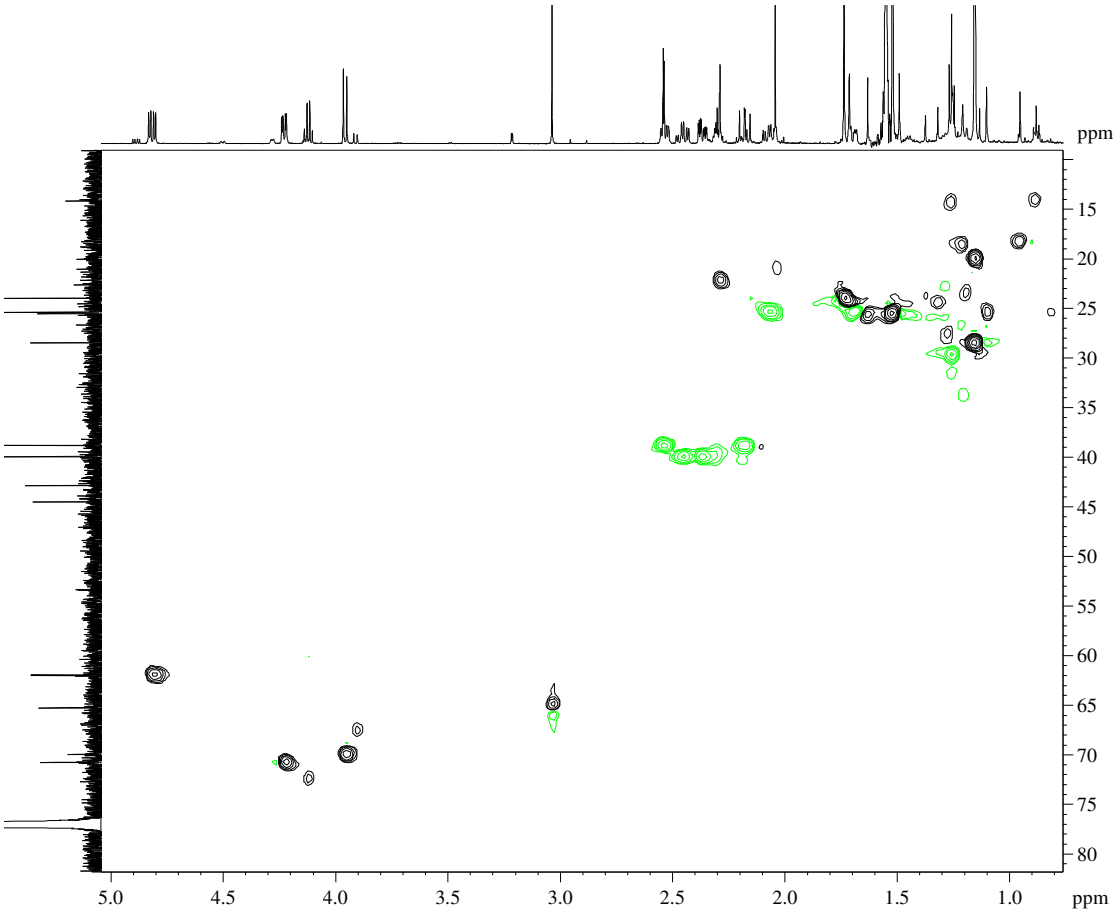

Figure S4.44 HSQC NMR spectrum of compound **4.8**

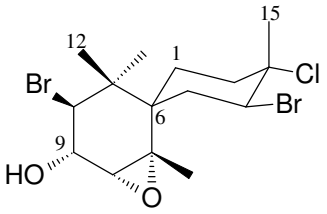

4.8

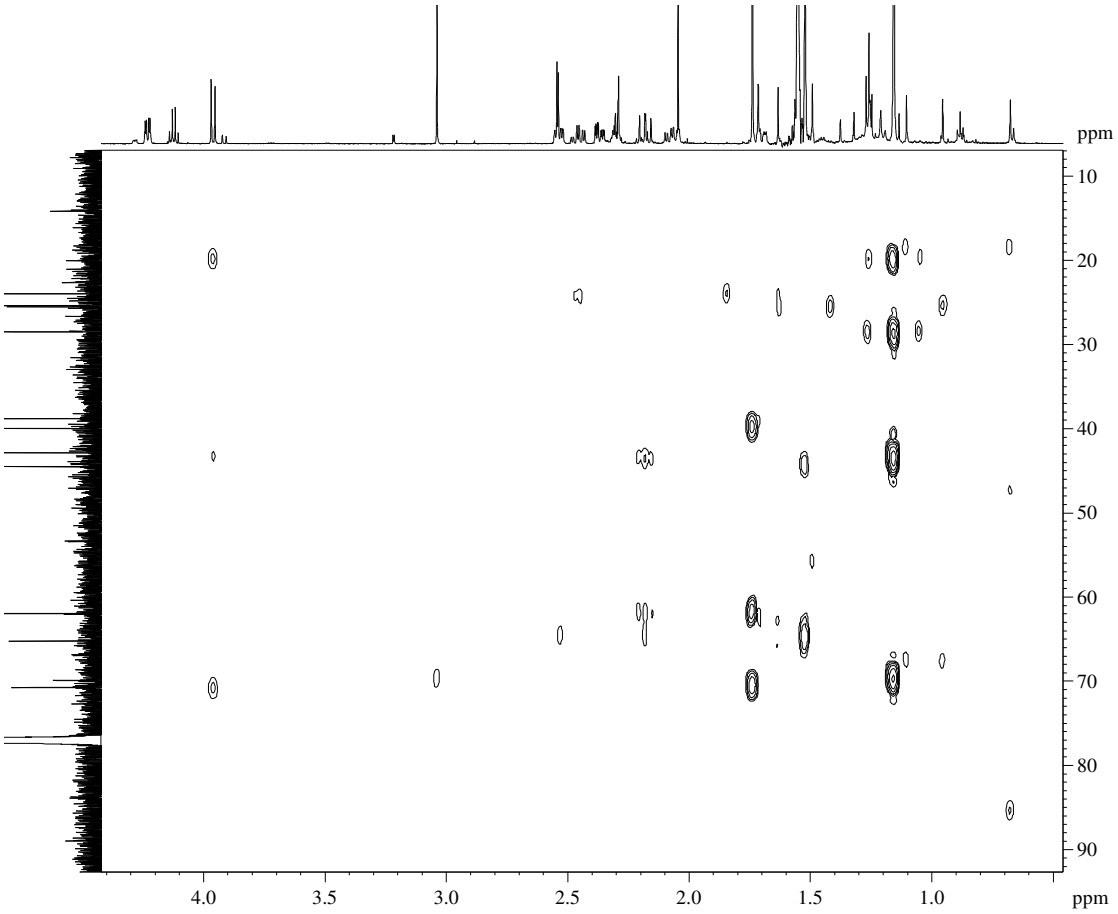

Figure S4.45 HMBC NMR spectrum of compound **4.8**

Chapter 5

Secondary metabolites from *Laurencia natalensis*

S5.1 Compound 5.1

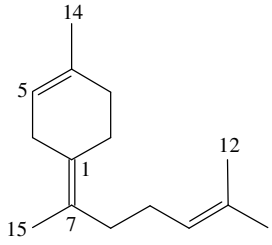

5.1

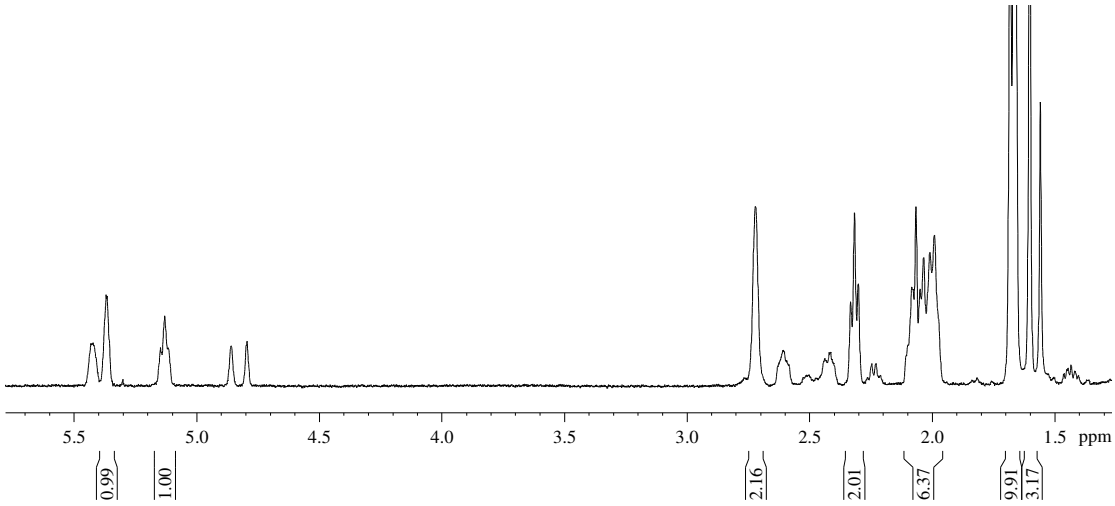

Figure S5.1[1]H NMR spectrum ($CDCl_3$, 600 MHz) of compound **5.1**

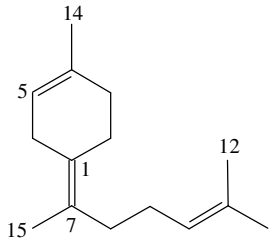

5.1

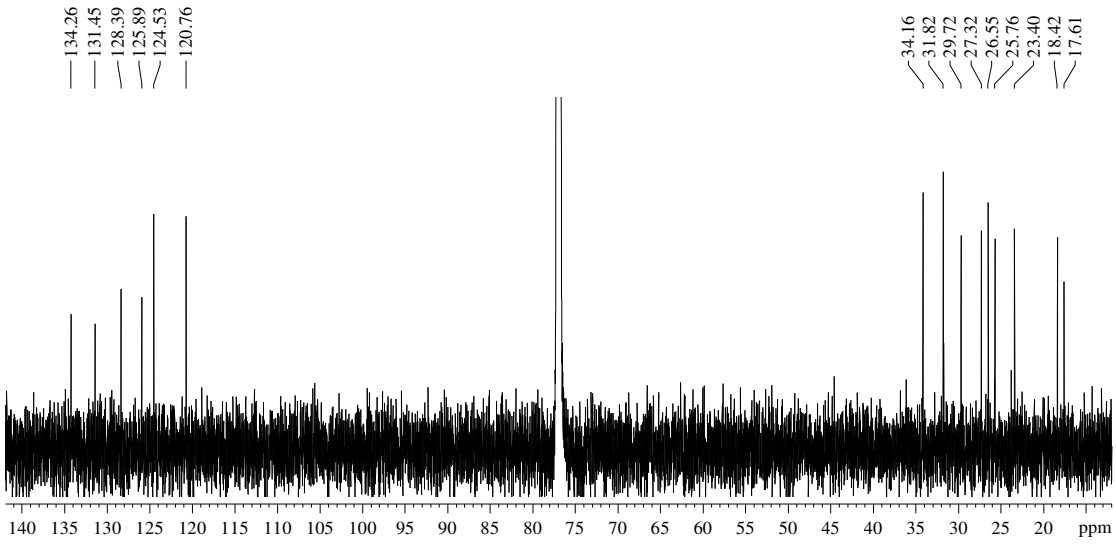

Figure S5.2 ^{13}C NMR spectrum ($CDCl_3$, 150 MHz) of compound **5.1**

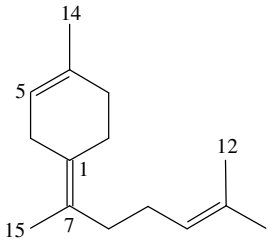

5.1

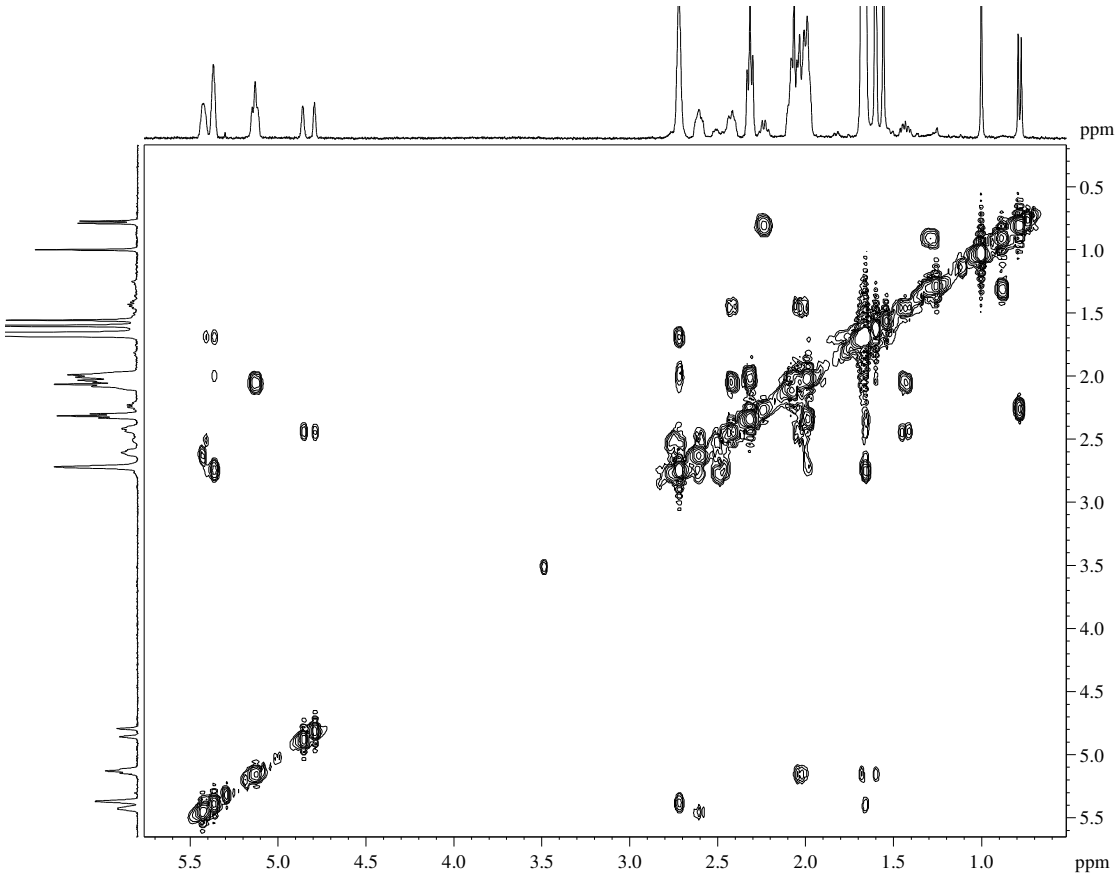

Figure S5.3 COSY NMR spectrum of compound **5.1**

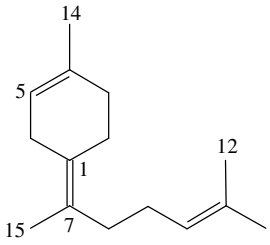

5.1

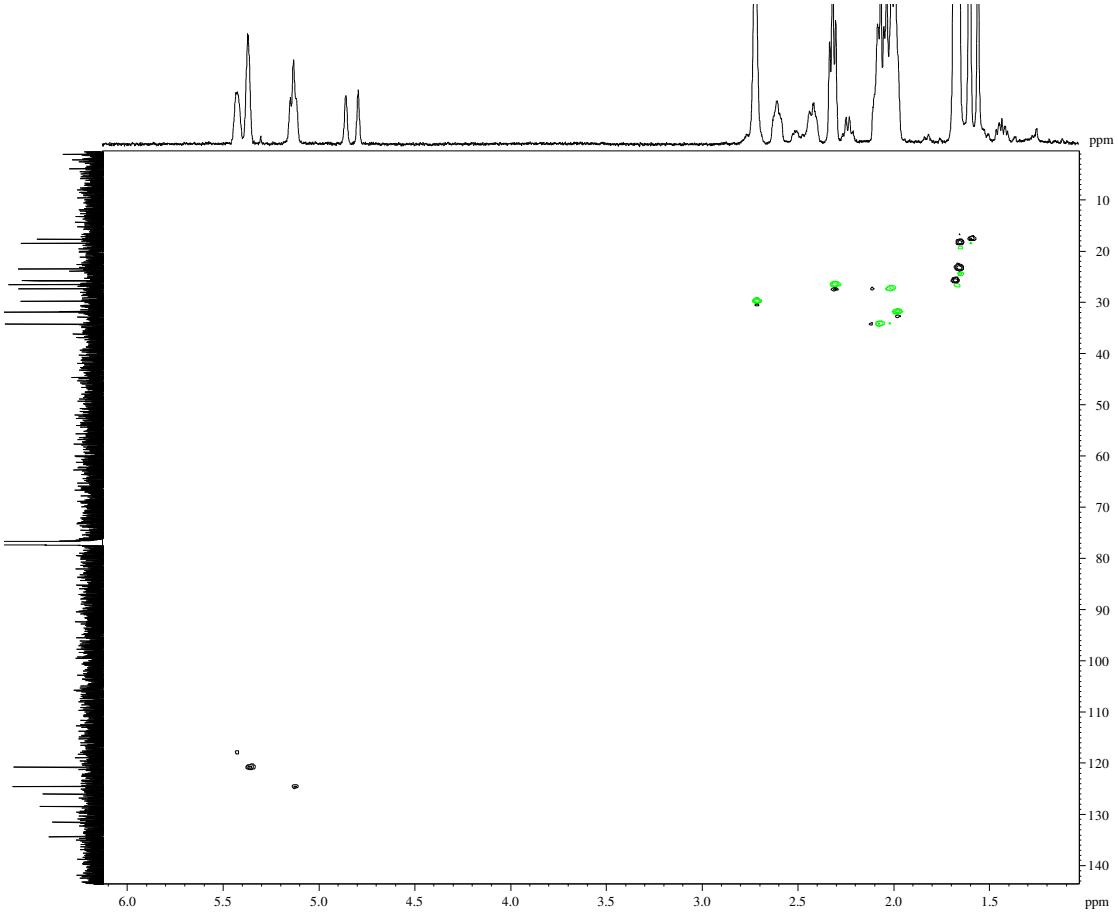

Figure S5.4 HSQC NMR spectrum of compound **5.1**

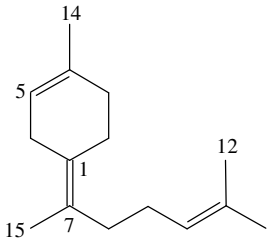

5.1

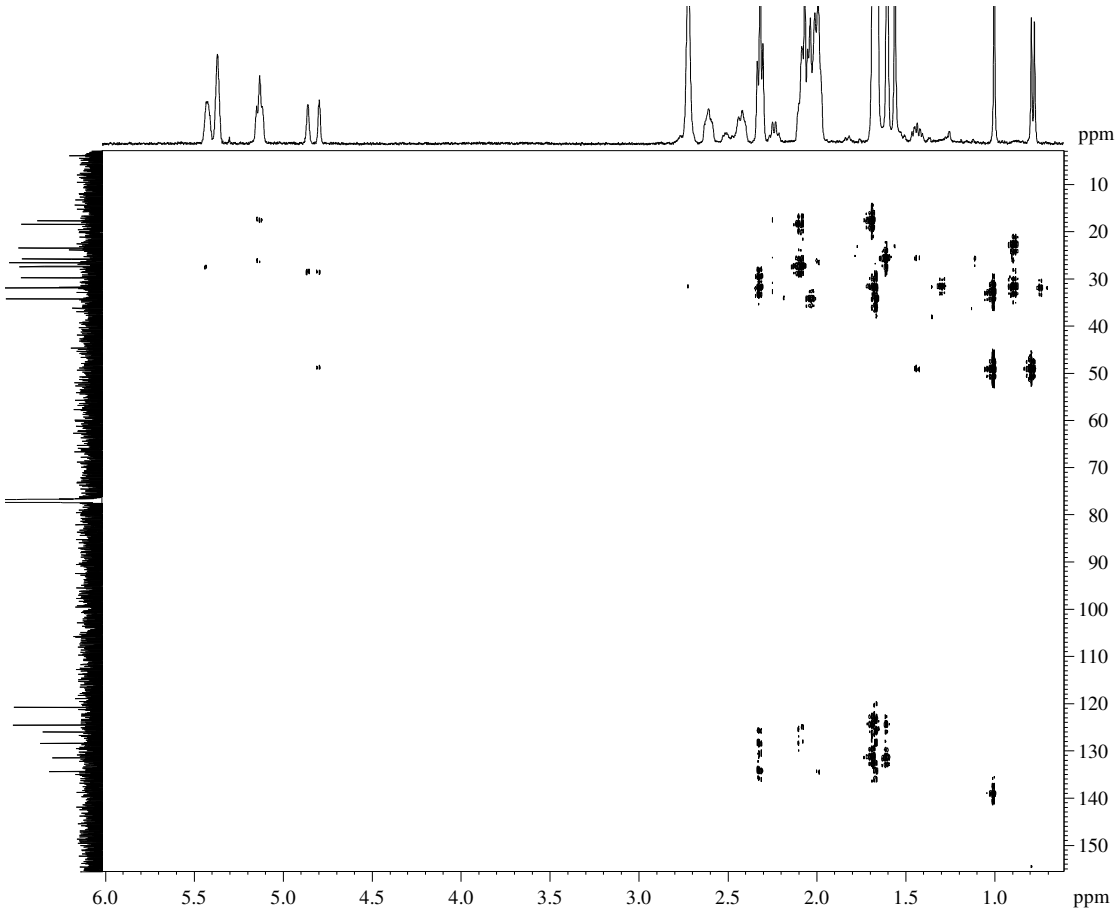

Figure S5.5 HMBC NMR spectrum of compound **5.1**

S5.2 Compound 5.5

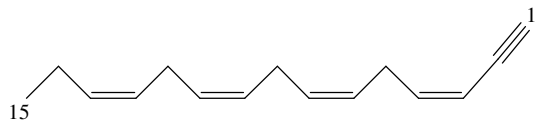

5.5

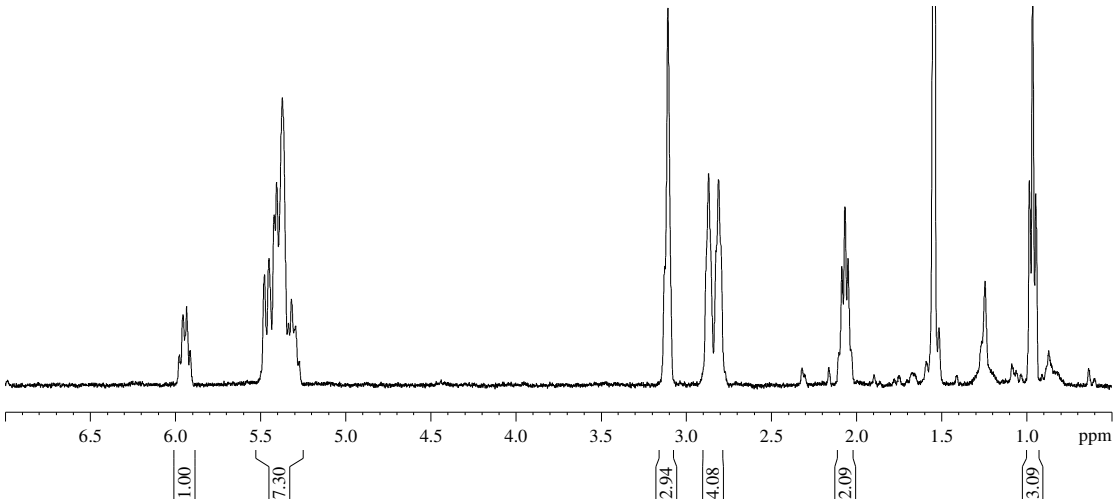

Figure S5.6 ^{1}H NMR spectrum ($CDCl_3$, 600 MHz) of compound **5.5**

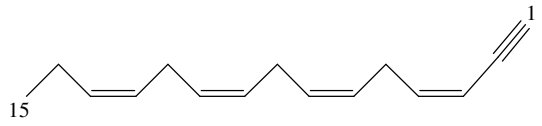

5.5

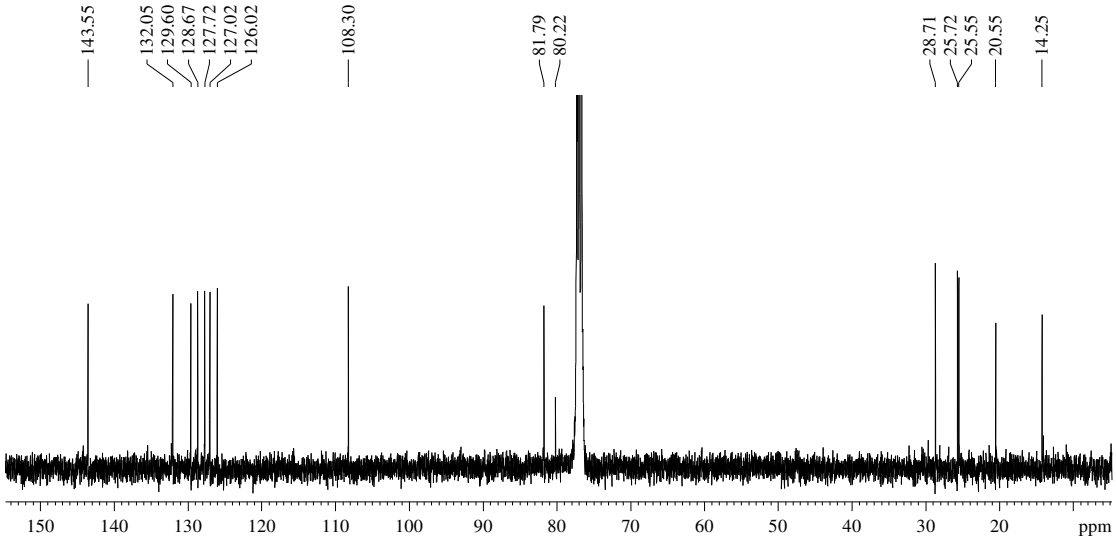

Figure S5.7 ^{13}C NMR spectrum ($CDCl_3$, 150 MHz) of compound **5.5**

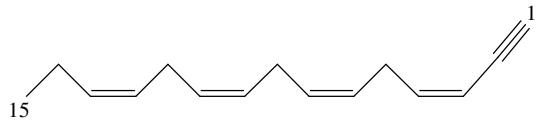

5.5

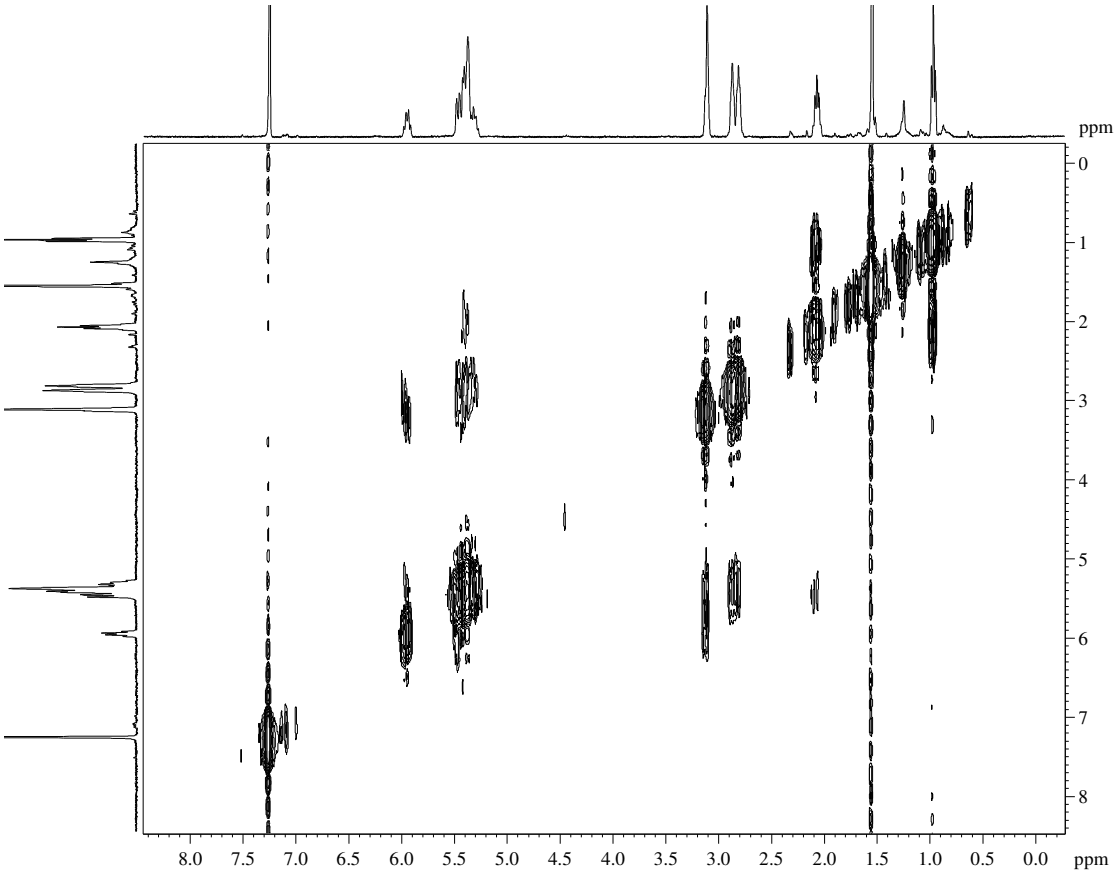

Figure S5.8 COSY NMR spectrum of compound **5.5**

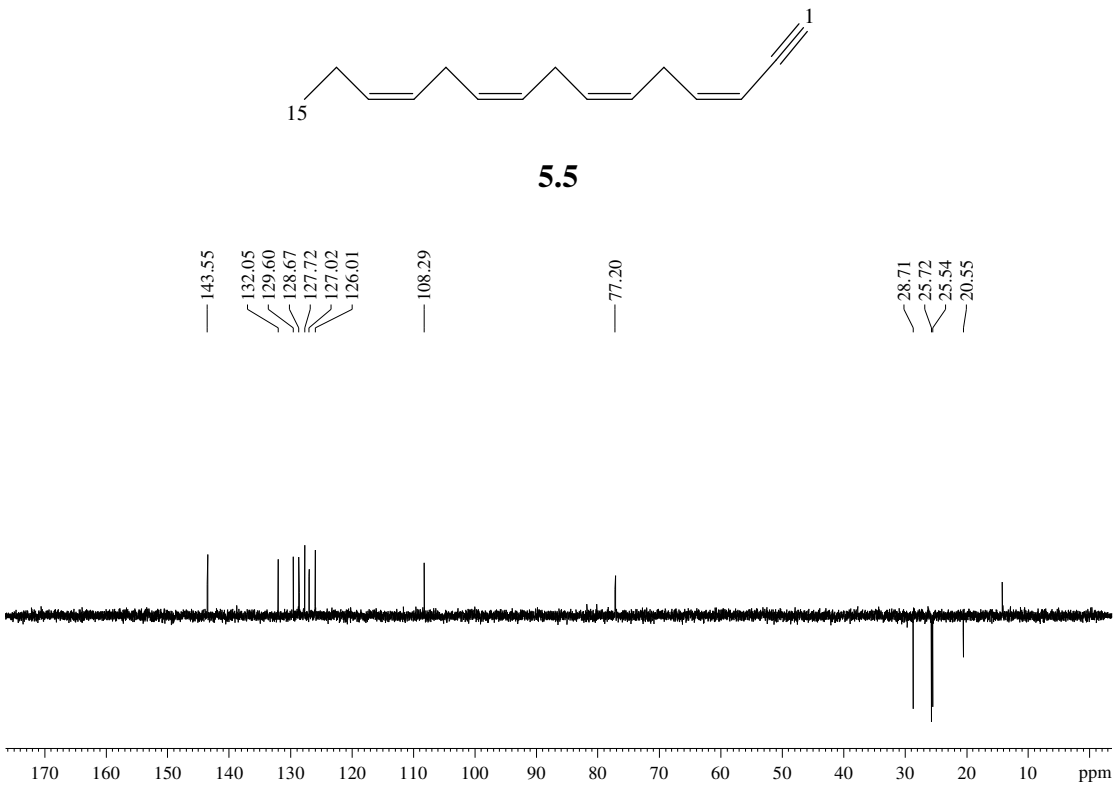

Figure S5.9 DEPT-135 NMR spectrum of compound **5.5**

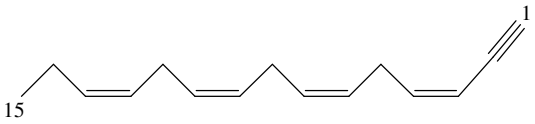

5.5

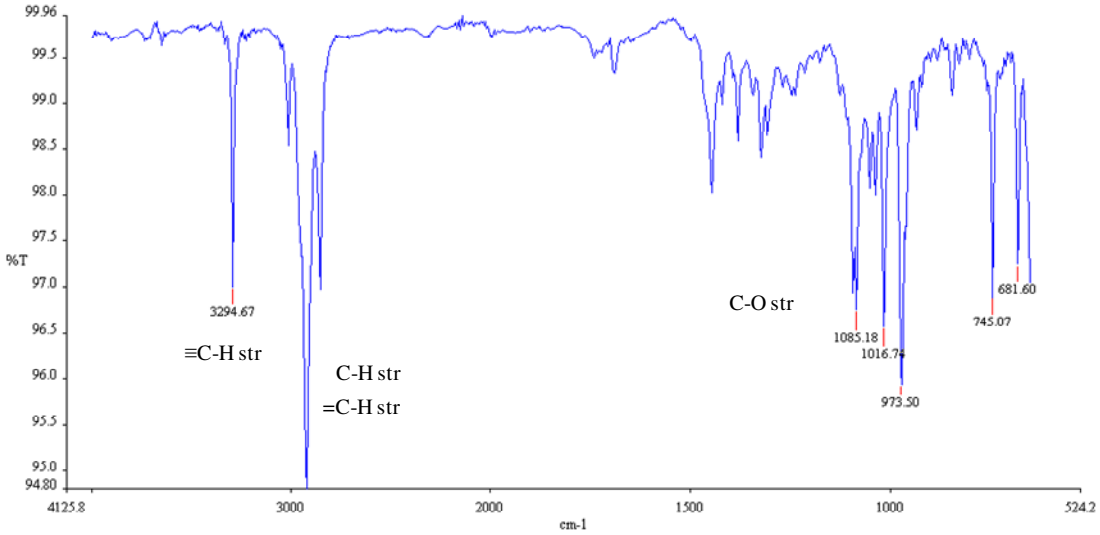

Figure S5.10 IR spectrum of compound **5.5**

S5.3 Compound 5.8

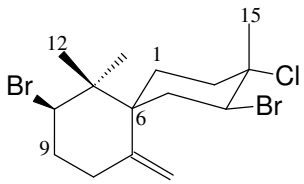

5.8

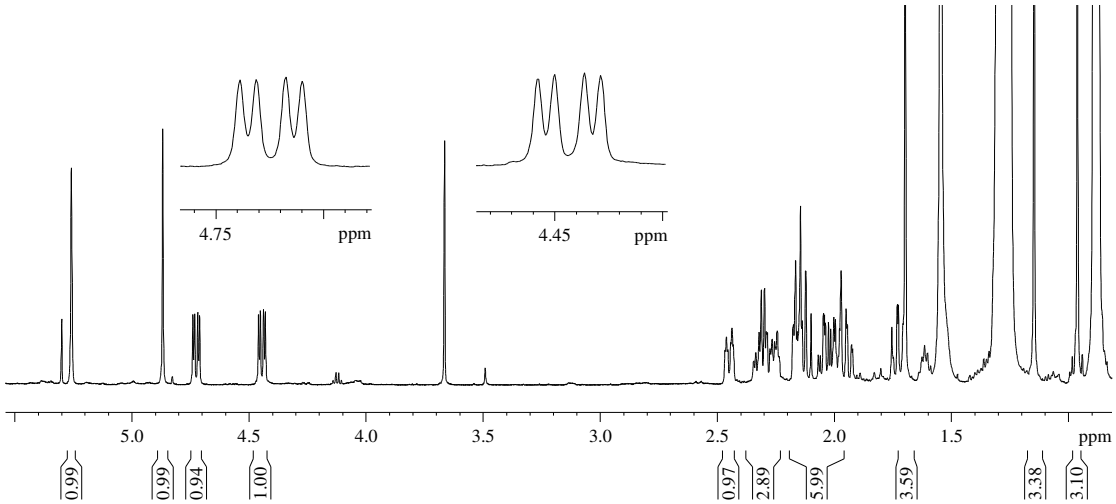

Figure S5.11 ^{1}H NMR spectrum ($CDCl_3$, 600 MHz) of compound **5.8**

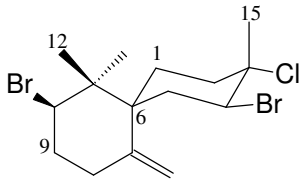

5.8

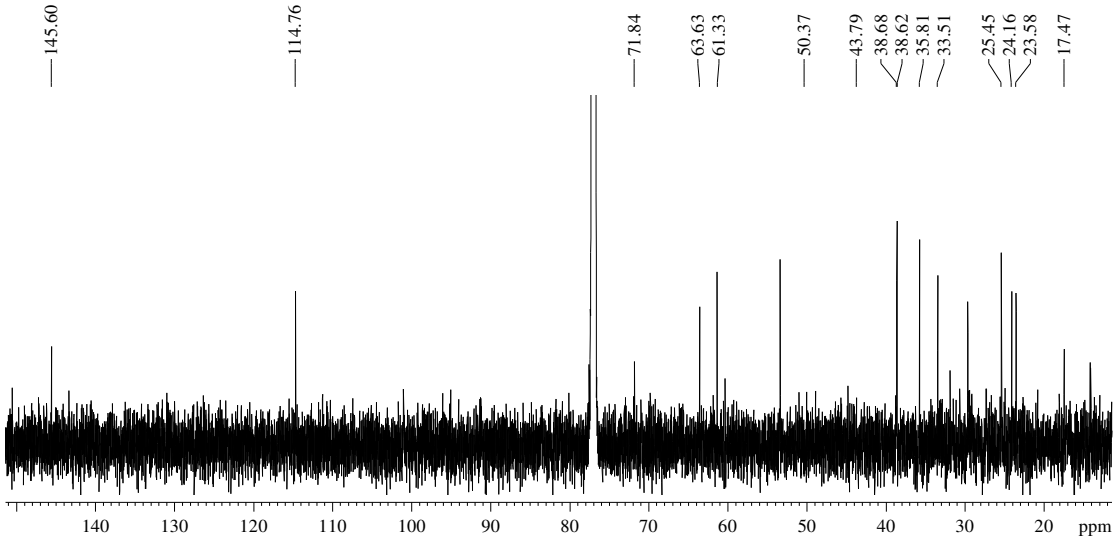

Figure S5.12 ^{13}C NMR spectrum ($CDCl_3$, 150 MHz) of compound **5.8**

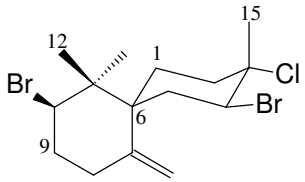

5.8

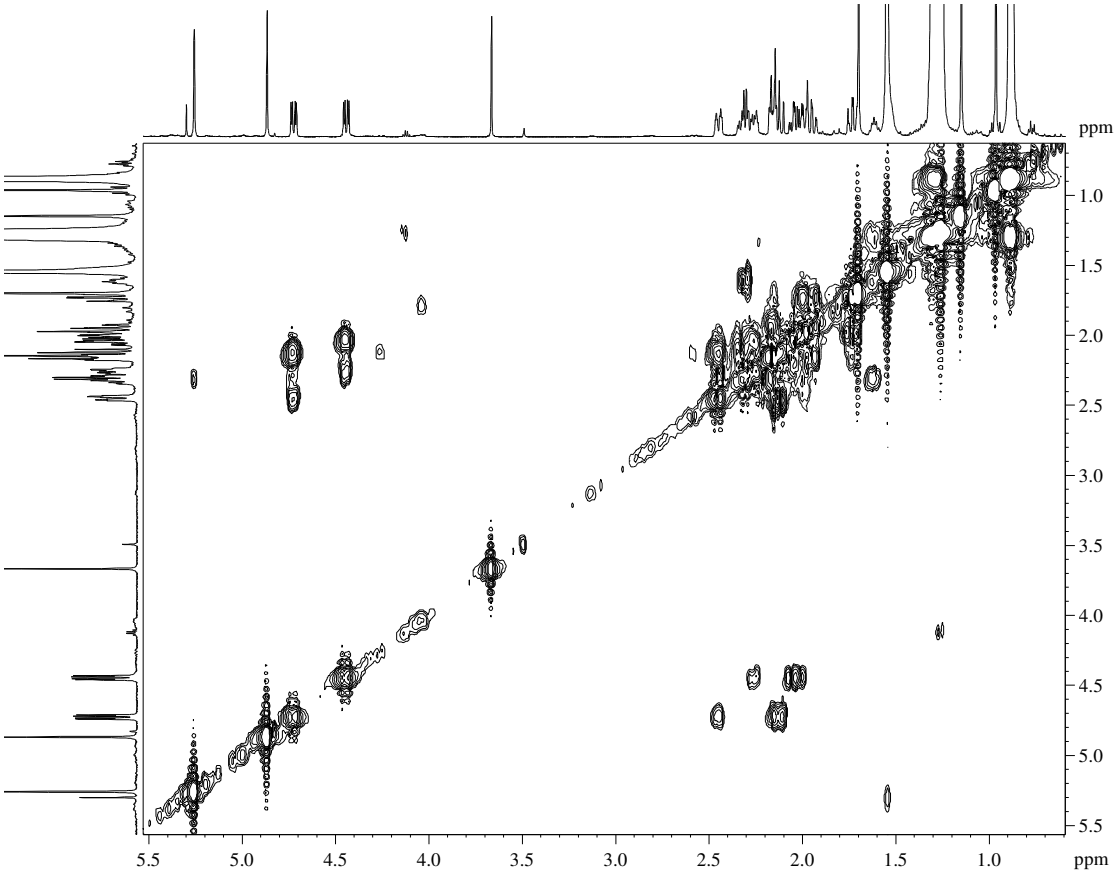

Figure S5.13 COSY NMR spectrum of compound **5.8**

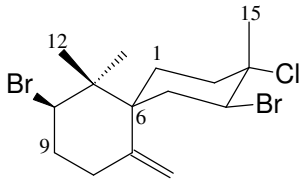

5.8

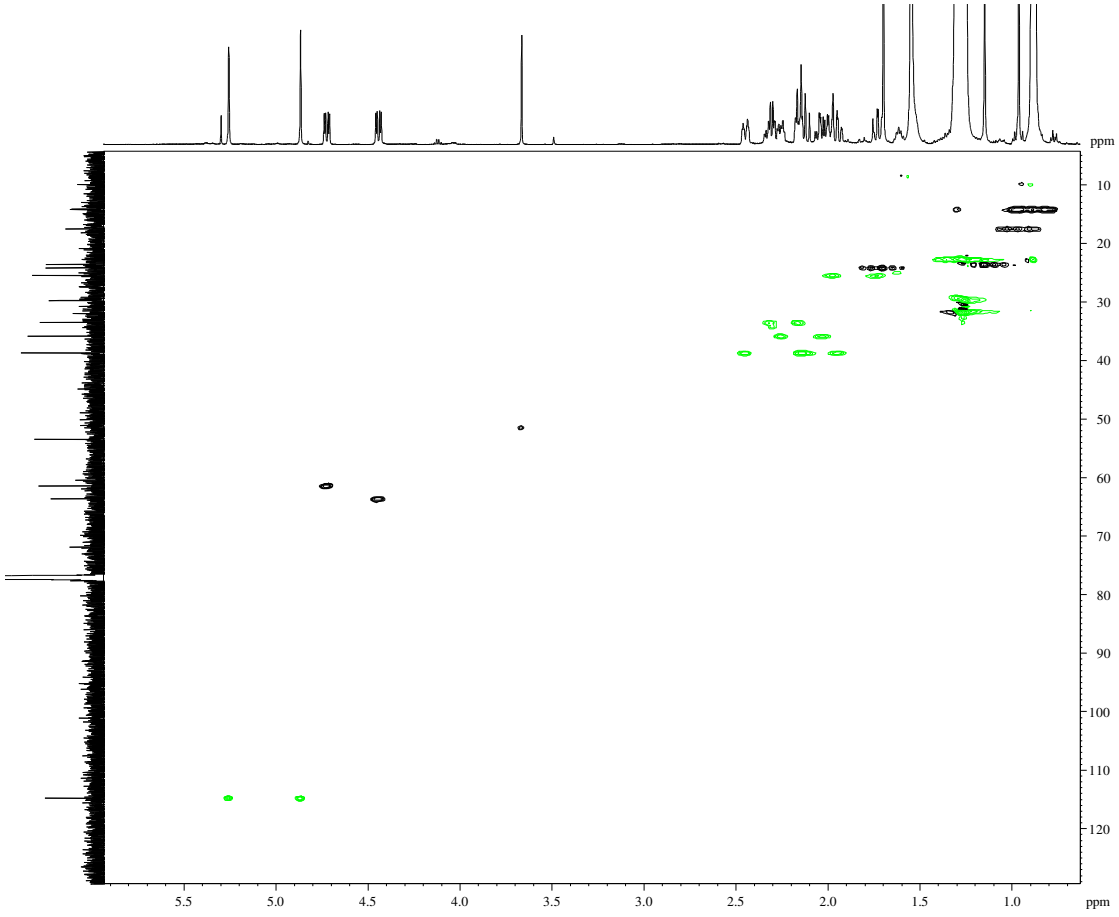

Figure S5.14 HSQC NMR spectrum of compound **5.8**

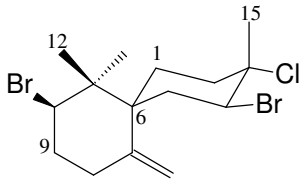

5.8

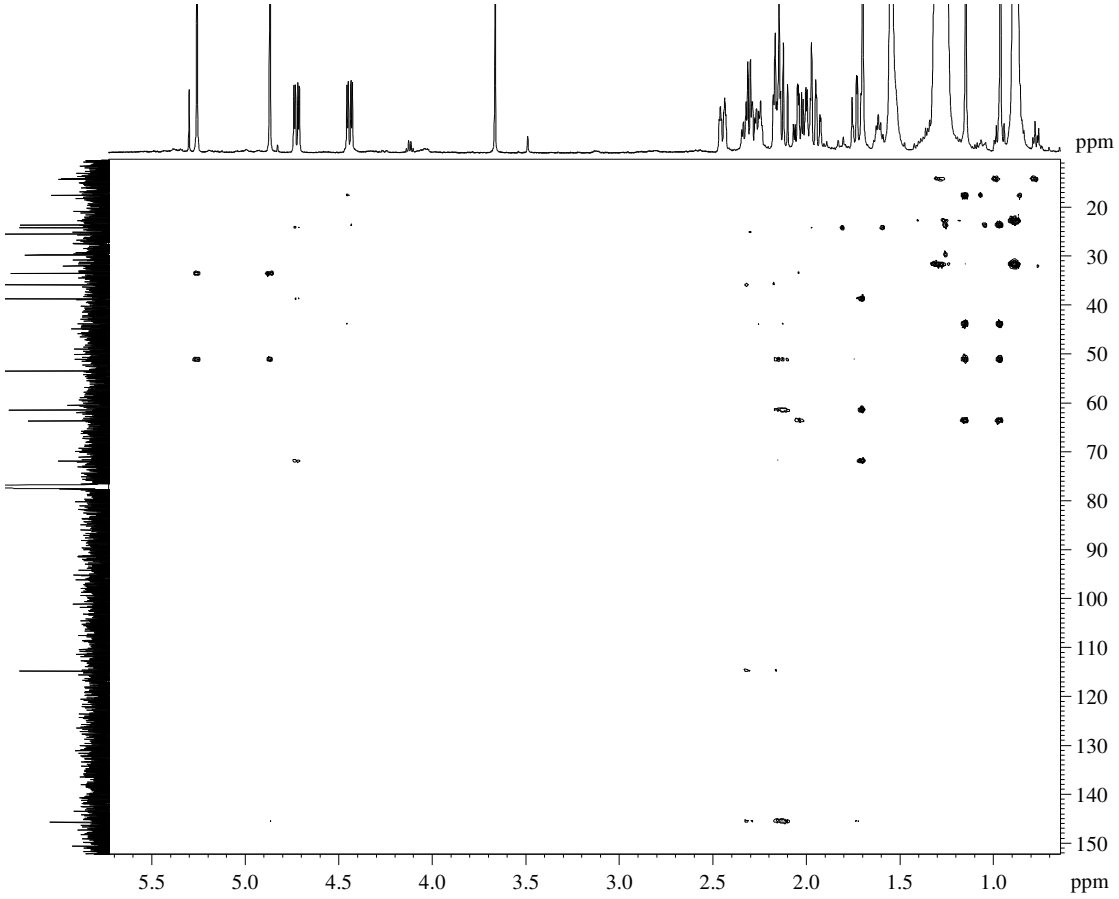

Figure S5.15 HMBC NMR spectrum of compound **5.8**

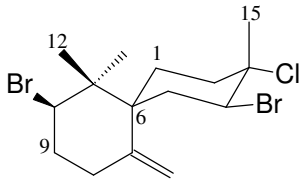

5.8

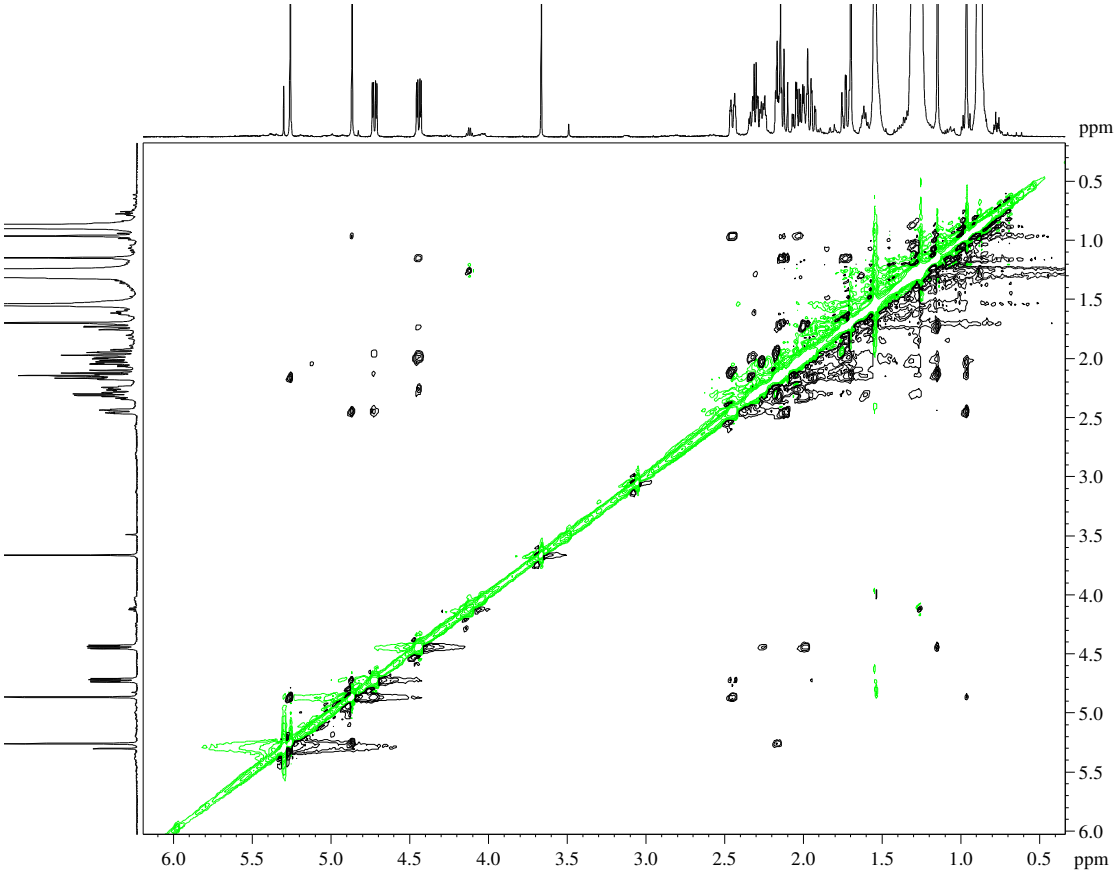

Figure S5.16 NOESY NMR spectrum of compound **5.8**

S5.4 Compound 5.9

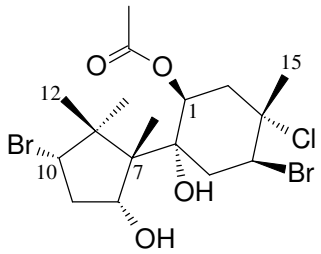

5.9

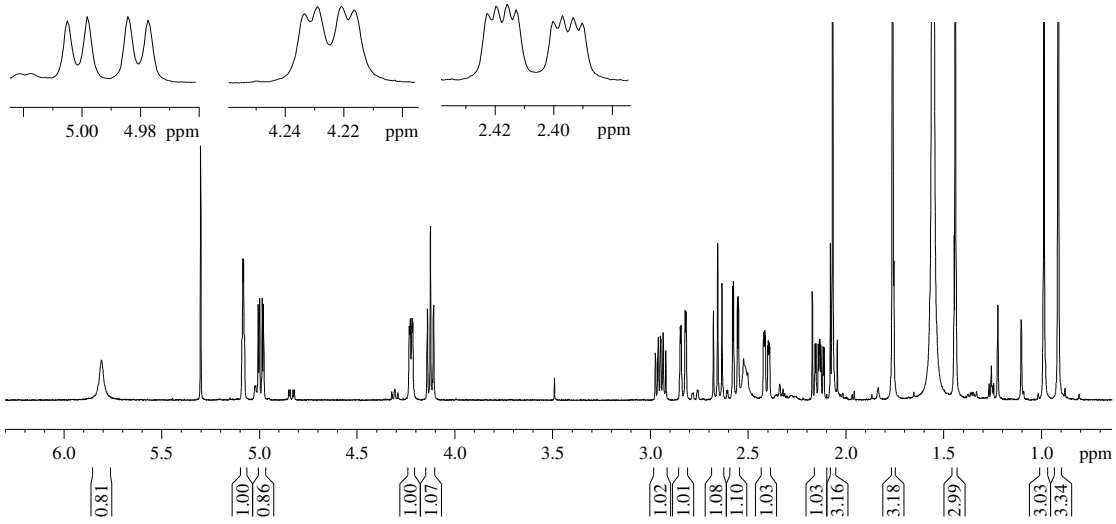

Figure S5.17 ^{1}H NMR spectrum ($CDCl_3$, 600 MHz) of compound **5.9**

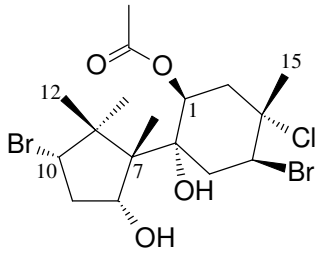

5.9

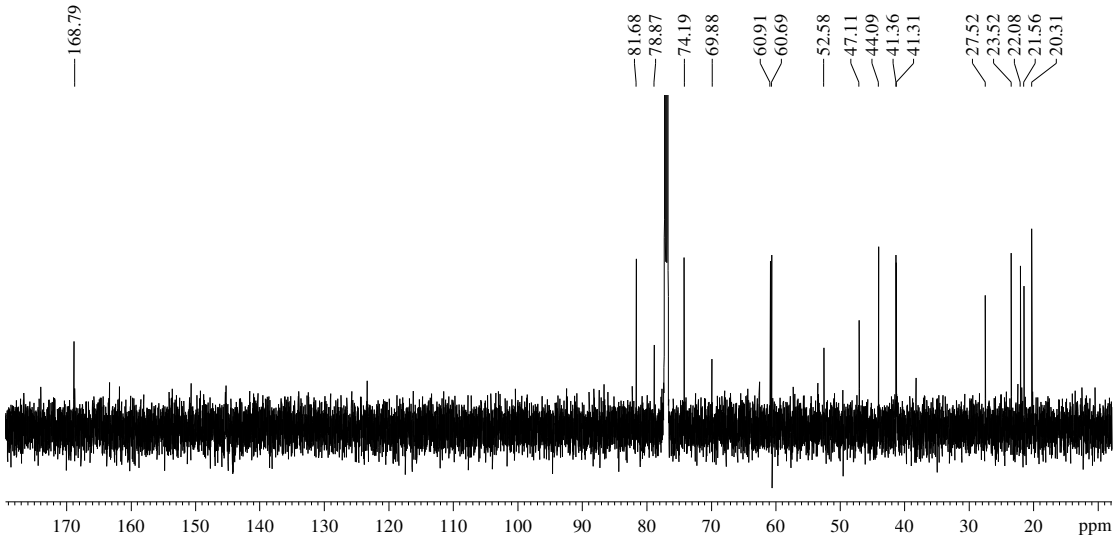

Figure S5.18 ^{13}C NMR spectrum ($CDCl_3$, 150 MHz) of compound **5.9**

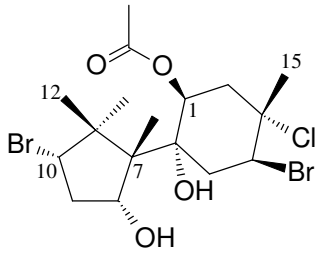

5.9

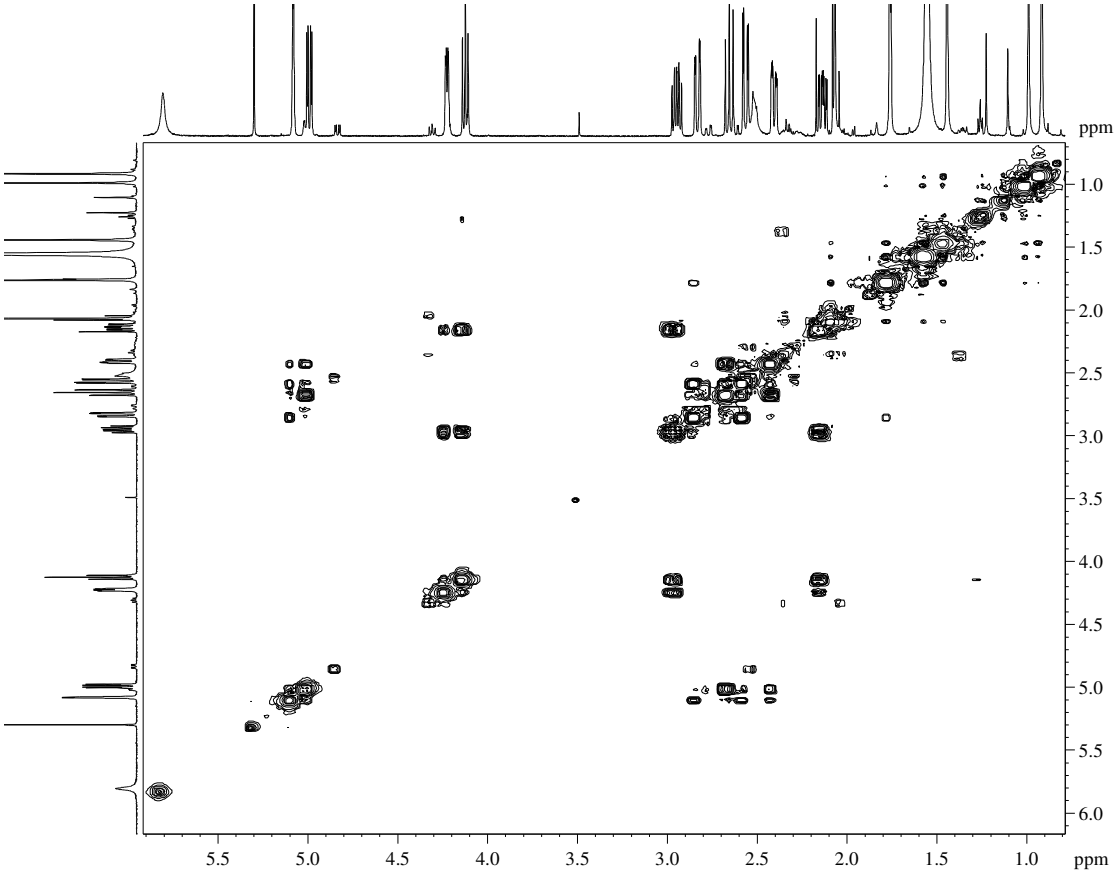

Figure S5.19 COSY NMR spectrum of compound **5.9**

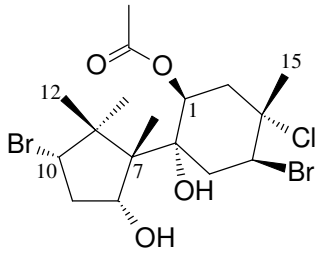

5.9

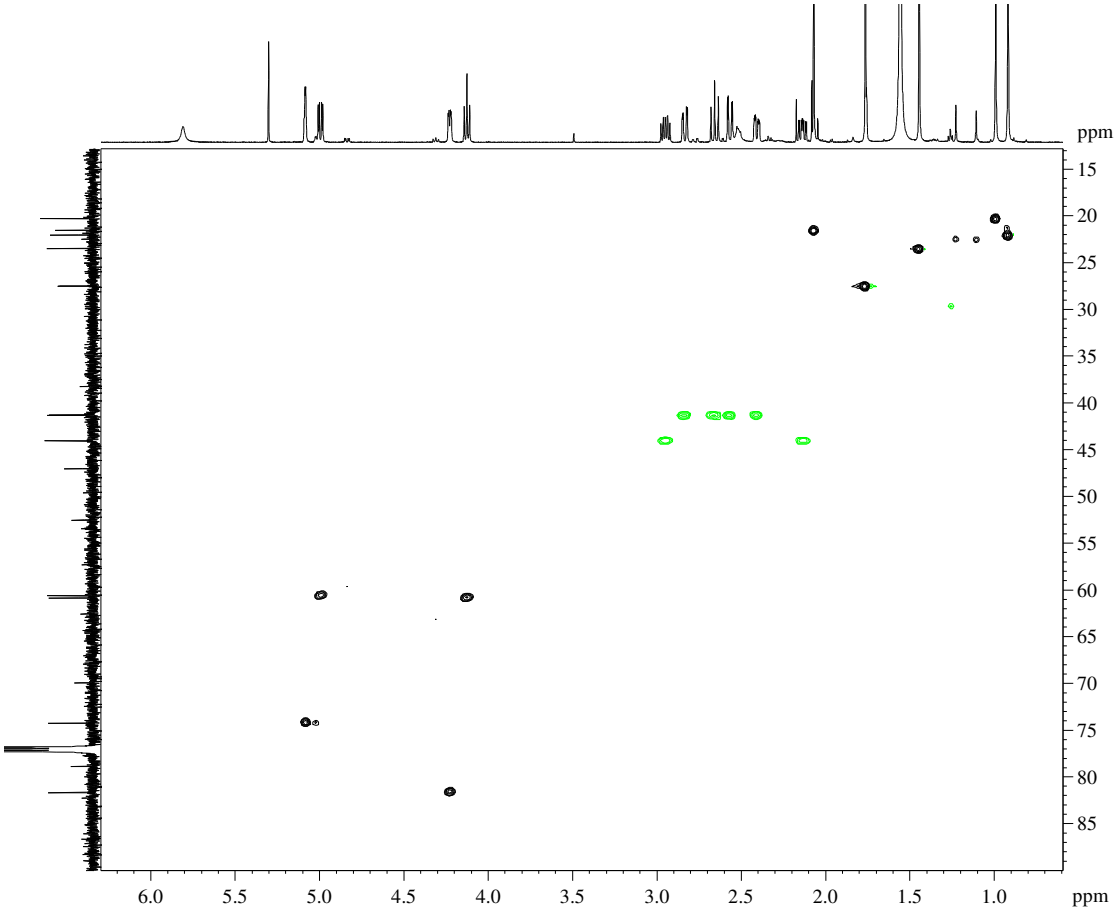

Figure S5.20 HSQC NMR spectrum of compound **5.9**

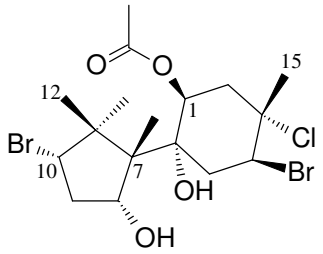

5.9

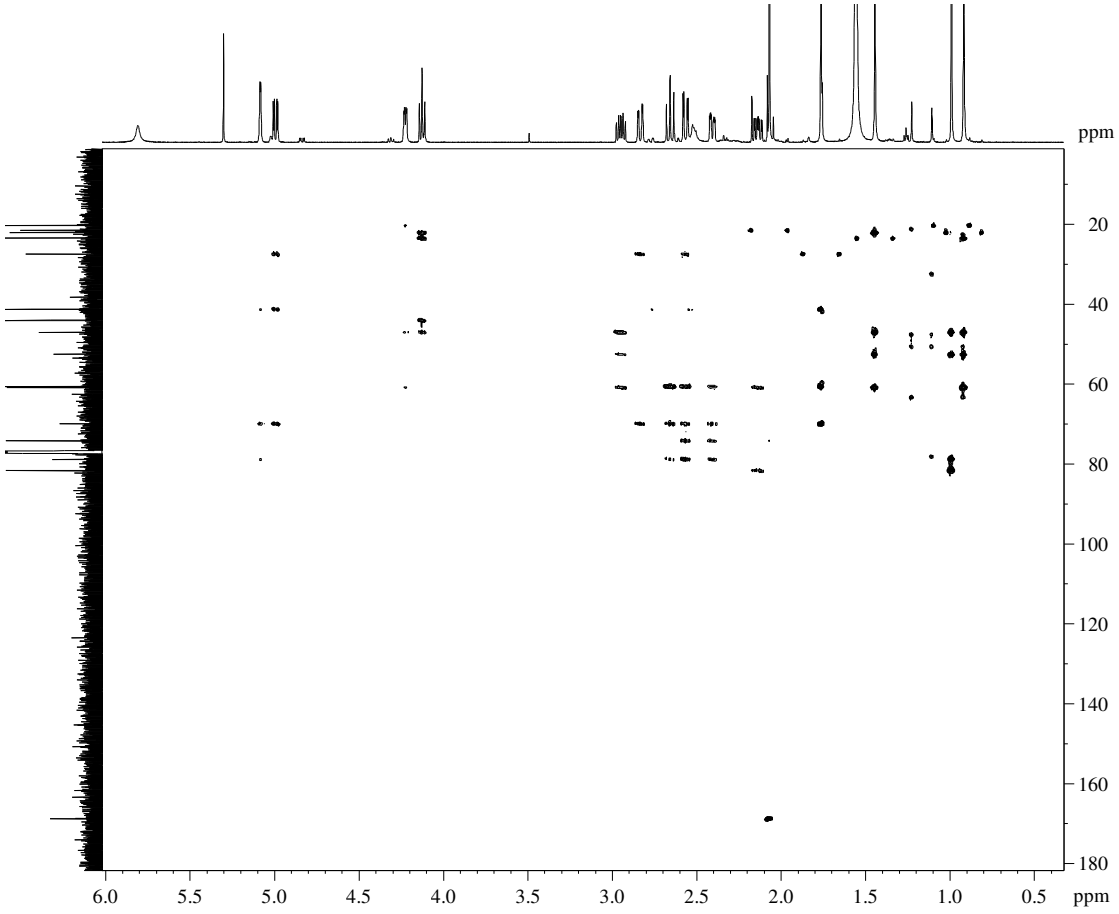

Figure S5.21 HMBC NMR spectrum of compound **5.9**

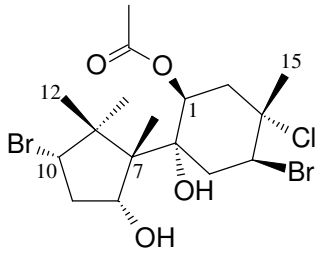

5.9

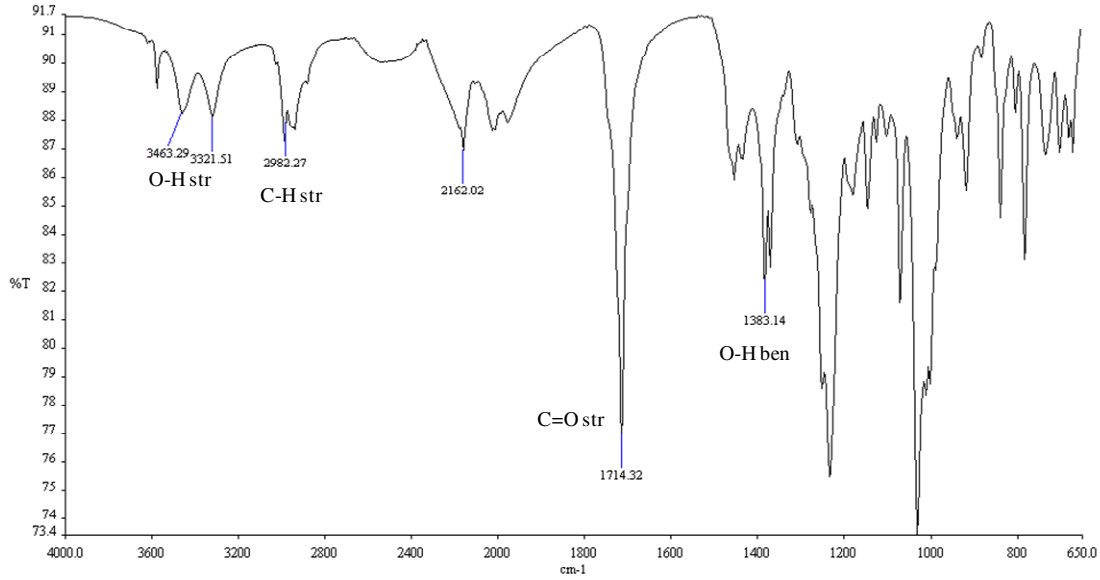

Figure S5.22 IR spectrum of compound **5.9**

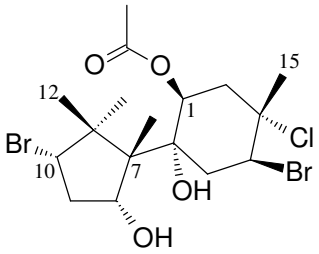

5.9

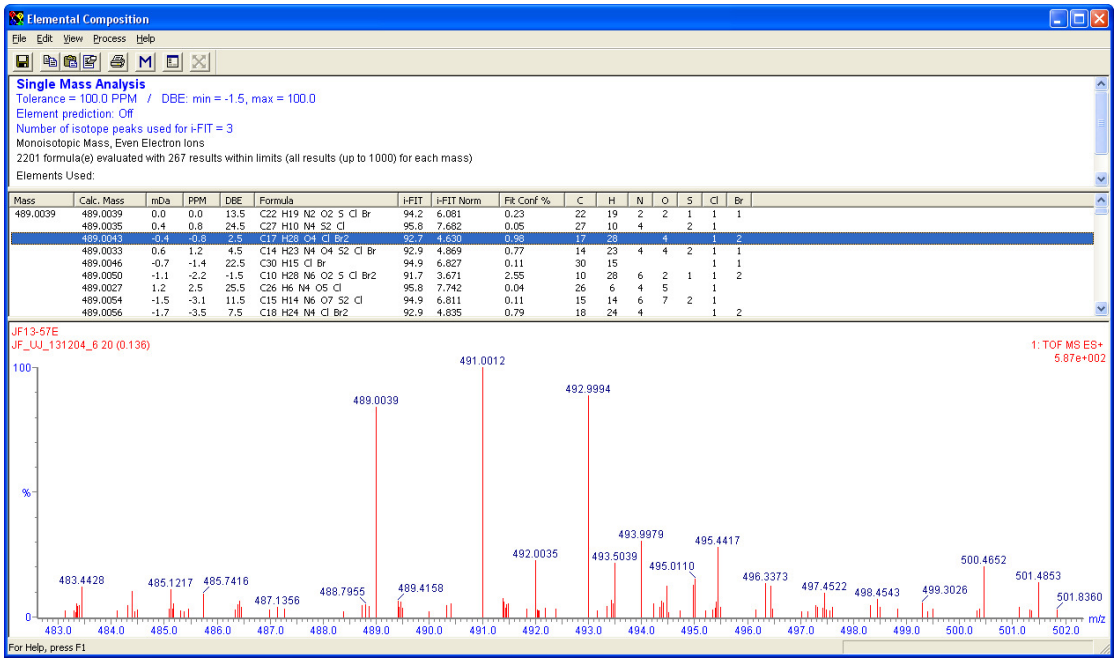

Figure S5.23 HRESIMS spectrum of compound **5.9**

S5.5 Compound 5.14

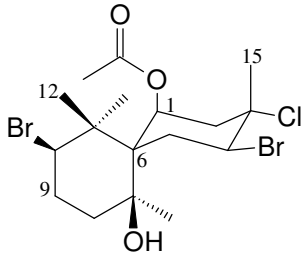

5.14

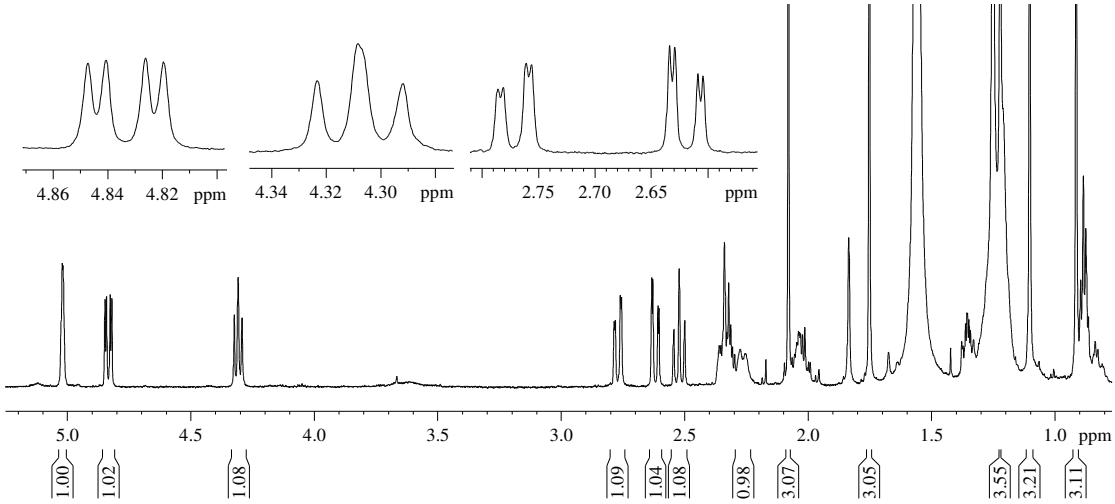

Figure S5.24 ^{1}H NMR spectrum ($CDCl_3$, 600 MHz) of compound **5.14**

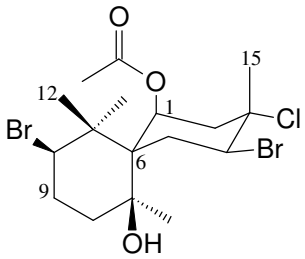

5.14

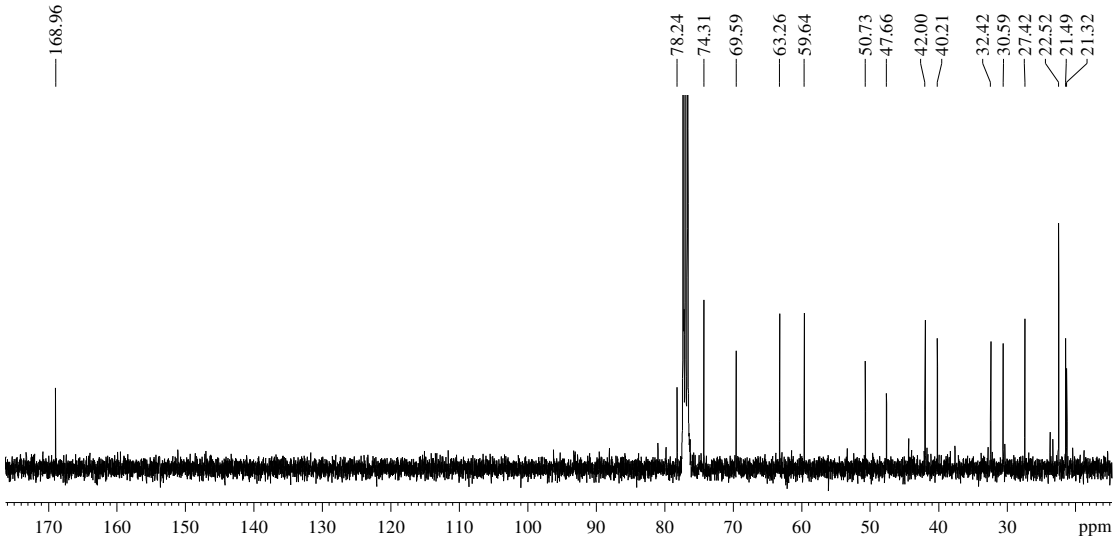

Figure S5.25 ^{13}C NMR spectrum ($CDCl_3$, 150 MHz) of compound **5.14**

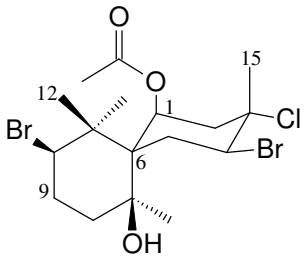

5.14

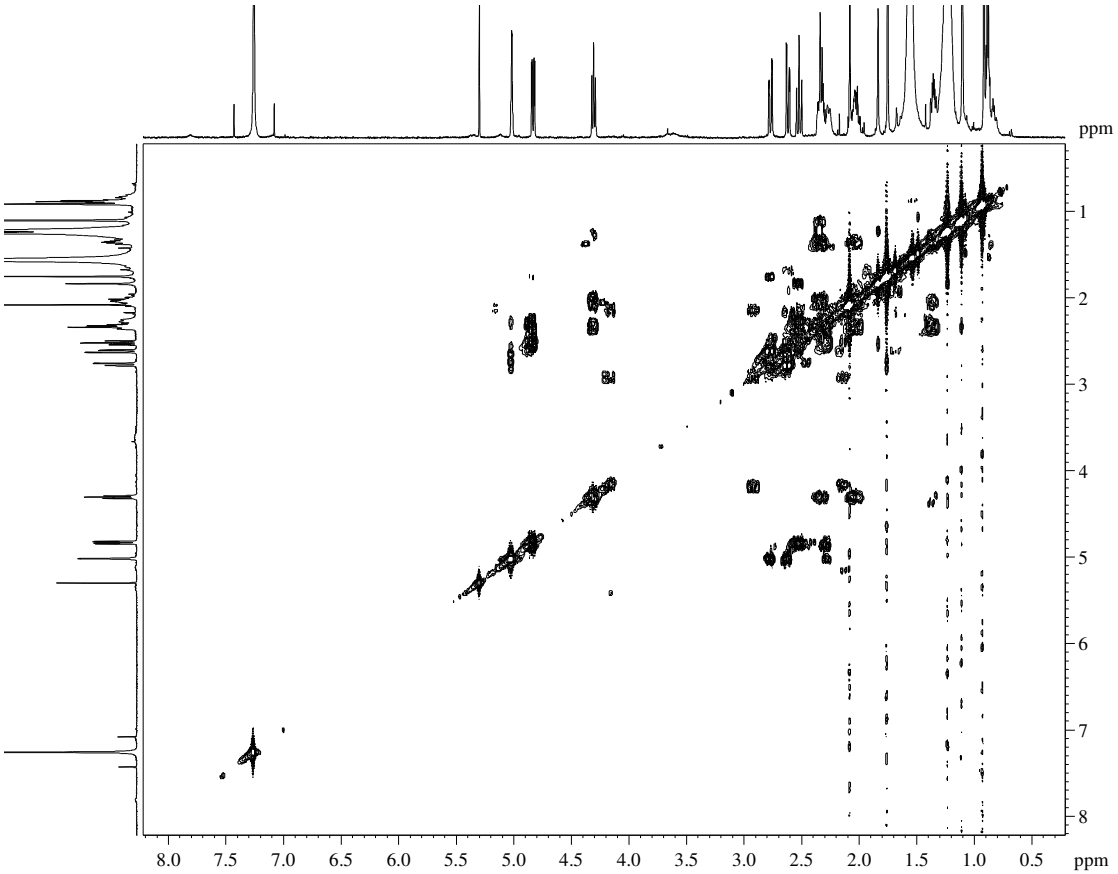

Figure S5.26 COSY NMR spectrum of compound **5.14**

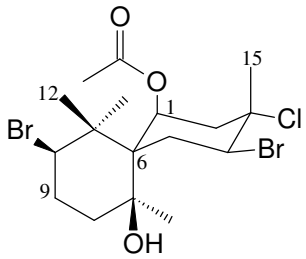

5.14

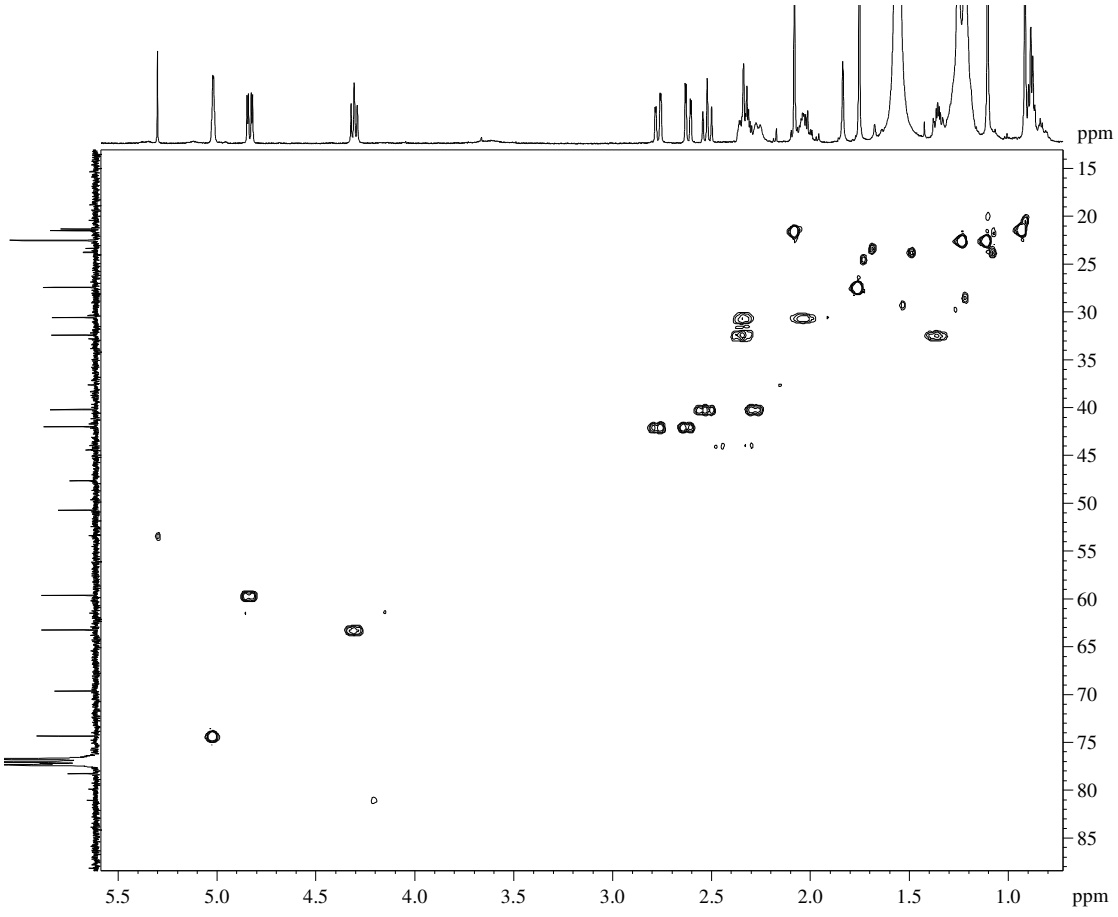

Figure S5.27 HSQC NMR spectrum of compound **5.14**

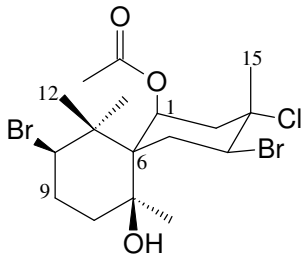

5.14

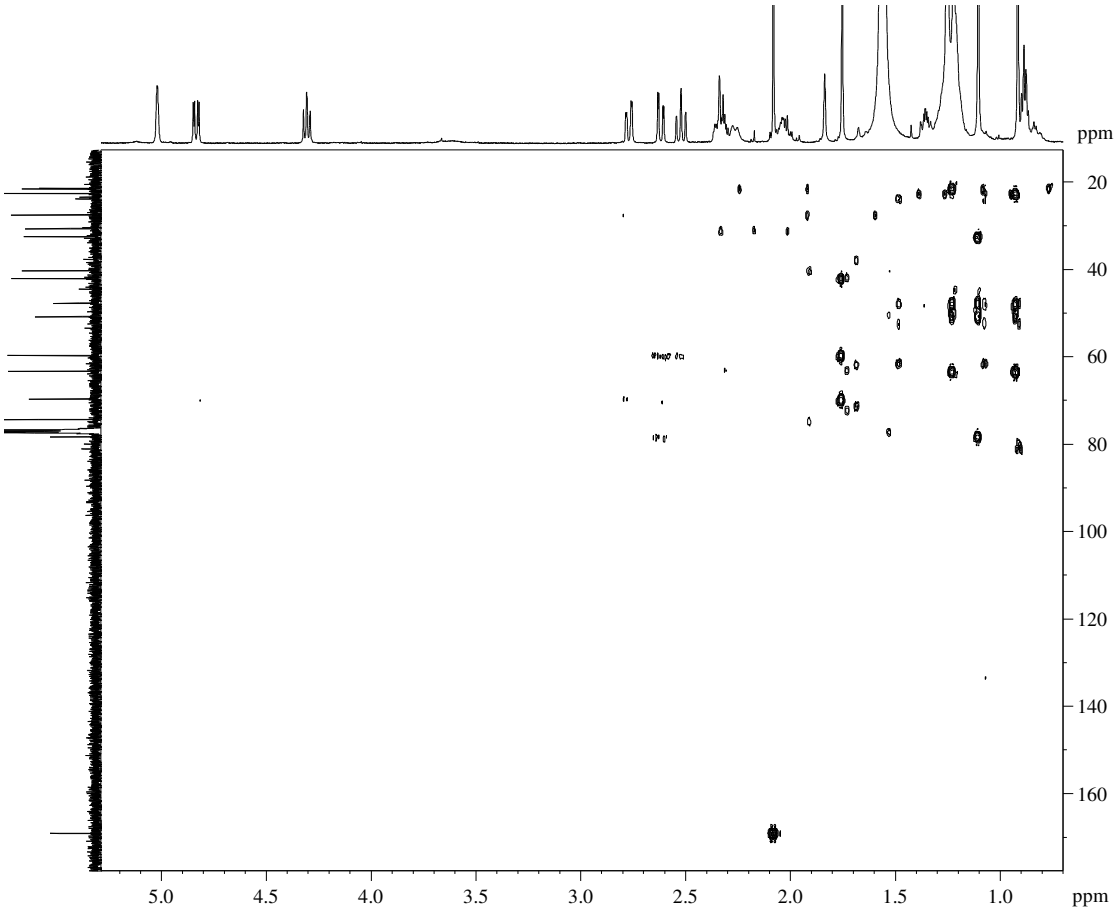

Figure S5.28 HMBC NMR spectrum of compound **5.14**

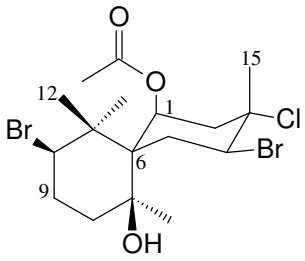

5.14

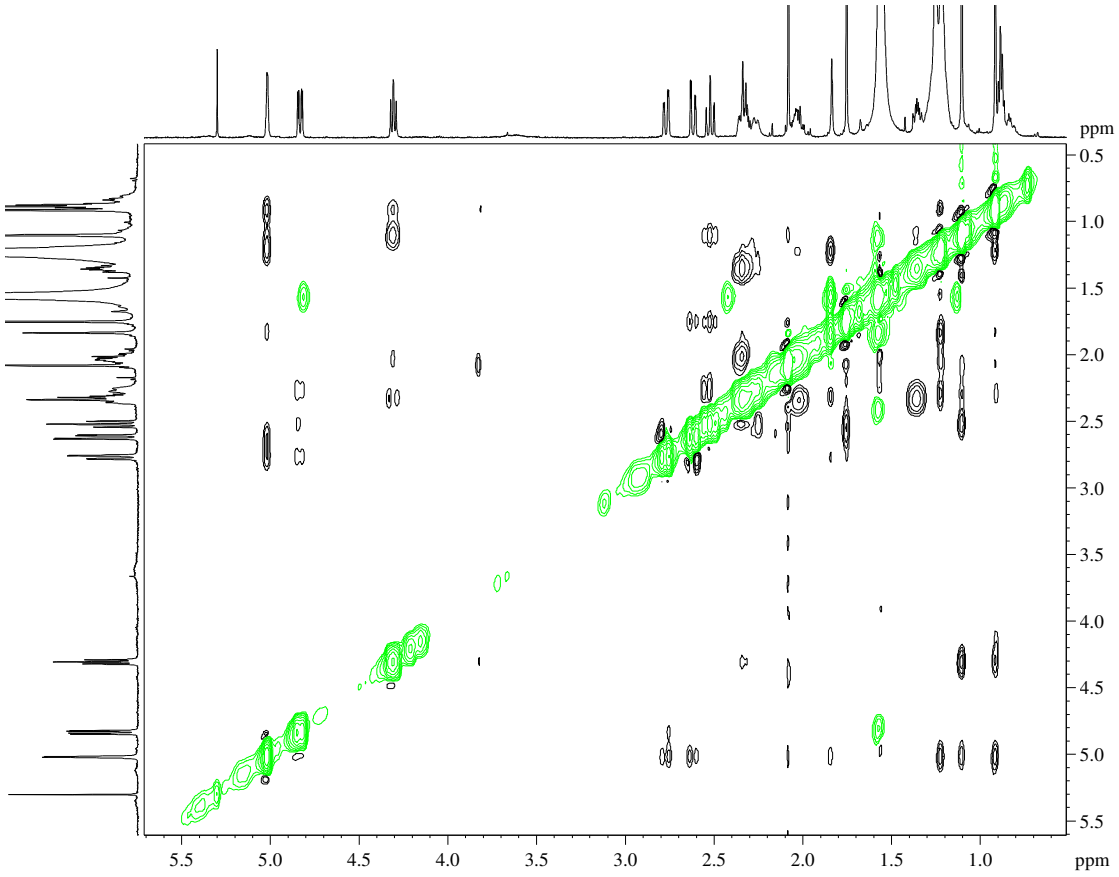

Figure S5.29 NOESY spectrum of compound **5.14**

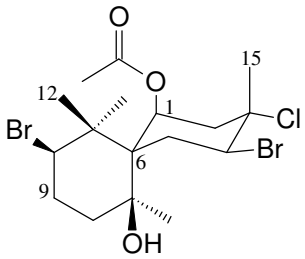

5.14

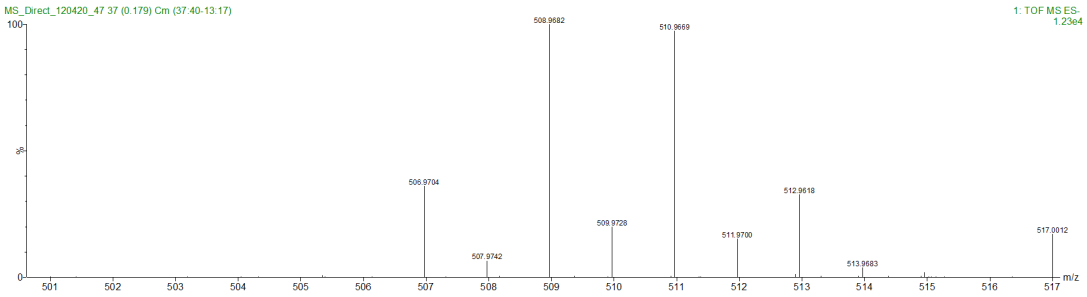

Figure S5.30 HRESIMS spectrum of compound **5.14**

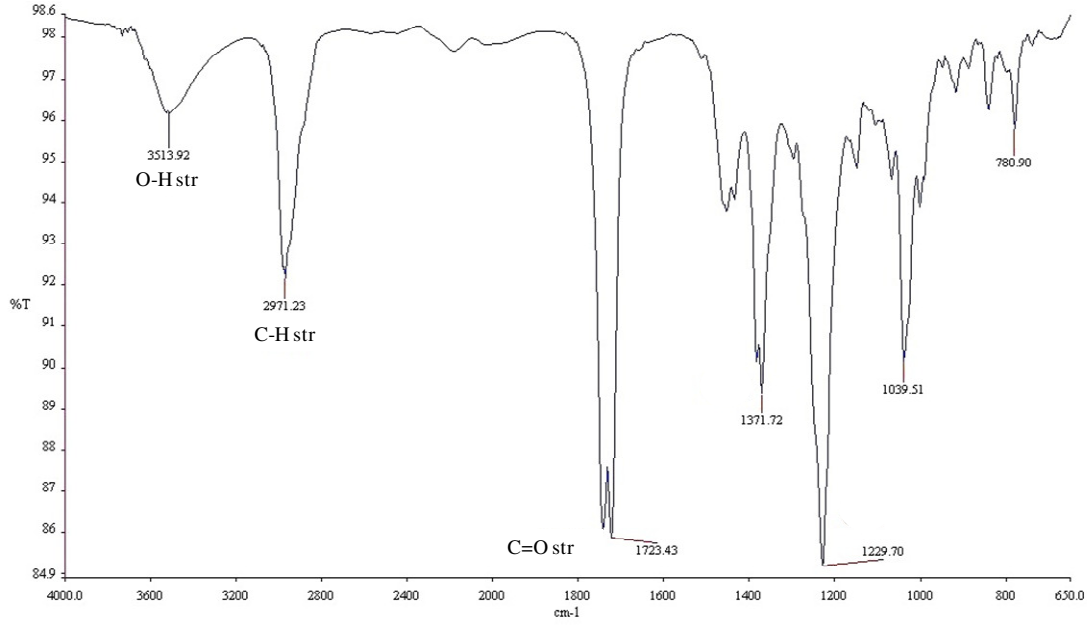

Figure S5.31 HRESIMS spectrum of compound **5.14**

Chapter 6

Secondary metabolites from *Laurencia complanata*

S6.1 Compound 6.1

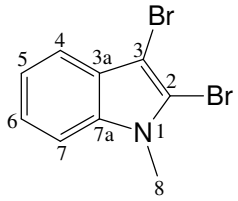

6.1

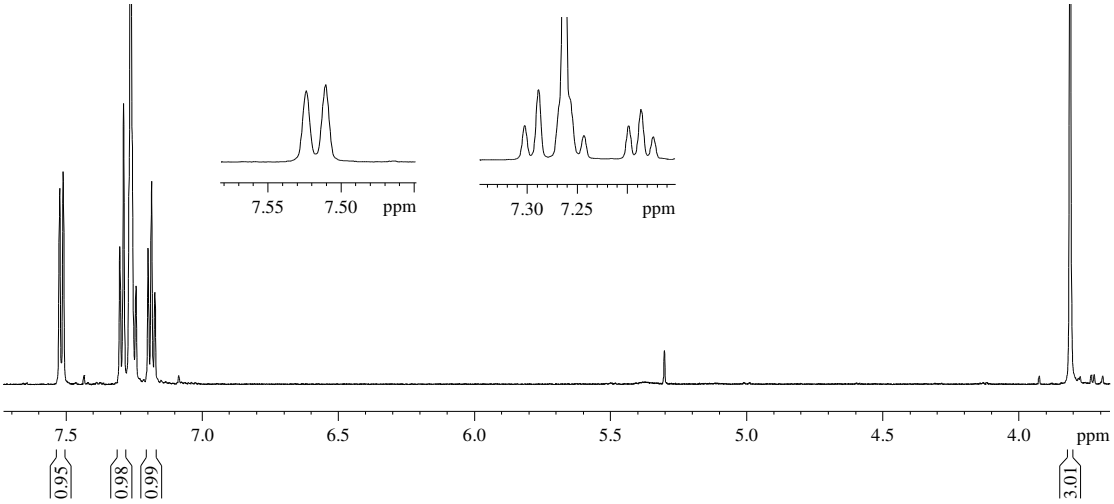

Figure S6.1: ^{1}H NMR spectrum ($CDCl_3$, 600 MHz) of compound **6.1**

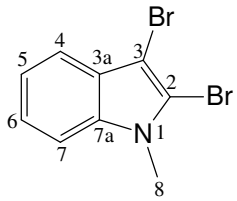

6.1

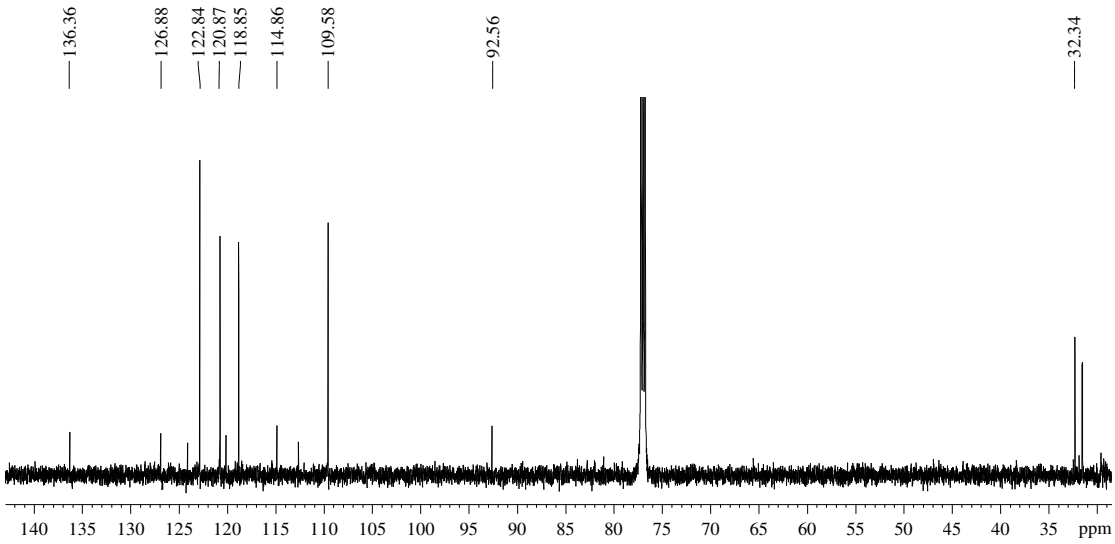

Figure S6.2: ^{13}C NMR spectrum ($CDCl_3$, 150 MHz) of compound **6.1**

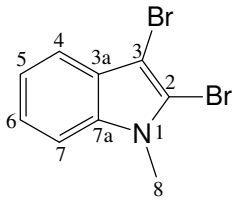

6.1

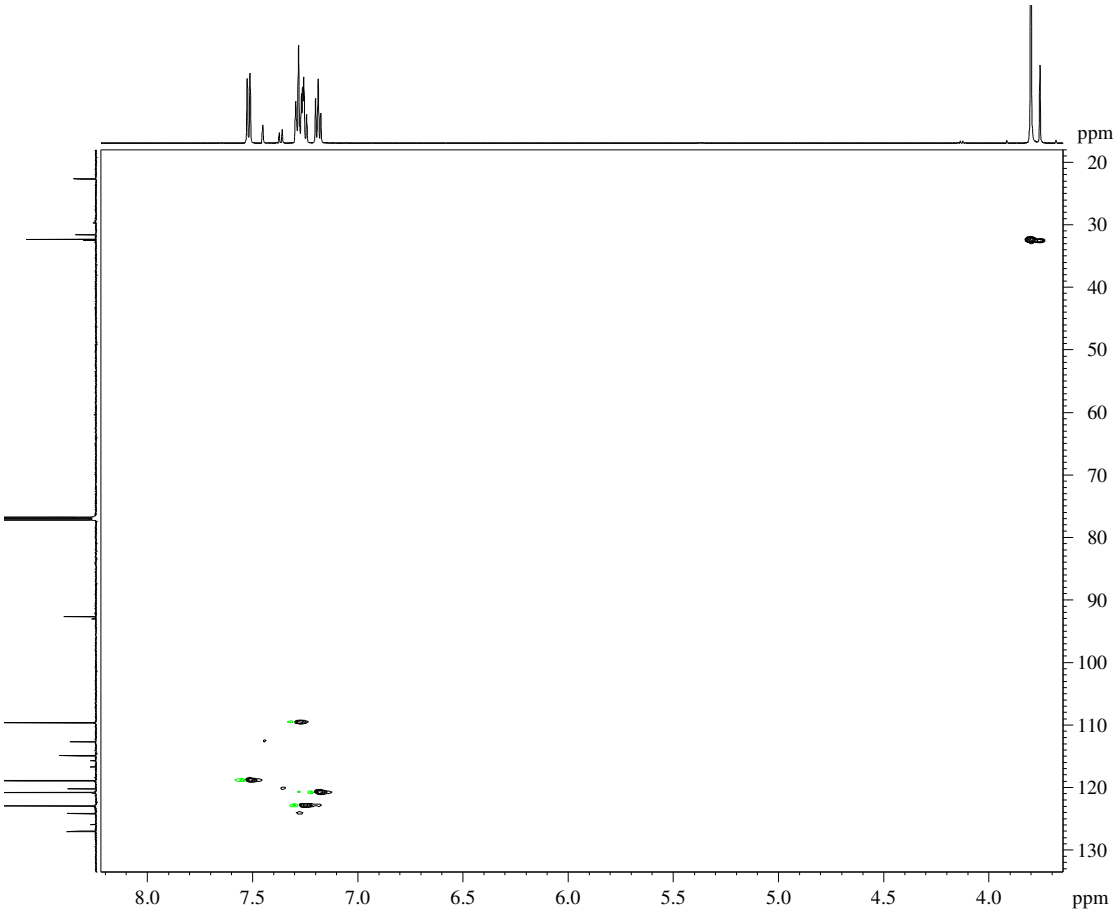

Figure S6.3: HSQC NMR spectrum of compound **6.1**

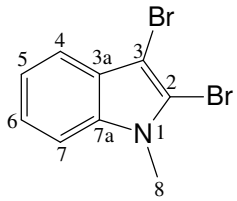

6.1

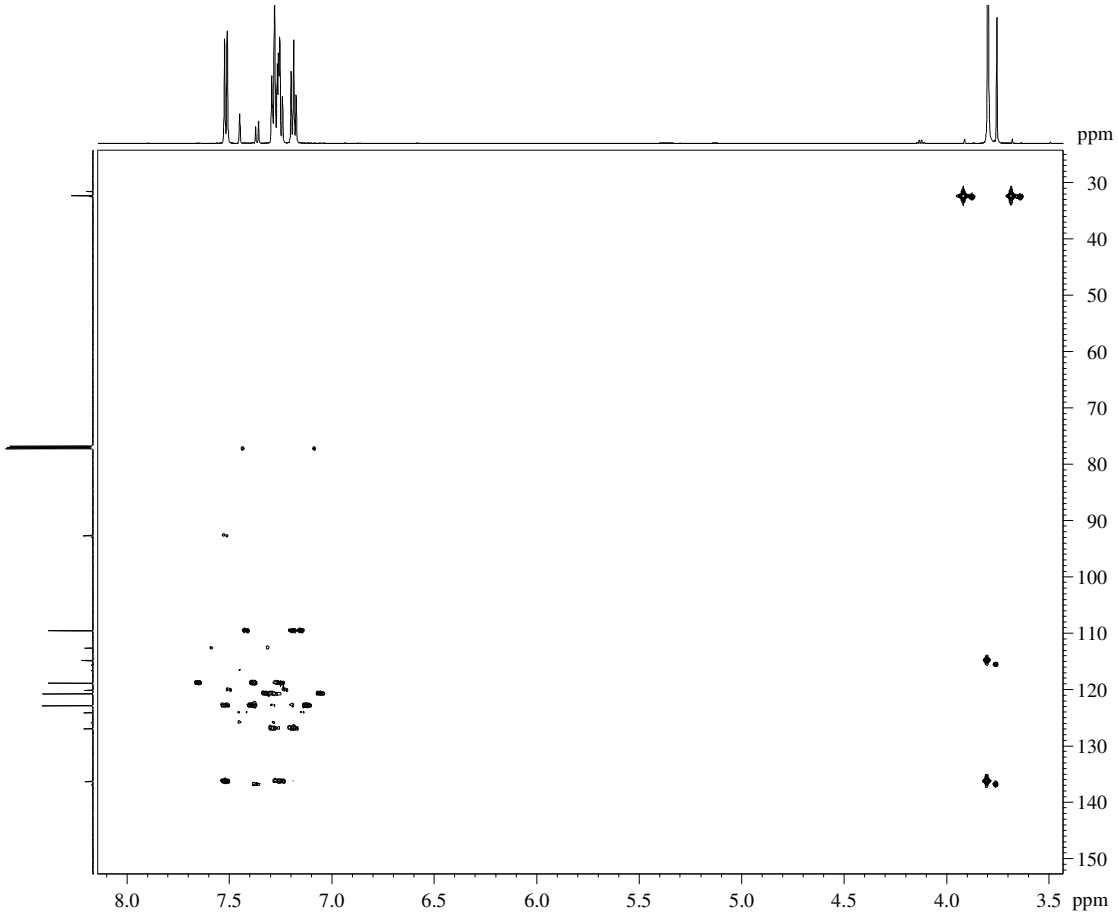

Figure S6.4: HMBC NMR spectrum of compound **6.1**

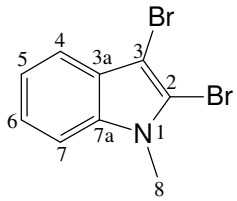

6.1

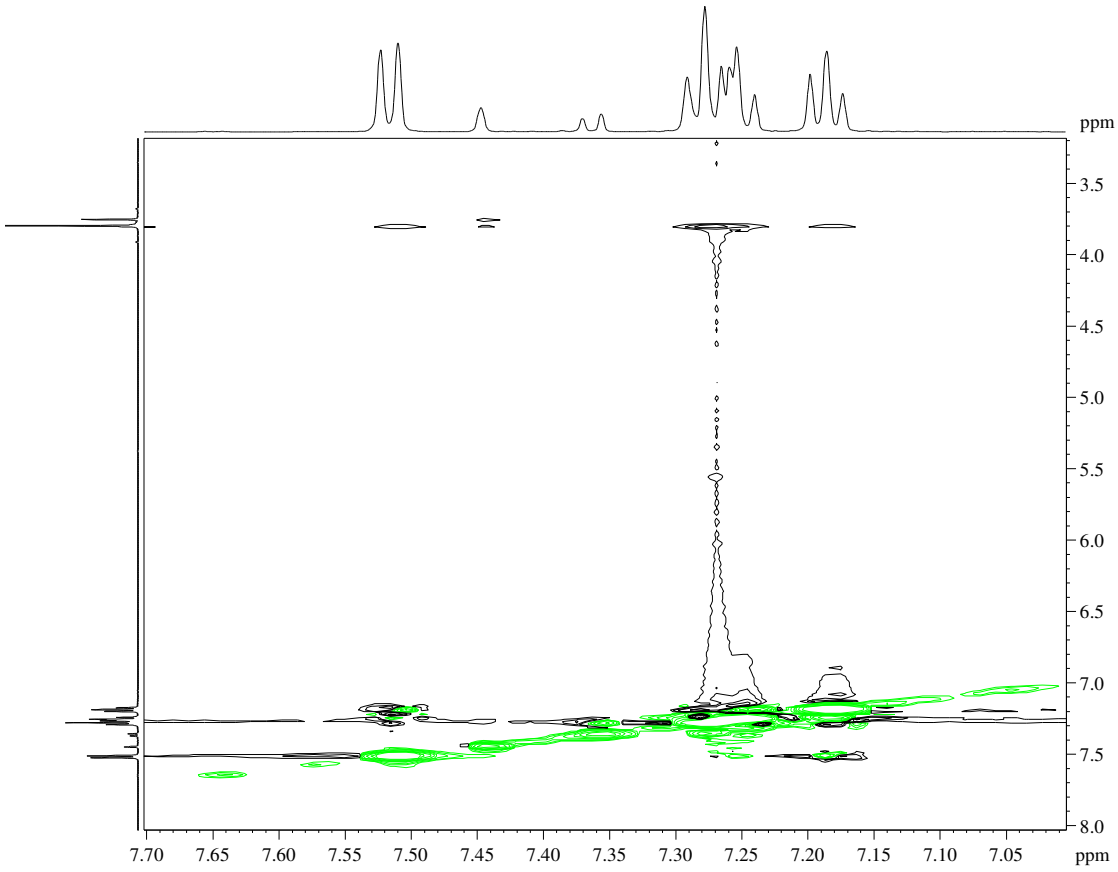

Figure S6.5: Expanded NOESY NMR spectrum of compound **6.1**

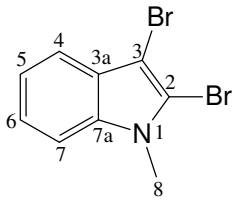

6.1

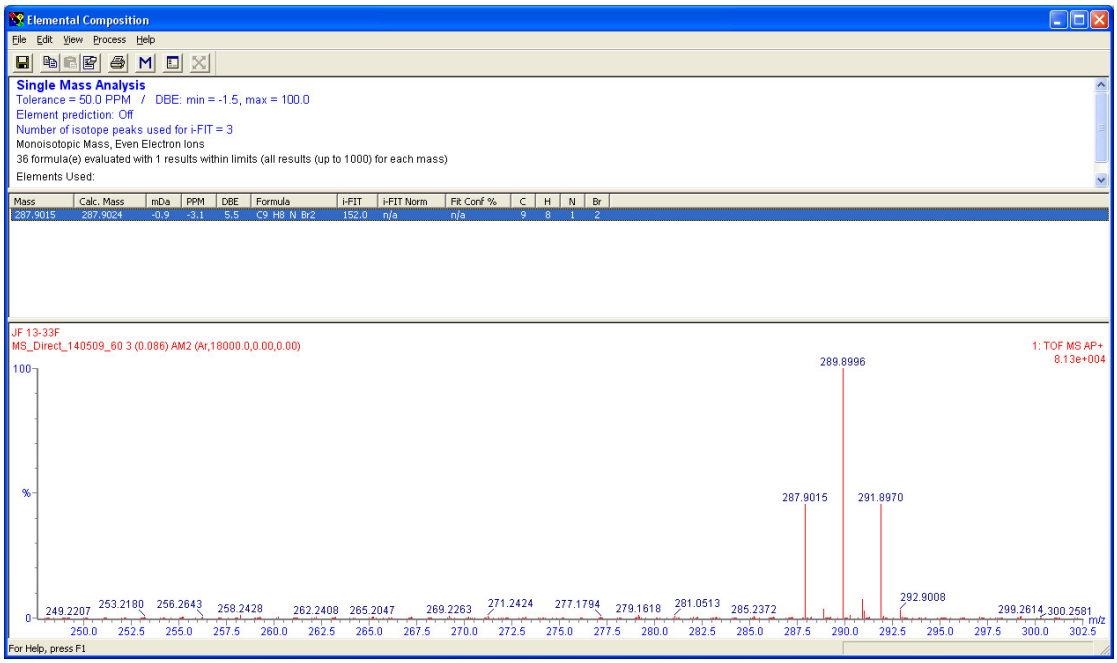

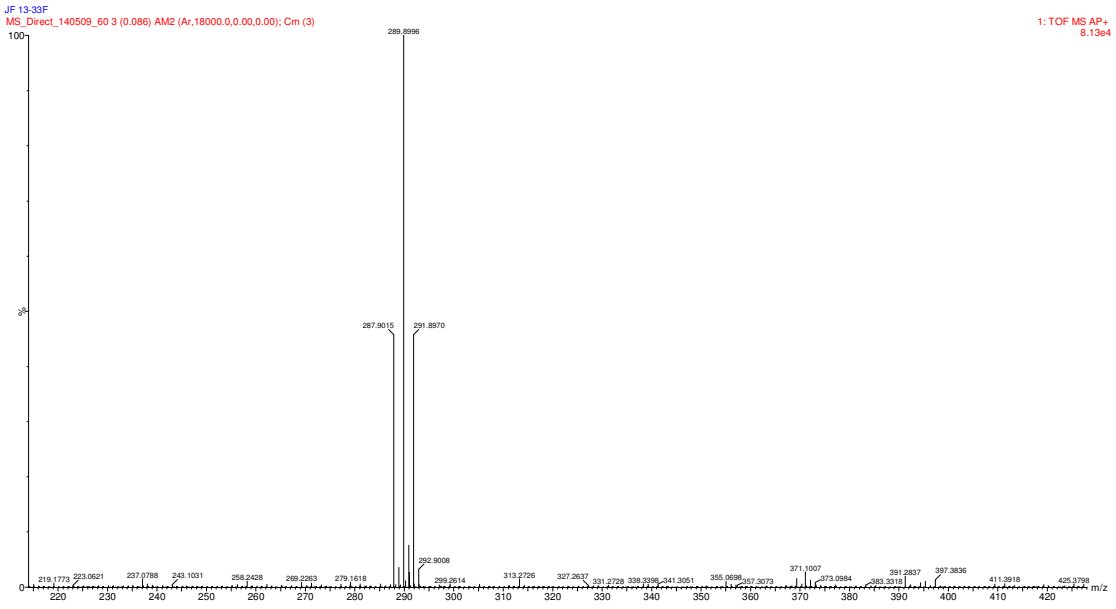

Figure S6.6: HRAPCIMS spectrum of compound **6.1**

S6.2 Compound 6.2

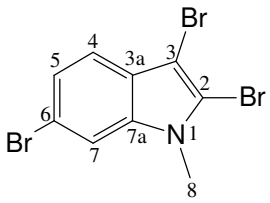

6.2

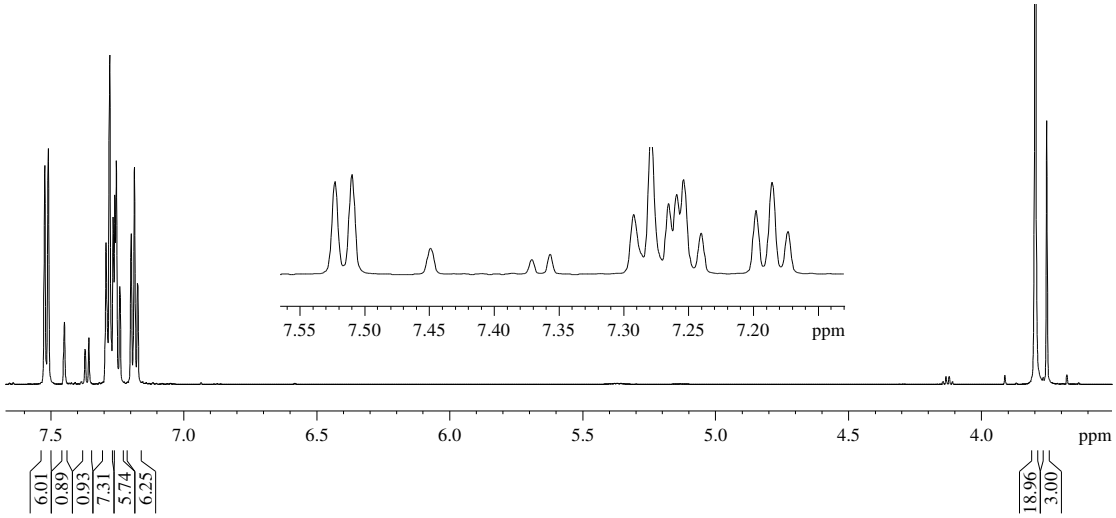

Figure S6.7: ^{1}H NMR spectrum ($CDCl_3$, 600 MHz) of compound **6.2**

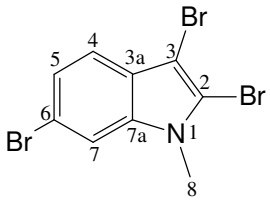

6.2

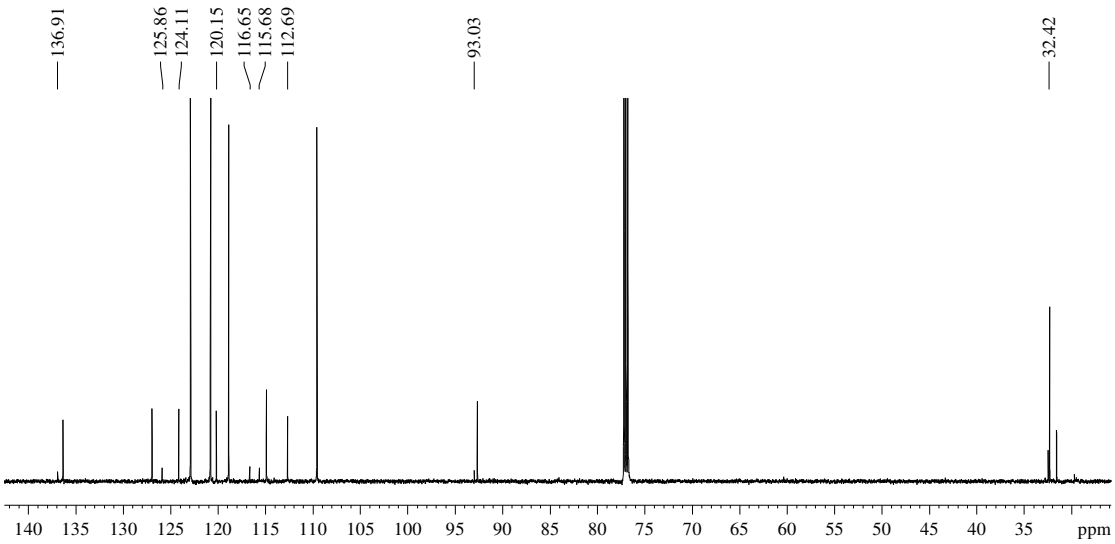

Figure S6.8: ^{13}C NMR spectrum ($CDCl_3$, 150 MHz) of compound **6.2**

Please note that NOESY correlations for compound **6.2** were obtained by analysis of NOESY spectrum of **6.1** (Figure S6.5), as the fraction contained a mixture of the two compounds.

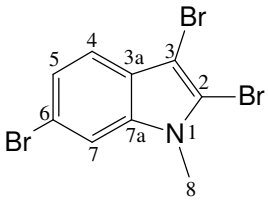

6.2

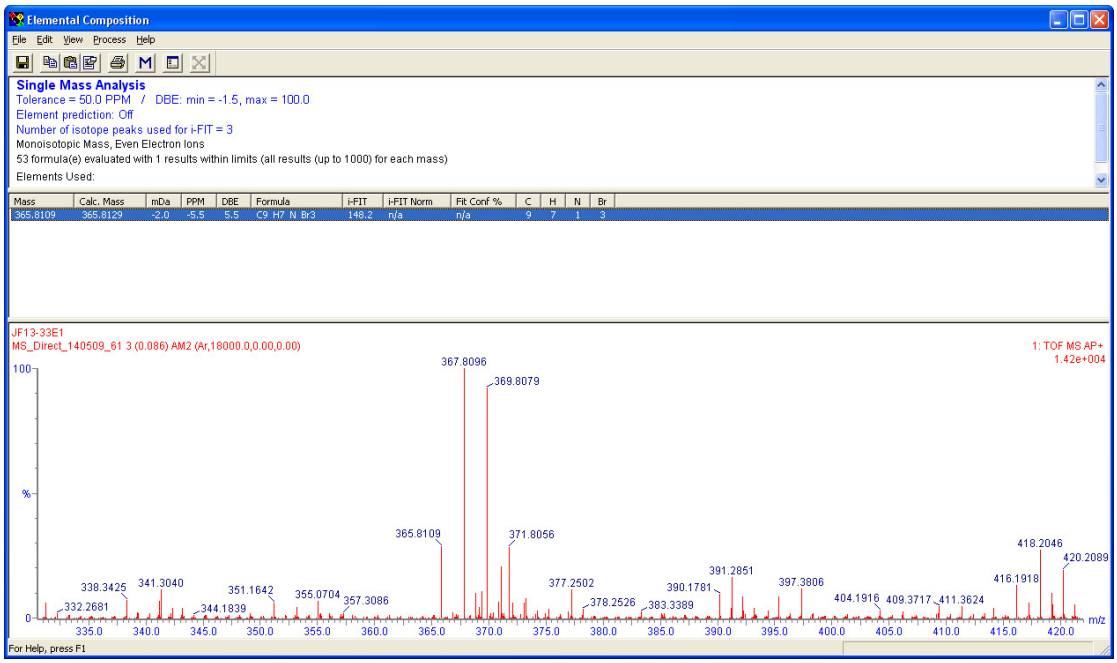

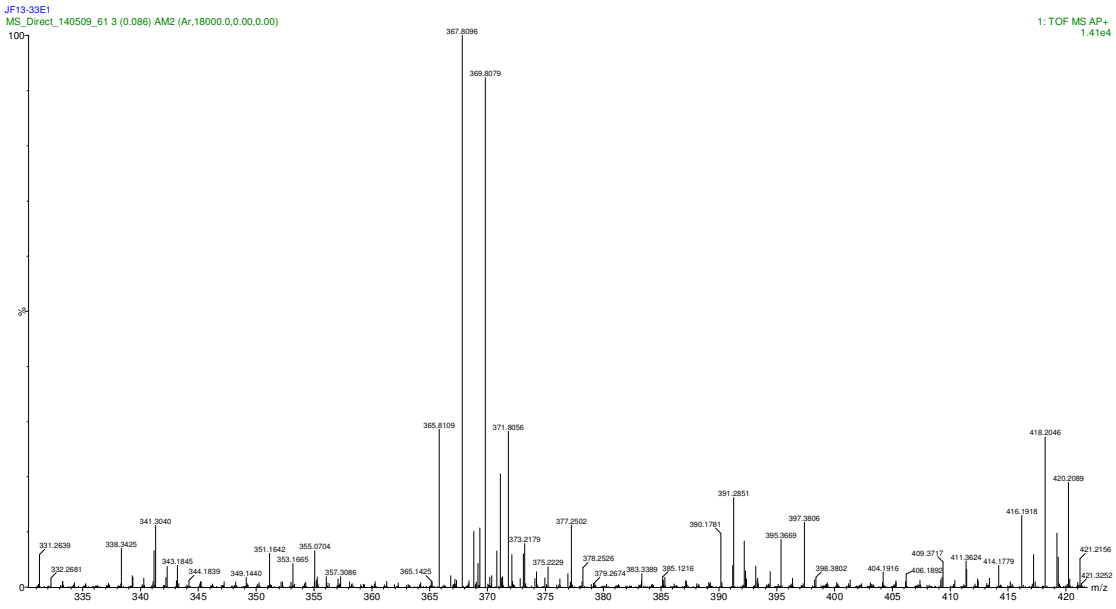

Figure S6.9: HRAPCIMS spectrum of compound **6.2**

S6.3 Compound 6.3

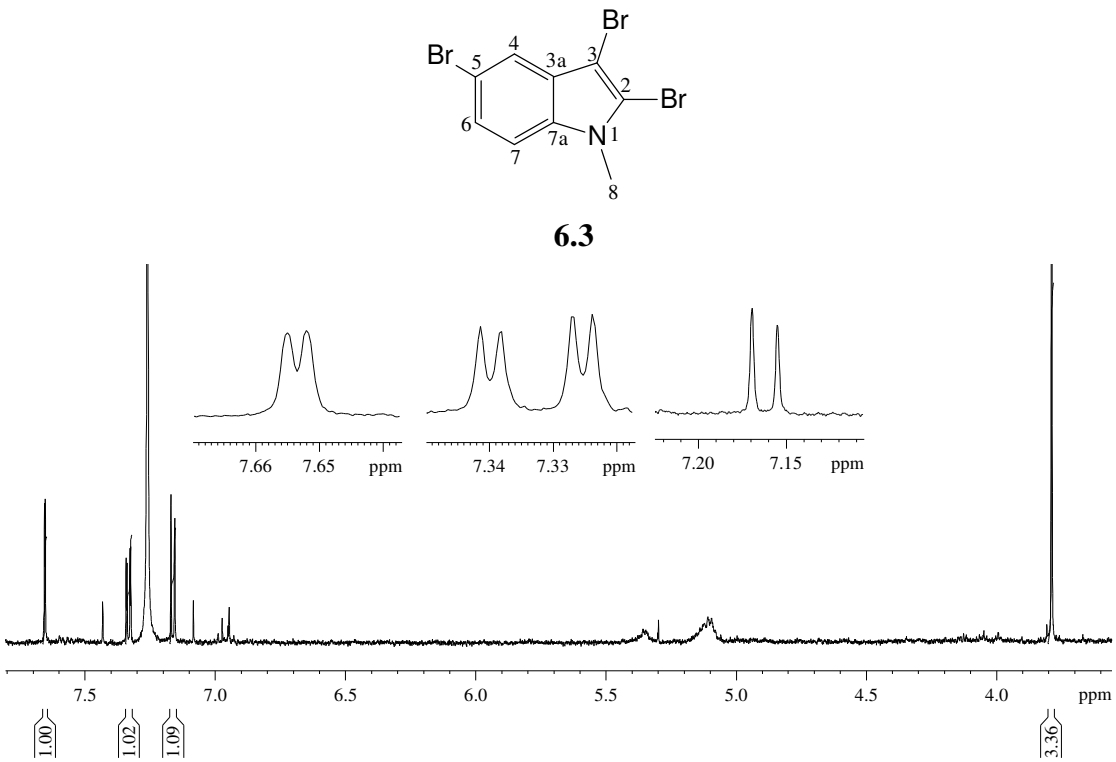

6.3

Figure S6.10: ^{1}H NMR spectrum ($CDCl_3$, 600 MHz) of compound **6.3**

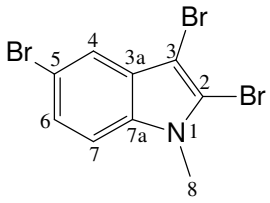

6.3

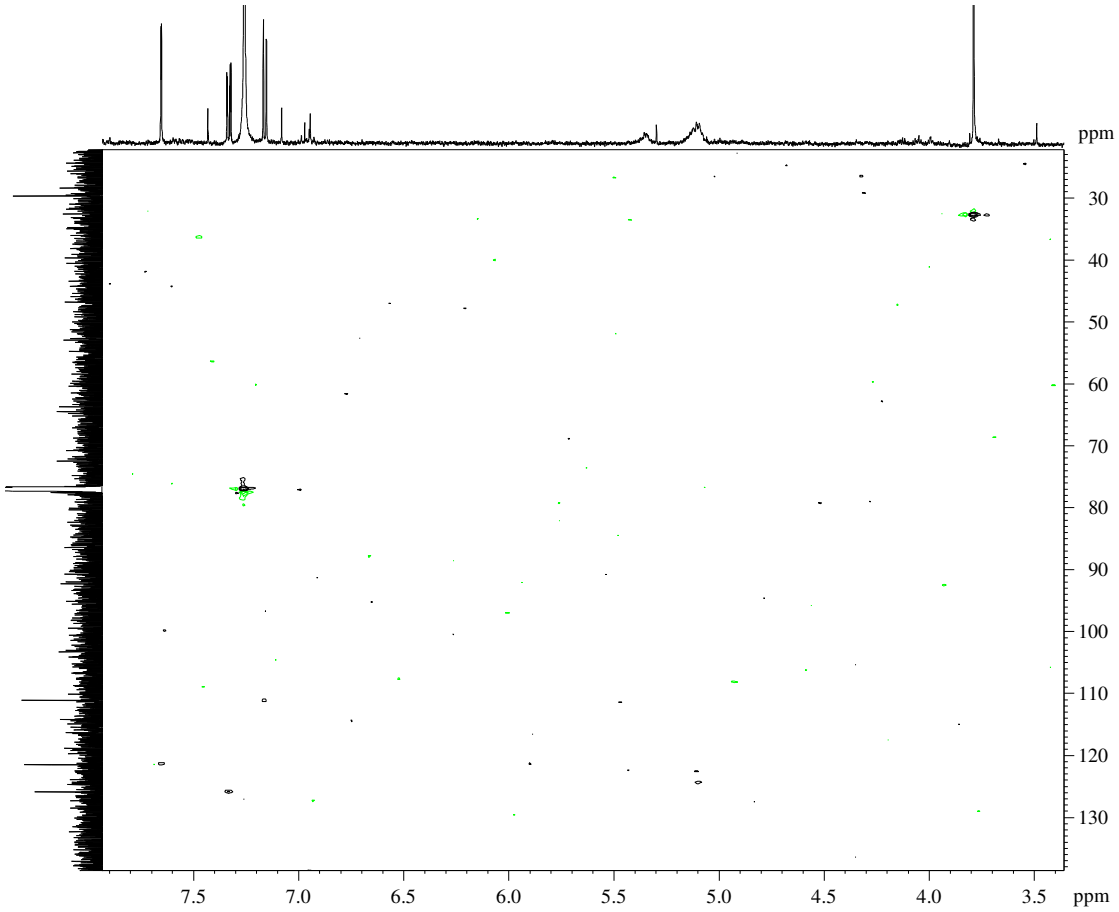

Figure S6.11: HSQC NMR spectrum of compound **6.3**

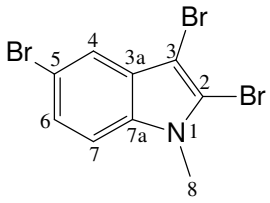

6.3

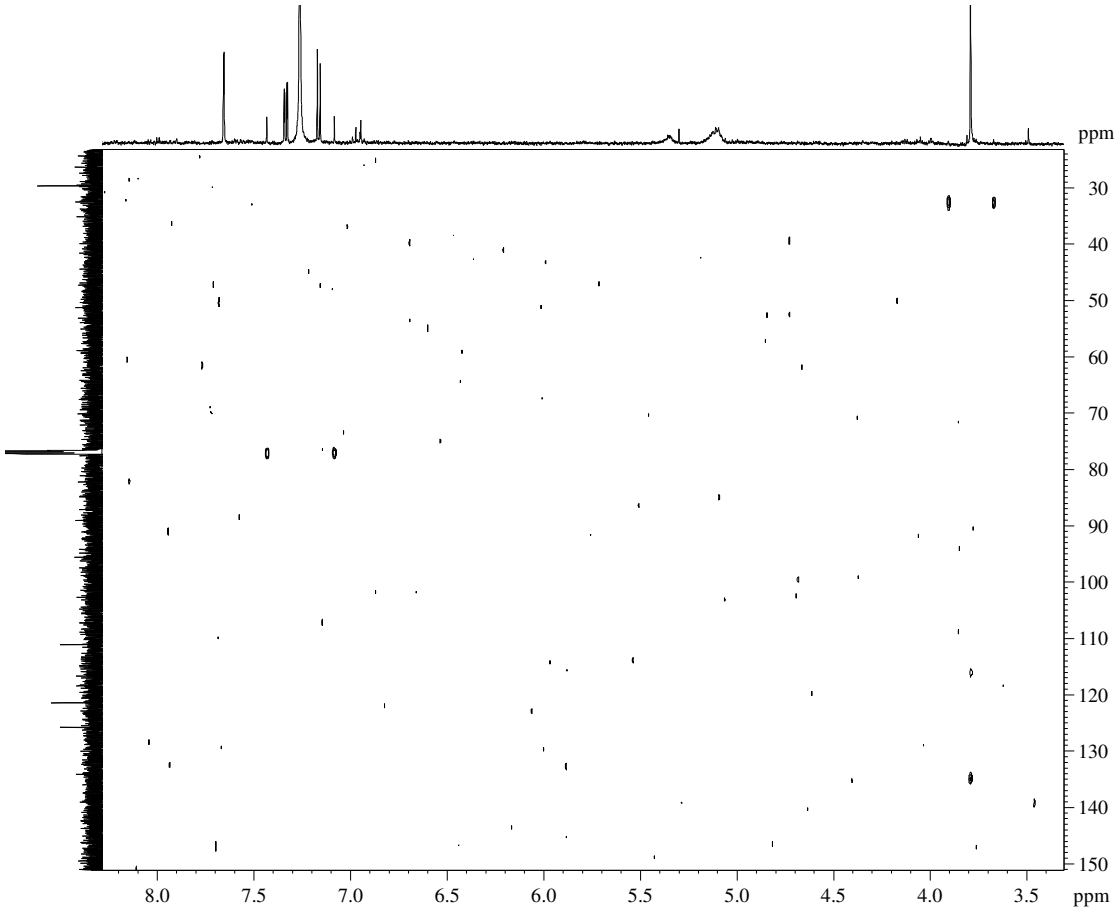

Figure S6.12: HMBC NMR spectrum of compound **6.3**

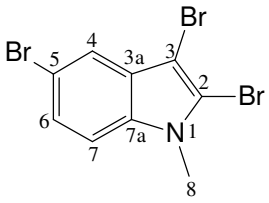

6.3

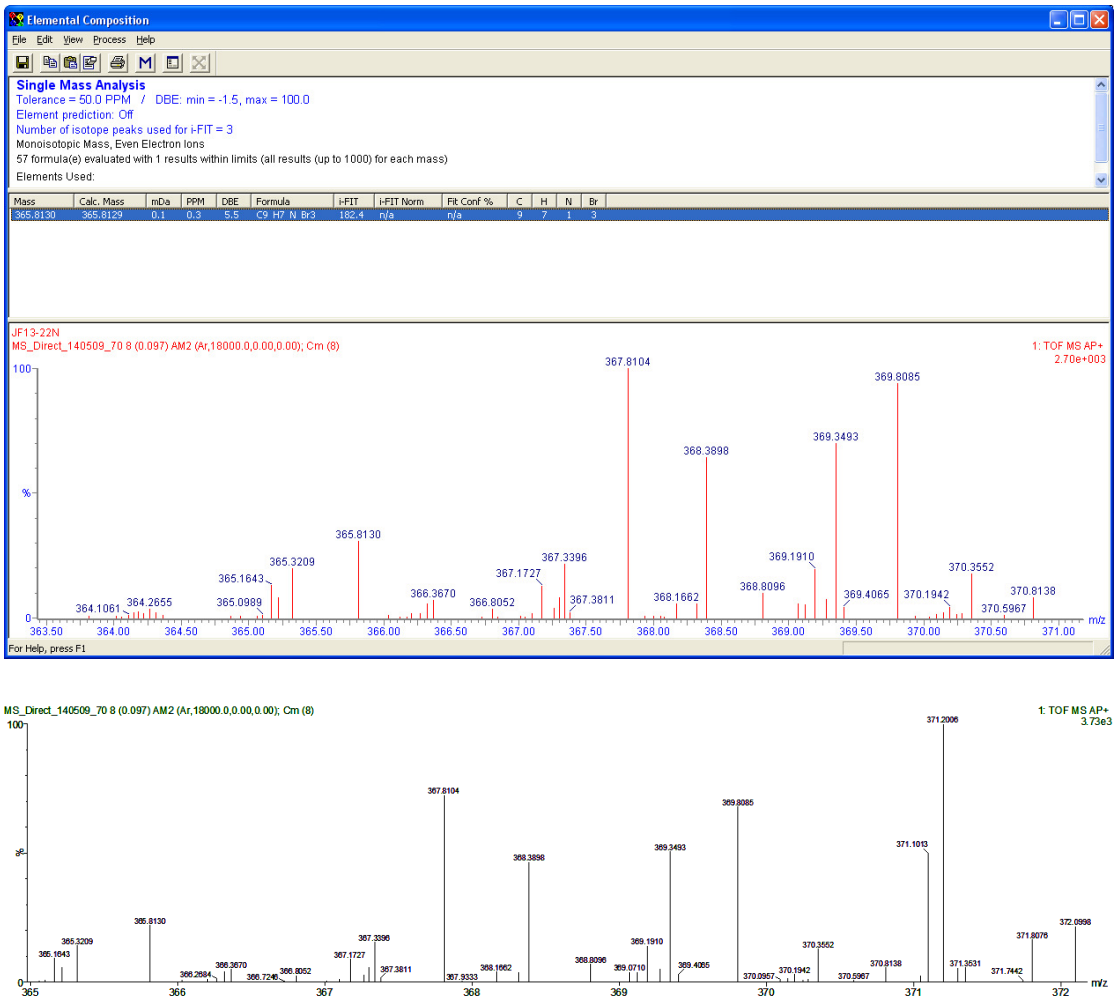

Figure S6.13: HRAPCIMS spectrum of compound **6.3**

S6.4 Compound 6.4

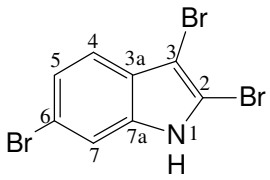

6.4

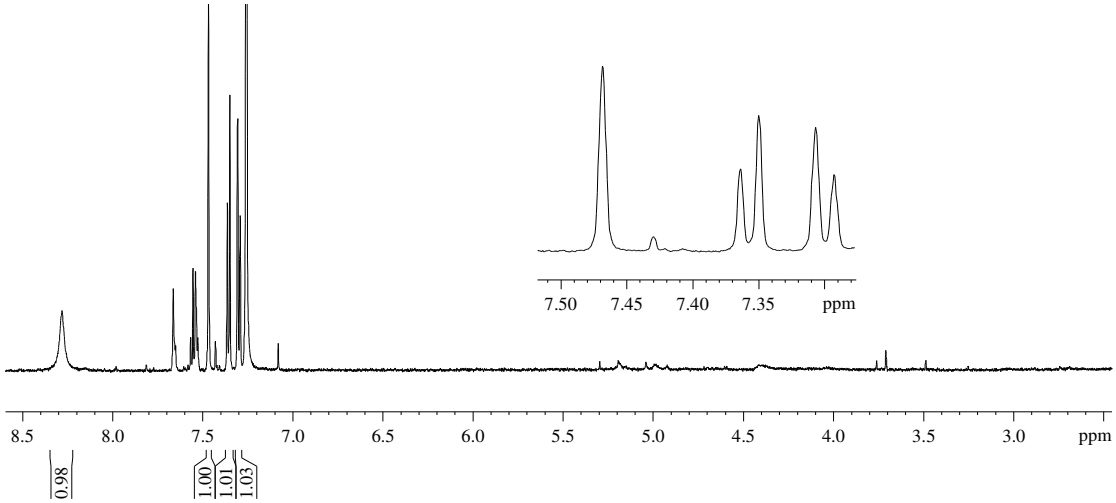

Figure S6.14: ^{1}H NMR spectrum ($CDCl_3$, 600 MHz) of compound **6.4**

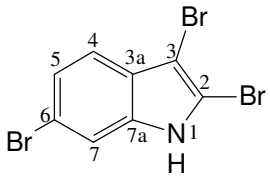

6.4

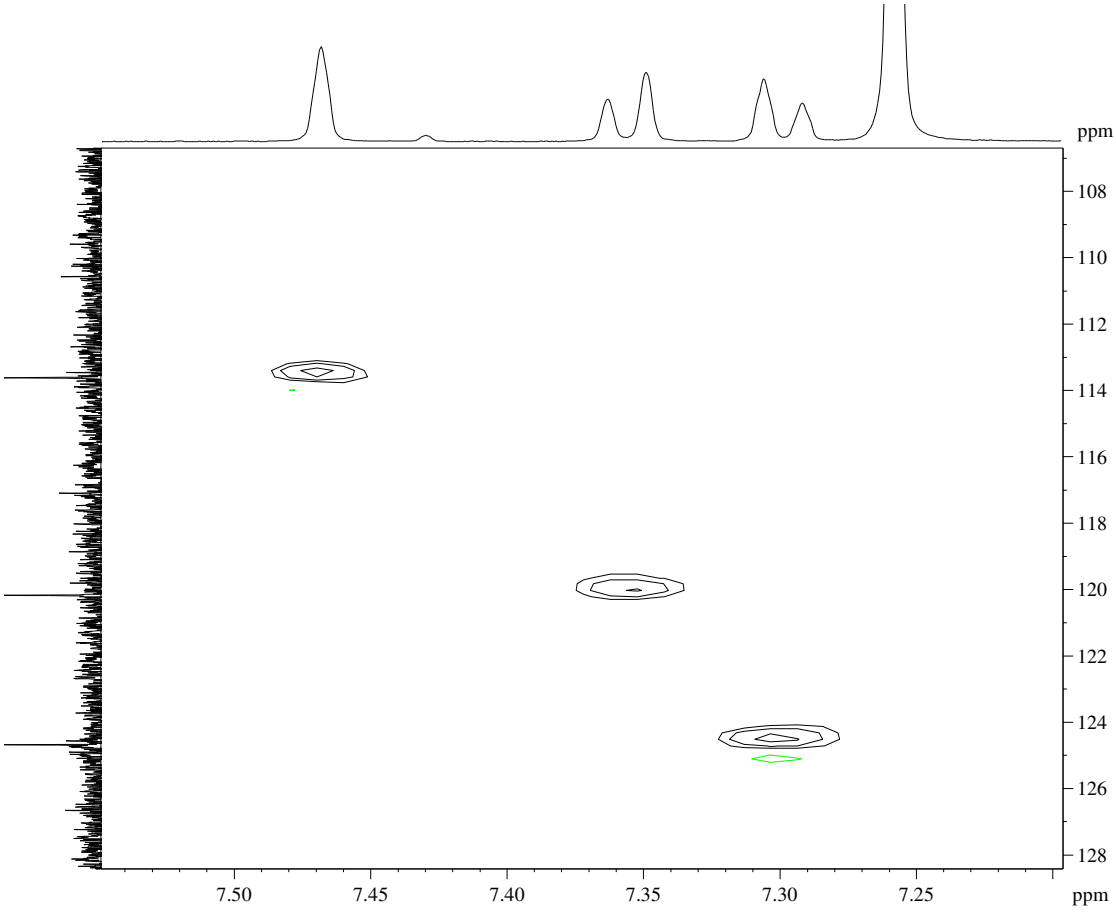

Figure S6.15: Expanded HSQC NMR spectrum of compound **6.4**

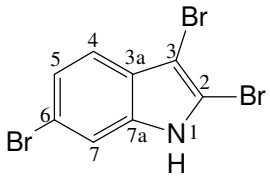

6.4

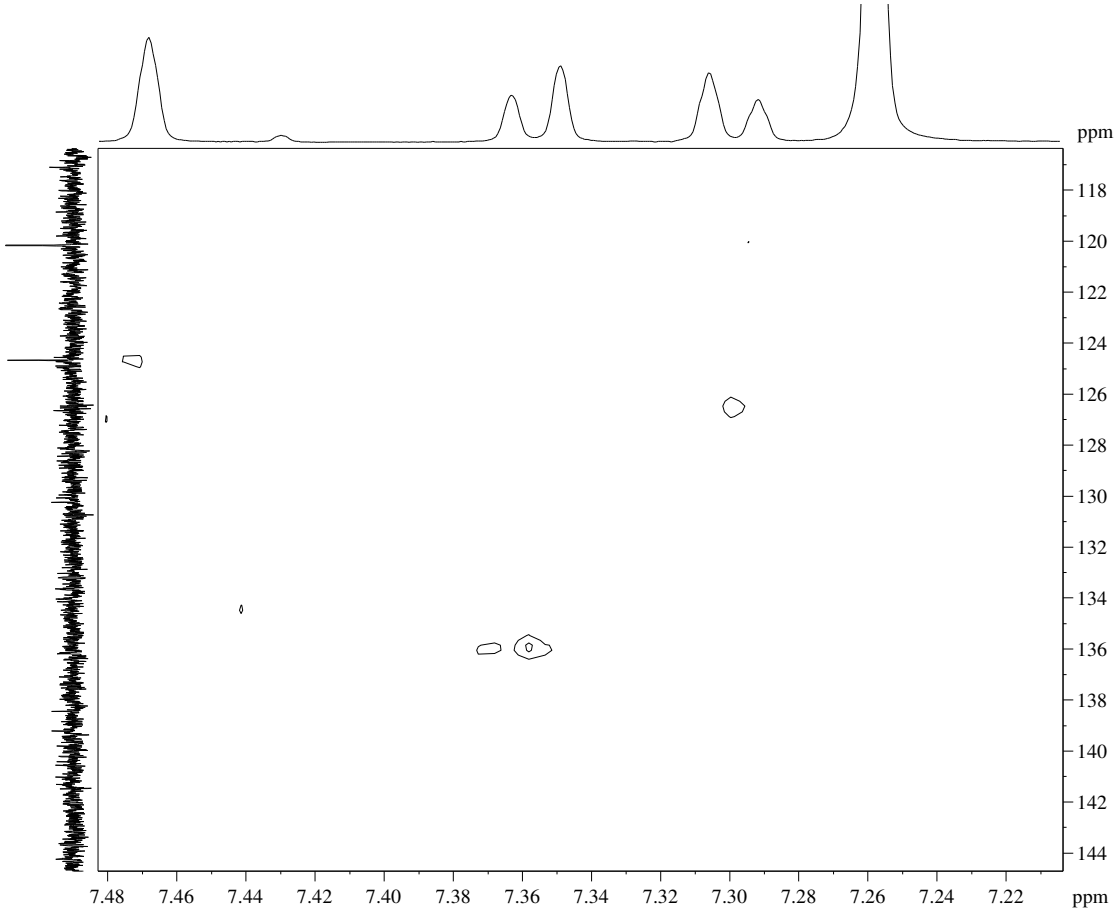

Figure S6.16: Expanded HMBC NMR spectrum of compound **6.4** showing quaternary carbons at δ_C 126.7 and δ_C 136.2

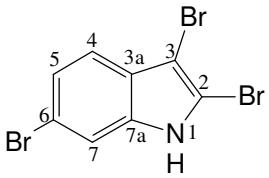

6.4

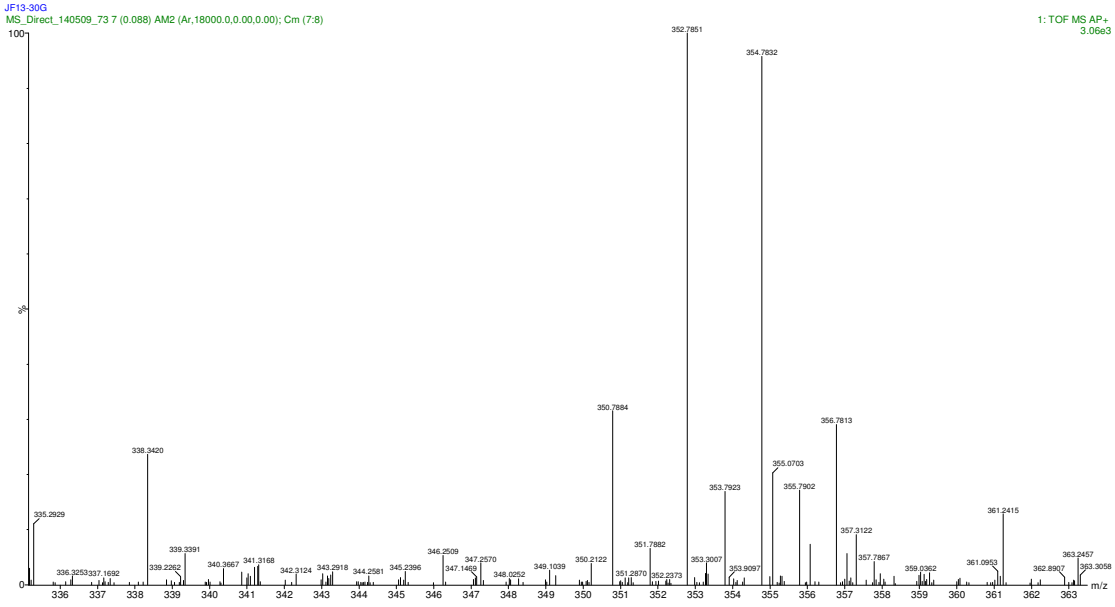

Figure S6.17: HRAPCIMS spectrum of compound **6.4**

S6.4 Compound 6.5

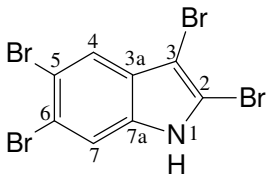

6.5

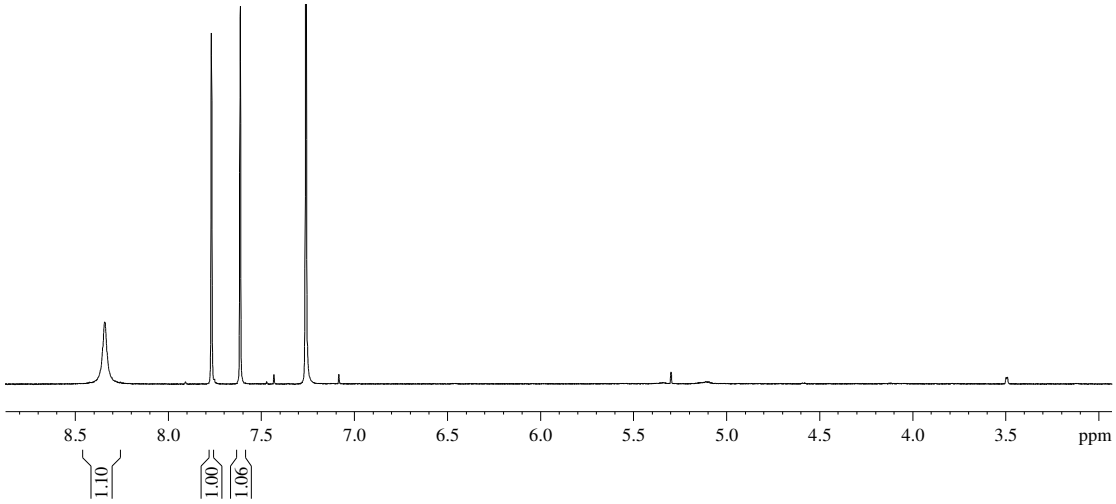

Figure S6.18: ^{1}H NMR spectrum ($CDCl_3$, 600 MHz) of compound **6.5**

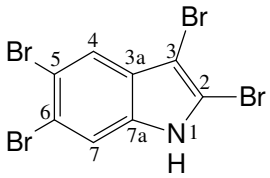

6.5

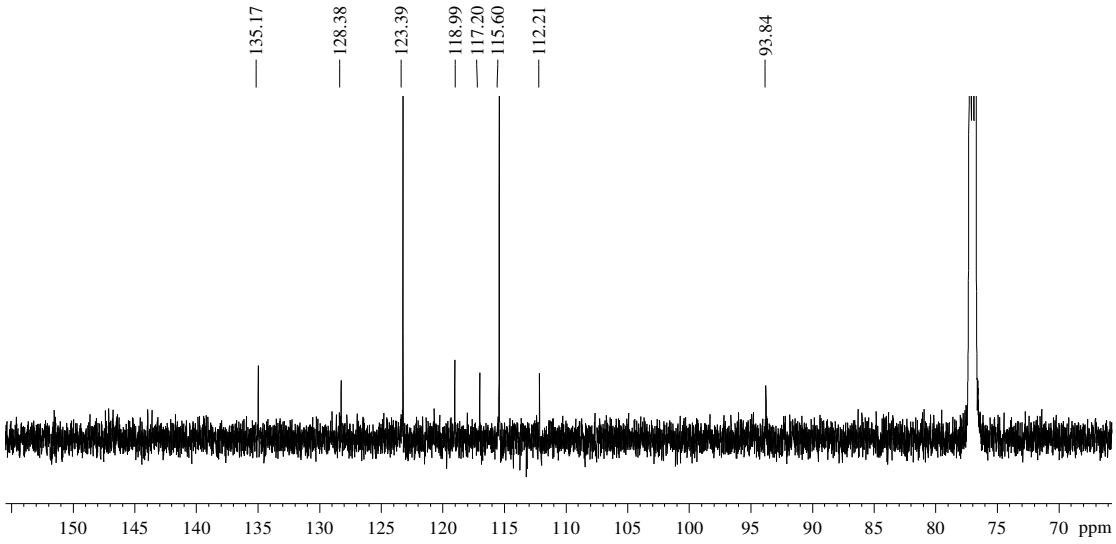

Figure S6.19: ^{13}C NMR spectrum ($CDCl_3$, 150 MHz) of compound **6.5**

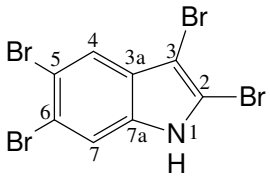

6.5

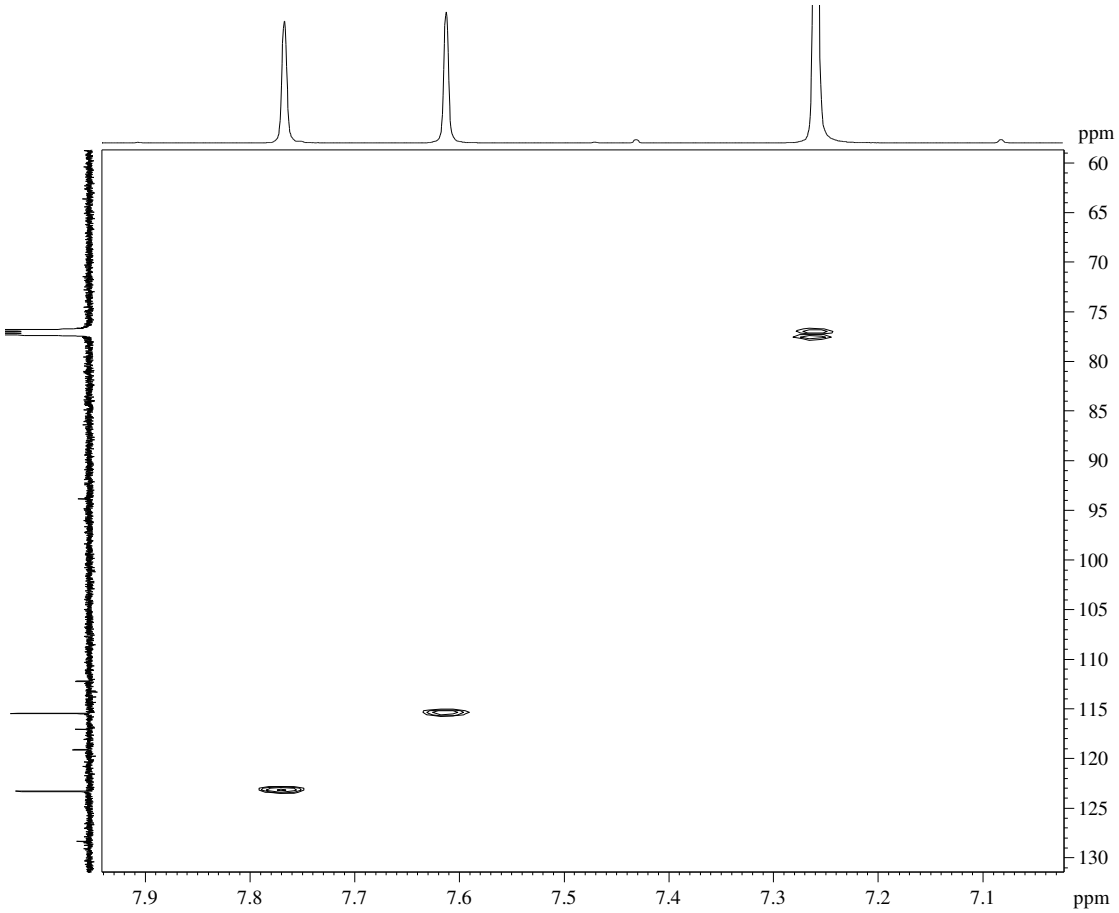

Figure S6.20: HSQC NMR spectrum of compound **6.5**

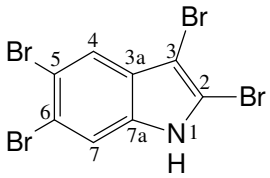

6.5

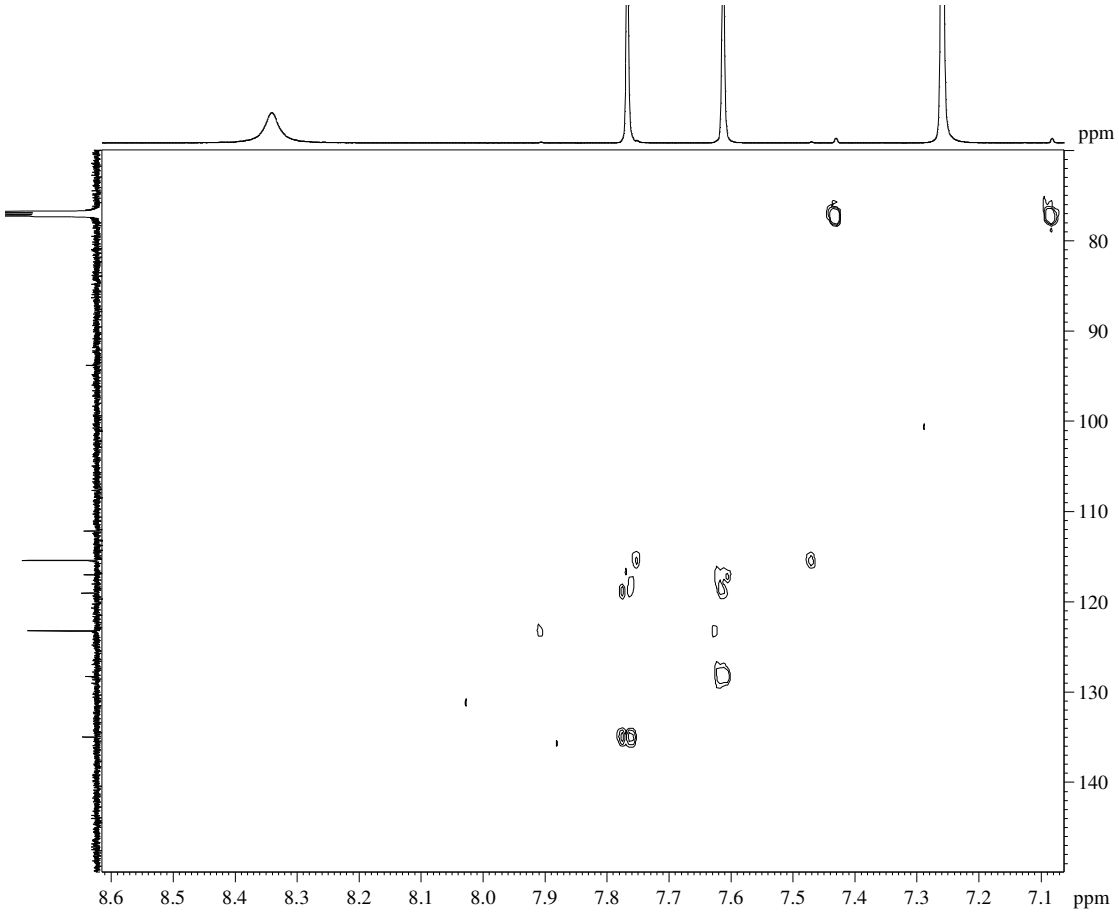

Figure S6.21: HMBC NMR spectrum of compound **6.5**

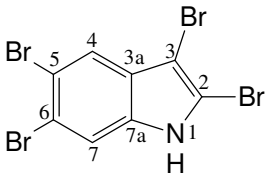

6.5

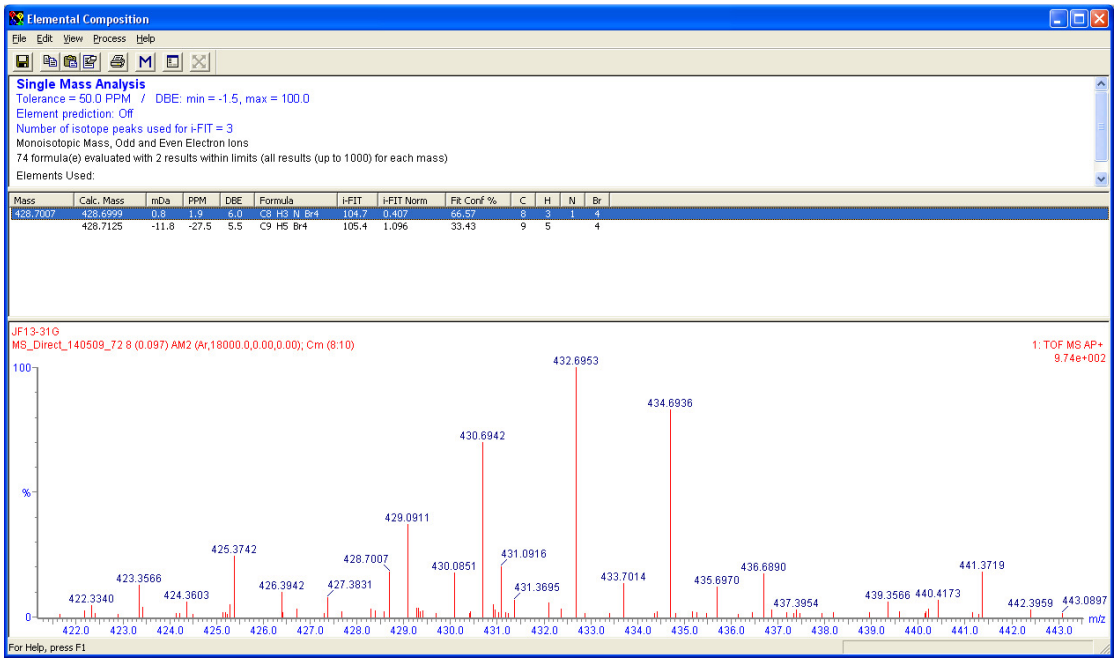

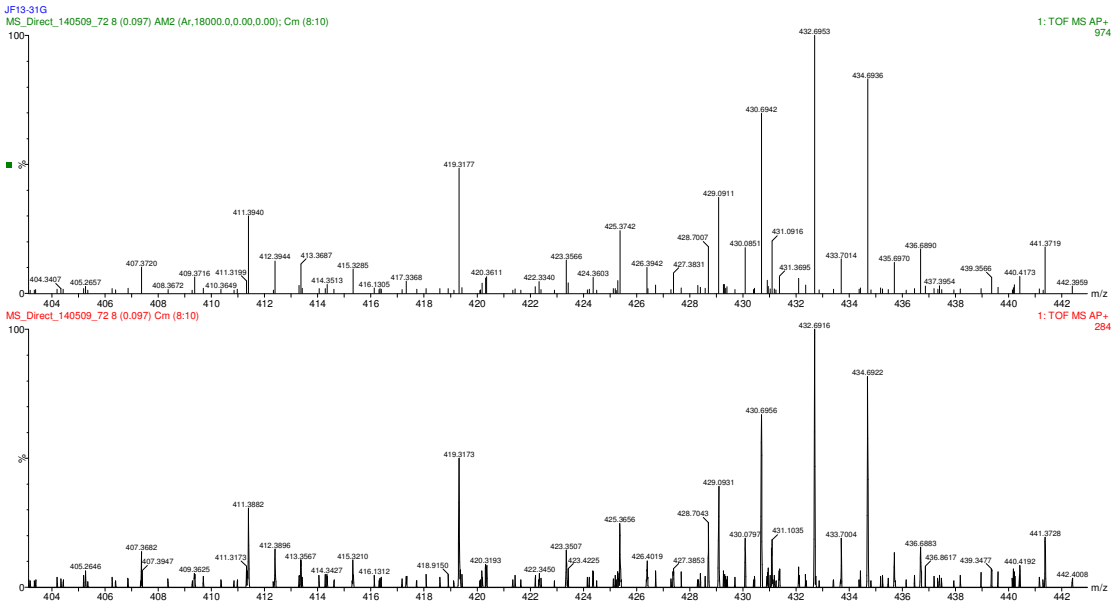

Figure S6.22: HRAPCIMS spectrum of compound **6.5**

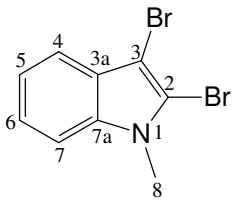

6.1

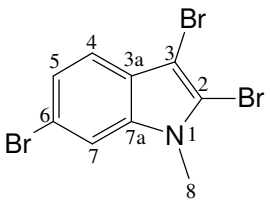

6.2

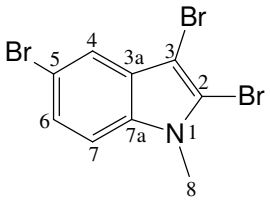

6.3

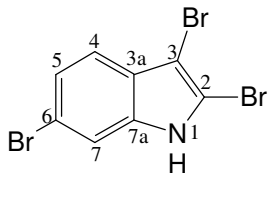

6.4

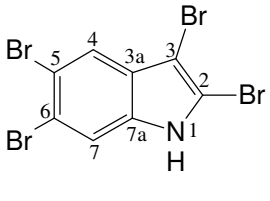

6.5

Table S6.1: ^{1}H NMR data ($CDCl_3$, 600 MHz) for compounds **6.1-6.5**

Proton No	6.1	6.2	6.3	6.4	6.5
4	7.52, d, 8.1	7.36, d, 8.5	7.65, d, 2.1	7.36, d, 8.6	7.77, s
5	7.19, t, 8.3	7.29, m	-	7.30, d, 8.6	-
6	7.26, m	-	7.33, dd, 8.8, 2.1	-	-
7	7.29, d, 8.1	7.45, s	7.16, d, 8.8	7.47, s	7.61, s
N-C**H$_3$**	3.81, s	3.76, s	3.79	-	-

Table S6.2: ^{13}C NMR data ($CDCl_3$, 150 MHz) for compounds **6.1-6.5**

Carbon No	6.1	6.2	6.3	6.4	6.5
2	114.9	115.7	116.3	110.6	112.2
3	92.7	93.0	92.4	93.8	93.8
3a	127.0	125.9	128.6	126.7	128.4
4	118.9	120.2	121.5	120.2	123.4
5	120.8	124.1	114.3	124.7	117.2
6	122.9	116.7	126.0	117.1	119.0
7	109.6	112.7	111.2	113.6	115.6
7a	136.4	136.9	135.8	136.2	135.2
N-**C**H$_3$	32.3	32.4	29.8	-	-

Chapter 7

Secondary metabolites from *Laurencia multiclavata*

S7.1 Compound 7.1

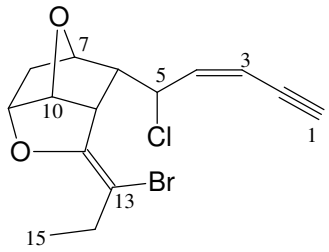

7.1

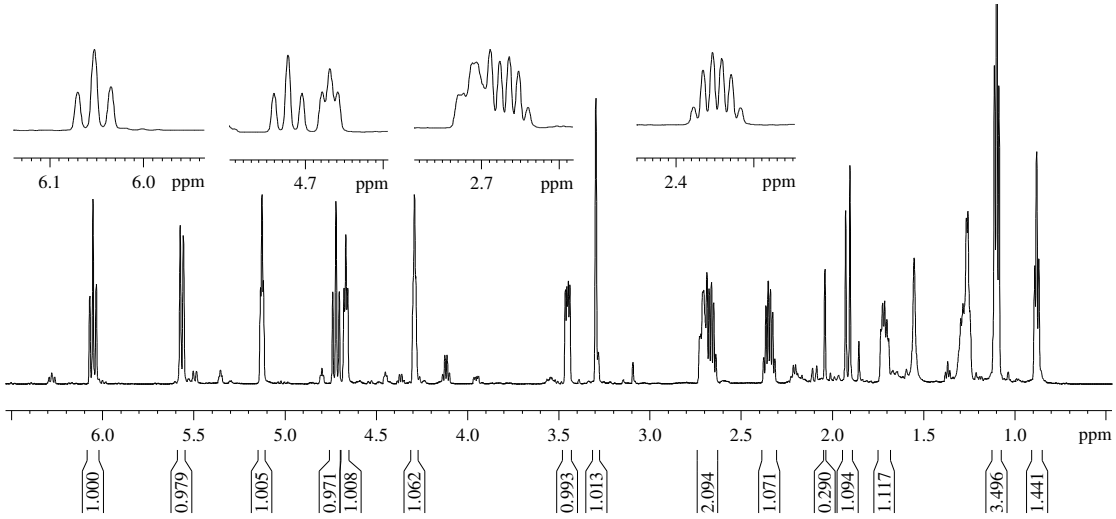

Figure S7.1: ^{1}H NMR spectrum ($CDCl_3$, 600 MHz) of compound **7.1**

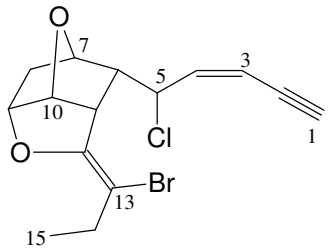

7.1

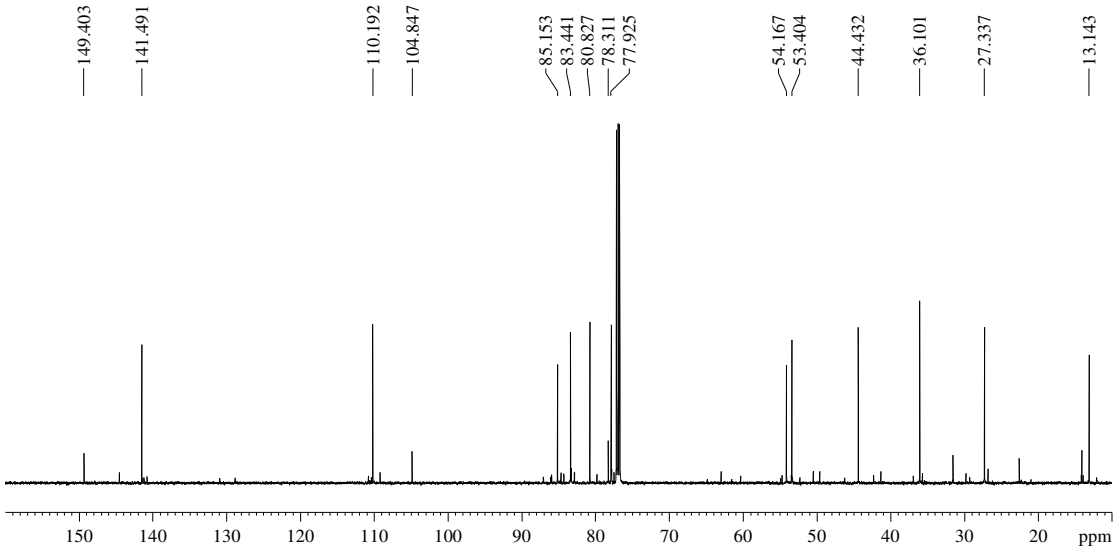

Figure S7.2: ^{13}C NMR spectrum ($CDCl_3$, 150 MHz) of compound **7.1**

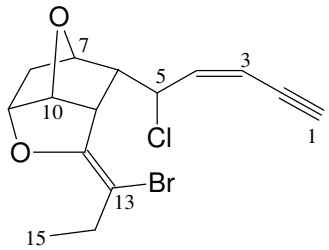

7.1

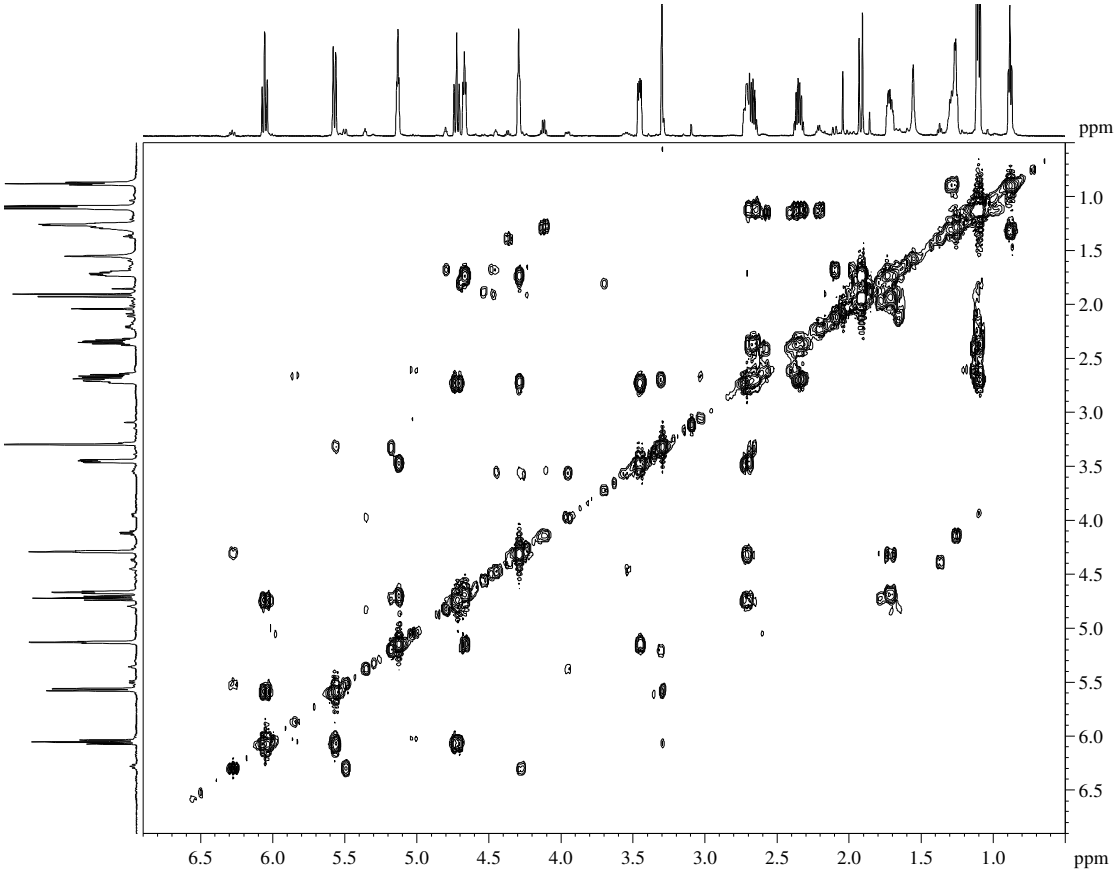

Figure S7.3: COSY NMR spectrum of compound **7.1**

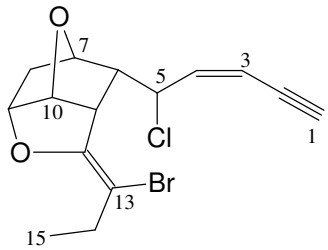

7.1

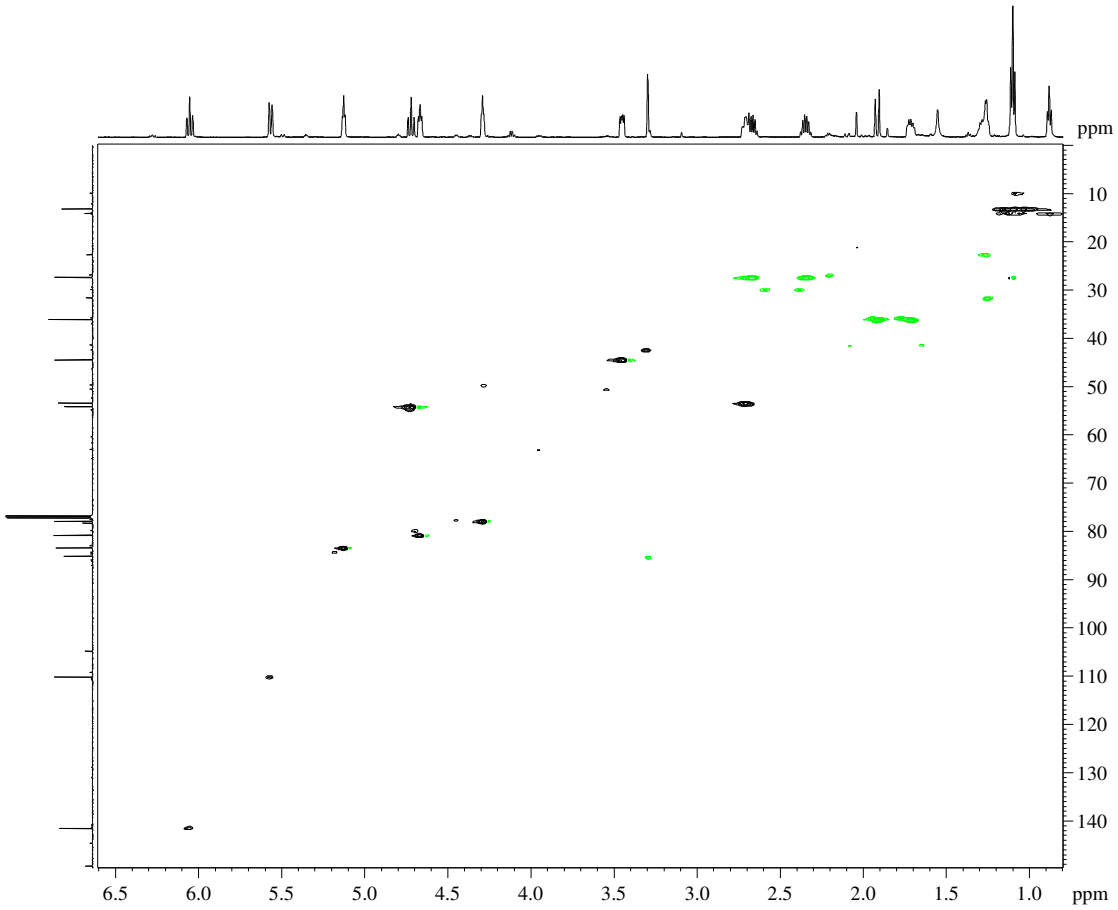

Figure S7.4: HSQC NMR spectrum of compound **7.1**

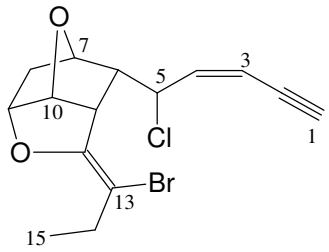

7.1

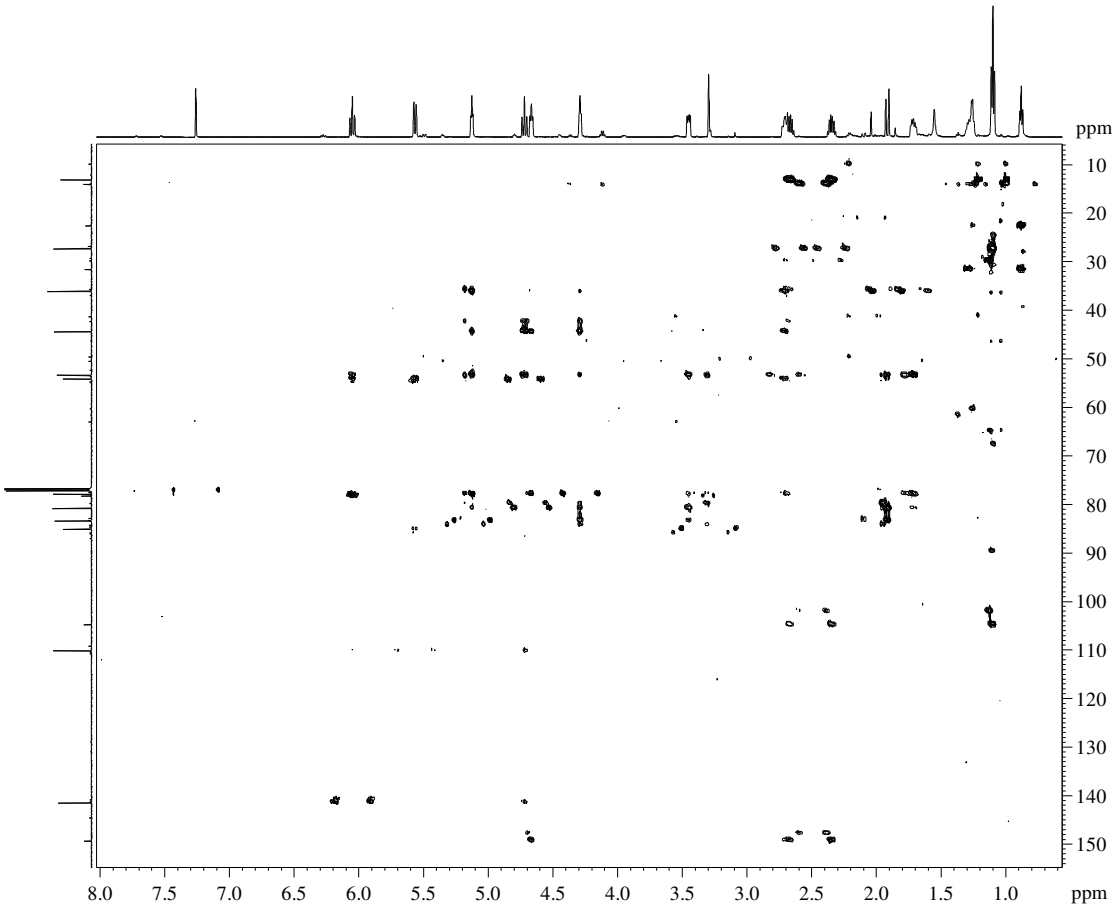

Figure S7.5: HMBC NMR spectrum of compound **7.1**

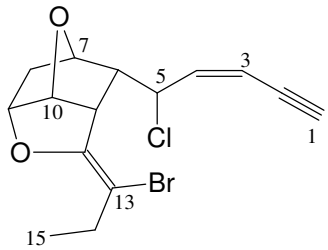

7.1

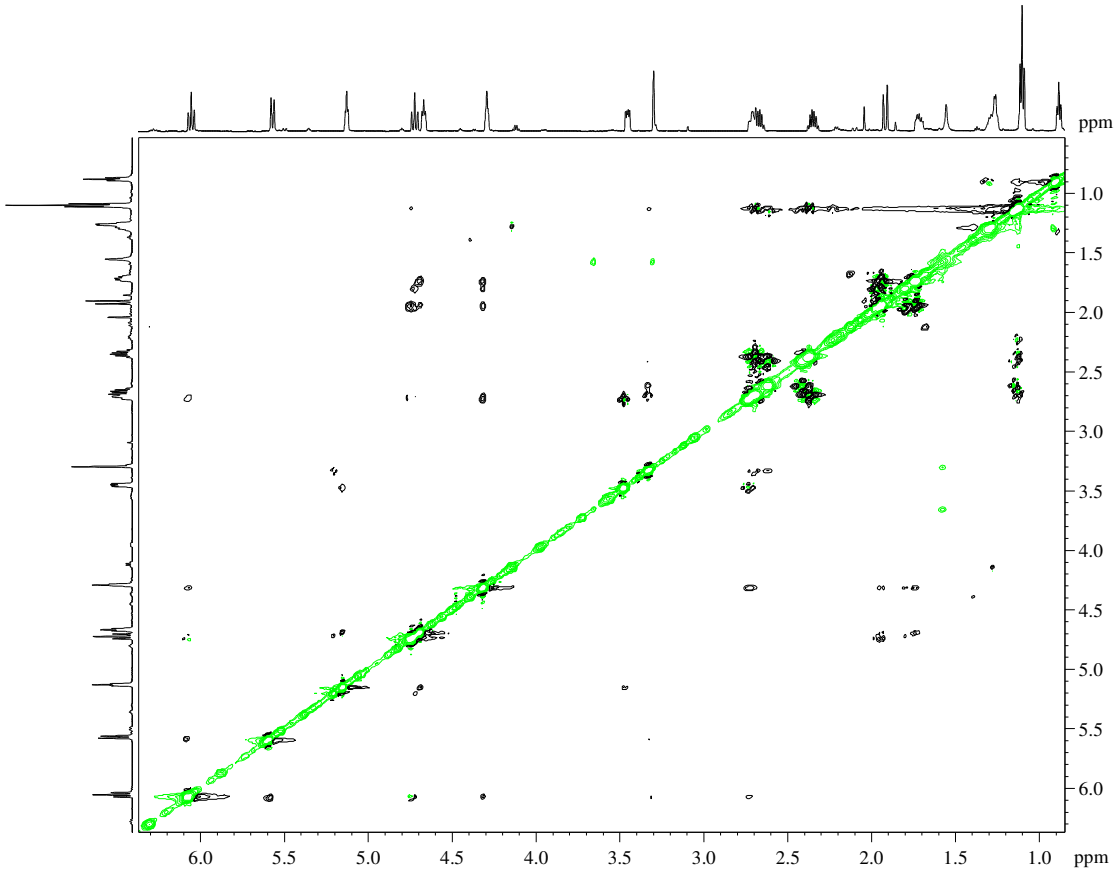

Figure S7.6: NOESY NMR spectrum of compound **7.1**

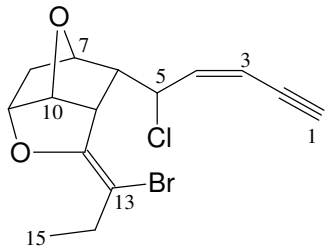

7.1

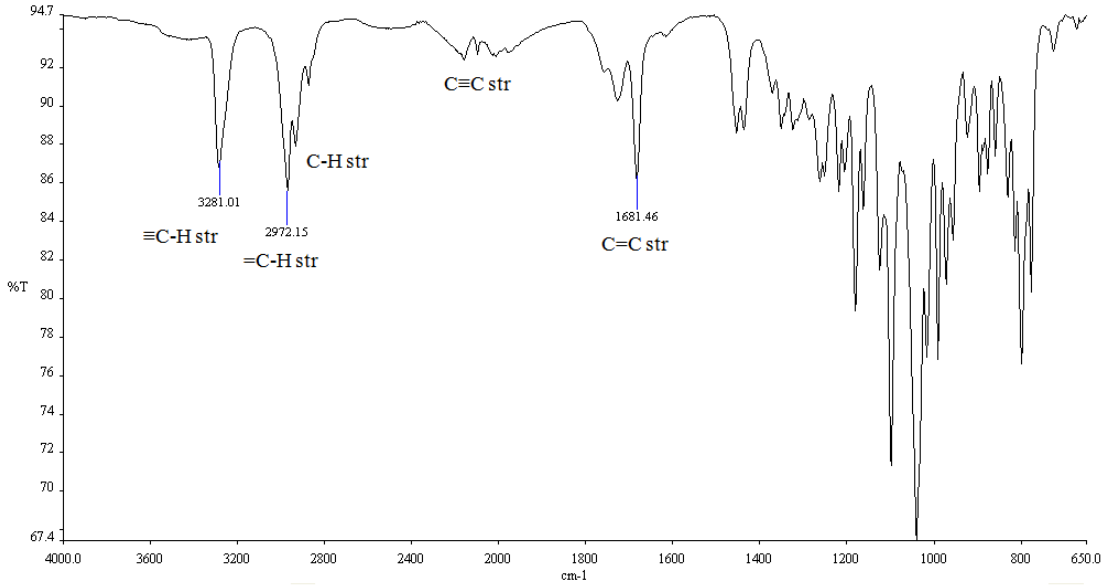

Figure S7.7: IR spectrum of compound **7.1**

S7.2 Compound 7.5

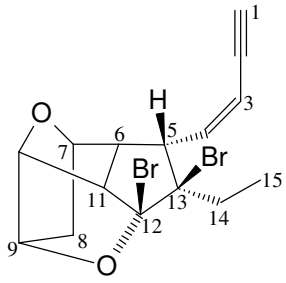

7.5

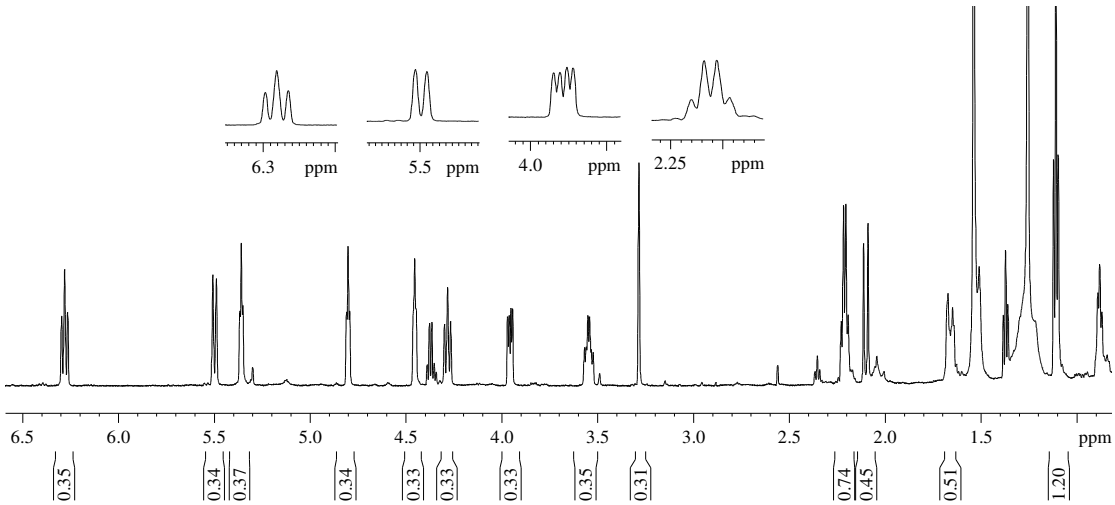

Figure S7.8: ^{1}H NMR spectrum ($CDCl_3$, 600 MHz) of compound **7.5**

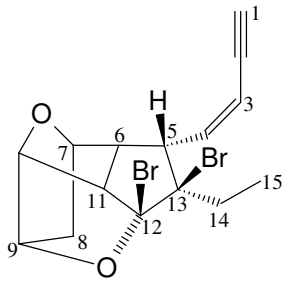

7.5

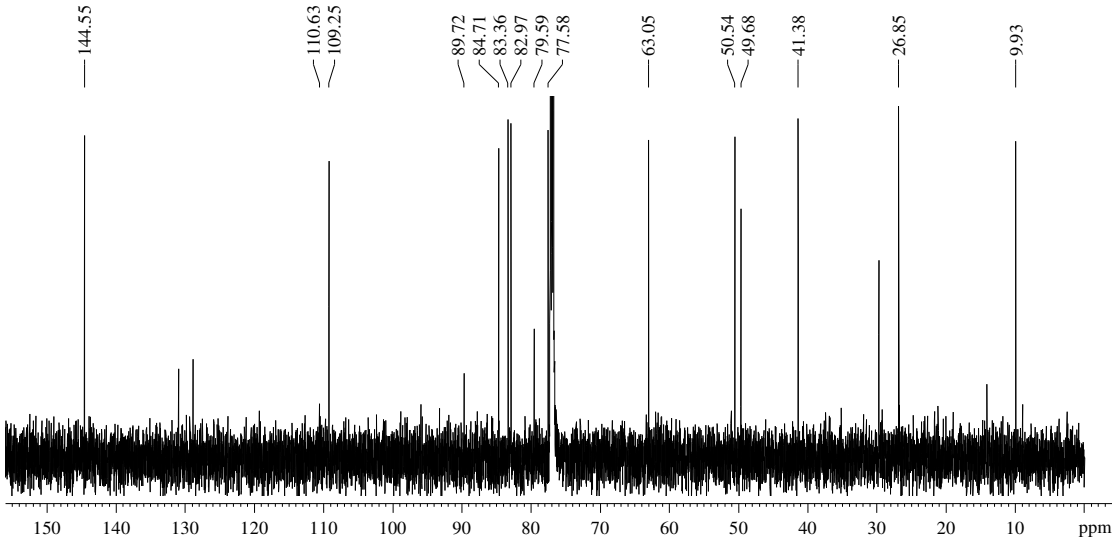

Figure S7.9: ^{13}C NMR spectrum ($CDCl_3$, 150 MHz) of compound **7.5**

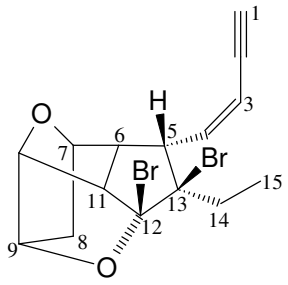

7.5

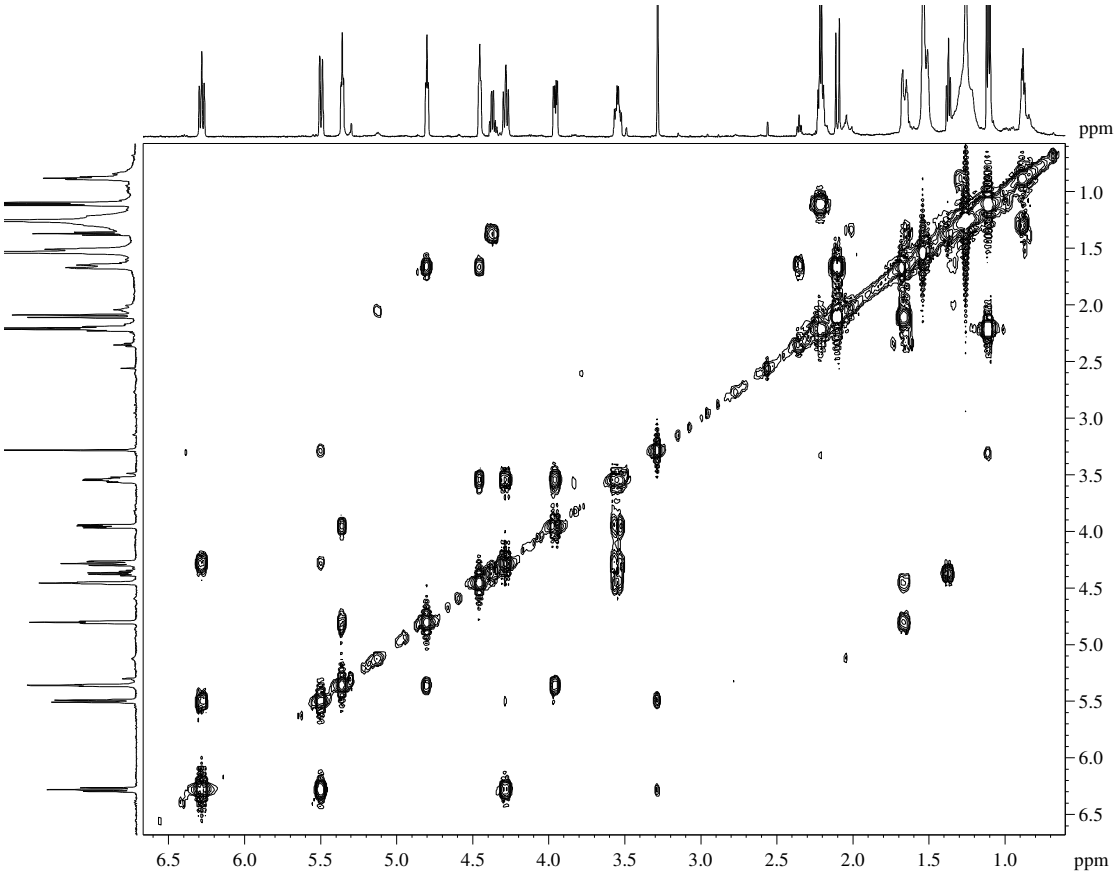

Figure S7.10: COSY NMR spectrum of compound **7.5**

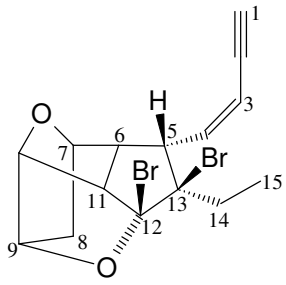

7.5

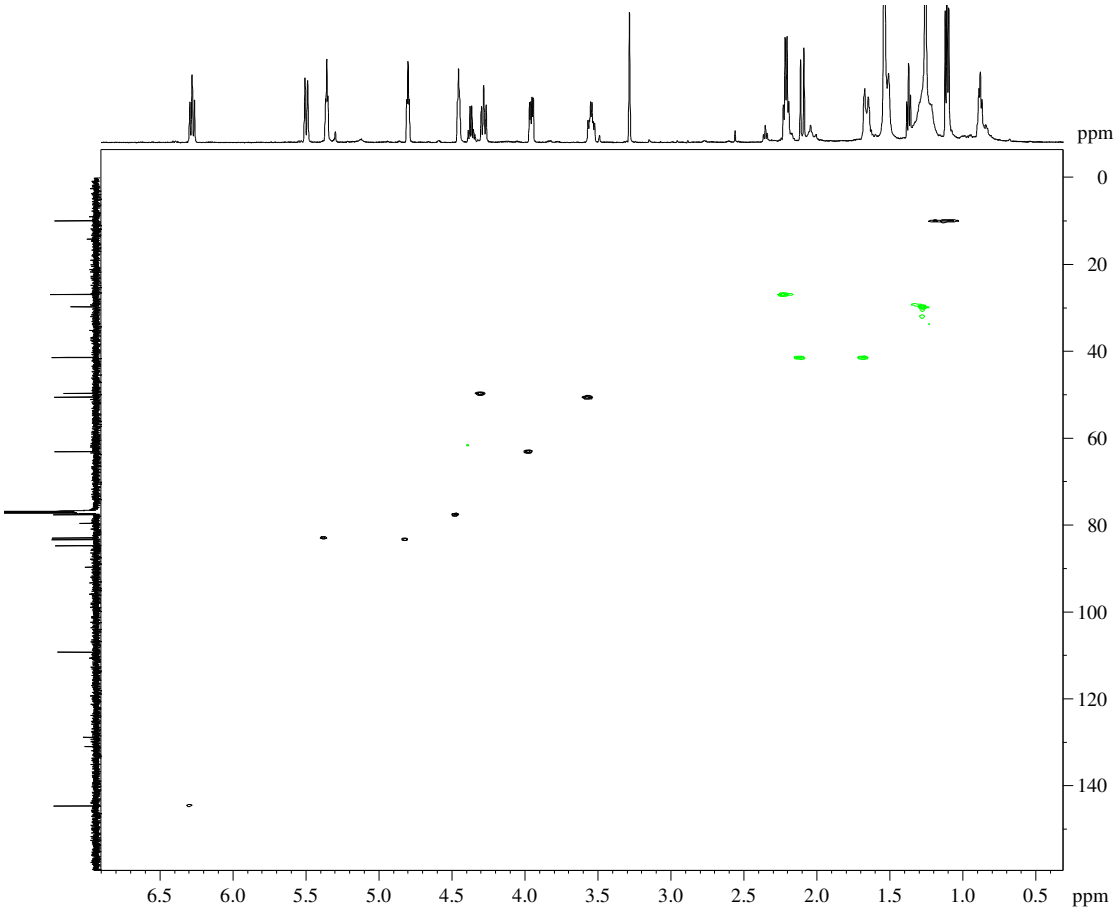

Figure S7.11: HSQC NMR spectrum of compound **7.5**

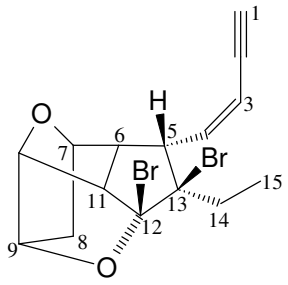

7.5

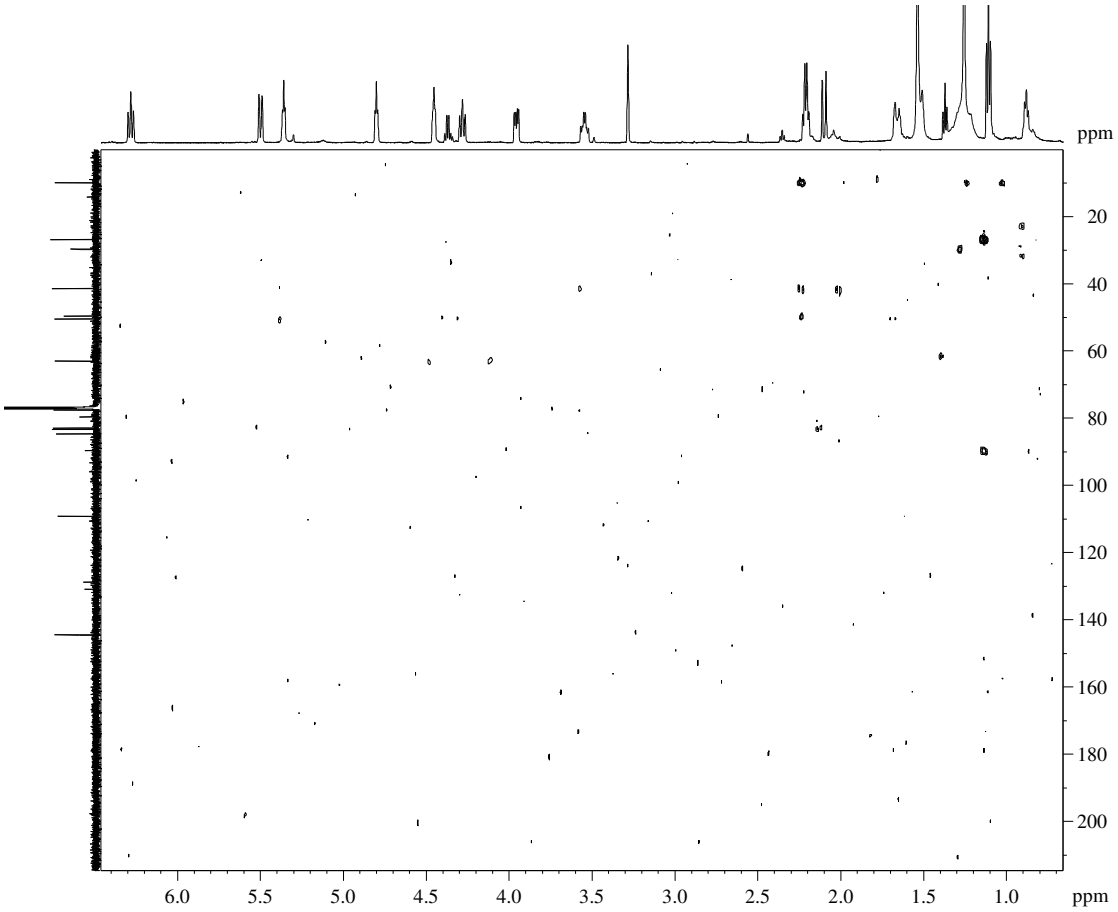

Figure S7.12: HMBC NMR spectrum of compound **7.5**

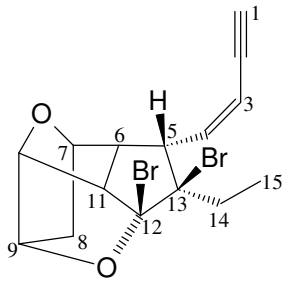

7.5

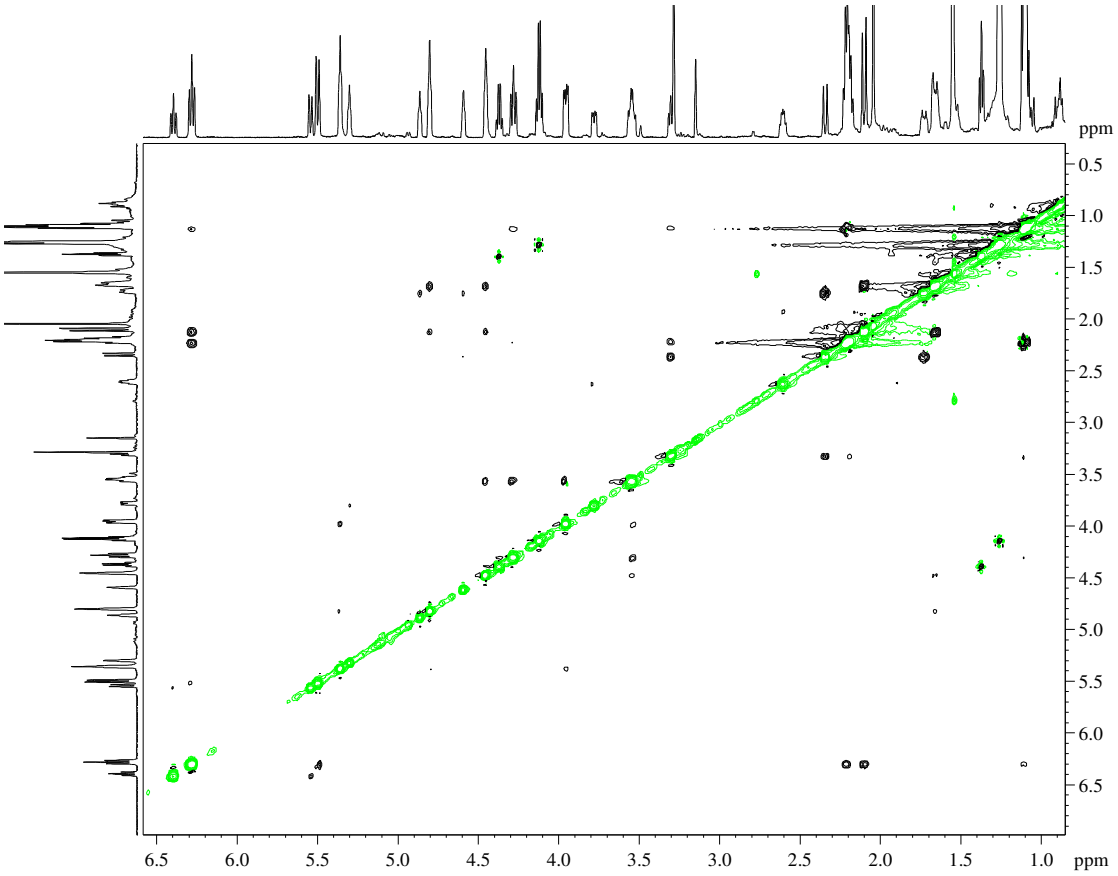

Figure S7.13: NOESY NMR spectrum of compound **7.5**

Please note that NOESY correlations for compound **7.5** were ascertained within the pre-purified mixture with its isomer compound **7.6.**

S7.3 Compound 7.6

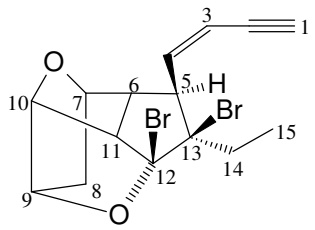

7.6

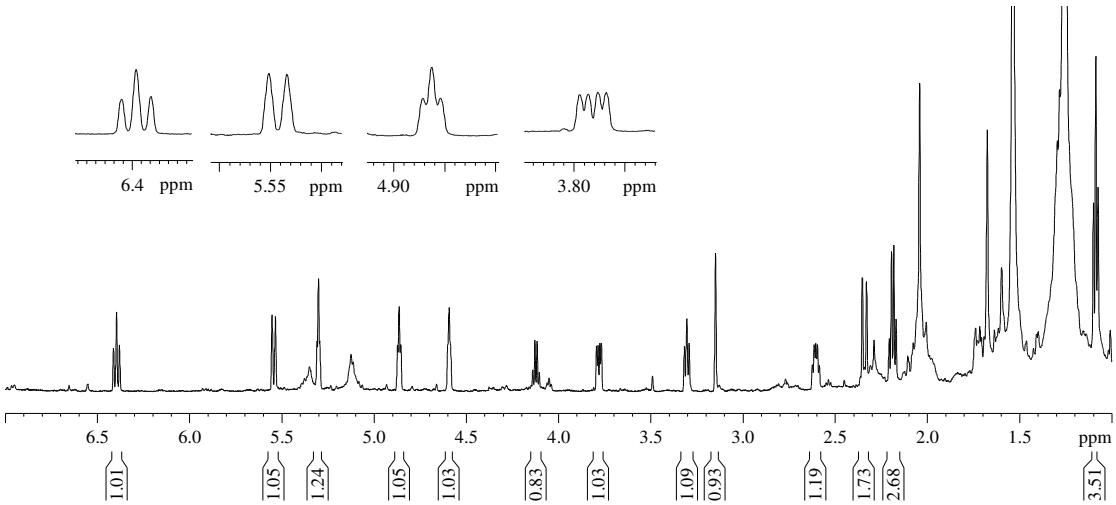

Figure S7.14: ^{1}H NMR spectrum ($CDCl_3$, 600 MHz) of compound **7.6**

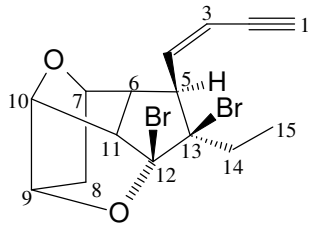

7.6

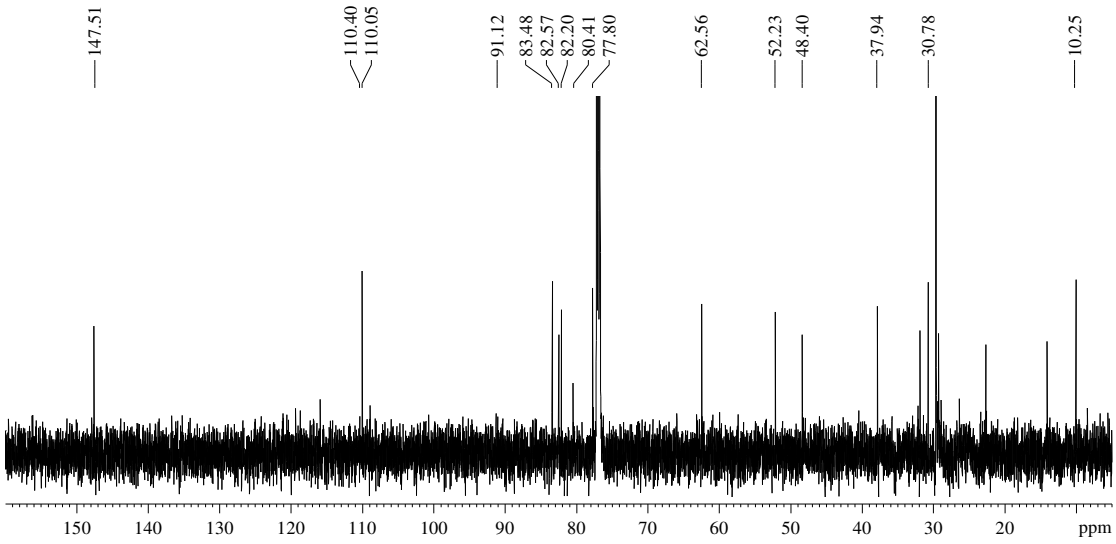

Figure S7.15: ^{13}C NMR spectrum ($CDCl_3$, 150 MHz) of compound **7.6**

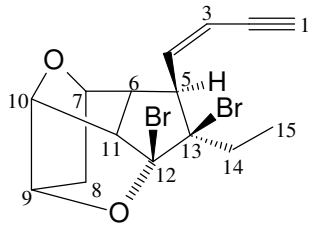

7.6

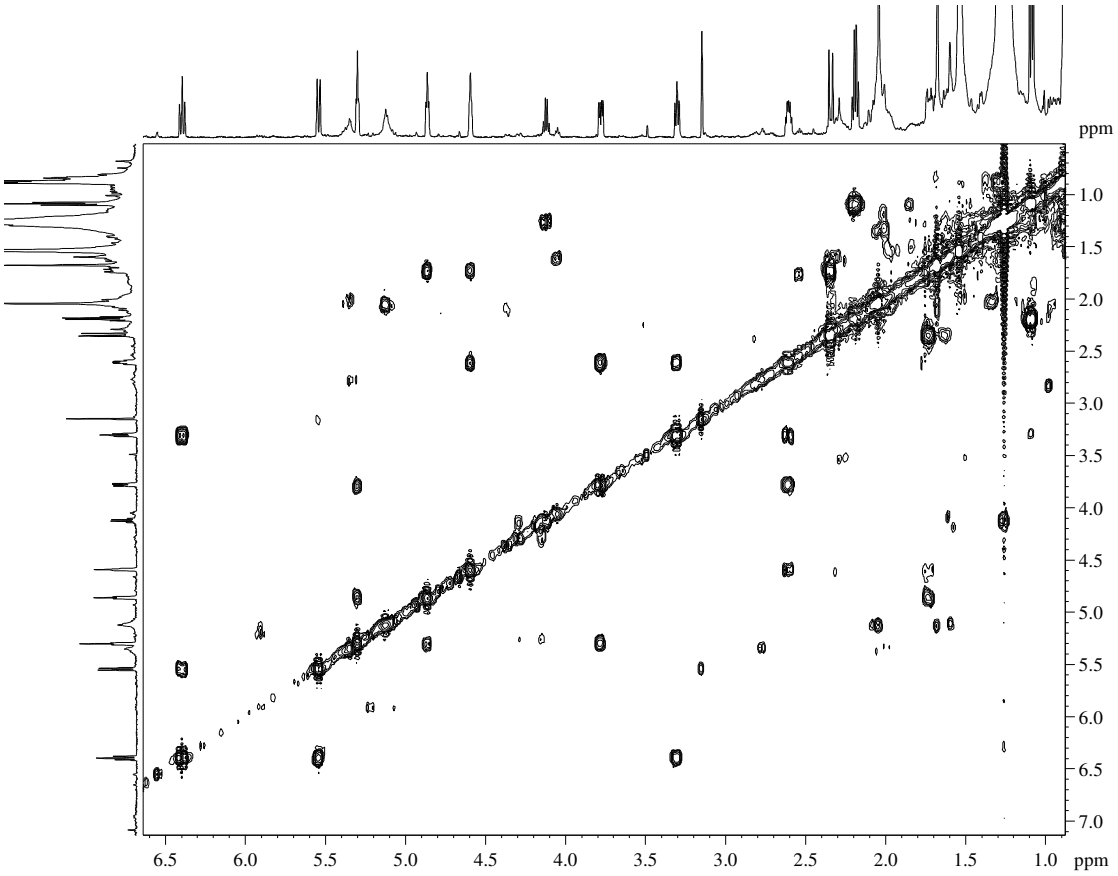

Figure S7.16: COSY NMR spectrum of compound **7.6**

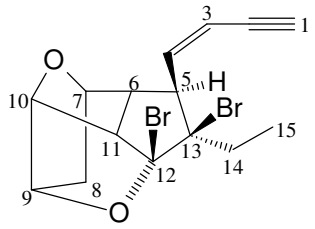

7.6

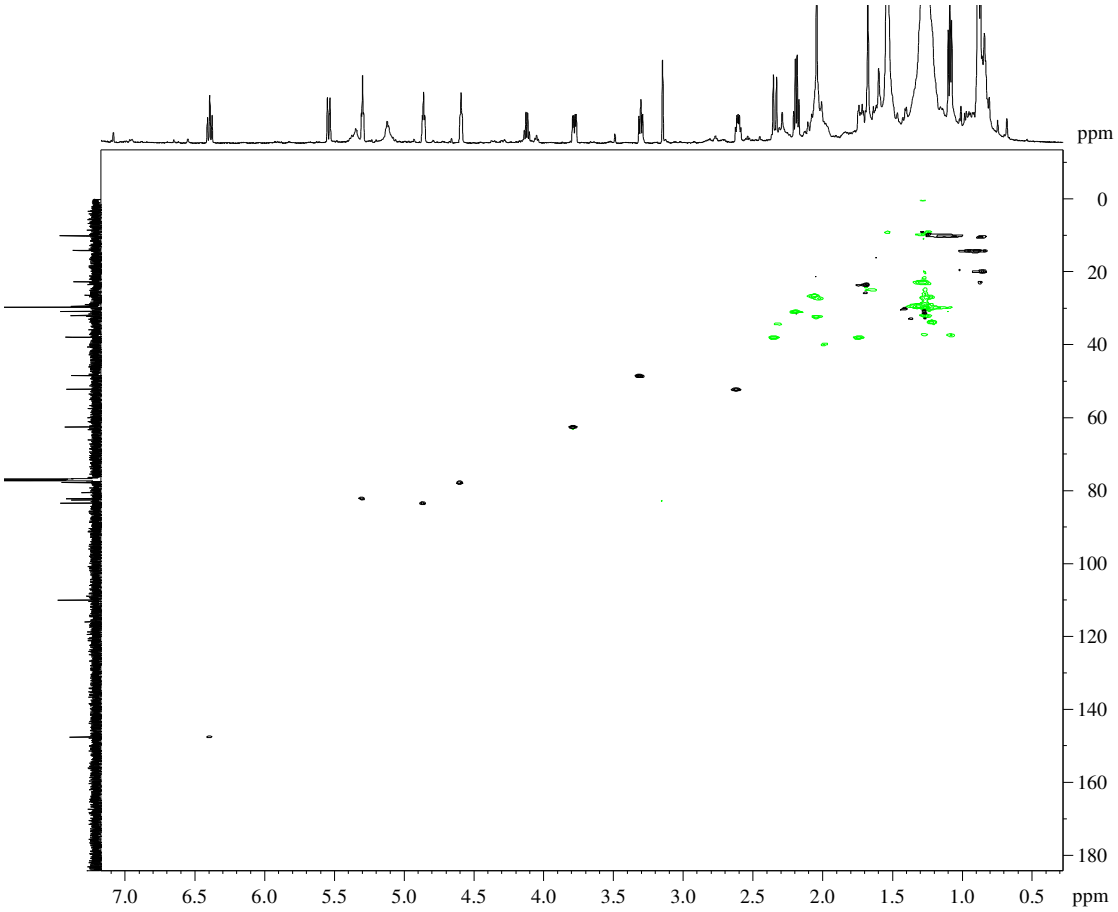

Figure S7.17: HSQC NMR spectrum of compound **7.6**

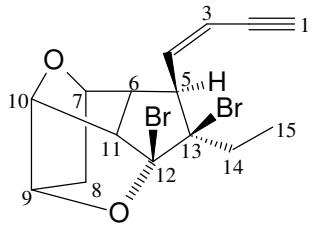

7.6

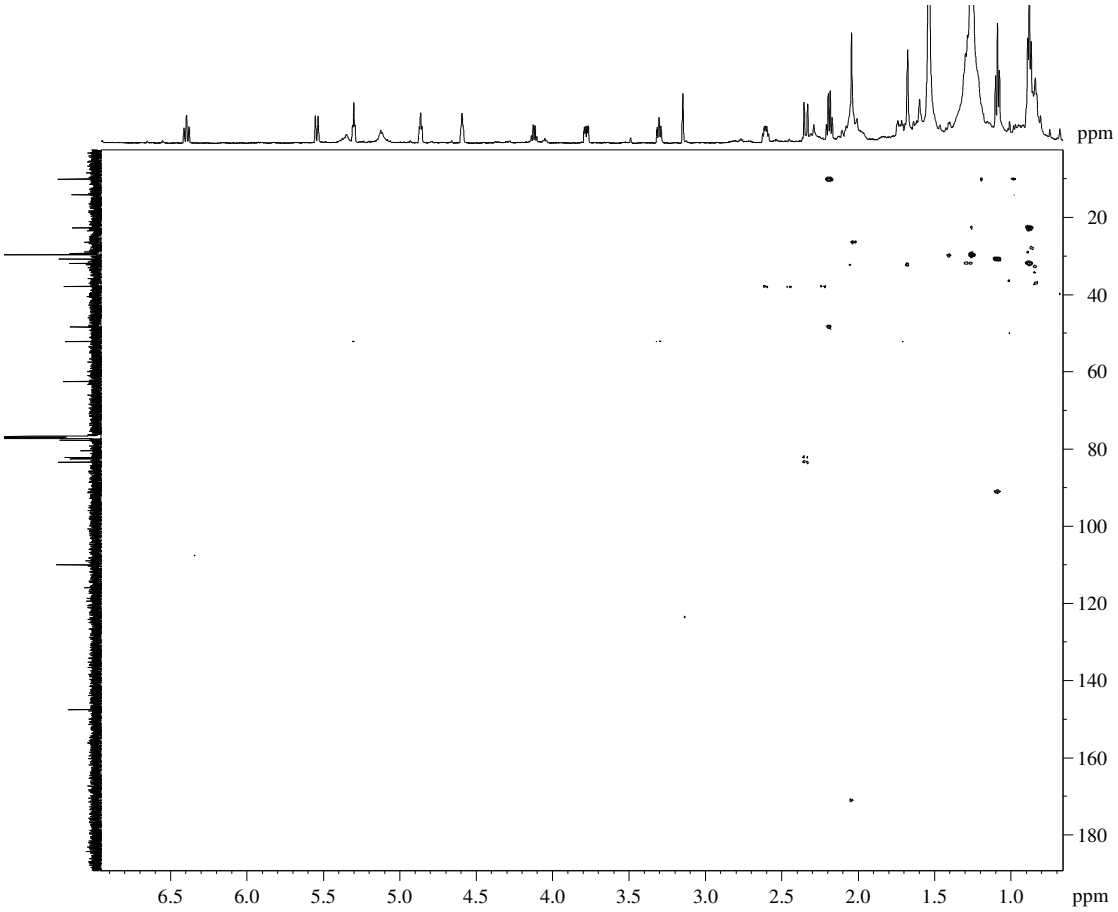

Figure S7.18: HMBC NMR spectrum of compound **7.6**

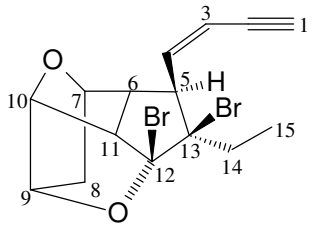

7.6

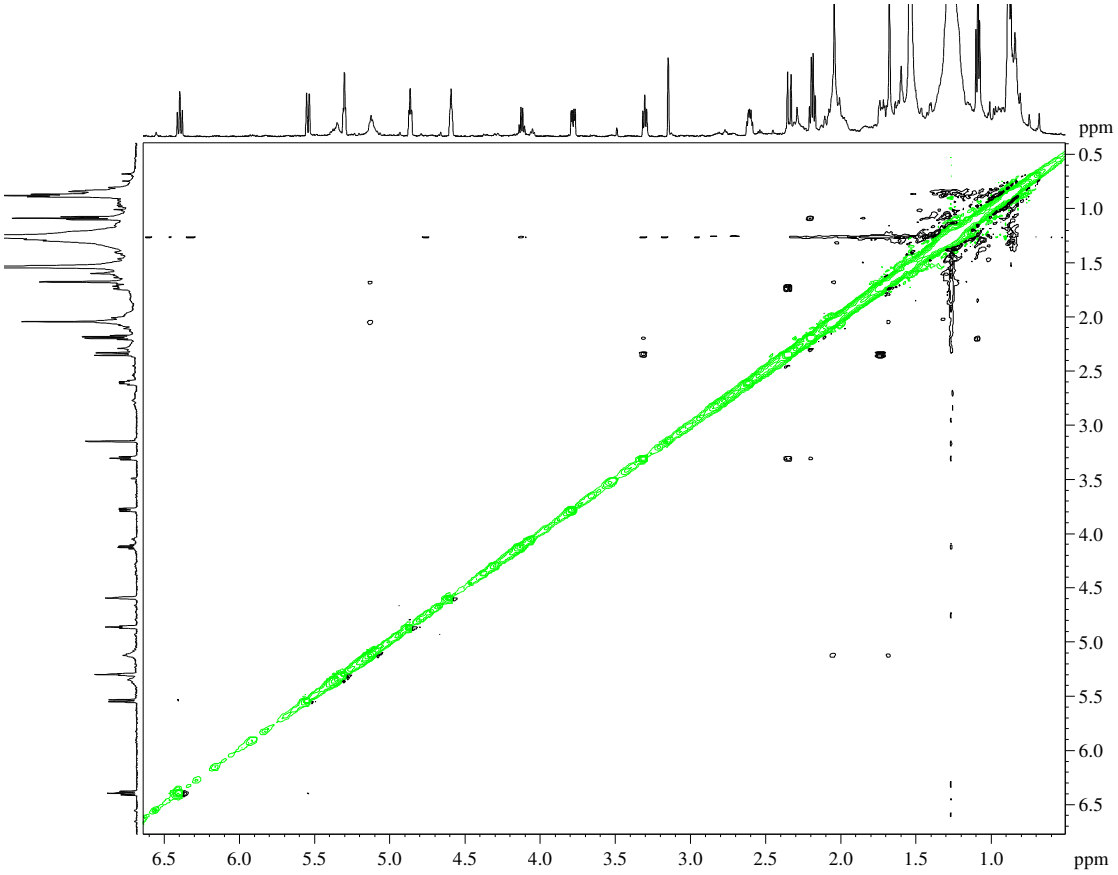

Figure S7.19: NOESY NMR spectrum of compound **7.6**

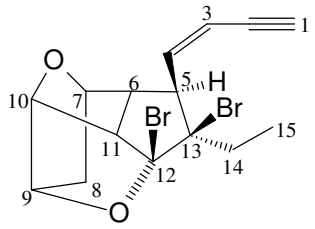

7.6

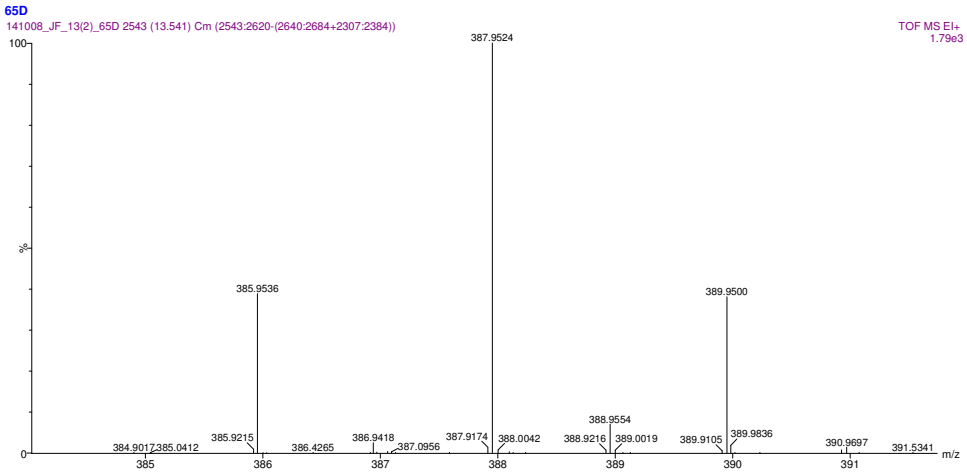

Figure S7.20: HREIMS spectrum of compound **7.6**

Chapter 8

Secondary metabolites from *Laurencia flexuosa*

S8.1 Compound 8.1

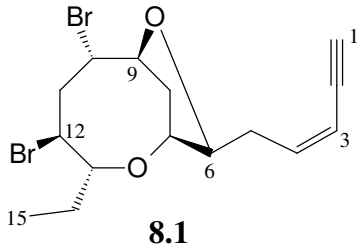

8.1

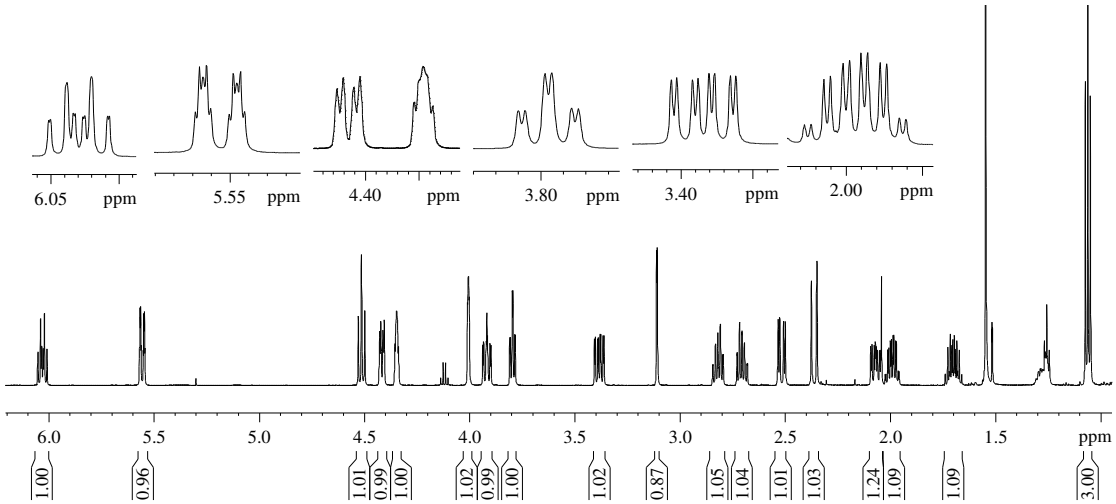

Figure S8.1: ^{1}H NMR spectrum ($CDCl_3$, 600 MHz) of compound **8.1**

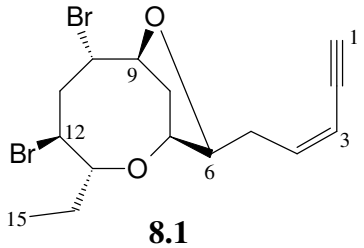

8.1

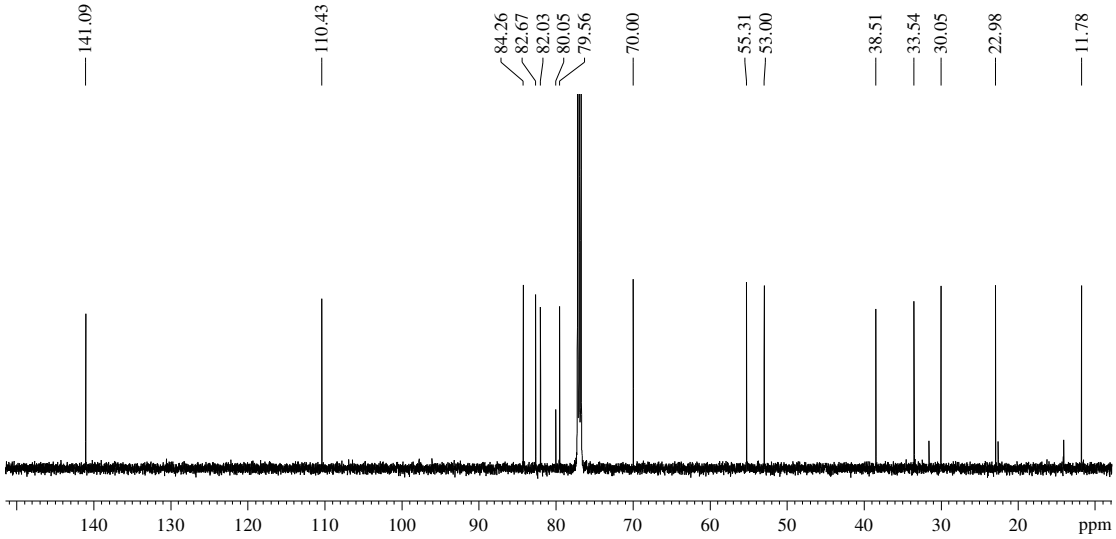

Figure S8.2: ^{13}C NMR spectrum ($CDCl_3$, 150 MHz) of compound **8.1**

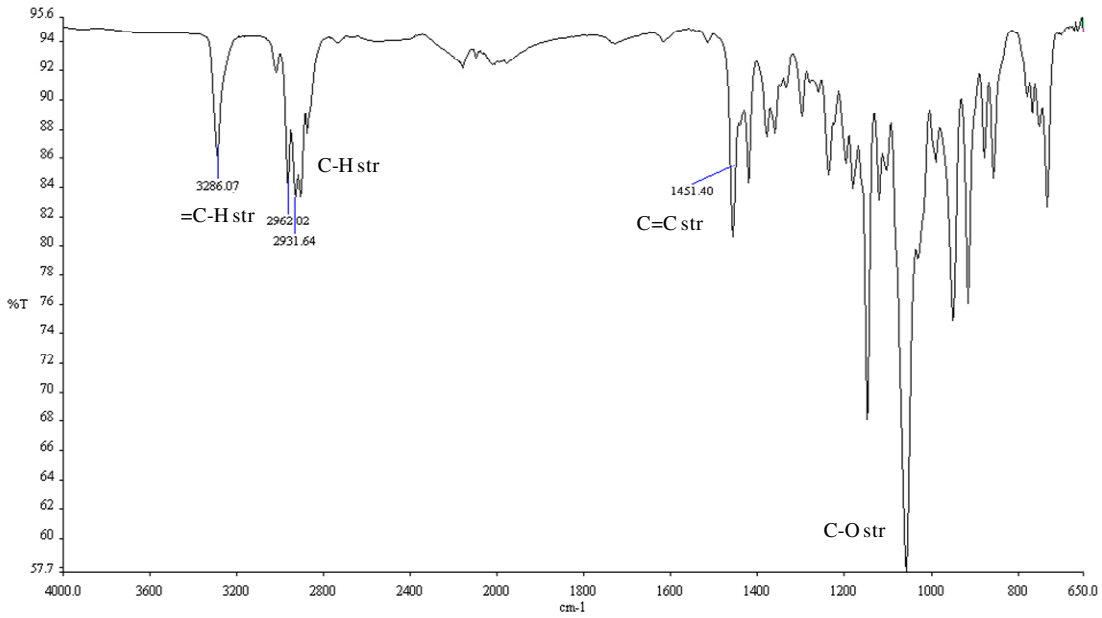

Figure S8.3: IR NMR spectrum of compound **8.1**

S8.2 Compound 8.2

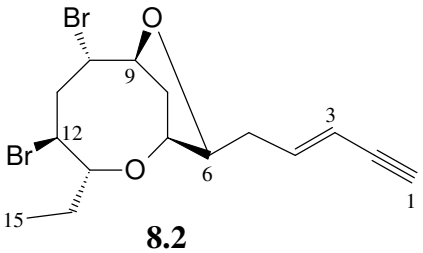

8.2

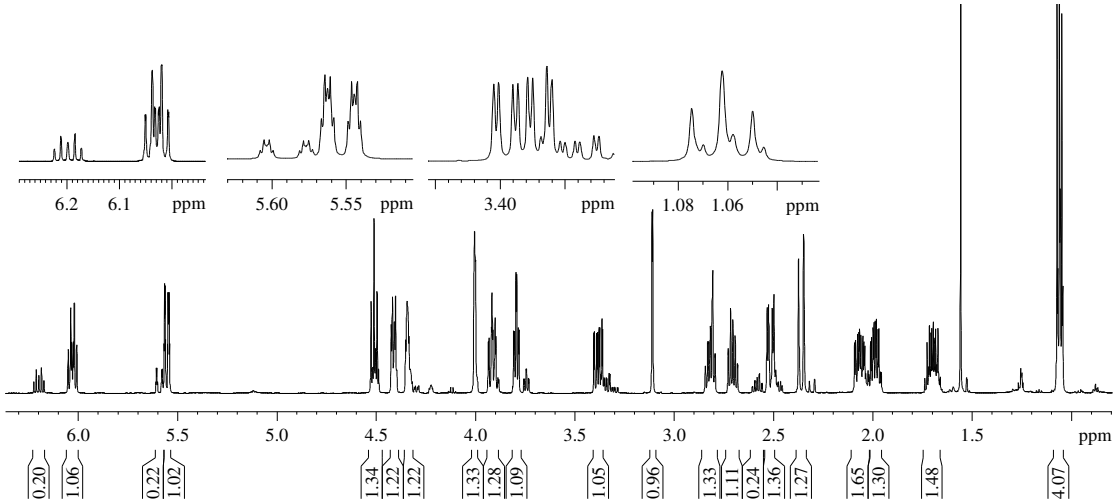

Figure S8.4: ^{1}H NMR spectrum ($CDCl_3$, 600 MHz) of compound **8.2**

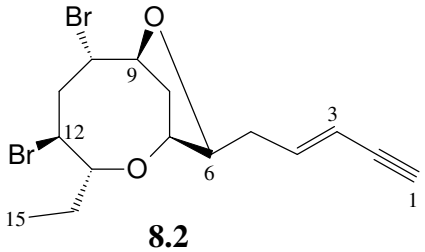

8.2

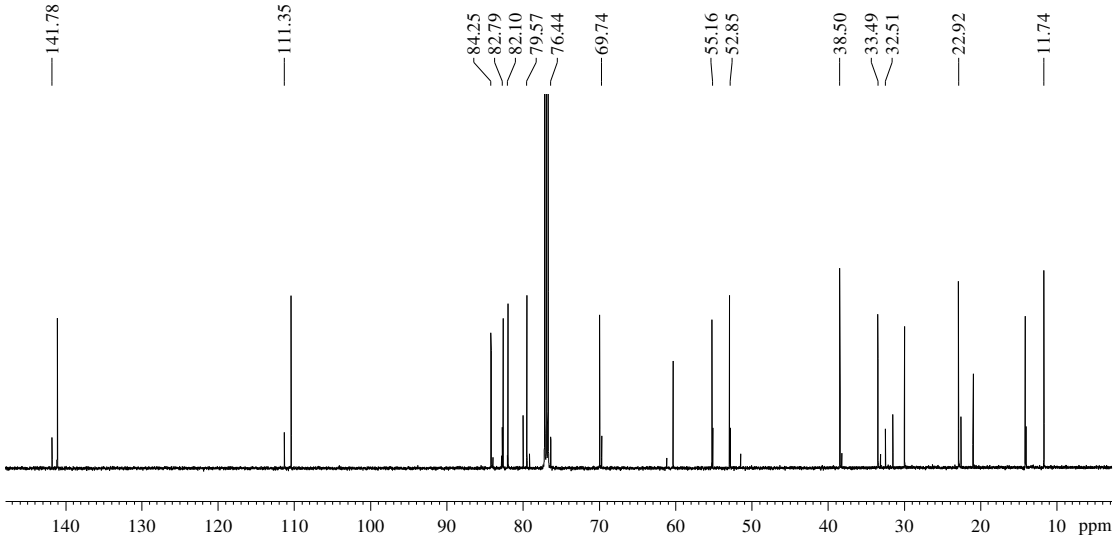

Figure S8.5: ^{13}C NMR ($CDCl_3$, 150 MHz) spectrum of compound **8.2**

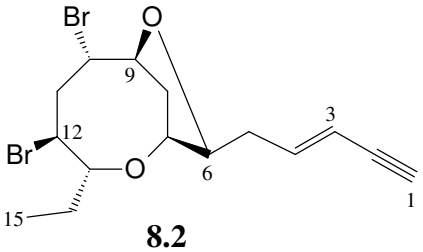

8.2

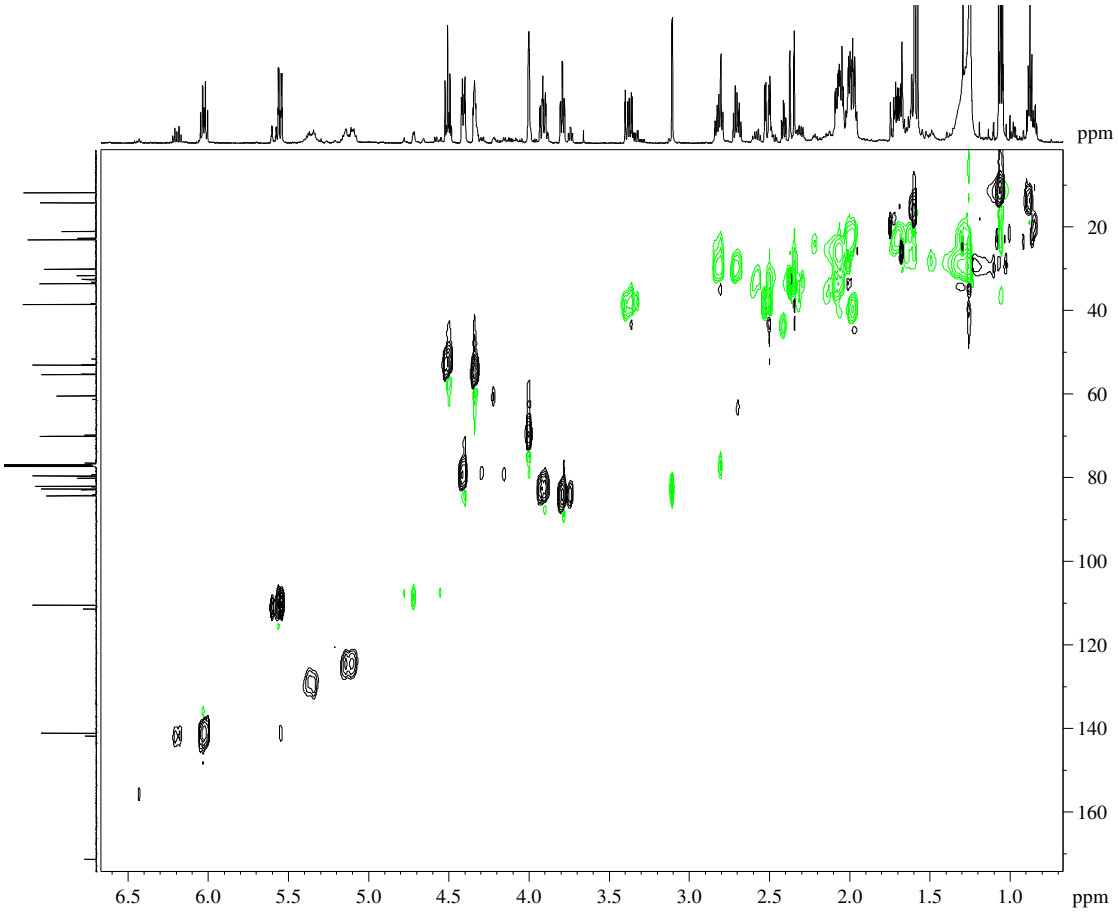

Figure S8.6: IR NMR spectrum of compound **8.2**

S8.3 Compound 8.5

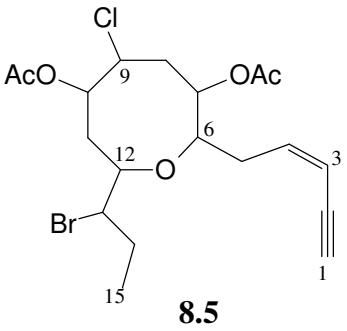

8.5

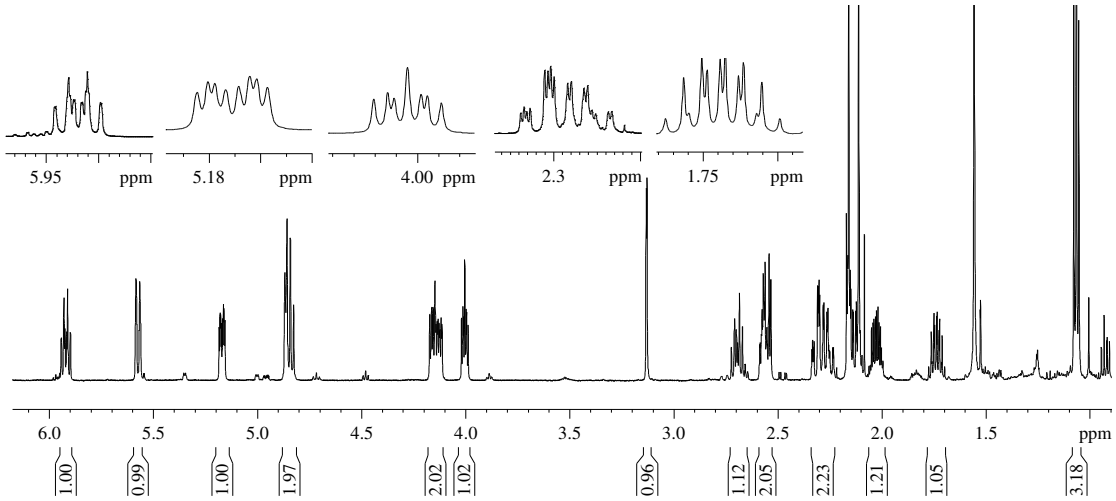

Figure S8.7: ^{1}H NMR spectrum ($CDCl_3$, 600 MHz) of compound **8.5**

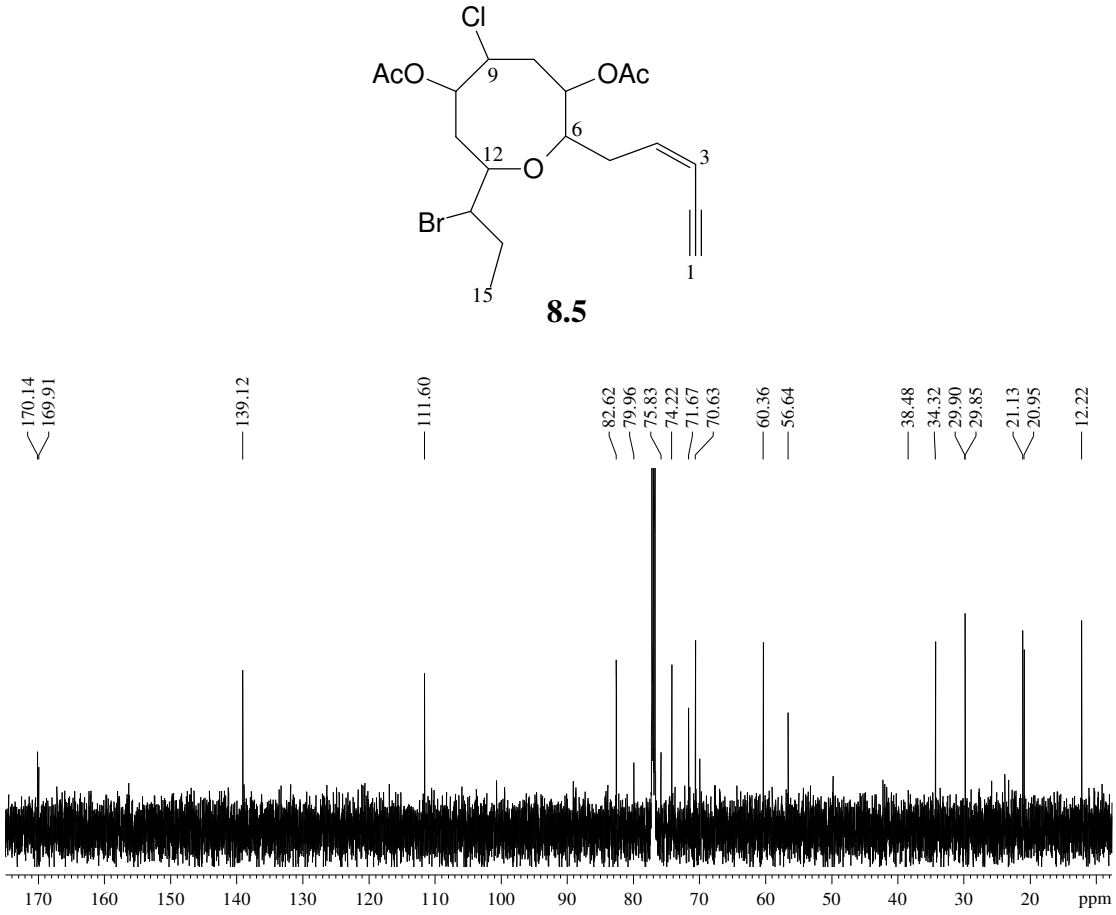

Figure S8.8: ^{13}C NMR spectrum ($CDCl_3$, 150 MHz) of compound **8.5**

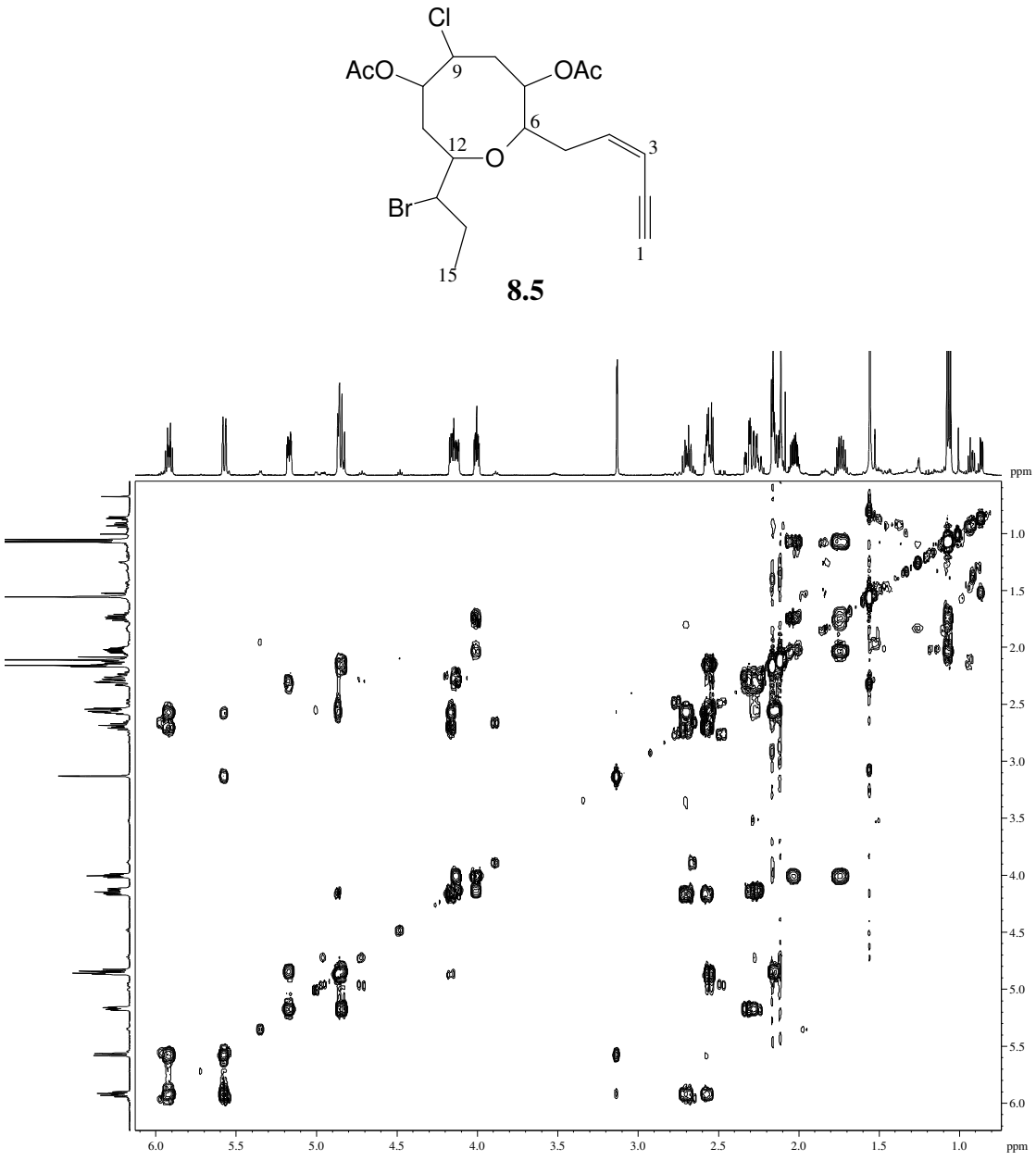

8.5

Figure S8.9: COSY NMR spectrum of compound **8.5**

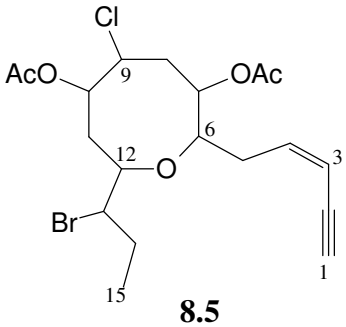

8.5

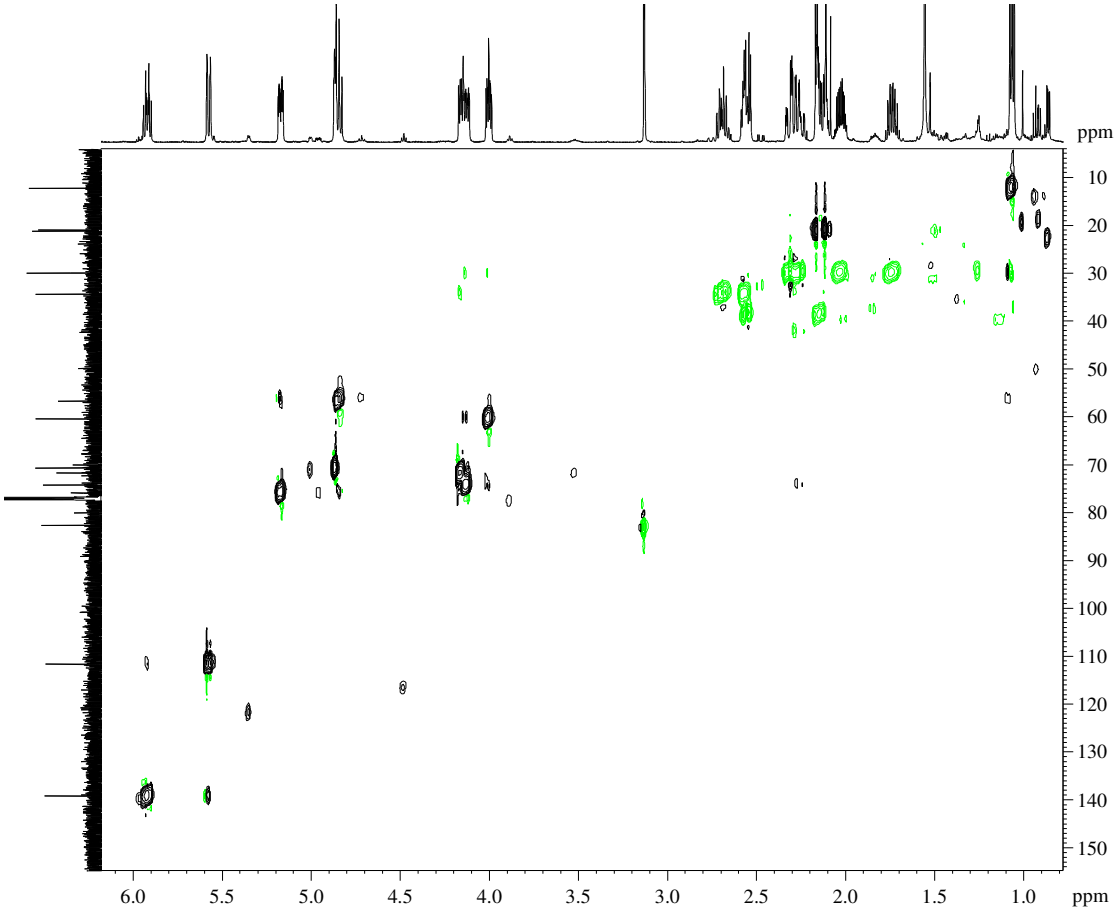

Figure S8.10: HSQC NMR spectrum of compound **8.5**

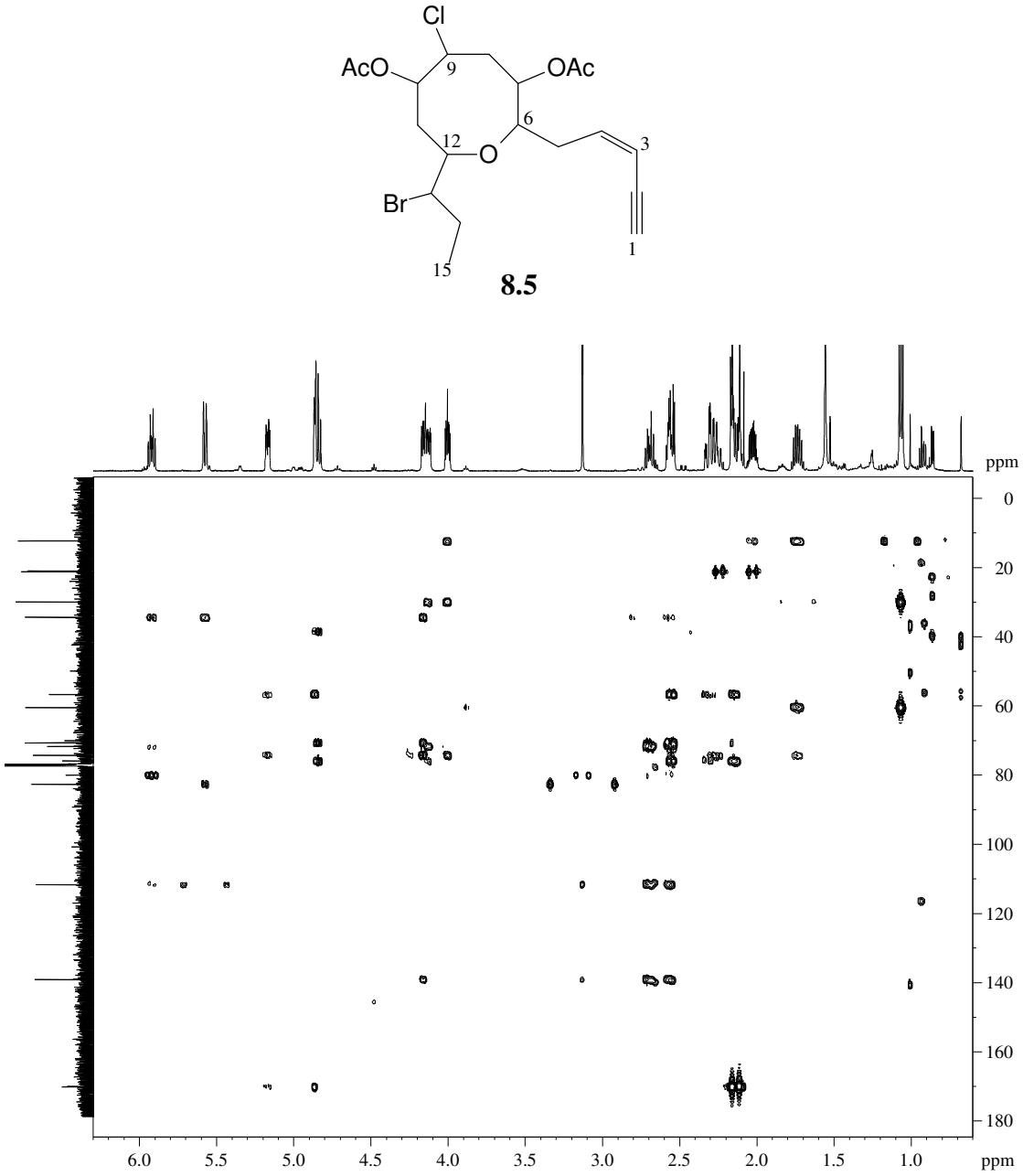

Figure S8.11: HMBC NMR spectrum of compound **8.5**

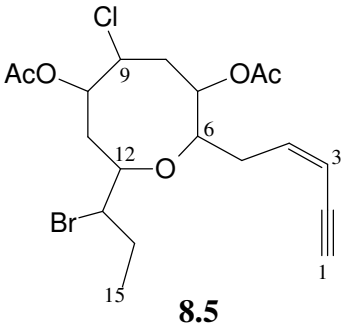

8.5

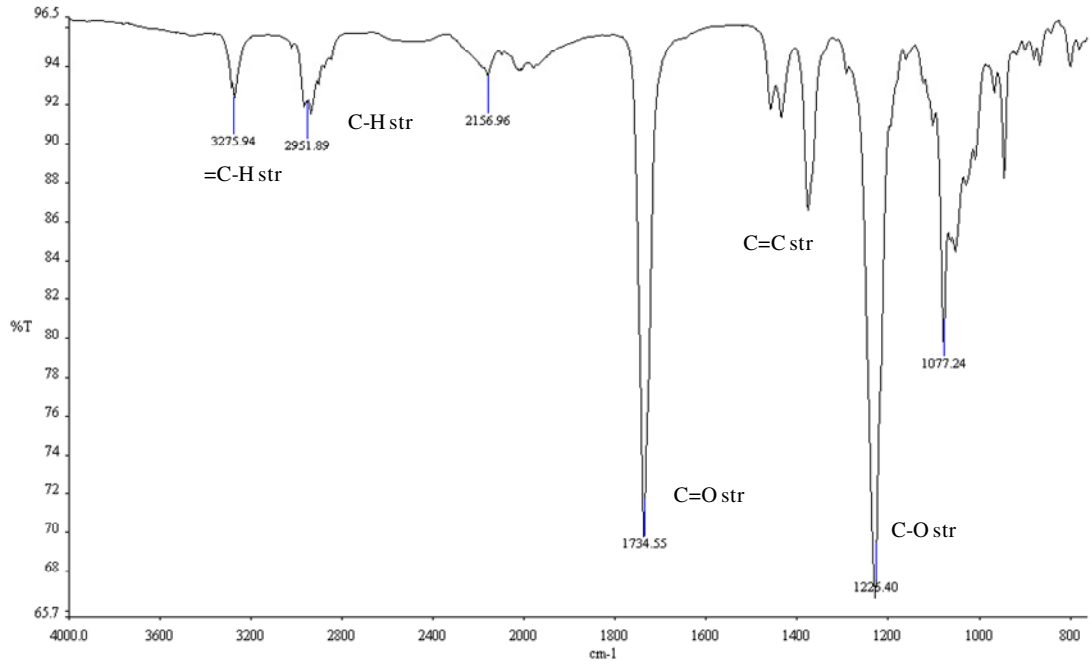

Figure S8.12: IR NMR spectrum of compound **8.5**

Chapter 9

Secondary metabolites from *Laurencia sodwaniensis*

S9.1 Compound 9.1

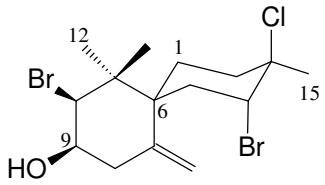

9.1

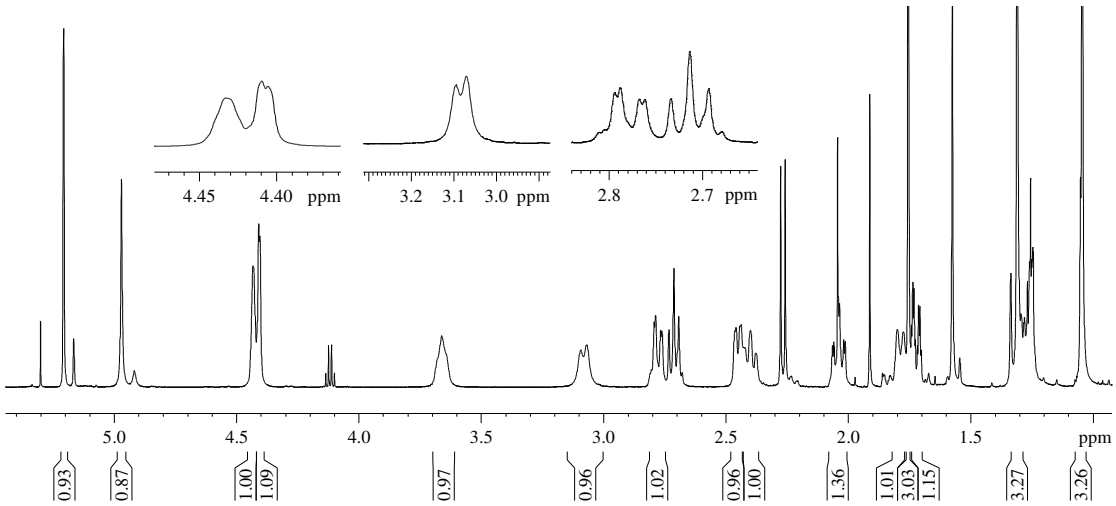

Figure S9.1: ^{1}H NMR spectrum ($CDCl_3$, 600 MHz) of compound **9.1**

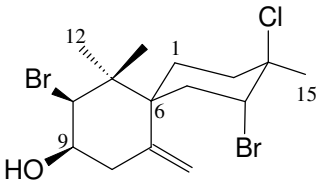

9.1

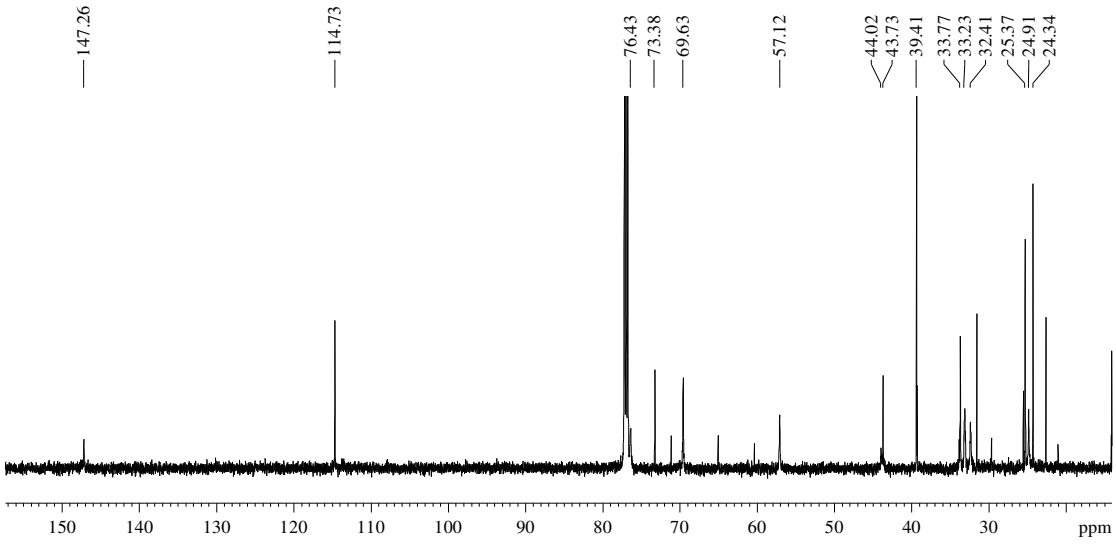

Figure S9.2: ^{13}C NMR spectrum ($CDCl_3$, 150 MHz) of compound **9.1**

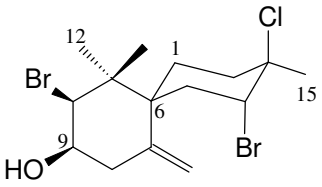

9.1

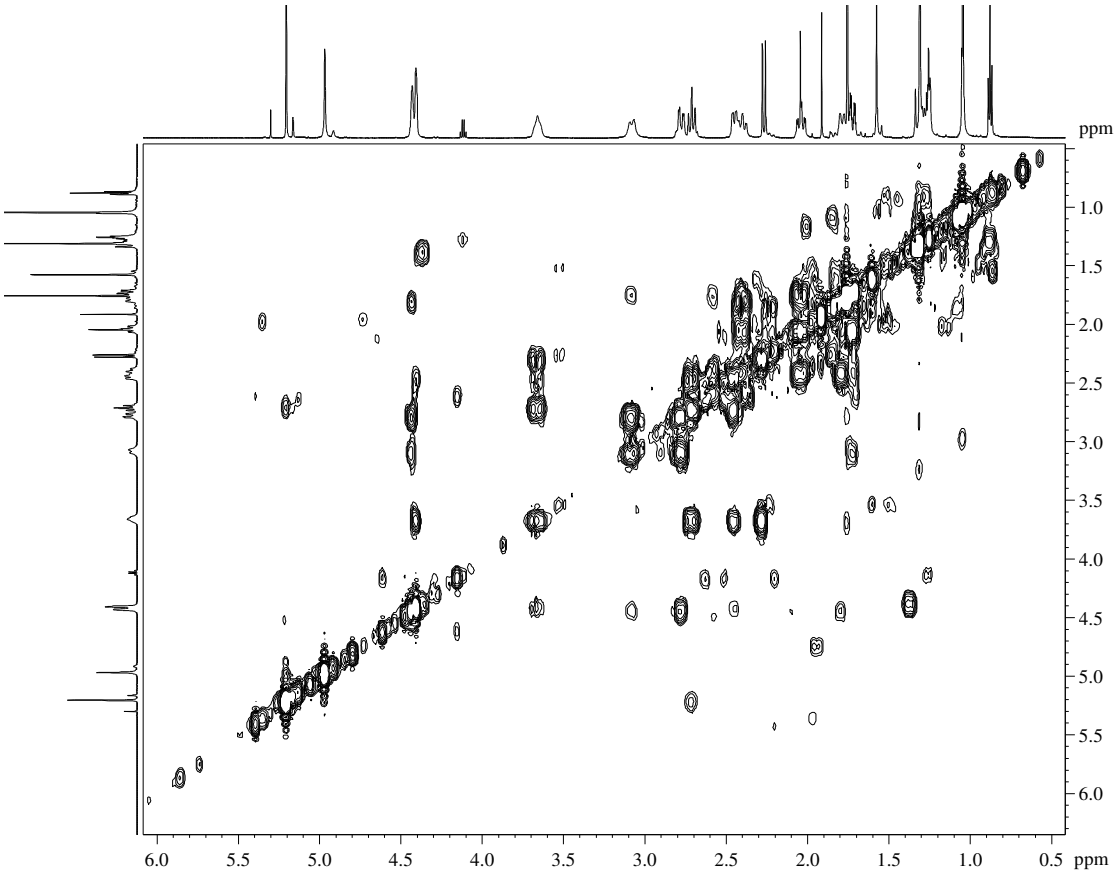

Figure S9.3: COSY NMR spectrum of compound **9.1**

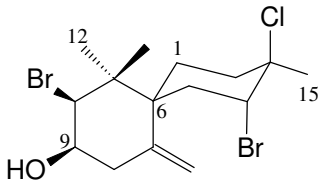

9.1

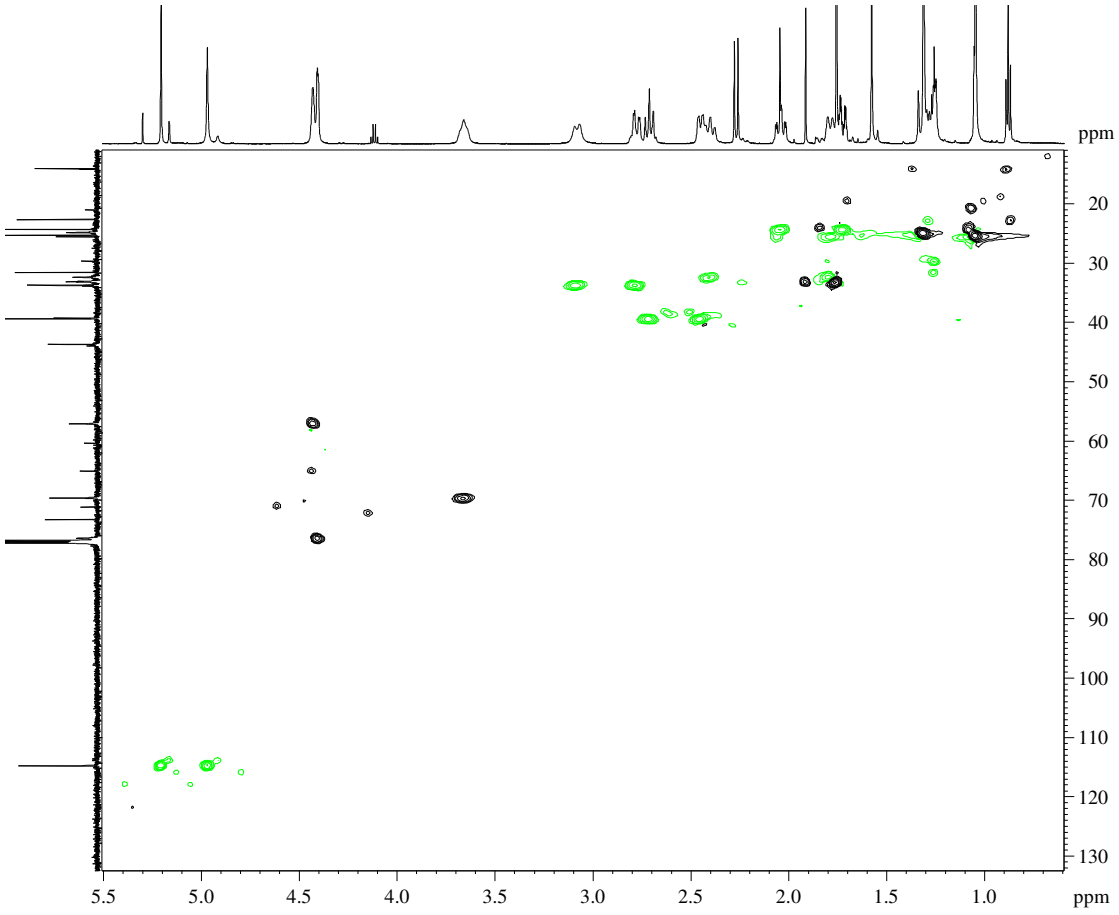

Figure S9.4: HSQC NMR spectrum of compound **9.1**

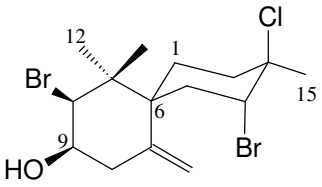

9.1

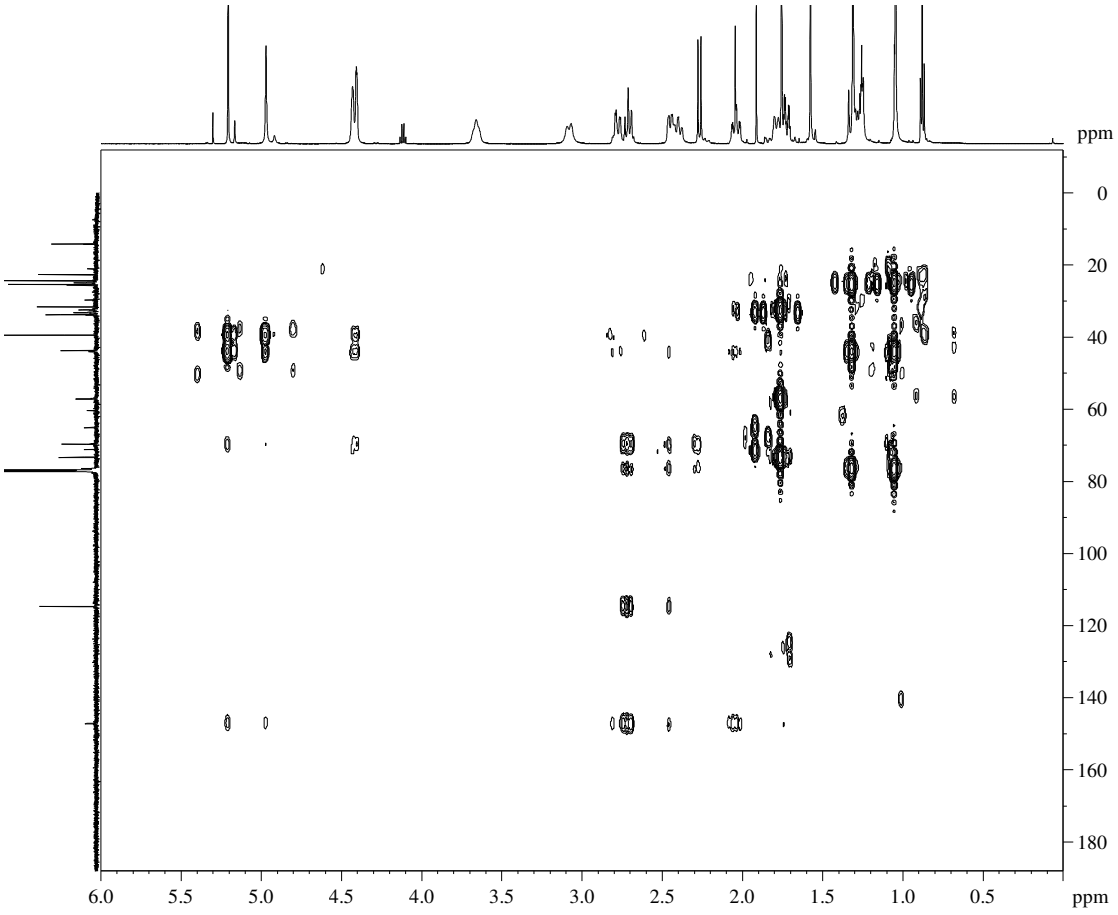

Figure S9.5: HMBC NMR spectrum of compound **9.1**

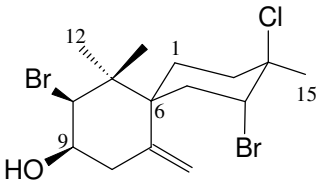

9.1

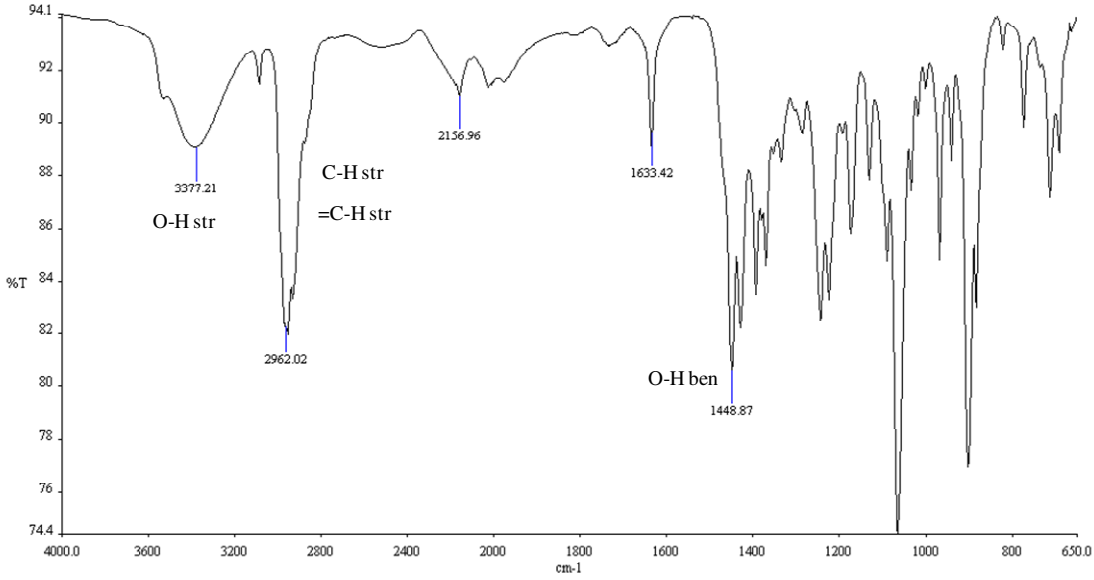

Figure S9.6: IR NMR spectrum of compound **9.1**

S9.2 Compound 9.3

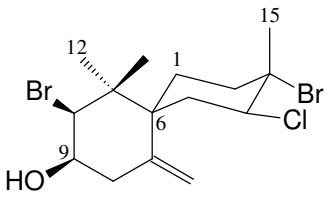

9.3

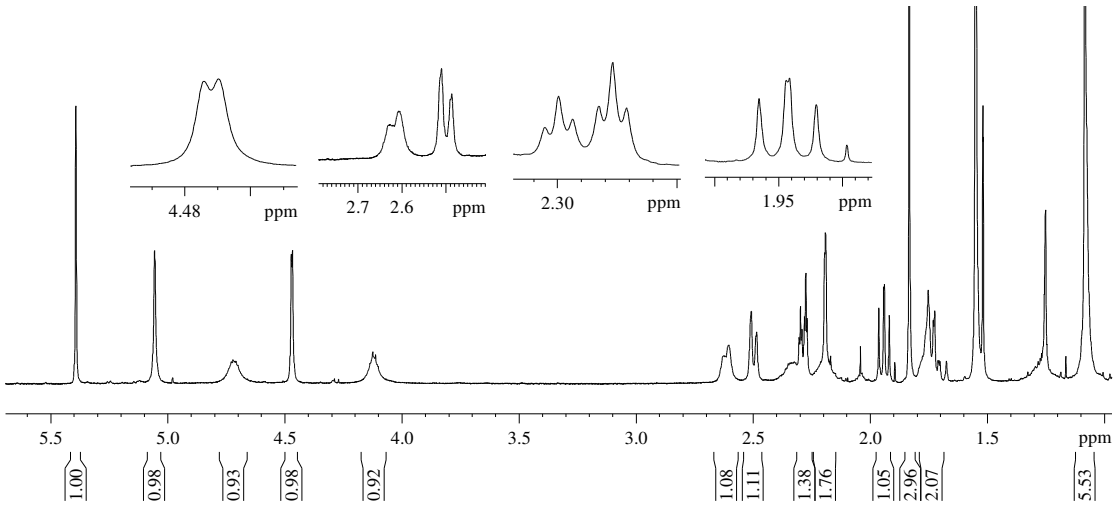

Figure S9.7: ^{1}H NMR spectrum ($CDCl_3$, 600 MHz) of compound **9.3**

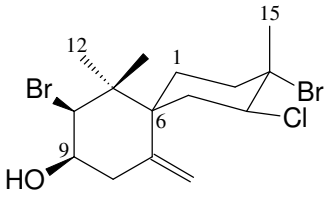

9.3

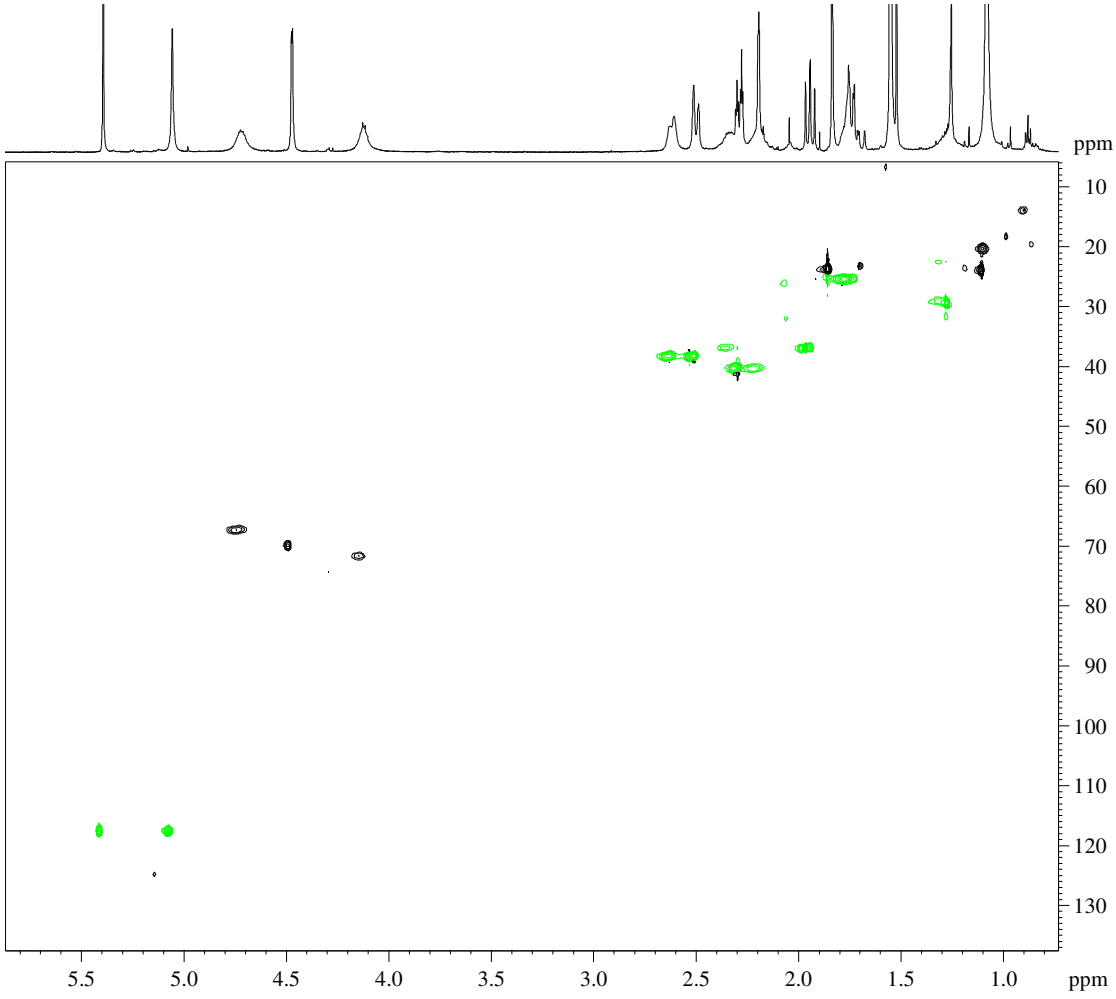

Figure S9.8: HSQC NMR spectrum of compound **9.3**

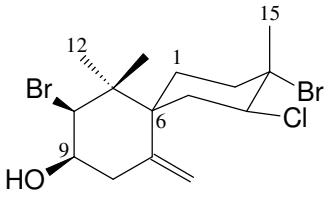

9.3

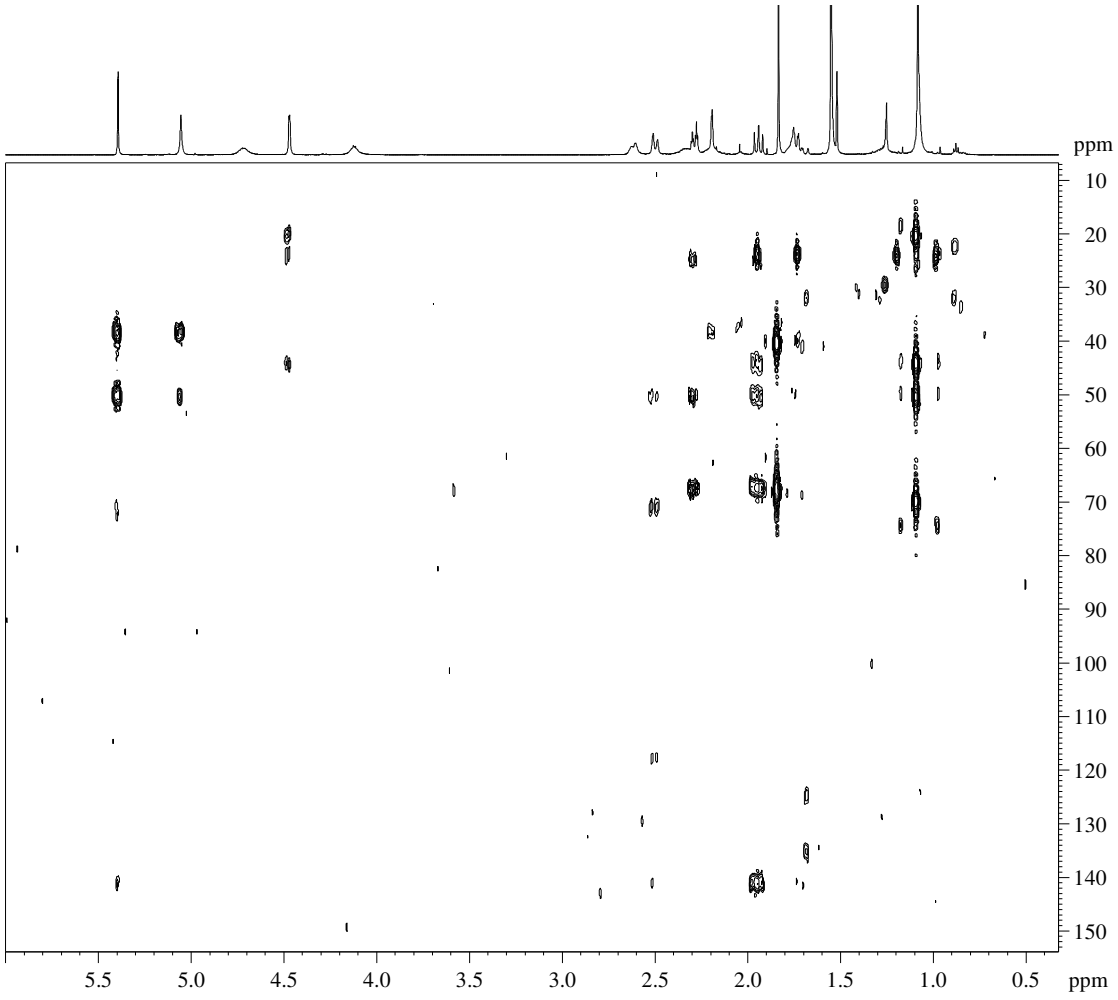

Figure S9.9: HMBC NMR spectrum of compound **9.3**

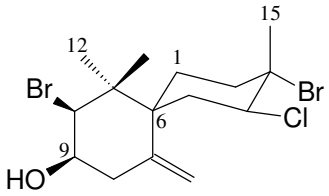

9.3

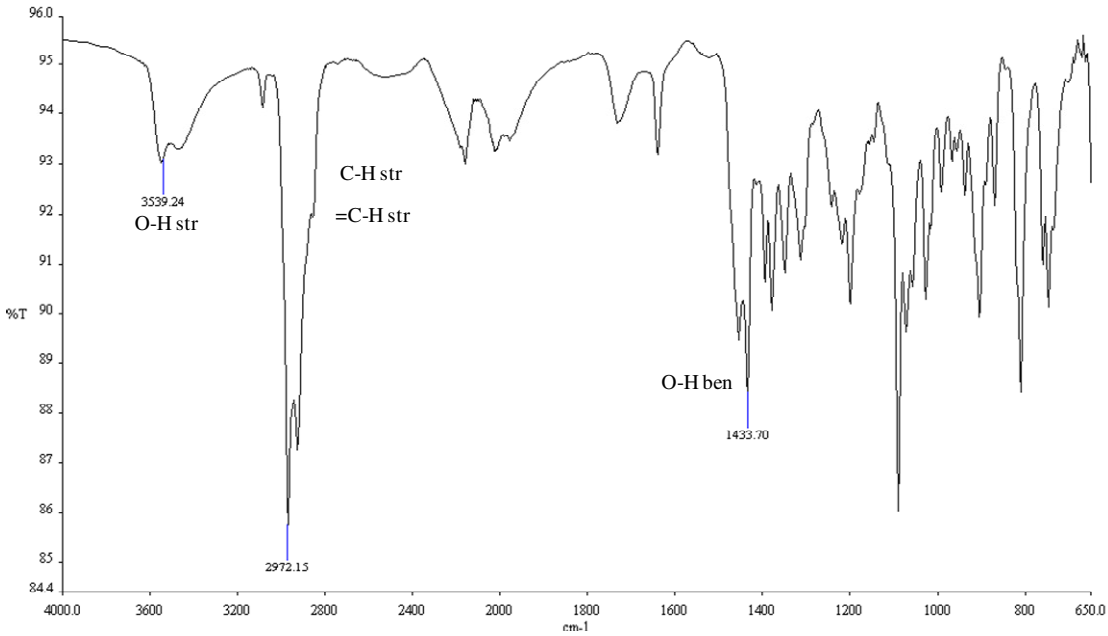

Figure S9.10: IR NMR spectrum of compound **9.3**

Chapter 10

Chemotaxonomic significance of metabolites isolated

From the *rbc*L sequence study done by (Francis, 2014)[1], the *Laurencia* spp. phylogeny tree in (Figure S10.1) was produced. Details of the phylogeny tree as presented by Francis (2014) are as explained below:

The phylogeny tree is based on a 50% majority-rule Bayesian inference of the South African *Laurencia* complex as inferred from the plastid *rbc*L gene region under a GTR + I + G model of sequence evolution.

Posterior probabilities (PP) ≥ 0.90 are depicted either adjacent to the relevant node or indicated by an arrowhead.

'A', 'G-J': unidentified morphotypes;

'K-P": *Laurencia* cf. *corymbosa* morphotypes;

#: *Laurencia obtusa* morphotype.

Species with sequences from or near type locality are underlined.

Country codes

A – Australia, **B** – Brazil, **C** – Cuba, **F** – France, **G** – Guadalupe, **I** – Ireland, **M** – Mexico, **NC** – New Caledonia, **P** – Philippines, **RSA** – South Africa, **S** – Spain, **USA** – United States of America, **T** – Taiwan, **V** – Venezuela

[1] Francis, C. M. **2014**. Systematics of the *Laurencia* complex (Rhodomelaceae, Rhodophyta) in southern Africa. PhD Thesis. University of Cape Town, Cape Town, South Africa.

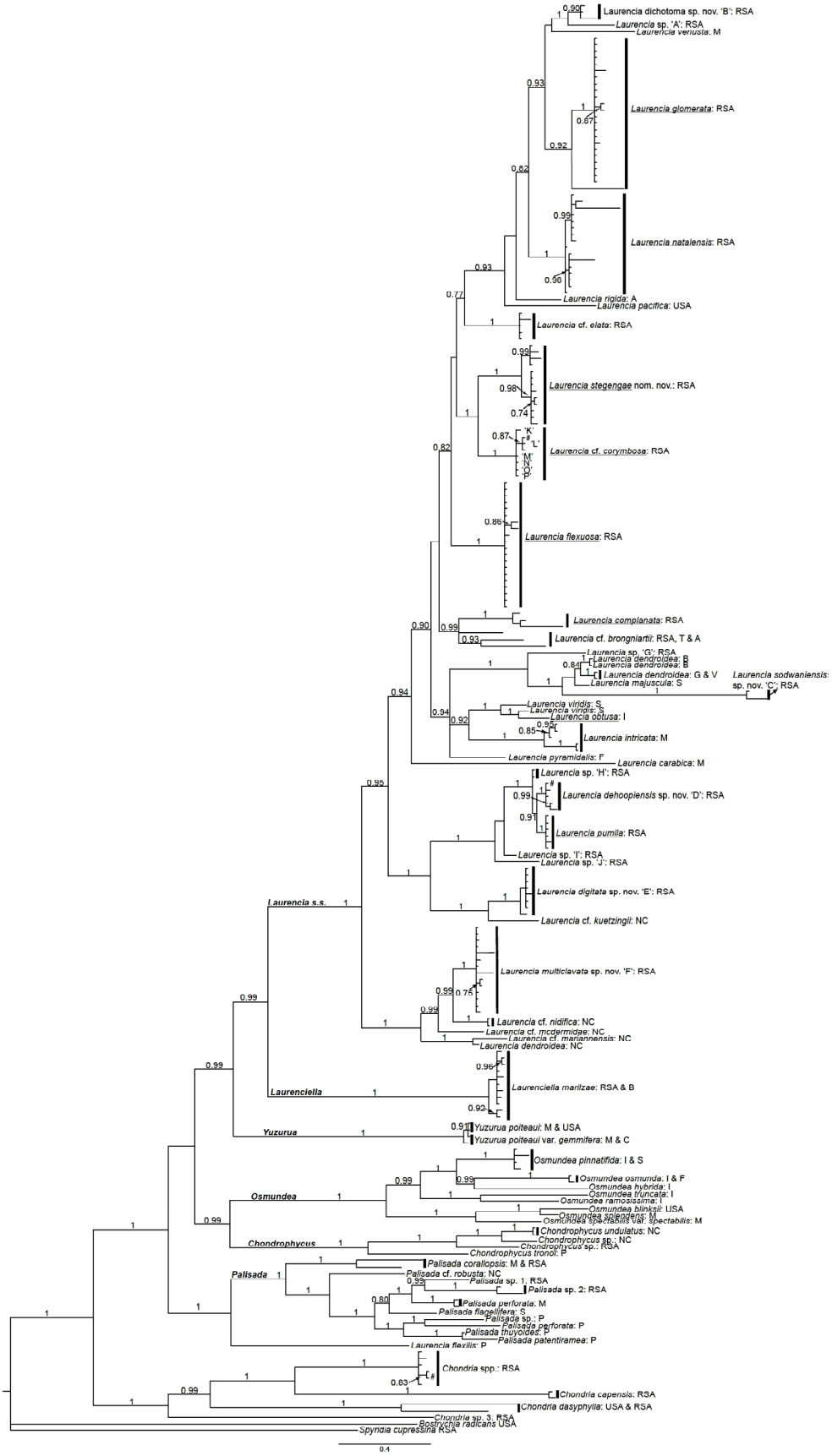

Figure S10.1: Phylogeny of *Laurencia* spp.

Chapter 11

^{1}H NMR profiling of crude organic extracts as a discriminatory tool for the identification of selected *Laurencia* spp.

S11.1 Additional ^{1}H NMR profiles

S11.1.1 *L. flexuosa* (KOS130823-2)

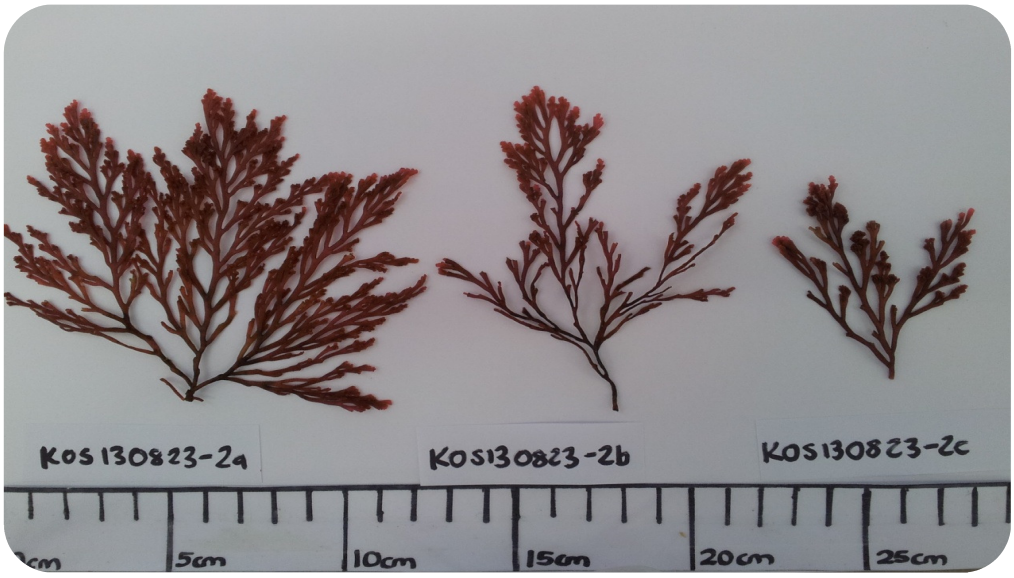

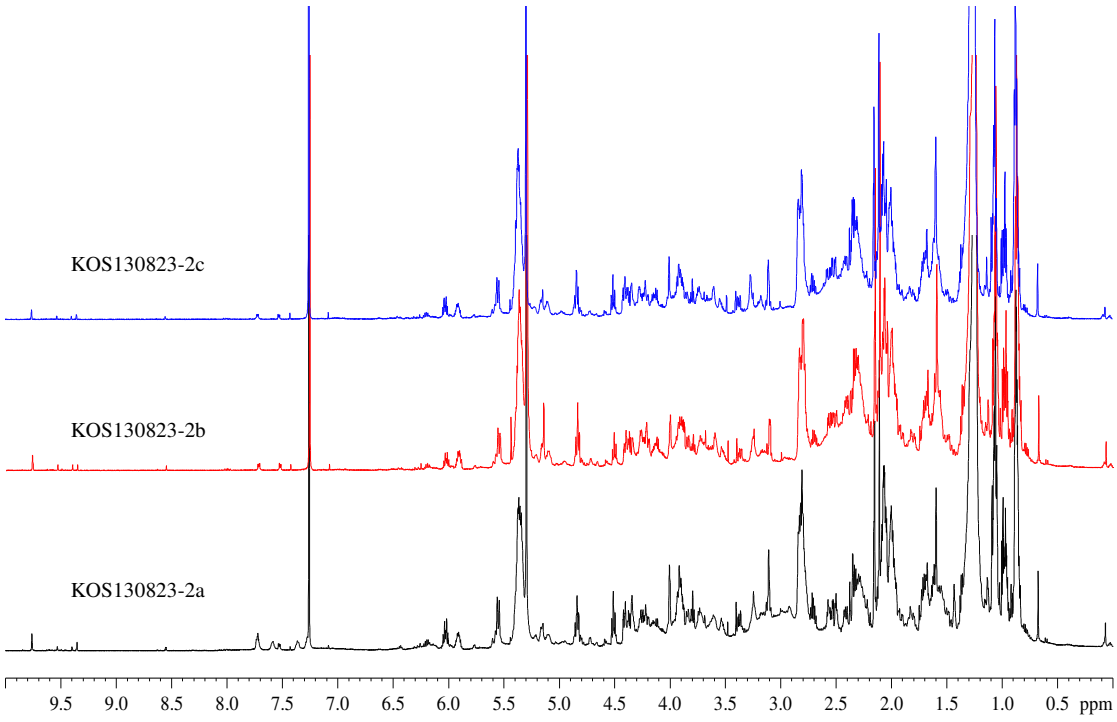

Figure S11.1 ^{1}H NMR ($CDCl_3$, 600 MHz) profiles of *L. flexuosa* (KOS130823-2)

S11.1.2 *L. flexuosa* (KOS130823-4)

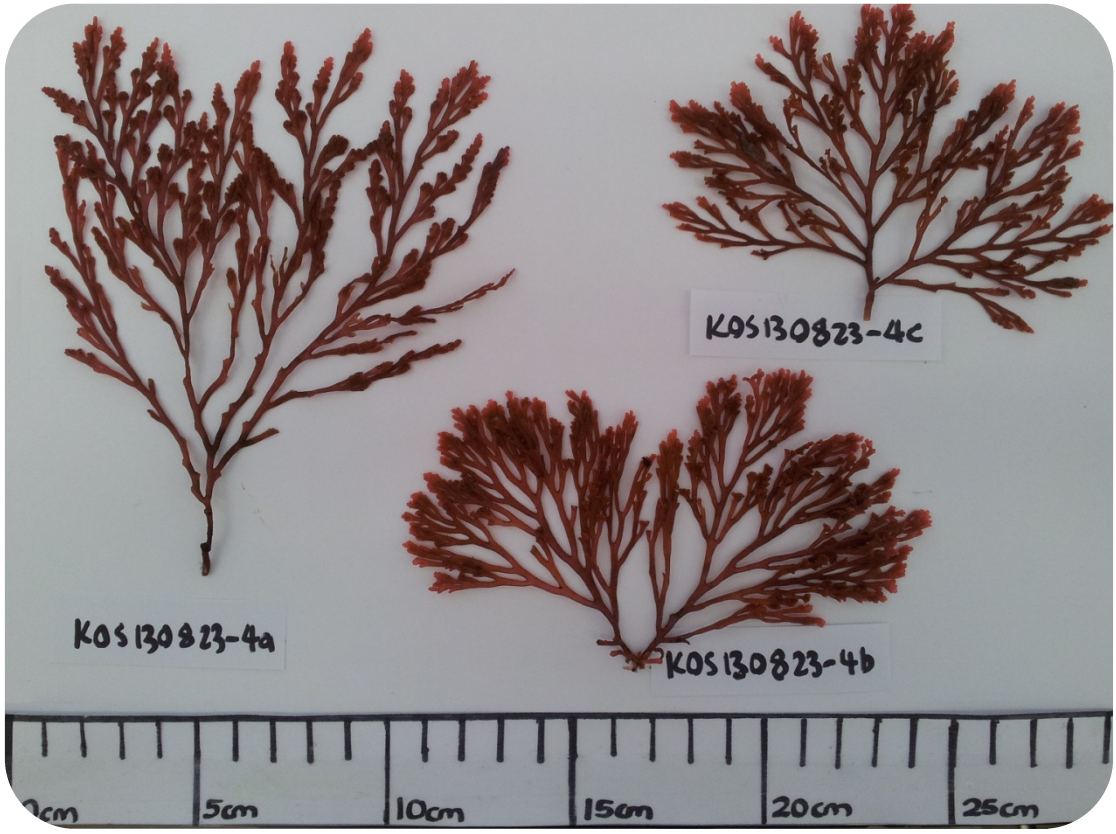

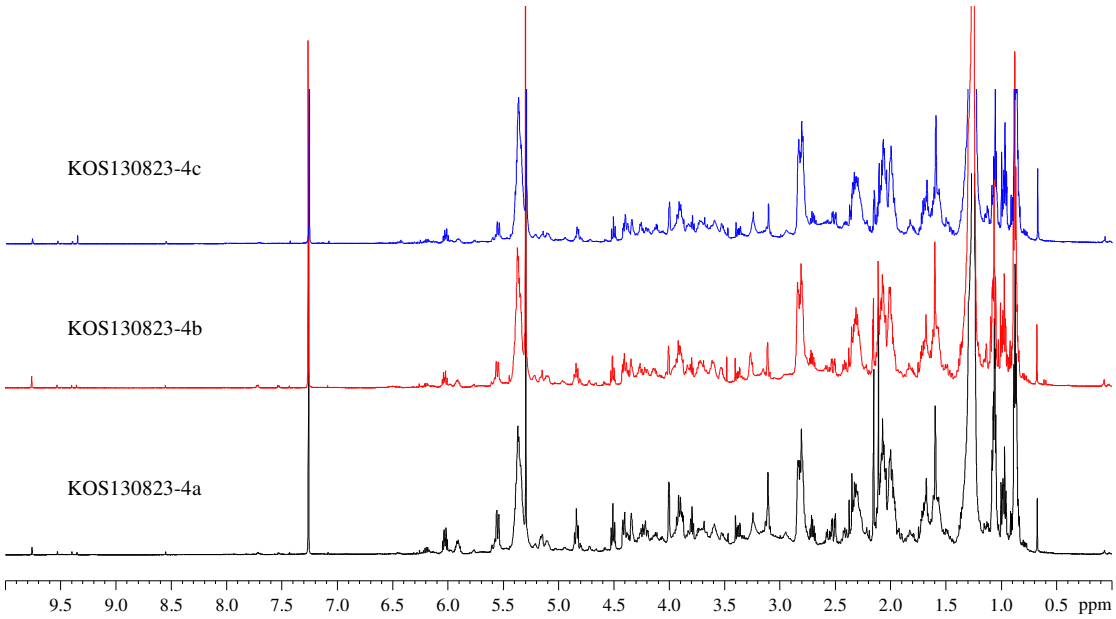

Figure S11.2 ^{1}H NMR ($CDCl_3$, 600 MHz) profiles of *L. flexuosa* (KOS130823-4)

S11.1.3 *L. flexuosa* (KOS130823-5)

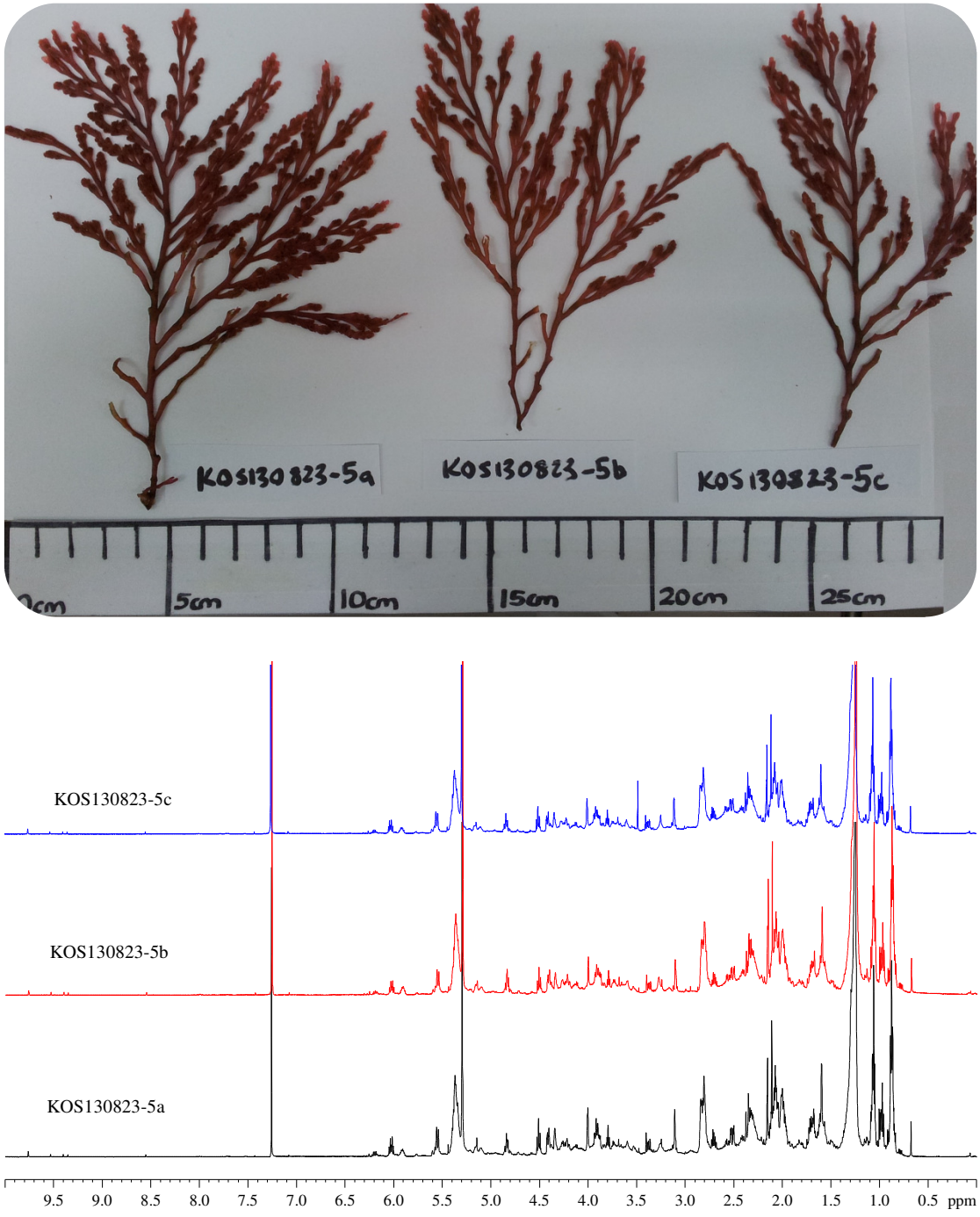

Figure S11.3 ^{1}H NMR ($CDCl_3$, 600 MHz) profiles of *L. flexuosa* (KOS130823-5)

S11.1.4 *L. flexuosa* (KOS130823-6)

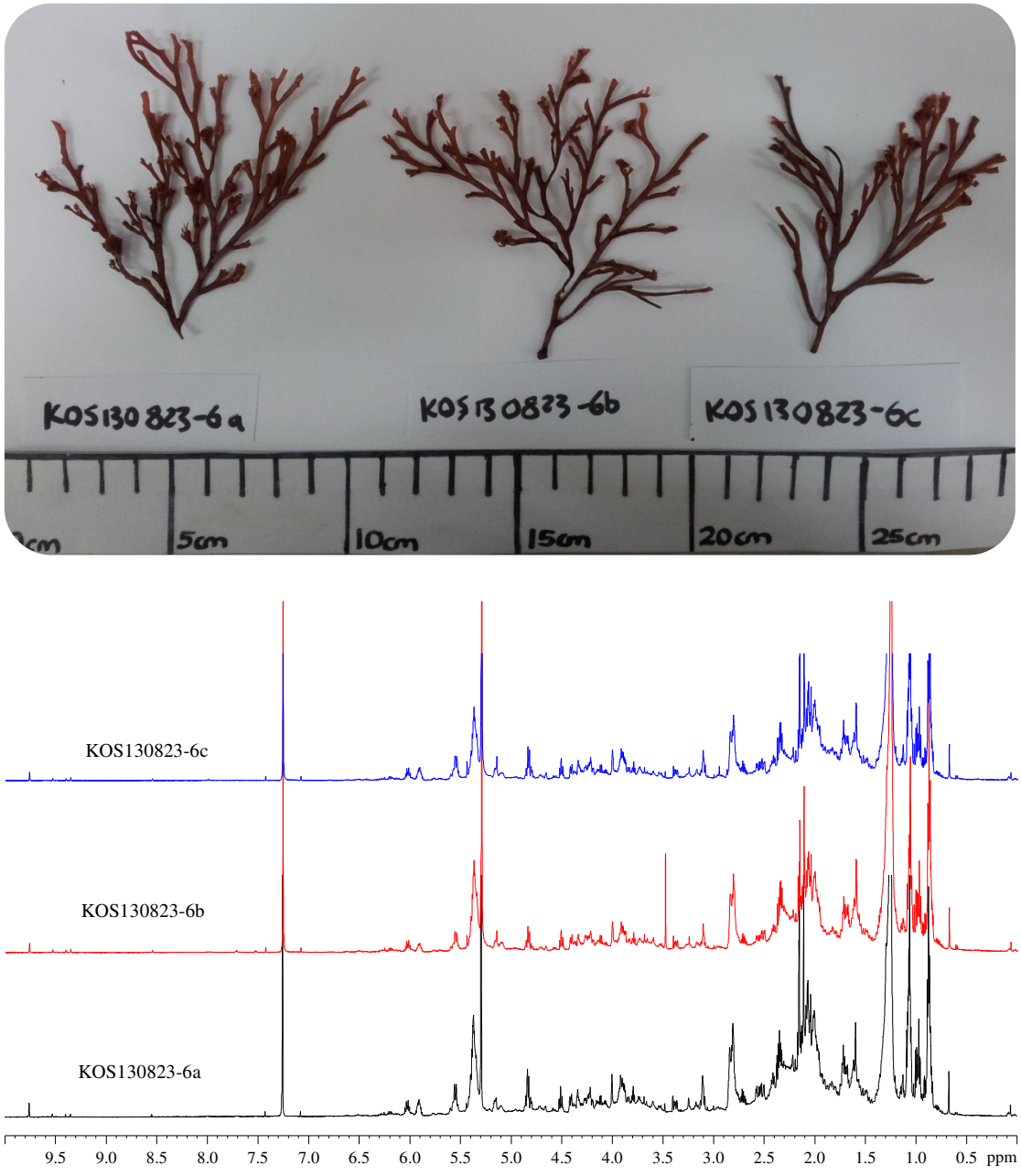

Figure S11.4 ^{1}H NMR ($CDCl_3$, 600 MHz) profiles of *L. flexuosa* (KOS130823-6)

S11.1.5 *L. flexuosa* (NDK130821-12)

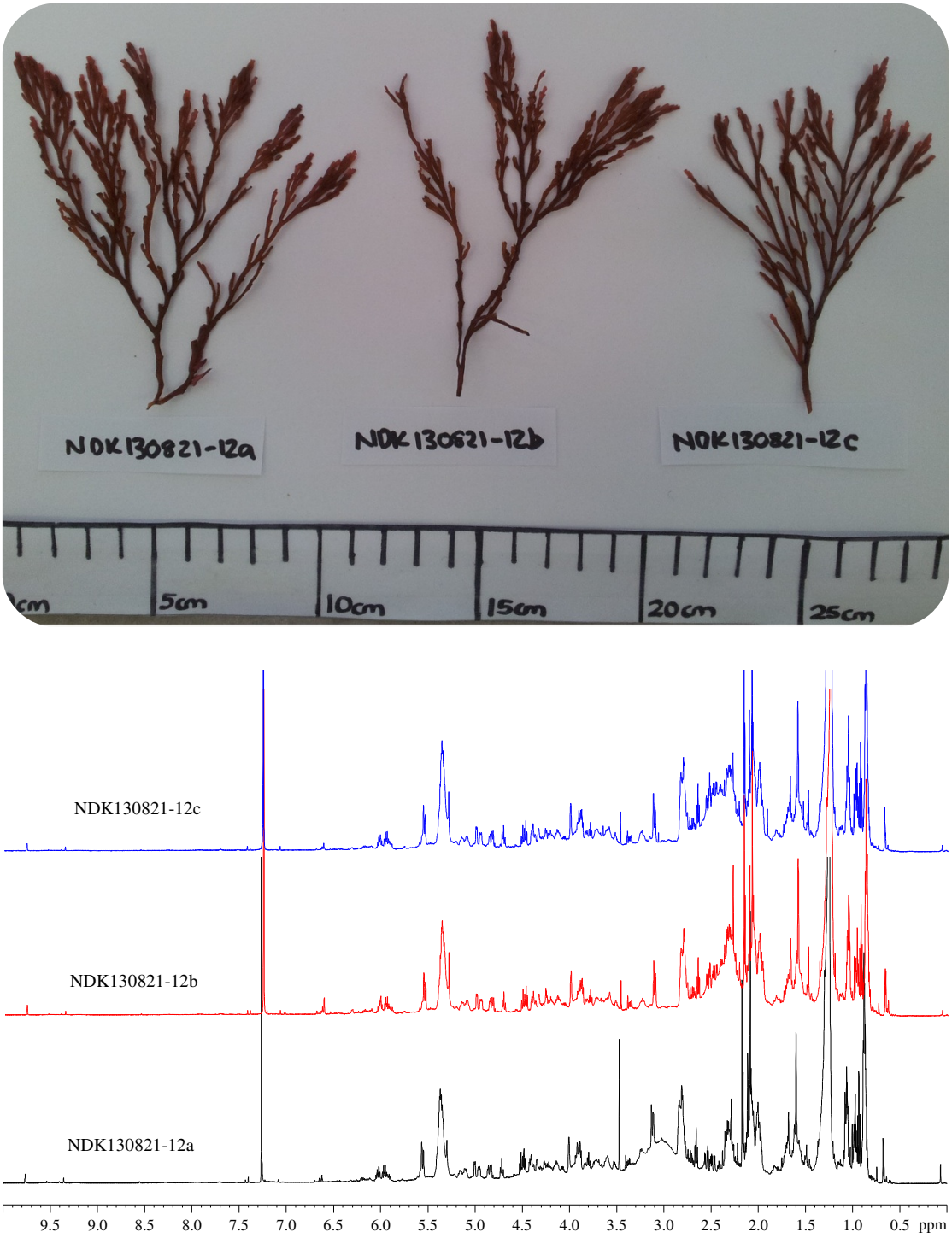

Figure S11.5 ^{1}H NMR ($CDCl_3$, 600 MHz) profiles of *L. flexuosa* (NDK130821-12)

S11.1.6 *L. flexuosa* (D1013)

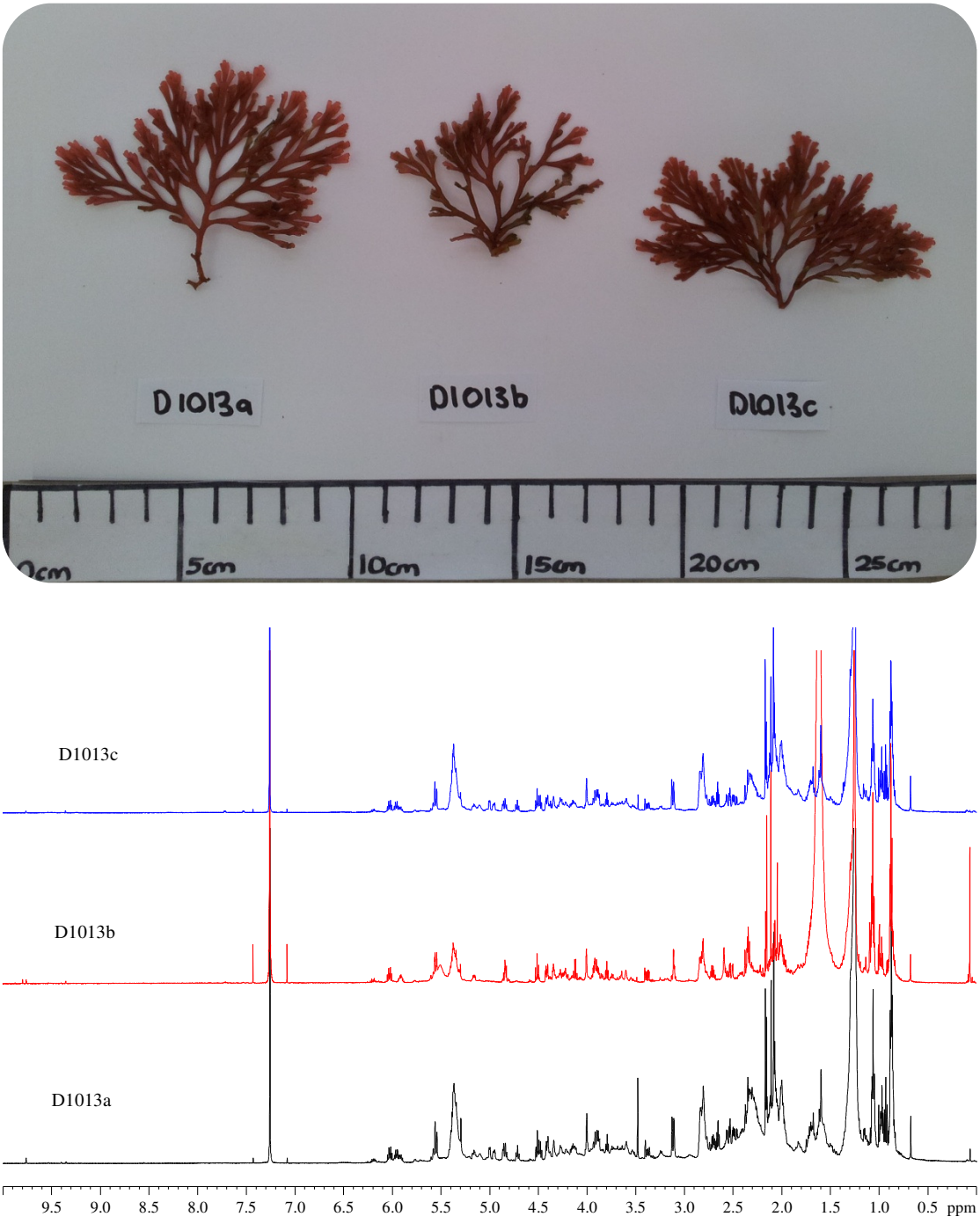

Figure S11.6 ^{1}H NMR ($CDCl_3$, 600 MHz) profiles of *L. flexuosa* (D1013)

S11.1.7 *L. flexuosa* (D904)

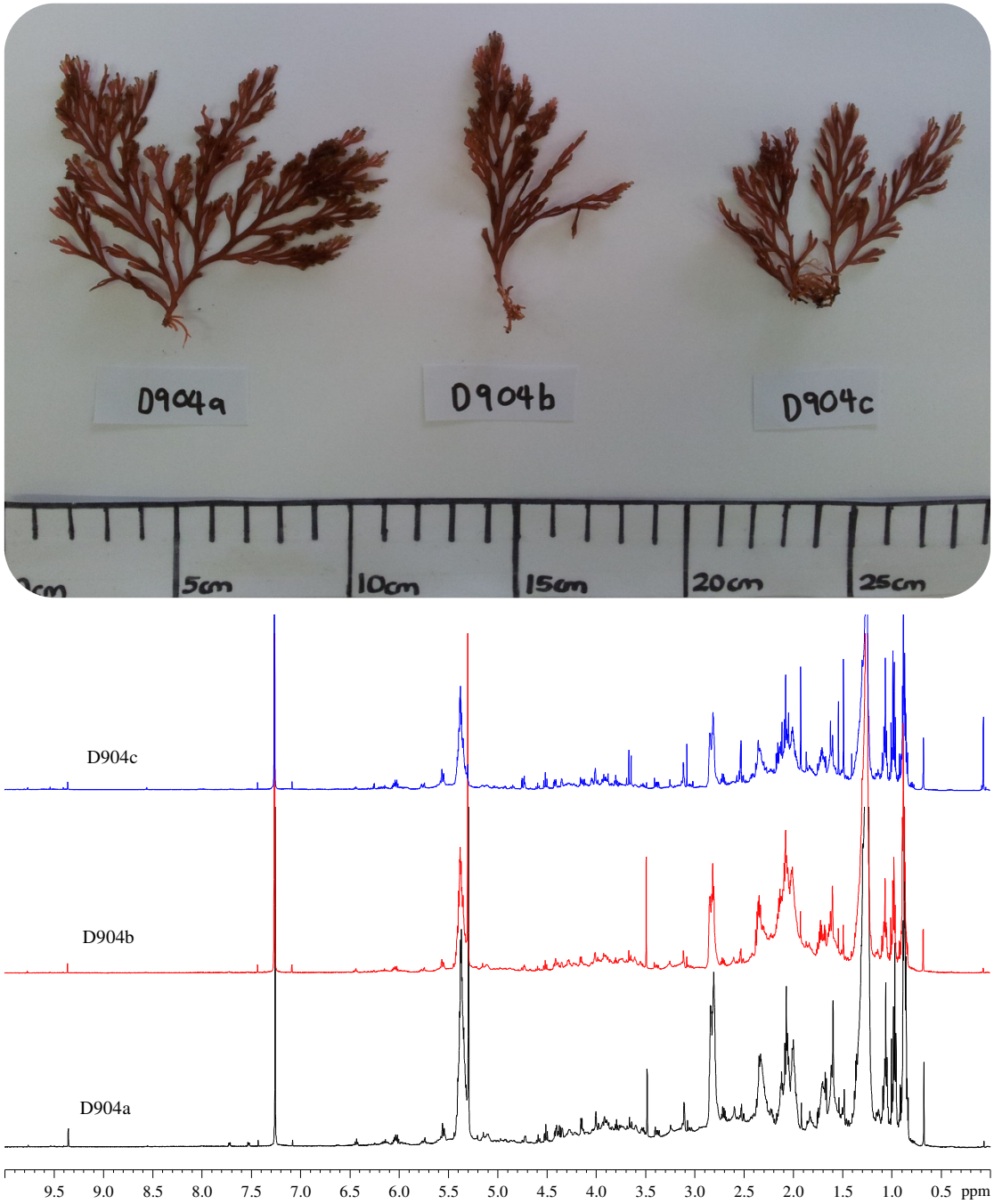

Figure S11.7 ^{1}H NMR ($CDCl_3$, 600 MHz) profiles of *L. flexuosa* (D904)

S11.1.8 *L. natalensis* (D1022)

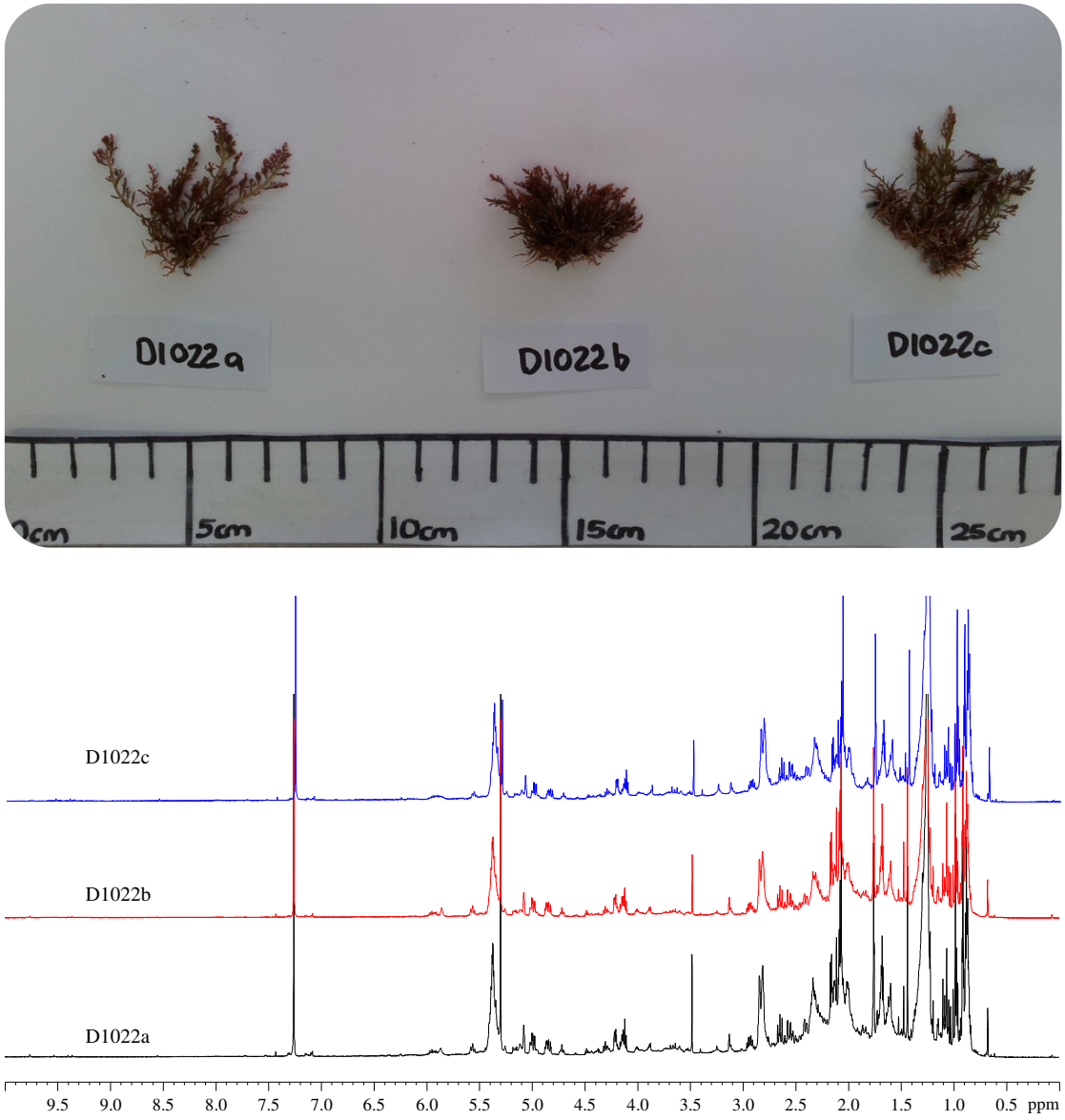

Figure 11.8: ^{1}H NMR ($CDCl_3$, 600 MHz) profiles of *L. natalensis* (D1022)

S11.1.9 *L. peninsularis* (D900)

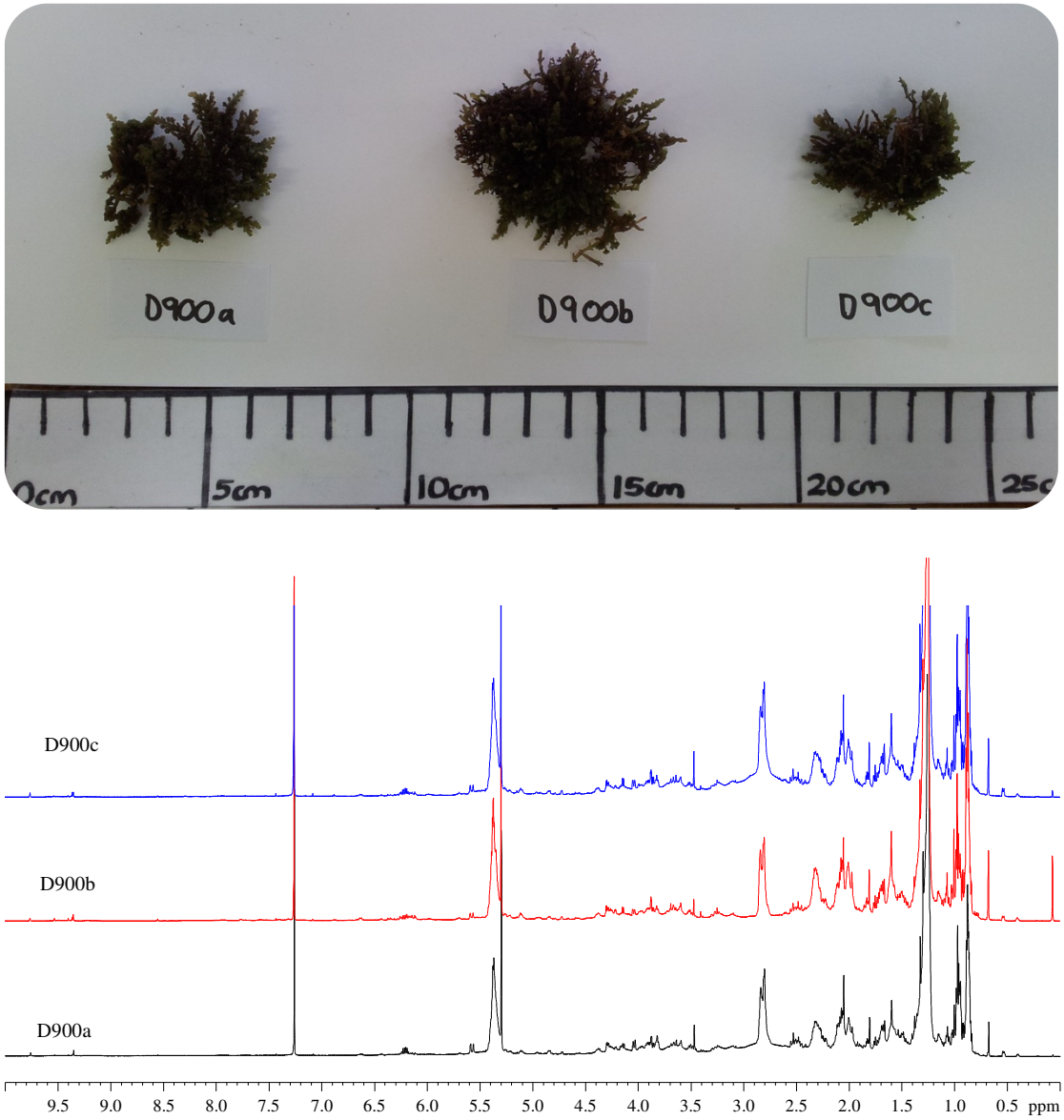

Figure S11.9 ^{1}H NMR ($CDCl_3$, 600 MHz) profiles of *L. peninsularis* (D900)

S11.1.10 *L. peninsularis* (GC120901)

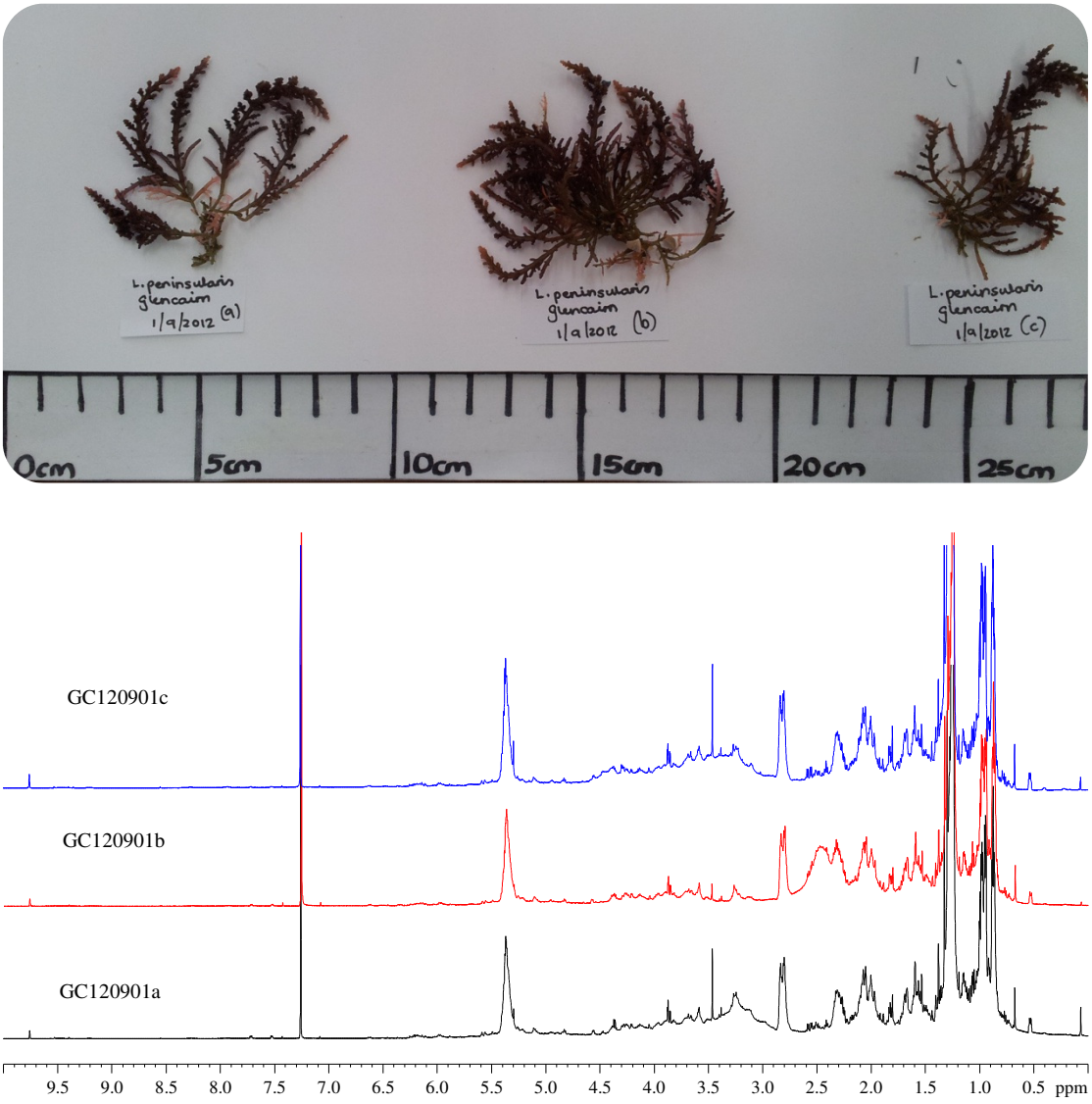

Figure S11.10 ^{1}H NMR ($CDCl_3$, 600 MHz) profiles of *L. peninsularis* (GC120901)

S11.1.11 *L. multiclavata* (D969)

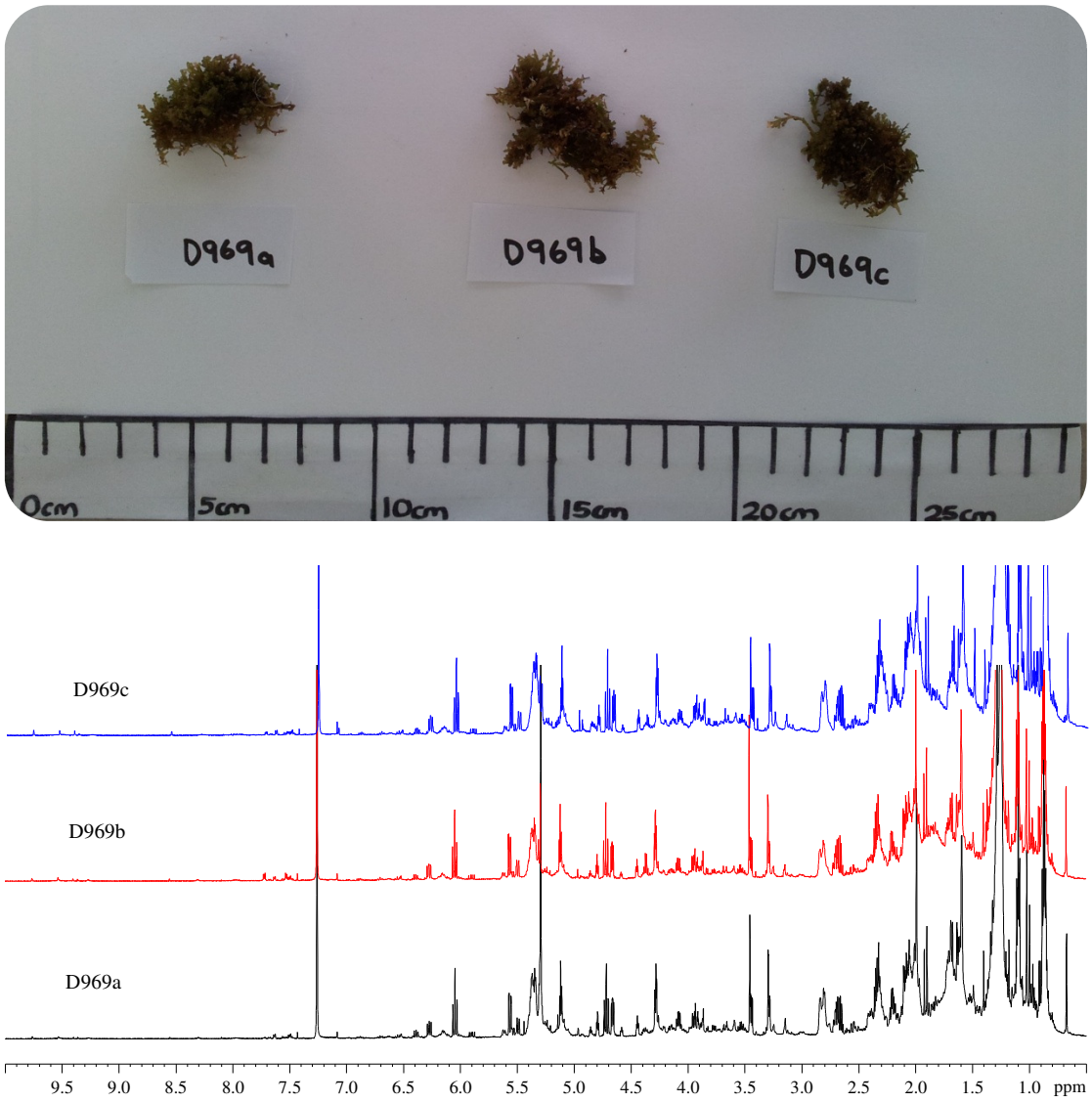

Figure S11.11 ^{1}H NMR ($CDCl_3$, 600 MHz) profiles of *L. multiclavata* (D969)

Appendix 1

Secondary metabolites from *Laurenciella marilzae*

S.A1.1 Compound A1.9

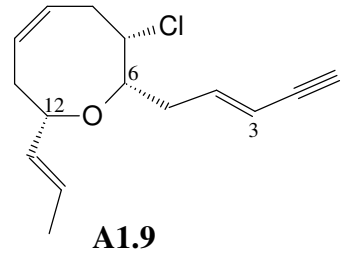

A1.9

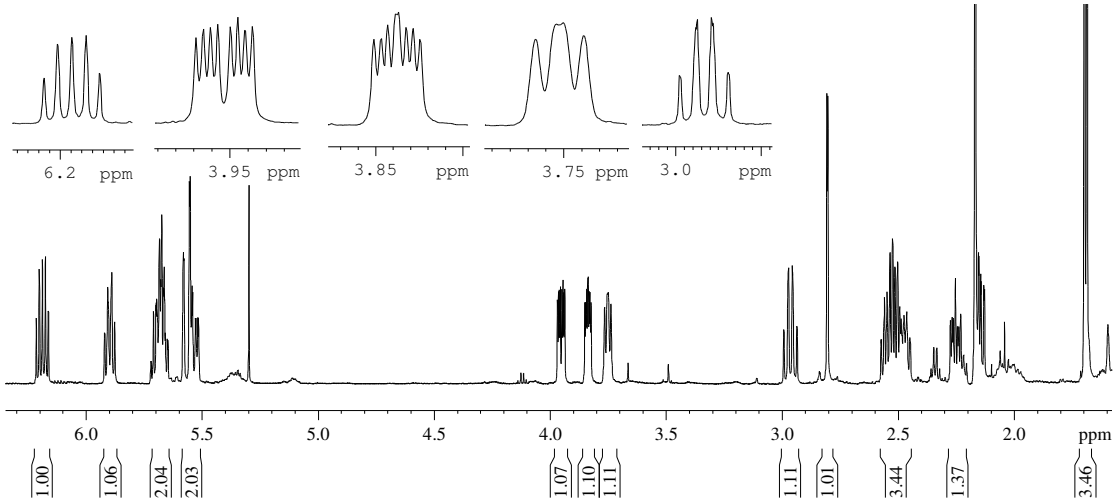

Figure S.A1.1.1: ^{1}H NMR spectrum ($CDCl_3$, 600 MHz) of compound **A1.9**

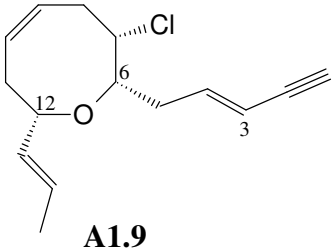

A1.9

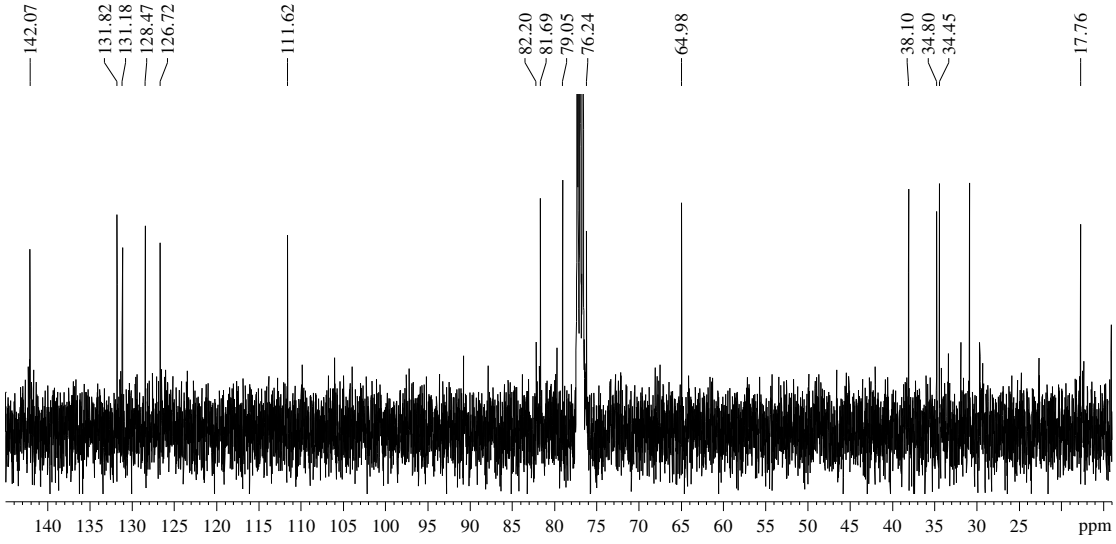

Figure S.A1.1.2: ^{13}C NMR spectrum ($CDCl_3$, 150 MHz) of compound **A1.9**

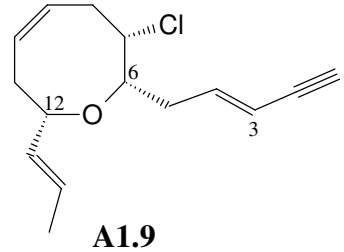

A1.9

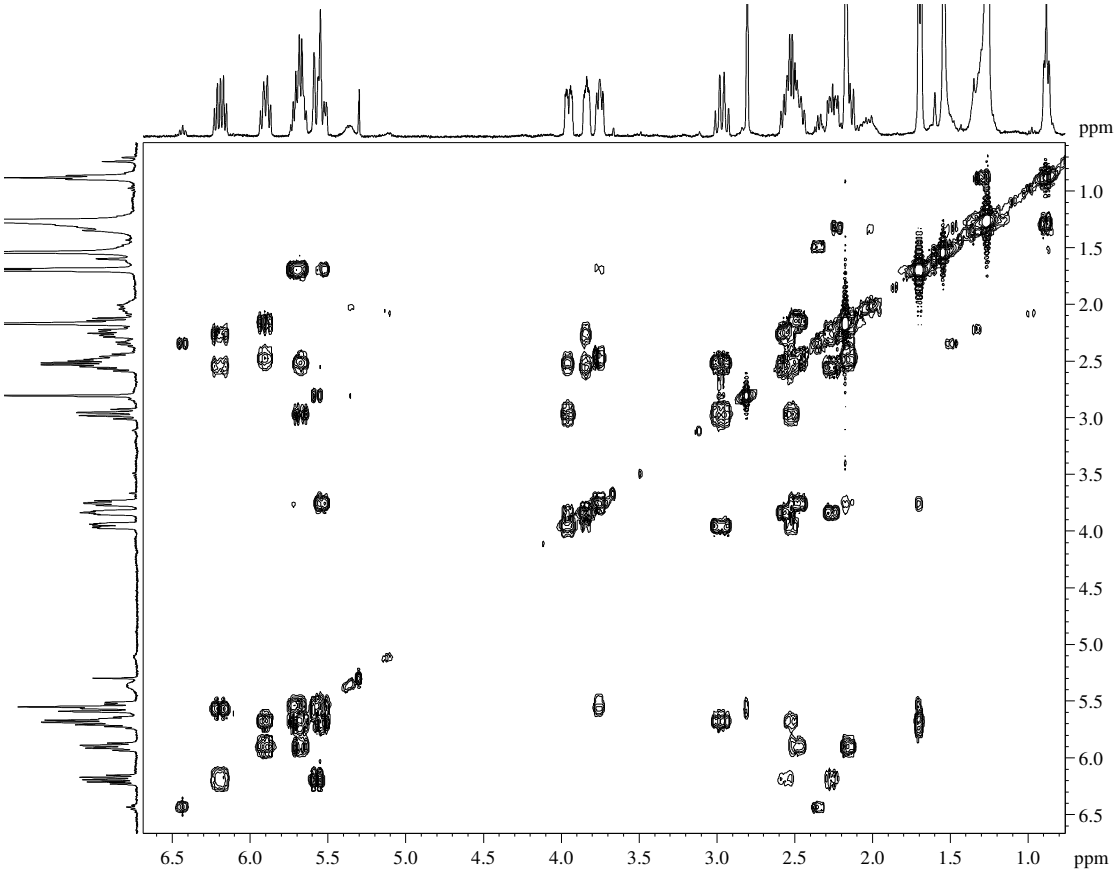

Figure S.A1.1.3: COSY spectrum of compound **A1.9**

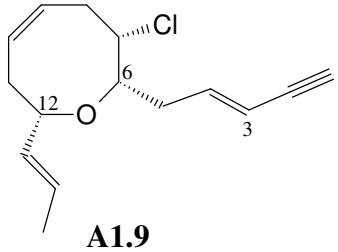

A1.9

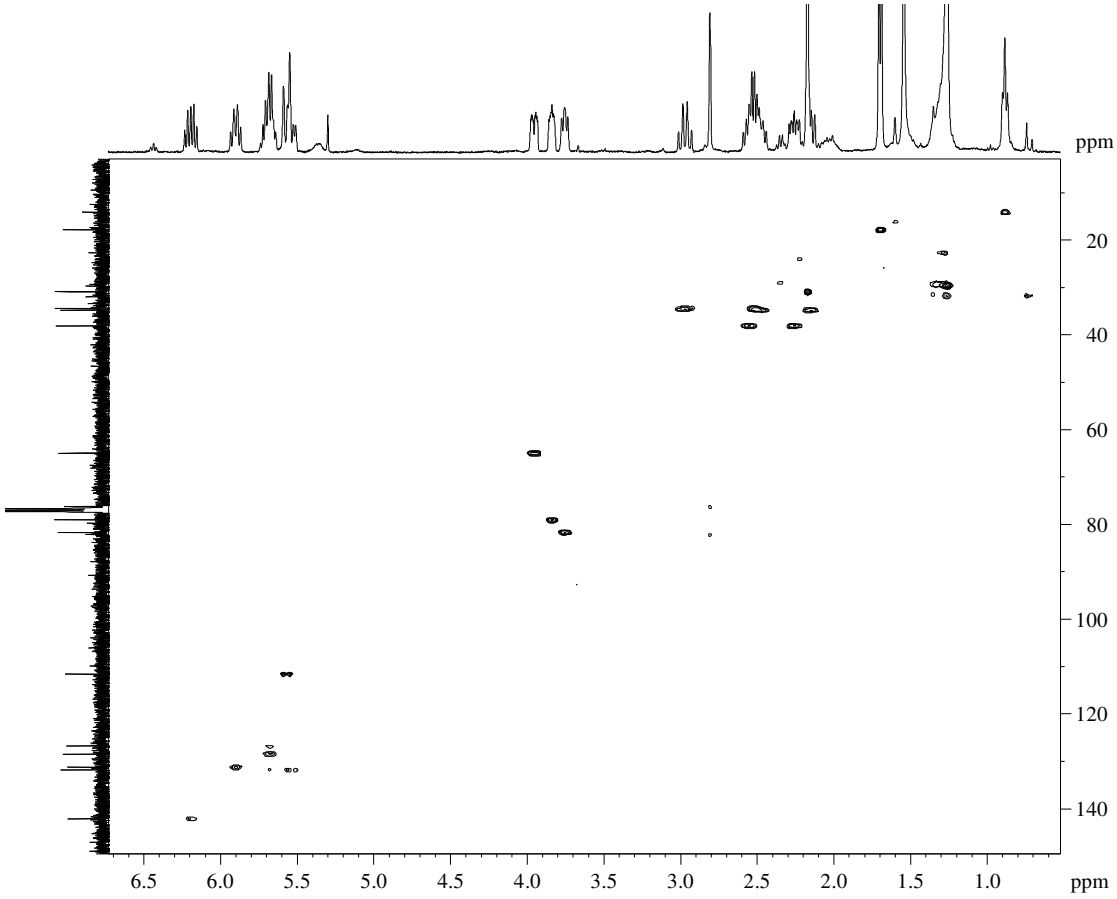

Figure S.A1.1.4: HSQC spectrum of compound **A1.9**

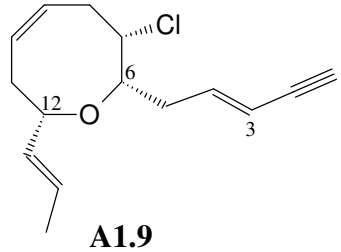

A1.9

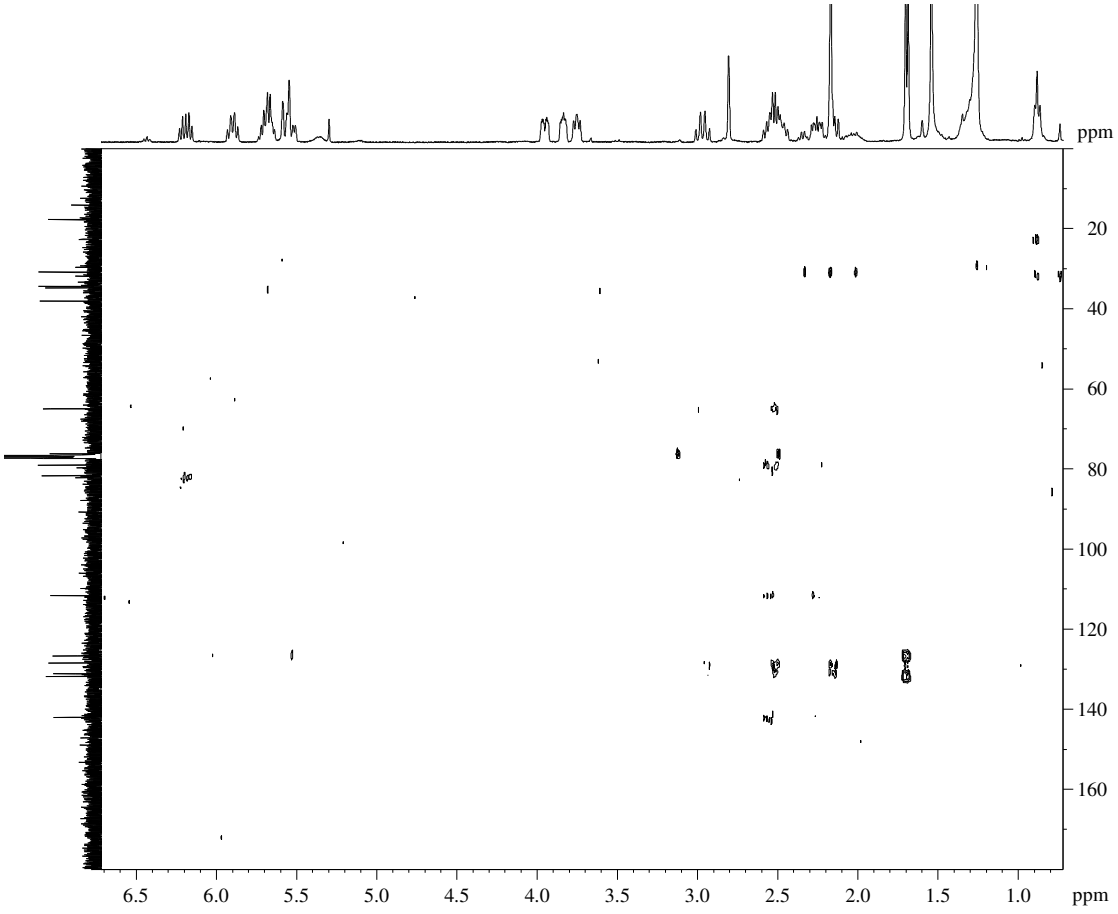

Figure S.A1.1.5: HMBC spectrum of compound **A1.9**

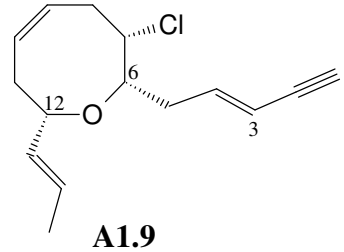

A1.9

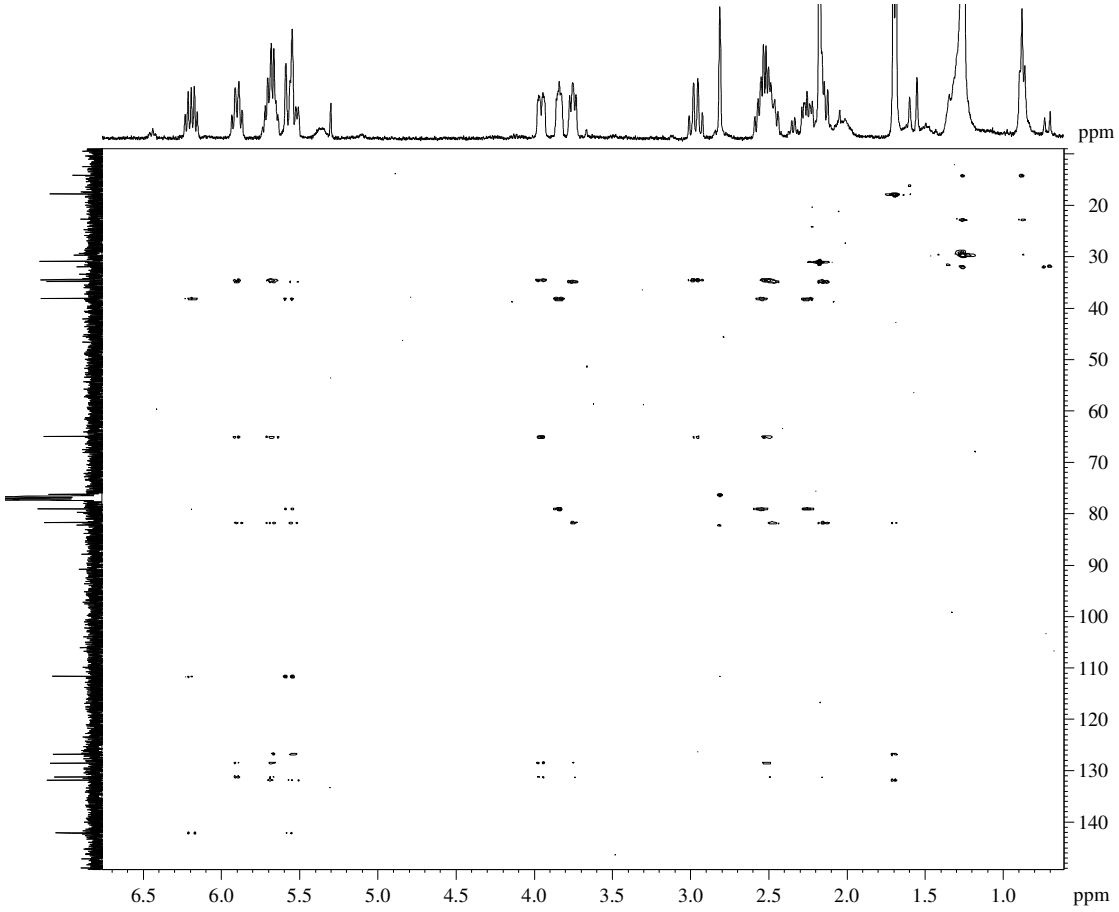

Figure S.A1.1.6: HSQC-TOCSY spectrum of compound **A1.9**

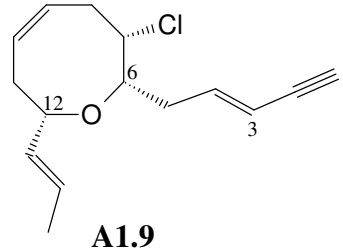

A1.9

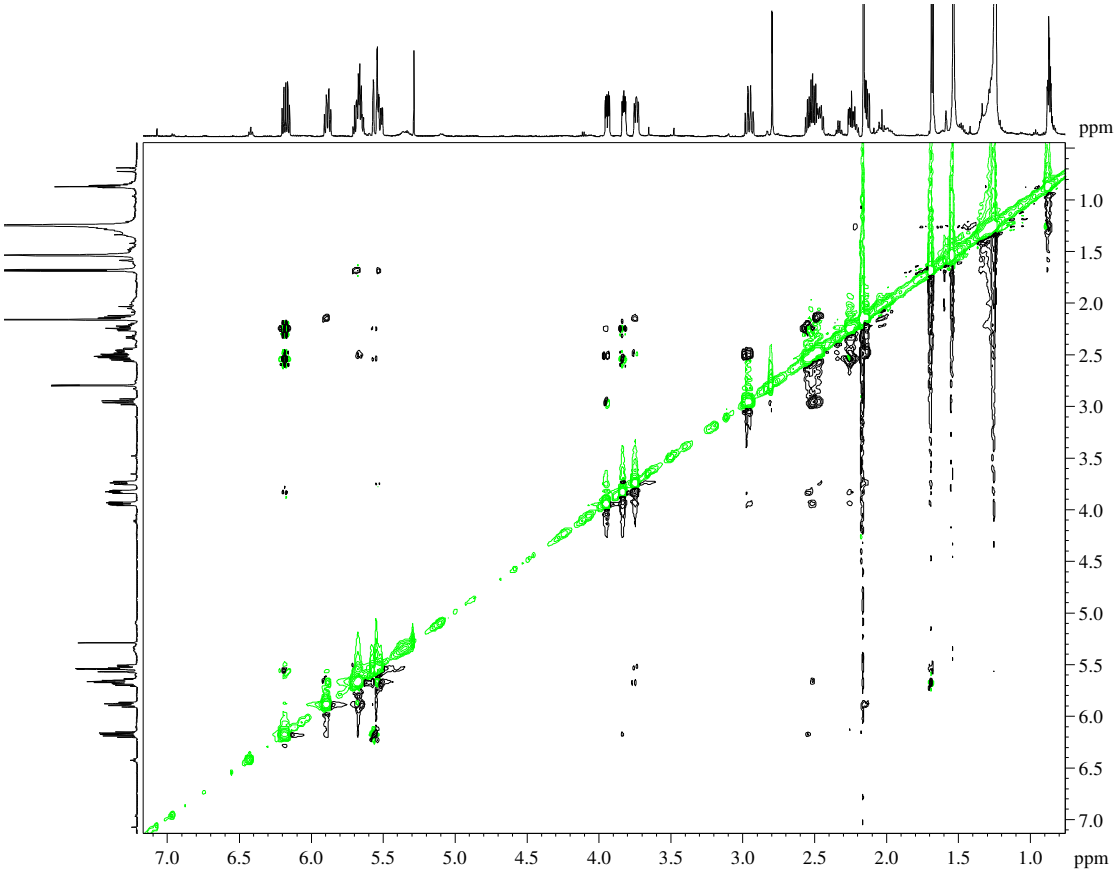

Figure S.A1.1.7: NOESY spectrum of compound **A1.9**

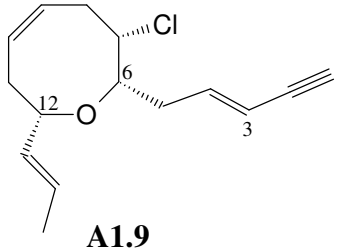

A1.9

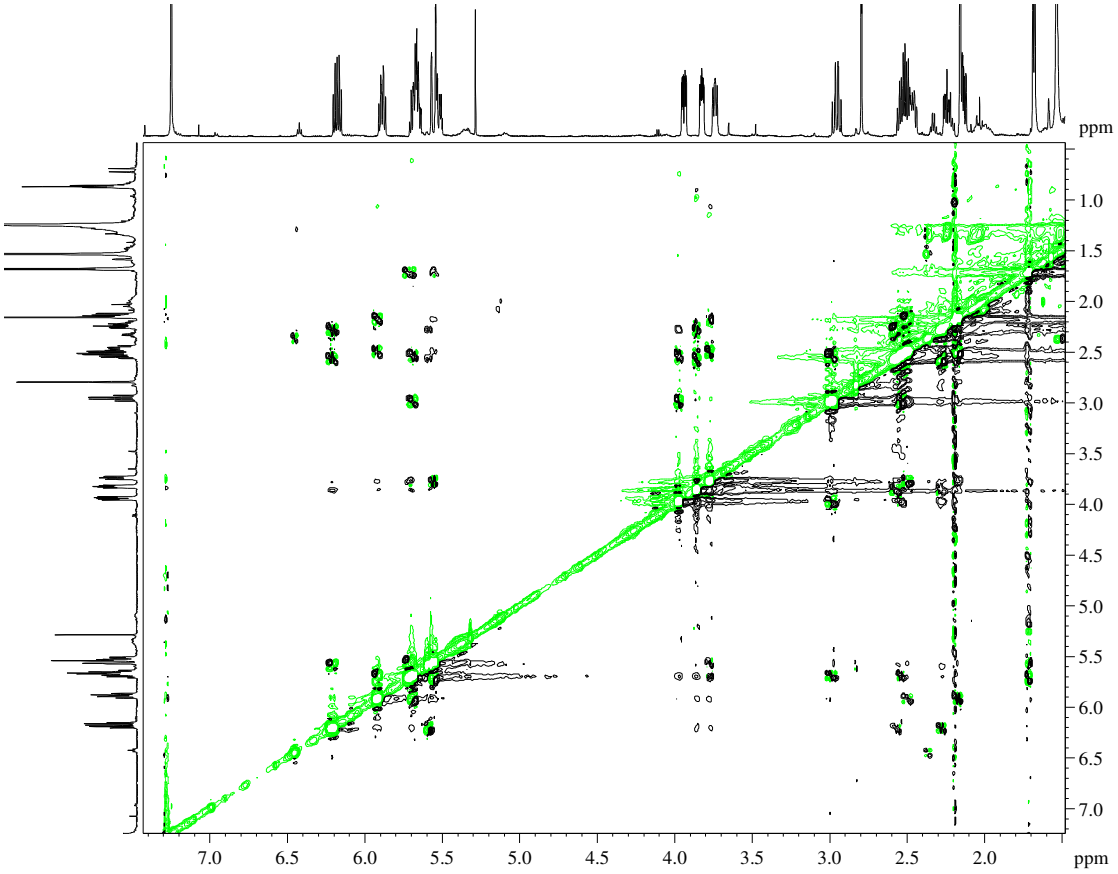

Figure S.A1.1.8: ROESY spectrum of compound **A1.9**

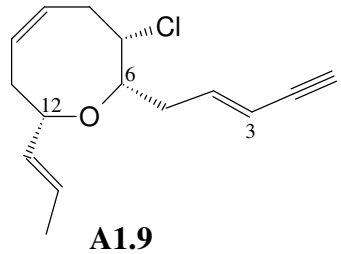

A1.9

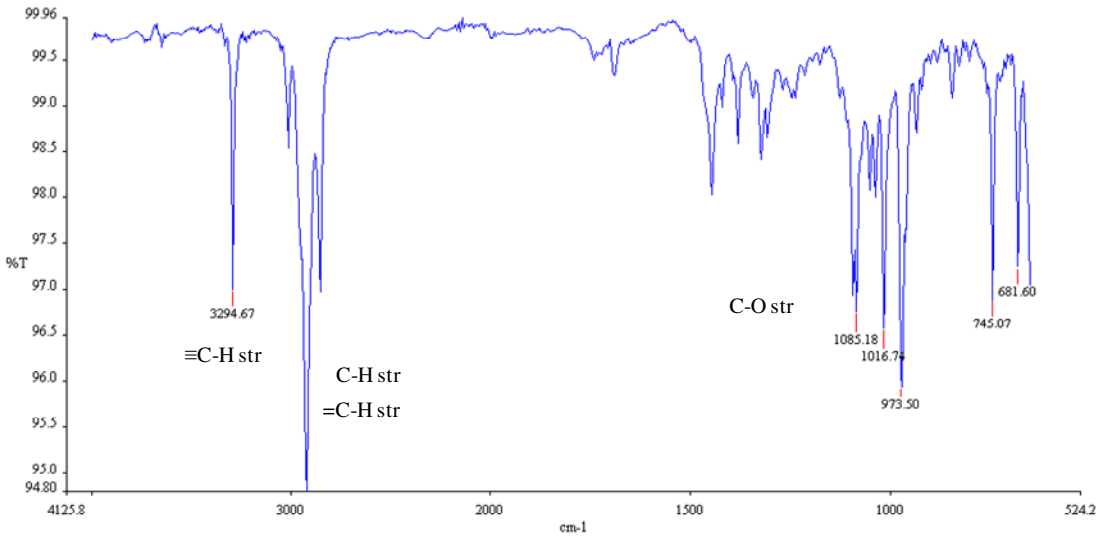

Figure S.A1.1.9: IR spectrum of compound **A1.9**